
Introduction

Each year, brief summaries of selected achievements at both the Ames-Moffett and Ames-Dryden sites of Ames Research Center are compiled as an annual report.

In this report for 1988 you may glimpse some of the challenging work recently accomplished in the areas of Aerospace Systems, Flight Operations and Research, Aerophysics, and Space Research. Here, you may sample the scope and diversity of the research that is now being done and the stimulating challenges that will be met in the future.

If you wish further information on any of the Ames research and technology programs, please write to the Chief Scientist, Dr. Jack Nielsen, MS 200-1A, NASA Ames Research Center, Moffett Field, CA 94035-5000, or call the number(s) at the end of each item.

W^m F. Ballhaus, Jr.

William F. Ballhaus, Jr.
Director

3-11-88
6021-1000

Table of Contents

	Page
INDEX	iii
AEROSPACE SYSTEMS.....	1
FLIGHT OPERATIONS AND RESEARCH	96
AEROPHYSICS	122
SPACE RESEARCH	178

For additional information on any item, you may telephone the Ames staff member(s) named at the end of that item. To call Ames-Moffett staff, commercial telephone users should dial 415-694- followed by the extension number. (Users with access to the Federal Telecommunications System (FTS) should dial 464- followed by the extension number.) To call Ames-Dryden staff, commercial telephone users should dial 805-258- followed by the extension number. (On FTS, dial 961- followed by the extension number.)

Index	Title	Author	Ames Moffett/ Ames Dryden	Organizational Division	Headquarters Program Office
Aerospace Systems					
	Three-Dimensional Viscous Drag Prediction for Rotor Flows	M. Chen M. Betzina	Ames Moffett	Full-Scale Aerodynamics Research	OAST-FF
	Rotating-Frame Laser Velocimeter for Rotor Testing	S. Dunagan	Ames Moffett	Full-Scale Aerodynamics Research	OAST-FF
	Particle Image Displacement Velocimetry	S. Dunagan C. Smith	Ames Moffett	Full-Scale Aerodynamics Research	OAST-FF
	Large-Scale Tilt-Rotor Performance and Rotor/Wing Interactions	F. Felker	Ames Moffett	Full-Scale Aerodynamics Research	OAST-FF
	Comparisons of Predicted and Measured Rotor Performance in Hover Using a New Free-Wake Analysis	F. Felker J. Light	Ames Moffett	Full-Scale Aerodynamics Research	OAST-FF
	Aeroelastic Stability Program	T. Graham R. Peterson	Ames Moffett	Full-Scale Aerodynamics Research	OAST-FF
	Hub Load Analysis of the SA349/2 Helicopter	R. Heffernan G. Yamauchi	Ames Moffett	Full-Scale Aerodynamics Research	OAST-FF
	Experimental Studies in System Identification of Rotor Dynamics	S. Jacklin	Ames Moffett	Full-Scale Aerodynamics Research	OAST-FF
	Study of Aeromechanical Problems with Active Controls	S. Jacklin	Ames Moffett	Full-Scale Aerodynamics Research	OAST-FF
	System Identification Techniques for Higher Harmonic Control of Rotorcraft Vibration	S. Jacklin	Ames Moffett	Full-Scale Aerodynamics Research	OAST-FF
	Calculation of Helicopter Rotor Blade-Vortex Interaction by Navier-Stokes Procedures	C. Kitaplioglu	Ames Moffett	Full-Scale Aerodynamics Research	OAST-FF
	Full-Scale Wind Tunnel Testing of the Helicopter Individual Blade Control System	B. Lau	Ames Moffett	Full-Scale Aerodynamics Research	OAST-FF
	Comparison of Vibration-Reduction Algorithms	J. Leyland	Ames Moffett	Full-Scale Aerodynamics Research	OAST-FF
	Rotor Blade Optimization	J. Light	Ames Moffett	Full-Scale Aerodynamics Research	OAST-FF
	Tilt-Rotor Download Research	J. Light J. Lee	Ames Moffett	Full-Scale Aerodynamics Research	OAST-FF
	Unsteady Rotor Airloads	T. Norman	Ames Moffett	Full-Scale Aerodynamics Research	OAST-FF

Index					Headquarters
	Title	Author	Ames Moffett/ Ames Dryden	Organizational Division	Program Office
Aerospace Systems (continued)					
	Visualization of Rotor Wakes by Using the Shadowgraph Technique	T. Norman J. Light	Ames Moffett	Full-Scale Aerodynamics Research	OAST-FF
	Numerical Methods for Vortical Flow Fields	P. Stremel	Ames Moffett	Full-Scale Aerodynamics Research	OAST-FF
	M-85 High-Speed Rotorcraft Concept	R. Stroub A. Louie	Ames Moffett	Full-Scale Aerodynamics Research	OAST-FF
	Tilt-Rotor Flutter Alleviation	J. van Aken	Ames Moffett	Full-Scale Aerodynamics Research	OAST-FF
	Hub-Drag Reduction	L. Young D. Sung	Ames Moffett	Full-Scale Aerodynamics Research	OAST-FF
	Free-Tip Rotor	L. Young D. Martin A. Louie	Ames Moffett	Full-Scale Aerodynamics Research	OAST-FF
	Tilt-Rotor Structural Aeroelastic Stability	C. W. Acree	Ames Moffett	Rotorcraft and Powered-Lift Flight Projects	OAST-FH
	Individual Blade Feedback Investigations	D. Balough	Ames Moffett	Rotorcraft and Powered-Lift Flight Projects	OAST-FH
	TRENDS Rotorcraft Data Base	M. Bondi	Ames Moffett	Rotorcraft and Powered-Lift Flight Projects	OAST-FH
	UH-60A Blade Design and Fabrication	J. Brilla E. Seto	Ames Moffett	Rotorcraft and Powered-Lift Flight Projects	OAST-FH
	Tilt-Rotor GTRS Status/Enhancement	G. Churchill	Ames Moffett	Rotorcraft and Powered-Lift Flight Projects	OAST-FH
	UH-60 Modern Technology Rotor Phase One Workshop	J. Cross J. Brilla	Ames Moffett	Rotorcraft and Powered-Lift Flight Projects	OAST-FH
	Supersonic Short Takeoff and Vertical Landing Fighter Design Studies	P. Gelhausen	Ames Moffett	Rotorcraft and Powered-Lift Flight Projects	OAST-FH
	Propulsion System for a Supersonic Short Takeoff and Vertical Landing Flight-Research Aircraft	D. Giulianetti P. Nelms	Ames Moffett	Rotorcraft and Powered-Lift Flight Projects	OAST-FH
	UH-60 DNW Risk Reduction Test	D. Jordan	Ames Moffett	Rotorcraft and Powered-Lift Flight Projects	OAST-FH
	UH-60 Dynamic Modeling and Shake Test	R. Kufeld	Ames Moffett	Rotorcraft and Powered-Lift Flight Projects	OAST-FH

Index	Title	Author	Ames Moffett/ Ames Dryden	Organizational Division	Headquarters Program Office
Aerospace Systems (continued)					
	Tilt-Rotor Advanced Technology Blades— Flight Ground Investigations	M. Maisel	Ames Moffett	Rotorcraft and Powered- Lift Flight Projects	OAST-FH
	Blade Root-End Flow Field for a Highly Twisted Low-Disc-Loading Rotor	M. Maisel P. Schumacher	Ames Moffett	Rotorcraft and Powered- Lift Flight Projects	OAST-FH
	Modern Technology Helicopter Rotor— BV-360 Flight Test	M. Maisel M. Watts	Ames Moffett	Rotorcraft and Powered- Lift Flight Projects	OAST-FH
	Tilt-Rotor Advanced Technology Blades— Airloads Investigation	M. Maisel M. Watts	Ames Moffett	Rotorcraft and Powered- Lift Flight Projects	OAST-FH
	U.S./U.K. Advanced Short Takeoff and Vertical Landing Aircraft Technology Program—Configuration Studies	P. Nelms C. White	Ames Moffett	Rotorcraft and Powered- Lift Flight Projects	OAST-FH
	Advanced Tactical Transport Technology	D. Riddle C. White	Ames Moffett	Rotorcraft and Powered- Lift Flight Projects	OAST-FH
	Parameter Identification Workshop—Identifi- cation of Rotor Inflow in Forward Flight	P. Talbot	Ames Moffett	Rotorcraft and Powered- Lift Flight Projects	OAST-FH
	Acoustics Laboratory	M. Watts	Ames Moffett	Rotorcraft and Powered- Lift Flight Projects	OAST-FH
	XV-15-702 Steel Blade Fatigue	B. Wellman	Ames Moffett	Rotorcraft and Powered- Lift Flight Projects	OAST-FH
	Networks for Image Acquisition, Processing, and Display	A. Ahumada A. Watson	Ames Moffett	Aerospace Human Factors Research	OAST-FL
	Perspective Displays and the Control of Motion	T. Bennett W. Johnson	Ames Moffett	Aerospace Human Factors Research	OAST-FL
	Traffic Alert Collision-Avoidance System (TCAS)	S. Chappell	Ames Moffett	Aerospace Human Factors Research	OAST-FL
	Integrated Rendezvous and Proximity Operations Displays	S. Ellis	Ames Moffett	Aerospace Human Factors Research	OAST-FL
	CRM Training Evaluation Project	C. Foushee	Ames Moffett	Aerospace Human Factors Research	OAST-FL
	Human Interface to the Thermal Expert System	D. Foyle N. Dorigi	Ames Moffett	Aerospace Human Factors Research	OAST-FL
	Individual Crew Factors in Flight Operations	C. Graeber	Ames Moffett	Aerospace Human Factors Research	OAST-FL

Index	Title	Author	Ames Moffett/ Ames Dryden	Organizational Division	Headquarters Program Office
Aerospace Systems (continued)					
	Human Factors Issues in Civil Medevac Operations	S. Hart	Ames Moffett	Aerospace Human Factors Research	OAST-FL
	Improved Flight Training Procedures	S. Hart	Ames Moffett	Aerospace Human Factors Research	OAST-FL
	Interpretation of Sensor Imagery	S. Hart	Ames Moffett	Aerospace Human Factors Research	OAST-FL
	Computational Human Engineering Research	J. Hartzell	Ames Moffett	Aerospace Human Factors Research	OAST-FL
	Visibility Modeling Tool—An A ³ I Project	J. Larimer	Ames Moffett	Aerospace Human Factors Research	OAST-FL
	Information Management and Transfer	A. Lee	Ames Moffett	Aerospace Human Factors Research	OAST-FL
	Virtual Workstation	M. McGreevy S. Fisher	Ames Moffett	Aerospace Human Factors Research	OAST-FL
	Cockpit Procedures Monitor and Error-Tolerant Systems	E. Palmer	Ames Moffett	Aerospace Human Factors Research	OAST-FL
	Operator Function Modeling: Cognitive Task Analysis in Supervisory Control	E. Palmer	Ames Moffett	Aerospace Human Factors Research	OAST-FL
	Computational Models of Attention and Cognition	R. Remington	Ames Moffett	Aerospace Human Factors Research	OAST-FL
	Aviation Safety Reporting System (ASRS)	W. Reynard	Ames Moffett	Aerospace Human Factors Research	OAST-FL
	Thermal Control Coating for Space Suits	B. Squire B. Webbon	Ames Moffett	Aerospace Human Factors Research	OAST-FL
	Advanced EVA Suit Technology	H. Vykukal	Ames Moffett	Aerospace Human Factors Research	OAST-FL
	Motion Processing in Humans and Machines	A. Watson	Ames Moffett	Aerospace Human Factors Research	OAST-FL
	Pyramid Image Codes	A. Watson	Ames Moffett	Aerospace Human Factors Research	OAST-FL
	Auditory Display Systems Research	B. Wenzel	Ames Moffett	Aerospace Human Factors Research	OAST-FL

Index	Title	Author	Ames Moffett/ Ames Dryden	Organizational Division	Headquarters Program Office
Aerospace Systems (continued)					
	International Aviation Technology Studies	L. Alton	Ames Moffett	Advanced Plans and Programs Office	OAST-FP
	International Rotorcraft Technology Studies	L. Alton	Ames Moffett	Advanced Plans and Programs Office	OAST-FP
	Electro-Expulsive Deicing System Demonstrated in Flight on Navy F/A-18 Hornet	L. Haslim	Ames Moffett	Advanced Plans and Programs Office	NAVAIR-SYSCOM
	Electro-Expulsive Deicers for Rotorcraft and Fixed-Wing Aircraft	L. Haslim	Ames Moffett	Advanced Plans and Programs Office	NAVAIR-SYSCOM
	Lightweight, Fire-Retardant, Crashworthy Aircraft Seat Cushioning	L. Haslim	Ames Moffett	Advanced Plans and Programs Office	TU
	Lightweight, Telescoping Rescue Boom for Helicopters	L. Haslim	Ames Moffett	Advanced Plans and Programs Office	TU
	U.S./Canada STOVL Technology Program	B. Lampkin	Ames Moffett	Advanced Plans and Programs Office	OAST-FP
	Aviation Technology Applicable for Developing Countries	J. Zuk L. Alton	Ames Moffett	Advanced Plans and Programs Office	OAST-FP
	Real-Time Simulation Computer Replacement	D. Astill	Ames Moffett	Flight Systems and Simulation Research	OAST-FS
	Neural Network Architecture	Y. Baram	Ames Moffett	Flight Systems and Simulation Research	OAST-FS
	Obstacle Avoidance	V. Cheng B. Sridhar	Ames Moffett	Flight Systems and Simulation Research	OAST-FS
	Dual-Lift Helicopter Slung-Load Systems	L. Cicolani	Ames Moffett	Flight Systems and Simulation Research	OAST-FS
	Ames' Crew Station Research and Development Facility Upgrade	L. Coe	Ames Moffett	Flight Systems and Simulation Research	OAST-FS
	Space Shuttle Simulation	A. Cook	Ames Moffett	Flight Systems and Simulation Research	OAST-FS
	Vertical Motion Simulator Upgrade Project	A. Cook	Ames Moffett	Flight Systems and Simulation Research	OAST-FS
	Simulator Evaluation of Controller Tools	T. Davis L. Tobias	Ames Moffett	Flight Systems and Simulation Research	OAST-FS

Index	Title	Author	Ames Moffett/ Ames Dryden	Organizational Division	Headquarters Program Office
Aerospace Systems (continued)					
	Satellite-Based Navigation	F. Edwards	Ames Moffett	Flight Systems and Simulation Research	OAST-FS
	Air Traffic Control Simulation and Development Facility	H. Erzberger	Ames Moffett	Flight Systems and Simulation Research	OAST-FS
	Graphical Interface for Air Traffic Control Automation Tools	H. Erzberger	Ames Moffett	Flight Systems and Simulation Research	OAST-FS
	Correlation of A109 Flight Test with Ground-Based Simulation	M. Eshow	Ames Moffett	Flight Systems and Simulation Research	OAST-FS
	Integrated-Flight/Propulsion-Control Research on the V/STOL Research Aircraft	J. Foster	Ames Moffett	Flight Systems and Simulation Research	OAST-FS
	Simulation Evaluation of Transition and Hover Flying Qualities of the E-7A STOVL Aircraft	J. Franklin	Ames Moffett	Flight Systems and Simulation Research	OAST-FS
	Flight Investigation of Automatic Position-Hold Systems for Rotorcraft	W. Hindson	Ames Moffett	Flight Systems and Simulation Research	OAST-FS
	Precision Landing Control for STOL Transports	C. Hynes	Ames Moffett	Flight Systems and Simulation Research	OAST-FS
	An Advisory System for Conflict Detection and Resolution	H. Lee	Ames Moffett	Flight Systems and Simulation Research	OAST-FS
	Aerodynamic Modeling for the V/STOL Research Aircraft	D. McNally R. Bach	Ames Moffett	Flight Systems and Simulation Research	OAST-FS
	Microburst Modeling Utilizing Airline Flight Data	T. Schultz R. Wingrove	Ames Moffett	Flight Systems and Simulation Research	OAST-FS
	Automated NOE Flight	B. Sridhar V. Cheng	Ames Moffett	Flight Systems and Simulation Research	OAST-FS
	Obstacle Detection	B. Sridhar V. Cheng	Ames Moffett	Flight Systems and Simulation Research	OAST-FS
	Mid-Field Path Planning	H. Swenson	Ames Moffett	Flight Systems and Simulation Research	OAST-FS
	Far-Field Mission Planning	N. Warner	Ames Moffett	Flight Systems and Simulation Research	OAST-FS
	CH-47/Cross-Coupling Studies	D. Watson W. Hindson	Ames Moffett	Flight Systems and Simulation Research	OAST-FS

Index					Headquarters
	Title	Author	Ames Moffett/ Ames Dryden	Organizational Division	Program Office
Flight Operations and Research					
	Altitude Acceleration Display for Hypersonic Aircraft	D. Berry	Ames Dryden	Research Engineering	OAST-OF
	Shuttle Launch Wind-Measurement Experiment	L. Bjarke	Ames Dryden	Research Engineering	OAST-OF
	X-29 Parameter-Estimation Research	G. Budd N. Matheny	Ames Dryden	Research Engineering	OAST-OF
	Integrated Trajectory Guidance Algorithms Flight-Tested	F. Burcham	Ames Dryden	Research Engineering	OAST-OF
	X-29A Turbulence Response Study	D. Crawford	Ames Dryden	Research Engineering	OAST-OF
	F-18 Off-Surface Flow Visualization	J. Del Frate	Ames Dryden	Research Engineering	OAST-OF
	Automated Flight Test Management System	L. Duke	Ames Dryden	Research Engineering	OAST-OF
	F-18 Surface Flow Visualization	D. Fisher	Ames Dryden	Research Engineering	OAST-OF
	X-29A Flight-Control Research	J. Gera	Ames Dryden	Research Engineering	OAST-OF
	The Effects of Aircraft Maneuver Dynamics on X-29A Aeroperformance	J. Hicks	Ames Dryden	Research Engineering	OAST-OF
	The Effects of Angle of Attack on Structural Damping on the X-29A Forward-Swept-Wing Airplane	M. Kehoe	Ames Dryden	Research Engineering	OAST-OF
	Thermal Analysis of Space Shuttle Orbiters	W. Ko	Ames Dryden	Research Engineering	OAST-OF
	Aircraft Performance Improvements with an Integrated Engine Flight-Control System	L. Myers	Ames Dryden	Research Engineering	OAST-OF
	In-Flight Simulation Study of Lateral Flying Qualities	B. Powers	Ames Dryden	Research Engineering	OAST-OF
	Development of a Real-Time Net Thrust Technique	R. Ray	Ames Dryden	Research Engineering	OAST-OF
	Titanium Honeycomb Panel Heating Tests	W. Richards	Ames Dryden	Research Engineering	OAST-OF
	Structural Divergence of Forward-Swept Wings	L. Schuster	Ames Dryden	Research Engineering	OAST-OF
	Throttle Response Criteria Research	K. Walsh	Ames Dryden	Research Engineering	OAST-OF

Index	Title	Author	Ames Moffett/ Ames Dryden	Organizational Division	Headquarters Program Office
Aerophysics					
	Balance Load and Alarm Monitoring System	R. Hanly	Ames Moffett	Aerodynamics	OAST-RA
	Development of a New Flow-Through Wind Tunnel Balance for Powered Model Testing	A. Roberts	Ames Moffett	Aerodynamics	OAST-RA
	NASA/Boeing Co-op	F. Steinle, Jr.	Ames Moffett	Aerodynamics	OAST-RA
	A Knowledge-Based Approach to Automated Flow-Field Zoning	A. Andrews	Ames Moffett	Fluid Dynamics	OAST-RF
	Behavior of Liquid Drops in Strong Electric Fields	P. Bahrami	Ames Moffett	Fluid Dynamics	OAST-RF
	Numerical Simulation of the Flow About the Integrated Space Shuttle Vehicle in Ascent	P. Buning J. Steger	Ames Moffett	Fluid Dynamics	OAST-RF
	Simulation of the "Suckdown" Effect	K. Chawla W. Van Dalsem	Ames Moffett	Fluid Dynamics	OAST-RF
	Pressure Gradient Effects on a Three-Dimensional Turbulent Boundary Layer	D. Driver	Ames Moffett	Fluid Dynamics	OAST-RF
	Transonic Navier-Stokes Project	J. Flores N. Chaderjian	Ames Moffett	Fluid Dynamics	OAST-RF
	Simulation of Rotor-Stator Interaction in a Multi-Stage Compressor	K. Gundy-Burlet M. Rai	Ames Moffett	Fluid Dynamics	OAST-RF
	Aeroelasticity Using the Euler Equations	G. Guruswamy	Ames Moffett	Fluid Dynamics	OAST-RF
	Aeroelasticity of Full-Span, Wing-Body Configurations	G. Guruswamy E. Tu	Ames Moffett	Fluid Dynamics	OAST-RF
	Hypersonic Flow Through a Narrow Expansion Slot for Scramjet Fuel Injection	C. Hung T. Barth	Ames Moffett	Fluid Dynamics	OAST-RF
	Computational Fluid Dynamics on a Massively Parallel Computer	D. Jespersen C. Levit	Ames Moffett	Fluid Dynamics	OAST-RF
	Transition to Turbulence in Plane Poiseuille Flow	J. Kim	Ames Moffett	Fluid Dynamics	OAST-RF
	Direct Numerical Simulation of Compressible Free-Shear Flows	S. Lele	Ames Moffett	Fluid Dynamics	OAST-RF

Index	Title	Author	Ames Moffett/ Ames Dryden	Organizational Division	Headquarters Program Office
Aerophysics (continued)					
	Accurate and Efficient Calculation of Equilibrium Gas Properties	Y. Liu M. Vinokur	Ames Moffett	Fluid Dynamics	OAST-RF
	Splashes in Microgravity	N. Mansour T. Lundgren	Ames Moffett	Fluid Dynamics	OAST-RF
	Passive Shock Control on a Supercritical Airfoil	G. Mateer	Ames Moffett	Fluid Dynamics	OAST-RF
	Space Shuttle Main-Engine Turnaround Duct Experiment	D. Monson	Ames Moffett	Fluid Dynamics	OAST-RF
	Low-Aspect-Ratio Wing Experiment	M. Olsen	Ames Moffett	Fluid Dynamics	OAST-RF
	Direct Numerical Study of Leading-Edge Contamination	P. Spalart	Ames Moffett	Fluid Dynamics	OAST-RF
	Experimental Study of Flow Unsteadiness Around an Ogive Cylinder at Incidence	G. Zilliac D. Degani	Ames Moffett	Fluid Dynamics	OAST-RF
	1988 Bayesian Learning Accomplishments: AutoClass	P. Cheeseman	Ames Moffett	Information Sciences	OAST-RI
	PI-in-a-Box: Intelligent On-Board Assistance for Spaceborne Experiments in Vestibular Physiology	S. Colombano D. Rosenthal	Ames Moffett	Information Sciences	OAST-RI
	Machine Learning and Planning	M. Drummond S. Minton M. Zweben	Ames Moffett	Information Sciences	OAST-RI
	Spaceborne VHSIC Multiprocessor System	H. Lum	Ames Moffett	Information Sciences	OAST-RI
	Real-Time Optical Pattern Recognition	E. Ochoa	Ames Moffett	Information Sciences	OAST-RI
	Conservation of Design Knowledge	C. Sivard M. Zweben	Ames Moffett	Information Sciences	OAST-RI
	A Knowledge-Based Approach to the Real- Time Control of Dynamical Systems	C. Wong B. Glass	Ames Moffett	Information Sciences	OAST-RI
	Human Interface to the Thermal Expert System	C. Wong N. Dorigi E. Drascher	Ames Moffett	Information Sciences	OAST-RI

Index

Title

Author

Ames Moffett/
Ames DrydenOrganizational
DivisionHeadquarters
Program
Office

Aerophysics (continued)

Discrete Particle Simulation of Compressible Flow	D. Baganoff J. McDonald W. Feiereisen	Ames Moffett	Thermosciences	OAST-RT
Simulation of Detonation-Wave-Enhanced Combustion	J. Cambier G. Menees H. Adelman	Ames Moffett	Thermosciences	OAST-RT
Computation of Nonequilibrium Hypersonic Flows	G. Candler	Ames Moffett	Thermosciences	OAST-RT
Aeroassist Flight Experiment to Use Ames-Developed Thermal-Protection Materials	H. Goldstein D. Leiser P. Sawko	Ames Moffett	Thermosciences	OAST-RT
Real-Gas Properties of Air and Air Plus Hydrogen Mixtures for Hypersonic Applications	R. Jaffe D. Cooper	Ames Moffett	Thermosciences	OAST-RT
Boron Nitride Coatings for Silicon Carbide Fibers	D. Kourtides	Ames Moffett	Thermosciences	OAST-RT
Fire-Resistant Composites for Aircraft Interiors	D. Kourtides	Ames Moffett	Thermosciences	OAST-RT
Three-Dimensional Simulation of Flow About the Aeroassisted Flight Experiment Vehicle	G. Palmer	Ames Moffett	Thermosciences	OAST-RT
Computer Simulation of NASP Nozzle/Afterbody Flows	S. Ruffin	Ames Moffett	Thermosciences	OAST-RT
Silicon Carbide Sewing Thread for a High-Temperature Thermal Protection System	P. Sawko	Ames Moffett	Thermosciences	OAST-RT
VIBSSH: Approximate Quantum-Mechanical Calculation of Vibrational Relaxation	S. Sharma W. Huo C. Park	Ames Moffett	Thermosciences	OAST-RT
Real-Gas Experiments at Hypersonic Speeds	A. Strawa	Ames Moffett	Thermosciences	OAST-RT
Mars Atmospheric Entry and Descent Using a High-Lift Vehicle	M. Tauber	Ames Moffett	Thermosciences	OAST-RT
Stagnation Streamline Reacting Flow Code Generalized for Any Gas Mixture	E. Whiting C. Park	Ames Moffett	Thermosciences	OAST-RT

Index					Headquarters
	Title	Author	Ames Moffett/ Ames Dryden	Organizational Division	Program Office
Space Research					
	Scientific Visualization of Geologic Data	W. Acevedo	Ames Moffett	Earth System Science	OSSA-SG
	Pilot Land Data System (PLDS)	G. Angelici W. Likens	Ames Moffett	Earth System Science	OSSA-SG
	Area Frame Development	T. Cheng R. Slye G. Angelici	Ames Moffett	Earth System Science	OSSA-SG
	Estimating Regional Methane Flux in Northern High-Latitude Ecosystems	G. Livingston L. Morrissey	Ames Moffett	Earth System Science	OSSA-SG
	Fast Airborne Gas Sensor	M. Loewenstein	Ames Moffett	Earth System Science	OSSA-SG
	Trace-Gas Flux, Canopy Chemistry, and Remote Sensing in Coniferous Ecosystems	P. Matson N. Swanberg T. Billow	Ames Moffett	Earth System Science	OSSA-SG
	Nitrous Oxide Flux from Tropical Forest Ecosystems	P. Matson G. Livingston P. Vitousek	Ames Moffett	Earth System Science	OSSA-SG
	Biogeochemical Cycling in Terrestrial Ecosystems	D. Peterson	Ames Moffett	Earth System Science	OSSA-SG
	Tropical Wetland Ecosystem Dynamics	K. Pope C. Duller	Ames Moffett	Earth System Science	OSSA-SG
	Atmospheric Optical Depths: Background Aerosols, Smokes, and Clouds	R. Pueschel	Ames Moffett	Earth System Science	OSSA-SG
	Condensed Nitrate, Sulfate, and Chloride in Antarctic Stratospheric Aerosols	R. Pueschel	Ames Moffett	Earth System Science	OSSA-SG
	Biospheric Monitoring and Vector-Borne Disease Prediction	P. Sebesta B. Wood K. Pope C. Duller	Ames Moffett	Earth System Science	OSSA-SG
	Remote Sensing of Biogeochemical Cycling Indexes of Western Coniferous Forests	M. Spanner D. Peterson	Ames Moffett	Earth System Science	OSSA-SG
	Biodiversity Project	L. Strong C. Hlavka	Ames Moffett	Earth System Science	OSSA-SG
	AVIRIS Data Quality for Coniferous Canopy Chemistry	N. Swanberg	Ames Moffett	Earth System Science	OSSA-SG
	Remote Sensing of Tropical Forest Types in Relation to Forest Fertility	N. Swanberg	Ames Moffett	Earth System Science	OSSA-SG
	ER-2 Ozone Measurements	J. Vedder	Ames Moffett	Earth System Science	OSSA-SG

Index	Title	Author	Ames Moffett/ Ames Dryden	Organizational Division	Headquarters Program Office
Space Research (continued)					
	Tracer Studies in the Stratosphere	J. Vedder	Ames Moffett	Earth System Science	OSSA-SG
	Remote Sensing of Aquatic Manganese Biogeochemistry	R. Wrigley L. Richardson	Ames Moffett	Earth System Science	OSSA-SG
	Gradients of Mineralization in Bone	S. Arnaud	Ames Moffett	Life Science	OSSA-SL
	Laboratory Studies of Reactions of Oxygen Atoms with Various Polymer Films	M. Golub T. Wydeven	Ames Moffett	Life Science	OSSA-SL
	Oxidation of CELSS Wastes Near the Critical Point of Water	T. Wydeven C. Koo Y. Takahashi	Ames Moffett	Life Science	OSSA-SL
	Research Animal Holding Facility	R. Hogan	Ames Moffett	Space Life Sciences Payloads Office	OSSA-SP
	KC-135 Parabolic Flight Investigations	P. Savage	Ames Moffett	Space Life Sciences Payloads Office	OSSA-SP
	General Purpose Work Station	G. Schmidt	Ames Moffett	Space Life Sciences Payloads Office	OSSA-SP
	SIRTF Prototype Secondary Mirror Assembly	P. Davis	Ames Moffett	Infrared Astronomy Projects Office	OSSA-SR
	Spherical Bearing for an Airborne Telescope	J. Eilers R. Averill N. Kunz J. Hirata	Ames Moffett	Infrared Astronomy Projects Office	OSSA-SR
	Helium-3 Cooler	P. Kittel	Ames Moffett	Infrared Astronomy Projects Office	OAST-SR
	Cool-Down of Primary Mirror for the SOFIA Telescope	S. Maa	Ames Moffett	Infrared Astronomy Projects Office	OSSA-SR
	Low-Background Evaluation of Large Integrated Infrared Detector Arrays	M. McKelvey N. Moss	Ames Moffett	Infrared Astronomy Projects Office	OAST-SR
	Cryogenic Optics Test Facility for 1-M-Class Mirrors	R. Melugin L. Salerno G. Sarver	Ames Moffett	Infrared Astronomy Projects Office	OSSA-SR
	SIRTF Pointing Control System Studies	N. Rajan	Ames Moffett	Infrared Astronomy Projects Office	OSSA-SR

Index

Title	Author	Ames Moffett/ Ames Dryden	Organizational Division	Headquarters Program Office
Space Research (continued)				
SOFIA Pointing Control System Studies	N. Rajan	Ames Moffett	Infrared Astronomy Projects Office	OSSA-SR
Infrared Black Coatings for the Submillimeter Region	S. Smith	Ames Moffett	Infrared Astronomy Projects Office	OSSA-SR
Tertiary Mirror Assembly	M. Sullivan J. Lee	Ames Moffett	Infrared Astronomy Projects Office	OSSA-SR
The Laboratory Study of Cometary and Interstellar Ice Analogs	L. Allamandola	Ames Moffett	Space Science	OSSA-SS
Isotopic Ratio Measurements Using a Diode Laser Spectrometer	J. Becker C. McKay	Ames Moffett	Space Science	OSSA-SS
Lightning Production of Hydrocarbons on Titan	W. Borucki Y. Ishikawa C. McKay	Ames Moffett	Space Science	OSSA-SS
Star Sensor Search for Venusian Lightning	W. Borucki J. Dyer J. Phillips	Ames Moffett	Space Science	OSSA-SS
Clay Energetics	L. Coyne P. Costanzo B. Theng A. Rice	Ames Moffett	Space Science	OSSA-SS
Mars Exobiology Research Consortium	L. Coyne	Ames Moffett	Space Science	OSSA-SS
Particle-Gas Dynamics in the Protoplanetary Nebula	J. Cuzzi	Ames Moffett	Space Science	OSSA-SS
Planetary Ring Structure and Dynamics	J. Cuzzi	Ames Moffett	Space Science	OSSA-SS
Early Biological Evolution and Atmospheric Carbon Dioxide – Searching for a Link	D. Des Marais	Ames Moffett	Space Science	OSSA-SS
Small-Particle Research on the Space Station	G. Fogleman J. Huntington G. Carle	Ames Moffett	Space Science	OSSA-SS
Minerals as a Source of Free Oxygen in Planetary Evolution	F. Freund S. Chang T. Wydeven	Ames Moffett	Space Science	DDF & SETI
On Salt-Entrapped Bacteria, Evolution, and Martian Exploration	L. Hochstein H. Stan-Lotter	Ames Moffett	Space Science	OSSA-SS

Index	Title	Author	Ames Moffett/ Ames Dryden	Organizational Division	Headquarters Program Office
Space Research (continued)					
	Are Magnesium Ions Primitive "Enzymes" in RNA-Type Replications?	A. Kanavarioti C. Bernasconi S. Chang	Ames Moffett	Space Science	OSSA-SS
	Gas Chromatographic Analysis of Model Titan Atmosphere at Low Pressures	D. Kojiro	Ames Moffett	Space Science	OSSA-SS
	Ecosystem Nitrogen Cycles as Modeled for Possible Ancient Martian Communities	R. Mancinelli	Ames Moffett	Space Science	OSSA-SS
	Mars Penetrator Instrumentation Design for Exobiology	J. Marshall D. Schwartz G. Carle	Ames Moffett	Space Science	OSSA-SS
	Cometary Impact and Chemical Evolution	V. Oberbeck C. McKay T. Scattergood G. Carle J. Valentin	Ames Moffett	Space Science	OSSA-SS
	Economical Signal-Processing Algorithms for SETI	B. Oliver	Ames Moffett	Space Science	OSSA-SS
	Progress in Signal Detection in SETI	B. Oliver	Ames Moffett	Space Science	OSSA-SS
	Submillimeter Observations of the Total Solar Eclipse of March 18, 1988	T. Roellig M. Werner G. Kopp E. Becklin F. Orrall C. Lindsey J. Jefferies	Ames Moffett	Space Science	OSSA-SS
	Modeling Metabolic Evolution on Mars	L. Rothschild R. Mancinelli	Ames Moffett	Space Science	OSSA-SS
	Astronomical Time-Series Analysis	J. Scargle	Ames Moffett	Space Science	OSSA-SS
	Collection of Model Titan Aerosols on Thin Wires	T. Scattergood V. Oberbeck J. Valentin J. Borucki G. Carle	Ames Moffett	Space Science	OSSA-SS
	Infrared Spectral Line Profiles of Supernova 1987a	F. Witteborn J. Bregman D. Wooden P. Pinto D. Rank M. Cohen	Ames Moffett	Space Science	OSSA-SS

Aerospace Systems

Three-Dimensional Viscous Drag Prediction for Rotor Flows

An analytical method to predict the drag force on the blades of rotorcraft in hover or forward flight is being developed. The objective is to provide an efficient design tool for the rotorcraft industry to predict the power required under conditions of simulated flight.

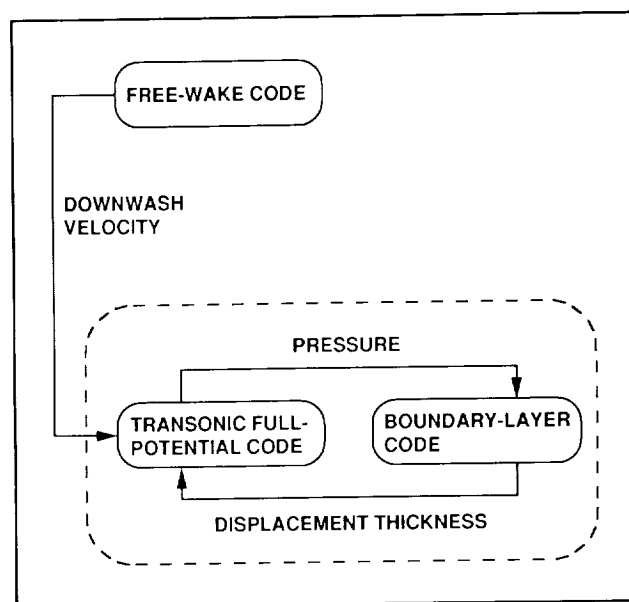
This method solves the three-dimensional boundary-layer equations in the rotating reference frame. This boundary-layer method is coupled with a full-potential method that solves the transonic full-potential equations in the rotating frame for rotor flows. The full-potential method provides the pressure distribution on the blade surface as the outer boundary condition to the boundary-layer method. The boundary-layer method then feeds the displacement thickness on the blade surface back to the full-potential method as a correction from the viscous effect. This process is repeated until the solutions converge.

The usual "marching" scheme for solving the boundary-layer equations breaks down when separation is encountered. To handle flows with bubble-type separation, an inverse method has been implemented. This method specifies an initial surface shear and then iterates to upgrade the surface shear by matching the viscous and inviscid pressures until the solutions converge.

The wake that is shed by the rotor blades has a crucial influence on the blade loading. The ability to take this effect into account is critical to the accuracy of the analysis. A free-wake analysis developed by Continuum Dynamics, Inc., under a contract with Ames Research Center, allows the effect of the wake on the blade loading to be included. To account for the influence of the wake, the free-wake method provides the downwash velocity on the rotor plane to the full-potential method. The flowchart shows the coupling of the three methods.

This method has been shown to accurately predict the drag force on a nonlifting rotor. Future work will focus on extending this method to lifting rotors in both hover and forward flight.

(M. Chen and M. Betzina, Ext. 5043/6856)

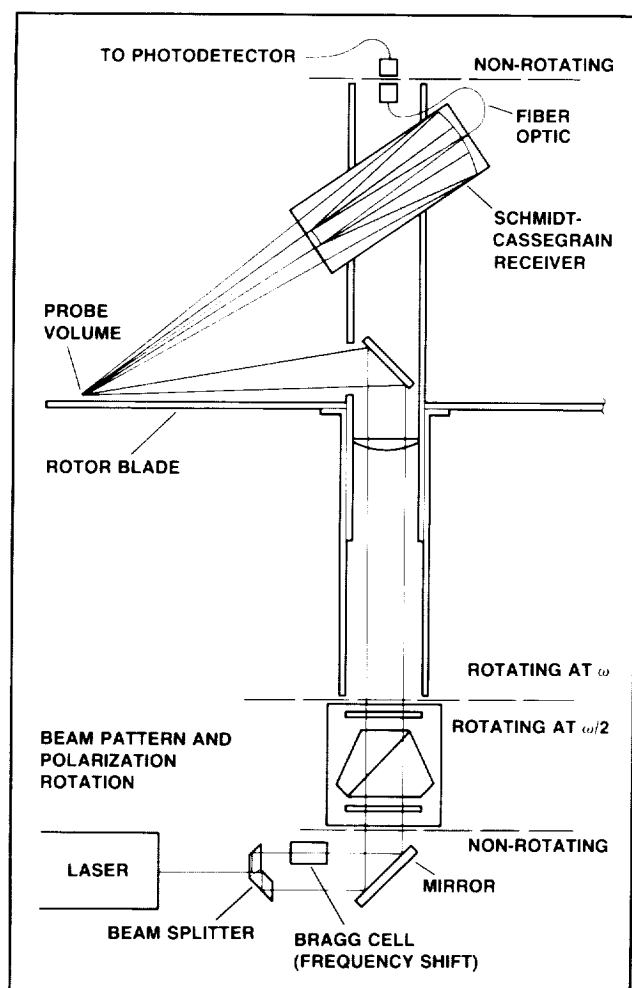


The coupling scheme of the boundary-layer, transonic full-potential, and free-wake codes

Rotating-Frame Laser Velocimeter for Rotor Testing

The no-slip condition at the surface of a rotary-wing, propeller, or turbomachinery rotor introduces a radial centripetal force component to the boundary-layer flow. Coriolis forces must also be included in the flow model. Some data indicate that these conditions may somehow delay boundary-layer separation and thereby may increase the lifting capability of a rotary wing. A detailed experimental evaluation of the boundary layer on a rotary wing is required to better understand this phenomenon.

Measuring the boundary-layer flow on a rotary wing is not an easy task. Previous attempts relied on instrumentation with a probe that was stationary in a laboratory or wind tunnel reference frame. Data were then sampled, and tagged with the blade azimuth position corresponding to the time of acquisition. Such an approach does not provide an ensemble measurement at a point that is stationary with respect to the wing, as would be needed for validation of a computational fluid dynamics prediction. Furthermore, most of the time the probe is far outside the wing boundary layer.



Optical layout for a single-channel, dual-beam, rotating laser velocimeter

Recent advances in moderate-range (1 to 3 meters) laser Doppler anemometers (LDA) suggest an approach that should provide a nonintrusive means of measuring the boundary-layer flow over a rotary wing. This approach is based on the use of an optical image rotator. The optical axis of a dual-beam LDA channel is aligned with the coincident mechanical axes of the image rotator and rotor shaft. An image rotator rotates an image being viewed through it at twice its angular rotation. Therefore, if the image rotator spins at one-half of the shaft speed, the two beams of the LDA will appear stationary with respect to the shaft. A lens and mirror may be arranged, as shown in the accompanying figure, to locate a probe volume in the boundary layer. A compact, off-axis, backscatter Cassegrain collector with a fiber optic coupler will transfer the

optical signal to photodetectors in the laboratory. A simple sliding tube assembly may be used to sweep out a boundary-layer traverse.

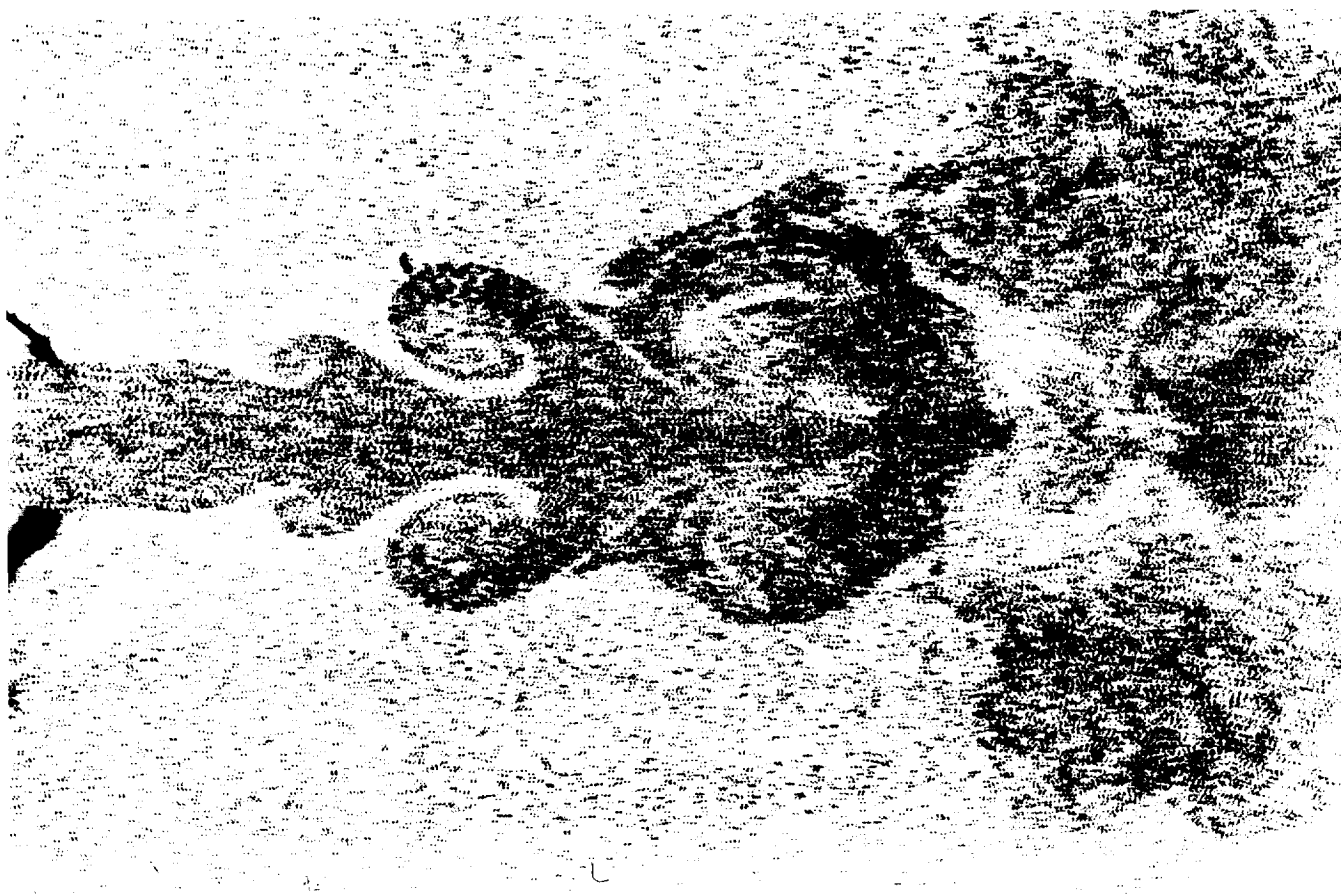
A dual-beam LDA with a Pechan prism image rotator has been assembled as a proof-of-concept demonstrator. This work has highlighted the extreme alignment sensitivity of the image rotator. It has also been shown that fringe contrast (which implies signal-to-noise ratio) in the LDA probe volume is consistent through the range of rotation, despite significant polarization variations arising from total internal reflection in the prism. A new mirror-type image rotator is planned to improve alignment and polarization qualities. A technique verification study is planned which uses a prototype test rig and spinning disk. This study will permit experimental redundancy and cross-checks with fixed frame instrumentation. The ultimate goal of this work is the measurement of three velocity components in the boundary layer of a hovering helicopter rotor operating at a high thrust coefficient.

(S. Dunagan, Ext. 5043)

Particle Image Displacement Velocimetry

An accurate velocity measurement capability is essential to the experimental evaluation of aerodynamic flows. If the measurement can be done non-intrusively, higher fidelity is achieved and very delicate flow mechanisms may be examined. Furthermore, if the measurement can be made simultaneously at many locations throughout the flow field, spatial gradients in the flow may be analyzed and important features, such as the vorticity field, may be quantified. Simultaneous measurement of many locations also permits very rapid documentation of a flow.

A recently developed experimental technique, particle image displacement velocimetry, has many of these attractive features. The principle of operation is quite simple. The highly collimated, high-power output of a pulsed laser is focused to a thin sheet of light using cylindrical and spherical optics. The alignment of the sheet in the test flow defines the plane in which velocity measurements will be made. Scattered light from particles entrained in the



Double-exposure photograph of air jet discharging into plenum

flow may be imaged on a film plane. Sequential photographs of this illuminated plane of the particle field may be obtained by repetitively pulsing the laser, or by firing two lasers in succession.

Interrogation of the multi-exposure photographic record by interferometric means provides very accurate information on the movement of particles in the time interval between pulses. In combination with the known (microsecond range) pulse separation time, this information permits the calculation of nearly instantaneous particle motion. If the particle size has been chosen to be small enough so that viscous forces dominate, then particle velocity and fluid velocity are equivalent. The velocity vector sign ambiguity may be resolved by introducing a velocity bias to the particle image field (by sweeping the camera), which is analogous to the introduction of a Bragg frequency shift in laser anemometry.

This technique previously has been proven for incompressible (water tunnel) studies at low speed. Recent work at Florida State University, sponsored by a grant from Ames Research Center, has been directed at obtaining measurements in air. The principal difficulty is that the smaller, lighter particles that must be used in air scatter much less light, so that a suitably exposed photographic record is difficult to obtain. However, measurements have been made in a high-aspect-ratio (two-dimensional) jet discharging into a plenum, at a mean jet discharge velocity of 4.5 meters per second and a Reynolds number of 2250. A typical photograph from this study is presented in the accompanying figure. The complex vortical structure of the jet as it breaks down may be clearly seen. The velocity vector data obtained from the "specklegram" is presented in the second figure. The uniform vector field in the plenum area repre-

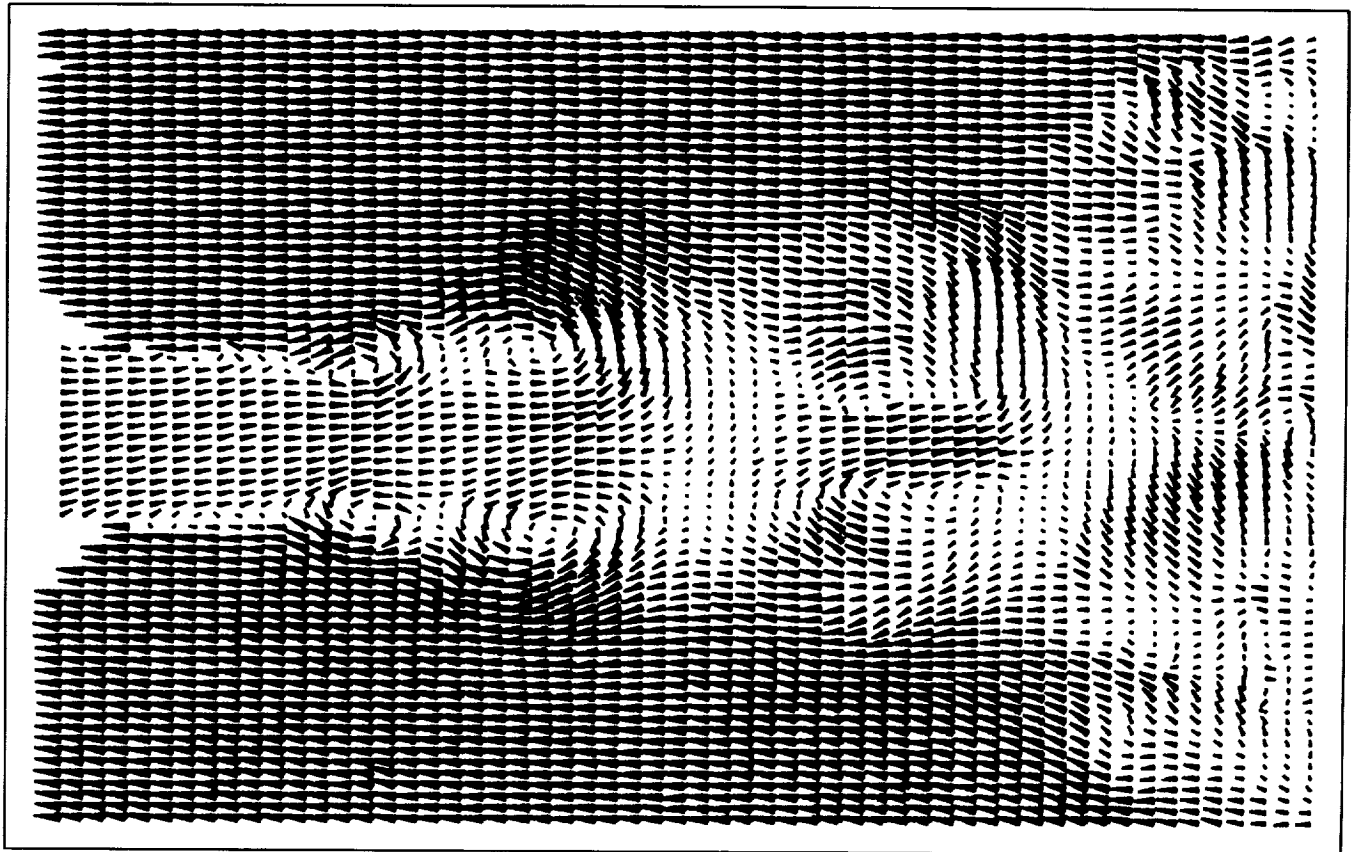
ORIGINAL PAGE
 REPRODUCED FROM WHITE PHOTOGRAPH

sents the superimposed velocity of the moving camera. Vorticity and other gradient data may also be obtained.

Future plans are directed at the application of the method to a small-scale wind tunnel test in which an

airfoil at a high angle of attack will be studied. Successful implementation will serve as a foundation for studies of large-scale rotor flows.

(S. Dunagan and C. Smith, Ext. 5043/4055)



Instantaneous velocity field of jet

Large-Scale Tilt-Rotor Performance and Rotor/Wing Interactions

A test of a 2/3-scale V-22 aircraft rotor in the 40-by 80-Foot Wind Tunnel was performed to measure rotor performance in forward flight and rotor/wing aerodynamic interactions in hover and forward flight. The test used the Ames Prop Test Rig, with its accurate rotor balance system, for measuring rotor performance and loads. This research program is a cooperative effort between NASA and the U.S. Navy.

The initial phase of the test effort focused on the download of a tilt-rotor wing in hover. A 2/3-scale

V-22 wing was fabricated and installed in the rotor wake at the correct position to represent the rotor/wing geometry of a V-22 aircraft. A large image plane simulated the presence of a second rotor and wing. Measurements of the wing download were acquired for a wide range of rotor thrust levels and wing flap angles. The effects of rotor rotation direction and rotor nacelle angle on download were also assessed. The test provided excellent data quality, including extensive measurements of steady and unsteady pressures on the wing surface. These data provide insight for the development of analytical methods.

The second phase of the test addressed rotor performance and rotor/wing aerodynamic interac-

tions in forward flight. However, problems with the rotor control system that compromised test safety prevented acquisition of all the data required to satisfy these test objectives. Based on the lessons learned in this test, an improved control system is being developed (along with other upgrades to the test apparatus) in support of a second test to be performed in 1989. This test will provide the first large-scale measurement of tilt-rotor performance, rotor and hub oscillatory loads, and rotor/wing aerodynamic interactions at speeds of up to 300 knots.

(F. Felker, Ext. 6096)



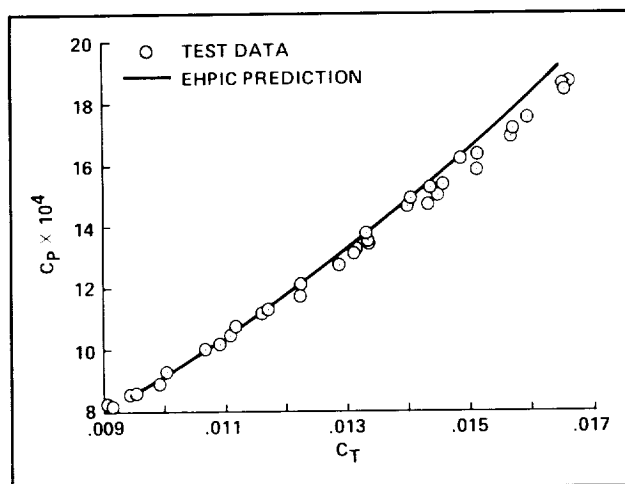
The 2/3-scale V-22 rotor and wing in the 40- by 80-Foot Wind Tunnel

Comparisons of Predicted and Measured Rotor Performance in Hover Using a New Free-Wake Analysis

A new free-wake analysis has been developed to predict the performance of rotors in hover and axial

climb. The analysis was developed by Continuum Dynamics, Inc., under the NASA Small Business Innovative Research program. The analysis determines the rotor wake geometry by using a novel influence coefficient/relaxation scheme that avoids the problems associated with time-marching approaches. The blade aerodynamic loads are found by using a vortex lattice lifting-surface analysis. The solution for the blade loading is fully coupled with the wake relaxation procedure, so artificial iteration between the blade and wake solution procedures is required. The only empiricism in the analysis is the use of standard two-dimensional airfoil tables to provide blade viscous drag data.

An extensive validation effort has been completed that assessed the ability of the analysis to predict the performance of a wide range of rotors in hover and vertical climb. The rotors considered for hover performance comparisons included two tail rotors with no twist or taper, five helicopter main rotors with moderate twist and varying amounts of taper, and three tilt rotors with large amounts of twist and taper. Good-quality isolated-rotor hover performance data were available for each of these rotors. The performance of two rotors in vertical climb was also computed. No effort was made to "tune" the analysis to improve the correlation with experiment, and every effort was made to make the calculations representative of what would be obtained by a skilled user who did not possess test data for the rotor of interest.



Comparison of predicted and measured hover performance—Bell-Boeing V-22 tilt rotor— -41° twist, 0.67 taper ratio

The results obtained were excellent, with the analysis generally predicting the rotor performance to within $\pm 5\%$ over a wide range of operating conditions. The calculations of rotor performance in vertical climb were found to be substantially more accurate than the predictions of commonly used momentum theory. The ability of the analysis to successfully predict the performance of such a wide range of rotors over such a wide range of operating conditions constitutes a significant advance in rotary-wing aerodynamics.

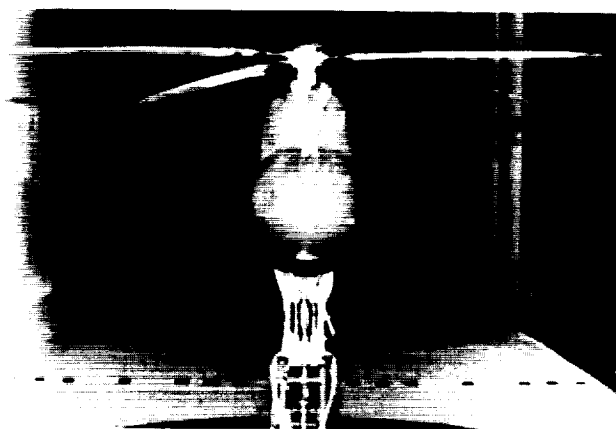
Current work is addressing several improvements to the analysis. An option for adding an image system to calculate the effect of the ground on rotor performance is being added. Previous analyses have relied on empirical relationships to account for the influence of the ground. Also, the code is being modified to operate efficiently on a vector processing computer. Initial results have shown that this modification can reduce the computation times by a factor of three.

(F. Felker and J. Light, Ext. 6096/4881)

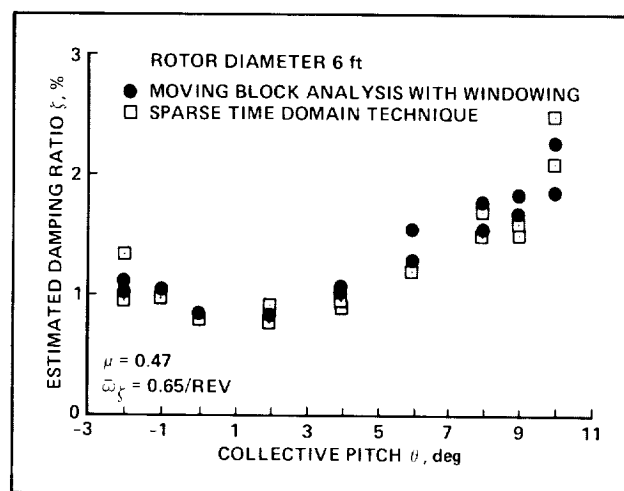
Aeroelastic Stability Program

Current-generation helicopter rotor systems are sophisticated mechanical systems that operate with very high loads in adverse aerodynamic environments. To relieve the high rotor-blade-root moments and maintain dynamic stability, helicopter rotor blades typically have several hinges, bearings, and/or dampers at the blade root. These mechanical devices operate in the rotating system and experience large oscillatory loads. They require frequent maintenance and can drastically reduce the reliability/serviceability of the rotor system. With high-strength composites coming of age, prototype rotor systems have been designed in which most or all of the hinges/bearings/dampers have been eliminated. These systems have lowered maintenance requirements, and have improved reliability and handling, without reducing performance or stability margins.

Full- and small-scale wind tunnel test programs, as well as some flight tests, have proven the concept of such designs as well as the structural and operational integrity of the rotor systems. However, several important areas of hingeless and bearingless



Small-scale bearingless rotor wind tunnel test



Forward flight results: lag-mode damping

rotor technology are not adequately understood. For example, the dynamic and aerodynamic characteristics of these rotors in forward flight have not been fully determined. One of the reasons these rotors present a challenge is because their aeroelastic couplings change with flight conditions. Also, analytical modeling techniques are just beginning to predict the aeroelastic stability of these rotors at moderate and high forward flight speeds.

To address these and other problems, two experimental programs have been pursued. First, a full-scale wind tunnel test program will further investigate the aeroelastic behavior of a BO-105 hingeless rotor system. This rotor system will be tested on the rotor test apparatus (RTA). A rotor balance is being acquired for the RTA and will be used to measure both steady and unsteady rotor forces and moments.

Second, a small-scale wind tunnel test program of a bearingless rotor (Boeing-Vertol ITR) was successfully completed at the University of Maryland, College Park. The photograph shows the bearingless rotor system in the Glenn L. Martin wind tunnel. Stability data were obtained in hover and forward flight. In addition to the analytical correlation of the stability data, two algorithms for estimating damping from transient data will be evaluated. A comparison of the two algorithms is shown in the figure.

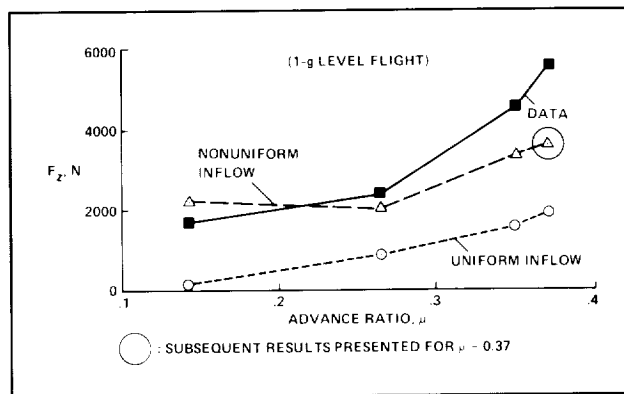
To expand the analytic capability of rotorcraft aeroelastic analyses, the finite-element capability developed by the University of Maryland is being extended to handle coupled rotor/body problems with composite blades and elastic body degrees of freedom in forward flight.

(T. Graham and R. Peterson, Ext. 6714/5044)

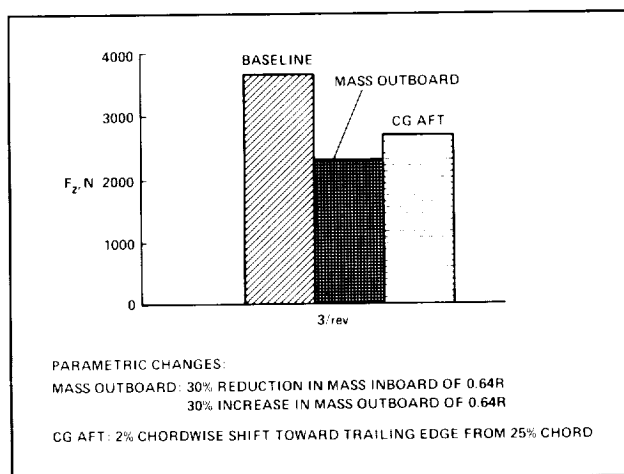
Hub Load Analysis of the SA349/2 Helicopter

Reducing helicopter vibration is desirable for many reasons, including increased crew and passenger comfort, and reduced wear on the aircraft. An understanding of the sources that generate vibration can aid in the development of rotorcraft with lower oscillatory loads. Examining helicopter forces and moments at the rotor hub, both experimentally and theoretically, is an important step toward understanding vibration. With this goal in mind, three aspects of hub loads were studied during the past year.

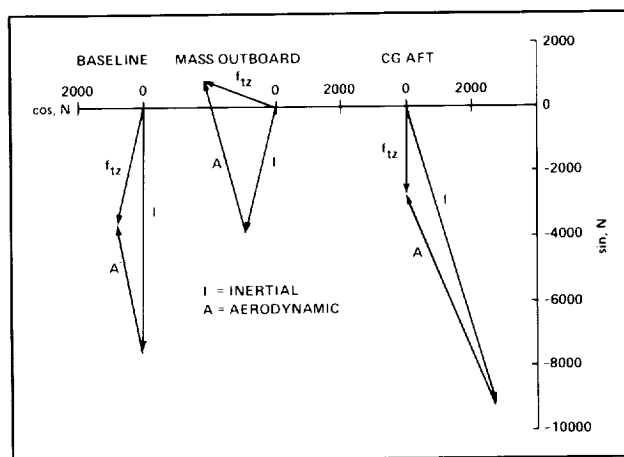
The first study compared predicted and measured hub loads in both the rotating and nonrotating reference frame. For a three-bladed rotor, such as the SA349/2, the fixed-frame hub vibration occurs at multiples of the three-per-revolution (3/rev) harmonic. The first figure shows a correlation of the 3/rev out-of-plane hub force component as a function of advance ratio. Predictions were made using both a uniform inflow and a nonuniform inflow (prescribed wake) model in the CAMRAD analysis (CAMRAD is a NASA-developed rotorcraft code). As evidenced by the figure, the correlation was significantly improved when a nonuniform-inflow model was used in the analysis. The predictions, however, matched the data better at low advance ratio.



Correlation between measured and predicted 3/rev out-of-plane hub force



Effect of shifting blade spanwise mass distribution and chordwise c.g. location on 3/rev out-of-plane hub force, F_z ($\mu = 0.37$)



Aerodynamic and inertial components of 3/rev out-of-plane hub force, F_z ($\mu = 0.37$)

In the second study, the effects of variations in the blade mass distribution and chordwise center of gravity (c.g.) location on the SA349/2 oscillatory hub loads were investigated theoretically. The concept of altering blade design to reduce hub loads has been examined both experimentally and analytically. The second figure shows the effects on the magnitude of the out-of-plane component of the hub force of 1) shifting the blade mass outboard, and 2) shifting the chordwise c.g. aft of 25% chord. Both alterations in blade design led to reductions in the out-of-plane hub force. These reductions were further scrutinized by separating the aerodynamic and inertial contributions to the total forces (as shown in the final figure for the out-of-plane hub force) and then decomposing these contributions into torsion and bending modal components.

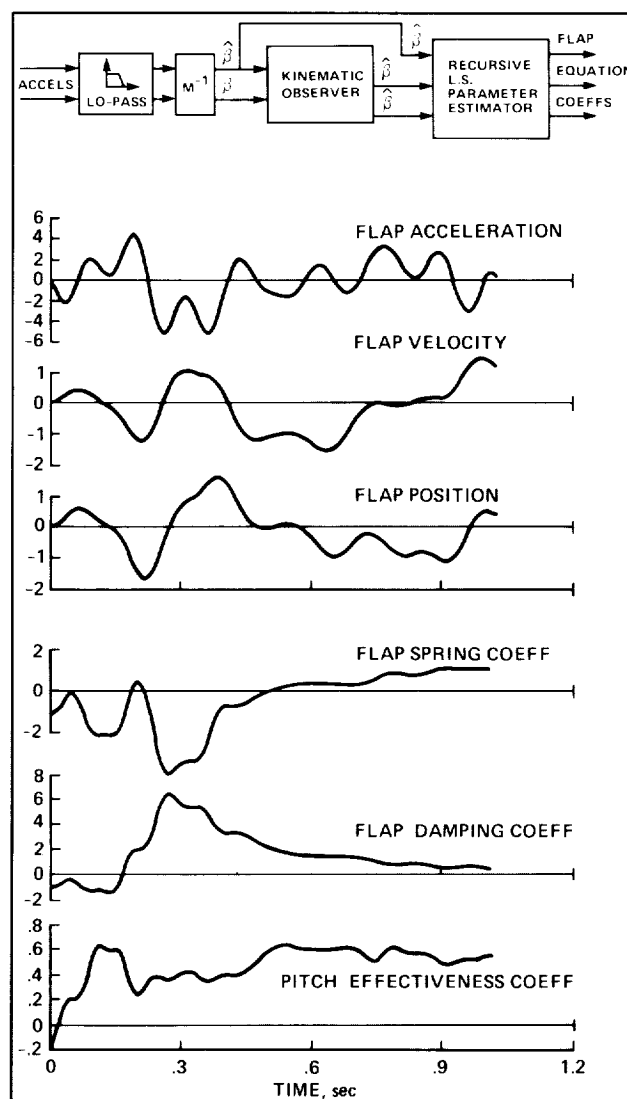
In the third study, a theoretical examination of employing higher harmonic control of the rotor to minimize the hub shear forces was conducted. An algorithm was developed that used 3/rev swashplate control to minimize the 3/rev hub forces. This was accomplished by introducing a controller between the trim and circulation/motion iteration sections of CAMRAD. The magnitude of the resulting combined hub forces was reduced by 95%.

This research represents the second phase of a cooperative program between NASA and the French Ministry of Defense. The purpose of this program is to learn more about the aerodynamic and dynamic behavior of helicopters by using SA349/2 flight-test data and current helicopter analyses developed in the United States and in France. The first phase of the program began with the 1984 flight test of the SA349/2 helicopter. Rotor blade structural and aerodynamic loads were measured for various thrust levels and advance ratios. The SA349/2 aircraft was flown again in 1987, thus initiating the second phase of this joint program. For this flight test, the rotor mast was instrumented to measure hub forces and moments. More detailed blade bending-moment data were also obtained. Several 1984 flight conditions were duplicated during the 1987 flight tests by matching advance ratio and thrust-to-solidity ratio. Collectively, results from the two flight tests provided a comprehensive data base.

(R. Heffernan and G. Yamauchi, Ext. 5043/6719)

Experimental Studies in System Identification of Rotor Dynamics

Efforts over the past few years have indicated the benefits of using kinematic observers for estimating helicopter rotor system states. The advantage of the kinematic observer scheme is that the state variables of the helicopter rotor can be estimated without requiring any aerodynamic modeling of the rotor flow field. The method employs blade-mounted accelerometers and provides greater algorithmic simplicity and computational robustness over



Kinematic observer estimation flow chart with flap mode state and equation parameter time histories

traditional extended Kalman filter identification approaches.

A series of experiments is under way at Princeton's Rotorcraft Dynamics Laboratory under the direction of Prof. Robert McKillip, Jr. These experiments use a dynamically scaled, three-bladed, 4-foot-diameter, model rotor which has miniature accelerometers such that both rigid and elastic blade response may be measured.

This year, a set of hover experiments was performed to provide a checkout of the interface between the new telemetry unit and the multichannel commutator/ decommutator system. Bandwidth checks were made on the model control system to check its acceptability for use in controlling rotor modes at frequencies beyond one per revolution. In addition, studies were made by using the forced response data to determine the best means of reducing "measurement spillover" effects in the reconstruction of the modal response and dynamic equation parameters. Several approaches to identify the blade modal flapping parameters were evaluated, with the best approach consisting of prefiltering the accelerometer data by using a sixth-order, Butterworth, low-pass filter prior to use of the data in the two-pass estimation scheme. This approach is indicated in the figure, along with the time history of flapping modal response and various equation parameters.

Results of these studies indicate that higher-mode participation in the accelerometer data is significant, as expected, but can be controlled through use of sensor prefilters prior to use of the data in the two-pass identification scheme. Alternate, higher-order state observers appear attractive for active control applications where Butterworth filtering might introduce excessive phase lags in the estimator response. The servo bandwidth was deemed acceptable for the closed-loop identification studies to be conducted soon, but it warrants improvement before attempting active rotor control.

(S. Jacklin, Ext. 6668)

Study of Aeromechanical Problems with Active Controls

The desire to reduce the mechanical complexity and weight of articulated rotor hubs has led to the development of hingeless and bearingless rotor hubs. Although these new rotor configurations are simpler and lighter, they can introduce many undesirable stability problems. A study to examine the use of active controls to suppress three rotor/ fuselage instabilities was conducted by Prof. Peretz Friedmann and Dr. Marc Takahashi at the University of California, Los Angeles. One of the instabilities was an aeromechanical air-resonance-type instability, and the other two were rotor aeroelastic instabilities.

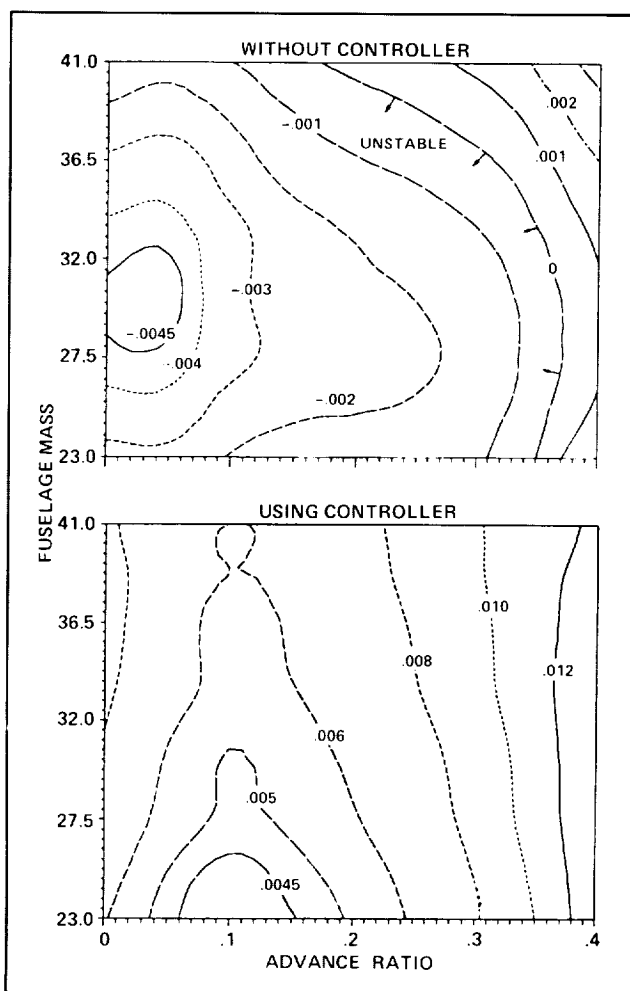
A primary contribution of this research was to first develop an improved formulation of the time-domain unsteady aerodynamics and an aeroelastic rotor model which included a torsional degree of freedom. This provided the basic aerodynamic model needed to study the effect of active controls on rotor stability. The methodology for solving the aeroelastic stability and response problem in forward flight was developed using an implicit formulation. It was found that the time-domain unsteady aerodynamics and torsional modeling terms were important to correctly predict hub shears and the effect of active control inputs.

This model was used to study the active control of rotorcraft air resonance in hover and forward flight with full-state and partial-state feedback. It was first found that partial-state feedback could not control the air-resonance problem. Subsequently, a simple multivariable compensator (having two conventional cyclic swashplate inputs and a single-body roll-rate measurement) was designed by using the loop-transfer recovery method. The method was shown to be capable of stabilizing a helicopter model that was deliberately selected to be unstable for the uncontrolled case. This is indicated in the figure, which shows the increase in lead-lag damping throughout a wide range of rotorcraft loading condi-

tions and forward flight speeds. Moreover, this approach to controlling air (and ground) resonance appears to be both practical and easily implementable. This approach will be tested on a coupled rotor/fuselage model, with hingeless blades, in a future wind tunnel test.

Lastly, the active control of coupled flap-lag and coupled flap-lag-torsional aeroelastic instabilities was also considered in this investigation. The results obtained thus far indicate that these instabilities are more difficult to suppress than the air and ground resonances because of the reduced robustness of the active controller.

(S. Jacklin, Ext. 6668)



Increased lead-lag regressing damping using active controller

System Identification Techniques for Higher Harmonic Control of Rotorcraft Vibration

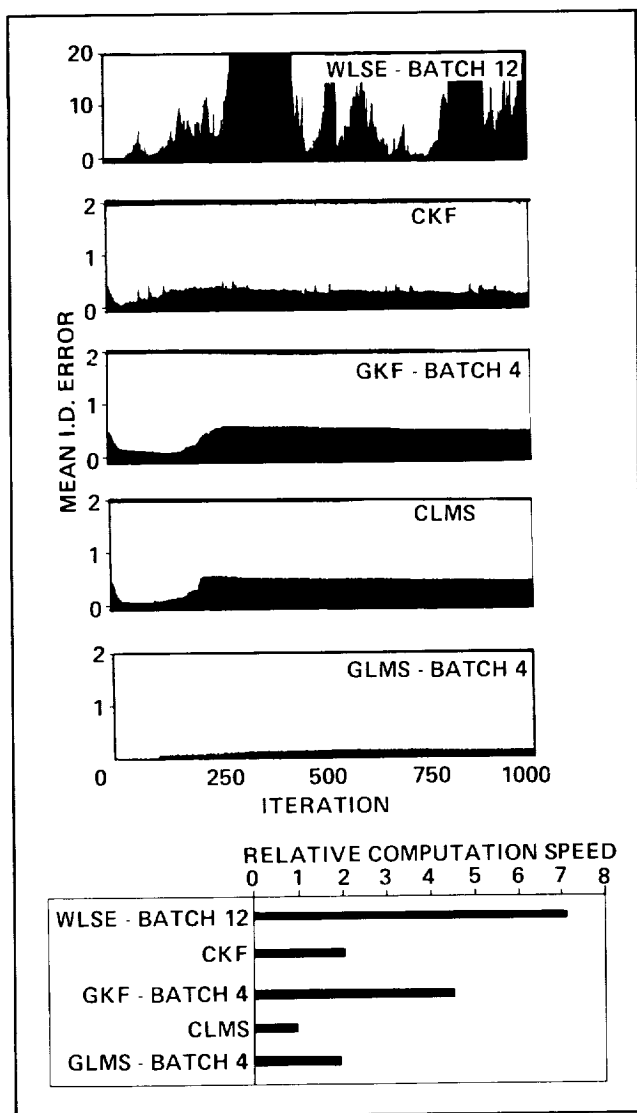
The rotorcraft operating environment presents a real challenge for system identification techniques. The high noise level of this environment alters the ability of identification techniques to distinguish measurement errors from actual changes in the system parameters.

Although the most widely advocated technique, the classical Kalman filter, can filter out this noise when properly tuned, the need to select its many tuning parameters to achieve stable and accurate identification discourages real-world application. This provides the motivation to find alternative identification techniques that can match or exceed the performance of the classical Kalman filter, yet are more easily implemented.

A numerical study was conducted at Ames Research Center to evaluate the performance of five frequency-domain, system-identification techniques by using a multi-input, multi-output simulation. These five techniques consisted of three previously proposed methods: (1) the weighted least square error (WLSE) approach in moving block format, (2) a classical Kalman filter (CKF), and (3) a classical least mean square (CLMS) filter; and two new methods: (1) a generalized Kalman filter (GKF), and (2) a generalized least mean square (GLMS) filter. The generalized methods were derived allowing for multi-step operation, rather than the single-step update approach used by their classical versions.

Open-loop identification performance was demonstrated to be very similar for all methods. However, in the closed-loop mode, as the vibration was reduced, the decreasing signal-to-noise ratio degraded identification performance. This is shown in the figure, which plots the matrix mean identification error for each of the methods.

Although the CKF method gave an order of magnitude better identification and computation speed than the WLSE method, it also required an order of magnitude more tuning time. Since vibration control using the WLSE method was seen to be feasible, the WLSE method represented a tradeoff of



Comparison of identification performance and computation speeds

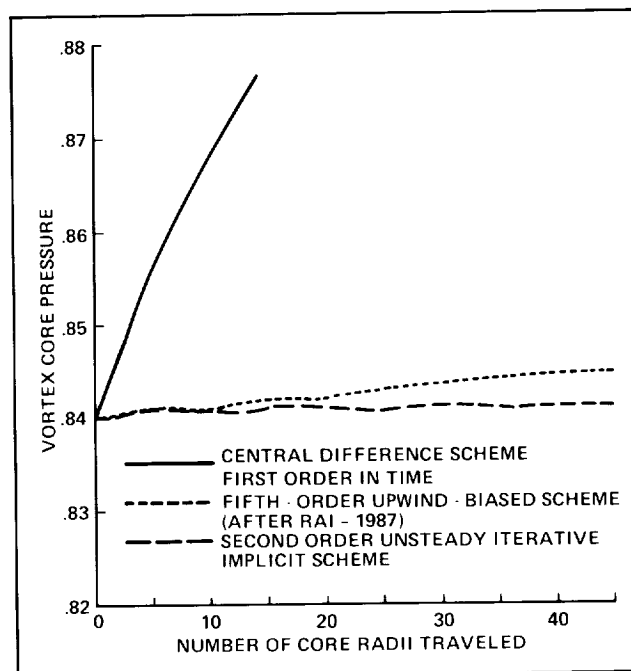
identification accuracy for tuning time. This was also seen for the GKF method, which produced a somewhat higher identification error than the CKF method, but used only half as many tuning parameters and was more stable. The CLMS and GLMS filters gave the best overall performance. These filters were easily tuned using only one tuning parameter. The CLMS technique gave identification accuracy similar to that of the CKF method, yet it was twice as computationally efficient. The multi-step GLMS method, while not as computationally efficient, exceeded the identification performance of the CKF method.

This study, therefore, advocates the use of the GKF, CLMS, and GLMS filters as viable alternatives to the prevalent CKF method. It is expected that the stability and tuning ease of these methods will encourage actual implementation. It is planned to experimentally test these identification methods in the Ames Research Center 40- by 80-Foot Wind Tunnel.

(S. Jacklin, Ext. 6668)

Calculation of Helicopter Rotor Blade-Vortex Interaction by Navier-Stokes Procedures

Blade-vortex interaction (BVI) is a well-known phenomenon that occurs in the flow field around a helicopter rotor and is one of the primary sources of noise and vibration. BVI is a very complex, three-dimensional, unsteady phenomenon. Previous computational studies of BVI have been based on either two-dimensional, unsteady or three-dimensional, steady models. These studies have provided valuable insight into the nature and physics of the problem and have laid the groundwork for further advances.

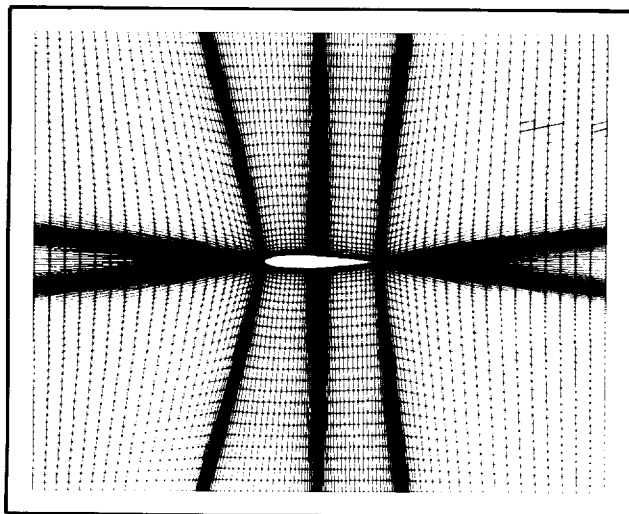


Vortex decay rates for different schemes

Recently, Scientific Research Associates (SRA), under contract to Ames Research Center, began one of the first efforts for the computation of three-dimensional, unsteady BVI at arbitrary vortex-blade intersection geometries. The proposed solution involves the use of a Navier-Stokes code with a linearized block/alternating-direction implicit solution algorithm. The problem is being approached in several stages, each successively more complex than the previous stage.

Several phases of the work have been completed. In the initial phase, the feasibility of using this basic approach was demonstrated by performing model three-dimensional calculations of a simple vortex interacting with an airfoil leading edge. These calculations, as well as the work of previous investigators, point to the importance of correctly modeling the vortex characteristics, and the boundary and initial conditions.

Therefore, during the second phase, work focused on improving the numerical scheme in order to reduce numerical errors in simulating vortex-dominated flows. The current scheme (which is second-order-accurate in time and second-order-accurate in space, and incorporates an implicit iterative procedure to reduce numerical "splitting" errors) yields a vortex as stable as the best previous models.

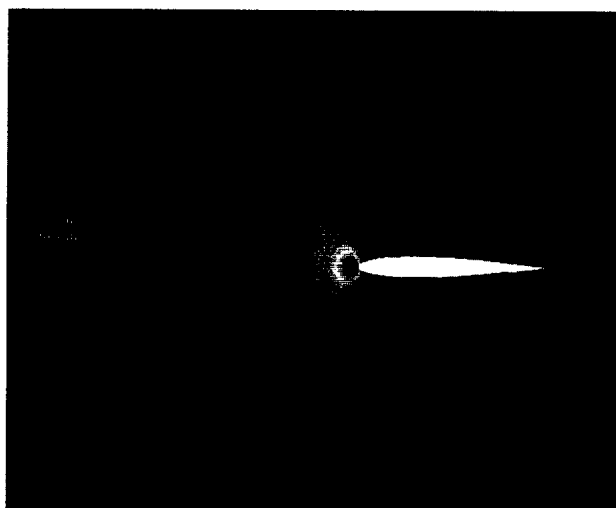


H-grid

During the third phase, two-dimensional calculations of vortex-airfoil interaction have been initiated using an H-type grid. A new version of the code with an improved turbulence model has allowed the calculations to be extended to higher Reynolds and Mach numbers more typical of real rotor blades.

During the next phases of the work, several two-dimensional test cases will be run to compare the results to other computations and to data. Next, the tip and rotational effects for a rotor blade will be modeled. Finally, fully three-dimensional, unsteady calculations will be performed. These last several phases of the work will require the computational resources of the National Aerodynamic Simulator at Ames Research Center.

(C. Kitaplioglu, Ext. 6679)



Pressure distribution

Full-Scale Wind Tunnel Testing of the Helicopter Individual Blade Control System

The Individual Blade Control (IBC) system provides a broad range of rotorcraft applications, including gust alleviation, attitude stabilization, vibration alleviation, blade lag-damping augmentation, stall

ORIGINAL PAGE
COLOR PHOTOGRAPH

flutter suppression, blade flapping stabilization, stall alleviation, and performance enhancement.

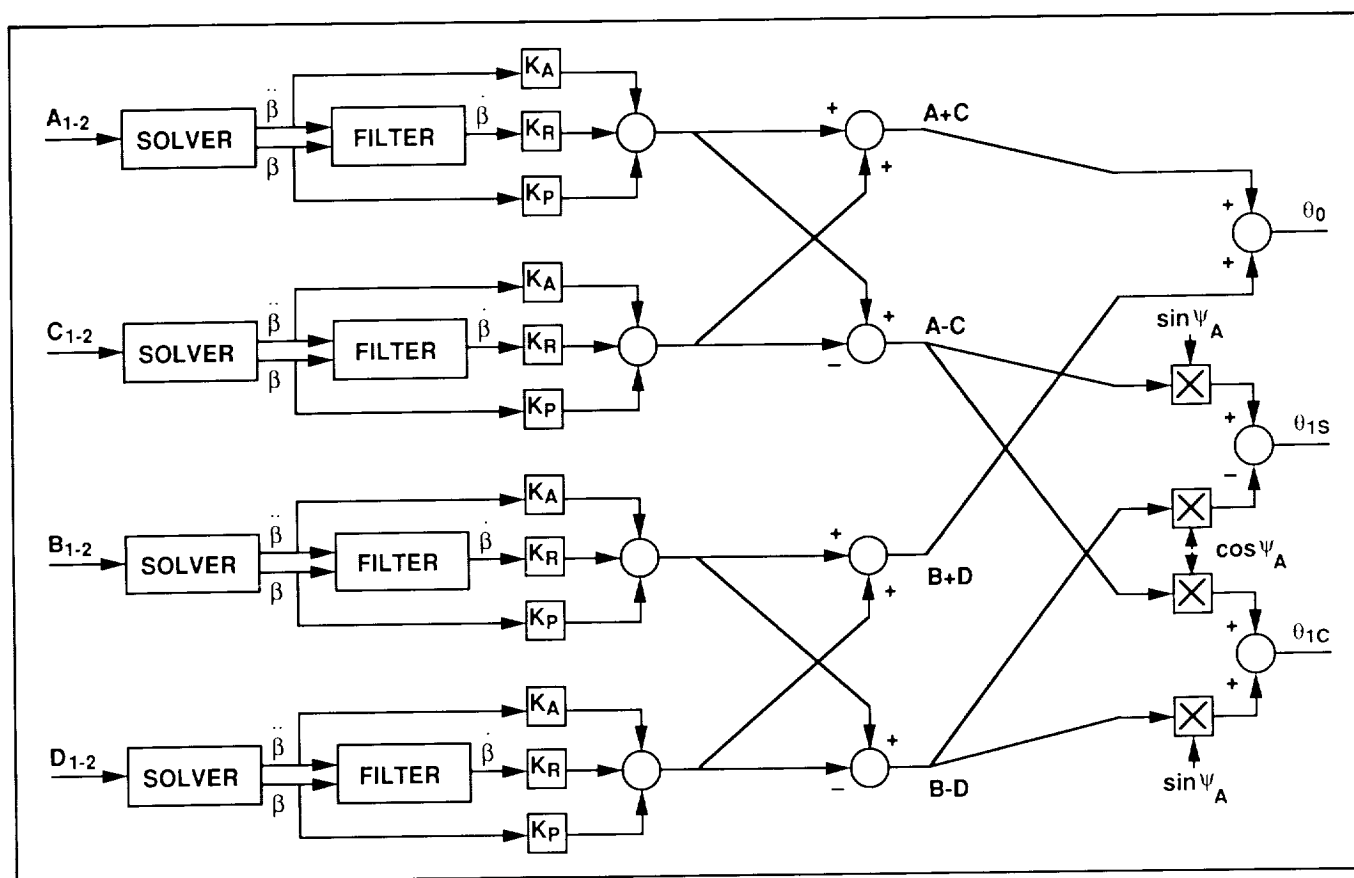
The concept of IBC embodies the control of each blade over a wide range of frequencies, using signals from individual blade-mounted accelerometers. The sensor signals are fed into a solver to calculate the blade modal responses (for example, blade lag angle and acceleration). The resulting signals are then integrated by the McKillip filter to yield the observed lag angle and rate.

The output of the filter becomes the input to the controller, which provides appropriate commands to the electrohydraulic pitch actuators. Since the actuators and the feedback loops rotate with the blades, a conventional swash plate is not required. However, by placing the actuators in the nonrotating system and controlling the blades through a conven-

tional swash plate, some IBC applications can also be achieved.

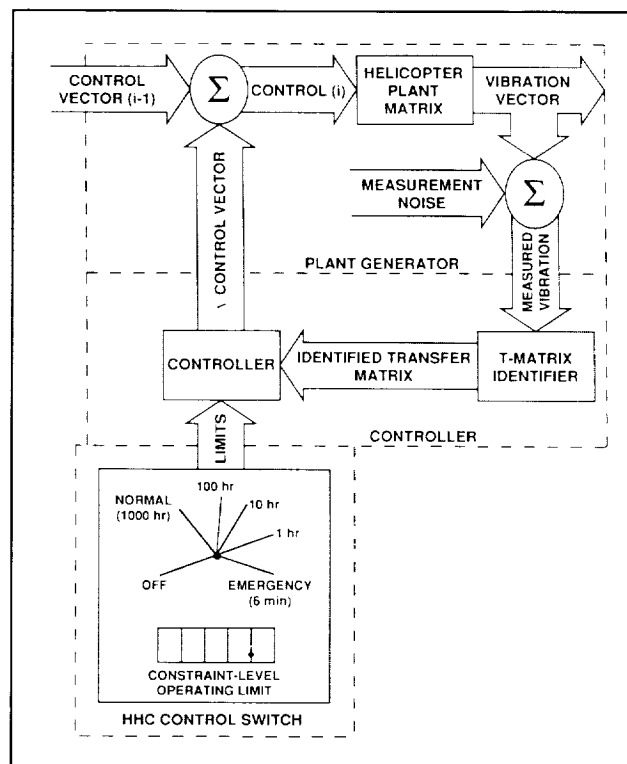
The theoretical background of the IBC concept has been well established in previous research sponsored by Ames Research Center grants/cooperative agreements with the Massachusetts Institute of Technology. To validate this concept, a Bell Model 412 rotor with 23-foot radius will be tested in the 40- by 80-Foot Wind Tunnel at Ames in the summer of 1989. The test objective is to conduct open-loop tests of blade in-plane damping augmentation and blade flapping stabilization, and to investigate the IBC system performance under the effects of deliberate failures of various components.

(B. Lau, Ext. 6714)



Schematic of flapping control system using the conventional swash plate for four-bladed rotor

Questions concerning the optimality of the control computation and the use of a single covariance lattice arose during this comparison. The actual optimal control problem was identified and a solution to a lower-dimension, but similar, problem was derived analytically. This solution defined a "bang-bang" optimal control scheme in which the optimal control was on its constraint envelope. Its position on this envelope was defined by analytically solving a system of nonlinear equations. A cursory attempt was made to solve the actual problem. Although a full analytic solution to this problem has not been derived at this time, the solution process clearly shows the bang-bang nature of the solution. This



Active control loop with HHC limiter switch

result strongly suggests a very suitable and appropriate way to regulate the active control from the cockpit.

As illustrated in the accompanying figure, a higher harmonic control (HHC) switch to constrain the operating control level would provide the pilot a rapid and simple means to employ up to the full HHC commands needed in the event of an emergency. This device could also keep track of time to the next required maintenance, which would be a function of the amount of time spent at each operating level.

(J. Leyland, Ext. 6668)

Rotor Blade Optimization

A method for optimizing rotor hover performance is being developed by Continuum Dynamics, Inc., under a contract with Ames Research Center. This Phase I Small Business Innovative Research contract is based on a free-wake hover analysis. The free-wake analysis uses curved vortex elements, a lifting-surface blade representation, and an efficient

wake-relaxation scheme. This work is based in large part on the unique relaxation scheme. The relaxation method provides influence coefficient arrays which relate rotor loads and wake geometry to the downwash distribution. The optimization work has expanded the arrays to account for changes in blade twist. The arrays are then coupled with a linear optimization scheme which provides an optimum blade twist distribution for given rotor and performance constraints. Preliminary results show rapid and efficient convergence to optimum configurations. Anticipated future work will examine variations in blade sweep, taper, or chord.

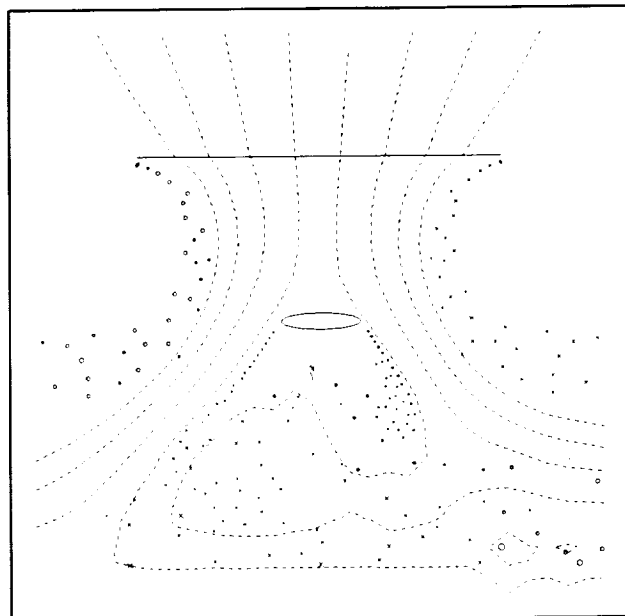
(J. Light, Ext. 4881)

Tilt-Rotor Download Research

A three-dimensional, unsteady panel method is being developed to predict the download of a tilt-rotor aircraft in hover. In the massively separated flow of a tilt-rotor wing, an oscillating wake is usually formed behind the separated region. The vorticity of different signs emanating from each side of the separated region tend to interact with each other. This makes the wake, as well as the wingloading, unsteady. An existing panel method analyzes the steady, separated flow, assuming a smooth and continuous wake shape. However, for unsteady, massively separated flows, this approach fails when a wake panel intercepts the wake shedding from the other side of the separation region.

To solve this problem, a new wake model is being developed which represents the wake by discrete doublet panels and marches the wake shape by the vorticity equations. A simplified, two-dimensional pilot code has been completed. In this code, the airfoil and rotor are represented by vortex panels, and the rotor slipstream and wake are simulated by the vortex tracing method. The two-dimensional code has demonstrated that the method is stable. Current research effort is concentrating on developing a three-dimensional, discrete wake panel model for unsteady load prediction.

A recently initiated grant with Stanford University will examine another method of tilt-rotor download prediction. This method will predict the download on a tilt-rotor wing by using a three-dimensional Navier-



Asymmetrical wing wake in ground-effect, two-dimensional panel method

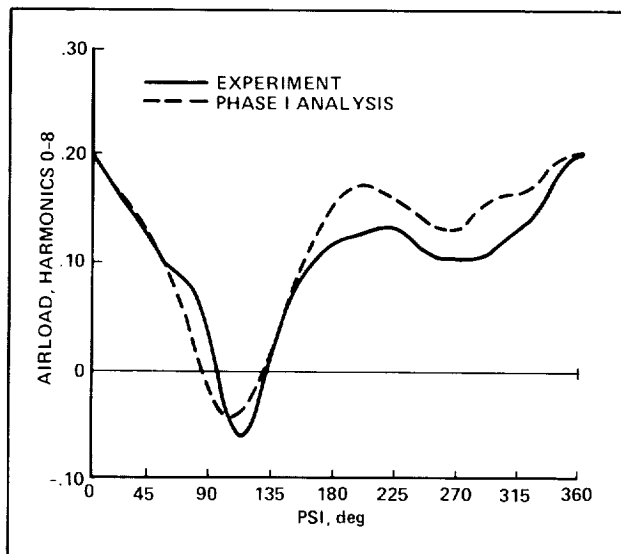
Stokes analysis. The thin-layer approximation is used because of computer memory and time constraints. The solution method is implicit and uses the Beam-Warming flux-splitting technique. A three-dimensional body-fitted grid is being developed for the problem. The domain of interest extends from the rotor plane to several chords below the wing, and beyond the wingtip. Inviscid boundary conditions (including pressures and velocities) on the rotor have been estimated by using a combination of blade element theory and momentum theory applied to a nonuniform actuator disk. The flow conditions in the rotor plane, but not on the rotor itself, have been predicted by using a three-dimensional panel method.

To validate these analyses, a small-scale download test is being planned at Ames Research Center. This test will use a scaled V-22 rotor system and two wings. The first wing will be used to examine the effect of upper surface blowing on download reduction by using two leading-edge slots and one trailing-edge slot. The second wing will be a model V-22 wing which will be used to examine the effect of rotor rotation direction and rotor/wing geometry variations.

(J. Light and J. Lee, Ext. 4881/4573)

Unsteady Rotor Airloads

Existing forward flight analyses cannot reliably predict the unsteady airloading on rotor blades, in particular the high-frequency vibratory loading in high-speed flight. Continuum Dynamics, Inc., under a contract with Ames Research Center, has successfully demonstrated that by coupling a novel, full-span wake model to a lifting surface loads analysis, very promising predictions of such loads can be obtained. Comparisons of predicted airloads with measured data from an H-34 main rotor show promising correlation (see figure). The new wake model features the use of curved vortex elements to model contours of constant vorticity in the wake and captures many important features of the wake-induced flow field absent from previous models.



Nondimensional airload for the H-34 rotor at $C_T = 0.0037$, $\mu = 0.39$, $r/R = 0.90$

In Phase II of this program, Continuum Dynamics will build on the demonstrated success of this initial effort to develop a complete and consistent forward-flight airloads analysis. The final code will

include the current lifting-surface model and multifilament wake, but with a new, efficient, far-wake model to permit the analysis of low-speed flight. Refinements in the treatment of trailing-vortex discretization and roll-up will be implemented, and enhancements in the modeling of compressibility effects will be undertaken. The final analysis will be designed to interact with a variety of advanced dynamics treatments and it will be correlated with a wide range of existing airload data.

(T. Norman, Ext. 6653)

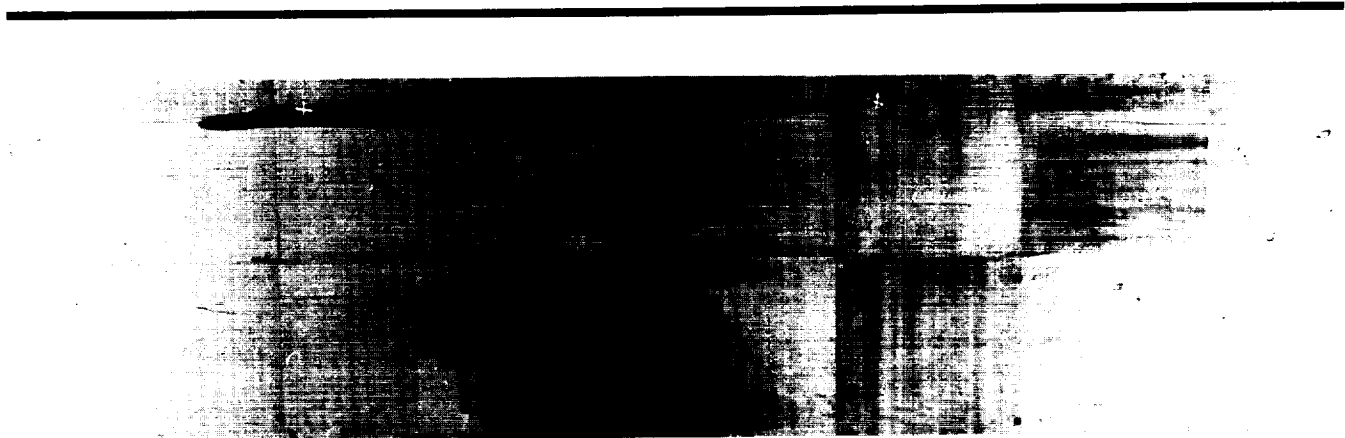
Visualization of Rotor Wakes by Using the Shadowgraph Technique

As part of a continuing study of rotorcraft flow fields by use of the wide-field shadowgraph technique, an experimental investigation was recently completed which documents the wake geometry of a hovering rotor with a novel, curved, swept-tip planform. The setup for this joint Army/NASA experiment consisted of a 7-foot-diameter model rotor tested in the Anechoic/Hover Test Chamber at Ames Research Center. Shadowgraphs were acquired at two thrust coefficients and three tip Mach numbers for a range of rotor azimuths.

A sample shadowgraph is shown in the figure. The tip vortex trajectories are identifiable in this figure as thin dark spirals emanating from the blade tips. Data from this investigation will be used to help validate new and existing hover-performance prediction codes.

Planning is currently under way to extend the shadowgraph technique to measure the wake geometry of rotors in forward flight. An upcoming small-scale rotor test in the Ames 7- by 10-Foot Wind Tunnel will provide sufficient information to assess the viability of this approach.

(T. Norman and J. Light, 6653/4881)



Sample shadowgraph at 1800 rpm and $\theta_c = 6^\circ$

Numerical Methods for Vortical Flow Fields

The numerical prediction for the strong interaction between vortical wakes and the viscous flow field about bodies is of considerable importance in the design analysis of rotorcraft. In general, these are strong interactions in which the rotor wake flows onto or passes very close to the other components of the aircraft. The effects of the vortex interactions are increased vibratory loading on the fuselage, decreased payload capabilities, and increased noise.

A numerical method for computing the aerodynamic interaction between an interacting vortex wake and the viscous flow about arbitrary two-dimensional bodies was developed to address this helicopter problem. That method solved the velocity/vorticity formulation of the Navier-Stokes equations. The computational mesh was concentrated near the body surface to resolve the boundary layer and was increasingly coarse farther from the body. The interacting vortex wake was modeled as an array of finite-core vortices. The core radius was variable and was independent of the mesh spacing.

The finite-core model eliminated the numerical diffusion associated with the coarse mesh spacing and provided for the accurate prediction of the vortex wake dynamics. This was true away from the body where the flow field was inviscid and was dominated by the rotor wake. Closer to the body, the flow was viscous and the convection of the rotor wake could no longer be considered inviscid. In this region, the interacting vortex wake interacted with the viscous separated wake and could no longer be modeled by

a finite-core model. At this point the finite-core vortex was distributed to the computational mesh and allowed to convect as part of the viscous solution.

Results for the flow about circular and elliptic cylinders were calculated. Results for the flow field without the interacting vortex wake compared very well with other numerical results and with results obtained from experiment, thus demonstrating the accuracy of the viscous solution. However, in calculating the flow about airfoils, the accuracy of the solution was lost. The solution was found to be both highly dependent on the mesh geometry and on the method used to accelerate the solution of the velocity equations. This dependency resulted from the loss of volume conservation. The discretized form of the velocity equation did not identically satisfy the discrete continuity equation. Results for flow about circular cylinders did not identify this discrepancy because an accurate solution could be obtained by converging the solution at each time step. However, when the flow about airfoils was calculated, the solutions would not converge, or they became unstable.

Calculations were conducted to evaluate the convergence and consistency of the solution for flow about airfoils. The primary concern of these calculations was to provide volume conservation during the solution of the velocity equations. The solution of the velocity equations was obtained by an SOR (successive over relaxation), an ADI (alternating-direction implicit), and a modified ADI technique. Iteration on the solution at each time step was used to couple the velocity and vorticity. In addition, a noniterative solution was obtained by coupling the vorticity transport equation with the velocity equations by implementing a block tridiagonal technique.

ORIGINAL PAGE
BLACK AND WHITE PHOTOGRAPH

The solution of the velocity equations by each of the above methods either resulted in violation of volume conservation, or did not converge, or both. The violation of the continuity equation was thought to be the cause of this discrepancy in the velocity formulation.

In order to satisfy volume conservation, a staggered grid and a fully coupled scheme were employed for the solution of the velocity/vorticity equations.

The staggered grid positioned the flow-field variables at separate physical locations. In this method, the definition of vorticity and the divergence of velocity were provided by central differencing over a single mesh cell, rather than over two mesh cells for a conventional grid. The staggered grid solution provided for the direct solution of the flow-field variables in a fully coupled manner requiring a single iteration per time step.

The coupled scheme solved for the vorticity and the velocity components by using an ADI scheme with a block tridiagonal formulation. After each time step, the divergence of the velocity was machine zero. This method was applied to the driven two-dimensional cavity problem. Results for this problem were in excellent agreement with other numerical investigations and results from experiment.

Currently, the staggered grid scheme is being applied to the three-dimensional cavity problem. Results have been obtained for the nonconvective form of the vorticity transport equation which demonstrate the symmetry of the problem and divergence of the velocity equal to machine zero. Currently, the convective form of the vorticity transport equation is being studied, after which the flow about three-dimensional bodies and the solution of vortex interaction in three dimensions will be addressed.

(P. Stremel, Ext. 6653)

M-85 High-Speed Rotorcraft Concept

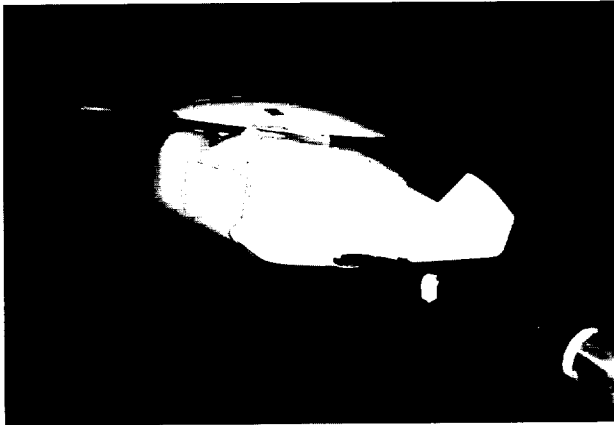
The helicopter, with its efficient hover capability and low-speed maneuver capability, has well served the contemporary military and civil communities. The higher speed capabilities, long sought by the user communities, have piqued the interest and innovativeness of designers for many years. As a result of studying a number of concepts about high speed, a new high-speed rotorcraft concept, designated as M-85, has been derived which may achieve a number of attractive performance goals such as 1) hover efficiency near the helicopter, 2) downwash field no worse than a CH-53E helicopter, 3) conversion from helicopter mode to fixed-wing mode that does not require a higher harmonic control system, 4) cruise speeds in excess of 500 knots, and 5) minimum flight speeds of 160 knots in fixed-wing mode.

Research effort in past years has been concentrated on the lift system and performance capabilities. The M-85 incorporates a rotating-wing system for generating basic lift 1) during hover, and 2) for low-speed flight up to conversion to the fixed-wing configuration used for high-speed flight. This lift system consists of a circular hub fairing, extending to approximately half of the rotor radius, and two or more individually controlled large chord blades. In hover mode, the hub fairing and the blades are rotating at the same speed.

While other system components were being investigated conceptually, a test at the NASA Langley Research Center 14- by 22-Foot Wind Tunnel was conducted to study the aerodynamic characteristics of the lift system in the fixed-wing mode at low-subsonic speed. Among the various configuration candidates, one has achieved a lift-to-drag ratio of 20. Preliminary performance calcula-

tions based on these test data have demonstrated the attractiveness of the M-85 concept. At the same time, the aerodynamics of several configurations are also being examined with the Ames panel-method code PMARC.

(R. Stroub and A. Louie, Ext. 6732/6976)



M-85 configuration and concept-evaluation test in the Langley Research Center 14- by 22-Foot Wind Tunnel

Tilt-Rotor Flutter Alleviation

The development of the next generation of tilt-rotor aircraft likely will be accompanied by an increase in maximum flight speed. Therefore the potential of whirl-flutter aeroelastic instability is also increased and could form a limiting factor to the maximum speed capability.

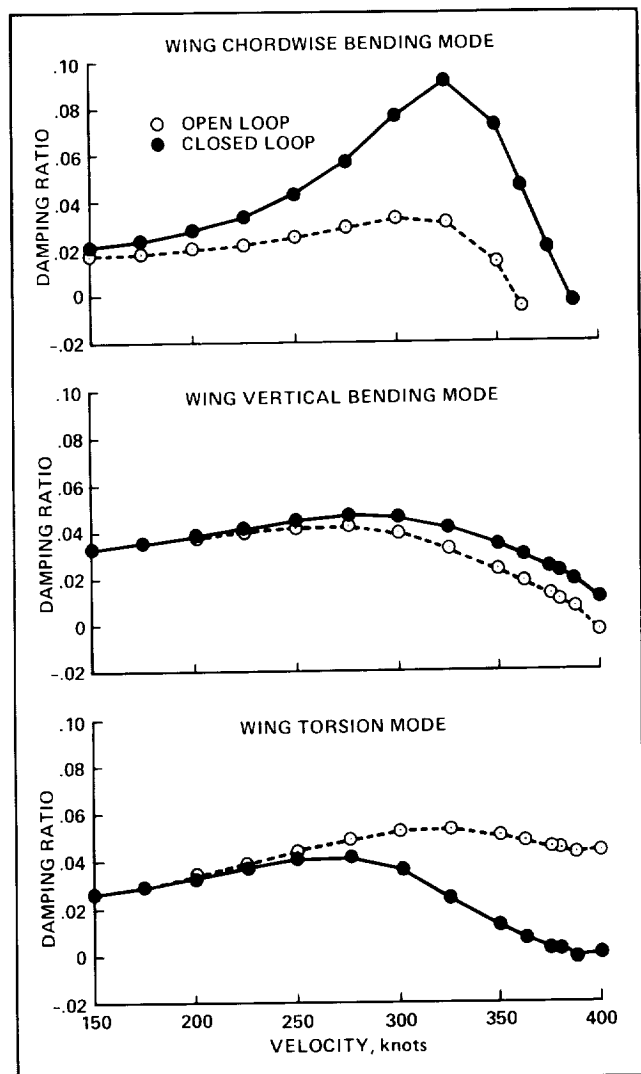
The University of Kansas Center for Research, Inc., under a cooperative agreement with Ames Research Center, is studying the potential payoffs of using active control for whirl-flutter delay/suppression.

A NASA-developed program, CAMRAD (Comprehensive Analytical Model of Rotorcraft Aerodynamics and Dynamics), is used to obtain a set of linear differential equations which describe the motion of the tilt-rotor aircraft at various speeds. The output of CAMRAD consists of the open-loop system matrices which describe the aircraft motion in the state-variable domain. These matrices form an input to a separate program which performs the closed-loop, active-control calculations. This program per-

forms an eigen analysis to determine the flutter stability for both the open- and the closed-loop systems. Time-response calculations are performed to estimate the magnitude of the required active control settings for closed-loop stability. The option exists to superimpose signal noise onto the closed-loop sensors.

It has been shown that the onset of whirl-flutter for the baseline aircraft, the XV-15, could be delayed by feeding back the wing accelerations (state variables) in the vertical and horizontal direction to the longitudinal cyclic (see figure).

Thus far, the effect of the feedback of pure state variables on the delay/suppression of whirl-flutter has been studied. A more realistic model of the actual



Modal damping in open loop and closed loop using active controller

sensor signal/output is being developed. The approach is consistent with that used in CAMRAD. An off-line structures program is used to calculate the free-vibration wing motion. The hub motion, resulting from this wing/body vibration, is a standard input to CAMRAD. The wing vibration characteristics also form an input to the active-control program and will be used to study the effect of the number of sensors and their location on the performance of various feedback control schemes in whirl-flutter alleviation.

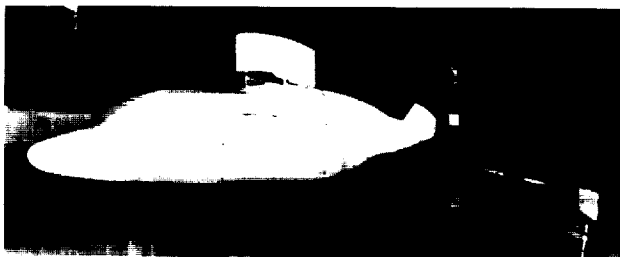
(J. van Aken, Ext. 6668)

Hub-Drag Reduction

Two principal activities are in progress for the Hub-Drag Reduction research program. First, a joint test was conducted by NASA Ames Research Center and the Army in the NASA Langley Research Center 14- by 22-Foot Wind Tunnel to verify and expand upon previously observed hub-drag reduction trends made in two tests in the Ames 7- by 10-Foot Wind Tunnel. Second, a joint test program between Bell Helicopter Textron, Inc., and Ames is in the preliminary stages of planning for a third test in the Ames 7- by 10-Foot Wind Tunnel.

Data reduction of the joint Army and NASA test in the Langley 14- by 22-Foot Wind Tunnel has been completed. The test results confirm the hub-drag reduction trends observed in the previous two Ames wind-tunnel tests, but do so with improved data accuracy and with reduced concern regarding blockage and wall effects on the drag trends.

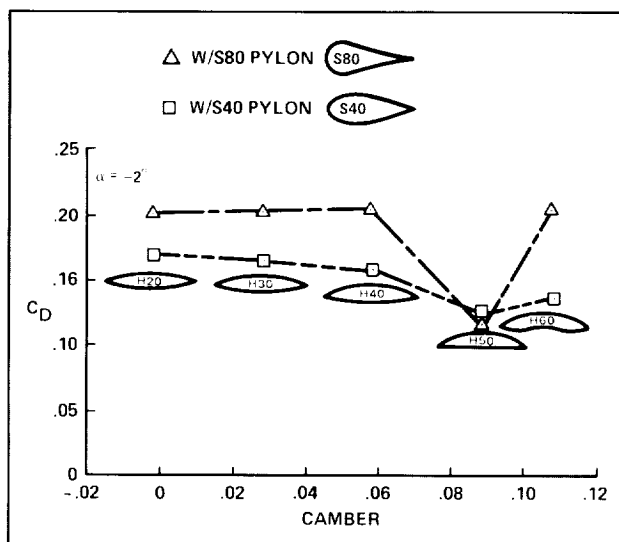
For a generic helicopter model having nonrotating hub fairings which do not incorporate blade shanks, the results from all three tests confirm that the minimum-drag fairing configuration tested was an



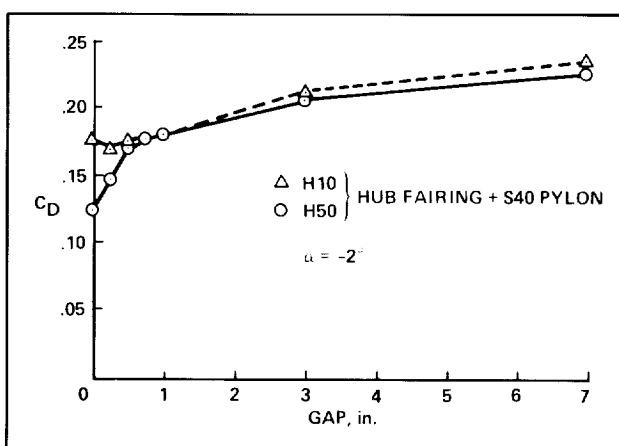
Joint NASA Ames and Army hub-drag test in the NASA Langley 14- by 22-Foot Wind Tunnel

integrated hub- and pylon-fairing combination having the following attributes: (1) a cambered hub fairing with a flat lower surface, (2) a pylon fairing having an approximate airfoil-type shape, and (3) minimal gaps between the hub and pylon fairings. In particular, the extreme sensitivity of the overall helicopter model drag to gaps between hub and pylon fairings was demonstrated in the latest wind tunnel test to a degree not matched previously.

The objectives of the proposed joint Bell Helicopter Textron, Inc., and Ames test in the 7- by 10-Foot Wind Tunnel are threefold: (1) to test low-drag fairings on a model of a production helicopter;



Effect of hub-fairing camber on drag



Effect of hub/pylon gap width on drag (cambered H50 and Symmetrical H10 hub fairings with S40 pylon)

(2) to explore practical hardware implementation issues by designing and testing fairings that can accommodate hub rotation, rotor-shaft motion, and blade shank integration; and (3) to quantitatively identify the interactional aerodynamic nature of the drag reductions observed for the low-drag fairings.

(D. Sung and L. Young, Ext. 4022)

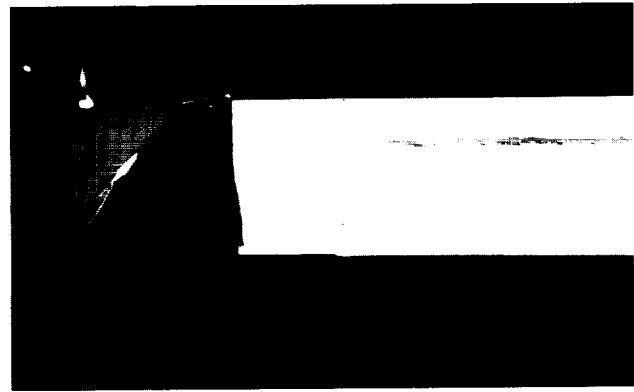
Free-Tip Rotor

A number of research activities are currently in progress to better understand the aerodynamic and dynamic characteristics of the free-tip rotor concept. These activities include (1) two semispan-wing tests in the Ames Research Center 7- by 10-Foot Wind Tunnel, (2) preparation for a proposed third entry in the 7- by 10-Foot Wind Tunnel, (3) modification of an unsteady panel-method computer code to predict forced- and free-vibration characteristics of free-pitching tips on semispan wings, and (4) continuing work on the design of a model rotor that incorporates both the free-tip rotor concept and advanced airfoil contours.

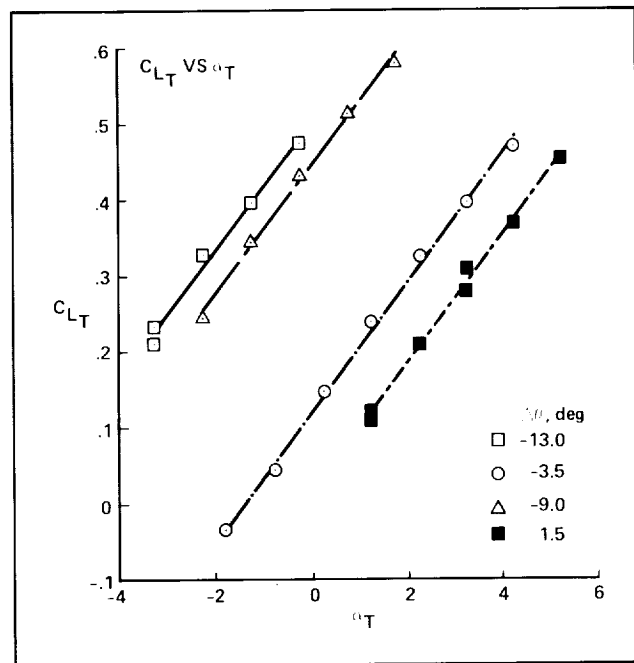
The first 7- by 10-foot test measured the low-speed, steady-state aerodynamic coefficients of a highly swept and tapered tip indexed at various incidence angles with respect to the inboard semispan wing. The tip planform tested during this semispan-wing test will be used in the advanced free-tip rotor model design. Additionally, analysis of the data is focused on establishing the functional dependence of the tip aerodynamic coefficients on the relative incidence angle between the tip and wing. Finally, the experimental results are being correlated with predictions from a panel-method computer code.

The second 7- by 10-foot test measured the free-vibration characteristics of free-pitching wingtips on a semispan-wing model, resulting in estimates of tip aerodynamic spring and damping. Additionally, semiempirical predictions of tip aerodynamic spring and damping are being correlated with the experimental test results.

Preparations are being made for a third semispan-wing test in the 7- by 10-Foot Wind Tunnel. This proposed test will investigate the forced-vibration response of a free-pitching wingtip caused by external, periodic aerodynamic excitation. The



Free-tip semispan-wing I test (flow visualization of leading-edge separation bubble)



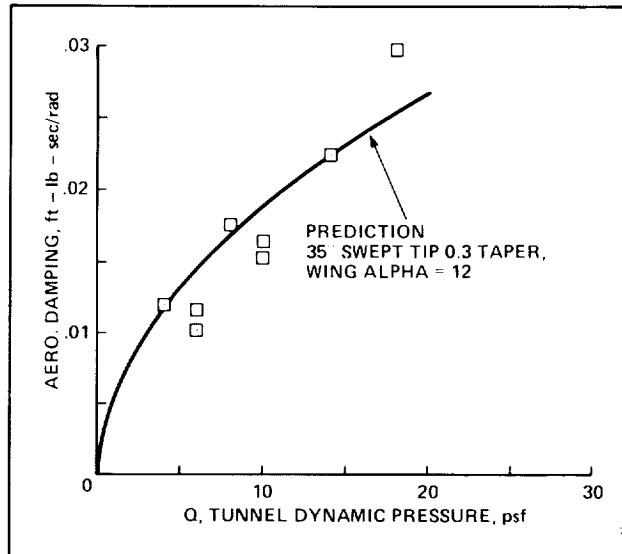
Free-tip semispan-wing I test (advanced tip planform)

objective of this test is to establish an empirical relationship between tip forced-vibration response and wing bending-moment vibration reduction.

Work is in progress to proceed beyond semiempirical methods for predicting free-tip forced- and free-vibration response. An unsteady, potential-flow, panel-method computer code is being modified to handle free-tip semispan-wing configurations. Prescribed tip motion has been implemented in the code and an evaluation of the results is being performed.

Finally, work continues on a model rotor detail design for an advanced free-tip rotor. Results from the semispan-wing tests have been incorporated into the design methodology. Additionally, preliminary dynamic analyses have been performed in-house on the model rotor so as to estimate interim-design blade frequencies, evaluate blade mass-distribution design alternatives, and estimate the stability of the rotor and its test stand.

(L. Young, D. Martin, and A. Louie, Ext. 4022/6976)

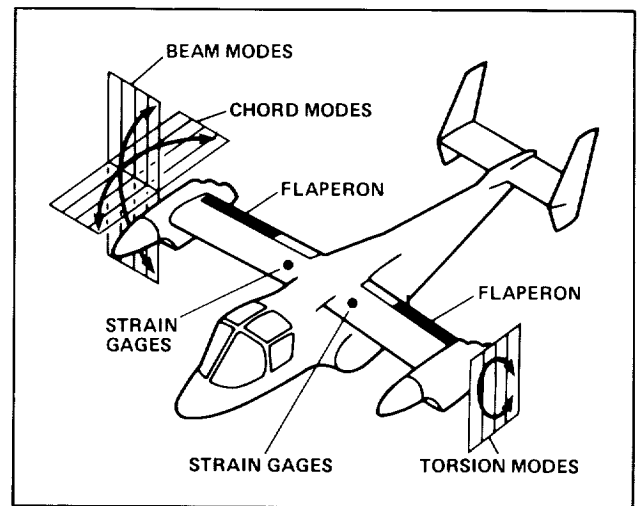


Free-tip semispan-wing II test

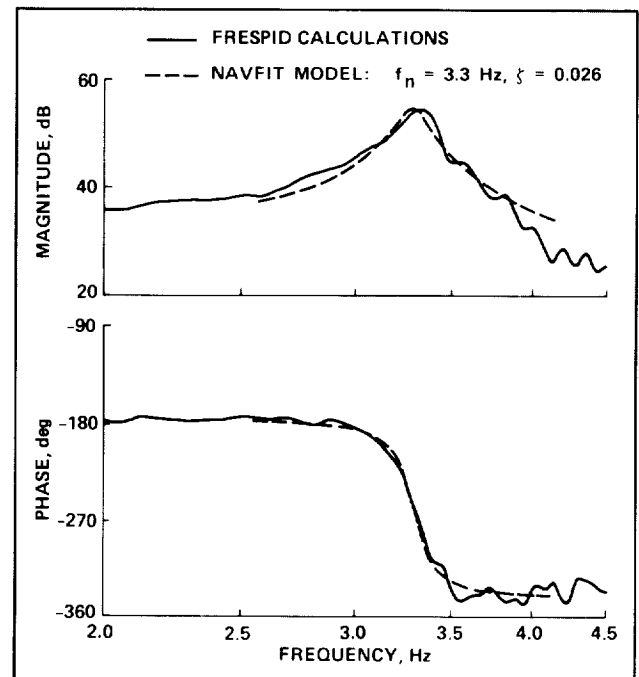
Tilt-Rotor Structural Aeroelastic Stability

The dual objective of the research is to develop flight-test and data-analysis techniques to document the aeroelastic stability characteristics of tilt-rotor aircraft and to verify existing prediction techniques.

The XV-15-703 tilt-rotor aircraft at Ames Research Center uses its flaperons to excite structural modes for which natural frequency and structural damping can be measured and analyzed. The research has two elements. The first is the development of flight-test techniques that provide strong structural mode excitation while minimizing multiple-mode coupling; frequency sweeps have proved to be the most productive approach. The second element is the development of analytical tools to analyze the



XV-15 aircraft, showing flaperons, strain gage locations, and wing modes



Symmetric beam mode frequency response

flight-test results, including the ability to separately analyze closely spaced modes; the most recent innovation is the use of coherence-weighted spectral curve fits. These techniques can also be applied to ground vibration tests.

Current investigations are being performed on the XV-15 configured with the new Advanced Technology Blades (ATB). The high mass and solidity of

the ATBs require close attention to coupled rotor/airframe dynamics. Flight and ground tests have demonstrated the inability of existing analytical methodologies to accurately predict rotor loads and stability. Hence, the ATB program encompasses efforts to improve the ability to calculate aeroelastic and aeroservoelastic effects in both low- and high-speed flight.

(C. W. Acree, Ext. 5423)

Individual Blade Feedback Investigations

The objective of the individual blade feedback investigations is to evaluate a control system that obtains rotor dynamic information from blade-mounted sensors and uses this information as a feedback source. This is part of a cooperative effort with Dr. Norman D. Ham of the Massachusetts Institute of Technology. Dr. Ham has developed a method for estimating the main rotor blade flapping and bending motion by using blade-mounted accelerometers. These accelerometer signals are processed with control algorithms which generate input command signals that can be implemented through a conventional swashplate. This type of control system has potential applications to gust alleviation, vibration reduction, and other rotor-associated dynamic phenomena.

During 1988 effort was focused on using this approach with the XV-15 tilt-rotor aircraft. Analytical findings indicate that successful alleviation of tilt-rotor "chugging mode" response can be obtained, as can reduction in wing/rotor interference effects.

Flight tests of a four-blade, open-loop system aboard a UH-60A Black Hawk helicopter are scheduled for 1989. These tests are designed to determine whether the blade-mounted accelerometers can generate useful feedback signals in flight.

(D. Balough and N. Ham, Ext. 3152)

TRENDS Rotorcraft Data Base

The object of the TRENDS data base operating system is to provide NASA with an "expert" rotorcraft system which not only makes rotorcraft flight-test data easily accessible to the user community, but provides all users of these data with the critical tools for rotorcraft research. Currently NASA has a data base operating system which provides access to three rotorcraft data bases using 5 gigabytes of on-line disk storage. TRENDS has been developed over a 5-year period, and is a leading data base operating system for rotorcraft research. It is being used by NASA and the major rotorcraft developers of the United States, and it provides them with sophisticated data-analysis routines along with powerful graphics.

This system runs on a VAX/785 computer system and uses many of the unique DEC/VMS operating system features, such as "keyed access." TRENDS supports the execution of rotorcraft math model programs within TRENDS to enable the comparison of simulation data with the actual flight-test data. The user-friendly interface provided for the running of the math model along with the archiving of these data will continue to be expanded within TRENDS. The aim of this program is to add to TRENDS not only a significant increase in the data storage capacity, but to add more math models, including output from CAMRAD and possibly NASTRAN. Finally TRENDS also provides a gateway for DATAMAP program users to access their pressure data by using all of the latest three-dimensional plot programs available in that system.

NASA is presently involved in various long-term rotor research programs to improve rotorcraft performance. These research programs will require the acquisition and storage of massive amounts of rotor system loads data. In 1989, 80 gigabytes of storage capacity will be brought on-line by using a laser disk jukebox system. NASA plans to use this new optical disk system by making TRENDS into a hybrid data base manager which will read data from both magnetic and optical disk storage systems.

(M. Bondi, Ext. 6341)

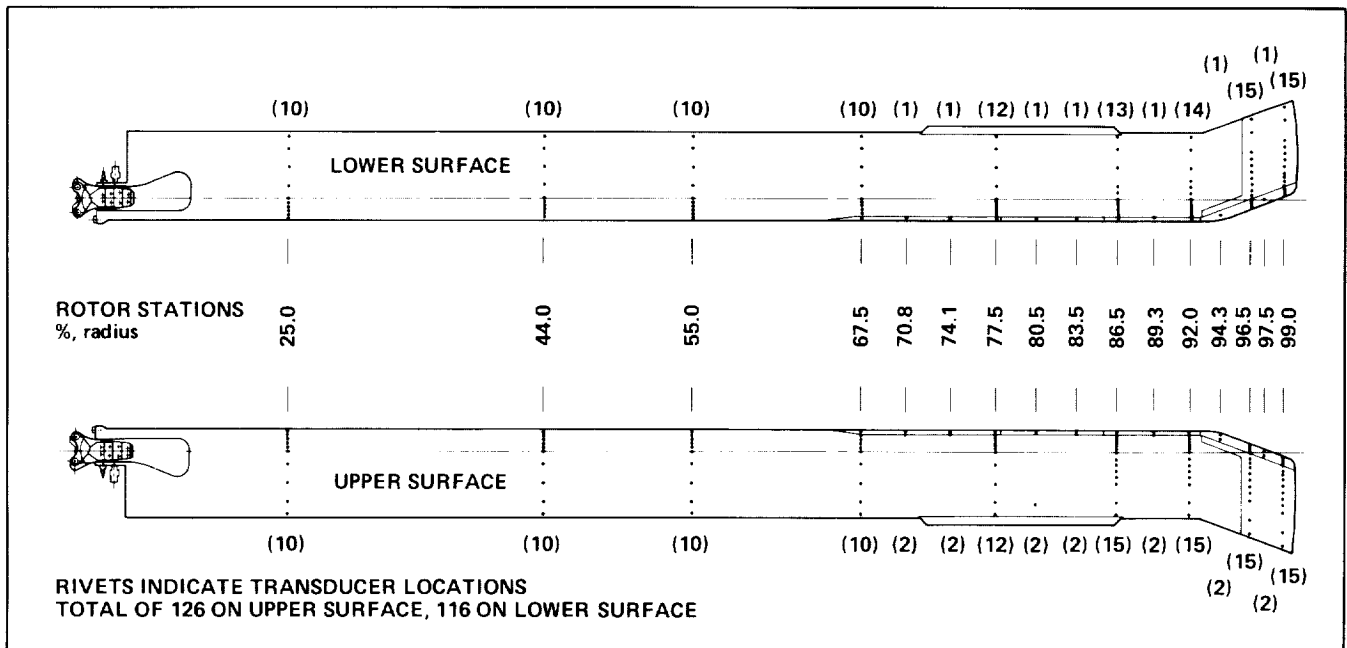
UH-60A Blade Design and Fabrication

Two specially instrumented UH-60A helicopter rotor blades have been designed and fabricated, to NASA specifications, with the objective of acquiring rotor airloads flight data. These data will be obtained while exploring the high-speed flight regime, testing the aerodynamic effects of maneuvers, investigating the effects of transition, and measuring the aircraft acoustic signature. The data will become part of a nationally available comprehensive rotor airloads data base to be used for the advancement of analytical methods.

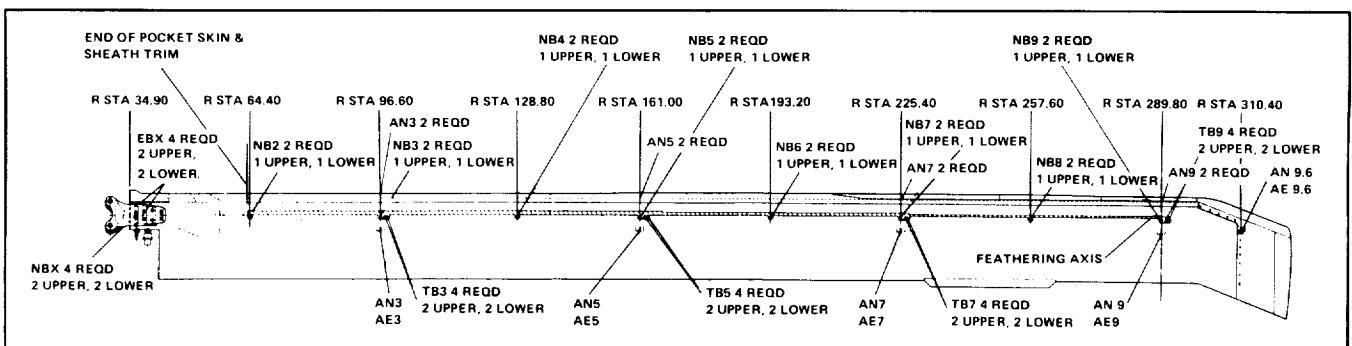
One rotor blade (see first figure) contains 242 miniature pressure transducers located in

chordwise arrays at nine radial stations. Temperature measurements are simultaneously recorded at 50 selected pressure-transducer locations. The other instrumented rotor blade contains 68 strain gages measuring normal and edgewise bending, and 20 accelerometers measuring normal and edgewise accelerations along the length of the rotor blade, as shown in the last figure. Both special rotor blades were fabricated, statically and dynamically balanced (whirl-tested), and calibrated at the contractor's facility before delivery to Ames Research Center in November 1988. The flight research program is scheduled to start in mid-1989.

(J. Brilla and E. Seto, Ext. 3152)



Pressure-instrumented blade layout for UH-60 rotor research program



Strain gage and accelerometer instrumented blade for UH-60 program

Tilt-Rotor GTRS Status/ Enhancement

The Generic Tilt-Rotor Simulations (GTRS) math model and computer program development was initiated in 1982, to provide the government with a tool for analyzing potential tilt-rotor aircraft and systems. The basic program utilized the models developed by Bell Helicopter Textron, Inc. (BHTI), and was modified by Systems Technology, Inc., to permit its use as a generic model. The modification consisted of reformatting the BHTI model and program structure to permit complete control of the configuration through input data changes. The model was then validated by correlating the computer program output with XV-15 flight-test data. Correlation deficiencies were eliminated by further refinements in the model. The GTRS program was released in January 1985 for use by government agencies and contractors.

Additional changes in the GTRS contracted for in 1985 enhanced its capability as a design and analysis tool. These changes provide interactive capability with the Tilt-Rotor Engineering Database System (TRENDS) for direct comparison of static and dynamic performance and response characteristics between GTRS outputs and flight-test results. The GTRS (Revision A) was to be released in December 1988, and is available to government agencies and contractors. User assistance in GTRS installation and training will be provided.

(G. Churchill, Ext. 6311)

UH-60 Modern Technology Rotor Phase One Workshop

Industry, government, and academia were invited to attend a week-long workshop in June 1988 to be introduced to the UH-60 helicopter Phase One flight-test data base. The specific objectives were to present what was done and how it was done; to introduce the associated nomenclature, test matrix, and sensors; to explain and demonstrate how to gain interactive access to the computer data base, and how to use the associated computer analysis and data-management programs; to provide the workshop participants with hands-on experience with the data base; and to compare rotor-control-load test

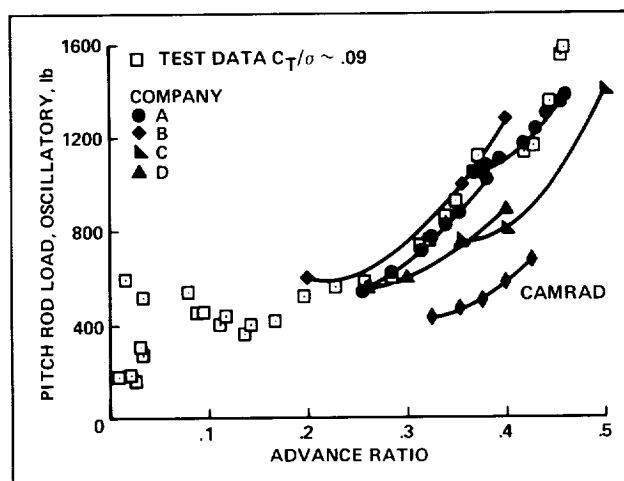
results with predictions provided by each of the industry participants, and by NASA.

The Phase One data base was acquired during a joint NASA-Army flight test conducted from February through June 1987. The testing included level flight, descents, and maneuvers from hover to 200 knots and up to 2 g's. The measurements included blades and rotor-control loads, fuselage vibrations, and rotor acoustics. Upon completion of the flight testing, an intensive effort was made by the test team to eliminate all erroneous and misleading data from the data base, which currently resides on government computers at Ames Research Center and is remotely accessible upon request.

Each of the industry participants was contacted to predict rotor control loads at high speed. As a part of the workshop, the contractors presented their results and discussed the techniques used to obtain them. NASA presented rotor-control-load predictions obtained from the comprehensive rotorcraft analysis program, CAMRAD. The figure presents the rotor-control-load predictions and test data as a function of rotor advance ratio. The results show that each participant predicted the load rise with airspeed reasonably well, but that improvements can still be realized.

The workshop served its purpose well by introducing the user community to the first of several newly available and easily accessible rotorcraft data bases. The prediction resulting from the contracts proved to be informative and generated interest among the user community.

(J. Cross and J. Brilla, Ext. 6571)



Control load predictions compared to flight-test results

Supersonic Short Takeoff and Vertical Landing Fighter Design Studies

Short takeoff and vertical landing (STOVL) capability will enhance the operability of future fighter aircraft. Five contracted studies to design STOVL fighter aircraft with different propulsion concepts have been completed. The results of four of those studies, the ejector-augmentor concept, the remote-augmented-lift-system concept, the vectored-thrust concept, and the tandem-fan concept, which were being conducted under the U.S./U.K. Advanced STOVL program, have been used to evaluate the strengths and risks associated with each concept. The results of the fifth study will be factored in outside the joint program.

The results of the contracted studies were evaluated by a team of government engineers, including members of the Air Force, Navy, and NASA. The concepts were evaluated for their levels of technology, and adjustments were made to normalize them. The conceptual designs were then resized to perform the design mission. The results of the normalization effort were reported to the Joint Assessment and Ranking Team who compared the results to the results of similar studies which were conducted in the United Kingdom.

Studies are continuing in-house to update the conceptual designs to improve the understanding of the various concepts, and to reduce the risks of proceeding with a flight program. These studies will follow the efforts of various contractors who are performing (1) follow-on studies to evaluate the use of a current technology engine in a demonstrator/research aircraft, and (2) design studies to evaluate the Navy's Advanced Capabilities Aircraft Desired Operational Capability.

(P. Gelhausen, Ext. 5701)

Propulsion System for a Supersonic Short Takeoff and Vertical Landing Flight-Research Aircraft

Pratt and Whitney of the United Technologies Corp. is under contract to Ames Research Center to evaluate a derivative of the PW5000 engine. This engine is a candidate for use in the propulsion system of a potential supersonic short takeoff and vertical landing (STOVL) flight-research/proof-of-concept demonstrator aircraft. This ground-based research program is a cooperative effort with Defense Advanced Research Projects Agency (DARPA) and the Air Force. Four powered-lift propulsion systems are under consideration: vectored thrust, ejector augmentor, remote augmented lift, and hybrid tandem fan. The contracted effort includes three authorized tasks: (1) concept definition and trade-off studies, (2) reaction-control-system (RCS) bleed tests, and (3) concept airframe integration.

Tasks 1 and 3 are nearing completion. Task 2 is completed. Matrices of steady-state and transient RCS bleed airflows were investigated. These ranged from maximum individual bleeds of 13.3% of overall compressor airflow from the compressor interstage and 10.1% from the diffuser exit (cabin bleed), to combined interstage and diffuser exit bleeds of 8.6% and 10.1%, respectively. No adverse effects on gas-generator performance resulted for these bleed conditions, which should meet RCS bleed airflow requirements for STOVL. The first flight of a potential research aircraft demonstrating STOVL operation, supersonic capability, and supermaneuverability could be in the mid-1990s. Detailed engine development plans are being formulated by Pratt and Whitney to meet this potential first-flight timeframe.

(D. Giulianetti and P. Nelms, Ext. 6338/6093)

UH-60 DNW Risk Reduction Test

A test of the Army rotary-wing test stand mounted on the Deutsch-Niederlandischer Windkanal (DNW) sting was conducted to investigate undesirable stand/sting vibrations during high-speed (~330 feet per second) tunnel operation in the 8- by 6-meter test section.

With the rotary-wing test stand mounted on the DNW sting, a brake-plate test was performed to investigate the damping and frequency response of the test stand in the static wind tunnel environment. The brake-plate test was performed in the X-Z (longitudinal-vertical) plane. The test stand was then instrumented with accelerometer and surface pressure taps before a tunnel wind-speed/sting-position survey to investigate the test stand response. The tunnel was operated with test section slats both opened and closed. Although the test stand did vibrate somewhat, the magnitude was not nearly as great as that experienced during the high-speed testing of the Boeing 360 model rotor, and hence it was no cause for concern.

Main rotor hub impedance tests were also performed on this test stand configuration.

(D. Jordan, Ext. 6159)

UH-60 Dynamic Modeling and Shake Test

As an important element of the UH-60 Modern Technology Rotor Program, an investigation to advance the fundamental knowledge of the rotary-wing aeromechanics that cause fuselage vibration is ongoing. Data from various sources have been collected and prepared for study. The data collected include the NASTRAN modeling, the shake test modal analysis completed under the DAMVIBS program, and the hub and fuselage vibration measurements from the UH-60 Phase I flight test. Both the NASTRAN modeling and the shake test were modified by the addition of weight to more accurately represent the flight-test vehicle. Comparisons have been made between flight test and analysis as the first step of the validation process for the integration of airframe and rotor models.

Finally, two contracts have been released to use flight-test data to estimate rotor/fuselage interaction. It is believed that these contracts will identify ways to reduce fuselage vibration. Data from additional accelerometers, blade pressures, and strain measurements will be available from the UH-60 Phase II flight-test program to improve the models.

(R. Kufeld, Ext. 4682)

Tilt-Rotor Advanced Technology Blades—Flight Ground Investigations

All composite rotor blades for the XV-15 Tilt-Rotor Research Aircraft have been fabricated by Boeing/Vertol under contract to Ames Research Center. The Advanced Technology (ATB) program consisted of

1. the design of blades which will allow greater low-speed maneuverability and improved high-gross-weight vertical takeoff and landing (VTOL) capability without penalizing high-speed performance, while simultaneously improving structural life;
2. the development of tooling and fabrication methodology suitable for highly twisted blade configurations;
3. the fabrication of a ship set of blades and spares;
4. a series of ground tests.

The remaining technical objective of this investigation is the evaluation of the ATB throughout the flight envelope of the XV-15 research aircraft.

Flight tests of the XV-15 (with the Advanced Technology Blades) during FY 1988 have revealed that high-control loads are encountered while operating in the helicopter mode at low forward speeds. Analytical predictions made before the flight investigations did not correctly estimate the magnitudes of the oscillatory load harmonics. An extensive evaluation of the data has identified several possible sources of the problem, including the contributions of blade dynamics and the effects of the rotor control system and control actuator dynamics. The on-going study of this load problem may lead to further refinement of the analytical tools in the areas of rotor airloads/wake predictions and control system modeling for tilt-rotor aircraft. The development of a

satisfactory resolution will demonstrate the validity of the analytical methods available for rotor loads and dynamics analyses.

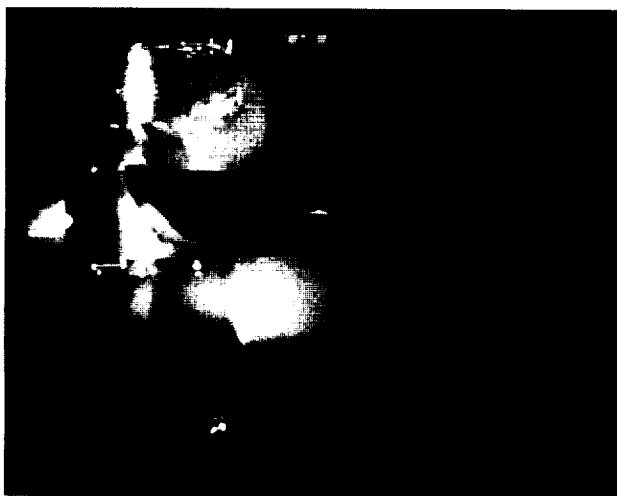
The expansion of the full flight envelope and the completion of the flight investigation with the Advanced Technology Blades on the XV-15 will be performed after the load issue is resolved.

(M. Maisel, Ext. 6372)

Blade Root-End Flow Field for a Highly Twisted Low-Disc-Loading Rotor

Several rotor performance codes underpredict measured static rotor performance at thrust coefficients above the point of maximum figure of merit. Similarly, predictions of windmill performance typically underestimate the power developed at high blade angles. Prior experimental blade pressure data by German and Russian researchers suggest that the inboard sections of the blades are capable of producing greater lift levels than would be expected based on two-dimensional airfoil data. The question of chordwise flow at the inboard blade stations was, therefore, addressed in a model-scale rotor test conducted in the Army Aeroflightdynamics Directorate Anechoic/Hover Test Chamber.

A three-bladed, 4-foot-diameter rotor with about 37° of blade twist (representing a typical tilt-rotor



Smoke flow visualization during hover test

blade) was used for the performance and inflow investigation. Smoke and tuft flow-visualization techniques failed to reveal firm evidence of a significant chordwise flow component. Model performance documented during the test will be used in further tilt-rotor download and airframe/rotor interaction studies.

(M. Maisel, Ext. 6311)

Modern Technology Helicopter Rotor—BV-360 Flight Test

The critical technologies required for the next-generation helicopter have been embodied in the Boeing Helicopter Company Model BV-360. This aircraft incorporates

1. an all-composite primary structure that offers reduced weight, reduced manufacturing costs, and reduced maintenance costs,
 2. a mixed-modulus, composite rotor hub (using graphite and fiber glass) that employs a fail-safe design, and elastomeric bearings that reduce maintenance and weight savings,
 3. tandem advanced high-speed rotor designs.
- While the major part of the development of this technology-demonstration helicopter is borne by Boeing/Vertol and its suppliers, Ames Research Center is participating in the investigation of the modern-technology rotor through a contract to fabricate, whirl test, and flight-test the forward Model 360 rotor.

The all-composite rotor reflects current state-of-the-art aerodynamic features. The blade uses relatively thin, new transonic airfoils that provide a 23% increase in cruise efficiency and a 4% increase in hover efficiency over previous aerodynamic configurations. The improved cruise-mode efficiency, coupled with reduced airframe drag, was predicted to permit cruise speeds in excess of 200 knots.

During FY 1988, the highlight of the Model 360 test program was the expansion of the flight envelope to 200 knots in level flight. Much of the approximately 80 flight hours involved investigations of specific technical issues that arose during the flight envelope expansion and the demonstration of satisfactory resolutions of these problems. The correction of vibration, loads, and performance prob-

ORIGINAL PAGE
BLACK AND WHITE PHOTOGRAPH

lems will validate improvements to the state-of-the-art methodology used. Flight-testing of further refinements and of steady and dynamic loads will be continued in FY 1989.

The contracted effort with the Boeing Helicopter Company was modified in 1987 to include the design and fabrication of a pressure-instrumented blade for the forward Model 360 rotor. The planned test program will augment other helicopter airloads investigations by providing data in a range of high flight speeds not available with current helicopters. The data will be added to the national rotorcraft airloads data base and will be used to validate aeroacoustics, dynamics, and aerodynamics models used in the design and prediction of advanced rotorcraft flight characteristics. During FY 1988 the Critical Design Review of the pressure-instrumented blade was accomplished, and NASA authorized Boeing to proceed with the fabrication of the blade. The test article will be completed in FY 1989.

The flight data will also be used to assess the effect of scale by comparing the results to information previously obtained from model-scale tests in the German/Dutch (DNW) wind tunnel. Full-scale rotor tests in the large-scale wind tunnel facility at Ames are being considered.

(M. Maisel and M. Watts, Ext. 6372)

Tilt-Rotor Advanced Technology Blades—Airloads Investigation

The time-varying distribution of airloads on the surface of the Advanced Technology Blade (ATB) will be measured throughout the flight envelope of the XV-15 Tilt-Rotor Research Aircraft. This unprecedented study will provide fundamental tilt-rotor performance, load, vibration, and acoustics data essential for improving predictive methodology in these disciplines. The information will be incorporated into a national rotor data base for the advancement of analytical methods. Model-scale wind tunnel tests will complement the flight data and will provide information on scale and wind tunnel effects.

To perform the flight investigation, one of the spare ATBs is being modified by the Boeing Helicopter Company to incorporate 200 imbedded miniature pressure transducers. During FY 1988, design

of the blade modification approached completion. The Critical Design Review and installation of the transducers is planned for FY 1989.

Work on a high-sample-rate Pulse Code Modulation (PCM) data system capable of detecting impulsive loads has begun at Ames Research Center. The PCM system will be contained within the rotating spinner and will use existing slip rings to transmit the data to the on-board recorder.

Small-scale ATB-configuration rotor blades incorporating miniature pressure transducers will be fabricated by Bell Helicopter Textron, Inc. Ames has contracted with Bell to prepare tooling for the model blades. Airloads testing will be performed in the Deutsch-Niederlandischer Windkanal (DNW) (Netherlands) facility on a model/drive system provided by the Army Aeroflightdynamics Directorate (Ames) and DNW.

(M. Maisel and M. Watts, Ext. 6372)

U.S./U.K. Advanced Short Takeoff and Vertical Landing Aircraft Technology Program—Configuration Studies

The governments of the United States and the United Kingdom are cooperating to further the technology for a supersonic, advanced, short takeoff and vertical landing (ASTOVL) fighter aircraft. This cooperative effort (the U.S./U.K. ASTOVL Aircraft Technology program) involves the U.S. Department of Defense, NASA, the U.K. Ministry of Defence (MOD), and the U.K. Royal Aircraft Establishment (RAE). Government teams have been established to focus on the definition of a joint U.S./U.K. technology program for ASTOVL concepts. The intent of this program is to mature those concepts sufficiently to judge their relative merits, and to support future program decisions, including the possibility of a flight-demonstrator/research aircraft.

This ground-based technology program is covered by a Memorandum of Understanding (signed by both governments in January 1986), which covers 5 years, with 1986 as the first year. The program focuses on a single-engine, single-seat, supersonic STOVL fighter/attack aircraft with excellent transonic

maneuverability and an all-weather capability. Four promising propulsion concepts, which have been identified as potentially feasible for this type of aircraft, are featured in this program: (1) vectored thrust, (2) ejector augmentor, (3) remote augmented-lift system, and (4) tandem fan.

There are three elements in the U.S./U.K. ASTOVL program: concept-evaluation studies, common technology programs, and concept-specific technology programs.

The concept-evaluation studies were contracted efforts to provide:

1. four aircraft configuration definitions, each featuring one of the four propulsion concepts,
2. aircraft mission performance, including sensitivities,
3. identification of critical technologies, including sensitivities,
4. a definition of ground-based technology-development plans, including an indicative cost estimate for conducting these plans.

These concept studies were conducted in the United States and the United Kingdom with no collaboration between contractors so as to provide two independent assessments of the relative merits of the concepts. Thus, collaboration in this element will be solely between government officials.

Under direction of the U.K. government (MOD and RAE), Rolls-Royce, Ltd., provided the engine data and British Aerospace Establishment (BAE) conducted the airframe studies for all four propulsion concepts. In the United States, Lewis Research Center had three engine companies under contract to generate engine data and to support the airframe companies in the integration process. They were Allison, General Electric, and Pratt and Whitney. Ames Research Center had the responsibility for the airframe contracts, which were initiated in January 1987. The four airframe contractors and their selected propulsion-lift concepts were General Dynamics (ejector augmentor), Grumman (remote augmented-lift system), Lockheed (tandem fan), and McDonnell Aircraft (vectored thrust). These studies were completed in early FY 1988.

Following completion of the concept studies, the U.S. Government conducted a "normalization" of the four U.S. designs to bring them to the same technology level. This normalization process was not necessary for the U.K. designs because only one airframe (BAE) and one engine (Rolls-Royce) company

conducted all four studies. The U.S. normalization activity was completed in June 1988. After completion of the normalization process, a joint assessment process was begun to assess and rank the concepts for the purpose of selecting the most promising for specific technology programs which could lead to a technology-demonstrator aircraft. The joint assessment process is to be completed in early FY 1989, and concept-specific technology programs will begin in late FY 1989.

(P. Nelms and C. White, Ext. 6093/5653)

Advanced Tactical Transport Technology

There is renewed Air Force interest in developing a military advanced tactical transport (ATT) aircraft to be introduced in the mid- to late 1990s. Evolving Air Force mission requirements may dictate that this airplane possess vertical and short takeoff and landing (V/STOL) field performance capability or, at the very least, short takeoff and landing (STOL) characteristics superior to those demonstrated during the YC-14 and YC-15 prototype programs. Combining these stringent field-performance requirements with superior cruise efficiency will require the meticulous blending of vehicle aerodynamics, propulsion integration, and stability and control technologies. A well-developed analytical capability will be used to the fullest extent possible during the configuration-development cycle. However, experimental data must be acquired in the hover and transition flight regimes to quantify the performance level of these advanced-technology transport concepts.

Under a Memorandum of Understanding between the Air Force Wright Aeronautical Laboratory (AFWAL) and Ames Research Center, a cooperative program is under way to define and assess several V/STOL military tactical-transport concepts which meet multiple mission requirements. The starting point for the program is the AFWAL lift plus lift-cruise transport design. With Air Force financial support, Ames personnel designed and fabricated a 7%-scale semispan model which was tested at Langley Research Center by Ames personnel. Wind tunnel data for the hover and transition flight regimes were acquired and analyzed. Design

guidance has been provided for advanced airfoils, and the wind tunnel data are being used to verify the computed characteristics.

Additionally, Ames and AFWAL will develop an alternate V/STOL transport configuration which uses a propulsive lift system other than lift plus lift-cruise. Assessment is under way of the potential of an upper-surface-blowing (USB) configuration for superior STOL and possible vertical takeoff and landing (VTOL). Ground measurements have been made of the USB flap flow field on the Ames Quiet Short-Haul Research Aircraft (QSRA). These data are being used to design and fabricate a modified flap system for a series of ground tests to determine augmented USB flow-turning efficiencies for VTOL operations.

Ames is pursuing for AFWAL the manufacture and testing of a nose-gear jump strut which would be installed and tested on the QSRA. The jump strut has potential application to future Air Force aircraft, such as the ATT, to provide for reduced takeoff distance.

(D. Riddle and C. White, Ext. 6085/5653)

Parameter Identification Workshop—Identification of Rotor Inflow in Forward Flight

By using a coupled model of rotor flapping dynamics and rotor dynamic inflow, we are attempting to identify parameters of the dynamic inflow model from helicopter flight measurements of blade flapping. This activity under The Technical Cooperation Program (TTCP) led to a joint workshop organized by Ames Research Center and the Royal Aircraft Establishment (RAE) at Bedford, England, hosted by the RAE in March 1988. With flight data on the Puma helicopter provided by RAE, researchers formulated coupled inflow flapping models and compared results on identified rotor and inflow parameters at the workshop. Some parameter estimates were comparable; however, more effort appears to be needed in deriving a reliable model structure before further attempts are made to identify coefficients in the model.

(P. Talbot, Ext. 5108)

Acoustics Laboratory

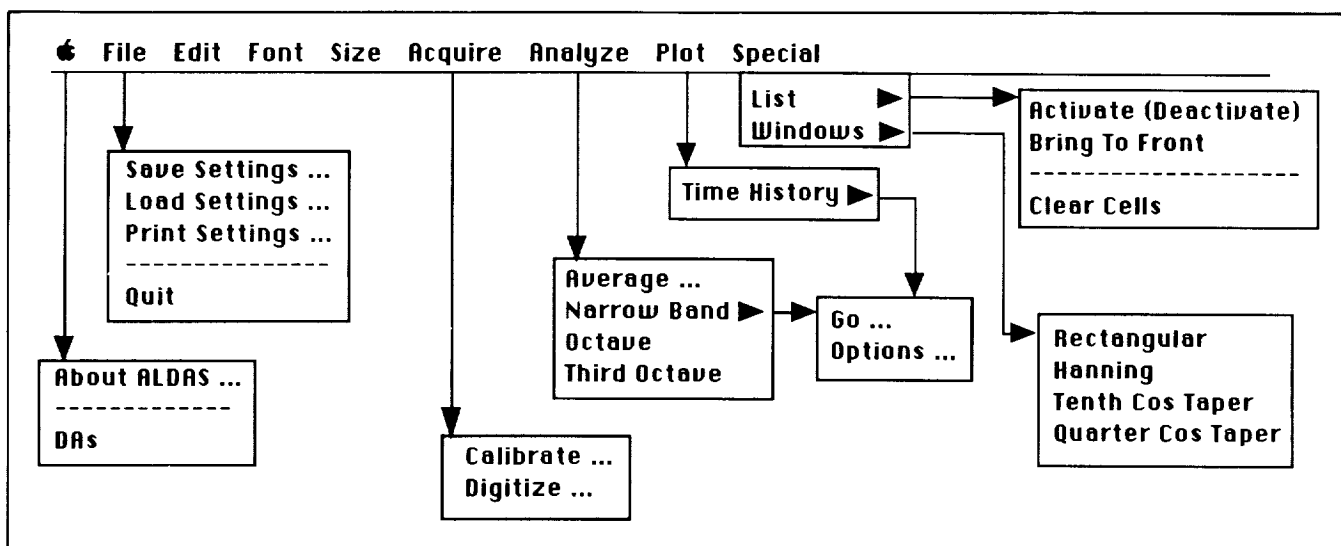
During FY 1988 a major effort was undertaken to upgrade the capabilities of the Rotorcraft Technology Branch acoustics laboratory. These upgrades include acquiring digitizing capabilities and new data-reduction capabilities which will greatly improve the speed and accuracy of analyzing the acoustics data obtained for both flyover and in-flight testing.

The new data-acquisition and analysis system is centered around a Macintosh II personal computer with internal analog/digital (A/D) cards. An interface program which controls these cards and processes the data is being developed in-house. This new system will be easy to use, transportable, and expandable to provide the required acoustics data-analysis capabilities in support of NASA rotorcraft flight-investigation programs.

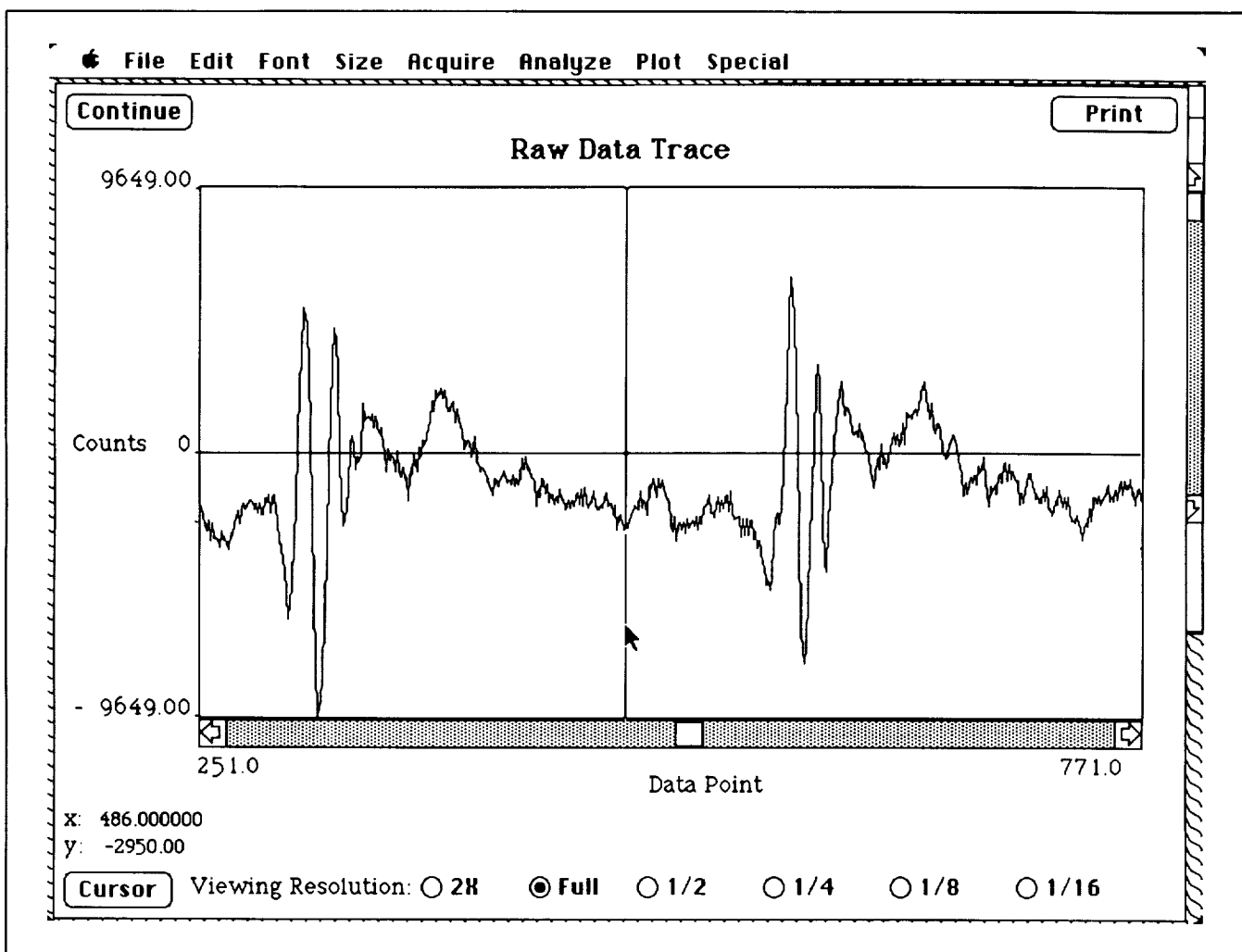
The Acoustics Laboratory Data Acquisition/Analysis Program (ALDAS) is being written for the Macintosh II personal computer to conform to the Apple Macintosh User Interface Guidelines, and is thus easy to learn and use. The first figure is a composite of the menu options available, and the last figure shows a screen image of the plot option. As seen from these figures, ALDAS makes heavy use of menus and on-screen controls. Features of ALDAS include automated channel calibration; any combination of four input channels for A/D conversion; narrow band, octave, and third-octave analysis; cursor for data values; variable viewing resolution; user-choosable display units; and several windows for fast Fourier transform analysis. ALDAS also has the ability to average data on a once-per-revolution pulse or on user-selectable data points.

The ALDAS program, along with the advances in A/D cards for personal computers, will greatly enhance the quick and accurate analysis of acoustics data obtained from both flyover and in-flight testing.

(M. Watts, Ext. 6574)



Menu options for ALDAS program



Sample viewing screen from ALDAS program

XV-15-702 Steel Blade Fatigue

Two stainless steel rotor blades on the XV-15-702 Tilt-Rotor Research Aircraft were found to have developed skin fatigue cracks. These chordwise cracks were approximately 9 inches long, starting just aft of the spar and extending to the trailing edge. They were discovered during routine inspection by Bell Helicopter Textron, Inc. (BHTI), personnel. Subsequent investigations by workers from the Ames Research Center Rotorcraft Flight Investigations Branch and the Test Engineering and Analysis Branch revealed that improper or inadequate treatment during manufacturing of the blade skin material left the material between metallic grains more susceptible to corrosion than the parent material. This condition, called intergranular corrosion, led to the initiation of cracks, which, when subjected to stresses induced by flight loads, propagated through the steel skin. As the blade spar was not involved, the failure was benign and did not cause any problems in flight.

The steel rotor blades installed on the XV-15-703 aircraft at Ames had been subjected to the same manufacturing process and therefore were suspect. Inspection showed that the -703 blades were free of skin cracks. These blades had been removed from the XV-15-703 aircraft for installation of the Advanced Technology Blades and were available for the -702 aircraft.

A safe operating procedure for flying with the steel blades was developed to allow BHTI to continue flight operations with the XV-15-702. BHTI developed a load spectrum that represented their current flight-research program. This information was used with fracture mechanics methods to calculate the time required for a hypothetical crack just below the limit of detectability to grow to critical size based on worst-case blade loads. Once a crack has reached critical size, it will grow without limits. This interval represents a detection "window," within which blade cracking may be detected before part failure. This interval was found to be 2 hours.

BHTI was given permission to continue their flight-research program using the steel blades from the -703 aircraft, but it was required to perform an eddy-current inspection at 2-flight-hour intervals. To

date, BHTI has flown these blades for 25 flight hours and has not found any evidence of rotor blade skin cracks.

(B. Wellman, Ext. 6311)

Networks for Image Acquisition, Processing, and Display

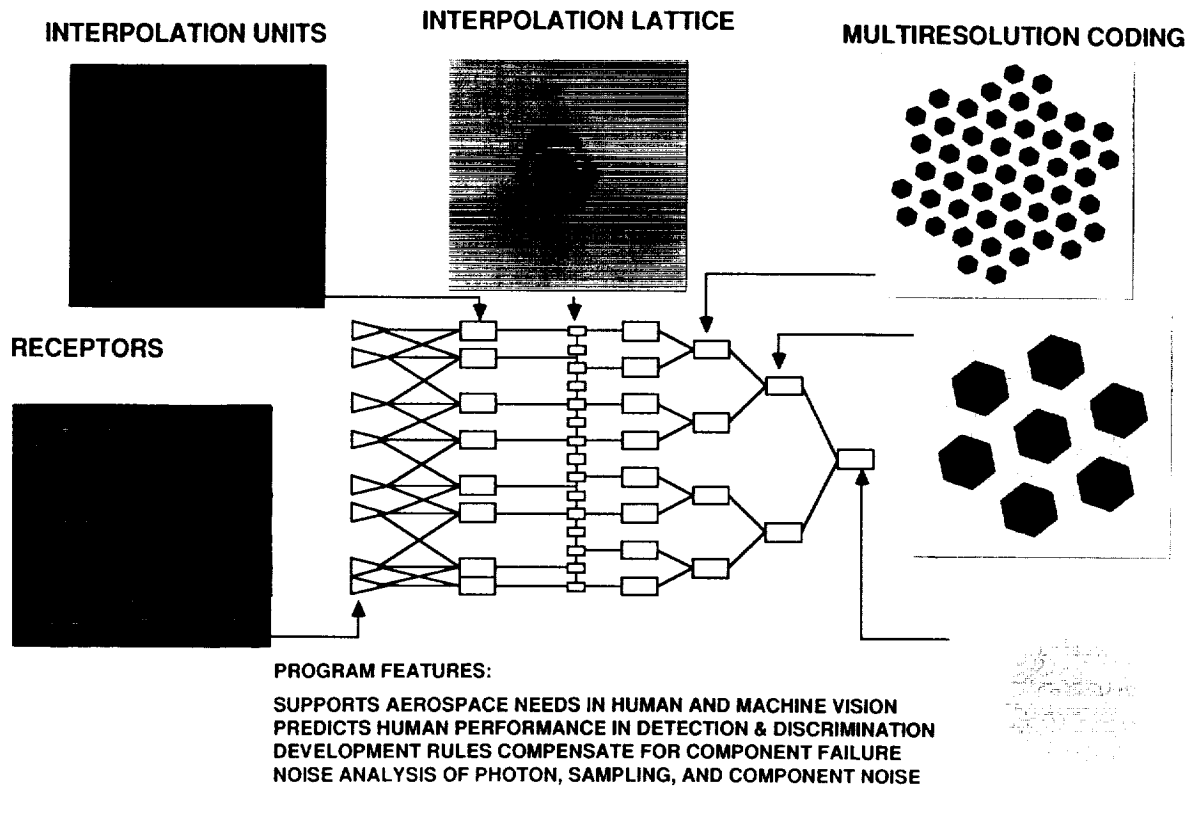
The human visual system has layers of networks which sample, process, and code images. Understanding these networks helps to understand human vision and to design autonomous vision systems based on network processing. Ames Research Center has an ongoing program to develop computational models of such networks. Part of the research is being done in collaboration with Stanford University.

The models predict human performance in detecting targets and in discriminating displayed information. In addition, the models are artificial vision systems sharing properties with biological vision that has been tuned by evolution for high performance. Properties include variable-density sampling, noise immunity, multiresolution coding, and fault tolerance. The research stresses the analysis of noise in visual networks, including sampling, photon, and processing unit noises.

Program accomplishments include the development of the following models and procedures:

1. models of sampling array growth with variable density and irregularity comparable to that of the retinal cone mosaic,
2. noise models of networks with signal-dependent and signal-independent noise,
3. models of network connection development for preserving spatial registration and interpolation,
4. multiresolution encoding models based on hexagonal arrays (hexagonal oriented orthogonal quadrature pyramid transform),
5. mathematical procedures for simplifying the analysis of larger networks.

(A. Ahumada and A. Watson, Ext. 6257/5419)



Networks for image acquisition, preprocessing, and coding

Perspective Displays and the Control of Motion

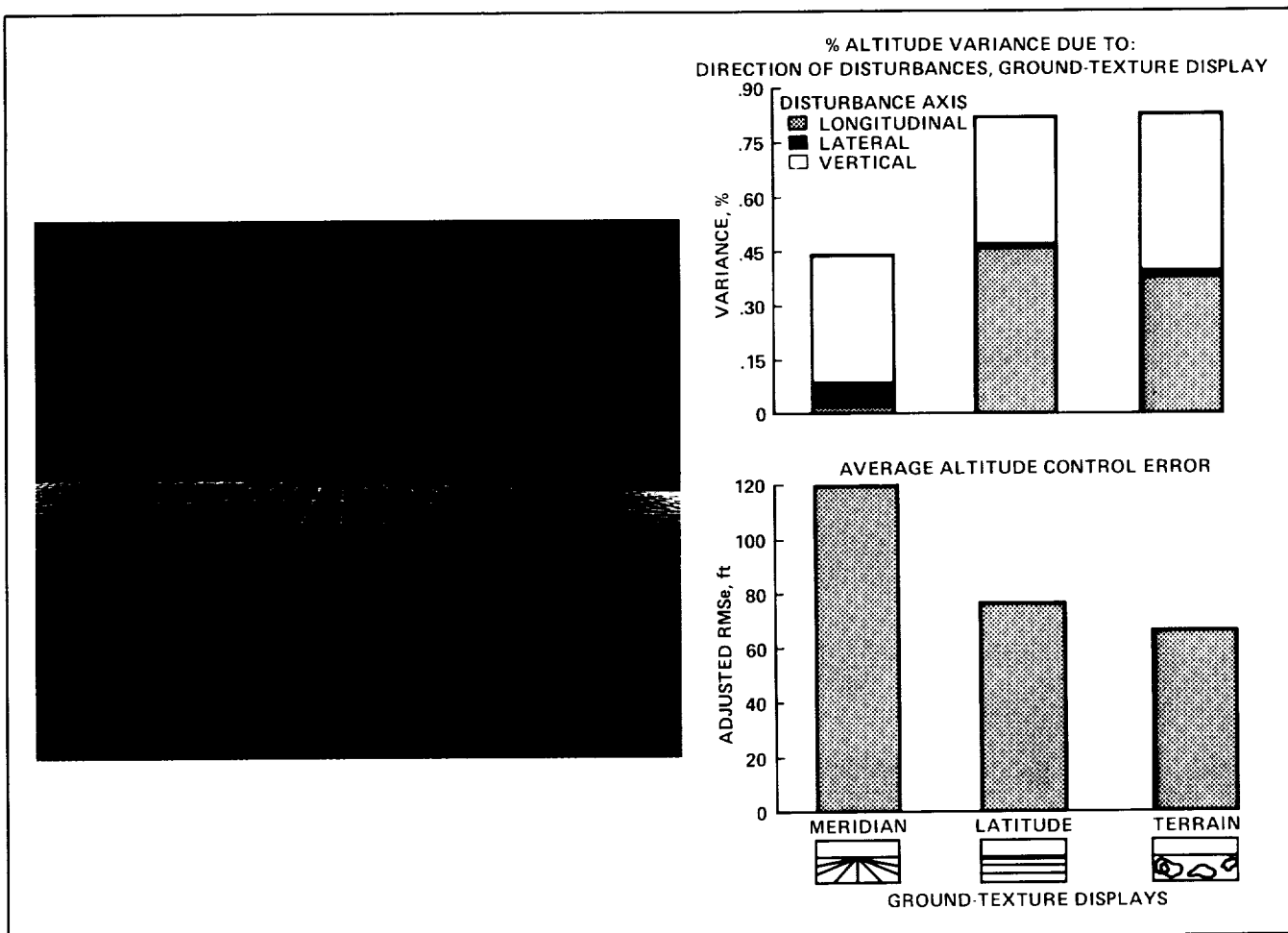
Helicopter pilots depend on visual cues to maintain vehicle orientation, altitude, speed, and heading. In low visibility, they must rely on panel- and helmet-mounted displays of sensor- and computer-generated imagery to augment the limited visual cues available. However, little is known about how pilots extract information about vehicle motion from visual cues, the relationship between optical cues and pilot control inputs, and the performance limitations imposed by different display mediums and formats. This information is urgently needed to design advanced displays capable of satisfying civil and military requirements for low-level operations at night and in low visibility.

A major research effort has been initiated to extend rotorcraft mission capabilities in degraded visual conditions. The specific objectives are to

- (1) determine which optical cues pilots use to regulate speed, heading, and altitude; (2) model the relationship between optical cues, control inputs, and performance for different maneuvers; (3) specify the minimum visual cues necessary to perform the most critical tasks projected for advanced rotorcraft; (4) quantify the range of pilots' performance capabilities with current and advanced panel- and helmet-mounted displays; and (5) develop and test improved visual display formats.

Aviation accident reports, part-task simulation results, and models of visual perception suggest that pilots may use inappropriate visual cues to maintain altitude. In a recent simulation, visual cues pilots may use to maintain altitude were evaluated using stylized perspective displays (e.g., lines parallel and/or orthogonal to the direction of flight, random dot patterns) alone or superimposed on simulated terrain.

As expected from previous studies, pilots confused movements in the meridian lines (texture par-



Perspective displays and the control of motion

allel to the direction of flight) because of lateral disturbances with altitude deviations. Unexpectedly, however, they were more prone to confuse movements in latitude lines (texture orthogonal to the direction of flight) resulting from longitudinal disturbances with altitude deviations. However, despite this, they still performed better with latitude texture than with meridian texture. The control strategy underlying these results is being investigated.

In FY 1989, flight research will be conducted to verify the simulation results in a realistic setting. Part-task simulations will be completed in which the relationship between optical cues, pilots' control inputs, and the accuracy with which pilots are able to maintain the speed and direction of vehicle motion in the presence of disturbances will be quantified. Data from these and other simulations will be used to

derive a formal computational representation of how pilots use optical information to regulate vehicle motion. The model structure will represent control activity, in the time domain, as a hierarchical set of pilot-selectable optical regulation strategies that couple optical conditions with control onsets.

Pilot performance was evaluated with helmet, panel, and out-the-window terrain displays that varied in quality, field of view (FOV), and field of regard (FOR) in simulated flight. In addition, the effectiveness of perspective grids positioned between the vehicle and the ground that were coupled to vehicle translation or translation and rotation was compared. As expected, altitude control was more accurate in hover and slalom tasks with a wider FOV (out-the-window). However, the grid display improved hovering performance significantly for the narrow FOR

(panel) display when it was coupled to vehicle translation, but not rotation.

When pilots use visually coupled devices to track targets during forward flight, vehicle control and/or target tracking may suffer. However, limited data are available about the performance envelope for three-dimensional target tracking with helmet-mounted displays. Thus, the influence of vehicle and target motion and target range, azimuth, and elevation on pilot performance will be determined in a series of part-task simulations.

(T. Bennett and W. Johnson, Ext. 5906/6187)

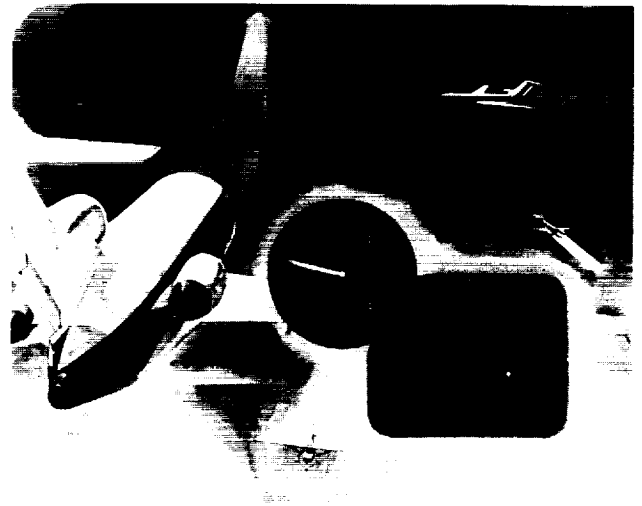
Traffic Alert Collision-Avoidance System (TCAS)

The Traffic Alert Collision-Avoidance System (TCAS) is a stand-alone system that can detect the presence of any transponder-equipped aircraft that is within a prescribed envelope around a TCAS-equipped aircraft. TCAS can provide the pilot with a visual display showing the relative position, distance, and altitude of other aircraft. TCAS evaluates the closure rates and flight geometry of other aircraft relative to itself. If TCAS calculates that a collision threat exists, it will issue visual and verbal maneuver commands to the pilot. TCAS can "see" other aircraft even though the pilot may not be able to, for example during conditions of reduced visibility or high workload.

The aviation industry looks to Ames Research Center for guidance in evaluating many human factor issues, such as

1. pilot interpretation of the information that TCAS makes available,
2. pilot acceptance of the display format chosen by the manufacturers,
3. pilot willingness to trust a system that commands him or her to make sometimes abrupt, evasive maneuvers because of unseen traffic,
4. pilot response time and success rate.

The aviation industry also looks to Ames for guidance in evaluating system configuration changes



A diagrammatic view of TCAS information as seen in a B-727 cockpit, showing command information on a vertical speed indicator and a planform display of the traffic visible in the sketch

introduced by industry and the integration of TCAS into the routine operating environment already existing in the cockpit.

Ames has conducted TCAS experiments using currently working airline crews flying typical airline flights to both terminal metropolitan destinations and outlying airports. These experiments explored:

1. TCAS with part- and full-time traffic display, and with no traffic display, just maneuver information
2. Pilot performance with and without target areas displayed on the vertical speed indicator
3. Pilot execution of the commanded maneuvers in different aircraft performance regimes

Two of the nation's major airlines now have a limited number of TCAS-equipped aircraft operating on routine daily flights within the national airspace system. Future research will explore optimizing TCAS maneuver guidance for the "glass cockpit," combining traffic with navigational information, and optimizing the voice command vocabulary to elicit proper pilot response.

(C. Billings and S. Chappell, Ext. 5718/6909)

ORIGINAL PAGE
BLACK AND WHITE PHOTOGRAPH

Integrated Rendezvous and Proximity Operations Displays

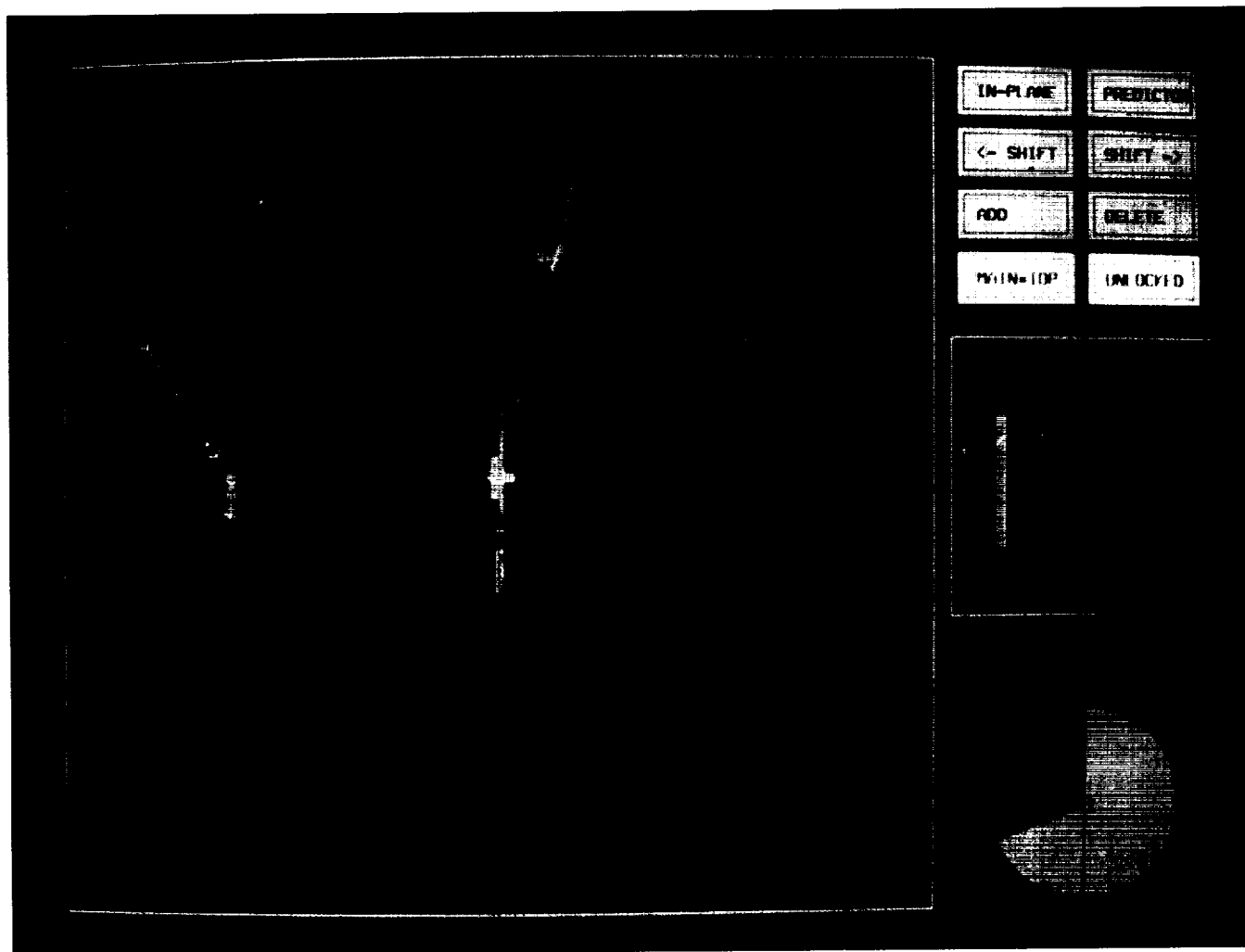
The purpose of this research program is to provide and evaluate display concepts for space station proximity operations (ProxOps) displays or other generic displays of relative orbital position. The display concepts will emphasize the use of metrical computer graphics to present spatial information to astronauts or other crewmembers.

The prototype ProxOps perspective display implemented in the Ames Research Center Proximity Operations Mockup has been supplanted by a substantially improved version currently implemented on an IRIS workstation. This display uses inverse dynamics to remove control nonlinearities associated with orbital maneuvering and provides a graphical tool for visualizing structural, plume-impingement,

and velocity constraints on orbital maneuvering. Two experiments evaluating performance of untrained users have been completed. Brief training periods are needed to learn to plan orbital maneuvers with this system.

Preliminary experimentation with the improved display has uncovered a new visual illusion associated with three-dimensional (3-D) interpretation of multi-orbital trajectories. Careful selection of the display's viewing direction may control this problem, but continued research into required geometric, symbolic, and computational enhancements is required to further optimize presentation of 3-D orbital information. This continued work will be conducted jointly by Ames Research Center, the Israel Institute of Technology (Technion), and U.C. Berkeley.

(S. Ellis, Ext. 6147)



Proximity operations planning display

ORIGINAL PAGE
COLOR PHOTOGRAPH

CRM Training Evaluation Project

Cockpit Resource Management (CRM) training is aimed primarily at improving crew coordination in the multipilot aircraft. CRM refers to a broad array of factors associated with effective team performance such as communication, interactional styles, leadership, and related characteristics. The extent of the crew coordination problem was identified in a systematic research program begun at Ames Research Center in the late 1970s, and this work has served as the catalyst for developing CRM training programs and techniques such as Line-Oriented Flight Training (LOFT). While it is a relatively new concept still in the process of maturing, CRM has achieved a remarkable degree of acceptance internationally. The U.S. Air Force (USAF) now requires crew coordination training in the transport fleet, and the Federal Aviation Administration (FAA) is expected to initiate a requirement for some form of CRM training in all air transport organizations.

Despite this high degree of acceptance, little is known about the effectiveness of CRM programs, and the long-term success of this training effort will depend upon an objective assessment of whether long-term improvement is associated with CRM training. The effectiveness question is difficult to address at present, in part because of the relative newness of the concept, but also because of the difficulty of collecting data on long-term behavior change that can be related to operationally significant performance.

Ames, in cooperation with the University of Texas, has undertaken a major longitudinal study of CRM training programs. This effort, partially funded by the FAA, involves systematic data collection in multiple organizations on key crew coordination dimensions expected to be related to performance and overall safety.

These data are collected prior to implementing CRM training, during the training process, and for a period of several years after initial exposure during the recurrent training process. Measures collected at each interval include systematic indications of attitude change and, on a random basis, crew performance in LOFT simulator sessions. In addition, access to incident data bases has been provided by all participating organizations as a means of looking at long-term trends. Five major U.S. air carriers, a

major foreign carrier, and the USAF Military Airlift Command are participating in the evaluation program.

Preliminary findings appear to indicate that awareness and positive attitude change are related to CRM training exposure, but the magnitude of change varies greatly across organizations and training programs. In addition, there is evidence that some individuals are more amenable to change than others. Thus far, it is too early to detect systematic behavior or performance differences.

It is expected that this program will provide a test of the effectiveness of CRM training techniques. FAA will use this evaluation program to make decisions about the direction of CRM training in the U.S. aviation system.

(C. Foushee, Ext. 6114)

Human Interface to the Thermal Expert System

The Human Interface to the Thermal Expert System (HITEX) is part of the Systems Autonomy Demonstration Project. In this project, a thermal expert system (TEXSYS) will monitor, advise, and diagnose faults on a thermal testbed developed by the Boeing Aerospace Company. The Ames Research Center Aerospace Human Factors Research Division is responsible for HITEX in a cooperative effort with the Information Sciences Division.

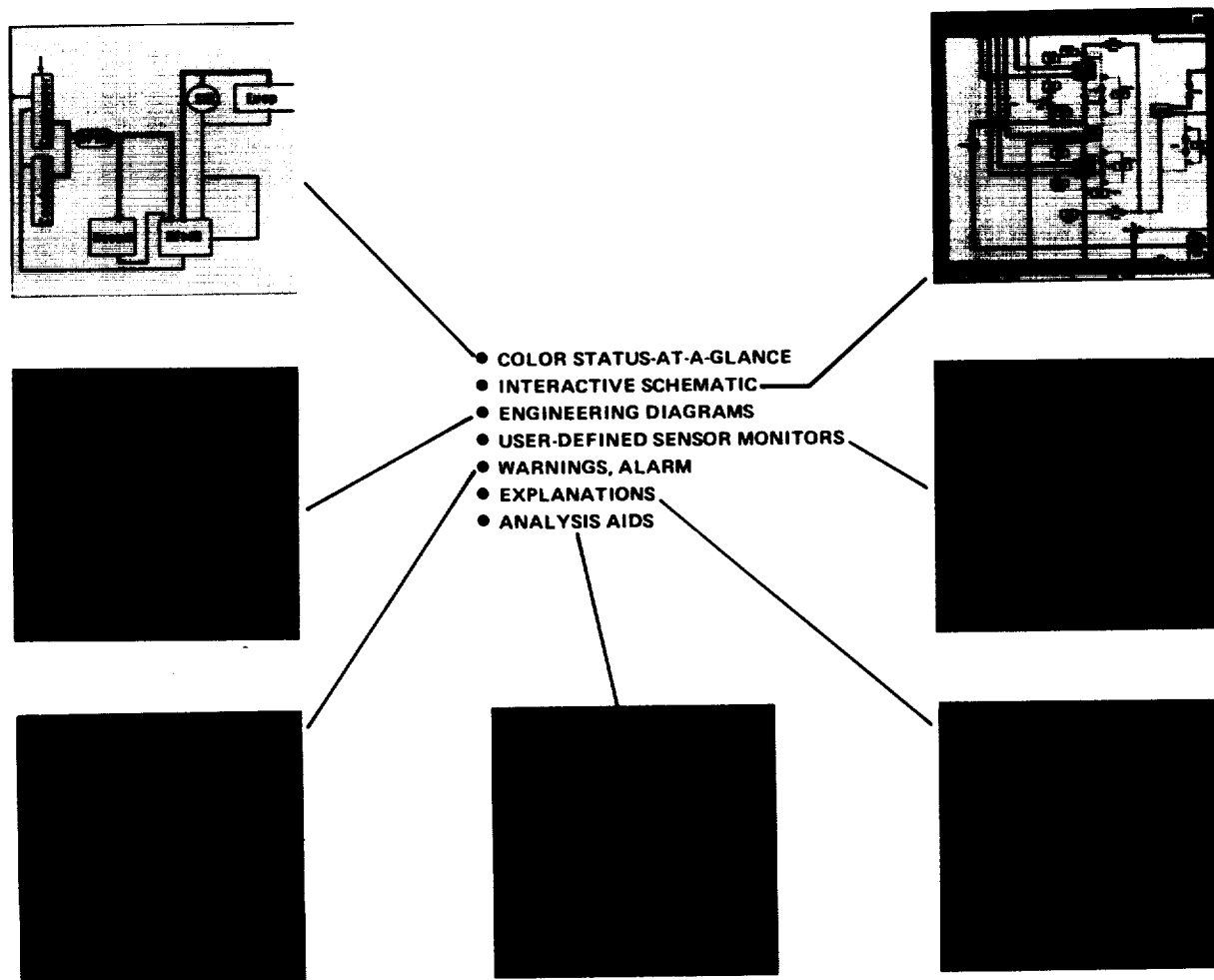
The goals of the HITEX are to provide a useful tool for thermal engineers to validate system performance, to provide flexible graphics to aid in finding and isolating information, and to accommodate users of varying skill levels. HITEX minimizes physical demands by using context-sensitive displays and customization, memory demands through immediate feedback and direct manipulation, and cognitive effort through flexible data presentation.

The operator will interact with two screens—the HITEX expert system screen and the graphical information display. The HITEX expert system screen will be implemented on a monochrome monitor and the graphical information display will be on a color monitor. The screens will be placed side by side and

will function as one large screen. A single keyboard and single mouse pointing device will be used. The user will be able to move the mouse from one screen to the other as if they were a single screen. Both screens will be driven by the one HITEX Symbolics,

which will communicate with both the Thermal Data Acquisition System and the TEXSYS.

(D. Foyle and N. Dorigi, Ext. 3053/3371)



Human Interface for the Thermal Expert System— Systems Autonomy Demonstration Project

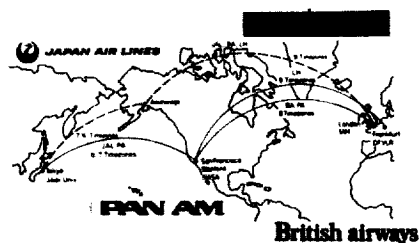
Individual Crew Factors in Flight Operations

The focus of this program is to assess the impact of fatigue and circadian rhythmicity on flight crew performance and to determine the contribution of factors associated with operational parameters, individual differences, and crew behavior. The approach is to combine limited laboratory and simulator

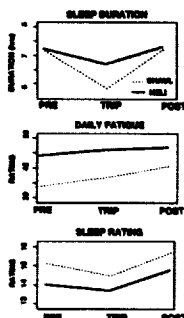
research with an extensive set of field studies documenting the physiological and behavioral responses of flight crews operating in a variety of flight environments.

This is the first major attempt to objectively study these issues in both commercial and military flight crews. Increasing pressure for smaller and more productive crews requires a better understanding of how and why pilot performance can be degraded.

ORIGINAL PAGE
COLOR PHOTOGRAPH



**HELICOPTER AND SHORT-HAUL
PILOT POPULATION COMPARISONS**



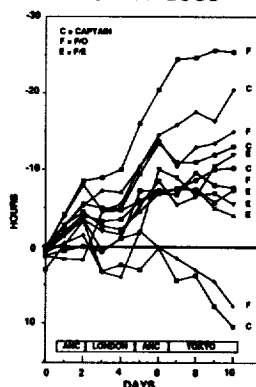
Flight crew fatigue

Another driver is the planned introduction of highly automated aircraft into the long-haul arena. By fully understanding the impact and operation of these factors, it will be possible to improve flight safety and efficiency by (1) developing guidelines for rulemaking and aircraft certification, (2) designing individual pilot coping strategies, and (3) making operational recommendations to air carriers.

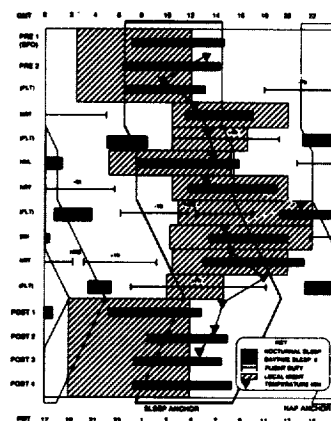
Research has concentrated on field studies using cockpit observers and continuous physiological monitoring in several types of flight operations:

1. Multisegment International Long-Haul Patterns (B-747 and USAF C-141)
2. Overnight Cargo Delivery (B-727)

**POLAR ROUTES: CUMULATIVE
SLEEP LOSS**



SINGAPORE TRIP PROFILE



FINDINGS

LONG-HAUL OPERATIONS

- INT'L COOPERATIVE POLAR ROUTE EEG STUDY – OUTBOUND DIRECTION CRUCIAL (EASTWARD WORSE)
- LARGE INDIVIDUAL DIFFERENCES IN SLEEP LOSS – DESIGN/OPS IMPLICATIONS FOR 2-PERSON COCKPITS
- SCIENTIFIC SCHEDULING GUIDELINES DEVELOPED

OVERNIGHT CARGO

- CAN PROVIDE UNIQUE INSIGHTS INTO CIRCADIAN DISRUPTION OF FLIGHT CREWS

N. SEA HELICOPTERS

- DAILY SLEEP LOSS SIMILAR TO SHORT-HAUL BUT POORER SLEEP AND GREATER FATIGUE

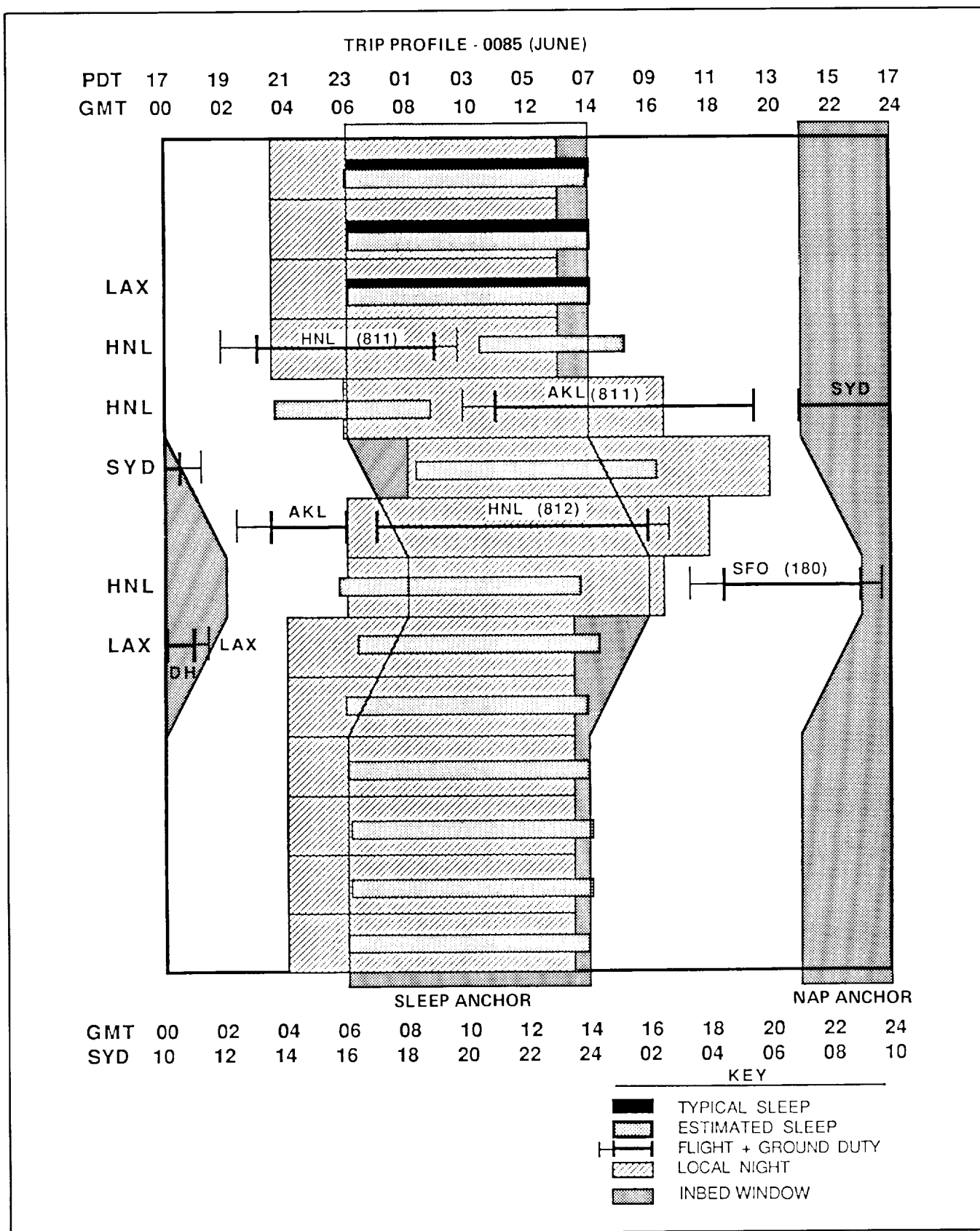
PILOT SELECTION

- IMPROVED SELECTION STRATEGIES ARE FEASIBLE

3. Extended Range North Sea Helicopter Transport (four rotorcraft types)

Additionally, a cooperative program with research organizations and airlines in West Germany, the United Kingdom, and Japan has enabled the collection of electroencephalography (EEG) sleep data during layovers on eastward and westward polar routes through Anchorage for comparison with home recordings made before and after the trips.

Data collection has been completed on long-haul crews, North Sea helicopter crews, and international polar crews. Technology transfer to the industry is occurring through interaction with the FAA aircraft



Application of circadian guidelines to aircrew scheduling

certification teams, two U.S. Pacific carriers, and the development with a U.S. manufacturer of a crew alertness support device for long-haul glass cockpits. The FAA, unions, and the management of two airlines have approved a full-mission, long-haul simula-

tion study and an in-flight EEG study of preplanned cockpit napping. Data collection will begin in February 1989.

(C. Graeber, Ext. 5792)

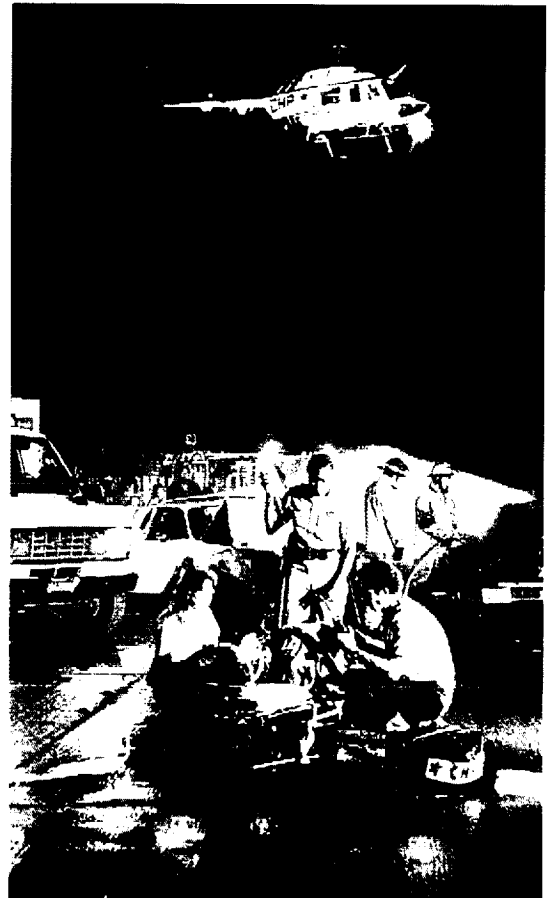
Human Factors Issues in Civil Medevac Operations

Although hospital-based Emergency Medical Service (EMS) helicopters play a critical life-saving role, they have the worst safety record of any segment of aviation. Since 1980, the EMS industry has averaged 12.3 accidents per 100,000 flight hours. In a recent survey, the National Transportation Safety Board (NTSB) cited weather-related factors as the most significant influence. These, coupled with program competition, demands by medical personnel,

crew schedules, and pilots' "can-do" attitudes, may produce an environment that precipitates errors and poor pilot judgment.

The high accident rate in civil EMS demands an immediate solution; however, imposing new regulations without the benefit of adequate research will not solve the problem. Thus, NASA researchers have initiated several activities in this area, capitalizing on their expertise in gathering and analyzing aviation incident data and knowledge about pilot error, workload, fatigue, circadian desynchronization, and other potentially relevant areas. In addition, the possibility

- SPONSORED TWO GOVERNMENT/INDUSTRY WORKSHOPS
- INITIATED ASRS/EMS SAFETY NETWORK
- COMPLETED TWO INFLIGHT EXPERIMENTS
- DEVELOPED PRE-FLIGHT RISK-ASSESSMENT PROCEDURE FOR EMS PILOTS
- INITIATED OPERATIONAL TEST OF RISK-ASSESSMENT PROCEDURE



Human factors issues in civil medevac operations

ORIGINAL PAGE
BLACK AND WHITE PHOTOGRAPH

of establishing an expanded program in cooperation with the FAA is being explored.

Two government/industry workshops were held for representatives from the private, public service, and military organizations responsible for medical evacuation where they shared common experiences, problems, and solutions. The EMS Safety Network was established within the framework of the Aviation Safety Reporting System (ASRS), with the support of the Helicopter Association International, National EMS Pilots Association, Airborne Law Enforcement Association, NTSB, and the FAA, among others. The network's goal is to develop a comprehensive data base of civil, public service, and military medevac incidents which can be analyzed to assess the effects of crew size, duty hours, procedures, missions, etc., on pilot workload, fatigue, judgment, and performance, and to compare the consequences of different approaches to medical evacuation.

Information from the EMS Safety Network, in conjunction with in-flight assessments of public service and hospital-based medevac crews will focus subsequent research efforts on the most critical areas. An in-flight evaluation of helicopter law enforcement crews was performed to assess the utility of research methods proposed for use in EMS helicopters. Subjective and physiological measures of crew workload were obtained and a detailed analysis of crew communications and activities was completed. Subjective ratings and the content of crew communications indexed crew workload. Verbal fluency for cockpit communications indexed fatigue.

An in-flight evaluation of EMS flight crews has begun and will be completed in 1989. This experiment will investigate (1) pilot workload, (2) pilot decision making, (3) cues used to maintain geographical orientation, and (4) communications.

Many EMS incidents and accidents have been attributed to poor pilot judgment; pilots accept or continue flights under deteriorating weather conditions or when other risk factors are present. To improve pilots' abilities to evaluate relevant factors and to make more appropriate decisions, a pre-flight risk assessment procedure, adapted from the U.S. Army and Coast Guard system, was developed. It will be tested in an operational setting and refined as needed. The final system will be publicly available.

(S. Hart, Ext. 6072)

Improved Flight Training Procedures

As the complexity of civil and military rotorcraft and their range of operational environments continue to increase, traditional training methods become less appropriate and training time and costs escalate. Thus, the need for more cost-effective procedures has become critical. Although it is clear that not all skills require the same level of physical fidelity for training devices, nor the same training philosophy, decisions about which methods are most appropriate for specific skills are based on tradition rather than scientific principle. The use of special-purpose computer "games" has been proposed as one method of reducing training costs; computer games are inexpensive, intrinsically motivating, and can require some of the same skills that are used in flying. However, the degree to which skills learned in this context generalize to flight training has not been determined.

The goal of this program is to identify the most efficient and effective methods of improving flight-related skills. A variety of training procedures have been evaluated to determine the situations in which they will, and will not, be successful. One approach, that of using computer games to develop more efficient learning strategies and time-sharing skills, has received particular attention. The rationale is that some of the skills normally acquired during training could be developed through exposure to a carefully constructed game that is structurally, rather than physically, similar to the task of flying.

An operational test of the concept was performed by researchers from Technion in the Israeli Air Force Flight School, funded by a NASA grant. One training method was applied to each of three groups of 20 Israeli Air Force pilot-trainees, matched on the basis of selection test scores. The experimental group received 10 hours of training on the game with specialized instruction to aid pilots in generalizing their game experience to flight school. The two control groups either received no game experience or played the game without specialized instruction. In all other respects, their flight-school experience was identical. The flying skills of all 60 trainees were assessed by Israeli Air Force flight instructors at the end of the second phase of flight training. It was found that the time-sharing skills and strategies

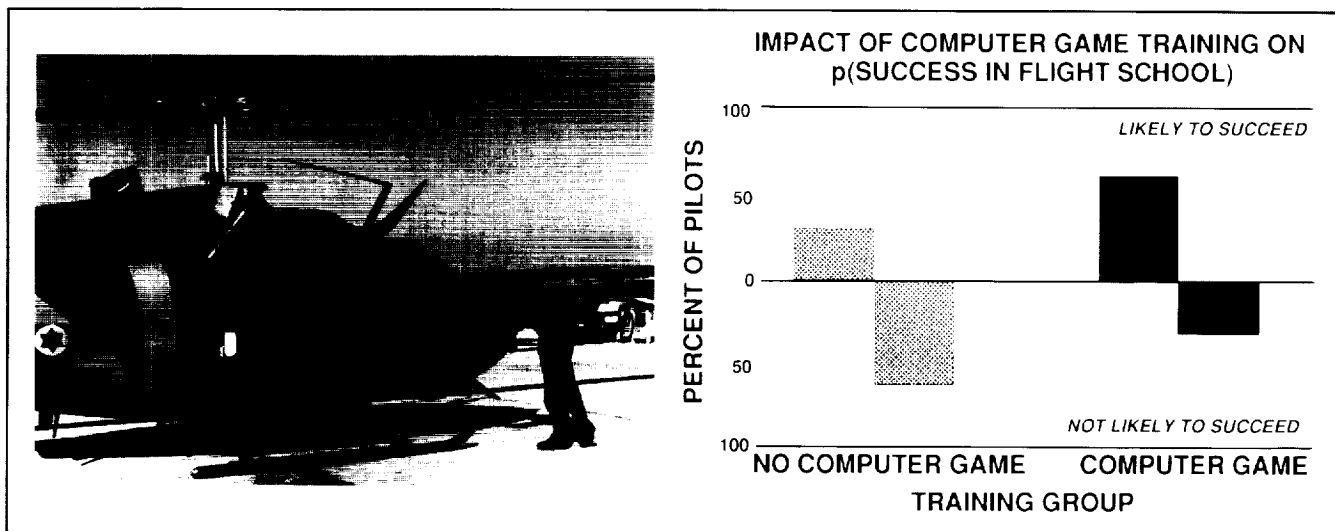
developed with the game increased by 30% the probability that trainees would complete flight school. Performance on the game appeared to predict success in flight school.

In FY 1989, final flight-school scores will be compared for the three training groups and the feasibility of using computer game trainers will be addressed in a final report. Data from the flight-school study will be used to develop an improved version of the game. A formal skill-oriented task-

analysis procedure will be developed to aid in designing computer game trainers for other applications.

Although the use of low-cost computer games as training tools has been proposed for years, this is the first operational test of the concept. Preliminary results are extremely encouraging.

(S. Hart, Ext. 6072)



Improved flight training procedures

Interpretation of Sensor Imagery

Helicopter pilots obtain visual information for low-level flight and obstacle avoidance directly from the environment, while occasionally referring to flight instruments. Helmet-mounted displays of infrared imagery with superimposed computer-generated symbology allow pilots to perform similar missions in reduced visibility, but pilots are generally unable to achieve the same level of performance that is possible with direct vision. Yet, far more attention has been devoted to developing hardware than to the difficulties pilots encounter using current and proposed visual aids.

NASA researchers analyzed helmet-mounted displays of thermal imagery from a human factors perspective. Three classes of problems were identified: (1) image quality, (2) physical configuration, and (3) difficulties in interpreting visual displays of ther-

mal contrasts. Image quality (e.g., contrast, resolution, field of view, etc.) generally depends on hardware limitations, many of which may be solved in the foreseeable future. Research is under way at Ames Research Center to identify the minimum requirements (from the perspective of the human user) to ensure adequate performance and to quantify performance limitations with alternative designs. NASA-supported research is being conducted at Technion to develop image stabilization techniques to resolve perceptual problems associated with the effects of vibration on helmet-mounted displays.

Among the problems related to physical configuration are the offset sensor location (below and in front of the pilot's eye position) and the monocular display format of current systems.

Research is under way to identify distortions in motion perception and range estimation associated with an offset eye point. While the monocular display

format leaves the unaided eye free to obtain peripheral motion cues, view cockpit instruments, and verify the identity of objects directly, differences in information available to the two eyes creates binocular rivalry. Pilots must selectively focus their attention on the information available to one eye or the other—a difficult and unfamiliar task—or simultaneously process different information from the two visual fields. Laboratory and simulation research is being performed to identify the perceptual and cognitive costs and benefits of monocular and binocular displays of static and dynamic images.

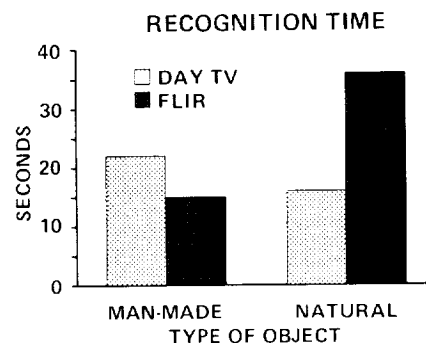
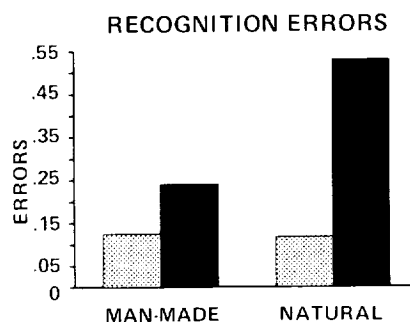
Visual representations of thermal contrasts may differ substantially from pilots' expectations about the appearance of natural or manufactured objects and the relative brightness and contrast of objects to their surroundings. This factor is unlikely to benefit from a technology solution. Preliminary research has been completed to compare object recognition and identification with television and thermal displays. Although performance was generally better with television displays, thermal images were superior for detecting manufactured objects (which tend to have a strong thermal contrast with the background).

OBJECTIVES:

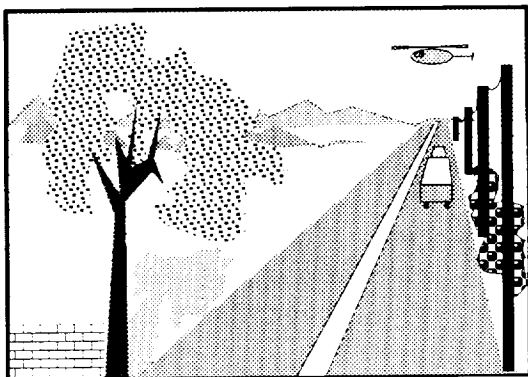
- DEFINE PILOTS' VISUAL REQUIREMENTS FOR HELMET-MOUNTED SENSOR DISPLAYS

FY88 ACCOMPLISHMENTS:

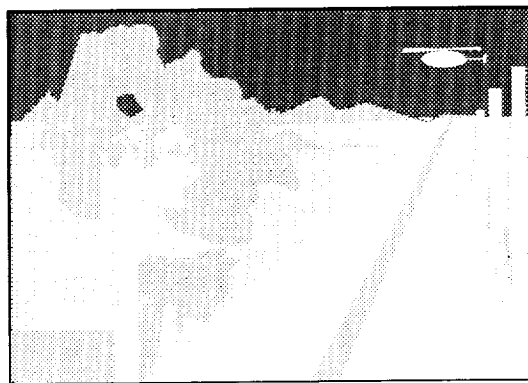
- IDENTIFIED PERCEPTUAL DIFFERENCES BETWEEN VIDEO AND INFRARED IMAGERY
- COMPARED OBJECT RECOGNITION WITH DYNAMIC VIDEO AND INFRARED DISPLAYS:
 - PERFORMANCE WORSE WITH FLIR
 - MAN-MADE OBJECTS EASIER TO IDENTIFY WITH FLIR THAN NATURAL OBJECTS
 - FLIR/VIDEO PERFORMANCE UNCORRELATED



DAY TV VIDEO IMAGE



FLIR IMAGE: "WHITE HOT"



Interpretation of sensor imagery

ORIGINAL PAGE
BLACK AND WHITE PHOTOGRAPH

Simulation research will be conducted to compare pilot performance with simulated out-the-window and infrared imagery to further quantify the relative importance of display parameters.

Training pilots to use helmet-mounted displays of thermal imagery is time-consuming and costly. Additional information is needed about the specific skills necessary to use such systems, and more efficient methods of developing these skills are required. A cost-effective microprocessor-based training system will be developed at Ames to improve pilots' performance with night-vision systems. It might present static and dynamic thermal and visual images for comparison, allow pilots to experiment with gain and polarity, demonstrate dynamic variations in thermal images, give pilots experience in focusing and shifting their visual attention, and demonstrate the effects of offset sensor location on range estimation. The system will integrate the results of the laboratory and simulation research.

Helmet-mounted infrared displays have been proposed for many advanced military rotorcraft and are being introduced into civil operations. However, little research has been performed to identify the costs and benefits of current and projected system designs from the perspective of the human users. Thus, little information is available about pilots' capabilities and limitations to aid designers in improving the systems. The goal of this program is to provide such information. The results of this comprehensive effort will contribute to improved system specifications and to design modifications that address the most significant human factors problems.

(D. Foyle, Ext. 3053)

Computational Human Engineering Research

The Army-NASA Aircrew/Aircraft Integration (A³I) project is a joint Army and NASA research effort to produce a Human Factors-Computer Aided Engineering (HF-CAE) system. The project's goal is to produce a human factors engineering tool to assist

design engineers in the conceptual phase of rotorcraft crewstation development and to anticipate crew training requirements. The system provides designers with interactive, analytic, and graphic tools which permit early integration and visualization of human engineering principles.

In the concept design phase, 70 to 80% of the life-cycle cost of an aircraft is determined. After hardware is built, mistakes are hard to correct and concepts are difficult to modify. Engineers responsible for developing crew training simulators and instructional systems currently begin work after the cockpit is built (too late to affect its design). The HF-CAE tool gives designers an opportunity to see it before they build it, to ask "what if" questions about all aspects of crew performance, including training, and to correct problems early. The system is focused on helicopters, but it is generic and permits generalization to other vehicles.

The HF-CAE system is similar in concept to computational tools such as finite-element stress analysis and computational fluid dynamics, which are used to improve designs and reduce costs. The results of the computational analysis are presented visually. The HF-CAE uses models of human performance and a computational simulation of manned flight to evaluate the cockpit design. The results are presented graphically and visually to the design engineers, often as a computer animation of manned flight.

The major elements of the HF-CAE system are (1) automated mission editor; (2) designer's simulation workbench, including aircraft dynamics and guidance models, human behavior/performance models, system function models, and workload models (workload models from Rotorcraft Human Factors Research Branch); (3) training requirements models; (4) three-dimensional computer-aided design utilities for cockpit layout, instruments, and controls; (5) anthropometric pilot model (graphic manikin); (6) designer's data, information and analysis center; and (7) simulation and integration executive control system.

The project began in fall 1984 and has completed three major phases of development toward a 1994 target date for a full prototype system. The cur-



Computer graphic tools for visualization of results of human factors-related design issues

rent phase focuses on the expansion of several elements of the system which was demonstrated during October and November 1988. The National Research Council's 2-year pilot performance model study is complete and is in the report phase. Two applied models of visibility and legibility are planned for inclusion in the system in the next phase.

(J. Hartzell, Ext. 5743)

Visibility Modeling Tool—An A31 Project

Computer-aided engineering (CAE) has revolutionized the way engineers create designs. It is now possible to use mathematical models of objects or processes to evaluate the performance of a design before the object is actually built. Classic examples

ORIGINAL PAGE
COLOR PHOTOGRAPH

include (1) the finite-element analysis of strength, used to evaluate the forces acting on structures such as bridges; and (2) the computational analysis of fluid dynamics, or computational fluid dynamic models, used to evaluate the lifting properties of wings.

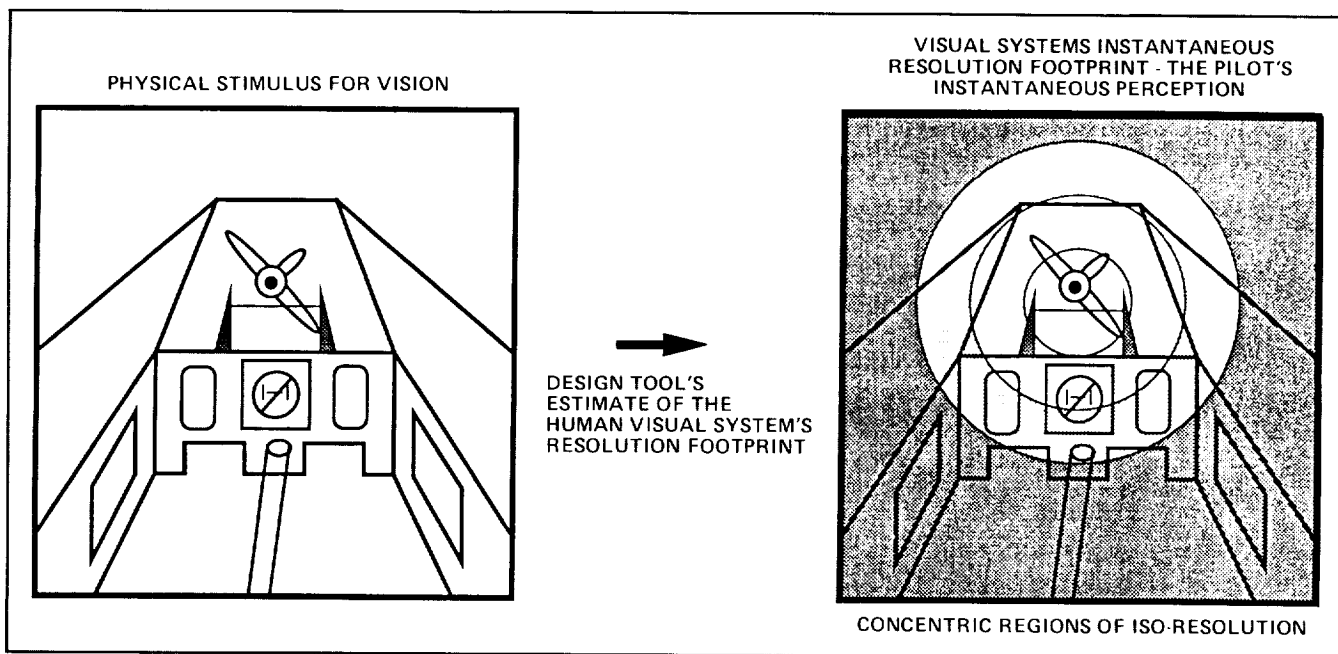
The Visibility Modeling Tool is a human factors (HF) CAE tool designed to help the crewstation design engineer obtain answers to questions about the visibility of information in potential avionic displays. The primary goal of this HF-CAE visibility tool is to evaluate potential designs before they are built; thereby it would reduce design costs, enhance the quality of the design engineer's product, and shorten the design time line. For this tool to be maximally useful, the evaluation that it provides to the engineer must be in an easily understood format; thus, user friendliness through graphics is another goal of the project. The Visibility Modeling Tool is being developed as an integrated component of the Army-NASA Aircrew/Aircraft Integration (A³I) project HF-CAE system.

To adequately model visibility, it is necessary to consider (1) the three-dimensional (3-D) geometry of the crewstation or cockpit; (2) the reflective and emissive properties of surfaces and objects in that space; (3) ambient lighting; (4) the pilot's or astro-

naut's eye points; (5) what he or she is looking at; (6) how this affects convergence and accommodation; (7) far, near, and retinal obstructions such as window posts, helmet margins, and retinal insensitivities; and (8) the current adaptation state of the pilot's visual system. All of these factors are being incorporated into the system at a level of realism that is adequate to generate reasonably valid estimates of visibility.

The program is a mixture of in-house effort and grants and contracts with leading scientists at universities and research institutions in the fields of vision research and computer graphics. This mixture of effort is vertically integrated and spans problems of basic vision science from the application of 3-D models to problems in computer-aided design (CAD).

Currently in place are two grants and a contract. In addition, there are collaborative agreements and a university consortium agreement on closely related topics in human vision. Much of the basic computer system architecture for the system has been developed and tested (i.e., communication protocols and system integration); there is a 3-D CAD system for rapid prototyping of cockpits and cockpit avionics; and a 3-D pilot manikin is currently being integrated into the system.



Visibility modeling applied to cockpit design and evaluation: computational models of human visibility, an A³I project/ASHFRD:ARC

In the next phase a computational model for the pilot's volume visual field will be added, and a model of the legibility of letters and symbols will be integrated into the system. Basic developmental work is proceeding on modeling accommodation, i.e., human optical blur, surface quality, and ambient lighting.

(J. Larimer, Ext. 5185)

Information Management and Transfer

The effective management and transfer of information within the National Airspace System (NAS) is critical to a safe and efficient air transportation system. Future NAS operations will require flight-deck information management systems designed for optimal transfer of airborne, ground, and satellite information to aircrews. Information management principles are required which define the information needed, and when and in what form it should be provided.

Ames Research Center has an ongoing research program to develop and verify design principles for, and demonstrate the viability of, advanced information management systems for future air transport operations. The program goals are to develop design principles for advanced flight-deck information management systems and to develop computer-aided design (CAD) technology to facilitate the integration of new information technology. As air-to-ground, as well as airborne, information transfer is a part of this research, aircraft-air traffic control integration in the future NAS will benefit from this effort.

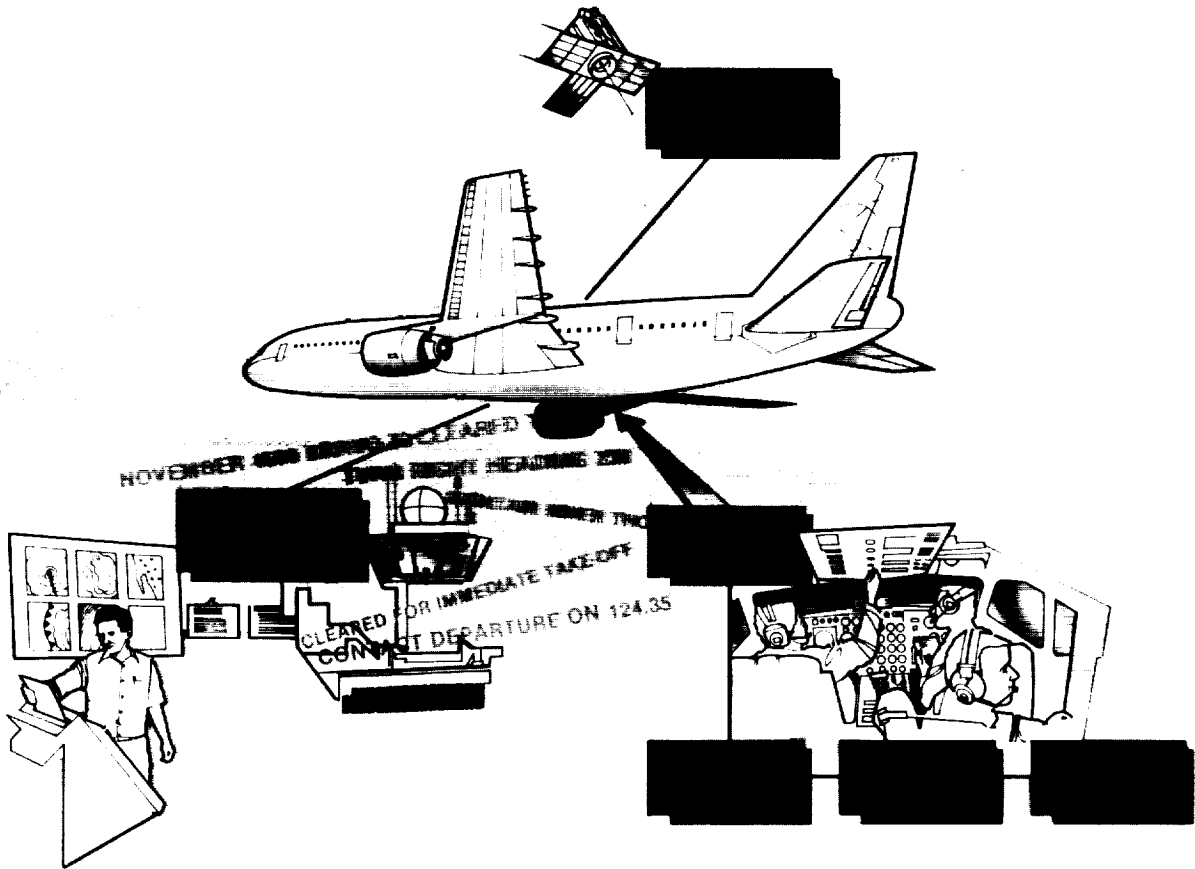
To attain the program goals by FY 1992, a multifaceted approach has been undertaken. This approach includes (1) the development of methodology for quantifying aircrew information requirements and information processing capacity during all flight phases, (2) the identification of current operational problems that could be eliminated by improved sys-

tem design, (3) the development and evaluation of prototypical information management systems, (4) the development of part system simulation technology as a low-cost design and evaluation tool, and (5) the development of CAD technology based upon information management principles.

During FY 1988 a number of efforts were successfully completed in support of the program objectives. A test instrument for quantifying aircrew information requirements and methods for deriving information load was developed. Analyses of Aviation Safety Reporting System (ASRS) incidents of air-ground information transfer were completed. In support of advanced communication management system development, linguistic analyses of communication problems resulting in accidents were completed, as was an aircrew survey of automation requirements of proposed data-link communications, and an MIT grant was initiated to develop an optimal automated clearance delivery system for advanced aircraft. With specific regard to weather information management, a study to determine minimal information transfer requirements for ground-based terminal radar was completed, as was an analysis of ASRS weather-related incidents.

Future efforts planned in support of this program are the development and evaluation of alternative measures of aircrew information load and the development of part systems simulation technology for use in computer-aided information system design. With regard to air-ground communication management, the development of an error-resistant data-link communications protocol is planned, as is the development of optimal interfaces for display-based communication systems. In weather information management, guidelines will be developed for flight-deck integration of ground-based weather information (such as low-level windshear and other severe weather avoidance information), and weather-related ASRS incidents will continue to be analyzed.

(A. Lee, Ext. 6908)



Information transfer technology

Virtual Workstation

The application of human capabilities outside of vehicles and shelters will be a vital element of space station, Moon base, and Mars exploration missions. While extravehicular activity (EVA) will account for much of the human presence, and automated robots will assist in many chores, telepresence and interactive visualization systems will provide essential complementary capabilities.

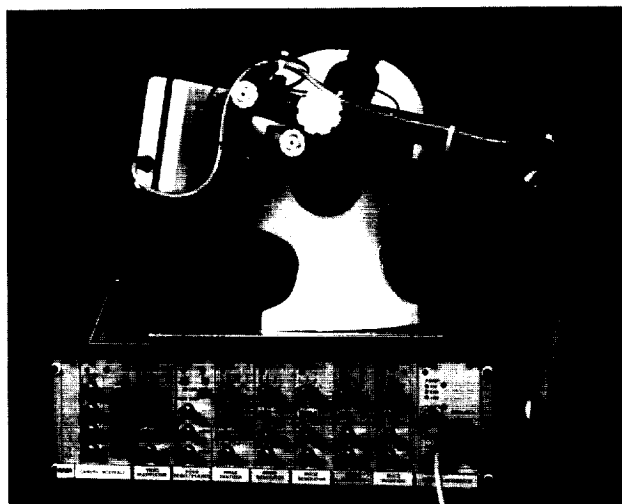
To support NASA's mission requirements for augmented human capability, Ames Research Center continues developing the Virtual Workstation. This device is a multisensory personal simulator and telepresence device. It consists of a custom-built, wide-field-of-view, stereo, head-mounted display; a custom video processor; magnetic head tracker; fiber optic gloves; magnetic gesture trackers; voice input/output; and an audio symbology generator. The

Virtual Workstation is being developed to enable greatly improved situation awareness in complex spatial environments; to enable high-fidelity telepresence for control of telerobots; to simulate workstations, cockpits, and module interiors; and to enable improved visualization interfaces for exploration of planetary surface data.

In 1988, the third-generation monochrome viewer and video processor electronics were completed. Ad hoc demonstration software was replaced by a system software library for programming the viewer, tracker, and glove, and an improved object data base format and its support tools. A directional acoustic signal processor, the "convolvotron," was designed and is being fabricated. Initial Operational Configuration (IOC) of the prototype system was achieved in 1988. The hardware and software were integrated into a stable configuration for user interface research, and generic development ended.



A user wearing the third-generation Virtual Visual Environment Display (VIVED) with a microphone for verbal control and earphones for both directional and nondirectional audio feedback, all mounted on a highly adjustable headset



The third-generation VIVED system, including headset and video processor

Currently, a major documentation effort nears completion, and technology transfer activities are rapidly increasing. Current focus is on applying this technology to NASA's missions and goals.

A new program to support the transition of this technology to Space Station Freedom was begun in October 1988. This program, funded by the Office of Space Station, will determine the design accommodations required to support the eventual installation of advanced head-mounted displays aboard

Space Station Freedom, and will develop advanced, flight-qualifiable prototypes.

Application software is under development for a joint effort between NASA Ames and NASA's Jet Propulsion Laboratory (JPL) in which the Virtual Workstation will be used to provide an alternate operator interface in telerobotics supervisory control. In another project, a highly dexterous, anthropomorphic end-effector (under development at JPL) and the Ames Virtual Workstation will demonstrate high-fidelity dexterous telepresence between Ames and JPL within the next 3 years.

As part of the Pathfinder Humans-in-Space Program, user interfaces for virtual exploration of planetary surfaces will be developed. Users will be able to explore the planets as integrated environments, not merely through individual pictures. As a spinoff to aeronautics research, specific plans are being developed to provide systems for use in rotorcraft helmet-mounted display research and computer-aided cockpit design tools.

(M. McGreevy, S. Fisher, B. Wenzel,
Ext. 6147/6789/6290)

Cockpit Procedures Monitor and Error-Tolerant Systems

The objective of this research is to develop the technology necessary for the design of error-tolerant cockpits. A key feature of error-tolerant systems is that they incorporate a model of pilot behavior. The system uses this model to track pilot actions, infer pilot intent, detect unexpected actions, and alert the crew to potential errors. In some sense, the goal is to develop an "electronic check pilot" that can intelligently monitor pilot activities.

We are pursuing a number of alternative ways to track operator activity and infer operator intent. We are investigating techniques based on (1) a rule-based script of flight phases and procedural actions, (2) operator function models, and (3) Bayesian temporal reasoning.

The first version of the script-based program was tested against protocol data from four Boeing 727 simulator flights. The program could detect procedural errors, but its ability to account for pilot actions from procedures done out of the normal

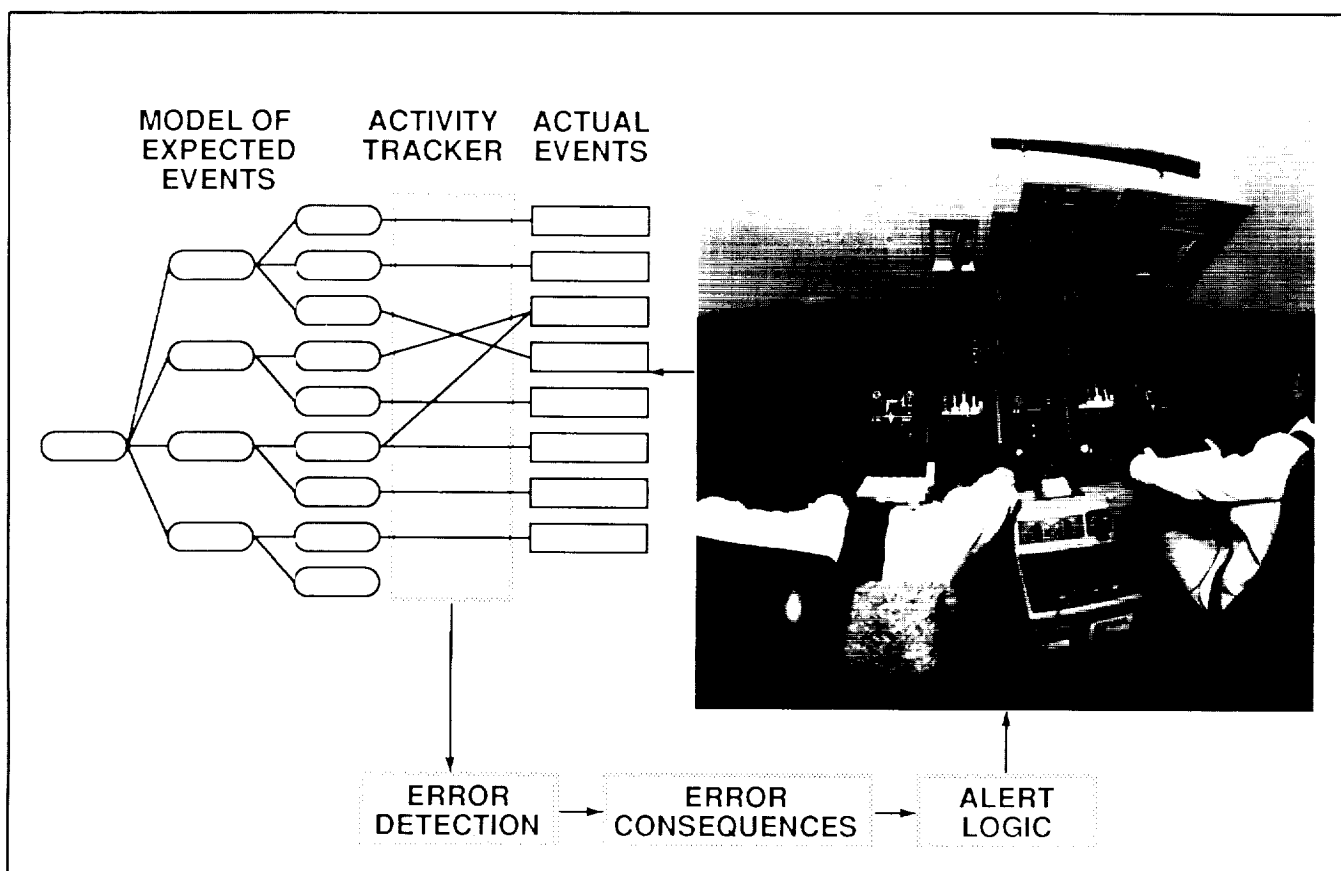
sequence was inadequate. A capability to explain unexpected actions by linking them to procedures that are nominally done or unstarted is being added to the program to remedy this problem. Under a grant to Georgia Tech, an intent-inferencing system, based on an operator function model, was developed and tested on data from a satellite communications system with good results. Under a contract to Search Technology, a prototype for an intent-inferencing system based on Bayesian reasoning was developed.

In 1989, we will compare these three methods against data from our 727 simulator. We also plan to initiate an empirical study designed to better understand how check pilots detect procedural errors and infer pilot intent.

The technology developed for the cockpit pro-

cedures monitor will be used to develop an interactive cockpit display to aid pilots in executing procedures. In its initial version, this "smart checklist" will graphically display the procedural script developed to track pilot actions. Modes of checklist operation will include both passively monitoring pilot execution of procedures and automatically executing procedures. Under a related Small Business Innovation Research contract, we will develop and test a procedure execution aid that can compose procedures that are appropriate for the current flight situation and equipment configuration. These methodologies will be used to develop and evaluate in full mission simulation a cockpit procedures monitor and a smart checklist in the Advanced Concepts Flight Simulator.

(E. Palmer, Ext. 6073)



Cockpit procedures monitor and error-tolerant systems

ORIGINAL PAGE
BLACK AND WHITE PHOTOGRAPH

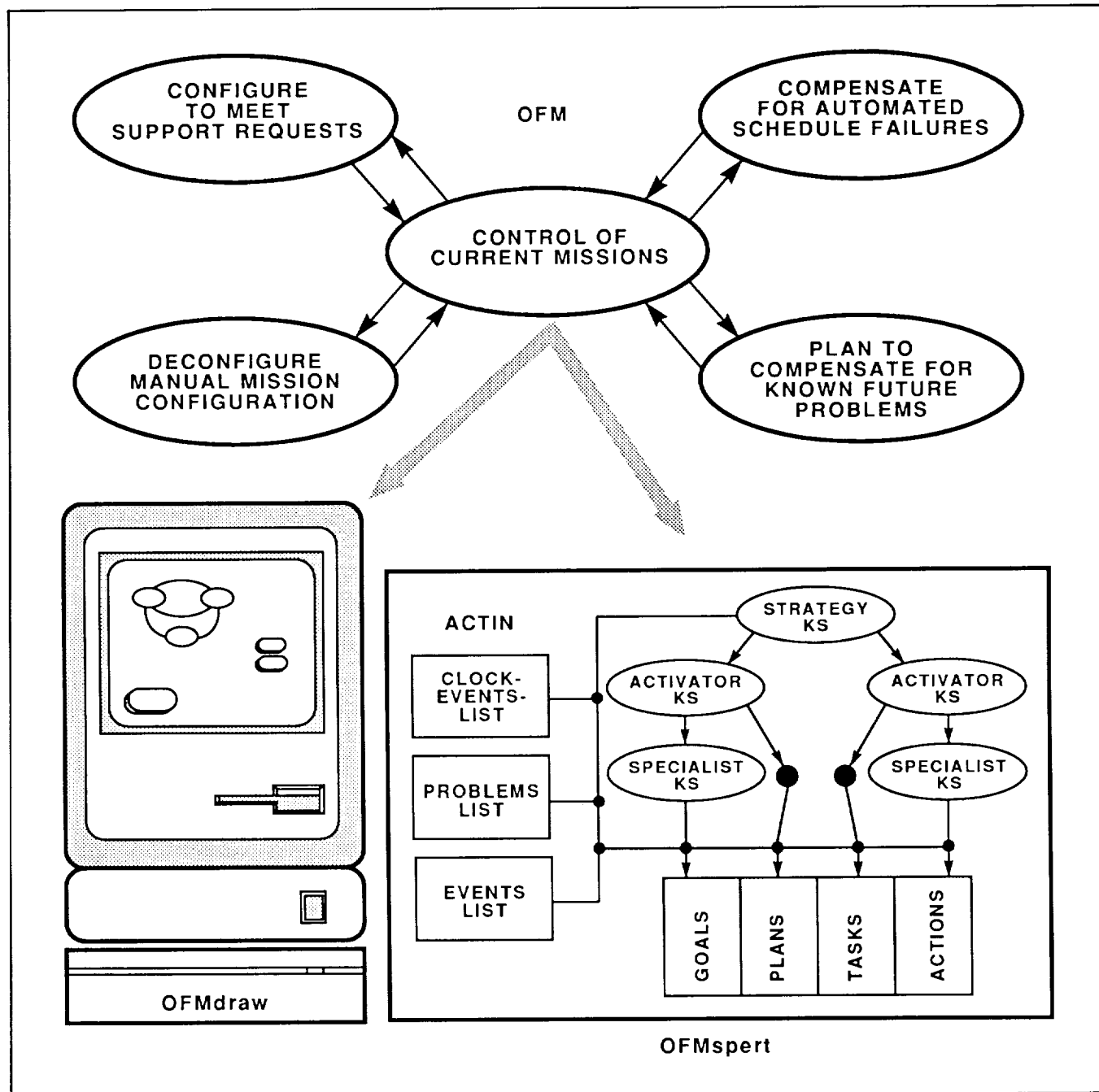
Operator Function Modeling: Cognitive Task Analysis in Supervisory Control

The Operator Function Model (OFM) project is composed of three related activities.

The first activity is a study of the use and development of models of operators in complex, auto-

mated space systems. The OFM methodology was extended to represent cognitive as well as manual operator activities. The network task model at its lowest level has both physical and cognitive actions. This enhancement extends the OFM structure to provide a tool for cognitive task analysis.

The second activity is the ongoing development of OFMdraw, which is a software tool that facilitates



Operator function modeling—an approach to cognitive task analysis in supervisory control

the construction of an OFM. OFMdraw is implemented on a Macintosh II in Smalltalk. Currently, OFMdraw can be used to construct a heterarchic network of nodes and arcs.

During 1988 most of our work was spent on OFMspert, the third activity in this project. OFMspert has two purposes: (1) it is a methodological extension of the structure of the original OFM to encompass explicitly the domain-specific information to function as a self-contained, on-line model of the human operator capable of real-time operator intent inferencing; and (2) it is intended to be able to dynamically assume responsibilities for portions of the supervisory control task in automated space systems. The intent inferencing portion of OFMspert was validated by verbal protocols of operators controlling a dynamic system and by comparing OFMspert's interpretations of operator behavior with those of a domain expert.

(E. Palmer, Ext. 6073)

Computational Models of Attention and Cognition

Human operators are severely limited in their ability to process and respond to multiple information sources. Aviation and space environments impose severe visual, auditory, and decision-making demands in situations where human failure can cause catastrophic results. Information overload has been identified as a major contributor to error in military aviation, especially helicopter nap-of-the-Earth (NOE) operations, and in critical monitoring tasks such as air traffic control and ground control of space missions.

The ultimate solution to problems arising from limitations on attention and cognitive capacities will come from optimal allocation of function between human and machine combined with optimal configuration of multimodal displays and controls. Realiza-

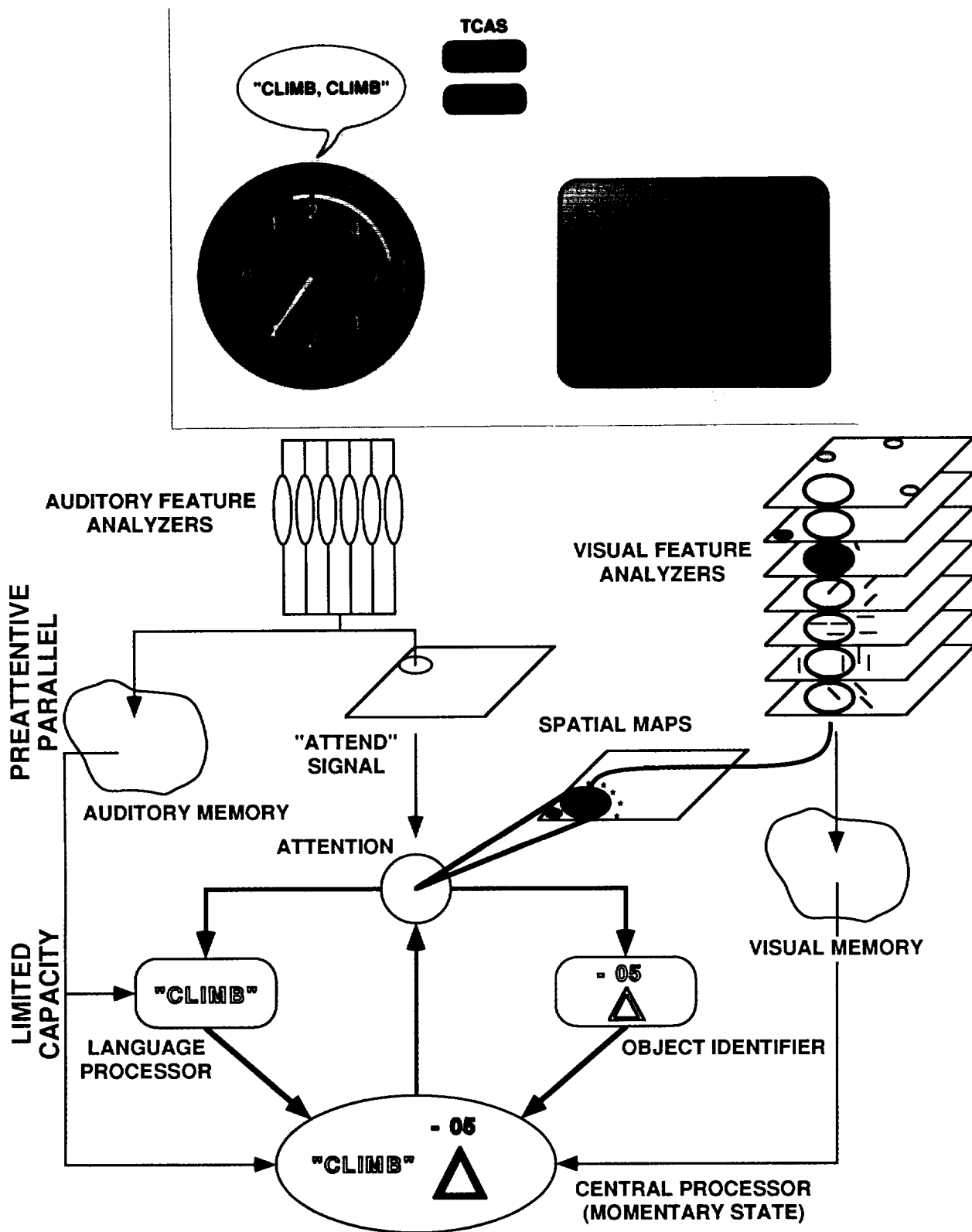
tion of such optimization depends on a deeper understanding of attentional control. This can be achieved by developing validated computational models of human information processing.

Ames Research Center has an ongoing research program in attention and human cognition focused on determining the mental resources underlying complex task performance. This research has identified stimuli that control attention and situations in which distraction will be unavoidable, making it possible to design displays that better capture and direct an operator's attention. Work on cognitive architecture has led to models of simple multitask settings that will aid in making decisions about the use of speech controls and displays, and the allocation of tasks between the human operator and automated subsystems. Current research will extend these findings to more complex task environments by (1) developing methods for mapping complex tasks onto underlying mental resources; (2) conceptualizing, implementing, and iteratively refining computational models of human cognition; and (3) developing quantitative models of the allocation, control, and mechanisms of human attention.

Several aerospace scenarios are being investigated as a basis for analysis and model development, including (1) ground control of manned and unmanned space operations, (2) helicopter NOE and search-and-rescue operations, and (3) air traffic control and anticipated Space Station proximity control operations. The figure depicts the hypothesized stimulus processing involved in decoding information from a Traffic Alert Collision-Avoidance System (TCAS) flight advisory display.

The research program involves extensive in-house research and model development while it supports related modeling efforts at universities. Related efforts at Ames address workload, methods of assuring proper levels of alertness in civil air transport, and pilot error.

(R. Remington, Ext. 6243)



Hypothesized stimulus processing involved in decoding information from a TCAS flight advisory display

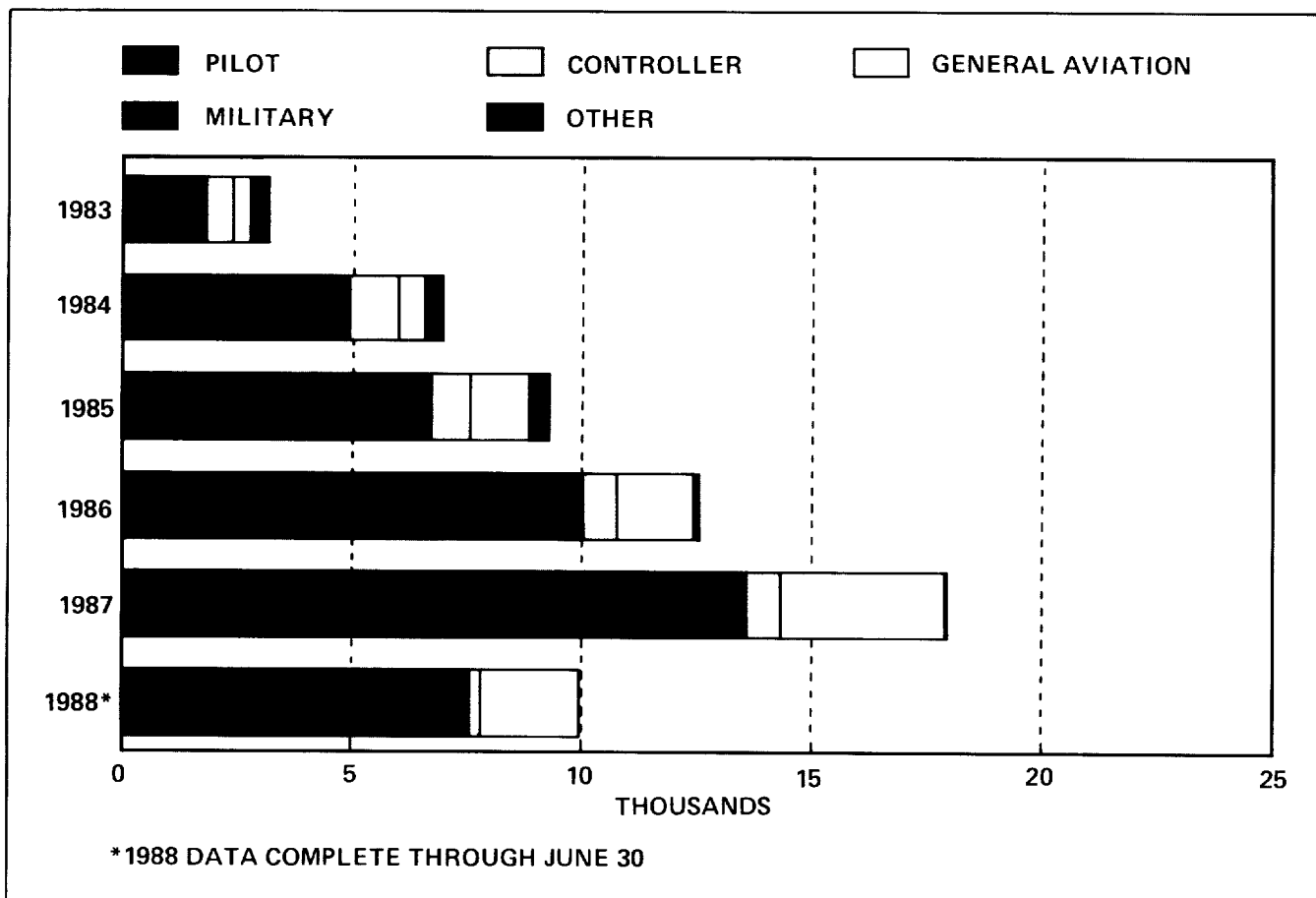
Aviation Safety Reporting System (ASRS)

The Aviation Safety Reporting System (ASRS) was established in 1976. It is managed by NASA at the request of the Federal Aviation Administration (FAA). The ASRS receives, processes, and analyzes voluntarily submitted aviation incident reports from pilots, air traffic controllers, and others. These reports describe both unsafe occurrences and hazardous situations. The ASRS offers incident reporters confidentiality, and the FAA provides limited immunity for unintentional aviation safety transgressions the reporters may have committed. In exchange, the program receives safety information which can be used to remedy reported hazards, to provide data for planning and making improvements to the National Airspace System, and to conduct research on pressing safety problems. The ASRS is particularly concerned with the quality of human performance in the aviation system.

The ASRS program is unique among aviation reporting systems. Its special qualities include the following:

1. proof of the concept of acquisition, analysis, and use of incident data,
2. unique methodology to capture otherwise inaccessible human performance data,
3. one-of-a-kind data base of actual incident information as reported by participants,
4. proven capability for diverse application to both research and operations,
5. ability to actively monitor the aviation system,
6. capability of effective technology transfer as evidenced by ASRS-type systems in other countries and disciplines,
7. world's largest repository of human performance information,
8. consistent support and use of the program by government and industry.

In addition to screening and processing report receipts for entry to a data base, the ASRS maintains



ASRS report intake

that data base and supporting computer hardware and software and interrogates the data base to satisfy the information requirements of government and industry. Report receipts can be statistically analyzed for trends and problem concentrations—although there are important theoretical limitations on the use of ASRS data for this purpose. Since its inception, the ASRS has published more than 35 research studies based on its data, covering the full spectrum of aviation activity; in addition, the program has issued 949 alerting messages and responded to 1,388 special data requests.

The ASRS currently operates under a Memorandum of Agreement with the FAA that is effective until September 1992. The program has achieved a productive and active rapport with FAA operational and research organizations and is consistently used by NASA, the National Transportation Safety Board, the Department of Defense, and the aviation community. A large and growing report volume continues to challenge ASRS resources; however, with increased FAA and NASA support, the program has the potential to significantly increase its operational and research activities.

(W. Reynard, Ext. 6467)

Thermal Control Coating for Space Suits

The Shuttle Extravehicular Mobility Unit and past suit configurations for Apollo and Skylab have used the Integrated Thermal Micrometeoroid Garment (ITMG) to provide thermal protection to astronauts performing extravehicular activity (EVA). The ITMG is a multilayer garment that lessens the incident thermal radiation. Several characteristics limit its practicality for use in a routine space station EVA, including restricted mobility, complex fabrication, relatively low resistance to atomic oxygen degradation and orbital debris penetration, and a limited lifetime.

The no-prebreathing requirement for space station EVA operations has led to the development and

evaluation of hard space suits. The hard suit structure allows designers to provide passive thermal control in the suit structure. Environmental influence on the suit can be minimized with a high-reflectance coating.

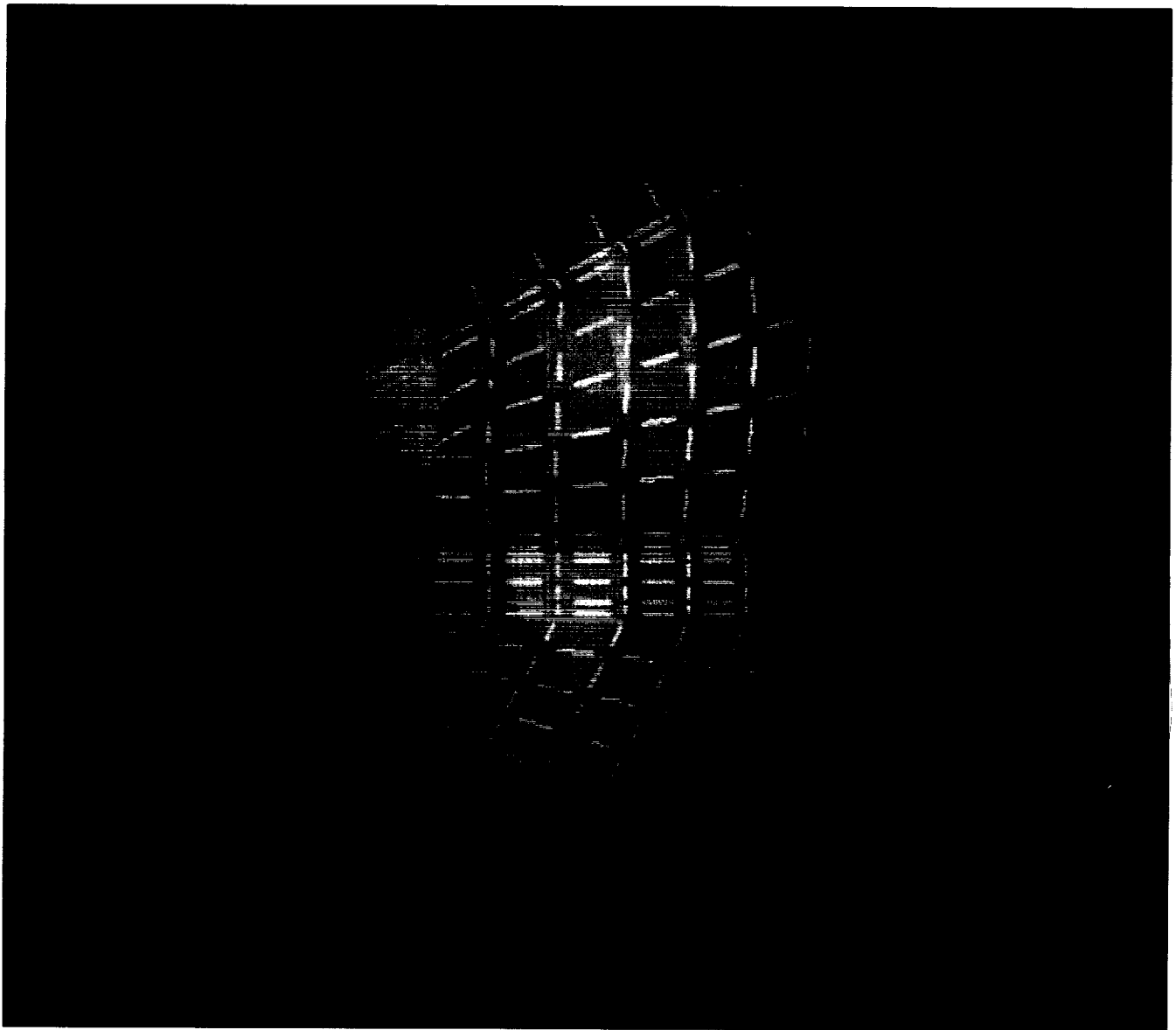
Materials testing on 10 candidate metal coatings was completed. Both polished and textured substrate surfaces were investigated. Samples have undergone corrosion and abrasion tests with subsequent determination of optical properties to quantify degradation. Additional testing included tape adhesion, salt spray fog, and thermal soak tests.

The plated gold coating on a polished surface exhibited consistently higher reflectance throughout the test protocol. Two suit elements have been plated with gold and will be instrumented for use in a thermal vacuum test. The test article will contain a pressurized, temperature-controlled, annular gas flow (to simulate ventilation in a suit limb) and will be subjected to simulated components of the space station EVA thermal environment.

Data from the test will be used to validate a finite-element computer model of the suit parts in the same environments. Preliminary analyses of the suit elements with a graybody reflectance of 98% in a cold environment (radiation to deep space only) yield structural temperatures of 68.3° F. Convective heating in this cold case is 2.25 Btu/hr-ft². Addition of direct incident solar radiation raises equilibrium temperatures to 71° F. Convective cooling is 1.36 Btu/hr-ft². These heating/cooling loads are lower than for past and current suit insulation. The high-reflectance coating isolates the suit from its thermal environment.

The model will be revised so that it will include infrared radiation sources. Infrared radiation will be a significant component of the thermal environment in some space station EVA scenarios. After validation of the model with empirical data, several realistic configurations will be analyzed by parametrically varying the model interior convection, suit-coating reflectance, and space environment. The model may be adapted for use in research of other thermal environments, such as the Lunar or Martian surfaces.

(B. Squire and B. Webbon, Ext. 5057/6646)



Resultant temperature for the gold-coated suit parts in a cold environment is 68.3°F

Advanced EVA Suit Technology

The Ames Research Center (ARC) has an ongoing program to address extravehicular activity (EVA) suit requirements for the space station. A product of this effort has been the development of the ARC AX-5 space suit. The overall objective of this program has been to provide a high-mobility suit that eliminates the need for prebreathing, provides increased hardware and systems life, minimizes maintenance, provides increased hazard protection, and accommodates a wide range of sizes.

As a part of the overall evaluation process, a series of tests has been established at the Johnson Space Center (JSC) to assess the performance of advanced suit concepts as compared to the current Shuttle Extravehicular Mobility Unit (EMU). These tests consist of mobility range comparison, torque/force work capability tests, general workstation performance assessment, and the EASE/ACCESS structure assembly simulation.

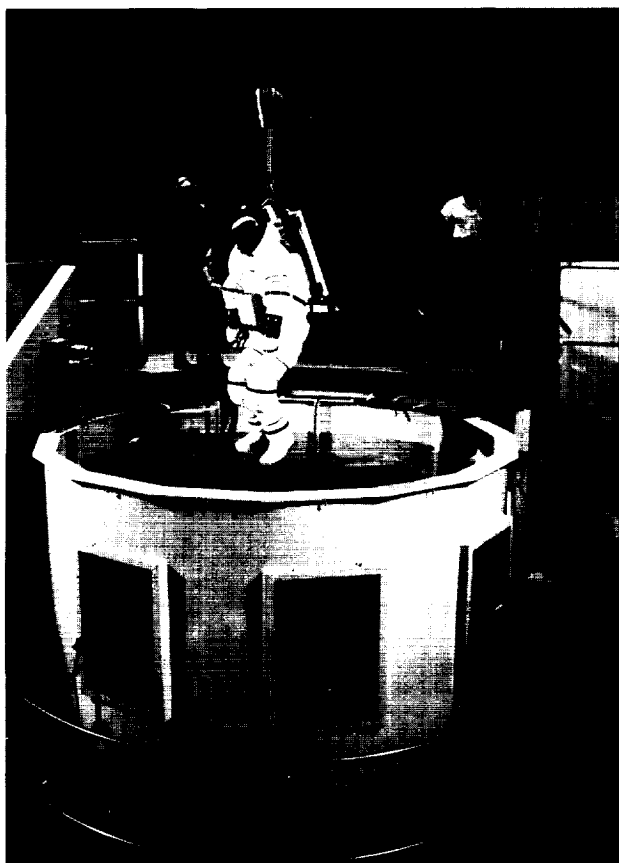
In early 1988, tests of the AX-5 mobility and range-of-motion were completed in the JSC Weightless Environment Test Facility (WETF). Although the

**ORIGINAL PAGE
COLOR PHOTOGRAPH**

hard data of these tests have not yet been analyzed for release by JSC, indications are that the AX-5 has considerably more mobility than the Shuttle EMU.

Currently, the AX-5 bearing assemblies are undergoing modification. Upon completion, tests will be resumed in mid-March 1989 at JSC to complete the test matrix. In addition, component mobility torque and life cycle tests will be initiated at ARC to complete the performance assessment of the AX-5. Subsequent upgrades are anticipated and will be incorporated into the AX-5.

(H. Vykukal, Ext. 5386)



The AX-5 hard space suit is lowered into a natural buoyancy test facility to undergo testing

Motion Processing in Humans and Machines

Humans navigate almost effortlessly through complex environments by relying on a sophisticated

visual capacity for estimating the motion of self and objects. Ames Research Center has an ongoing research program to understand and model the human motion-sensing mechanism, and to develop algorithms for motion sensing in autonomous vision systems. This research will have important applications in the areas of robotics, obstacle avoidance, autonomous vehicles, and nap-of-the-Earth flight, and will also provide insights into the motion information required by pilots for flight control. Part of this research is performed in collaboration with Stanford University.

Accomplishments include new algorithms for estimating two-dimensional image velocity fields from image sequences, and algorithms for estimating three-dimensional motion parameters from the two-dimensional velocities. We have also completed a study on the dependence of human direction-of-motion judgments on the contrast of picture elements. Results show strong contrast-dependent biases, which are a powerful means of distinguishing between alternative models and which may have practical consequences in themselves.

(A. Watson, Ext. 5419)

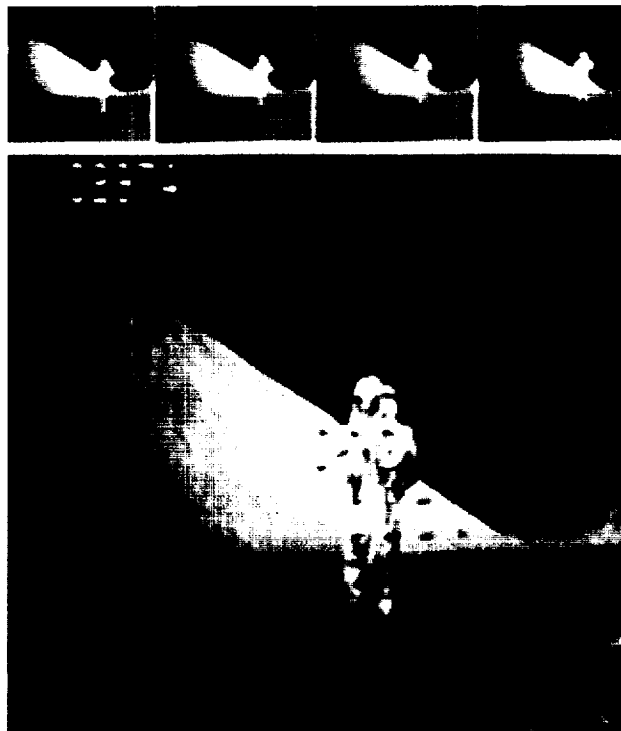


Image motion estimates obtained from simulated human visual processing

ORIGINAL PAGE

BLACK AND WHITE PHOTOGRAPH

Pyramid Image Codes

Vision systems, both human and machine, transform the spatial image into a coded representation. Particular codes may be optimized for efficiency or for extraction of useful image features. We have explored image codes based on the primary visual cortex in humans and other primates. Understanding these codes will advance the art in image coding, autonomous vision, and computational human factors.

In the primary visual cortex, imagery is coded by features that vary in size, orientation, and position. We have devised a mathematical model of this transformation, called the hexagonal oriented orthogonal quadrature pyramid (HOP). In a pyramid

code, features are segregated by size into layers, with fewer features in the layers devoted to large features. Pyramid schemes provide scale invariance, and are useful for coarse-to-fine searching and for progressive transmission of images.

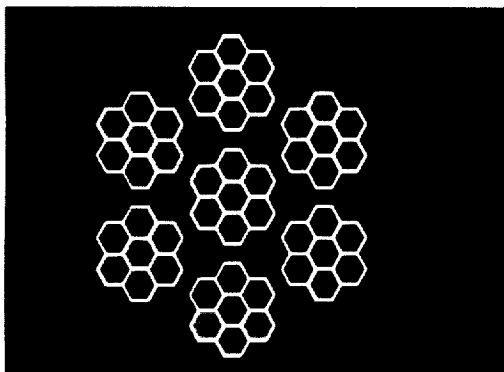
The HOP transform is novel in three respects: (1) it uses a hexagonal pixel lattice, (2) it uses oriented features, and (3) it accurately models most of the prominent aspects of the primary visual cortex. The transform uses seven basic features (kernels) which may be regarded as three oriented edges, three oriented bars, and one nonoriented "blob." Application of these kernels to nonoverlapping, seven-pixel neighborhoods yields six oriented, high-pass pyramid layers, and one low-pass (blob) layer. Subsequent high-pass layers are produced by recur-

IMAGE CODES REQUIRED FOR

- AUTONOMOUS VISION
- IMAGE STORAGE & TRANSMISSION
- MODELING HUMAN VISION

HEXAGONAL ORTHOGONAL ORIENTED PYRAMID (HOP)

- EASY TO COMPUTE AND INVERT
- HIGHLY EFFICIENT
- MATCH HUMAN VISION
- HEXAGONAL LATTICE



ORIENTED, ORTHOGONAL KERNELS

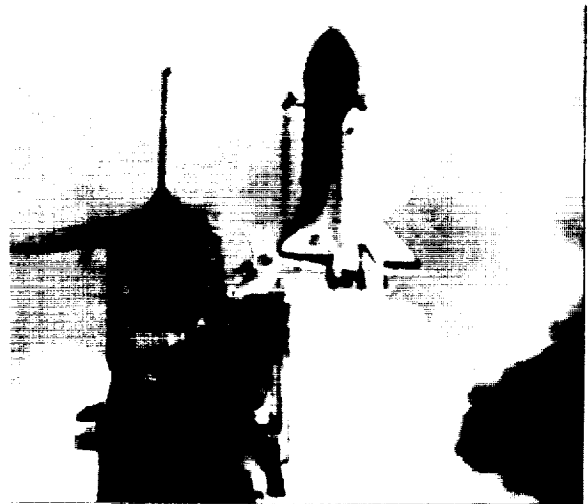
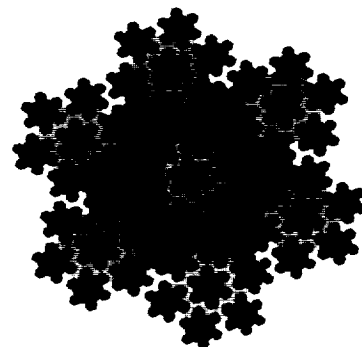


IMAGE CODED AT 1 BIT/PIXEL



PYRAMID OF KERNELS

Pyramid image codes

**ORIGINAL PAGE
COLOR PHOTOGRAPH**

sive application of the seven kernels to each low-pass layer.

Preliminary results on use of the HOP transform for image compression show that 24-bit color images can be coded at about 1 bit/pixel with reasonable fidelity. Future work will explore related codes and more detailed comparisons to biological coding, and applications to motion processing and shape perception.

(A. Watson, Ext. 5419)

Auditory Display Systems Research

Auditory cues can provide a critical channel of information in complex spatial environments; in periods of high visual workload; and when visual cues are limited, degraded, or absent. Some or all of these conditions will be present in such space station operations as (1) the monitoring and control of autonomous and semiautonomous telerobots, (2) the conduct of extravehicular activity (EVA) and the use of visor displays, and (3) the management of complex on-board space station systems. Auditory information can also enhance the utility of virtual environment displays such as NASA's Virtual Workstation.

Spatial auditory displays require the ability to generate localized sound cues in a flexible and dynamic manner. Ames Research Center is currently investigating the underlying perceptual principles of auditory displays and is also developing a prototype signal processor based on these principles. Rather than use a spherical array of speakers, the prototype will maximize portability by synthetically generating three-dimensional sound cues in real time for delivery through earphones. Unlike conventional stereo, sources will be perceived outside the head at discrete distances and directions from the listener. This is made possible by numerically modeling the effects of the outer ears (the

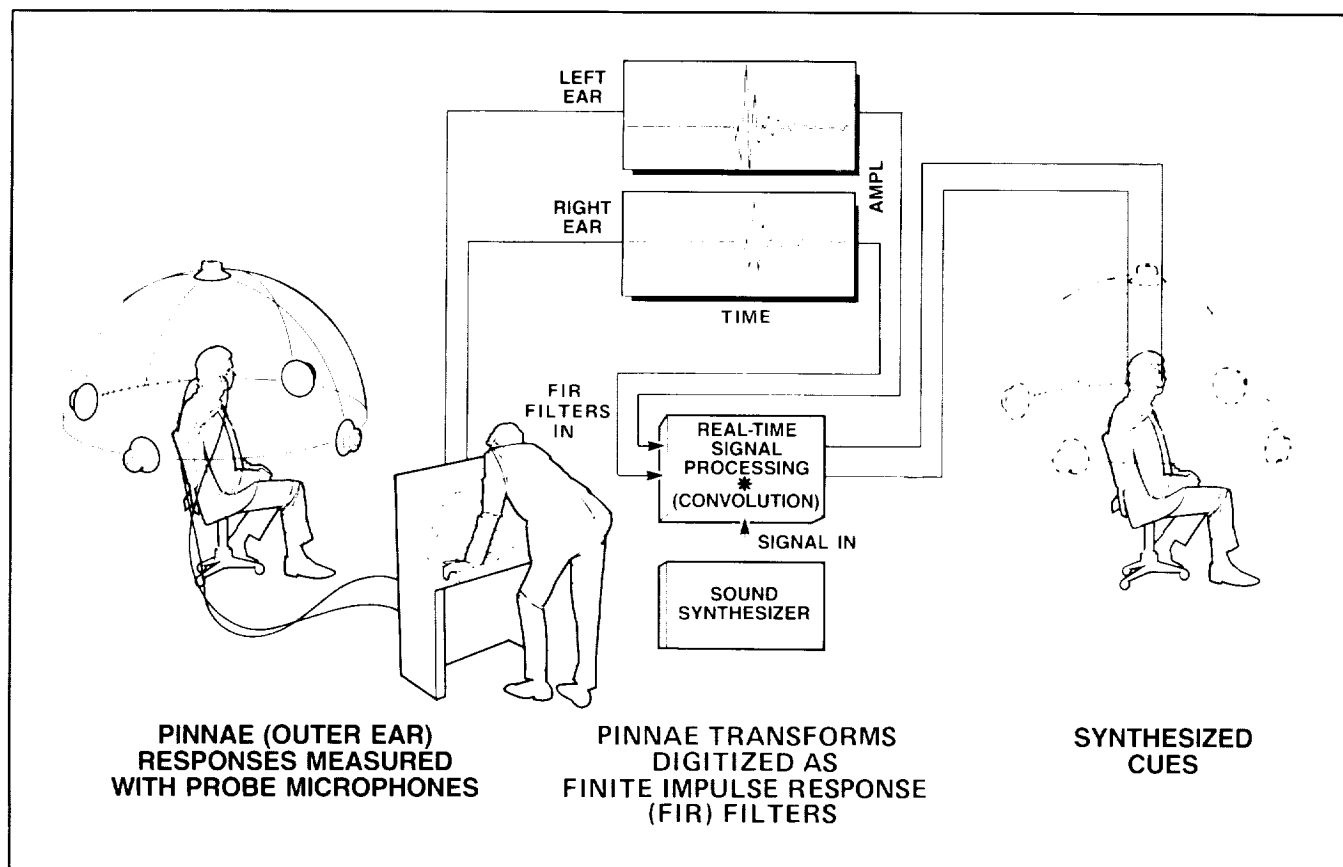
pinnae) on the sounds perceived at various spatial locations. These "pinnae transform filters" can then be applied to arbitrary sounds (voices, for example) to cause them to seem spatially located.

A nondirectional audio display, based on well-established electronic sound synthesis standards, is also under development. An initial version of an auditory symbol editor was completed. This system will enable researchers to investigate auditory symbology for communication of meaning apart from verbal content. In addition, experience in the integration of this system with the Virtual Workstation will benefit the later incorporation of the spatial audio display system.

Cooperative research with Dr. Frederic Wightman of the University of Wisconsin, Madison, is under way. This research includes perceptual validation of the synthesis technique in both the practical and the more basic areas. Practical issues include required computational resolution and signal bandwidth. Basic issues include acoustic determinants of individual differences in localization behavior. In 1988, a real-time signal processor (the "convolvotron") was designed, and a wire-wrapped prototype was fabricated. When integrated with a head-tracking device, the initial version is capable of synthesizing three localized sources which can be independently stabilized in fixed positions or in motion trajectories relative to the listener.

Plans include adaptation of Dr. Wightman's measurements of the pinnae transform filters for use in the convolvotron, evaluation of the perceptual validity of the convolvotron-generated directional audio, and implementation of the processor as a printed circuit (PC) board for greater reliability and ease of replication. A PC-based convolvotron capable of presenting four independent and simultaneous directional sound sources is scheduled for completion in 1989. The convolvotron will be incorporated into the Ames Virtual Workstation and will undergo system calibration and performance evaluation in specific applications.

(B. Wenzel, Ext. 6290)



Three-dimensional auditory display: synthesis technique

International Aviation Technology Studies

A study of international aviation technology markets and resources is progressing. Data on the world aviation market such as research and development, education, capital expenditures, forecasts, aircraft types, companies, agreements, applications, civil or military, employment, trade balance, etc., have been collected and sources have been identified. Informal documents on some countries and related subjects have been produced and a Hypercard filing system has been initiated for related documents. In 1989, important trends in international aviation technology which may have implications for U.S. technology will be identified, and the potential for developing forecasting models will be assessed.

(L. Alton, Ext. 5887)

International Rotorcraft Technology Studies

An evaluation of the potential advantages of the tilt-rotor vehicle technology for a specific emergency medical service (EMS) application continues. The feasibility of rotorcraft-based EMS in the Caribbean Basin was assessed using data on population, motor vehicles, and motor vehicle accidents. A discrete-event Monte Carlo simulation model permitting a comparative analysis of conventional rotorcraft and the tilt-rotor aircraft as EMS vehicles for use on a personal computer was expanded and improved. This model compares the relative performance of these vehicles and evaluates the required number and location of EMS centers and rotorcraft in Puerto Rico and the Lesser Antilles.

The model accepts data such as the locations and categories of hospitals, the number and capacity

of rotorcraft at each hospital, the region in which a given percentage of accidents will occur, and other data relating to rescue time, response time, etc. The program output includes the average wait time before an accident victim is reached, the average rescue time before the victim is taken to the nearest appropriate hospital, the number of accident victims that were not rescued because no rotorcraft was available, and the number of hours per week each rotorcraft flies.

Simulation analyses show that two tilt-rotor vehicles could perform more effectively for the region than three helicopters, with significantly less average rescue time and fewer out-of-range accidents. Rotorcraft manufacturers and operators are using these results in planning and marketing activities.

This generic model is being applied to a broader scope of public service and commercial missions, combinations of missions, transportation alternatives, and locations in a study with the University of Puerto Rico. Design characteristics for effective tilt-rotor operations have been identified and were communicated to appropriate organizations. A tilt-rotor feasibility study by the Port Authority of Puerto Rico will incorporate the results of this research.

(L. Alton, Ext. 5887)

Electro-Expulsive Deicing System Demonstrated in Flight on Navy F/A-18 Hornet

An icing flight-test series designed to validate the effectiveness of a NASA Ames Research Center-patented ice-protection system has been successfully completed for NASA by the Naval Air Test Center, Patuxent River. The Electro-Expulsive Deicing System (EEDS) was tested on the engine inlet of a U.S. Navy F/A-18 Hornet fighter-attack carrier aircraft. That sharp inlet lip is particularly susceptible to ice accretion. As the accreted ice subsequently breaks off the inlet, fragments are ingested by the engine, causing severe foreign-object damage.

The Navy has lost at least five F/A-18 engines (F-404) and the Canadians have suffered 26 losses

according to Navy information sources. Recognizing the critical need for a practical solution to the inlet icing problem and foreseeing the potential of the Ames system, the Naval Air Systems Command provided all the necessary funding to the NASA program to expedite the development work.

The program was organized, the test artifacts were made, and the icing flight tests were executed, while invoking the most stringent safety requirements, all in record time. This endeavor is an excellent example of the team cooperation of NASA, Navy, Marines, Air Force, and contractor (freely donating participation), and of their dedication to a program with so high a flight safety potential.

The test also represents the first time a retrofittable deicing boot device has been demonstrated to be effective as an ice protection system for that type of high-performance aircraft. The thin EEDS leading-edge tape deicer combines the properties of rain/sand erosion with the ability to pulverize any accreted ice. Thus, when the pulsing rate was sufficiently frequent (e.g., every 3-5 seconds), the EEDS demonstrated its ability to perform not only as an effective deicer, but as an excellent anti-ice system as well. Adaptation of this technology for civil transport application is under way.

(L. Haslim, Ext. 6575)



Icing flight test of electro-expulsive deicing system on engine inlet of F/A-18 Hornet behind spray boom of Air Force NKC-135 icing spray tanker

ORIGINAL PAGE
BLACK AND WHITE PHOTOGRAPH

Electro-Expulsive Deicers for Rotorcraft and Fixed-Wing Aircraft

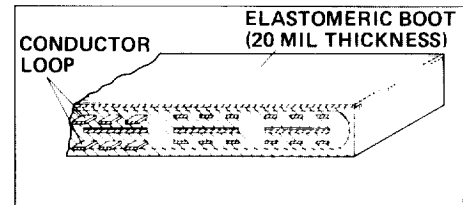
A dynamic new deicing system has been patented which promises to extend the operational capability of current aircraft into harsh icing environments with greater safety. The Electro-Expulsive Separation System has attracted strong interest from

the commercial airline industry, the Federal Aviation Administration, general aviation, and the military because of its immediate potential as a simple, yet potent, ice protection system. The retrofittable device uses brief pulses of electrical current to pulverize ice accumulations into tiny fragments which are forcefully ejected harmlessly into the airstream.

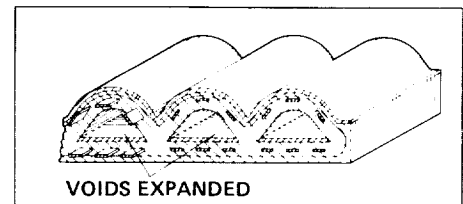
A major technological impediment to extending helicopter operations into the all-weather flight

ADVANTAGES OVER CONVENTIONAL SYSTEMS

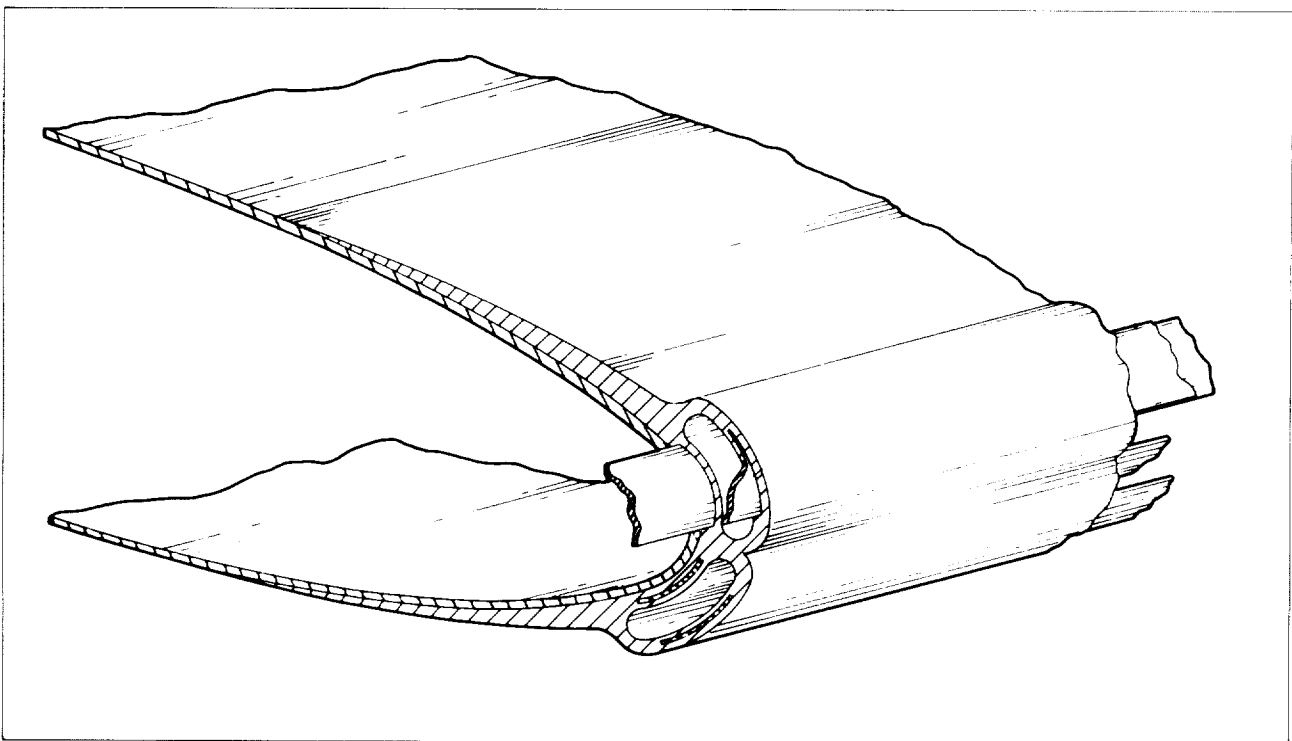
- FLEXIBLE, CONFORMS EASILY
- LOW POWER REQUIREMENT (TYPICALLY 500 Watts FOR LARGE A/C) 50 Watts/sq m VICE 25,000 Watts/m² (2300 Watts/ft²) FOR TYPICAL ELECTRO-THERMAL
- VERY EFFECTIVE DEICER: BOTH CRACKS OFF AND EJECTS ICE
- POSITIVE ACTION: 2-3 ORDERS OF MAGNITUDE ABOVE REQUIRED 25-35 g-FORCE TO EJECT ICE
- IMPROVED A/C PERFORMANCE/UTILITY IN ALL WEATHER
- LARGE WEIGHT/SPACE REDUCTION
- IMPROVED MAINTAINABILITY/RELIABILITY
- ECONOMY OF AIRFRAME CONSTRUCTION—CAN BE RETROFITTED
- RUNS ON A/C PRIMARY DC/AC BUSS



DEICING BOOT-INACTIVE



DEICING BOOT-EXPULSION PHASE



DEICING BOOT AFFIXED TO AIRFOIL (TYPICAL CONFIGURATION)

Electro-Expulsive Deicing System

regime is the lack of rotor-blade ice protection. The sensitivity of the blades to ice accumulation is well recognized. Anticipated weight and power penalties for existing helicopters have been cited as a major reason users have been reluctant to incorporate ice protection on existing helicopters.

A low-cost, low-powered, and lightweight solution to the problem of icing protection for helicopter rotor blades is available as a result of efforts of Ames Research Center personnel. This next-generation ice protection system consists of a flexible, highly durable polyurethane boot that is readily bondable onto almost any substrate, and requires no mechanical moving parts or pneumatic inflation to shed ice effectively from aircraft surfaces. When pulsed with the current spike, the elastomeric boot cyclically, expulsively expands, exerting an accelerating force ranging up to thousands of g's to throw off any accreted ice.

The operation could be described as snapping a "small rug to shake out the dust." In the relaxed state, the thin deicer boot is flat against the airfoil surface with no significant voids in its interior. However, during fabrication of the low-temperature rubber boot, there are enclosed, unbonded sections included (resembling knife slits) which are completely surrounded by the elastomer. These slits are in between and in parallel with a series of high-voltage ribbon conductors embedded in the rubber.

When a bank of capacitors in the power supply is discharged into the conductors in a zoned-sequence pattern, the large pulse of electricity



Icing wind tunnel test of NACA 0012 airfoil with ice accreted in 120-knot airstream

(about 3000 amperes discharged in less than a few tenths of a millisecond) suddenly induces these conductor pairs to repel one another with a violent and powerful force. This force causes the slit-voids to expand vigorously (as in the rug-snapping simile) to throw off any ice buildup. The voids immediately collapse again owing to the elastic rebound of the boot material, and thus the operation cycle has virtually no adverse effect on aerodynamic performance because of the rapidity of its action.

This Ames innovation uses one-thousandth of the power of electrothermal deicers and weighs one-tenth as much as existing systems. Numerous icing wind tunnel tests and flight tests have demonstrated its capability to remove ice ranging from the thickness of frost to an inch or more of glaze ice. Further, the tests demonstrated the efficacy of the device to function as an anti-icer (with frequent pulsing) as well as a deicer.

Although originally focused at helicopter use, the Navy is the first to recognize this concept's use for high-performance aircraft. An accelerated Navy-funded program has been under way to develop the Electro-Expulsive Deicer System for application on the F/A-18 Hornet and the V-22 Osprey. Successful icing flight tests on the Hornet have provided the Navy with sufficient confidence in the system to warrant procurement consideration.

(L. Haslim, Ext. 6575)

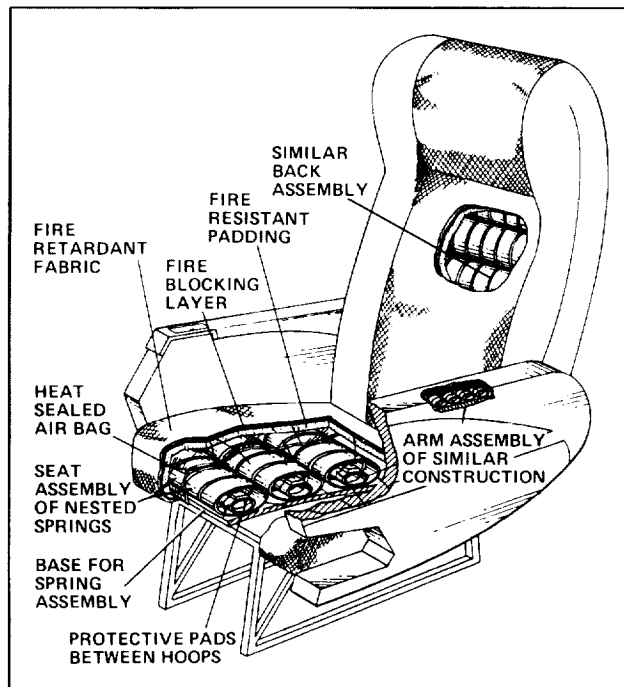


Accreted ice pulverized into airstream, 20 milliseconds after impulse

ORIGINAL PAGE
BLACK AND WHITE PHOTOGRAPH

Lightweight, Fire-Retardant, Crashworthy Aircraft Seat Cushioning

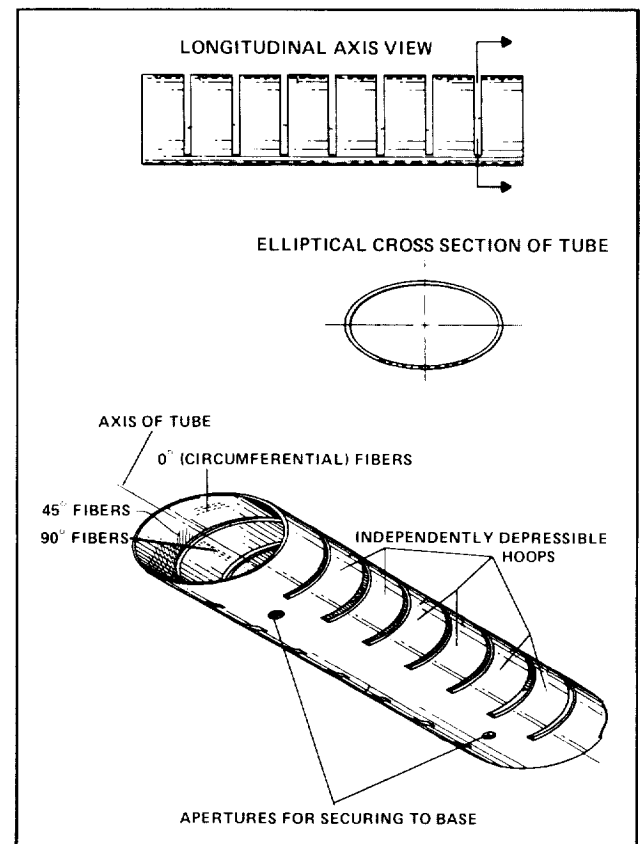
The recently patented fire-retardant aircraft seat cushioning provides both comfort and safety. The seat design consists of central elliptical tubular spring supports made of fire-resistant and fatigue-durable composites surrounded by a fire-blocking sheath. The cushioning is made crashworthy by incorporating energy-absorbing, visco-elastic layers between the nested, elliptical-hoop springs, a highly desirable feature for helicopter application. The design is intended to provide comfortable seating that meets aircraft-loading requirements without using the conventional polyurethane foam materials. Polyurethane foams emit lethal hydrogen cyanide gas and other toxic vapors when combusted.



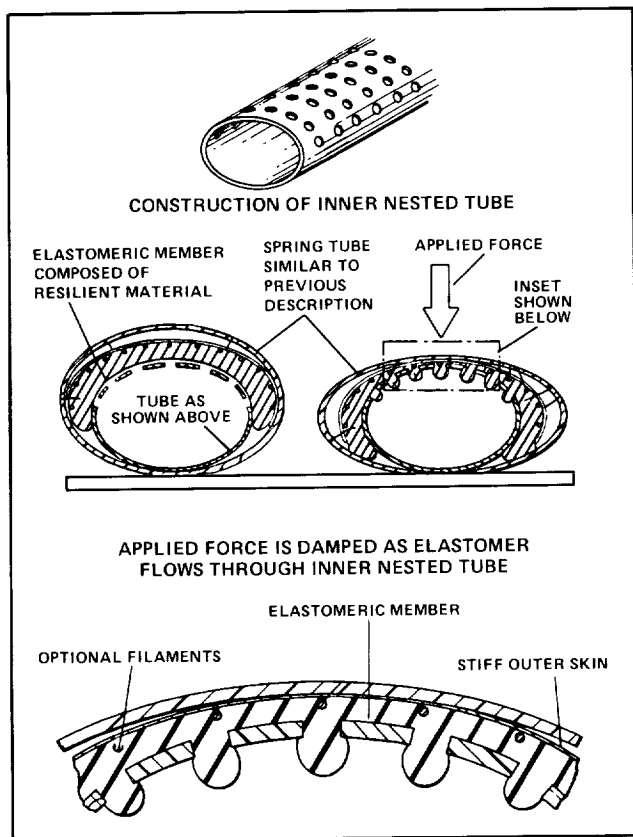
Aircraft seat

Aside from its fire-resistant and energy-absorbing characteristics, the seat cushion is lightweight, economical and simple to fabricate, easily maintained, and structurally strong. The first prototype cushioning is being fabricated, in anticipation of rigorous fire-testing by the Federal Aviation Administration. While the immediate development thrust is focused on acceptance of the cushioning as a standard for civil aircraft seat design in the near future, this novel concept is attracting significant automotive interest as well.

(L. Haslim, Ext. 6575)



Basic spring unit composed of a fabric reinforced composite



Nested springs used with inner elastomeric lining

Lightweight, Telescoping Rescue Boom for Helicopters

The HH-65A Dolphin helicopter entering the U.S. Coast Guard inventory does not have the capability of landing in water that its predecessors had. This shortcoming frequently requires crew members to jump into the open sea during a rescue, thereby increasing the overall risk. To improve the effectiveness and utility of their search and rescue helicopters, a Memorandum of Agreement exists between NASA and the Coast Guard to develop a concept for a lightweight, telescoping rescue boom for these helicopters. Ames Research Center has contracted with a leading helicopter corporation to fabricate a prototype version of the Ames rescue boom for flight-testing on the Dolphin.

Modern composite technology is used to achieve the desired properties. The retractable boom is designed to project the existing rescue hoist cable end to the front of the helicopter, within the pilot's

vision and beyond the main rotor's downwash. Upon engagement, the cable falls free from the extendable boom and is winched up in the conventional manner. Design provisions permit the boom to pivot from the longitudinal axis to the 30°, 45°, and 90° starboard positions as needed. The 90° position coincides with the rotorcraft's main door, where the crewmember can assist in the rescue. For rescues where tip-path obstructions exist (ship masts, bridges, buildings), the boom may be extended an additional 3 meters beyond the normal extension. Angled red and green light beams, projecting horizontally, are used to triangulate the proper safe distance (e.g., where they coincide) from the rotor tip to effect the rescue.

This device is expected to greatly improve the capabilities of rescue helicopters encountering conditions such as rough seas, mountainous terrain, and even high-rise building fires.

(L. Haslim, Ext. 6575)

U.S./Canada STOVL Technology Program

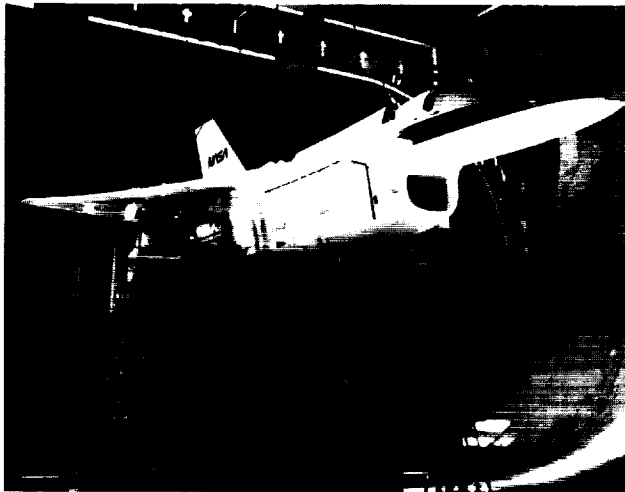
NASA, the Department of Defense Advanced Research Projects Agency (DARPA), and the Canadian Department of Regional Industrial Expansion (DRIE) are conducting a program to investigate the aerodynamics and propulsion characteristics of a full-scale model of General Dynamics' E-7 short takeoff and vertical landing (STOVL) aircraft. The program will have two phases. Phase I, the current activity, is the result of a Letter of Agreement between NASA and DRIE. In Phase II, under a DARPA/DRIE Memorandum of Agreement, a GE F110 engine will be installed in the model and an investigation and validation of a flight/propulsion-control system will be made at Lewis Research Center. It is anticipated that further wind tunnel investigations also will be performed at Ames Research Center.

The model, powered by a Rolls Royce Spey 801-SF engine, is presently installed in the 40- by 80-Foot Wind Tunnel in preparation for its initial tests. The accompanying figure shows the model during its installation in the tunnel. Subsequent investigations with this model will be done in the 80- by 120-Foot Wind Tunnel and at the Outdoor Aerodynamic Research Facility.

In hover, the aircraft thrust will be generated by chordwise ejectors on either side of the fuselage in the wing-root area. These ejectors will be fed by the engine-fan air at a pressure ratio of approximately 3.0, and by an aft-engine core thrust which is vectored vertically. In the cruise mode, the fan air will be directed aft through a second nozzle and the ejector areas closed by fairing doors. The core thrust will be vectored horizontally. The aircraft is designed to have a supersonic dash capability.

A program review of Phases I and II was held in Ottawa, Canada, in May 1988. Both government and industry participants gave status reports on their ongoing and planned activities.

(C. White, Ext. 5653)



Model of E-7 STOVL aircraft during installation in the 40- by 80-Foot Wind Tunnel

Aviation Technology Applicable for Developing Countries

Analysis of aviation technologies useful in formulating aviation or development plans to the year 2000 for the emerging countries of the world has been completed and a report has been drafted. The Caribbean Basin was used as a specific application.

Aviation technology was organized in the following categories: current technology in the region, applicable technology used in other regions, significant trends in technology, and technology issues regarding developing regions. Categories covered in

"The Significant Trends in Technology" section were next-generation conventional takeoff and landing aircraft, general-aviation aircraft, rotorcraft applications, rotorcraft technology, lighter than air, used aircraft upgrading, and computer/satellite advances.

The rapid growth of aviation technology and passenger and cargo traffic that has occurred in the past is projected to continue. These aviation technologies, if planned for and properly used in developing regions, offer the possibility of "leapfrogging" current technology to arrive in the 21st century and bypassing many of the major costs involved in present technology (such as extensive air traffic control ground infrastructure; new and extended airports; and road, rail, port, and communication systems in remote areas).

The next-generation transport aircraft, with improved infrastructure and management methods, will provide lower cost air transportation to the region from the United States and the rest of the world. The new short-haul air-transportation capability, if looked at from an overall systems and intermodal viewpoint, can offer many unique economic development opportunities. Satellite technology will enable rapid, economical capabilities in areas such as navigation, communications, weather forecasting, training, and maintenance assistance.

(J. Zuk and L. Alton, Ext. 6012)

Real-Time Simulation Computer Replacement

Ames' Simulation Laboratory (Simlab) has acquired a very fast real-time computer, the AD 100, to perform very high frequency math model computations. The AD 100 and associated computers are being integrated into the simulation facilities with the objective of their being operational within 6 months after acceptance from the vendor. A second constraint is that the operational system must meet a set of baseline requirements established by the user community.

The AD 100 is a fast (20 million floating-point operations per second) computer with a large (16-megabyte) data memory, and an integral input/output (I/O) capability. The I/O system contains an input/output control processor (IOCP) which operates

ORIGINAL PAGE
BLACK AND WHITE PHOTOGRAPH

in parallel with the AD 100 to provide an efficient means for handling real-time, hardware in-the-loop requirements.

The two main tasks for this project are to interface this IOCP with the existing Simlab remote I/O system and to convert the existing FORTRAN simulation programs and support software to the AD 100 programming language called ADSIM.

The AD 100 was accepted from the vendor in August 1988. The project is on schedule to complete the integration into Simlab in January 1989. The IOCP has been interfaced with a test bed consisting of Simlab I/O hardware through a VME interface. Most of the simulation support software is coded, checked out, and running on the AD 100. The math model for the first aircraft simulation has been coded, and the aircraft performance has been verified in static conditions. Checkout of the dynamic phase is imminent.

The introduction of the AD 100 computer into the Simlab will allow complex real-time simulations to be solved at much faster rates than were previously possible. This will improve fidelity by allowing higher-frequency-content models to be simulated.

(D. Astill, Ext. 6171)

Neural Network Architecture

Multidimensional pattern-recognition problems, such as the ones arising in machine vision and navigation, require massive information storage and processing capabilities. Recent advances in neural network technology suggest that such problems may be more effectively solved by these parallel processors than by conventional sequential computers. However, previously proposed neural network structures, based on fully connected neurons have been

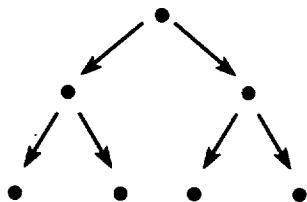
shown to have limited capabilities. Rosenblatt's original perceptron (1960), based on one-way communication between neurons, has been shown to lack a reliable pattern-recognition capability. However, a more recent structure based on a two-way communication, proposed by Hopfield (1982), has been shown to have a very limited information-storage capacity.

Recent research at Ames Research Center has shown that the main deficiency of the Hopfield model is in the full connectivity assumed to exist between the neurons, which are the information-processing units of the network. New network structures, which consist of interconnected nested subnetworks (each comprising relatively few fully connected neurons), have been proposed.

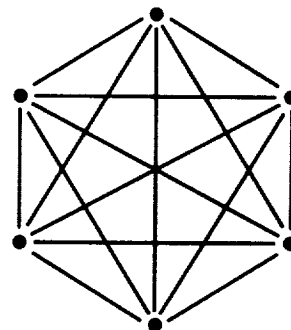
A nested network structure is shown in the attached figure. For comparison, the connectivity concepts employed by the Rosenblatt and the Hopfield models are also shown. The nested network structure consists of four layers of subnetworks corresponding to different spatial frequencies, each comprising five interconnected neurons. (For graphical clarity, not all the interneuron connections within a subnetwork are shown.) The nested structure allows for the storage and retrieval of subpatterns of different sizes, which may constitute meaningful information in their own right or may jointly form larger patterns. Storage of only a few subpatterns in each subnetwork results in a large storage capacity of patterns and subpatterns in the nested network, so the network maintains its high stability and error correction capability.

Future research will further examine the capabilities of the proposed network structures as associative memory and pattern-recognition devices and their applications to machine vision and navigation.

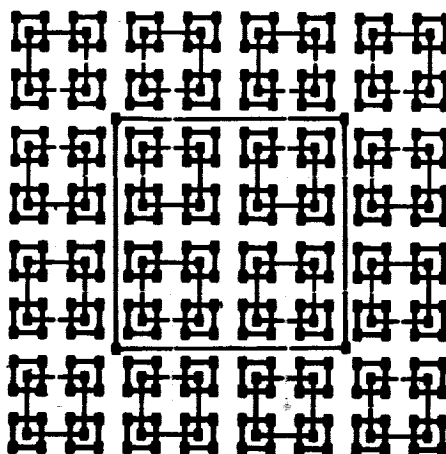
(Y. Baram, Ext. 5427)



ROSENBLATT'S PERCEPTRON (1960)
ONE-WAY CONNECTIVITY



HOPFIELD'S NETWORK (1982)
TWO-WAY, FULL CONNECTIVITY



NESTED NEURAL NETWORK
PARTIAL, TWO-WAY CONNECTIVITY

Neural network architectures

Obstacle Avoidance

Obstacle avoidance is the lowest-level function of the automatic-guidance structure conceived for nap-of-the-Earth (NOE) rotorcraft flight. The objective of this function is to track a reference trajectory provided by the higher-level path planners using INS data, while simultaneously making decisions to deviate from the reference trajectory to avoid obstacles revealed by the obstacle-detection subsystem.

Obstacle avoidance represents the only guidance function that uses online information of the out-

side world; consequently, it is a critical component of automated NOE flight. Methodologies developed for the obstacle-avoidance function will also be useful to other industrial (e.g., mobile robots); civil (e.g., planetary rovers and civil aircraft amid thunderclouds); and military (e.g., autonomous land vehicles) applications. In spite of the similar needs of these other applications, the obstacle-avoidance techniques studied under these applications have been limited to situations in which the obstacle information exceeds that available in the NOE rotorcraft situation.

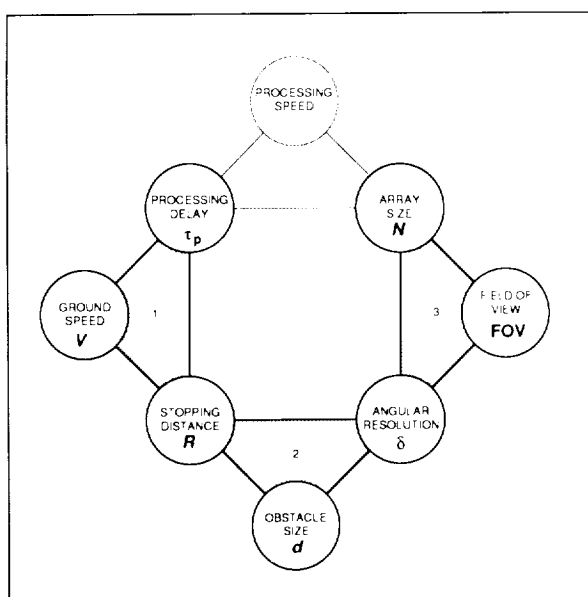
ORIGINAL PAGE
COLOR PHOTOGRAPH

Functional analysis of generic sensor requirements has been carried out to establish sensor capabilities required for rotorcraft NOE flight. The approach emphasizes systematic deductions based on clearly stated assumptions. In that way, controversial conclusions based on conflicting assumptions can be easily resolved. The analysis has led to the conclusion that automatic NOE flight in a hostile environment can benefit the most from a carefully designed obstacle-detection system which involves both active and passive sensors.

The analysis has also identified the nature of obstacle information available to the obstacle-

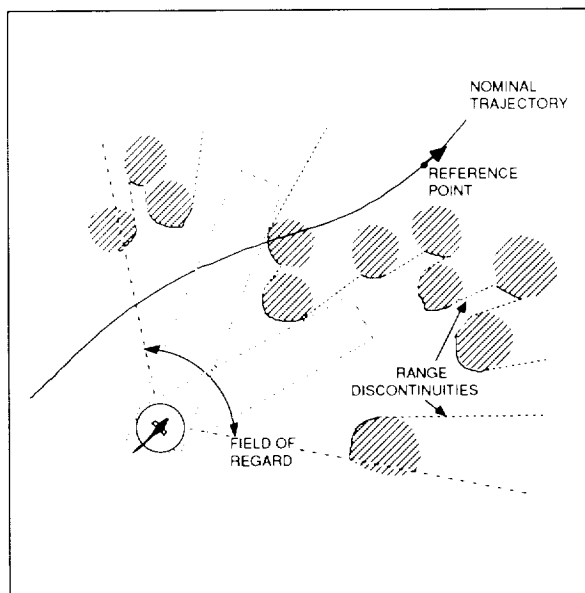
avoidance function. A guidance concept that observes such limitations is being developed and its viability has been verified in a two-dimensional framework using computer simulations. The subsequent effort is to develop the full three-dimensional guidance algorithm, and to test it with detailed simulations, including realistic dynamic and sensor models.

(V. Cheng and B. Sridhar, Ext. 5424/5450)



FUNCTIONAL ANALYSIS OF SENSOR REQUIREMENTS VIA VARIABLE DECOUPLING

1. VEHICLE PERFORMANCE
2. OBSTACLE CHARACTERISTICS
3. SENSOR PARAMETERS



GUIDANCE STRATEGY

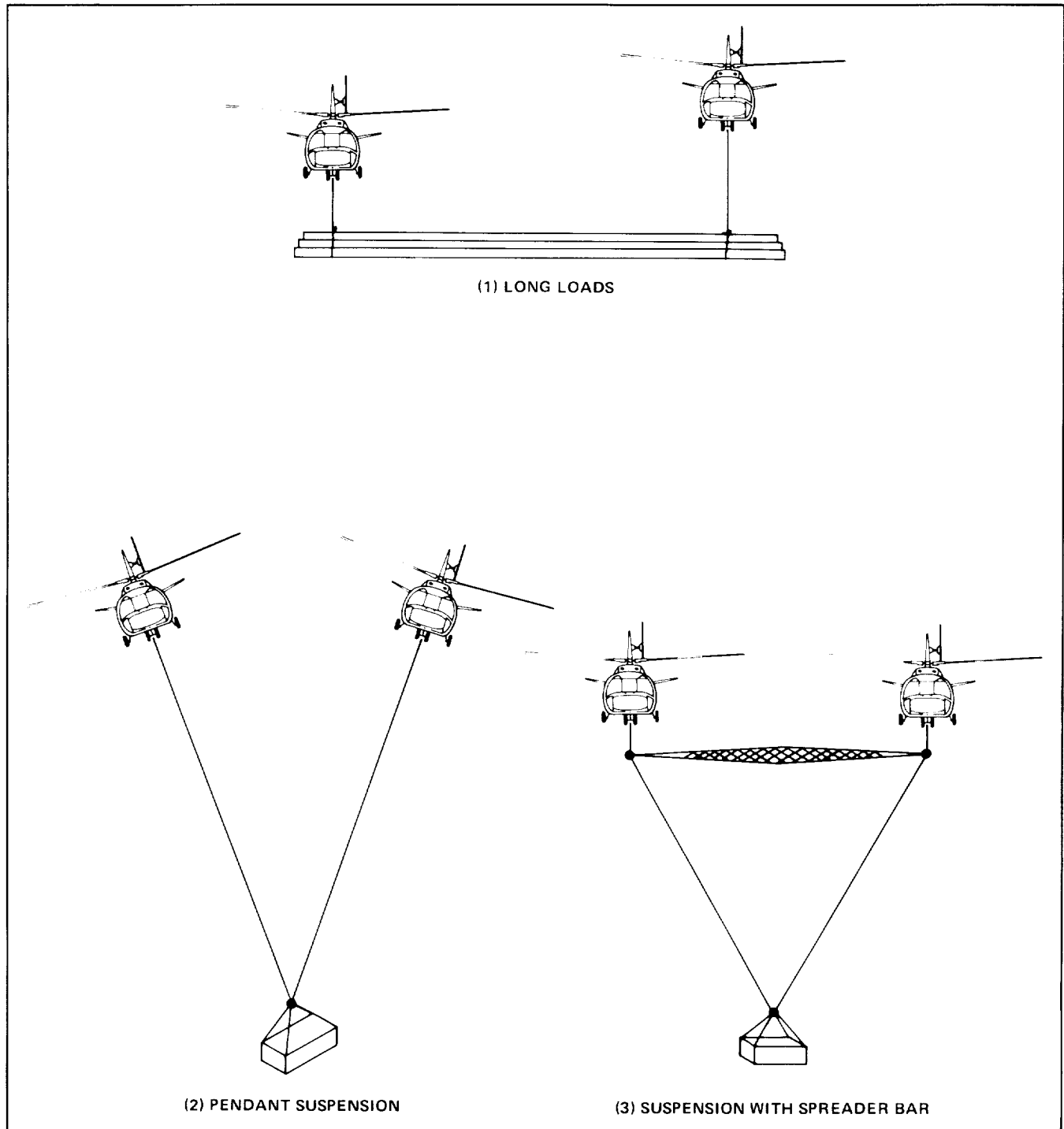
- TRACK REFERENCE POINT ON NOMINAL TRAJECTORY
- AVOID OBSTACLES BY GOING "AROUND" THEM
- DETECT POTENTIAL OPENING BASED ON RANGE DISCONTINUITIES

Obstacle avoidance

Dual-Lift Helicopter Slung-Load Systems

A study to derive simulation equations for dual-lift systems has been successfully completed. The

development of a suitable trajectory-control system is seen as the principal task in achieving operational feasibility of dual lift, and this motivates the effort to obtain a system model for analysis and simulation. Simulation equations which are valid for general flight



Dual-lift systems

conditions and which exactly represent the rigid-body dynamics of the constituent bodies have not previously been available.

The dual-lift systems of current interest (see figure) are examples of slung-load systems. In general these can be adequately modeled as systems of n rigid bodies connected by straight-line links or cables which carry force along the link only and are otherwise massless with no external forces. Simulation equations representing all such systems were derived from d'Alembert's principle. Three formulations are given which account for elastic or inelastic cable models and for any appropriate choice of the generalized coordinates representing the system's degrees of freedom.

If the cables are modeled as inelastic, then constraints are imposed (c in number) and the number of degrees of freedom is $d = 6n - c$. Previous methods of deriving simulation equations led to the required inversion of a $d \times d$ matrix ($d = 20$ for the dual-lift system (3) shown in the figure) for which an analytical inverse is unknown. A method has been found which requires the inverse of a much smaller $c \times c$ matrix ($c = 4$ for the dual-lift system (3)).

Results have been obtained for the 3 dual-lift systems of the figure. Equations for elastic or inelastic cable models for all three systems are readily integrated in a single simulation. Additional results for single helicopter systems have been obtained for comparison with previous work on slung-load simulations.

(L. Cicolani, Ext. 5446)

Ames' Crew Station Research and Development Facility Upgrade

The computer-generated imagery system on the Crew Station Research and Development Facility (CSRDF) is being upgraded from a Singer Link System to a General Electric Compuscene IV. Acceptance of the fully integrated system is scheduled to occur in the spring of 1989.

The CSRDF, a joint development program with Ames Research Center and the U.S. Army Aeroflightdynamics Directorate, was accepted in September 1987. The Singer System, on loan to Ames from the U.S. Army, was integrated into the

CSRDF as part of the initial delivery. In January 1988 the Singer System was returned.

A General Electric Compuscene IV was selected to replace the Singer System. In addition to providing sufficient scene capacity to concurrently display 15 moving models (as well as projectiles, articulated parts, and weapons effects), the system also provides hardware-generated texture. This texture capability allows fine patterns to be applied to the polygons that build the scene without affecting the system load. This provides the extremely high resolution, high level of detail in the scene required by low-level flight.

Numerous other features such as video gamma correction, sensor controls, shading, translucency, collision detection, line-of-sight ranging, and weapon impact detection are provided by the Compuscene IV. This upgraded capability will allow realistic simulation of the modern, complex, high-workload environments required in combat-mission scenarios.

(L. Coe, Ext. 6171)



Compuscene IV visual scene in Ames' Crew Station Research and Development Facility

Space Shuttle Simulation

The Space Shuttle program uses the Ames Research Center's Vertical Motion Simulator (VMS) to study Shuttle handling qualities and control systems during landing and rollout. The simulation conducted during July and August 1988 addressed the following objectives:

ORIGINAL PAGE
BLACK AND WHITE PHOTOGRAPH

1. to confirm flight rules and STS-26 baseline systems,
2. to examine the effects of new hardware models and crosswind landings, specifically tire-failure modeling,
3. to continue design and integration studies of the baseline system + direct control + redundant nose-wheel steering + carbon-carbon brakes,
4. to provide systems evaluation and proficiency training for the crews.

During this 6-week simulation, 1725 approaches and landings were performed, with 10 orbiter configurations, having gross weights of from 185,000 to 256,000 pounds. The new models incorporated and studied included tire failures, nose-wheel steering (NWS), and tire wear. Subsystems examined included the flight-control system, tires, drag chutes, carbon-carbon brakes, and beryllium brakes.

Earlier simulations of the Shuttle have used the Ames-developed computer-generated visual data bases of the Edwards Air Force Base, Kennedy Space Center, and Dakar landing sites. The four new visual data bases (all for transatlantic sites) constructed for this investigation were (1) Benguerir, Morocco; (2) Banjul, Gambia; (3) Zaragoza, Spain; and (4) Morón, Spain.

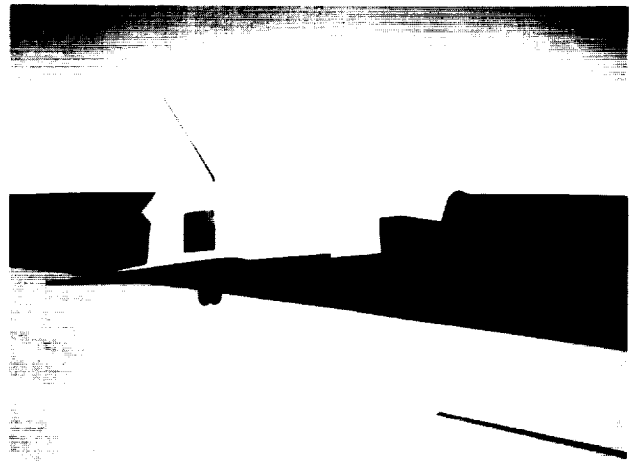
In addition to the STS-26 crew, the pilots of STS-27 through STS-31 and 23 other pilot-astronauts were provided evaluation and familiarization flights.

Specifically for STS-26 flight rules, it was determined that, for the nominal system, handling qualities were Level 1 (satisfactory) for crosswind peaks of less than 12 knots.

For the new hardware-failure models, the study identified the worst-case tire-failure scenarios, and determined that the present NWS system will not handle all tire failures for crosswind conditions greater than 15 knots, particularly for landing weights equal to or exceeding 240,000 pounds. Manual switching for redundant NWS was considered to be acceptable.

It was determined that the drag chute reduced loadings on all other rollout systems, but that, initially, there is a requirement for deploying the drag chute in the reefed configuration.

All the test objectives of this simulation were met, with an extremely high overall simulation system reliability of 90%.



Ames' vertical motion simulator computer-generated image of Space Shuttle

A follow-on Shuttle simulation is scheduled on the VMS for April 1989. At that time we intend to conduct further study of NWS control laws for heavyweight vehicles, drag chutes, carbon-carbon brakes with the antiskid system in the simulation loop, and the integration of the above three systems.

(A. Cook, Ext. 5162)

Vertical Motion Simulator Upgrade Project

The vertical motion simulator (VMS) at Ames Research Center was returned to service in July 1988 after extensive upgrade modifications to the motion-generation system. The VMS is a large, 6-degree-of-freedom (6-DOF) flight simulator used for various aerospace research programs, from fixed-wing aircraft and rotorcraft to the Space Shuttle. Because unique performance capabilities were needed for rotorcraft simulations, an Army-funded project defined and developed a new 4-DOF motion generator with improved performance capabilities. This hydraulically actuated, 4-DOF system has been integrated with the VMS to give a fully independent, 6-DOF motion-generation system.

The improved motion capabilities (1) include the addition of an independent longitudinal degree of freedom, and (2) more than double the maximum accelerations attainable in the three rotational axes.

ORIGINAL PAGE
BLACK AND WHITE PHOTOGRAPH

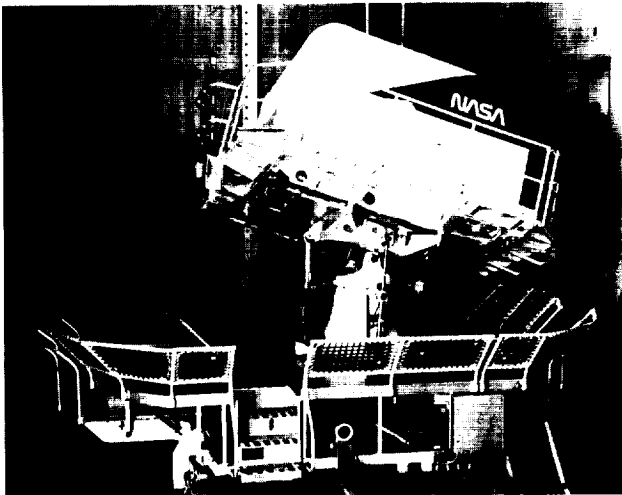
This new 4-DOF system sits atop the lateral carriage, which sits upon the vertically moving beam of the VMS. A cone-shaped structure is mounted on the longitudinal carriage and rotates about the vertical axis to provide yaw. The pitch and roll motions are provided by a gimbal assembly atop the cone structure. All three rotations are driven by hydraulic servo actuators. The simulator cockpit is then mounted on top of the gimbal.

The VMS upgrade project was a major, coordinated effort over a 2-year period, with much of the design effort and subsystem fabrication accomplished before that.

The VMS was taken out of service for only 1 year for hardware installation and integration. During this time, several other refurbishment and upgrade tasks were also accomplished to improve the overall VMS capability.

The new motion system interfaces with the previously existing motion platform and with the system of interchangeable cabs. Because of this compatibility, the improved performance capabilities are now available to all Ames and national research programs such as Space Shuttle, MV-22, C-17, Light Helicopter, Experimental, and numerous other research and development investigations.

(A. Cook, Ext. 5162)



Upgraded four-axis motion system on the Ames vertical motion simulator

Simulator Evaluation of Controller Tools

The effectiveness of automation aids for air traffic management and the effect of such aids on airline operations was recently evaluated in a combined air traffic control and piloted simulation at Ames Research Center. The initial evaluation concerned the use of the Descent Advisor, an automation aid for arrival traffic management at an Air Route Traffic Control Center (ARTCC).

The objective of this study was to assess the effectiveness of Descent Advisor tools in sequencing and spacing arrival traffic. Under various traffic conditions, nine subject controller teams used Descent Advisor tools developed at Ames to solve a range of traffic management problems such as

1. predicting aircraft arrival times,
2. meeting spacing requirements at a feeder fix,
3. resolving spacing conflicts at the fix,
4. merging traffic vectored off route into the traffic flow on standard arrival routes,
5. correcting time errors accumulated by individual aircraft during their descent.

In addition, the controllers were asked to evaluate other aids such as the use of multiple colors in the display, a mouse input device for interaction with



Training controllers to use the Descent Advisor automation aid

ORIGINAL PAGE
BLACK AND WHITE PHOTOGRAPH

the Descent Advisor tool, menu-driven controller functions, and a graphical timeline that displayed current traffic time schedules to the fix. The overall response from the subject controllers was strongly favorable. The controllers found the Descent Advisor to be an effective aid that reduced workload and allowed them to initiate control strategies earlier in the approach than is possible without this tool.

The Man-Vehicle Systems Research Facility Boeing 727 simulator was linked, via voice and data link, with Advanced Concepts Air Traffic Control Simulation. The simulator provided a realistic measure of the time precision that current airline crews could achieve at a feeder fix by following profile descent advisories issued by controllers using the Descent Advisor automation tool. In addition, the pilots evaluated the acceptability of the advisory-assisted descents. Other issues addressed were mid-descent advisories to correct any accumulated error in the descent, the effects of different wind conditions on pilot performance, and procedures for route intercepts during descent.

A total of 29 airline crews participated in the simulation and executed 180 descents that spanned the entire speed envelope of the 727 aircraft. Preliminary results show most aircraft that were following the controller's advisory arrived at the feeder fix within 30 seconds of their scheduled arrival time. Previous experiments showed that pilots who were executing pilot-discretionary descents could only be expected to arrive at the fix within 100 seconds of their scheduled time, which is inadequate for optimal traffic flow. In addition, a mid-descent correction procedure was demonstrated that eliminated virtually all error in arrival time. The pilots were enthusiastic in their support of the concept and could foresee no major operational problems in executing advisory-assisted descents.

In a followup simulation now being conducted, a terminal radar control position and a flow-management position will be included; in addition, Langley Research Center's TSRV 737 four-dimensional-equipped piloted simulator will be connected to the Air Traffic Control simulation via transcontinental voice and data links.

(T. Davis and L. Tobias, Ext. 5452/5430)

Satellite-Based Navigation

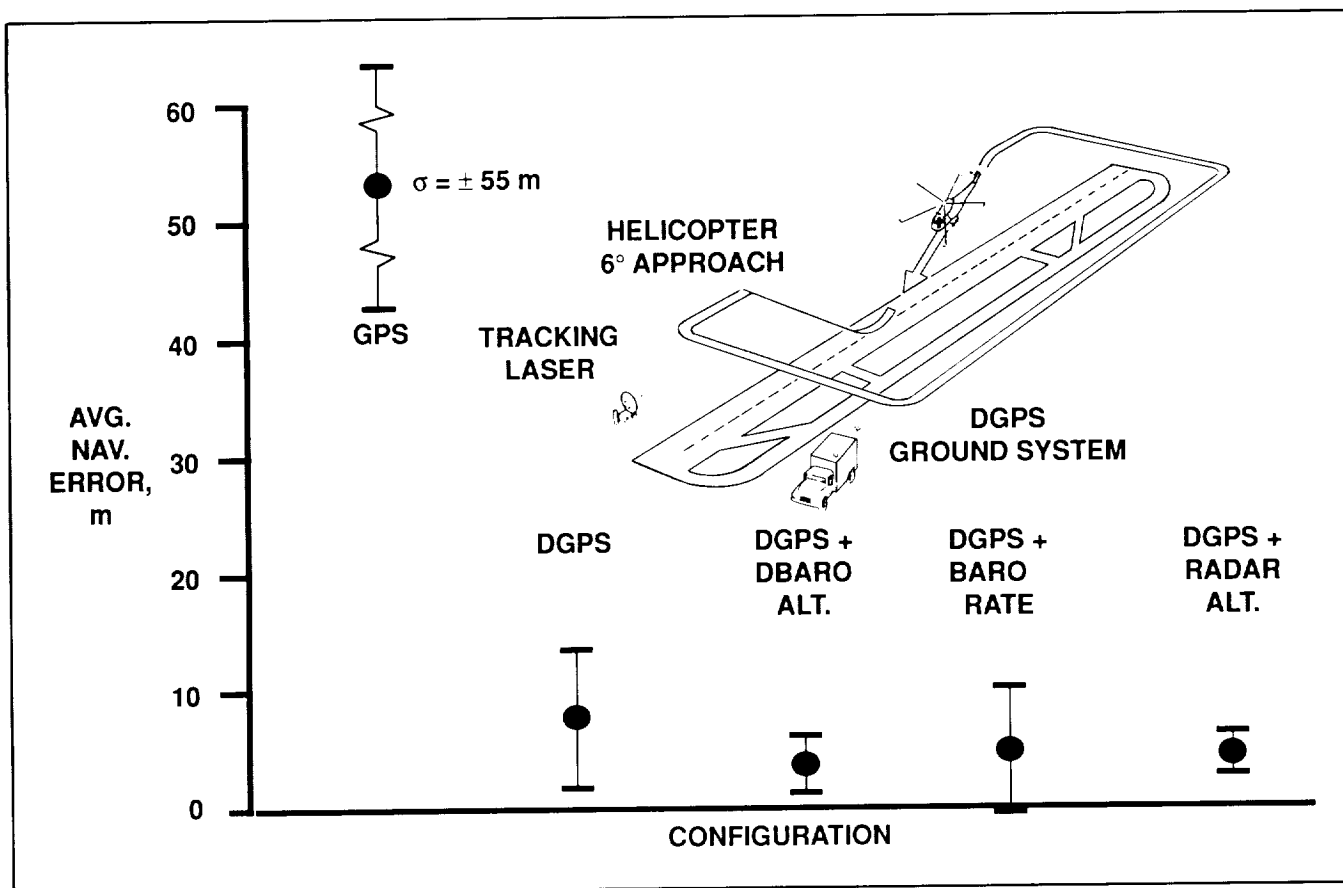
The objective of this research is to evaluate the use of the NAVSTAR Global Positioning System (GPS) to support helicopter automated low-altitude aircraft operations and helicopter nap-of-the-Earth (NOE) flight.

A particularly attractive alternative mechanization of GPS is differential GPS (DGPS), which provides significant improvements in performance when compared to a conventional GPS. A major attribute of DGPS for NOE helicopter flight is that it does not require a direct line of sight between the helicopter and the ground station because correction signals can be relayed through a satellite link. The additional performance obtained may prove sufficient to support precision hover, and autonomous low-altitude flight, instrument approach, and landing operations into areas not currently served by ground-based guidance aids. Offshore explorations, operations into remote and mountainous terrain, and inter- and intra-city emergency medical rescues are examples of helicopter missions that can be supported by differential GPS.

An in-flight evaluation of the DGPS concept using the civil, coarse acquisition signal (C/A code) was completed in FY 1987. The airborne and ground-based components for the concept were developed and successfully flight-tested, incorporating real-time differential corrections that were data-linked from the ground station. A reconfigurable navigation algorithm in the airborne computer was programmed to accept inputs from various on-board sensors to improve the vertical axis performance. During the past year these data have been analyzed.

A summary of the vertical axis performance for several system configurations is shown in the figure. The results show that significant improvement in performance can be obtained by including a differential barometric altitude correction (DBARO) with the GPS range correction in the uplinked information.

Ames Research Center is utilizing the theoretical and experimental studies conducted under the previous DGPS Helicopter Terminal Approach Program to evaluate the relative performance of various GPS precision-code concepts. An appropriate concept will be selected for development on a NASA flight-



Differential Global Positioning System C/A code vertical axis performance

test vehicle to support the automated NOE test program. Performance of the candidate system will be evaluated through simulation and ground and in-flight testing.

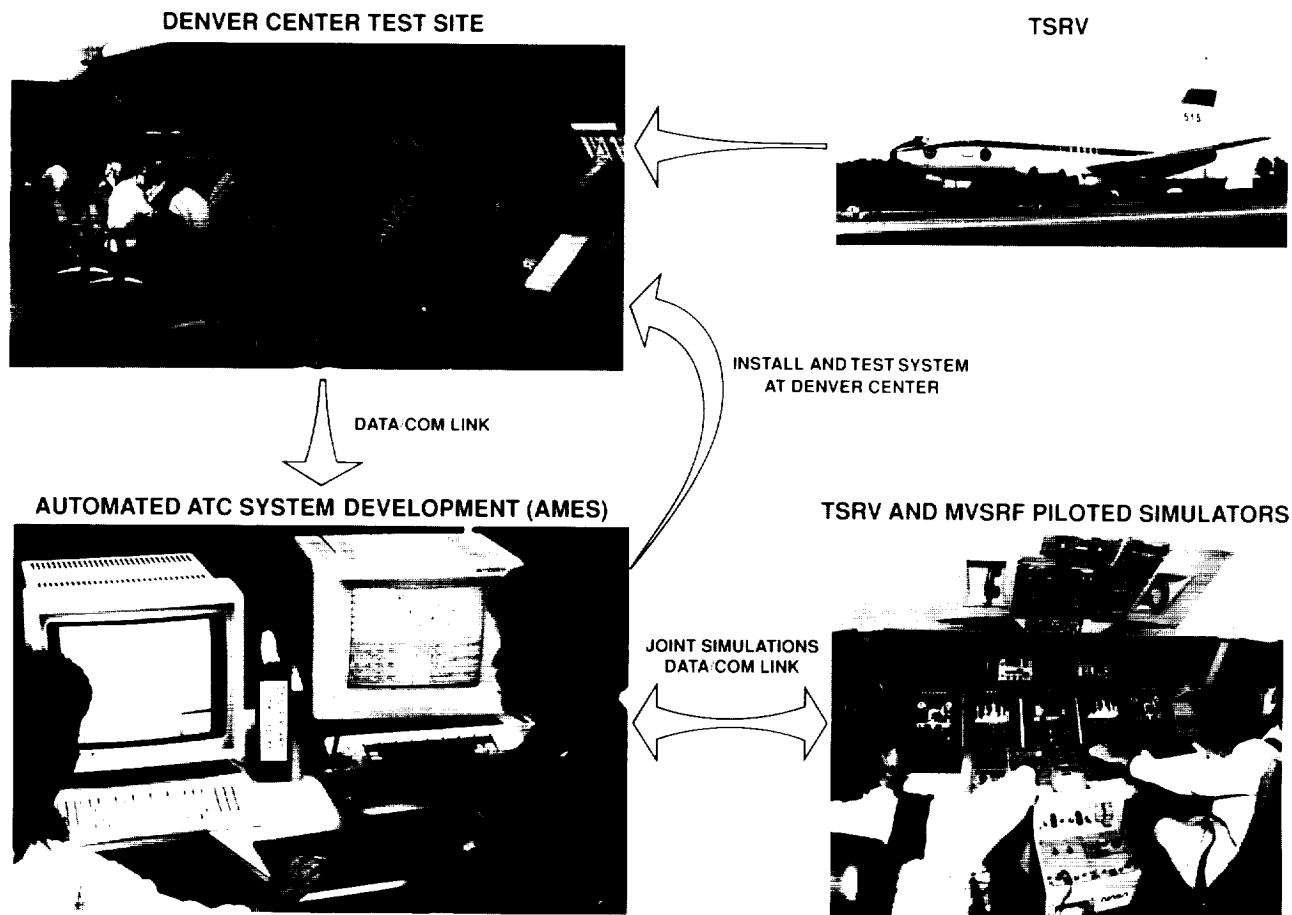
Future plans include

1. the examination of the GPS and the inertial navigation system for precise flightpath control during rotorcraft low-altitude precision hover and NOE flight,
2. the evaluation of Precise Positioning Service differential GPS to support fixed-wing aircraft terminal-approach operations,
3. the development of integrity-monitoring tools for the differential GPS ground-reference system to detect GPS system anomalies and alert users more quickly.

(F. Edwards, Ext. 5437)

Air Traffic Control Simulation and Development Facility

An indispensable element of a comprehensive research program in air traffic control (ATC) automation is a facility for realistically simulating ATC concepts and validating automation software. A second generation of such a facility (originally developed at Ames Research Center in the 1970s) recently was put on line and played a key role in the May 1988 real-time simulation of the Descent Advisor automation tool. In addition to providing a controller-interactive simulation environment, the facility also has been designed for validating automation systems that are to be tested in a live traffic environment at an ATC center.



NASA-FAA automated air traffic control tests

Essentially, the new facility consists of an interconnected network of color graphics workstations and a file server made by Sun Microsystems. During the running of a real-time simulation, the workstations are configured as radar controller suites (which also host the automation tools) and as pseudopilot stations. Each pseudopilot station can simulate the flights of 10 to 15 aircraft in real time. The pseudopilot stations model aircraft performance realistically, and they provide an extensive set of simple and compound autopilot and navigation modes, including so-called four-dimensional (4-D) flight management. The pseudopilots receive clearances and vectors from the controller and enter them into the pseudopilot station, thus simulating pilot response.

The facility includes a prototype version of the future Sector Suite Display, which is the key component of the Federal Aviation Administration's Advanced Automation System. This 20- by 20-inch superhigh-resolution color graphics system made by Sony has been integrated into the Sun network. The display will be used as an enroute or terminal radar controller station during the next simulation scheduled for early FY 1989.

A new six-channel voice communication system and a data link connect the facility to the Boeing 727 piloted simulator located in the Man-Vehicle Systems Research Facility (MVSF) at Ames. A similar voice and data-link connection has also been established with the TSRV-737 simulator at NASA Langley Research Center. The participation of piloted aircraft

simulators in an ATC simulation is required when pilot operational procedures are at issue.

The facility is designed to interface with and display live traffic data from the Denver Air Route Traffic Control Center at Longmont, Colorado. Special modems are located at each site, and a 15-kilobyte lease line has been installed to send the data from the Denver Center to the Ames facility. The data link is now feeding live ATC data into the facility.

Access to the live data at the Ames facility will play a crucial role in the development of test systems for the Denver Center as well as in basic research. Thus, comparing the simulated and live traffic flows will help to assess the fidelity of the ATC simulation. Also, researchers at Ames will be able to observe traffic flows at any time, so they can capture infrequent or unusual traffic conditions such as those caused by a rapidly moving weather front. However, the most important use of the live data will be for expediting software validation of test systems before their installation at the Denver Center.

(H. Erzberger, Ext. 5425)

Graphical Interface for Air Traffic Control Automation Tools

Ames Research Center, in a cooperative program with the Federal Aviation Administration, is conducting research on automation tools for managing terminal-area traffic. A major challenge in the design of automation tools for air traffic control (ATC) is the specification of an effective interface between the controller and the complex algorithms needed for manipulating aircraft trajectories in space and time, known as 4-D guidance. Although 4-D guidance concepts were originally developed for on-board flight-management systems, researchers at Ames have recently adapted these concepts to various ground-based ATC automation problems.

Work is now focused on exploiting interactive computer graphics methods in the design of the controller interface. A graphical interface for a class of automation tools, collectively called a Descent Advisor (DA), has been implemented on a Sun Microsystems workstation. The DA tools incorporating this interface are designed to assist a radar controller in managing the flow of arrivals at a feeder

gate into the terminal area. Essentially, the interface generates graphical representations of the spatial and time relationships between aircraft converging at the feeder gate. It also permits the controller to issue commands to the DA tools by manipulating a mouse or trackball. These commands, which are accessed through a set of on-screen control buttons, provide time-controlled descent clearances and spacing advisories for selected aircraft.

The photograph shows the controller's display configured for the Denver Air Route Traffic Control Center sectors that direct traffic to the Drako feeder gate. In the scenario illustrated in the figure, the controller has selected DA tools to provide descent information for the two aircraft shown in yellow which are converging on Drako along standard airline routes. The controller has previously specified 10-mile spacing between aircraft arriving at Drako, the point where traffic is handed off to the terminal controller. The appropriate descent clearances to achieve this spacing were calculated and are displayed, along with other information, in the clearance window at the top of the screen.

Thus, XAA404 should start its descent at 59 n.mi. from the Denver VOR (point shown in purple labeled TOD for Top of Descent) and fly a Mach-0.72, 320-knot descent profile at idle power. The DA tool predicts that XAA404 will be the first to arrive at Drako and will be followed by XTA321 at a distance of 10.0 n.mi. behind the leading aircraft.

The spacing distance resulting from these descent and speed clearances is shown by blue markers at and near Drako. The relative time separation and the arrival time of these two aircraft are shown on a so-called time line located at the left side of the screen. The time line, in 1-minute increments, displays the time that the aircraft are predicted to arrive at Drako within approximately the next 30 minutes. Because current time is at the bottom of the screen and future times are near the top, the time scale (along with predicted aircraft arrival times) moves steadily toward the bottom as time passes. The relative time separation at Drako between the two selected aircraft is seen to be about 2 minutes.

The absolute arrival times can also be read off. They come into play when the controller has to deliver aircraft at times specified by a scheduler or metering system. The yellow vertical bars on the time line indicate the arrival time range available by



Graphical interface for air traffic control automation tools

changing the aircraft speed within the flight envelope. Thus, this graphical interface allows the controller to monitor and control the traffic flow either by distance or time spacing criteria.

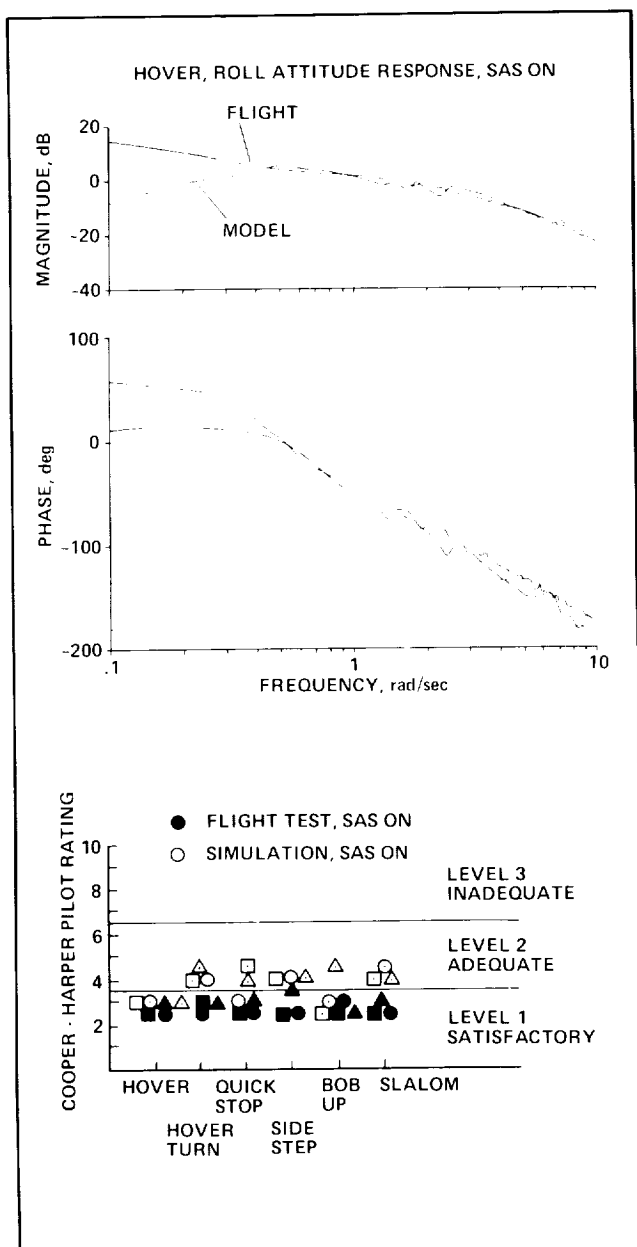
An extensive controller interactive ATC simulation of the DA tools was successfully completed in May 1988. Design is also progressing on an interactive graphics display for a flow-control/scheduling advisor system, which will provide optimized arrival times for display on the time line.

(H. Erzberger, Ext. 5425)

Correlation of A109 Flight Test with Ground-Based Simulation

A 3-year research program to validate a mathematical model of the Agusta A109 helicopter was completed this year. The study was conducted jointly by the United States and Italy under the auspices of the Memorandum of Understanding between the U.S. Army and the Italian Ministry of Defense. The technical work was performed by the U.S. Army Aeroflightdynamics Directorate, C.A.G. Agusta

ORIGINAL PAGE
COLOR PHOTOGRAPH



A109 flight-simulation correlation

(Italy), and the Italian Air Force, along with NASA personnel and facilities at Ames Research Center.

The subject of model validation was chosen because of the expanding role of piloted simulation in both the research community and in industry, wherein the math model is a major element and must be accurate if the simulation results are to be extrapolated reliably to the flight environment.

The A109 model development and validation began with the use of a generic rotorcraft model,

generated previously by NASA for use in real-time simulation, and known as ARM COP. The validation included quantitative time- and frequency-domain comparisons of the model and aircraft response characteristics, as well as subjective piloted comparisons through nap-of-the-Earth flight tests which were repeated in simulation. The results of the validation indicate that the A109 model is quantitatively a good approximation to the real helicopter when the Stability Augmentation System (SAS) is included. However, because of the lack of cues available to the pilot, the total piloted simulation exhibits slightly degraded handling qualities when compared with those seen in flight.

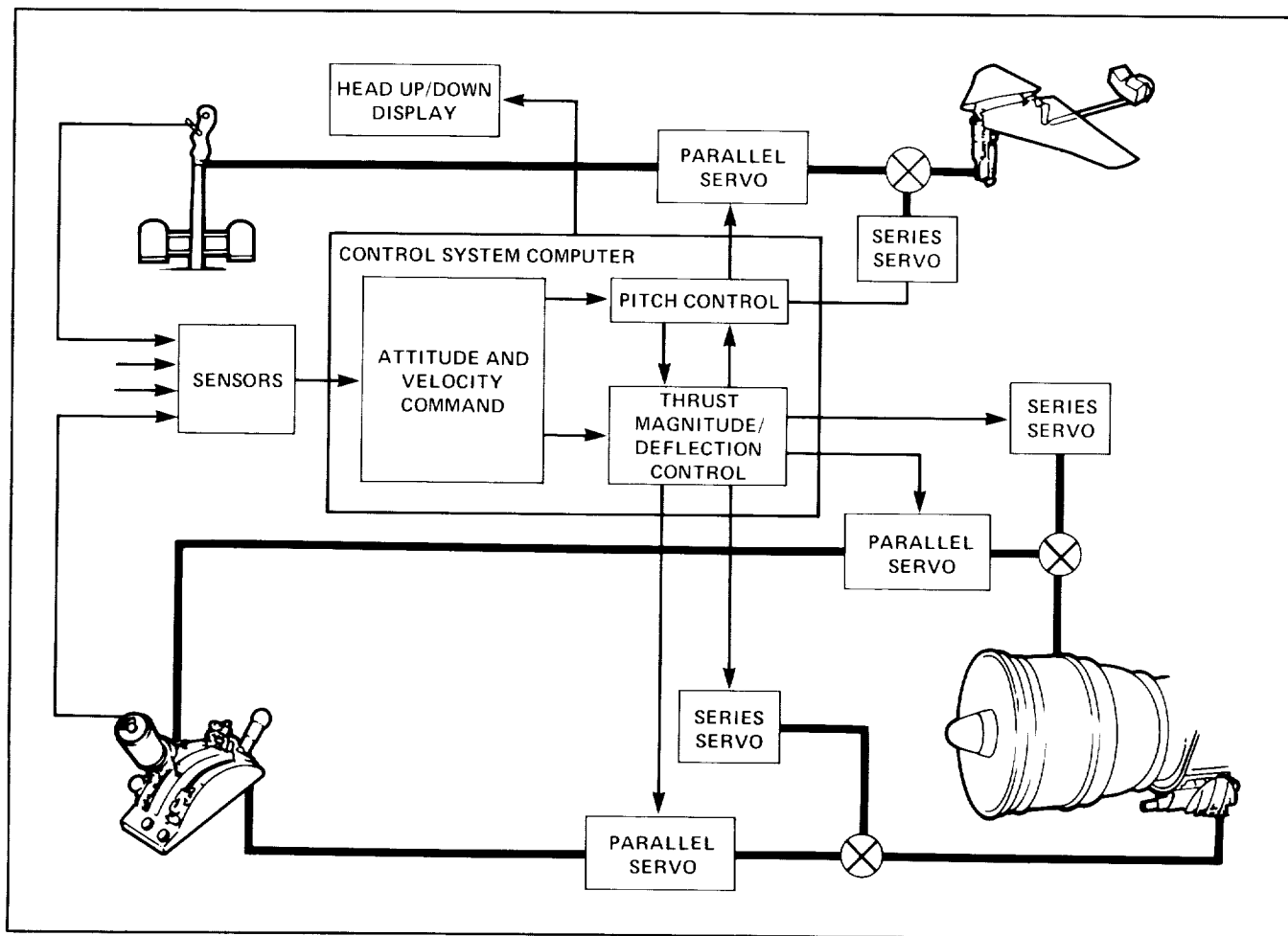
The validated model has been used as the baseline for a handling qualities investigation of centerstick force requirements, in support of Army efforts to develop a new rotorcraft handling qualities specification. The methods used to validate the model have been documented and will be useful in future efforts to validate real-time rotorcraft models for piloted simulation.

(M. Eshow, Ext. 5272)

Integrated-Flight/Propulsion-Control Research on the V/STOL Research Aircraft

The major technological barriers to routine vertical landing operations of vertical and short takeoff and landing (V/STOL) fighter-class aircraft in adverse weather and low-visibility conditions are (1) the complex interaction of kinematics, aerodynamics, and propulsive forces and moments during the conversion from airborne to jetborne flight, and (2) the resulting poor handling qualities and limited control authorities these interactions create. Ames Research Center is conducting a flight research program to integrate the propulsive and aerodynamic controls in ways which provide enhanced flightpath precision and mission capability, but which minimize the design requirements for "extra" propulsive capability (e.g., bleed air requirements).

The Flight Systems and Simulation Research Division is developing an integrated attitude and thrust vector control system to be flown on the



VSRA longitudinal/vertical control system

V/STOL research aircraft (VSRA), a YAV-8B Harrier aircraft. The system, outlined in the figure, will be fly-by-wire with mechanical backup and will use two flight computers to provide fail-safe operations.

This year, several significant development milestones were achieved.

1. A major hardware goal was achieved with the delivery and formal acceptance of the digital flight computers. These computers, which are based on the Motorola 68020 microprocessor, will allow flight software to be written in a higher-order language. This will give the researchers direct access to their control algorithms for more efficient experimentation.
2. The flight software is being developed by an in-house staff using structured software design methods and the computer-aided software engineering tool, Excelerator. A software critical design

review was successfully completed this year, allowing coding to begin.

3. In a parallel effort, work has begun on the design of the servo control unit under a contract let to GEC Avionics of Rochester, England. This unit is the interface between the two flight computers and the 10 servo actuators that drive the aircraft propulsion and flight controls, performing servo loop monitoring and flight computer command error detection for fail-safe operation. The preliminary design review for this unit was completed this year.

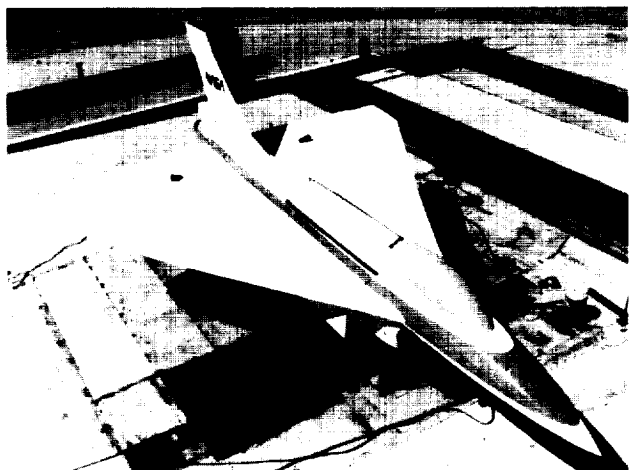
Plans are to begin installation of the equipment in the aircraft during 1989, with the first flight scheduled for late 1989.

(J. Foster, Ext. 5826)

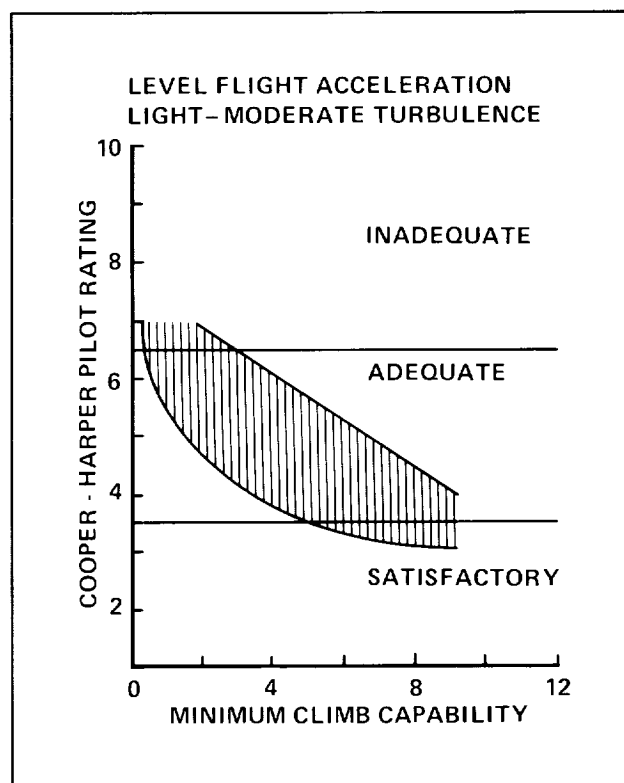
Simulation Evaluation of Transition and Hover Flying Qualities of the E-7A STOVL Aircraft

In recent years, NASA has been engaged in the development of technology for supersonic fighter/attack aircraft with a short takeoff and vertical landing (STOVL) capability. As part of this effort, a variety of airframe and propulsion system concepts have been defined and assessed through analytical studies; further, key technical issues associated with each concept, or common to more than one, have been identified for resolution. One of the critical areas of technology for these aircraft is the integration of flight and propulsion controls, specifically for the purpose of achieving good flying qualities in hover and throughout the low-speed operational envelope associated with the transition between hover and cruise flight. Ames Research Center, in particular, has been engaged in a research program (composed of analytical studies, ground-based simulations, and flight experiments) that addresses this critical technical concern.

One of the propulsion system concepts being pursued in this endeavor is the augmentor ejector, based on development work carried out by de Havilland of Canada and Ames. The airframe configuration most recently associated with this concept is the E-7A model developed by General Dynamics. A substantial amount of low-speed aerodynamic data has been acquired from powered-model tests of this configuration at Ames and Langley Research Centers and at de Havilland.



E-7A STOVL aircraft model



STOVL transition evaluation

A reasonably well-defined configuration, accompanied by an extensive definition of low-speed aerodynamic and propulsion characteristics, was in hand. So it was considered worthwhile to begin to assess some of the key issues associated with flight and propulsion control integration and flying qualities for hover and transition flight. Accordingly, to begin that assessment, the first of a series of ground-based simulation experiments was conducted. Objectives of the simulation were to define the acceptable transition flight envelope for the aircraft, determine control power used during transition flight and hover, and evaluate the integration of the aircraft's flight and propulsion controls.

Transition performance was characterized by the minimum climb or acceleration capability that exists at the most restricted portion of the transition corridor between hover and forward flight. Results indicate that fully satisfactory transition can be achieved with a minimum climb capability of 9–10° at this region of the corridor. The envelope becomes marginally adequate when the minimum climb capability is reduced to 2–3°.

Satisfactory flying qualities can be achieved for deceleration to hover in instrument conditions, for airfield landings, and for recovery to a small ship when attitude and velocity stabilization and command augmentation modes were provided. Satisfactory to adequate flying qualities were obtained for these same tasks when only the attitude command mode was used. This left the pilot to perform the task of thrust management that is required to control flightpath and speed in transition flight and translational velocities in hover.

(J. Franklin, Ext. 6194)

Flight Investigation of Automatic Position-Hold Systems for Rotorcraft

A flight investigation was conducted to help identify the system requirements and the design procedures necessary for a precision automatic hover system for the next generation of tactical military rotorcraft. Design requirements for these systems include prolonged drift-free regulation of position, and the capability to minimize position errors during tactical maneuvers (such as pedal turns and bob-ups) while operating in strong winds. Position-error objectives for this type of system, which is intended to be used close to obstacles, are related to the dimensions of the helicopter and the confined areas in which it may operate. Considering the off-axes maneuvering capability that is required, these objectives are more stringent than have been required in the past.

The research was conducted with the NASA/Army CH47B Variable Stability Helicopter. It included consideration and development of the navigation sensors and the signal-processing that was needed to furnish precise, transient-free position and velocity data to the system. For the design of the position-hold control law, a simple analytical model was used. Its simplicity was justified on the basis of standard analytical robustness tests, and its effectiveness was validated using flight-test data. The position-hold system was integrated in a multi-mode advanced stability and control system for the helicopter that permitted the pilot to easily select the combination of split-axes flight-control modes appro-

priate for the maneuvers conducted during the tests. Performance data for the system when operating in winds as strong as 40 knots were obtained, and were shown to meet the design objectives for the system.

(W. Hindson, Ext. 5008)

Precision Landing Control for STOL Transports

A flight evaluation of a high-precision manual landing control and display concept for short takeoff and landing (STOL) transports was completed using the NASA Quiet Short-Haul Research Aircraft (QSRA). A head-up display presents flare commands to the pilot, who executes a simple, repeatable nominal flare maneuver. Height and height-rate errors relative to the desired trajectory are fed back to a low-authority (± 0.05 -g), direct-lift-control system that drives spoilers and throttles so as to null the errors resulting from wind gusts and pilot deviations. This integrated cockpit display and closed-loop control constitutes a trajectory augmentation system that extends the QSRA flight control from augmentation of attitude, flightpath angle, and airspeed to augmentation of the trajectory itself. The pilot can easily override the low-authority closed-loop control, and a monitored simplex system is adequate for safety.

Touchdown dispersion was achieved that was approximately equal to that obtained during aircraft carrier trials with this same aircraft (± 18 feet). The pilots were hooded to touch down, and they rated the flare and landing task as satisfactory to adequate using the Cooper-Harper scale. Additional work is needed to extend the statistical data base and to cover a greater range of atmospheric disturbances. These evaluations were performed in the context of STOL operations with a powered-lift transport (6° approach glidepath at lift coefficient 5, to a landing in a 200-foot-long touchdown zone on a STOL runway 100 feet wide by 1700 feet long). However, the results are broadly applicable to all highly augmented vehicles with head-up displays that operate in environments in which high-precision guidance is available.

(C. Hynes, Ext. 6004)

An Advisory System for Conflict Detection and Resolution

One of the crucial functions of an air traffic controller is to detect and resolve potential conflicts. Ames Research Center is developing a computerized advisory system to assist the controller in predicting and resolving potential conflicts between aircraft. Rather than the straight-line extrapolation of current speed, altitude, and heading that is implemented in today's conflict alert logic, the new design uses techniques of 4-D (four-dimensional) guidance developed at Ames to accurately predict potential conflicts between aircraft that are flying complex trajectories. Furthermore, a hierarchy of resolution techniques, derived from an extensive interview of a controller expert, forms the basis of resolution advisories. The intent of the advisories is to assist controllers in tactical decision-making within the terminal area.

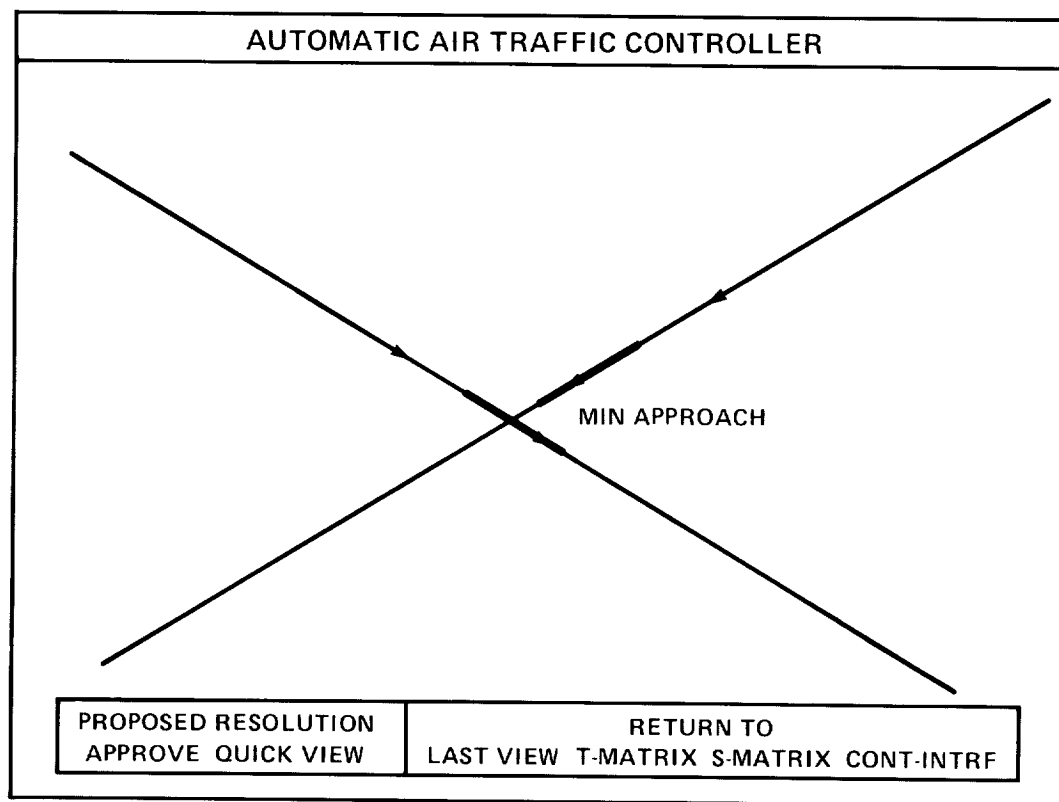
Potential conflict detection involves monitoring the predicted interaction pattern for all aircraft to determine the distance and altitude separation between any combination of aircraft pairs. The method is based on calculating 4-D trajectories for all aircraft from the current time to the look-ahead time, usually 10 minutes, to create the future interaction pattern of the aircraft. Generation of aircraft trajectories is based on 4-D guidance algorithms, which translate the current aircraft position, flight plans, and vectoring commands into reference trajectories. The detected potential conflict pairs are stored in a global conflict-detection matrix, each element of which designates the time of conflict if no action is taken.

Conflict pairs with the earliest time until conflict are resolved first. The potential conflict is resolved by altering the speed profile, the altitude profile, or the horizontal trajectory of one of the aircraft in the pair, without changing the overall time schedule for the remaining aircraft or creating a new conflict. The result of each resolution is a sequence of time-ordered guidance commands. The composite of all sequences, arranged in chronological order, is displayed to the controller as a sequence of advisories.

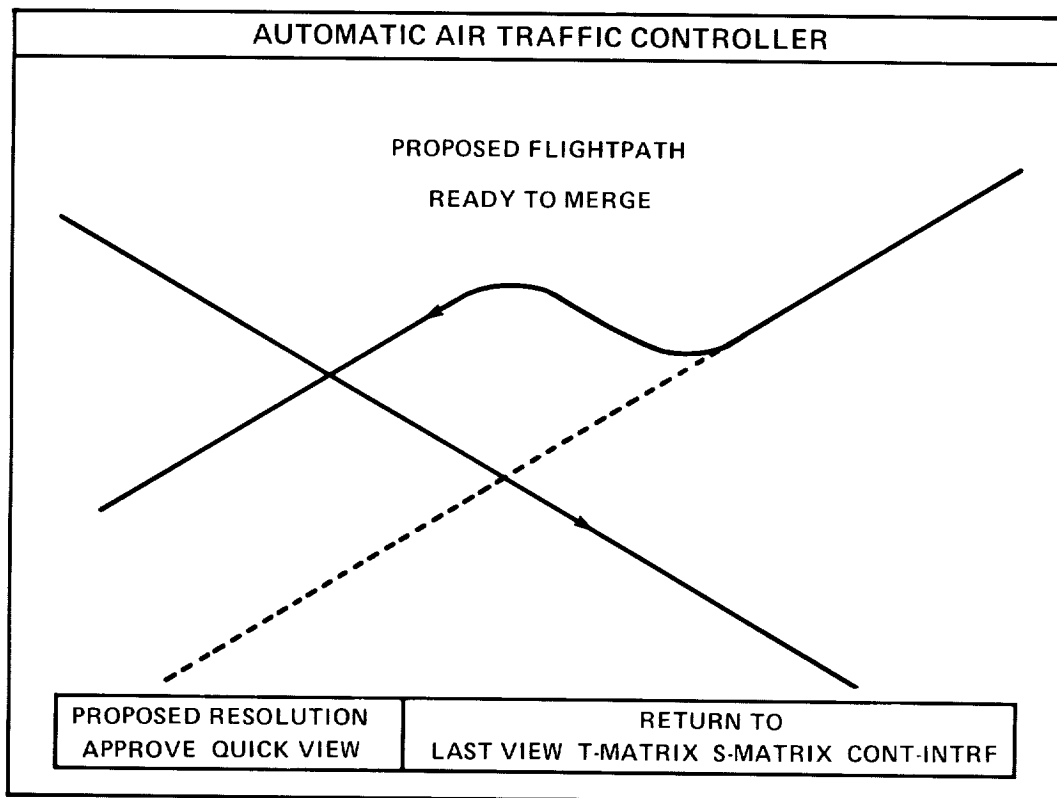
The first figure shows a screen display of a potential conflict between two aircraft on converging routes. The heavy line segments identify the regions where the pair would violate the minimum separation distance. The two dark triangles on the flightpaths indicate the location where the separation distance would be the least. The second figure displays the proposed resolution to this conflict. One aircraft is maneuvered to fly antiparallel to the other and to be separated by at least the specified minimum separation distance. After the potential conflict has been resolved, this aircraft executes a maneuver to merge with the originally planned flightpath.

The concept is being implemented in a Symbolics 3675 computer in three languages: (1) ART (Artificial Reasoning Tool) for knowledge-based rules, (2) LISP for parameterized and information transfer between the knowledge-based rules and the algorithms, and (3) FORTRAN for 4-D guidance algorithms. This concept will be evaluated by controllers, using the air traffic controller Advanced Concepts Simulation Facility at Ames.

(H. Lee, Ext. 5435)



(a)



(b)

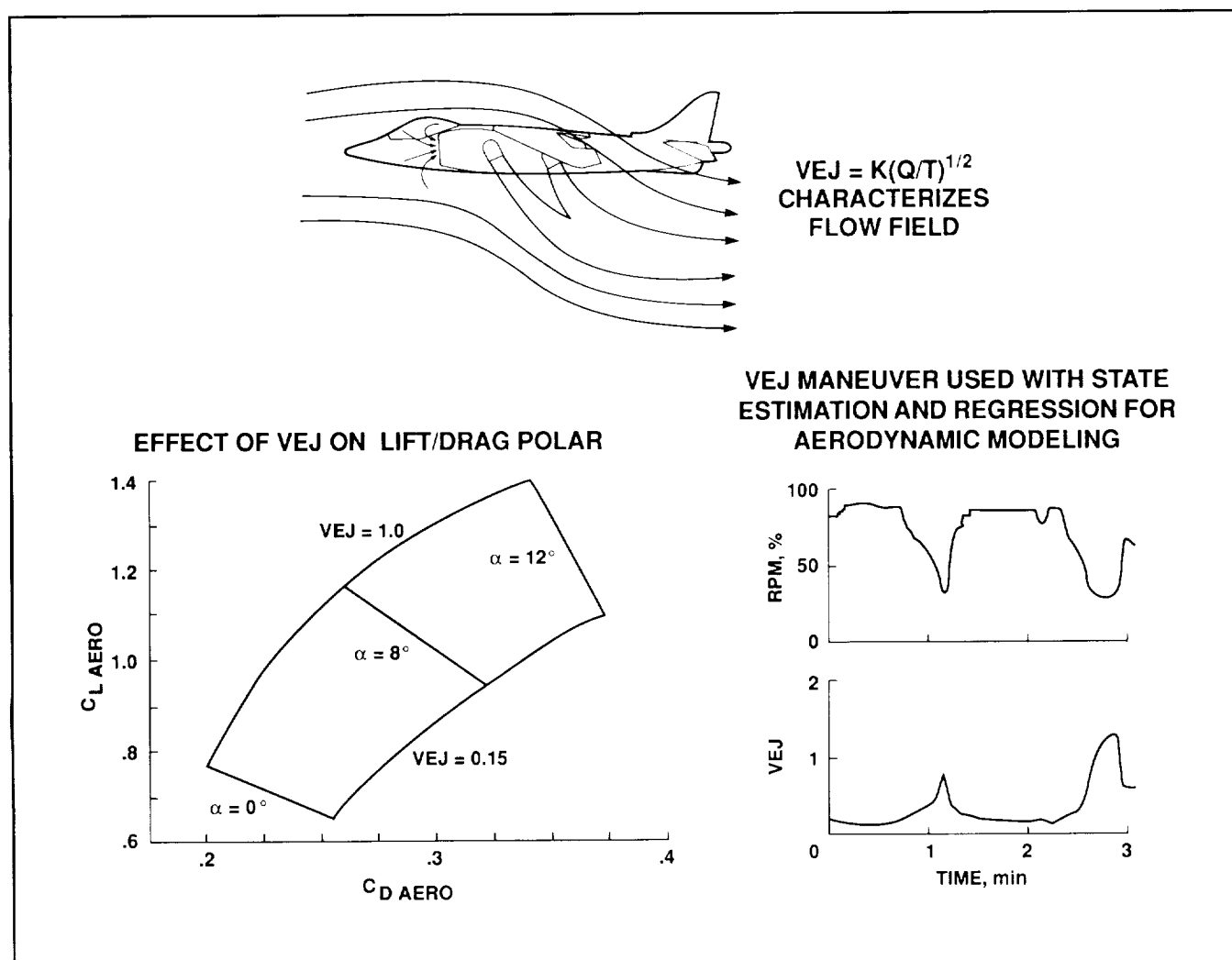
An advisory system for conflict detection and resolution

Aerodynamic Modeling for the V/STOL Research Aircraft

This program is to identify a full-envelope aerodynamic model of the V/STOL Research Aircraft (VSRA), YAV-8B Harrier, from flight-test data. The model must represent VSRA body forces and moments over a flight envelope that includes hover and transition to forward flight and back to hover, as well as short takeoff and landing operation and normal cruise. The new aerodynamic model is needed to update a VSRA simulation that supports ongoing research in advanced control, display, and guidance concepts for short takeoff and vertical landing (STOVL) aircraft. The model is to be determined through the use of linear regression, a procedure that

is well suited to identifying a highly nonlinear model. An advantage of the regression method is that it allows a computationally efficient analysis of full-envelope flight data. Good results, however, are dependent on data quality. The use of tracking data with state-estimation techniques provides the necessary corrections to flight measurements from gyros and accelerometers and ensures overall data consistency.

One characteristic that sets the VSRA apart from conventional aircraft is that it exhibits thrust-induced aerodynamics which are significant during transition between hover and conventional flight, and during low-speed flight. A useful measure of thrust-induced aerodynamics is the equivalent jet velocity ratio (VEJ), which is proportional to the square root of the ratio of dynamic pressure to engine thrust.



Modeling of thrust-induced aerodynamics

A flight-test maneuver was designed to accurately identify VSRA thrust-induced aerodynamics. During this maneuver, VEJ is varied at several fixed nozzle and flap settings. A large change in VEJ can be realized by varying thrust while the angle of attack (AOA) is held nearly constant. In the first segment of the maneuver, thrust is slowly added (while using pitch control to hold AOA) until a maximum thrust setting is reached. Then thrust is slowly reduced, again holding AOA, until a minimum thrust setting is reached. A large change in VEJ can also be realized by varying dynamic pressure at low thrust levels. During the second segment of the maneuver, thrust is reduced, and the aircraft is "pushed over" into a high-speed dive followed by a "pull-up." The data from this set of maneuvers should lead to better modeling of the thrust-induced aerodynamics associated with V/STOL aircraft.

The first set of VSRA flight tests has been completed. Maneuvers were designed to cover the complete flight envelope. Each maneuver included 3-5 minutes of coverage under continuous radar tracking. The flight records are being processed to provide a consistent data set that can be used to provide total and engine forces and moments. Once the VSRA data base is complete, records from several maneuvers may be concatenated to cover the envelope for model identification. The software for model representation and parameter identification is now being developed.

(D. McNally and R. Bach, Ext. 5440/5429)

Microburst Modeling Utilizing Airline Flight Data

Low-level microbursts are a continuing problem that must be better understood, in the interest of aircraft safety. One way to investigate the nature and cause of severe microburst encounters is through analysis of airline flight records. In the past, such

analysis was hindered by insufficient data, but more recent microburst encounters have involved modern airliners with digital flight-data recorders. These digital records, along with air traffic control radar position records, provide a means to determine and analyze the microburst wind environment.

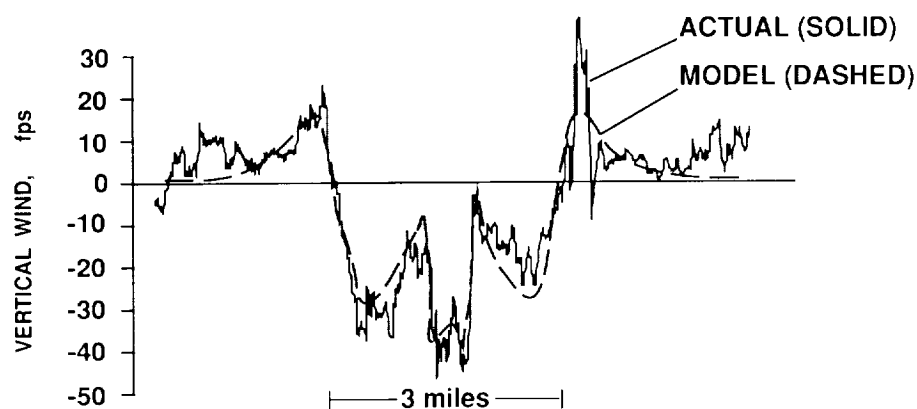
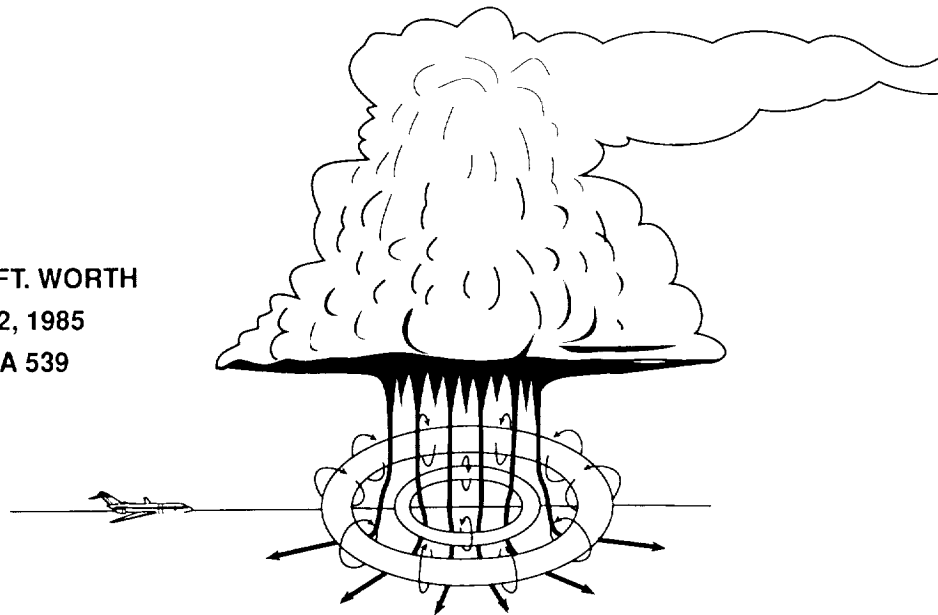
As part of the investigation by the National Transportation Safety Board, researchers from Ames Research Center have analyzed the flight and radar records from two airliners that penetrated the microburst at the Dallas/Ft. Worth (DFW) airport on August 2, 1985. The accident aircraft, Delta 191, encountered the microburst on final approach and contacted the ground about 1 mile short of the runway. The aircraft following, American 539, made a go-around 110 seconds after the accident and traversed the microburst at an altitude of about 2,500 feet above the ground. The results for Delta 191 show that the aircraft encountered a strong downflow, followed by a strong outflow, accompanied by large and rapid changes in the vertical wind. The results for American 539 during the go-around indicate a broad pattern of downflow in the microburst, with regions of upflow at the extreme edges.

The wind pattern in the DFW microburst has been identified through the development of a multiple-ring vortex model, which shows excellent agreement with the vertical wind profile (see the figure). The results show a large vortex ring at the outside edge of the microburst, and they clearly indicate a smaller vortex ring embedded in the downflow.

This Ames analysis of the airline flight data is the first to provide an accurate reconstruction of the winds within a microburst. The development of a multiple-ring vortex model provides the first evidence of rings embedded in the microburst downflow. The study provides a realistic wind field model that can be used in flight simulators to better understand the control problems in severe microburst encounters.

(T. Schultz and R. Wingrove, Ext. 5440/5429)

- DALLAS-FT. WORTH
- AUGUST 2, 1985
- FLIGHT AA 539



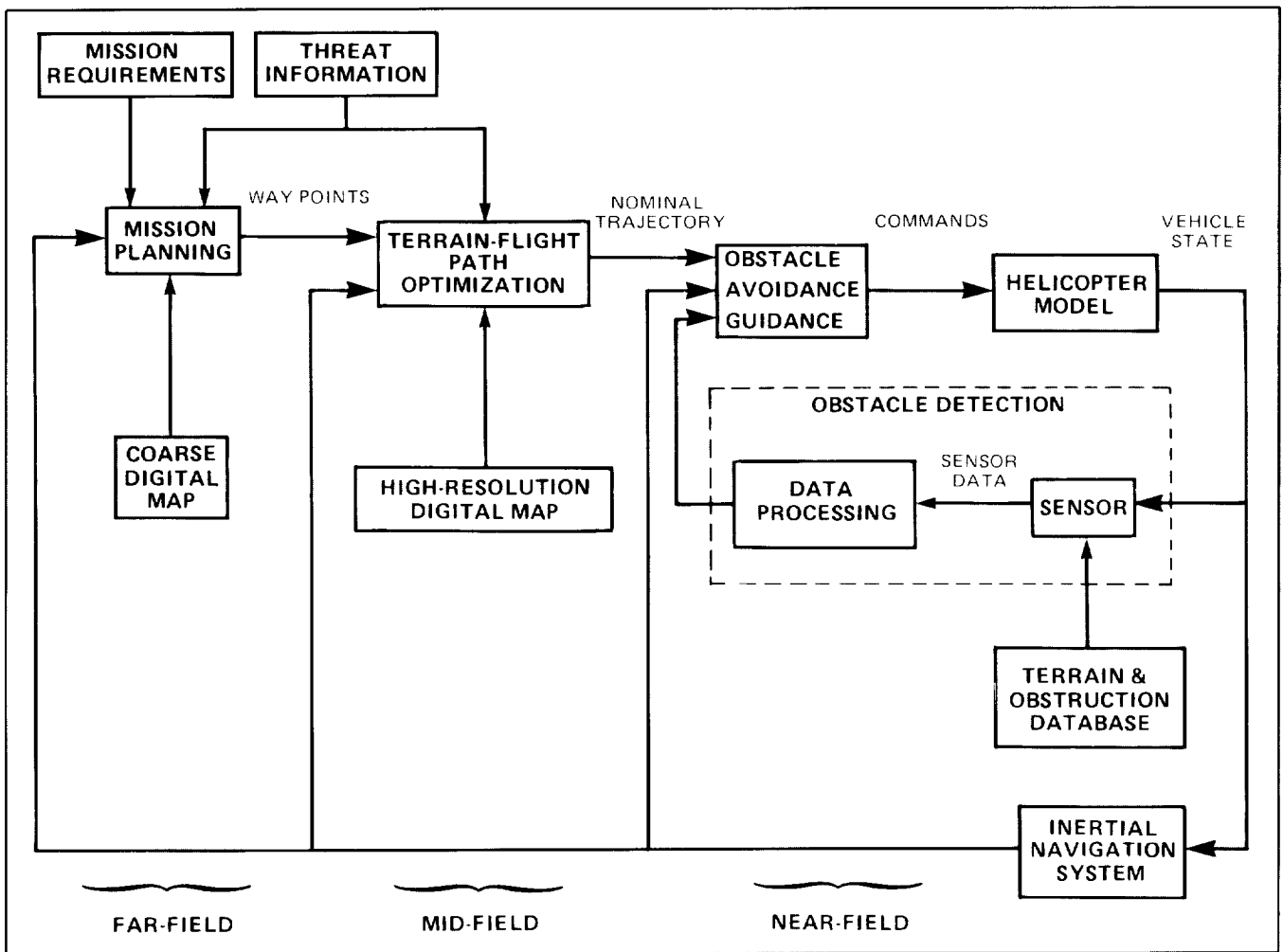
Vortex-ring model of DFW microburst

Automated NOE Flight

In high-threat battle areas, military rotorcraft must fly close to the Earth's surface to utilize the surrounding terrain, vegetation, or human-made objects to minimize the risk of being detected. The combination of piloting task and mission functions is extremely taxing for a two-pilot crew, and potentially prohibitive for a one-pilot crew. Computer-aiding with enhanced sensors has been identified as central to alleviating the difficulties in this mission scenario.

The automated nap-of-the-Earth (NOE) flight program is a cooperative NASA/Army program aimed at the development of technology leading to enhanced low-altitude/NOE flight-path management and control through computer-aiding. The long-term objective is to work toward achieving a pilot-centered automated NOE flight capability.

To achieve this goal, the program has decomposed the NOE guidance problem into three levels of functions: far-field, mid-field, and near-field. These three functions can be realized naturally in three



Automatic NOE guidance structure

feedback loops shown in the figure. The outermost loop, far-field mission planning, represents the highest level of decision-making. It aids the pilot in selecting goals and intermediate waypoints to satisfy mission requirements and avoid threats. The coarse route defined by the goals and waypoints is dynamically refined by the mid-field path optimizer. The near-field function deals with obstacle detection and obstacle avoidance.

The specific research in each of these areas is covered under the following research highlights:

1. far-field mission planning,
2. mid-field mission planning,

3. obstacle detection,
4. obstacle avoidance,
5. neural networks for autonomous guidance.

To address the system issues, a preliminary design for a "return-to-base" autonomous guidance capability has been completed and will be tested in simulation at McDonnell Douglas Helicopter with a follow-on test at Ames. Under a separate effort, a specification for a single-axis, automated NOE capability that has the potential of early flight validation has been initiated.

(B. Sridhar and V. Cheng, Ext. 5450/5424)

Obstacle Detection

The objective of this program is to develop obstacle-detection algorithms for the autonomous guidance of vehicles and, in particular, for rotorcraft nap-of-the-Earth (NOE) flight. The reliable detection of obstacles is a key element in advancing the automation of rotorcraft.

Research in this area has focused on

1. developing an in-house capability to process sensor data by using image-processing and computer vision methods,
2. developing the obstacle-detection algorithms,
3. developing algorithms for estimating the range to obstacles,
4. evaluating the algorithms using real and simulated data.

Several image-processing algorithms which constitute the basic blocks necessary to detect obstacles, in image data from low-light-television (LLTV) and forward-looking infrared (FLIR) sensors, have been developed on the Megavision 1040 XM image-processing system. These algorithms will be tested using real flight data and simulated data from the Ames Vertical Motion Simulator. The in-house work is augmented by a contract with Honeywell Systems Research Center and by a Small Business Innovation Research contract conducted by Space Computer Corporation.

A significant accomplishment during 1988 was the development of a simulation consisting of rotorcraft dynamics, image-object geometry, and estimation algorithms on the VAX computer.

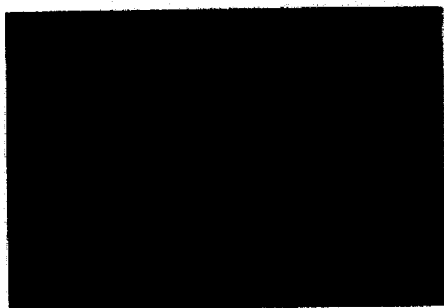
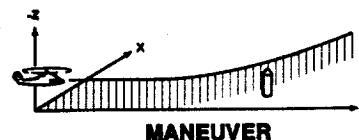
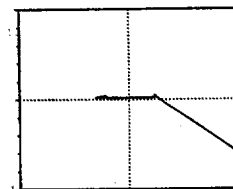


IMAGE PROCESSING SYSTEM



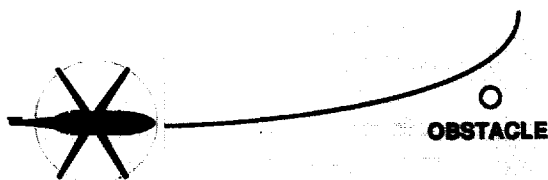
MANEUVER



MOTION IN IMAGE PLANE

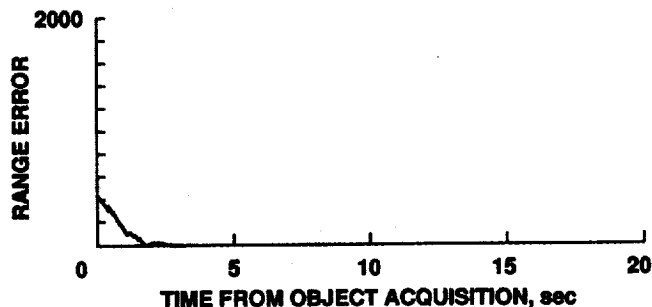
VAX BASED IMAGE SENSOR SIMULATION

DEVELOPED AND EVALUATED A RECURSIVE PROCEDURE FOR IMPROVED RANGING TO ISOLATED TARGETS



OBSTACLE

Obstacle detection



ORIGINAL PAGE
COLOR PHOTOGRAPH

The figure shows a rotorcraft flying along the y-axis at a constant altitude and speed, then making a left turn. As the rotorcraft moves, the image corresponding to the object moves in the image plane. The tip of the object is selected as an isolated target for range determination.

The simulation is being used as a test bed to study how range accuracy to the object is affected by the estimation technique, measurement interval, rotorcraft maneuvers, relative geometry between the rotorcraft and the object, and errors in the position and orientation of the rotorcraft. This simulation will be converted to a three-dimensional computer graphics simulation and used to integrate the obstacle-detection algorithms with ongoing research efforts in obstacle avoidance.

Techniques for obstacle detection resulting from this effort will be considered as candidates for detecting hazards during the terminal-descent phase of a Mars landing.

(B. Sridhar and V. Cheng, Ext. 5450/5424)

Mid-Field Path Planning

The mid-field path-planning problem can be characterized by a real-time precise path definition that is based on knowledge of the terrain, threats, and mission objectives. Terrain-Following/Terrain-Avoidance (TF/TA) research for high-performance aircraft is an example of the mid-field path-planning problem. As part of the automated nap-of-the-Earth program, a research effort has been conducted to adapt TF/TA concepts from fixed-wing aircraft to helicopters, and to use TF/TA to examine the control/display requirements for the pilot/system interface of an automated helicopter low-altitude flight system.

The baseline algorithm is a forward-chaining dynamic programming technique. The algorithm calculates a 30-second trajectory, known as a patch, which is updated every 6 seconds. Although conceptually correct, the algorithm was not adequate for pilot acceptance. The two primary problems discovered during an initial piloted simulation were:

1. an undesirable oscillation in guidance about the nominal path, caused by necessary discretized control values,

2. discontinuous guidance commands at each update, caused by a mismatch between the actual helicopter position at the update and the estimated helicopter position used to compute the trajectory.

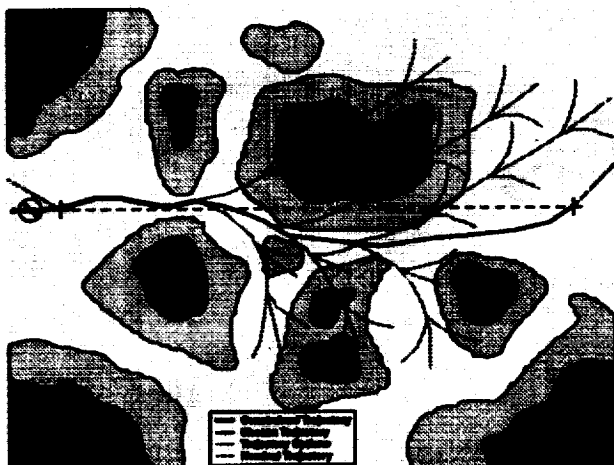
The first problem was resolved by adding two additional terms to the cost function. To resolve the second problem, the discontinuity at the system update, several methods were developed. The preferred method constrained the trajectory for a period equivalent to the time required for the update and the length of the trajectory displayed to the pilot. Beyond this point, the algorithm had the opportunity to adapt to new information such as changing terrain features or threat information. These modifications led to a much smoother TF/TA trajectory, with a negligible increase in vulnerability.

A flight-path-oriented head-up-display (HUD) was developed for maximum pilot understanding and minimum pilot workload. The HUD symbology included pathway-in-the-sky, phantom aircraft, and flight-path vector/predictor cues. A second piloted simulation, which successfully demonstrated the modified guidance algorithm and associated HUD symbology, recently has been conducted at the Ames Research Center Interchangeable Cab (fixed-base simulation facility). Two Ames test pilots participated, with each pilot making numerous simulation runs over several complex courses. Results showed that precise TF/TA flightpath control can be easily maintained at or below 100 feet above ground level with moderate pilot effort.

The current TF/TA guidance algorithm depends upon the assumption of constant speed throughout the flight. Work will be initiated to extend the system to handle variable speeds, including hover. Work in the near future will also include the integration of the TF/TA system with the obstacle-avoidance techniques currently under development.

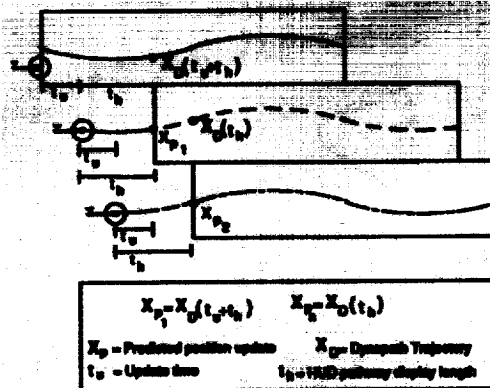
A complementary mid-field path-planning method is being developed under a grant with the Georgia Institute of Technology. This method solves the two-point boundary-value problem with the aid of a series of transformers to obtain a true, continuous, optimal feedback solution. The method has been demonstrated in off-line computer simulations and shows promising results.

(H. Swenson, Ext. 5469)

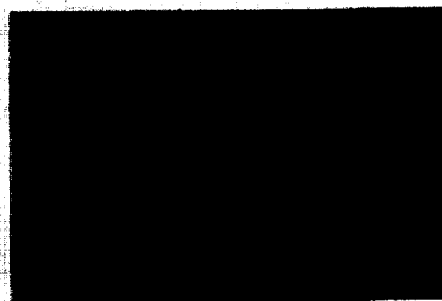


REAL-TIME OPTIMAL TRAJECTORY COMPUTATION

- CONSTRAINED ADAPTIVE SEARCH GUIDANCE
- LOW ALTITUDE PILOT ACCEPTABILITY



CONSTRAINED ADAPTIVE SEARCH



FLIGHT PATH CENTERED HUD SYMBOLOGY

- FLIGHT PATH VECTOR/PHANTOM AIRCRAFT
- PATHWAY-IN-THE-SKY SYMBOLOGY

Automated low-altitude path planning for rotorcraft

Far-Field Mission Planning

The objectives in far-field mission planning for the automated nap-of-the-Earth (NOE) program are to define, develop, and demonstrate an effective route planner/replanner for low-altitude/NOE helicopter flight. The planner would support the fully autonomous flight of a single-pilot scout/attack helicopter by reducing peak workloads, providing better management of fuel and other resources, minimizing threat exposure, and making real-time changes in the mission plan to meet changing objectives.

Three candidate mission route planners are in various stages of development.

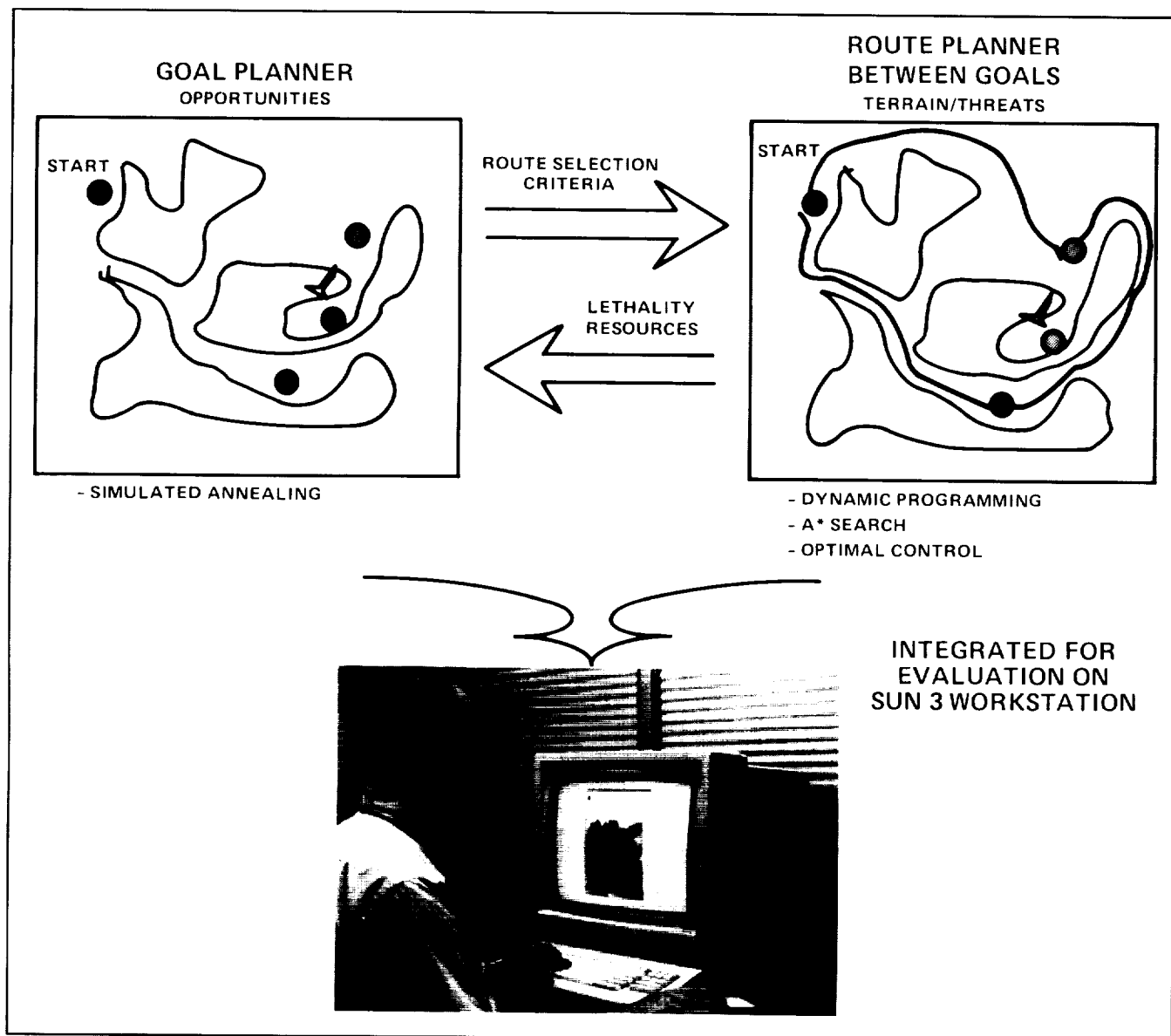
1. A Small Business Innovation Research Phase II contract to TAU Corp., provided a mission route planner using a dynamic programming algorithm to

produce a globally optimum plan. An early version of this software is operational. This software is being updated to incorporate features developed by TAU during performance of the Phase II contract.

2. A second contract with the Charles Stark Draper Laboratory has developed concepts for a goal planner using a heuristically guided, simulated, annealing algorithm for goal selection and sequencing.

Between goal objectives, this planner uses an A-star search to provide a route and accurate forecasts of fuel, time, and lethality of the path. Phase II of this contract has been initiated to incorporate the algorithms into a complete mission planner.

3. A third route planner, based on optimal control theory, is being developed under a grant to the Georgia Institute of Technology. The solution to the two-point boundary-value problem is reduced to a



Far-field planning

one-dimensional search scheme by the use of an adjoint-control transformation. This results in a numerically efficient algorithm to generate an optimal plan.

During 1988, an interactive, color graphics display was developed on a SUN 3/160 workstation in the Aircraft Automation Laboratory. This display provides an interactive user interface to control the inputs and operation of the far-field mission-planning software. Routes computed by the planners are displayed graphically on a color map of the terrain that is color-coded to indicate elevation as defined by

digital terrain elevation data. Potential threats are displayed in red, with the extent of their coverage indicated for the flight altitude of the helicopter. Other data from the planners are displayed numerically and graphically.

A test scenario is being developed to examine and compare the three route planners and to integrate the preferred route planner with the goal planner on the SUN 3/160 workstation. The best features of one or more of the three route planners will also be incorporated into a route planner to be used in the Helicopter Operations Planner (under devel-

opment by the U.S. Army) for use in experiments on the Crew Station Research and Development Facility.

(N. Warner, Ext. 5443)

CH-47/Cross-Coupling Studies

In-flight simulation provides a valuable opportunity for validation and supplementation of handling-qualities results obtained in ground-based simulation. In addition, the authenticity of simulator flight-evaluation tasks and corresponding pilot-control techniques can be verified with full-fidelity motion and visual cues. An in-flight simulation experiment investigating the effects of pitch-roll cross coupling for near-terrain flight was conducted on the NASA/Army CH-47B helicopter. This research was an extension of an earlier, piloted, ground-based simulation investigation of the same subject conducted on the Ames Research Center Vertical Motion Simulator.

The NASA/Army CH-47B is a variable stability helicopter equipped with an explicit-model-following flight-control system. A model of an unaugmented helicopter with cross coupling was developed for the

experiment. The model used variations in physical rotor parameters to generate cross coupling. The evaluation task was chosen to be representative of nap-of-the-Earth maneuvering flight. The handling-qualities results obtained in flight validate the conclusions of the previous simulation experiment.

The handling qualities of highly coupled aircraft are very sensitive to a combination of pilot technique, task demands, and the frequency-dependent characteristics of the coupling response. These frequency-dependent characteristics are determined by both the type of cross coupling and the on-axis rate damping of the aircraft. Pilot technique, in terms of learned control crossfeeds, can improve performance and lower workload for particular types of coupling. Pilot learning on one cross-coupled configuration was shown to have a direct effect on the next, and could make rapid adaptation to new coupling characteristics difficult. This could be important in the event of a failure of the flight-control stability-augmentation system in near-terrain flight. The pilot-control techniques demonstrated in flight were generally more consistent in terms of aggressiveness and handling-qualities ratings than were those derived from ground simulation.

(D. Watson and W. Hindson, Ext. 4037)

Flight Operations and Research

Altitude Acceleration Display for Hypersonic Aircraft

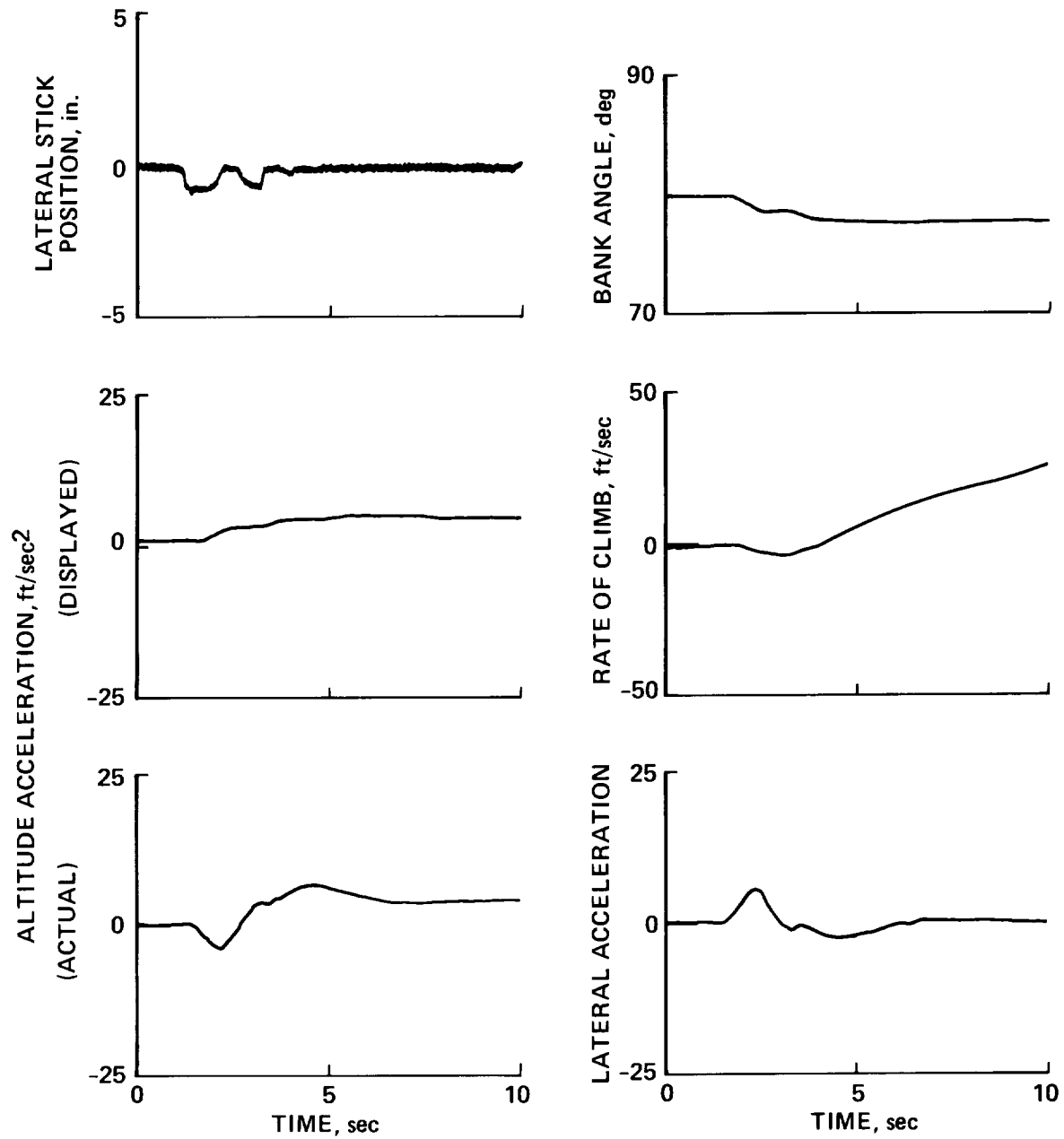
Flight simulation studies of hypersonic aircraft are being conducted in support of the National AeroSpace Plane program. A technique adopted by pilots for trajectory control during these studies is bank-angle modulation to control rate of climb (\dot{h}). Bank-angle changes alter the component of lift in the vertical direction, and result in changes in \dot{h} . Since \dot{h} response is very sluggish at hypersonic speeds, altitude acceleration (\ddot{h}) is also displayed to the pilot to provide lead information and confirmation that the bank-angle change is in the right direction. However, for some configurations, the \ddot{h} response to a bank-angle change is initially in the wrong direction. In some cases, this characteristic is severe enough that precise control is nearly impossible.

Analysis indicates that the \ddot{h} reversals are primarily due to dutch-roll-mode motion induced during the bank-angle change. Since these motions

are transitory, it was decided to remove the dutch-roll contamination computationally from the \ddot{h} display, and circumvent the difficulties associated with trying to suppress the transitory motions with the flight-control system. This would allow the pilot to see the \ddot{h} associated with bank-angle change free of dutch-roll contamination.

The figure illustrates the aforementioned display and pilot technique. A pilot is in the loop simulator run at Mach 16. The vehicle is initially in a steep right turn. The pilot applies a lateral stick input to the left to reduce bank angle, increase the vertical component of lift, and increase the rate of climb. The displayed \ddot{h} smoothly reflects the influence of the bank-angle change without reversals. The initial response of the actual \ddot{h} is in the wrong direction, is followed by an overshoot in the right direction, and finally settles to a steady value. In the steady state, the actual and displayed values are the same. The lateral acceleration is proportional to the side forces generated by the dutch-roll motion. The difference between the actual and displayed \ddot{h} is the dutch-roll motion.

(D. Berry, Dryden Ext. 3140)



Bank-angle modulation for rate-of-climb control

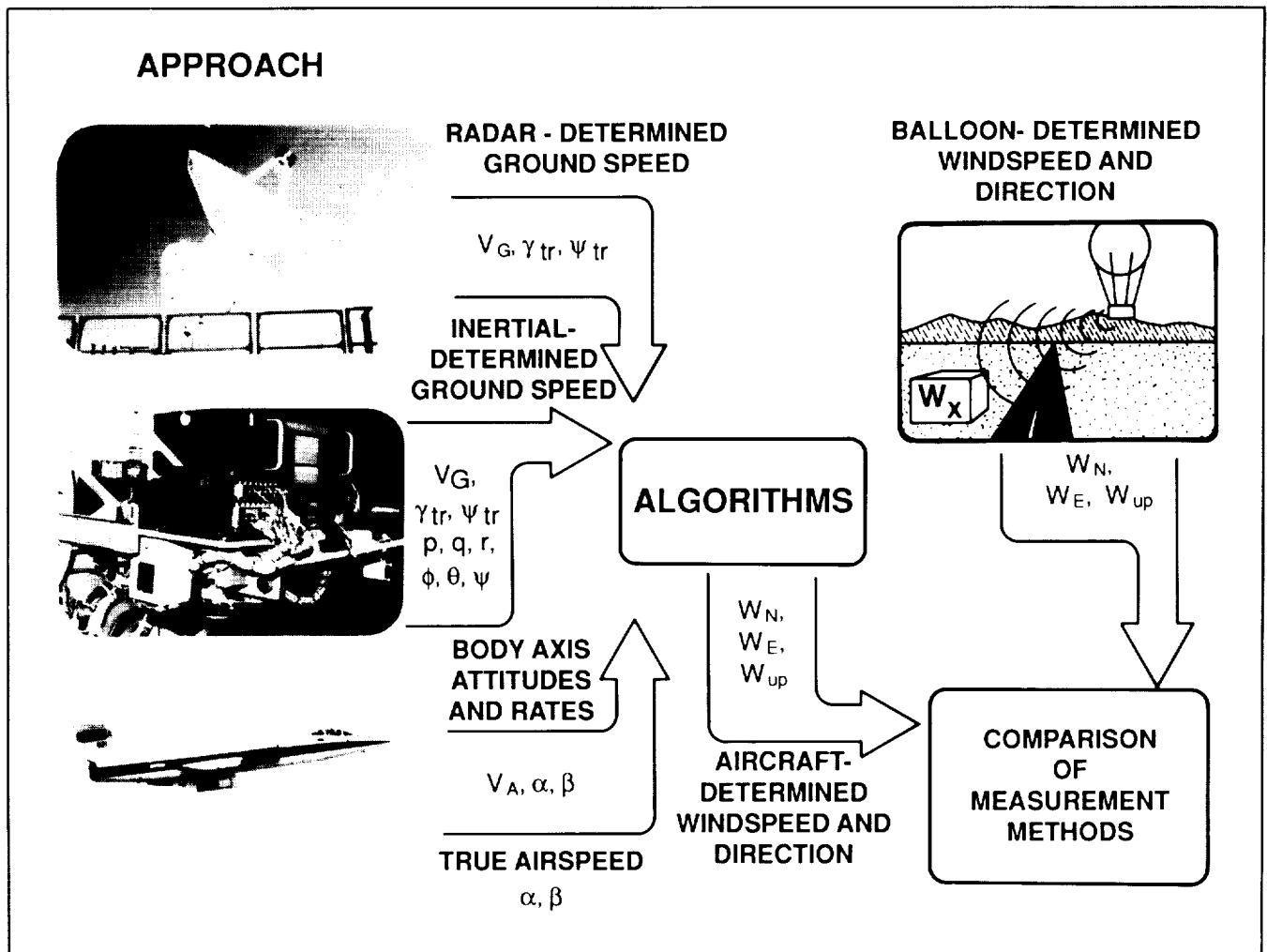
Shuttle Launch Wind-Measurement Experiment

Currently, Shuttle prelaunch wind profiles are measured 3.5 to 4 hours before scheduled lift-off using Jimsphere balloons tracked by FPS-16 radar. These wind profiles are used to predict launch trajectories and loads. If it appears that load limits will be exceeded, a no-go recommendation will be made. Because the wind can change significantly in 3 to 4 hours, margins are added to the balloon-measured wind values. A more rapid profiling technique which could be used closer to the scheduled time of lift-off might make it possible to reduce these margins.

At the request of Johnson Space Center, the NASA Ames-Dryden Flight Research Facility initiated an experiment to determine the feasibility of using an

instrumented high-performance aircraft to measure wind profiles more quickly. The following specifications were established: (1) FPS-16 radar tracking precision of 0.5 meters per second; (2) rapid profile to 60,000 feet; and (3) real-time calculation of winds. Once this phase of the experiment is concluded, recommendations will be made for implementation at Kennedy Space Center.

An F-104 is used for this experiment. It has conventional NASA/NACA instrumentation to provide air data and flow angles. An LTN-90 ring laser gyro inertial navigation system (INS) has been added to measure inertial speeds and angles along with Euler angles and rates. The aircraft is tracked with FPS-16 radar to provide an alternate measurement of inertial speeds and angles. Wind profiles calculated using aircraft measurements are compared with those



Shuttle launch wind shear measurement program

measured by a Jimsphere balloon launched during or just before the flight. The first figure shows the different measurements needed to calculate wind profiles.

The flight-test measurements were accomplished in three parts: (1) system checkout and air-speed and flow-angle calibrations; (2) subsonic/low-altitude profiles; and (3) supersonic/high-altitude profiles. In order to even come close to the accuracy goals of this experiment, the accuracy of the air-data and flow-angle parameters must be an order of magnitude greater than currently is expected in flight tests. Considerable work has therefore been done (and is still continuing) on the air-data and flow-angle calibrations.

The subsonic/low-altitude ($h < 40,000$ feet) flight tests were completed to see whether the concept worked before subjecting the INS to the more severe environment above 40,000 feet. The supersonic/high-altitude flights consisted of the following: a Mach = 0.9 climb to about 45,000 feet, a turn to an accelerating dive to about 30,000 feet, continued acceleration to Mach > 1.4, a supersonic climb to 60,000 feet, a supersonic descent to below 45,000 feet, a turn and deceleration to Mach = 0.9, and continued descent to below 10,000 feet. The second figure shows a typical comparison of balloon-measured and aircraft-measured wind profiles.

The flights for this phase of the experiment have been completed and analysis is ongoing. An

onboard computer that would compute wind values is being developed. Meanwhile, software has been developed to compute wind values in real time on the ground. A decision on whether to demonstrate this capability at Kennedy Space Center will be made soon.

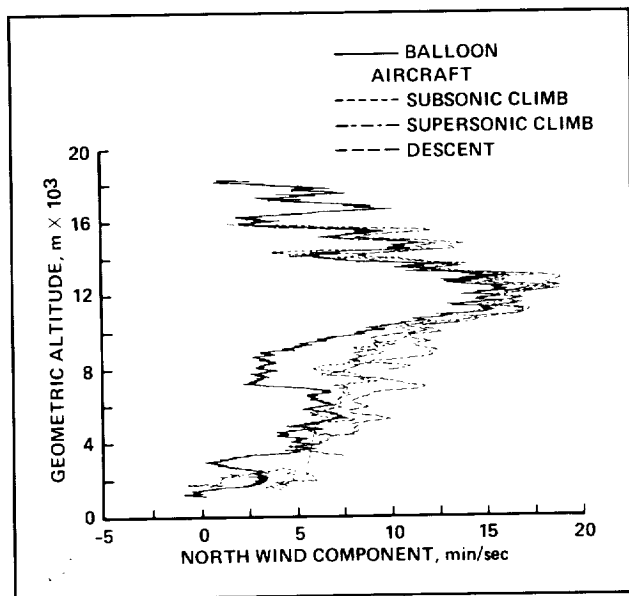
(L. Bjarke, Dryden Ext. 3706)

X-29 Parameter-Estimation Research

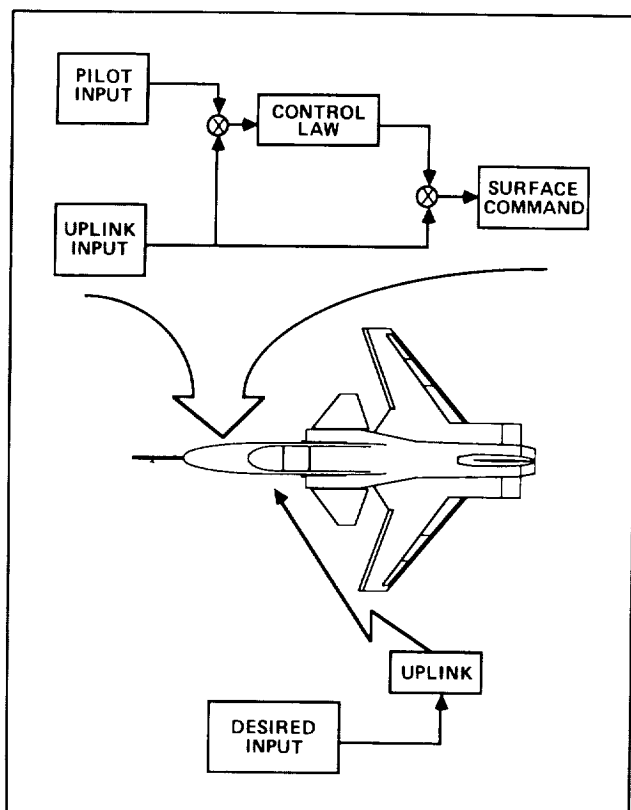
The X-29A research aircraft is being used to flight test the forward-swept wing (FSW) concept integrated with three-surface longitudinal control, close-coupled canard, thin supercritical airfoil, aero-elastic tailoring, and a high level of longitudinal instability. Of primary interest is the determination of aerodynamic stability and control parameters for the FSW configuration. Obtaining the aerodynamic parameters from flight will assist in the validation of predictive numerical codes and provide insight into the beneficial aspects of the forward-swept geometry.

The flight-test maneuvers consist of a series of control surface doublets designed to excite the aircraft dynamic response as much as possible within the flight control system (FCS) limits. (Conventional pilot-generated stick inputs resulted in surface derivatives that tended to be highly correlated with each other or with other aircraft variables such as pitch rate; thus, the extraction of individual surface effectiveness derivatives was not possible.)

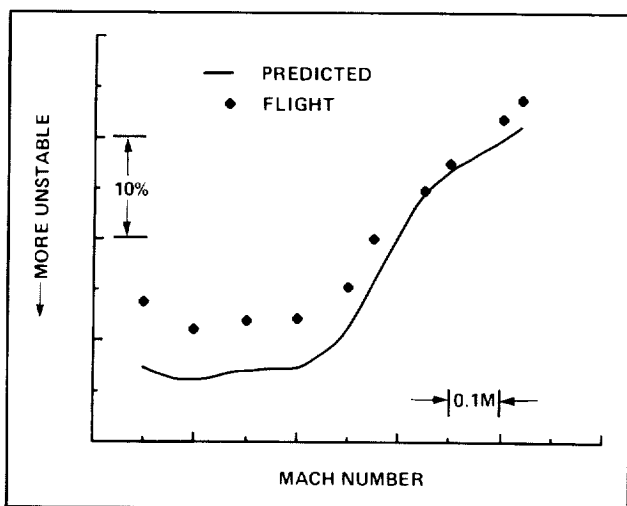
Flight testing to obtain aerodynamic stability and control data in the 1-g flight envelope has been completed. The high level of pitch instability, combined with a highly augmented aircraft and an FCS mechanization which commanded the three longitudinal surfaces in unison necessitated the use of individual rather than combined control surface doublets to excite the aircraft response. The ground-based Remotely Augmented Vehicle (RAV) Facility shown in the first figure was used to uplink individual control surface doublets, which were then combined with the on-board FCS signals, producing aircraft dynamics that contained independent noncorrelated information allowing derivative extraction.



F-104 flight 1239



X-29 RAV uplink system



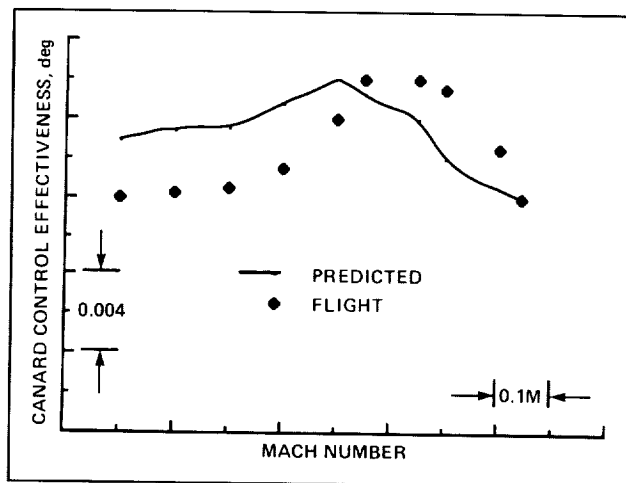
X-29 static margin

A computational parameter estimation technique utilizing a maximum likelihood minimization method was used for analyzing the flight data. Parameters measured include longitudinal static pitch stability and canard control effectiveness (C_m-D_c). The

second figure shows a comparison between wind-tunnel-predicted and flight-derived longitudinal static margins. At low Mach numbers, the aircraft displays a high degree of static pitch instability. With increasing Mach number, the aircraft becomes more stable as the center of pressure shifts aft. The aircraft is more stable than predicted, implying that the aerodynamic center is farther aft than predicted. In the third figure, C_m-D_c is shown to be a strong function of Mach number. The rapid rise in effectiveness occurs in the transonic region.

High-angle-of-attack data will be gathered during the next research phase. The resulting data base will offer information on forward-swept technology for comparison with predictive numerical methods while enhancing the design process of future fighter aircraft.

(G. Budd and N. Matheny, Dryden Ext. 3377/3728)



X-29 canard control effectiveness

Integrated Trajectory Guidance Algorithms Flight-Tested

Advanced integrated trajectory guidance algorithms (applications of earlier research conducted at Ames by Dr. Heinz Erzberger) have been flight-tested on the F-15 Highly Integrated Digital Electronic Control (HIDEC) airplane at Ames-Dryden. These algorithms can be used to calculate the minimum flight time or minimum fuel needed to reach a given end point. In addition, an advanced algorithm

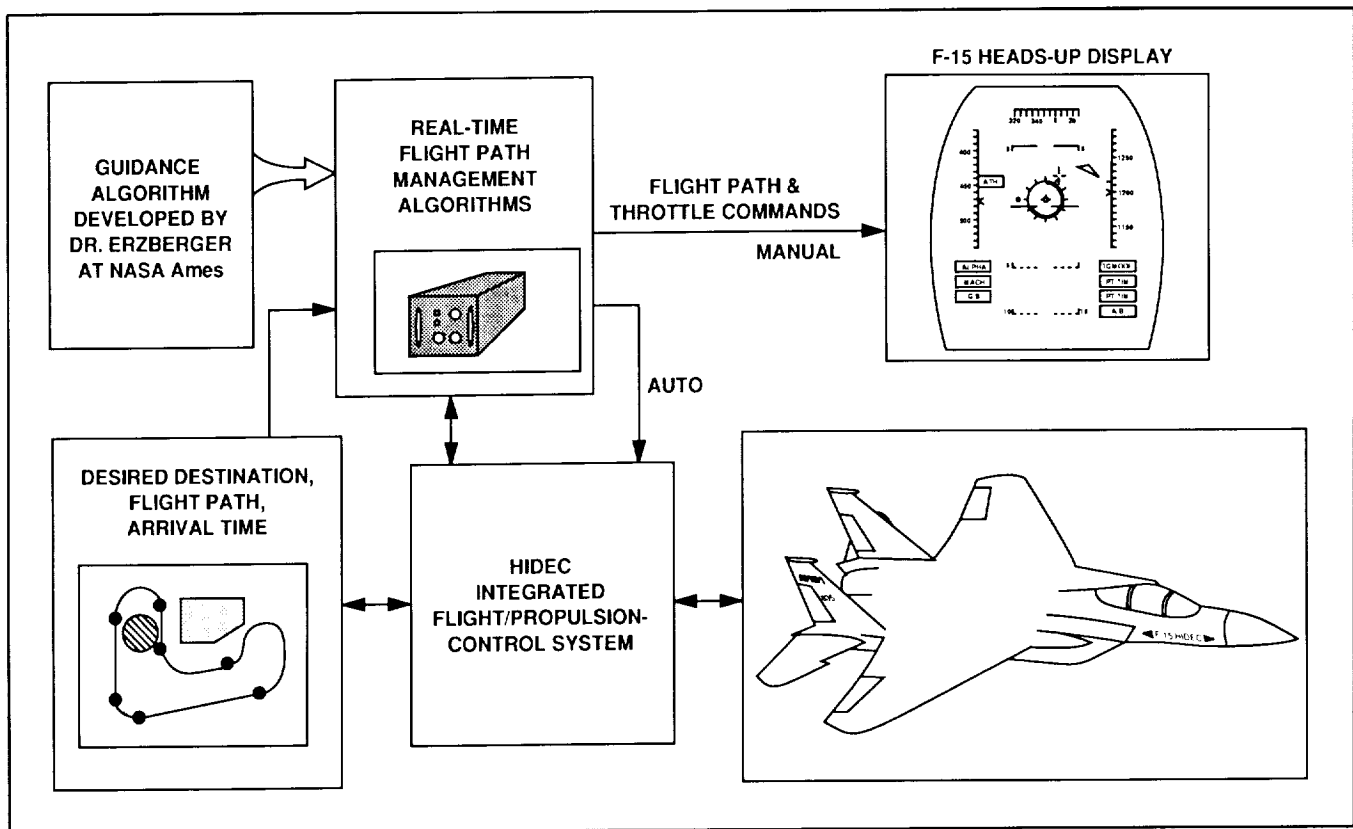


Diagram of the advanced trajectory guidance algorithms for the F-15

can be used to solve a four-dimensional problem, when the time is also specified—in this case, to calculate the minimum fuel for a given time of arrival.

The ability to calculate optimum trajectories in near-real time with on-board computers is of major interest for civil aviation because it allows recomputation of trajectories after weather or air traffic control diversions. The new algorithms are of even greater importance for military missions where changes in threats or targets occur routinely. In addition, the effects on trajectories of afterburning engines and supersonic speeds can be taken into account, a unique capability of these guidance algorithms.

In the HIDEC flight research the algorithms are processed in the on-board computer, which has access to information from the integrated flight/propulsion-control system as well as input on the desired flightpath. Flightpath commands for normal acceleration, roll rate, and throttle are generated by the computer. The command information is displayed on the F-15 heads-up display, where it may be implemented by the pilot. In an automatic mode,

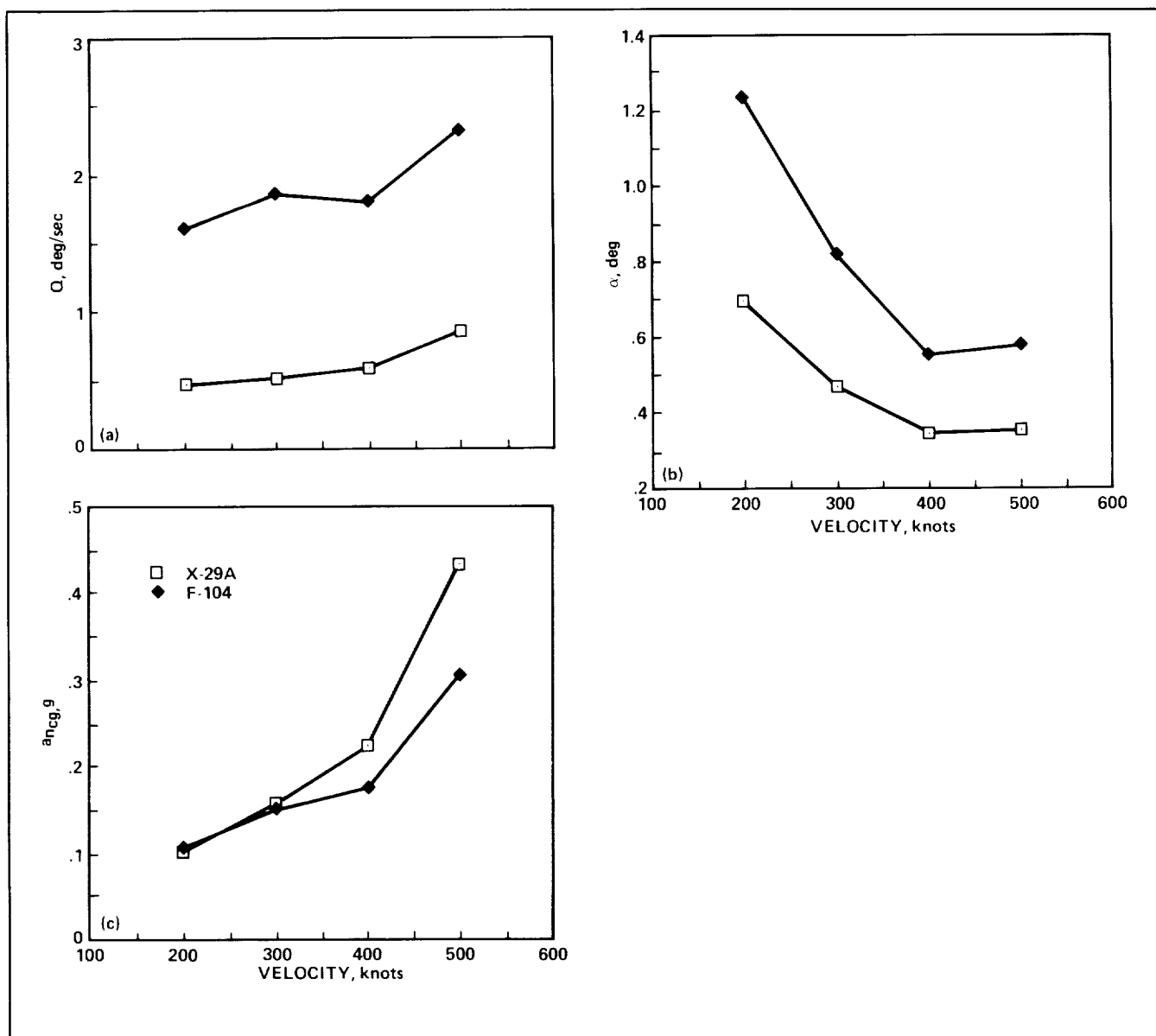
the flightpath and throttle commands are implemented through the HIDEC system, and the pilot may perform other tasks while the system automatically flies the optimum trajectory. Trajectories are updated approximately every 30 seconds.

During the flight testing, path captures were demonstrated, and manually flown optimum trajectories were compared to pilots' estimated optimum trajectories. A fuel saving of 3% was demonstrated in an all-subsonic mission segment. Larger fuel savings are projected for segments which require the use of afterburning and supersonic speeds.

(F. Burcham, Dryden Ext. 3126)

X-29A Turbulence Response Study

During the envelope expansion of the X-29A aircraft, pilots noticed that the response of this aircraft to atmospheric turbulence was significantly different

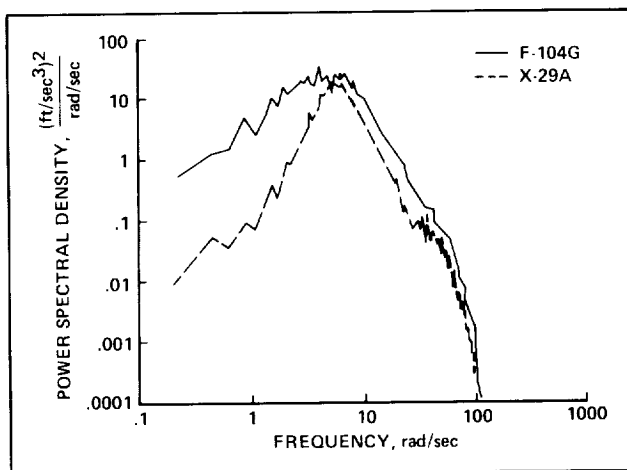


Biased standard deviation. (a) Pitch rate, (b) angle of attack, (c) center-of-gravity normal acceleration

than that of any aircraft they had flown. Pilot comments were, "The aircraft had a soft, uncommanded heaving motion"; it was "smooth edged," with "no sharp accelerations or bobbing"; "it feels like there's no pitching and no α change, no high-g onset." The cause of this unique response was unknown, but was thought to be a function of the X-29A's static longitudinal instability and high-gain/high-bandwidth flight-control system. A research plan was conceived to evaluate the turbulence response of the X-29A compared to a statically stable aircraft.

It was necessary that the stable aircraft in the experiment have the same wing loading as the X-29A, and an instrumentation system with the required parameters and at least a 40-Hertz rate. The aircraft chosen was NASA F-104G #826. This aircraft has a high degree of longitudinal static stability and has a wing area and an empty weight nearly identical to those of the X-29A.

The research plan called for simulated turbulence responses along with flight-test data. The simulation studies were performed with Ames-Dryden's



Power spectral density of center-of-gravity normal acceleration rate (jerk)

highly accurate 48th-order linear model of the X-29A and a simple linear model of the F-104. Models were compared in their responses to stick doublets, discrete alpha gusts, and continuous turbulence produced by a Dryden model. Flight data were collected in constant-altitude and constant-speed runs (2-minute duration) through atmospheric turbulence. The X-29A and the F-104 were in loose wingtip-to-wingtip formation with minimal pilot inputs. X-29A data were telemetered and recorded in the ground station while F-104 data were recorded aboard the aircraft. All data were analyzed for root-mean-square, standard deviation, and power spectral density.

The simulation and flight-test results were consistent and agreed well with pilot comments. The figure shows biased standard deviations of pitch rate, angle of attack, and center-of-gravity normal acceleration (ANCG) from the flight tests. (Biased means that pilot longitudinal stick inputs have not been factored out of these values.) These data show the much higher F-104 pitch rate and alpha changes. Normal acceleration at the center of gravity shows the X-29A's higher g's at high speed. This is a function of the X-29A's higher ANCG/alpha at high speed. The second figure shows the X-29A's much lower g-onset at low frequency. The heaving motion

may be caused by the flight-control system reacting quickly to the aircraft's pitch-up tendency. This would negate the pitching motion, and would appear as direct lift.

Future work will include the creation of a larger statistical data base, updates of the F-104 linear model, simulation correlation, turbulence model validation, and further investigation into the exact dynamics responsible for the unusual turbulence response.

(D. Crawford, Dryden Ext. 3007)

F-18 Off-Surface Flow Visualization

One of the research objectives for the F-18 High Angle of Attack Research Vehicle is to investigate the characteristics of the vortical flow structures which can play a large role in high-angle-of-attack flight. A technique to visualize the off-surface vortical flow has been developed. Smoke, generated by a smoke cartridge designed for this application by the U.S. Army Chemical Research, Development, and Engineering Center in Aberdeen, MD, is injected into the flow at several locations. The smoke is entrained in the vortical structures (forebody vortices and leading-edge extension (LEX) vortices) and traces them. The smoke flow is recorded using a 35-millimeter still camera and four video cameras.

Typical results using smoke for the visualization of the F-18 LEX vortices are shown in the first figure. In this case the smoke was emitted from a port near the LEX apex. The camera used to obtain these photos was mounted on the right wingtip. Note that as the angle of attack increases, the vortex breakdown location moves forward.

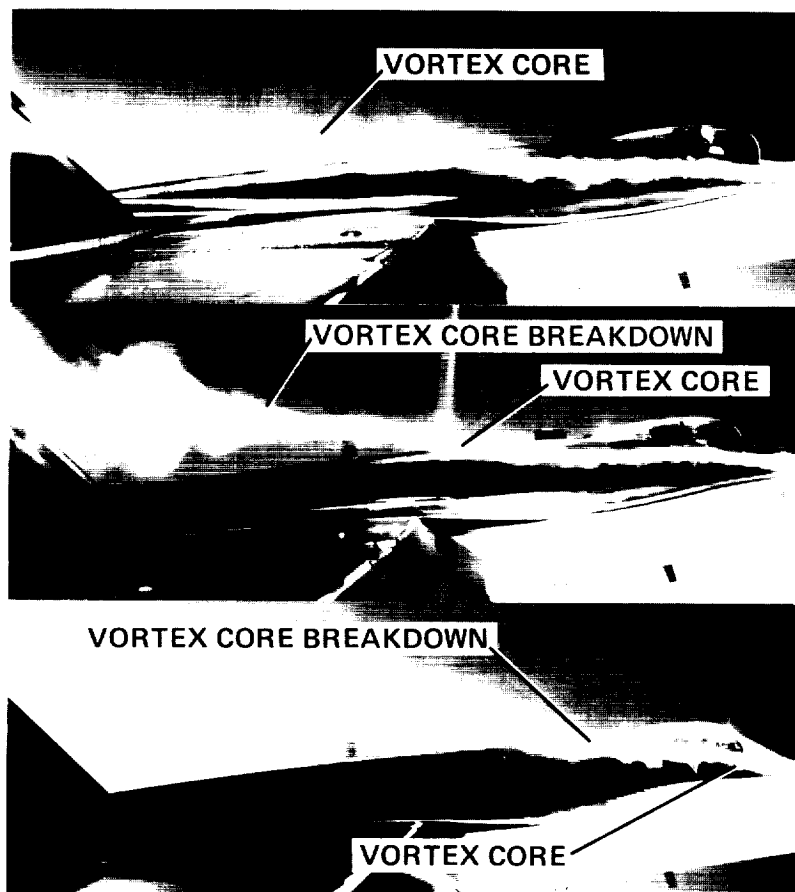
The second figure shows the LEX vortex breakdown position plotted against angle of attack. Note that the data gathered using smoke to visualize the vortex correlates well with that gathered using naturally occurring condensation.

(J. Del Frate, Dryden Ext. 3704)

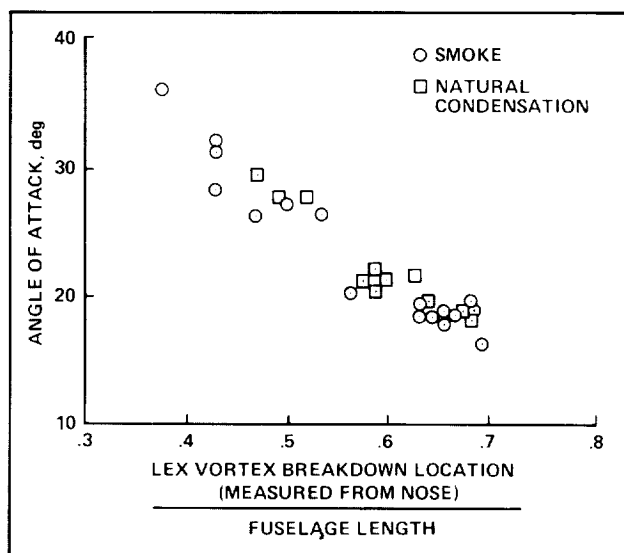
ANGLE OF ATTACK 15.0°

20.8°

34.6°



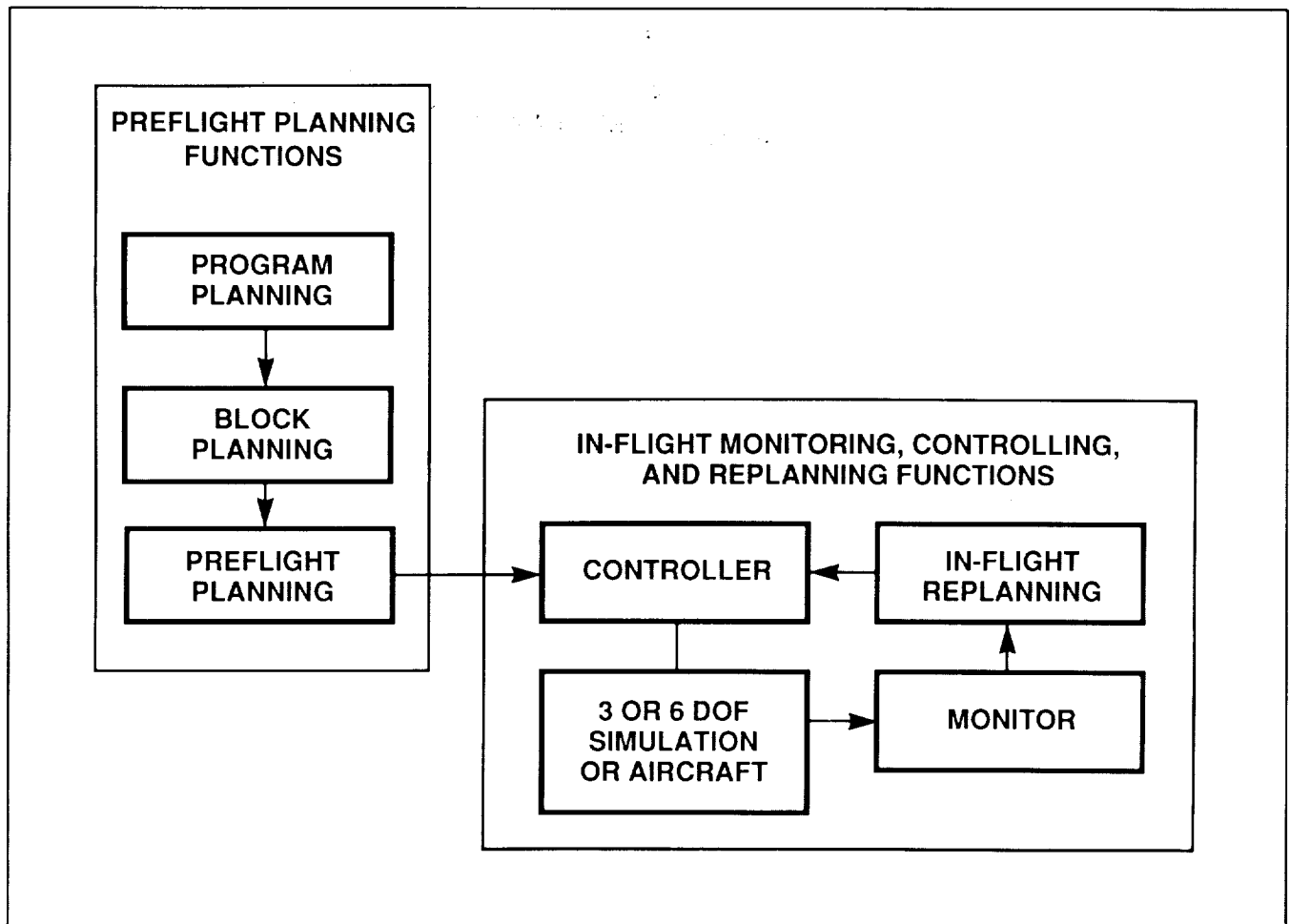
Examples of in-flight flow visualization with smoke generator system on F-18



The ATMS demonstrated flight-maneuver scheduling, a real-time controller for flight-test maneuvering, the close-coupling of symbolic and

numeric processing, and real-time maneuver monitoring.

(L. Duke, Dryden Ext. 3802)



Automated Flight Test Management System (ATMS) overview

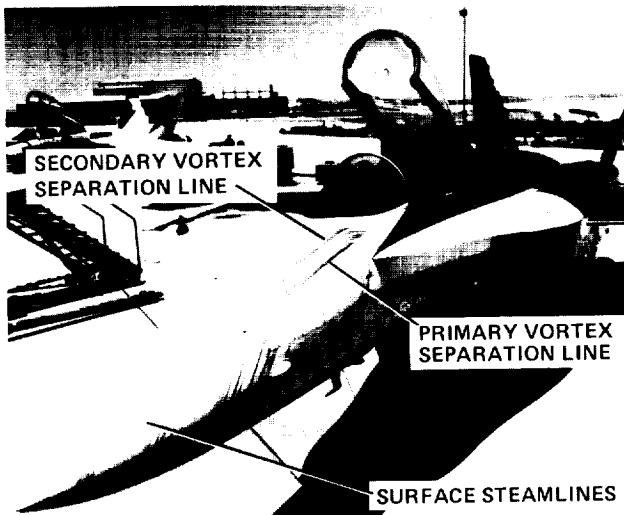
F-18 Surface Flow Visualization

Flow-visualization systems have been developed on the F-18 to visualize the vortical flow on the forebody and leading-edge extensions (LEX) when the aircraft is at high angles of attack. An emitted-fluid technique is used to mark the surface streamlines and regions of separated flows. This technique consists of releasing a small quantity of propylene glycol monomethyl ether and dye from surface orifices while the aircraft is stabilized. The flight conditions are held constant for about 1.5 minutes while the fluid evaporates and the dye sets or dries. The dye

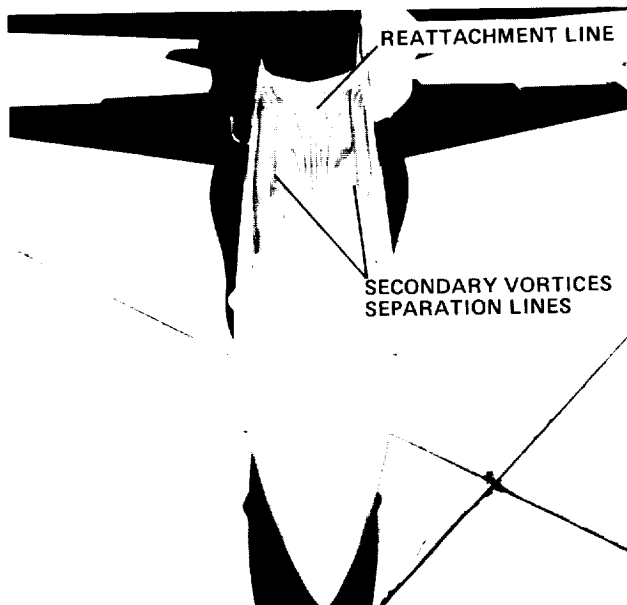
patterns of the surface streamlines and separated-flow regions are documented by photographing the surfaces after each flight.

Results of using this technique on the F-18 forebody for an angle of attack of 30° are shown in the two postflight photographs. An interpretative cross-section flow model showing the structure of the flow about the forebody for symmetrical flow is illustrated in the third figure.

Two primary and two secondary vortices were formed on the leeward side; the separation and reattachment lines are noted. As can be seen in the photographs, the remaining dye from this technique



Postflight visualization of surface streamlines and lines of separation on F-18 forebody, $\alpha = 30^\circ$

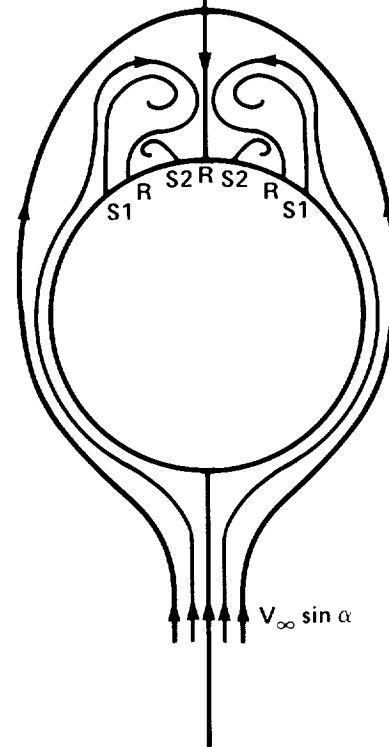


Head-on view of forebody

clearly showed the surface flow streamlines. Where the streamlines merge, the flow lifted from the surface and rolled up into streamwise vortex cores. Along the streamlines where the flows merge, the separation lines for the vortices were defined. Both the primary and secondary separation lines can be seen. A reattachment line on top of the forebody where the streamlines diverge is also noted.

(D. Fisher, Dryden Ext. 3705)

ORIGINAL PAGE
BLACK AND WHITE PHOTOGRAPH



Model of flow about forebody, symmetrical flow
(cross-sectional view)

X-29A Flight-Control Research

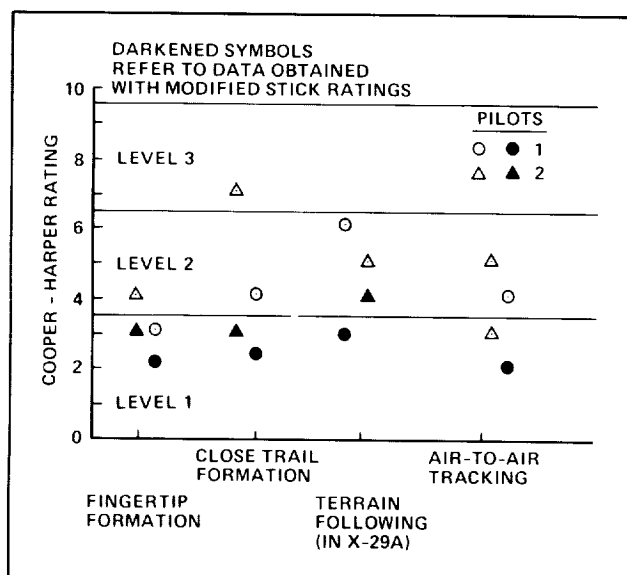
Although the X-29A research airplane was primarily designed to demonstrate the aerodynamic and structural advantages of forward wing sweep, the flight-control system of the airplane also incorporates several features that are of current interest in research on flight dynamics and controls.

Highly Relaxed Static Stability. The X-29A is flying with static instability levels that are unprecedented for manned airplanes. These instability levels allowed addressing the issues of (1) flight safety of this type of airplane during initial envelope clearance, (2) the applicability of military specifications on

dynamic stability, and (3) tradeoffs between dynamic stability and maneuverability.

Degraded Flight Control System Modes. These modes were designed into the flight-control system to be activated in the event of failure of various sub-systems, such as the attitude/heading reference system, the air-data system, and the angle-of-attack sensing system. Research to date shows that with the level of static instability of the X-29A, each degraded mode must incorporate variable gains, and that the degraded modes should have provisions for easy testability.

Speed Stability and Landing-Approach Characteristics. The high degree of stability augmentation of the X-29A results in an apparent neutral speed stability; that is, large changes in airspeed are possible without any changes in stick position or force. The pilots found this characteristic desirable in all flight phases except in the final approach during flare. During a series of evaluation approaches it was found that the introduction of a pitch stick force proportional to the airspeed difference from 175 knots resulted in desirable landing characteristics. This investigation included the evaluation of landing characteristics at low approach speeds, one of the benefits of forward wing sweep. Because of poor over-the-nose visibility at airspeeds below 140 knots, no firm conclusions could be reached from this study.

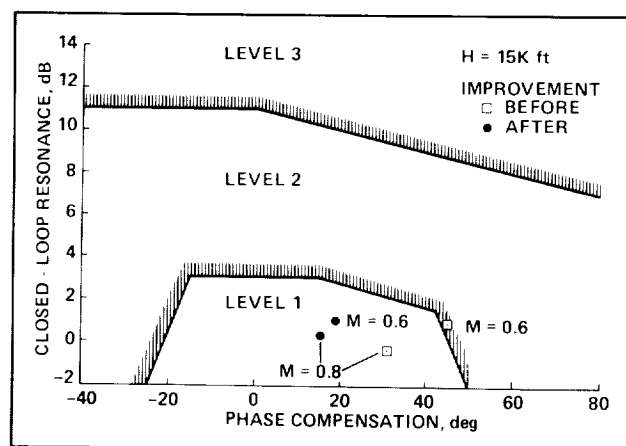


Flying qualities ratings before and after stick harmony modification

The flight-control system includes a precision approach control mode that controls flightpath and airspeed simultaneously. Although this system was not fine-tuned after the initial flight-test data became available, the results showed that the unusual configuration of the X-29A does not exclude the use of such systems.

Response to Atmospheric Turbulence. One of the pleasant surprises of the X-29A flight tests was the response of the airplane to atmospheric turbulence. Because of the very steep lift curve slope of the wing, the airplane was expected to have poor riding qualities in rough air. Both flight-test data and pilot comments showed that the airplane's primary response is a heaving motion instead of pitching into the gusts. Since the three separate pitch-control surfaces do not reach their trim position instantaneously during flight through rough air, the root-mean-square normal acceleration response appears to be attenuated by the flight-control system. Experiments are being conducted by flying a statically stable airplane in loose formation with the X-29A to compare their responses to atmospheric turbulence.

Control Stick Harmony. Studies of initial handling qualities showed that the pitch stick displacement of the X-29A is too large in comparison with the roll stick displacement. The control system was subsequently modified to reduce the pitch stick throw but preserve the original stick force per g. This simple modification resulted in at least a one-point improvement on the Cooper-Harper rating scale in



Handling qualities improvement resulting from using the Neal-Smith criterion

overall handling qualities of the airplane, as can be seen in the first figure.

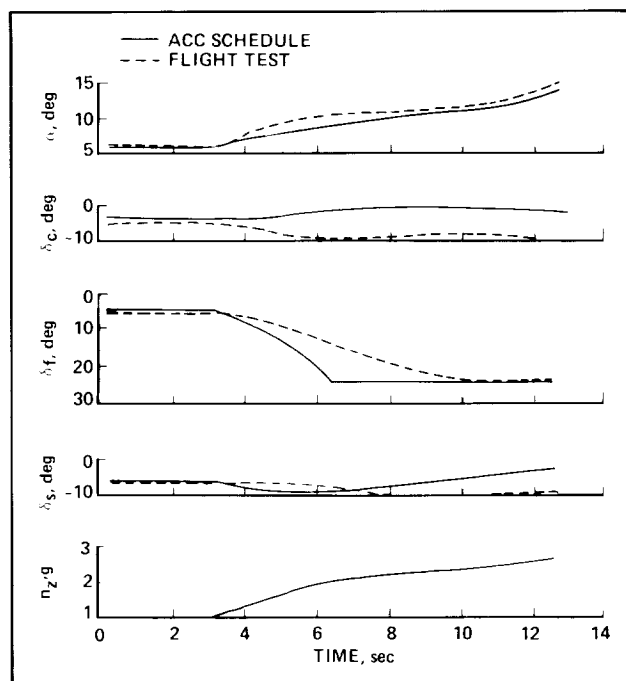
Improved Agility. Pilot opinion of the flying qualities of the X-29A indicated preference for less sluggish pitch response and higher maximum rolling velocities. To improve pitch handling, a scheme that uses initial flight data in conjunction with the well-known Neal-Smith handling qualities criterion was used. The second figure shows the improvement resulting from this modification. The flight-control computer software was also modified to command faster roll rates. Initial results from flight testing of these modifications indicate substantial improvements in the agility of the airplane without compromising dynamic stability levels.

(J. Gera, Dryden Ext. 3795)

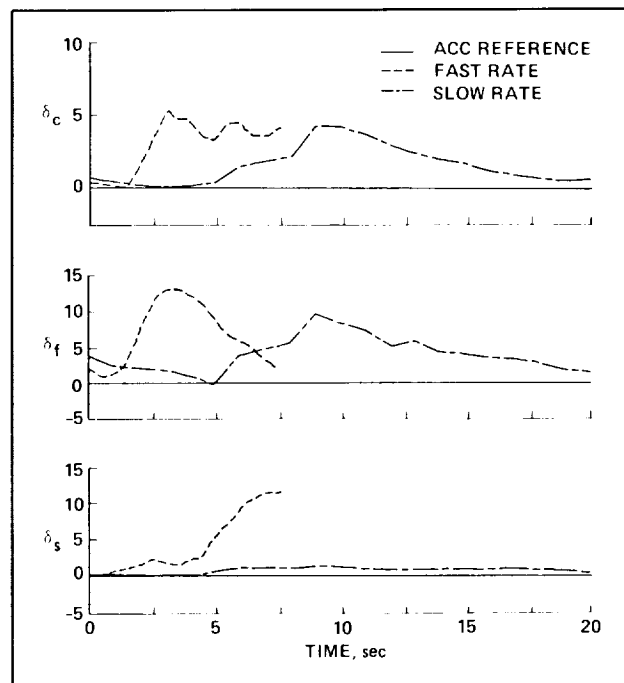
The Effects of Aircraft Maneuver Dynamics on X-29A Aeroperformance

The effects of control-surface scheduling lags on aeroperformance of the X-29A were investigated. These control-surface lags arose during very dynamic flight maneuvers, from inherent design characteristics of the flight-control system. The flight-control system of the X-29A aircraft was designed primarily to stabilize a highly statically unstable airframe. The automatic camber control (ACC) loop feature was designed to provide optimum lift-to-drag ratio for best aeroperformance for trimmed, stabilized flight. The wing-mounted trailing-edge flaperons tracked the automatic cambering schedule at a slow rate of 2° per second so as not to interfere with the short period control of the aircraft. During rapid maneuvering, this slow tracking rate resulted in large control-surface deviations from the optimum configuration and significant aircraft drag penalties of up to 15% in the subsonic speed regime.

The phenomenon was investigated in flight during the X-29A aeroperformance flight research phase as a function of maneuver rate and Mach



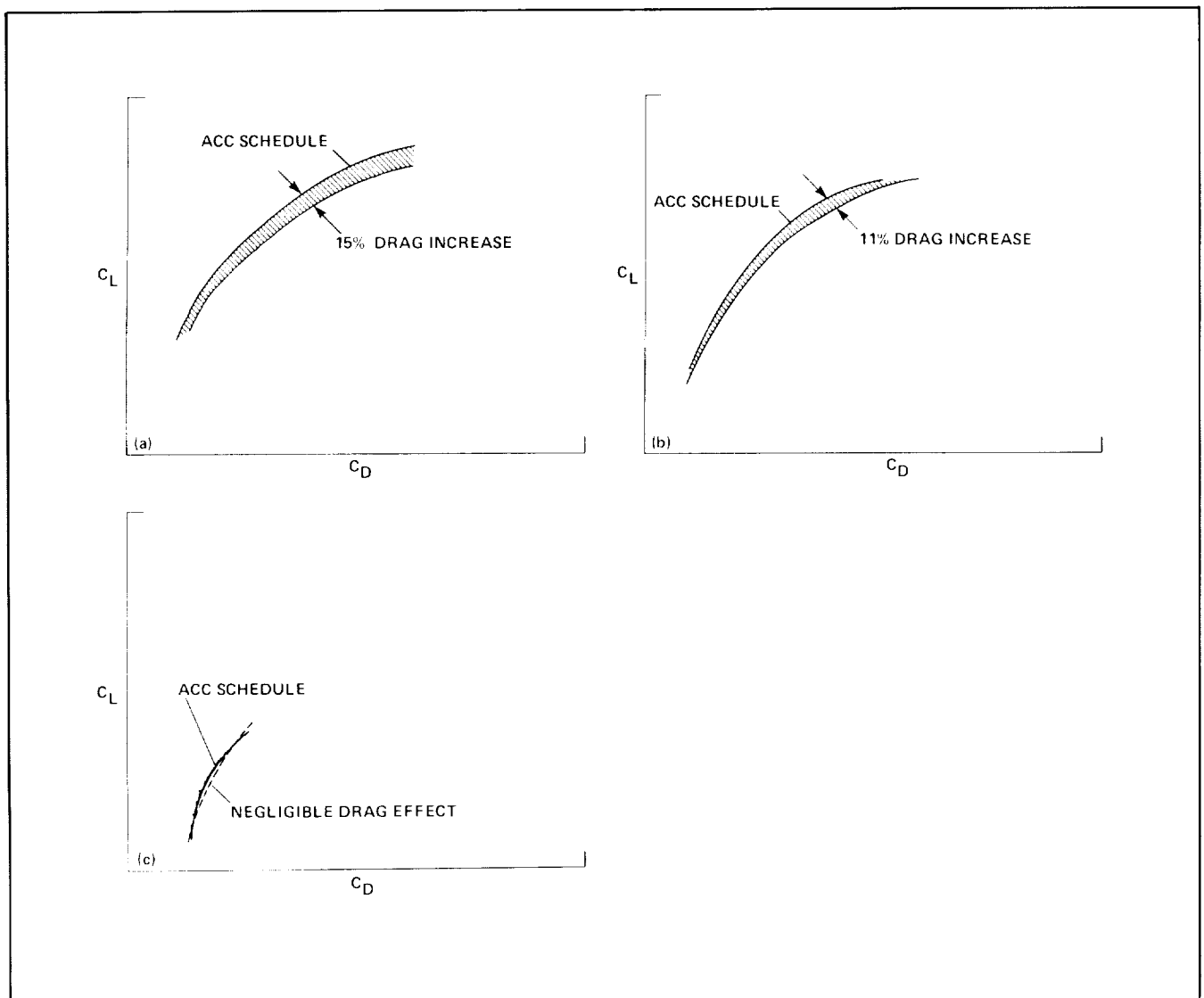
Off-ACC schedule effects



Control surface off-ACC reference increment during dynamic maneuvers

number. The dynamic-maneuver test techniques flown included the constant-Mach number pushover-pullup and wind-up turn. The pushover-pullup was flown at increasingly higher g-onset rates from the 1-g, wings-level, stabilized flight condition to a pushover to 0 g, a pullup to 2 g, and a recovery to 1-g flight. The constant-Mach-number wind-up turn was flown from the 1-g level-flight condition by increasing the normal load factor at varying g-onset rates in a turn until the aim load factor or angle of attack was reached. G-onset rate varied from 0.07 to 0.15 g/sec for "slow" maneuvers to about 0.5 to 0.7 g/sec for "fast" maneuvers. Test Mach numbers flown were 0.60, 0.90, and 1.20 at 30,000 feet.

Dynamic flight conditions caused all the control surfaces to lag several degrees from the ACC schedule. The forward-fuselage-mounted canards lagged as much as 13° , the wing flaperons lagged as much as 20° , and the aft-fuselage-mounted strake flaps lagged as much as 10° . Given a slow maneuver rate or enough time to track back to the optimum camber schedule, the control surfaces would track the ACC schedule during quasi-stabilized flight. Increasing maneuver rate caused larger control-surface deviations and aggravated the problem, since the control surfaces did not have enough time during the maneuvering flight to track back to the optimum schedule.



Maneuver dynamics effects on aeroperformance. (a) Subsonic case, (b) transonic case, (c) supersonic case

Subsonically the resulting drag increase from the optimum lift-to-drag polar was as much as 15%. As the airspeed was increased to Mach 0.90, the drag penalty effect began to wash out as a result of increasing flight-control-system limits on maximum flaperon travel. The maximum difference in this case was about 11%. Supersonically at Mach 1.20 there was no measurable drag penalty, because of the restricted travel of the flaperons.

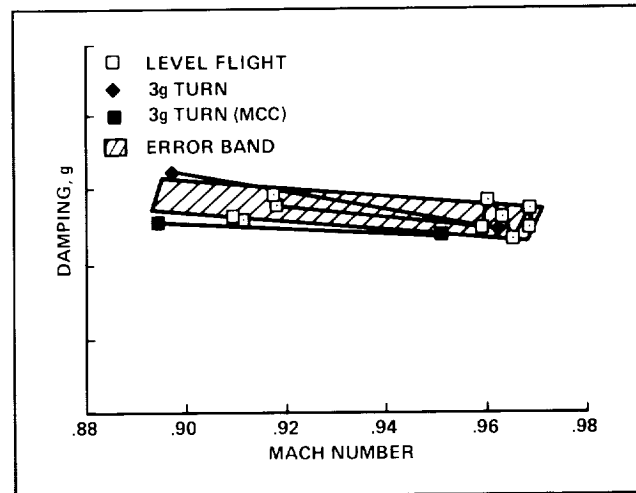
Although there was a conservative design compromise in the flight-control system to ensure aircraft stabilization, the flight-control laws can be designed to track the ACC schedule for best aeroperformance during maneuvering flight as well as in stabilized flight.

(J. Hicks, Dryden Ext. 3301)

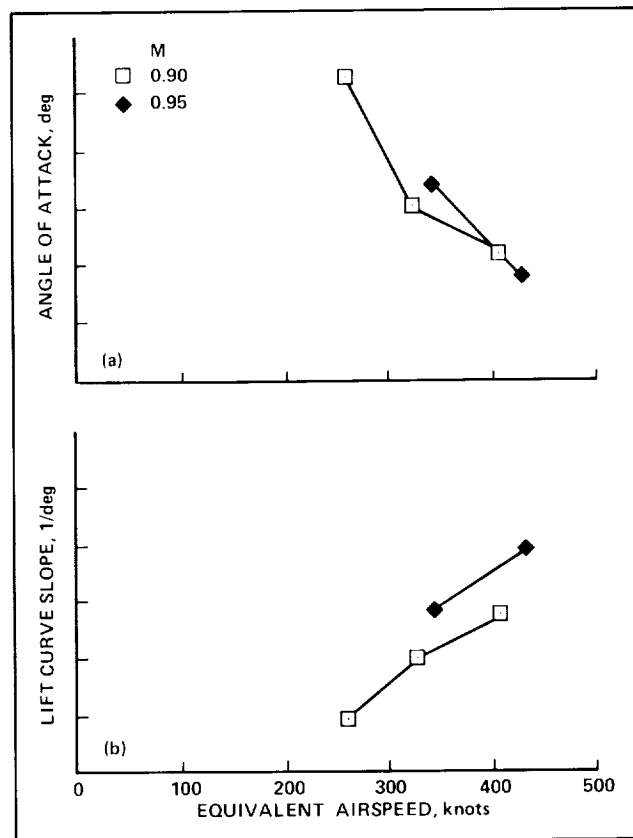
The Effects of Angle of Attack on Structural Damping on the X-29A Forward-Swept-Wing Airplane

Computer analyses, wind-tunnel tests, and flight tests have indicated that for unswept and aft-swept wings, flutter speeds and damping decrease with increasing wing angle of attack in the transonic Mach number region. Supercritical airfoils also can appreciably reduce the flutter speed of a wing in the transonic region. A flight investigation was conducted on the damping characteristics of the X-29A forward-swept-wing airplane at several angles of attack in the transonic region, at three different altitudes. This study provides the first in-flight data on the effects of angle of attack on structural damping for forward-swept wings using a thin, supercritical airfoil.

Three different angles of attack were obtained at each Mach number flown. The first was achieved by straight and level flight. This was followed by a 3-g turn flown in the automatic camber control mode, which allows the flaperons to deflect to an optimum position. To obtain higher angles of attack at a given Mach number, a 3-g turn was flown in the manual camber control (MCC) mode with the flaperons set at 0°.



Symmetric wing bending modal damping at an altitude of 40,000 feet



Measured lift-curve slope and angle of attack for straight and level flight conditions. (a) Angle of attack, (b) lift curve slope

The damping did not change as a function of angle of attack. An example of damping as a function of Mach number for the symmetric first wing bending mode at 40,000 feet is shown in the first figure. The damping measured at angles of attack above those required for straight and level flight are shown to be within the data scatter band for the straight and level damping values. Data were similar for other structural modes at the other altitudes tested.

Aerodynamic pressure and wing deformation data were obtained as angle of attack was varied. Shown in the second figure are variations with equivalent airspeed of the lift-curve slope and angle of attack at straight and level flight conditions for Mach numbers of 0.90 and 0.95 in the automatic camber control mode. It can be seen that the lift-curve slope increased for each Mach number as the equivalent airspeed was increased, which indicates an increasing leading-edge up-twist of the wing per degree angle of attack at the higher equivalent airspeeds.

This work contributes to the overall data base for angle-of-attack effects on structural damping in the transonic Mach number region.

(M. Kehoe, Dryden Ext. 3708)

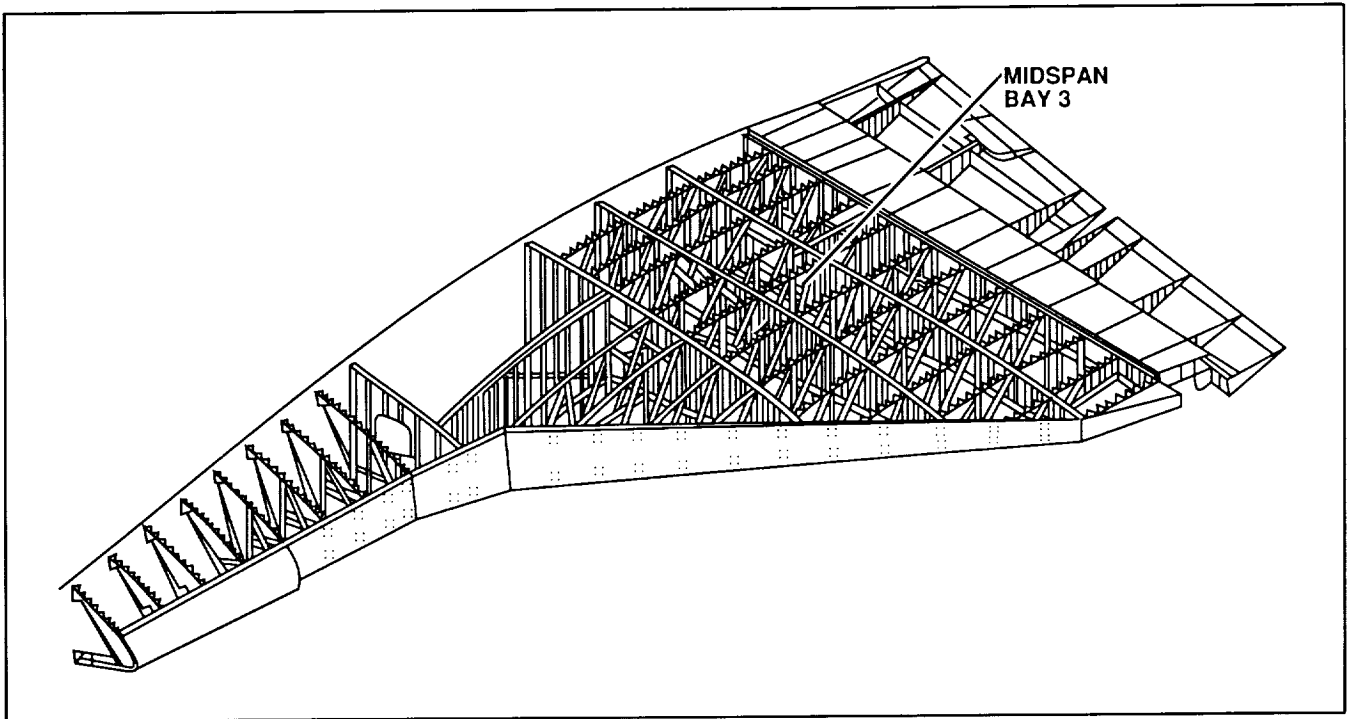
Thermal Analysis of Space Shuttle Orbiters

In thermal analyses of complex aerospace structures such as space shuttle orbiters, finite-element methods are usually used. In setting up finite-element thermal models of complex structures, the use of excessively fine elements may cause the number of radiation view factors to be astronomical, resulting in prohibitive computation time and/or computer space requirements for the transient-heat-transfer analyses. (For wing-box-type structures, each time the number of radiation elements is doubled, the number of radiation view factors is nearly quadrupled.) Thus, in finite-element thermal analysis of orbiter-type structures, the highest level of element density is determined by time constraints and/or by the memory capacity of the computer used.

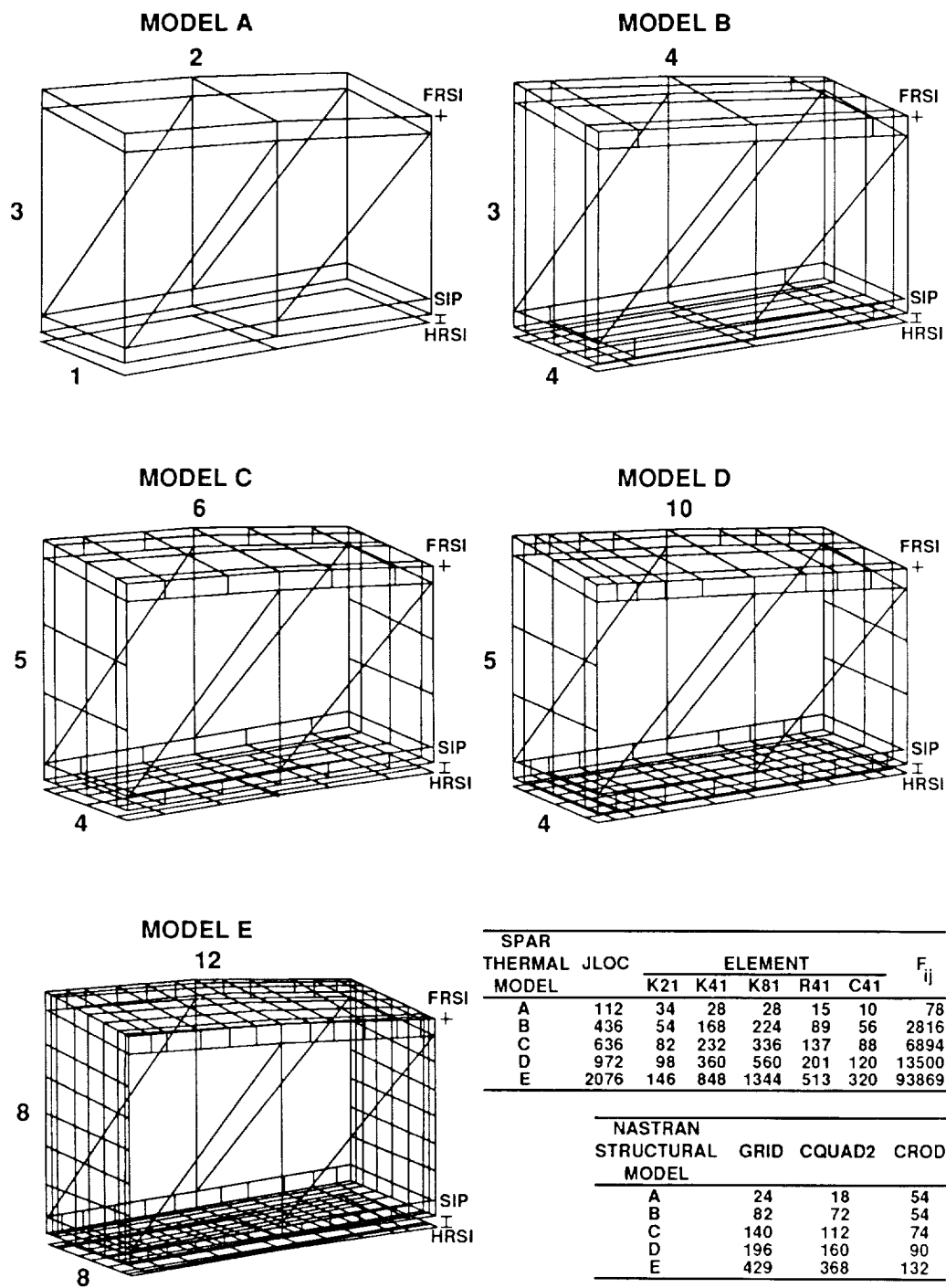
In order to establish the element density level for the thermal model of the entire wing, which could give accurate temperature predictions, one cell of the orbiter wing (located at midspan bay 3, as shown in the first figure) was selected for studies of the effect of element density on accuracy of temperature predictions (second figure). As can be seen in the third figure, a reasonable element density for the orbiter-type structure is eight elements between the two adjacent spar webs and six elements between the two adjacent ribs.

The results of this study form the basis for determining the element density level required in the thermal modelings of other aerospace structures similar to the orbiter structures.

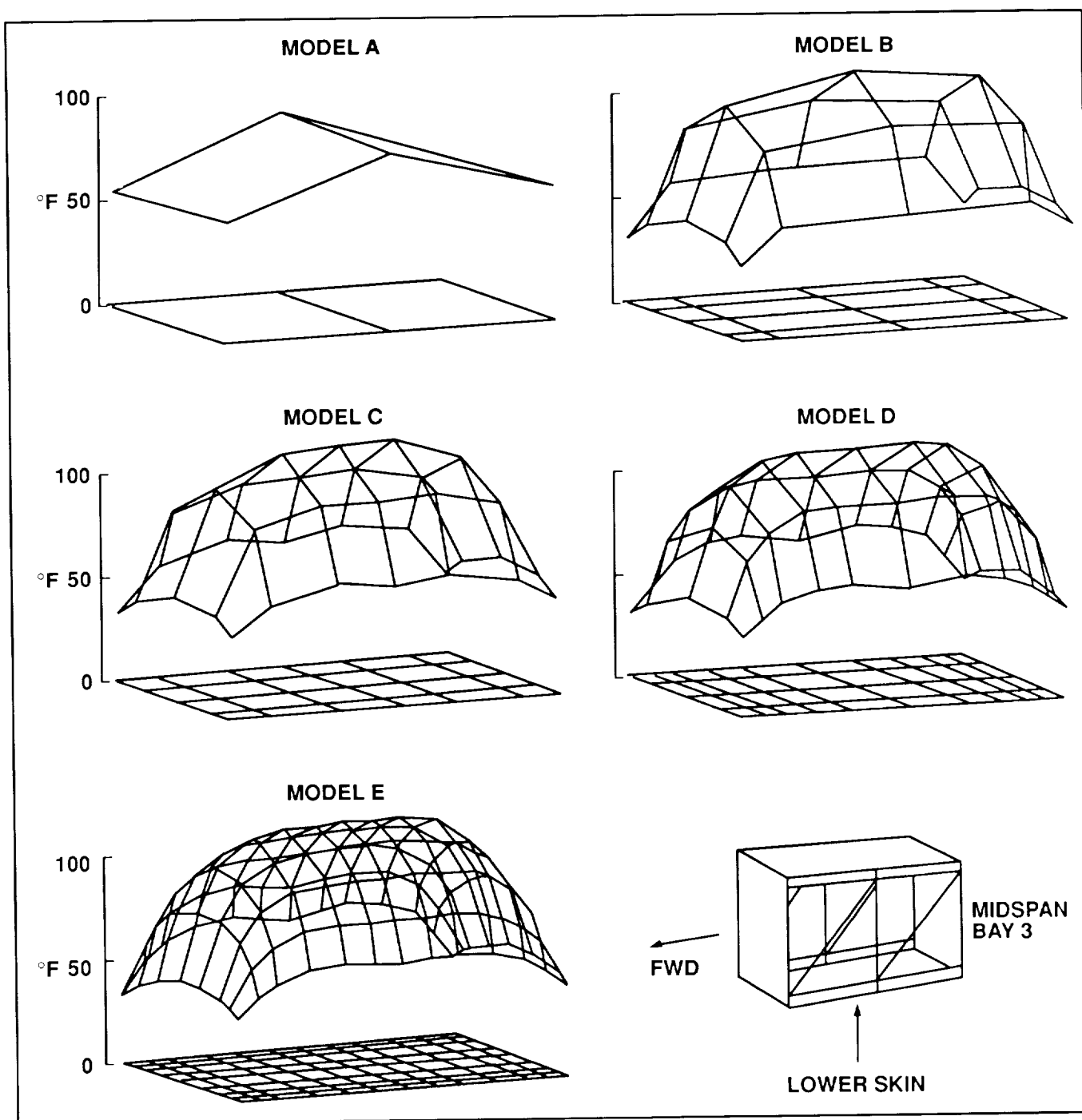
(W. Ko, Dryden Ext. 3581)



Space shuttle orbiter wing structure



Spar thermal models set up for orbiter wing midspan bay 3



Distributions of orbiter wing lower skin temperatures predicted from different thermal models. Time = 1700 seconds, STS-5 flight

Aircraft Performance Improvements with an Integrated Engine Flight-Control System

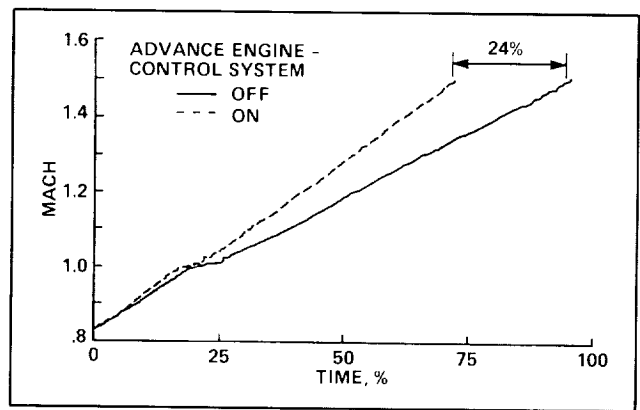
In a conventional engine control system, the engine stall margin is large enough to accommodate the worst-case combination of engine- and airplane-induced disturbances. In the Advanced Engine Control System (ADECS) mode, the stall margin is modulated in real time based on current requirements. This permits the unneeded stall margin to be traded for increased engine performance in the form of increased thrust, reduced fuel flow, or lower operating temperatures. This trade is implemented by uptrimming the engine pressure ratio (EPR).

The ADECS research was conducted at the Ames-Dryden Research Facility on an F-15 airplane. A digital electronic engine control (DEEC) was installed on both of the F100 engine model derivative (EMD) engines in the airplane. A digital electronic flight-control system, which contains the ADECS logic, was also installed on the airplane. These digital systems communicate with each other through a digital data interface and bus controller.

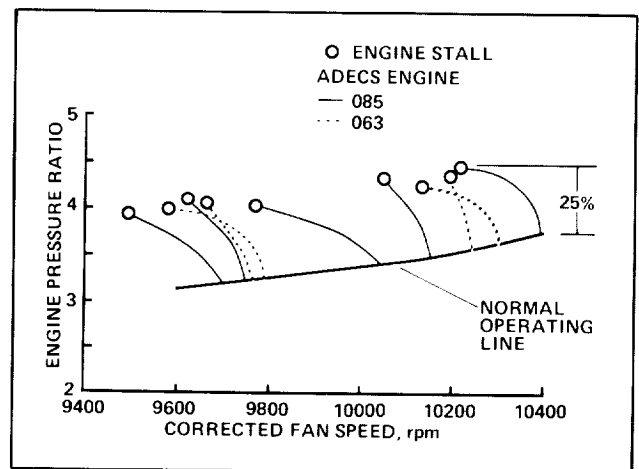
Thrust is increased by uptrimming EPR in parts of the flight envelope where excess stall margin and fan-turbine-inlet-temperature margin exist. The EPR uptrim logic resides in the digital flight-control computer and determines the proper EPR command to send to the DEEC to obtain higher thrust.

Results obtained from flights with one of the two F100 EMD engines equipped with the ADECS were reported in 1987; thrust increases of up to 10% were shown. In 1988, both engines were equipped with the ADECS system and additional aircraft performance benefits were obtained.

The additional thrust obtained with EPR uptrim was effective in improving aircraft performance. When angle of attack is low at this condition, the uptrim command is maximized because the inlet distortion is low. For test flights flown back to back, and after correction for differences in aircraft gross weight, the improvement in aircraft performance during a constant-altitude acceleration at maximum power at 50,000 feet is shown in the first figure. The time for acceleration from Mach 0.8 to Mach 1.5 is 24% less with the ADECS on. The improvement in specific excess power with the ADECS on for this



Maximum-power aircraft acceleration at 50,000 ft



Fan map showing stall margin of both ADECS engines

acceleration is about 10% at Mach 0.8 and 45% at Mach 1.5.

The effect of EPR uptrim on a 350-knot, intermediate-power climb from 10,000 to 40,000 feet was a significantly higher rate of climb, with a 14% improvement at 40,000 feet. With EPR uptrim, the time to climb from 10,000 to 40,000 feet was reduced 13%.

In order to validate the methodology used in the stall-margin calculation, intentional in-flight engine stalls were accomplished by increasing the values in the EPR command. The second figure shows a fan map representing fan pressure ratio versus corrected fan speed. Both ADECS engines were individually stalled. The data indicate that both engines have a stall margin of about 20-25%. This provides confi-

dence that the ADECS concept is not unique to a particular engine, but has general application.

ADECS is the first integrated flight- and propulsion-control system to be demonstrated in flight on an aircraft specifically configured for integrated-controls research. It will be possible to implement a wide range of integrated flight- and propulsion-control modes aboard future aircraft. Such modes will increase total vehicle effectiveness without significant weight or cost penalties.

(L. Myers, Dryden Ext. 3698)

In-Flight Simulation Study of Lateral Flying Qualities

An extensive flight research program, using the USAF variable-stability NT-33 aircraft, examined the interaction of the pilot controller feel system and the aircraft/flight-control-system dynamics on lateral flying qualities. The program was jointly conducted by NASA Ames-Dryden and the Calspan Corporation.

With highly augmented aircraft such as the X-29 research airplane, it was found to be advantageous to use complex control laws to produce very high levels of damping in all axes. This produced a very short roll-mode time constant in combination with a large time delay, for which there were no adequate design criteria. In addition, the X-29 pilot stick characteristics were significantly different than in previous aircraft, and the current practice of including the stick response in the calculation of overall time delay appeared to be invalid, judging from pilot evaluations. There was a need, therefore, to extend the handling

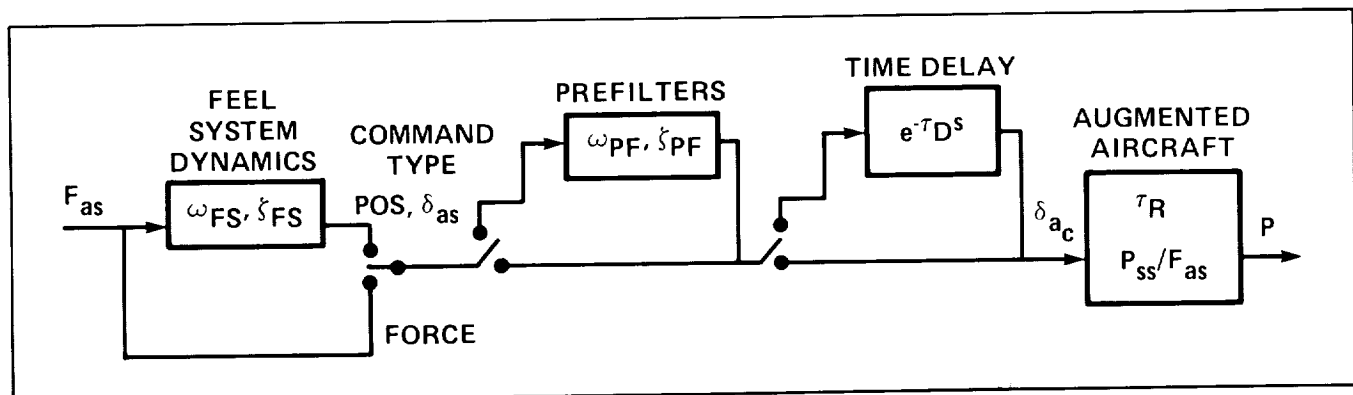
qualities data base to include these aircraft design variables.

The two major objectives of the research program were (1) to extend the data base to include systems with very low roll-mode time constants in conjunction with large time delays, and (2) to determine the contribution of the feel system to the overall measure of time delay.

The experimental setup is shown in the first figure. The primary variables were stick feel system frequency, roll-mode time constant, prefilter dynamics, and pure time delay. Both stick-position and force-command inputs were used with feel system frequencies from 8 to 26 rad/sec. Additional time delays varied from 0 to 250 msec, and roll-mode time constants varied from 0.15 to 0.45 sec. These variables were combined with several prefilters to produce the systematic variations of the end-to-end time delay in order to examine the contribution of the various components.

The primary evaluation tasks were the air-to-air tracking task and the approach and landing task. Forty-two flights totaling 56 flight hours were flown by three evaluation pilots. The data obtained included pilot ratings, comments, and task-performance records.

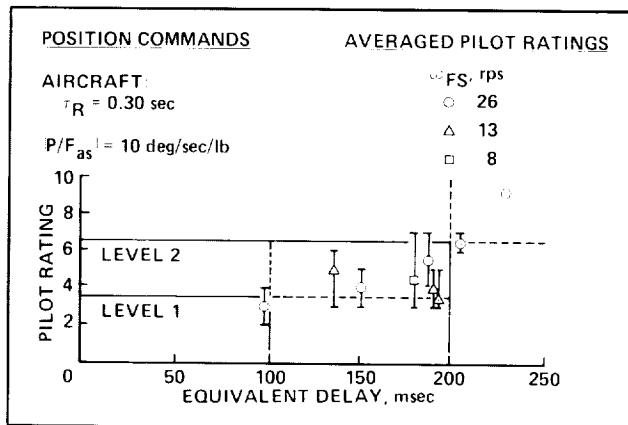
The tests indicated that there is a need to specify lower limits on roll-mode time constant as well as the upper limits that are currently specified in the Military Specifications, and that these limits are a function of time delay. It was also shown that the lag associated with the stick characteristics could be represented as equivalent time delay if the delay was measured from the force input; an example is shown in the second figure. However, the qualitative effect of the delay due to the stick characteristics was considerably dif-



Experimental setup

ferent than an equal amount of delay in the control system. With further analysis these results may be useful in creating design specifications for future aircraft.

(B. Powers, Dryden Ext. 3732)



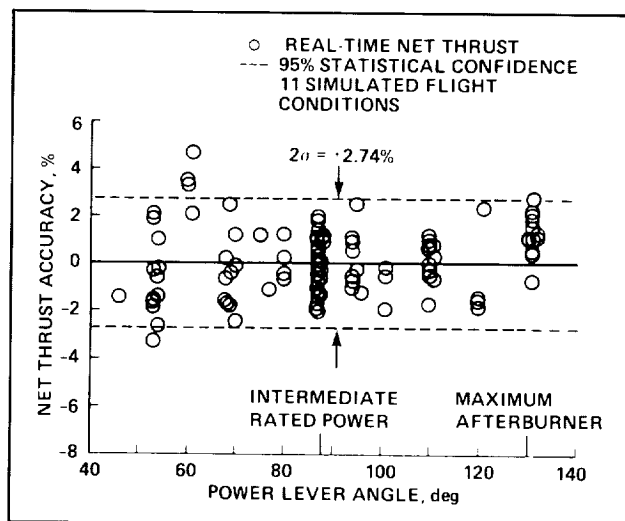
Power-approach evaluation—pilot rating data with the equivalent time delay measured from force input

Development of a Real-Time Net Thrust Technique

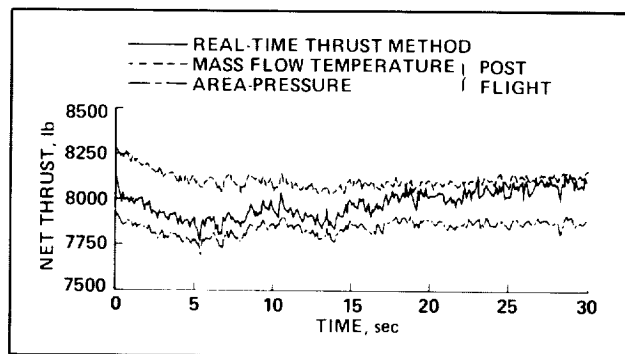
A new real-time net thrust technique was developed, in support of performance testing of the X-29A, to compute and graphically display aeroperformance flight results in real time. This real-time aeroperformance analysis capability allowed quick, accurate, post-maneuver evaluation of maneuver technique and data quality, thus increasing the productivity of the flight program. A key element of this project was the concurrent development of a real-time, in-flight, net thrust algorithm based on the simplified gross thrust method of the Computing Devices Company (Ottawa, Ontario, Canada).

The simplified gross thrust method has been evaluated by NASA on the F100 and J85 engines and was found to have the real-time advantages of minimal instrumentation and computational requirements. The method was developed for and applied to the F404-GE-400 engine using ground-test data obtained during extensive test-cell calibration of the engine for thrust.

The gross thrust algorithm calculates thrust based on a one-dimensional isentropic flow analysis



Accuracy of the real-time net thrust method



Comparison of in-flight thrust calculation methods

in the engine afterburner section and exhaust nozzle. The algorithm requires gas-pressure measurements from three afterburner locations, as well as free-stream static pressure. The afterburner pressures include the turbine exhaust total pressure and the afterburner entrance and exit static pressures. Calibration coefficients were determined during calibration of the gross thrust algorithm from data gathered on the flight-test engine at the NASA Lewis Research Center, and a $\pm 1.80\%$ thrust accuracy was achieved.

Net thrust is computed from gross thrust minus ram drag. Ram drag is the product of inlet mass flow and aircraft velocity. Real-time inlet mass flow was determined by calculating the mass flow rate at the afterburner entrance, using flow parameters determined in the gross thrust algorithm and the turbine discharge total temperature measured by existing

engine instrumentation. This mass flow rate is used to compute the inlet mass flow rate by accounting for bleed air extraction and fuel mass addition using an empirical model developed from calibration data. Aircraft velocity is obtained from the aircraft air data system.

The real-time net thrust method was also calibrated against Lewis calibration data to correct for simplifying assumptions, and a $\pm 2.74\%$ net thrust accuracy was achieved. Because the mass flow is calculated in the engine afterburner section where the gas flow is well mixed, inlet flow distortion effects are minimized.

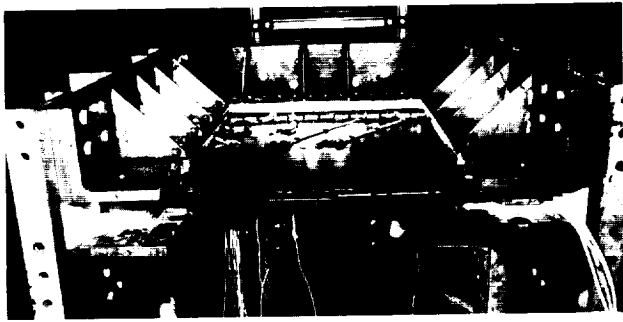
Gross and net thrust values were computed in real time at up to 12.5 samples per second. A real-time graphics display was developed to present time histories of gross and net thrust values and the measured afterburner pressures. This display enhanced safety of flight monitoring of the propulsion system by allowing real-time evaluation of engine performance. Comparisons of the real-time net thrust method to the standard postflight method have proved the real-time method to be both accurate and reliable. Because of the minimum computational requirements, real-time net thrust can readily be computed aboard the aircraft, providing valuable information to an integrated-controls or thrust-vectoring control system.

(R. Ray, Dryden Ext. 3687)

Titanium Honeycomb Panel Heating Tests

Titanium honeycomb panels were identified in the 1960s as one of several candidate concepts for use on high-speed aircraft. In early investigations, honeycomb panels exhibited problems with the bonding between the face sheets and the honeycomb core. Improved bonding techniques such as the Liquid Interface Diffusion (LID) method have resulted in the reemergence of honeycomb panels as leading candidates for the outboard wing panels of a Mach 5 aircraft.

Two LID-bonded titanium honeycomb panels have been tested in the Flight Loads Research Facility at Ames-Dryden to evaluate the integrity of the core/face sheet bonds in a simulated Mach 5



Mach 5 cruise vehicle (artist concept)



Titanium honeycomb panel instrumented with thermocouples and strain gages



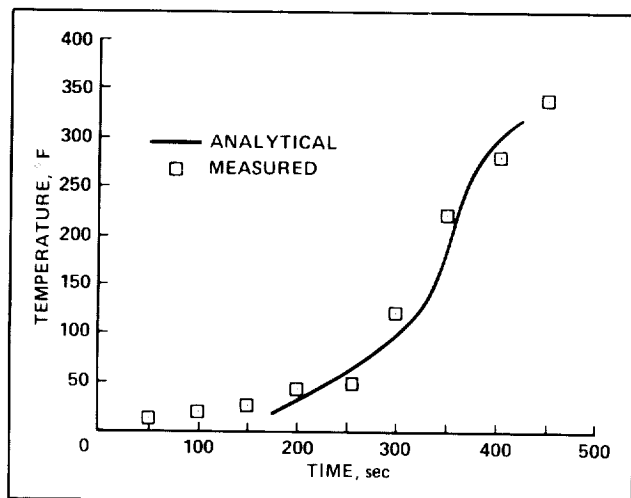
Test fixture with instrumented panel installed

temperature environment. Over 100 thermal cycles have been conducted on 2- by 2-foot wing panels. The panels consist of two 0.060-inch face sheets bonded to a 3/4-inch honeycomb core. Thermocouples and strain gages were installed on a symmetric octant of the upper and lower face sheets.

The stress levels associated with Mach 5 heating were attained by applying (1) a 350°F temperature

gradient through the panel thickness by heating the top surface of the panel with radiant quartz lamps, and (2) a quasi-fixed end restraint to prevent the panel from bending out of plane during heating. The resulting temperature, strain, and deformation measurements were compared to finite element model analysis to help determine the overall validity of this new wing panel concept. Good agreement is shown.

(W. Richards, Dryden Ext. 3562)



Comparison of measured and predicted gradients at center of panel

Structural Divergence of Forward-Swept Wings

The X-29A forward-swept wing flight-test data were examined. Subcritical-divergence/dynamic-pressure extrapolation techniques were investigated using FLEXSTAB analytical data and the X-29A flight data. The structural flight data consisted of in-flight measurements of wing deflections using the electro-optical Flight Deflection Measurement System installed on the X-29A aircraft, and wing-load measurements using calibrated strain-gage instrumentation. Supersonic flight data at Mach 1.2 were collected and preliminary analysis has been completed.

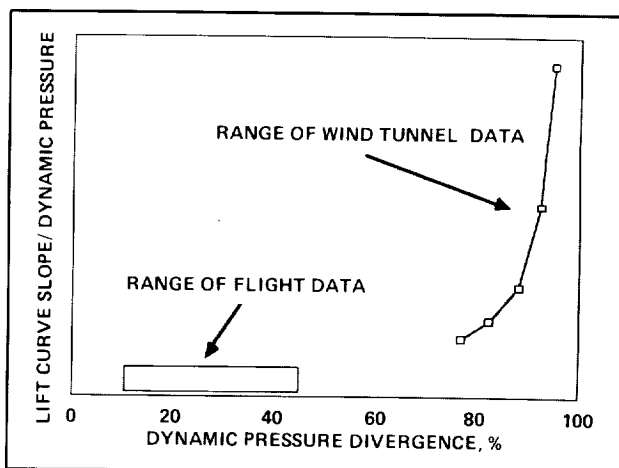
Data-analysis techniques have been refined in several ways. The original application of the divergence prediction techniques called for plotting the slope of a load or twist versus angle of attack. However, because of variations in dynamic pressure

during the flight-test maneuvers, it was found that the load or twist data should be divided by the current dynamic pressure at each point within the maneuver before taking the slope. Then the slope can be multiplied by the average dynamic pressure of the maneuver to obtain the data required on the load or twist per unit angle of attack.

Because of the extrapolative nature of the subcritical divergence-prediction techniques, precise flight-data analysis is required. Aerodynamic characteristics must be determined to the highest possible accuracy, and maneuvers must be performed within narrow specifications.

As a result of the current work, several recommendations are taking shape with respect to the envelope-expansion aspects and data-quality requirements of the divergence-prediction program.

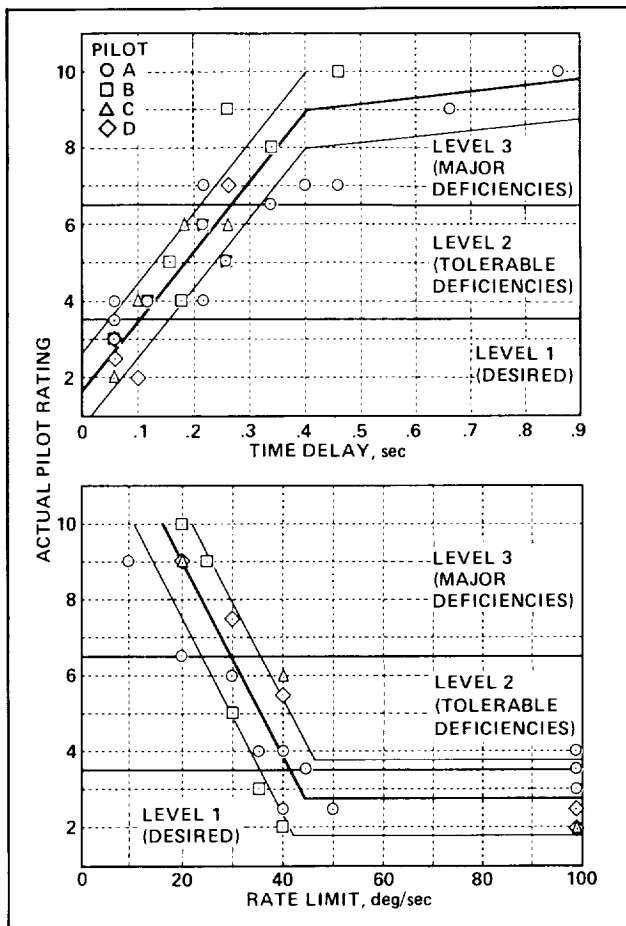
(L. Schuster, Dryden Ext. 3919)



The extrapolation problem

Throttle Response Criteria Research

Preliminary flight-test evaluations were conducted to determine the optimum high-performance-aircraft and engine-dynamic-response characteristics for precision-formation flight tasks. A variable electronic throttle control system was developed and flight-tested on a NASA Ames-Dryden TF-104G aircraft with a J79-11B engine. Ten research flights were flown to evaluate the effects of throttle gain, time delay, and fuel-rate limiting on engine handling



Effect of total throttle-control-system time delay and rate limit on pilot rating

qualities. The evaluations were accomplished at about 15,000 feet altitude and 350 knots indicated airspeed.

The evaluation pilot's objective was to fly in close wingtip formation with a lead aircraft, maintaining an approximately 5-foot wingtip clearance, and fore and aft position, as accurately as possible. It was not necessary to follow the lead aircraft position transients exactly, but the new position was to be captured quickly and accurately. Peripheral evaluations were conducted to investigate the effects of lead compensation for throttle control systems with significant time delay. Handling-quality effects of lag filters were also evaluated.

The evaluation data shown in the figures are in the form of Cooper-Harper pilot ratings versus increasing throttle-control-system time delays and decreasing rate limits. The data show definite trends of handling-quality degradation. Pilot comments obtained during the evaluations substantiate this. Threshold values for the three handling-quality levels, including the optimum values, of these key variables are shown. The ± 1 pilot-rating boundaries result in a data correlation of about 70%. Frequency data on response of compressor speed and longitudinal acceleration to pilot throttle input indicate a strong correlation of input with compressor speed but not with acceleration. The results of this test program provide a foundation for the development of throttle-control-system design guidelines.

(K. Walsh, Dryden Ext. 3686)

Aerophysics

Balance Load and Alarm Monitoring System

A microprocessor-based system for processing the combined static and dynamic signal from strain-gage balances into separate static and dynamic components was designed, fabricated, and evaluated in service as a prototype in the Ames Research Center Unitary 11- by 11-Foot Transonic Wind Tunnel. The system compares these components with a permissible envelope, displays the results, and provides an alarm when limits are approached. Use of this system will ensure that safety of operation is increased and in-service failure of balances resulting from excessive loading will be prevented. The balance load and alarm monitoring system will be integrated into the control of the model attitude so that an automatic reduction of model loads can take place if limits are exceeded. The work is being performed by Raman Aeronautics Research and Engineering, Inc.

(R. Hanly, Ext. 6262)

Development of a New Flow-Through Wind Tunnel Balance for Powered Model Testing

A new flow-through balance was developed to measure the aerodynamic forces generated by an advanced propfan, full-span-transport wind tunnel model with dual-powered propulsion simulators. The balance was calibrated under actual flow conditions in the Propulsion Simulator Calibration Laboratory at Ames Research Center. It has a demonstrated accuracy of $\pm 0.1\%$ of full-scale gage capacity under flow-off conditions. With flow, following the application of temperature, pressure, and momentum corrections, a $\pm 0.5\%$ accuracy was attained. The calibrated flow envelope of the balance is 40 to 160°F, 15 to 1500 pounds per square inch, and a mass flow rate from 0 to 7.0 lbm/sec.

Historically, highly accurate sting-mounted, flow-through balances have generally been difficult to develop because of two major problems: (1) temperature, pressure, and momentum variations associated with the airstream significantly affect the zeros, prime sensitivities, and interactions of the various gages, and (2) accurate calibration facilities and techniques to properly account for these effects are scarce.

Relative to the basic design, the sensitivity of this new balance to high-energy airflow effects has been minimized by incorporating the following design features:





1. an internal chamber with equal opposing areas that cancel most of the pressure and momentum forces on the metric portions of the balance,
2. flexible longitudinal bellows to increase fatigue life,
3. an axial-load measuring beam/flexure system located at the center of the balance to minimize the effects of longitude temperature gradients,
4. a single-piece construction to eliminate mechanical hysteresis effects.

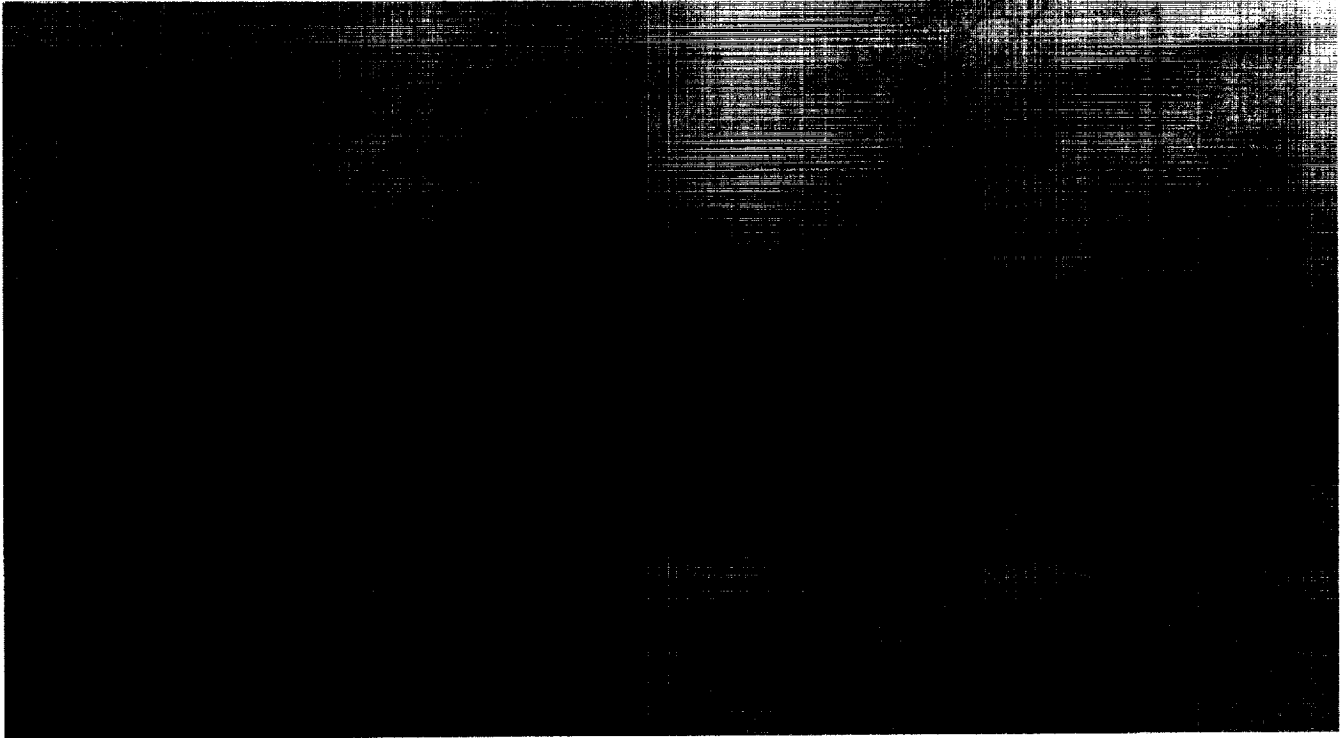
These design elements are illustrated in the first two figures.

The second problem, obtaining a balance calibration under realistic flow conditions, was addressed in the Propulsion Simulator Calibration Laboratory at Ames. The balance was calibrated for a range of temperatures, pressures, and mass flow rates to assess the individual effects and correction algorithms were developed to account for each. To confirm the validity of these correction algorithms, a test case was run where the temperature, pressure, mass flow, and balance loads were varied simultaneously. Initial no-flow conditions were taken at 78°F. Airflow through the balance was initiated with 140°F air at 1000 pounds per square inch and a flow rate of 2.8 lbm/sec. The forward normal gage was incrementally loaded up to 2800 pound force. The uncorrected results of this test case are shown in the third figure. The fourth figure shows the results after applying the correction algorithms. As shown, all flow-on induced deviations were corrected to within $\pm 0.5\%$ of full-scale deviation.


(A. Roberts, Ext. 6272)



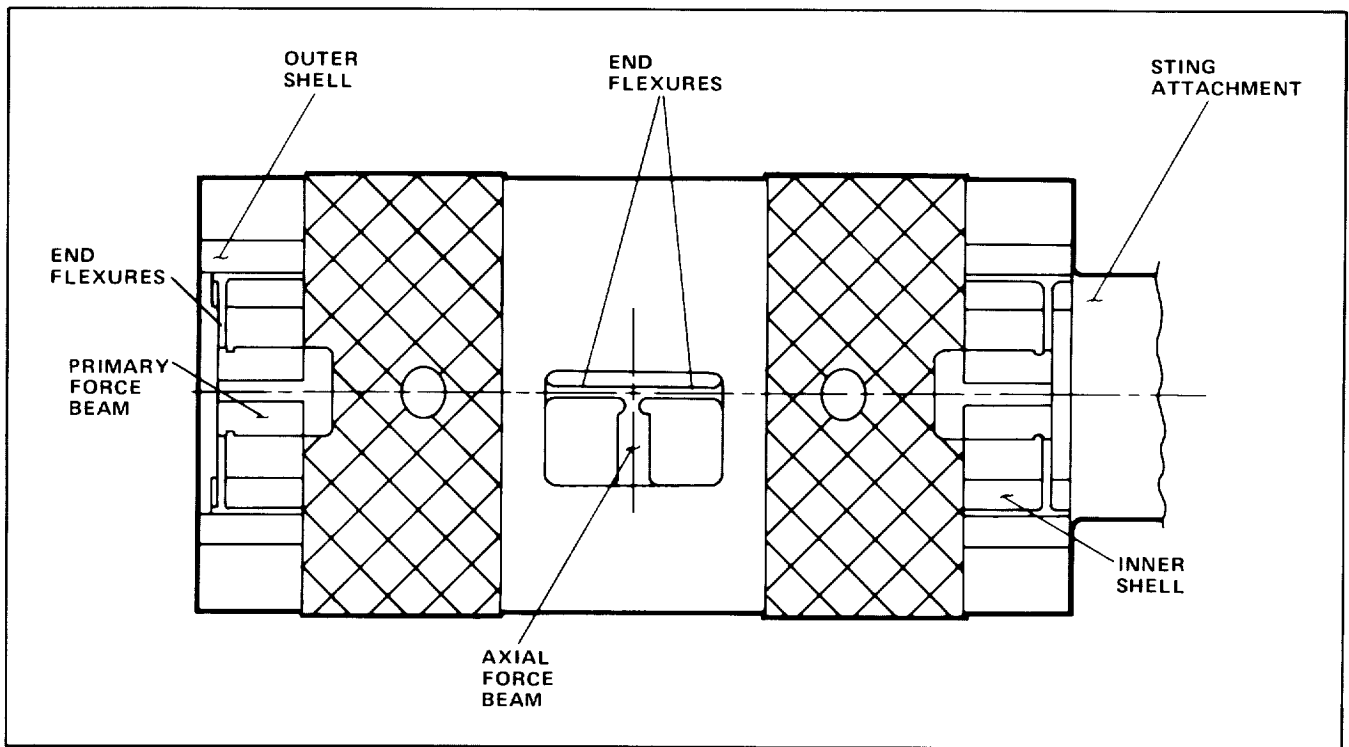
 EXTERNAL ATMOSPHERE
 HIGH ENERGY AIR FLOW
 METRIC PORTION OF THE BALANCE
 NON-METRIC PORTION OF THE BALANCE



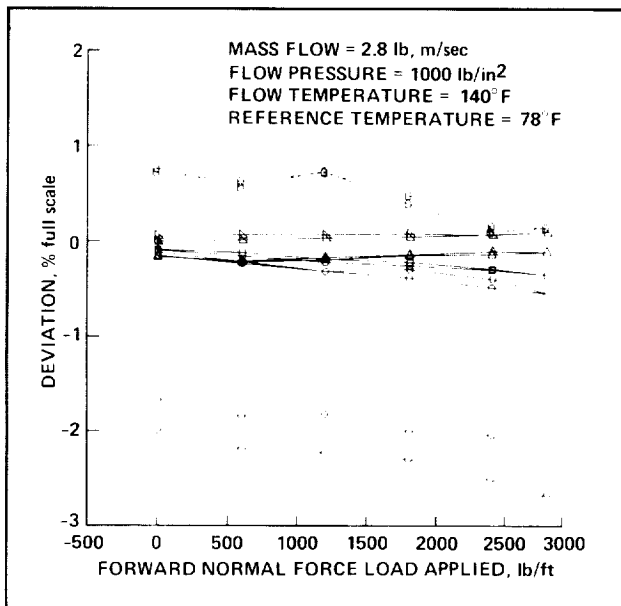
Flow path across the metric break, cutaway view

ORIGINAL 
COLOR PHOTOGRAPH

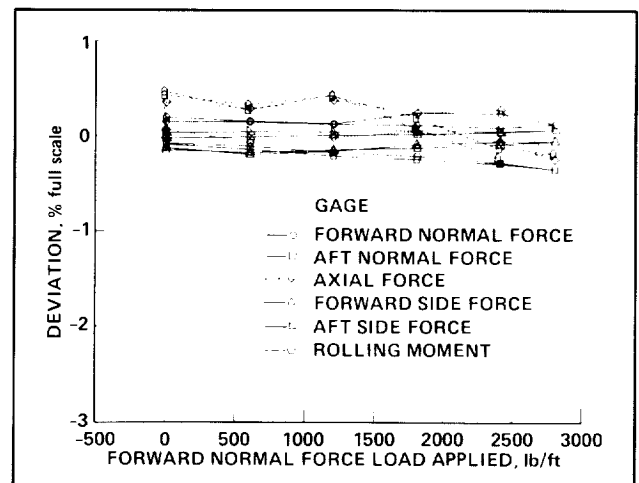
ORIGINAL PAGE
COLOR PHOTOGRAPH



Six-inch flow-through balance, side view



Indicated deviations of the test case results for all gages versus the forward normal force gage being loaded. Initial conditions were taken with a cold balance

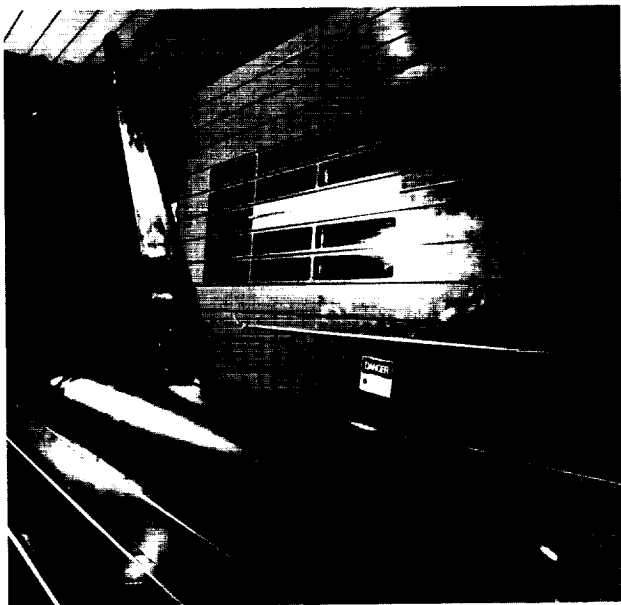


Indicated deviations of the test case results for all gages versus the forward normal force gage being loaded following application of all correction algorithms

NASA/Boeing Co-op

Ames Research Center and Boeing cooperated in a series of tests of semispan models to improve the wing design and the application of tunnel-wall interference technology to large models tested at transonic speeds. The tests used models that are the largest ever tested in the Ames 11- by 11-Foot Transonic Wind Tunnel and are near the practical limit relative to the size of the test section. Use of the large models resulted in Reynolds numbers that are three-fourths the size of full-scale numbers. Results of these tests established the need to evaluate designs at high Reynolds numbers and to perform substantially more computations, including multiple off-design conditions. Additionally, the off-design conditions require fine-gridding for the computations to adequately capture the double-shock structure inherent in off-design conditions. Evaluation of overall flow quality in the 11-foot wind tunnel shows that corner-type vortices exist, which affect semispan test results, and that a viable means of correcting transonic data for adverse flow quality, including wall-interference effects, is required.

(F. Steinle, Ext. 5848)



Advanced transport wing configuration tested

A Knowledge-Based Approach to Automated Flow-Field Zoning

Three-dimensional grid generation continues to pace the progress of computational fluid dynamics research and application. The difficulties of generating a computational grid (caused primarily by geometric complexity, the need for selective grid refinement, and current computer limitations) can be alleviated through the decomposition, or zoning, of a flow field into simpler regions, or zones. Users of such zonal grid approaches have discovered that to reap the benefits of zoning a flow field, it must be done quickly and efficiently. Those two requirements are difficult to satisfy because the element essential to both—zoning expertise—is scarce, is not easily taught, and is not well understood or formulated, and criteria for judging the quality of zonings varies from expert to expert. The growing consensus is that flow-field zoning should be automated.

To lay the foundation for an automated zonal grid-generation capability in three dimensions, a knowledge-based system was developed to demonstrate the feasibility of automating flow-field zoning in two dimensions. The system is called Expert Zonal Grid generator (EZGrid) and is written in C, Franz Lisp, and MRS. MRS is a logic programming language which processes symbolic propositions (facts and if-then rules) using pattern matching and logical deduction. For example, given the fact (man Socrates) and the rule (if (man x) then (mortal x)), MRS could deduce that Socrates is mortal.

EZGrid contains over 400 rules that enable it to automatically design flow-field zonings and generate the necessary computational boundaries and zonal interface curves for representative two-dimensional aerodynamic configurations. Input to EZGrid consists of geometric data (usually files of x,y coordinates), inflow conditions (free-stream Mach number, angle of attack, etc.), a profile of the user's zoning bias (indicating the subjective importance or acceptability of aspects of a zoning such as simplicity, orthogonality, location of singularities, etc.), and a qualitative description of the shape and configuration of the geometry. Zonal boundary-coordinate data

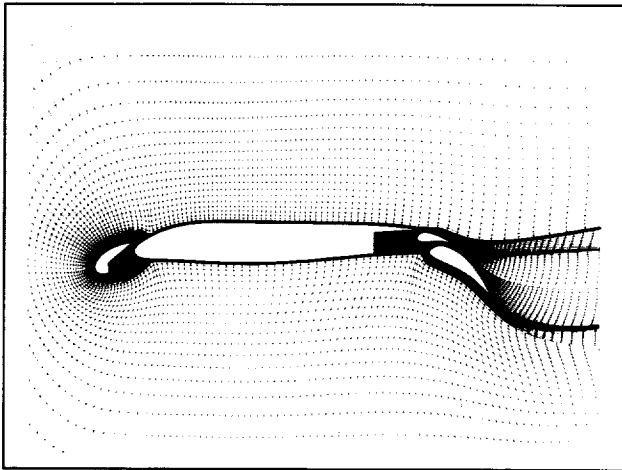
ORIGINAL PAGE
BLACK AND WHITE PHOTOGRAPH

files (with grid topologies implicitly defined) are output in a form which can be accepted directly by a grid generator. In addition, an evaluation of the zoning based on the user bias profile is provided.

The figure shows a seven-zone viscous grid for a four-element, high-lift airfoil in transonic flow at a 4° angle of attack. The zoning and grid topologies were generated automatically by EZGrid. The zonal grids were generated interactively using an existing grid generator.

The success of using a knowledge-based approach for automated flow-field zoning in two dimensions is encouraging. Future efforts to streamline three-dimensional grid generation will probably involve some degree of automation using knowledge-based techniques.

(A. Andrews, Ext. 6741)



Seven-zone grid for a four-element airfoil

Behavior of Liquid Drops in Strong Electric Fields

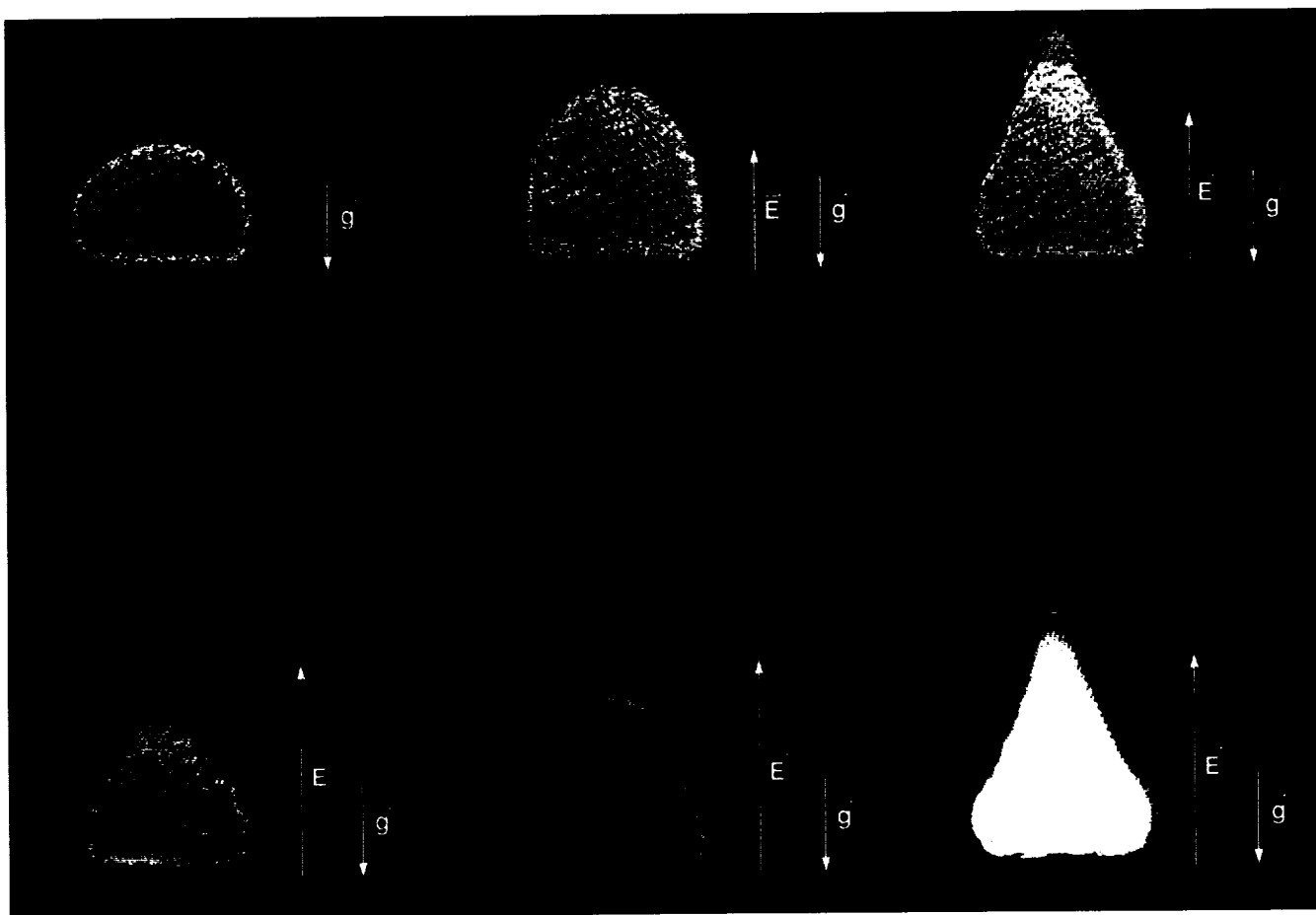
As part of a new initiative in low-gravity fluid dynamics research at Ames Research Center, experiments were performed to study the deformation, oscillation, and jetting of fluid droplets under strong electric fields. Technological concerns in this research area include the processing of materials in space, as well as terrestrial applications (for example, electrostatic spraying of paints and separation processes).

The experiments showed that extensive deformation of the drops occurs with increasing electric field strength. When stronger electric fields were applied, onset of drop oscillations was observed, with frequencies of about the second mode of free-drop oscillations. The motion, however, was modified by the presence of the surface electrical charge and was followed by ejection of thin jets and droplets. The first-order interactions of surface phenomena with the bulk fluid motion are significant factors in many space-based industrial processing schemes.

Images in the figure were taken from a droplet supported atop a 2-mm-diameter pedestal, using black and white high-speed video equipment. The images were enhanced by a digital image-processing technique used in the Ames Fluid Mechanics Laboratory.

A concurrent numerical study is under way which employs a generalized vortex technique. The motion is assumed to be axisymmetric in a vacuum, or in a low-density gas, where surface tension plays a key role.

(P. Bahrami, Ext. 4964)



Instability of a water drop in 1 g

Numerical Simulation of the Flow About the Integrated Space Shuttle Vehicle in Ascent

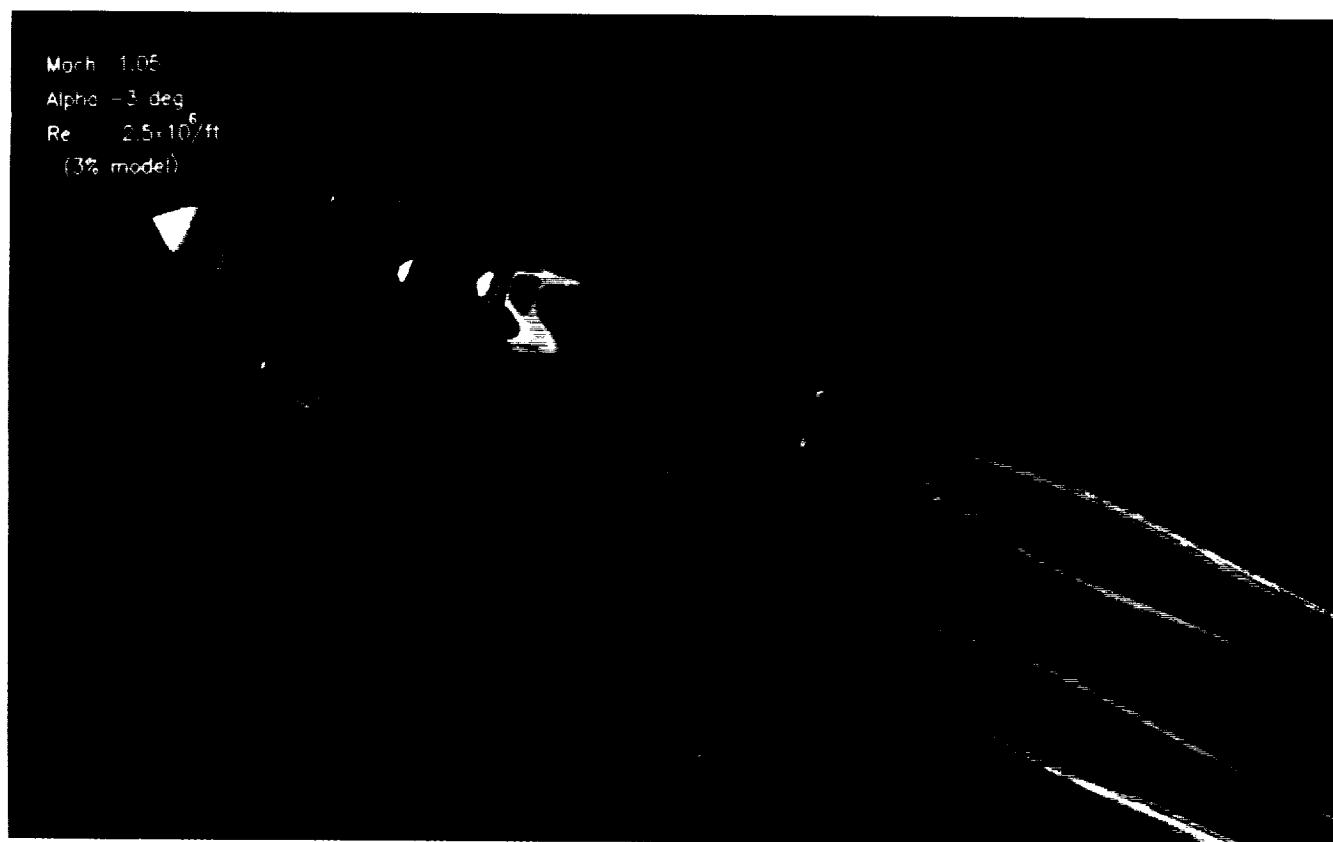
With the collaboration of the Johnson Space Center, a long-term effort has been initiated to compute the time-dependent flow over the integrated Space Shuttle vehicle during its ascent mode for various nominal- and abort-flight conditions. Although numerical computations have limitations, they can complement the existing experimental data base, and, because solutions of the entire three-dimensional flow field are obtained, they can provide additional insight into the flow physics.

Because of the complexity of the integrated vehicle, an overset (Chimera) composite-grid

approach was chosen for the discretization process. A body-conforming grid was used to represent each component—the orbiter, the external tank (ET), the solid rocket booster (SRB), an SRB plume, and some “attach” hardware. The code Pegasus, as provided by CALSPAN Field Services located at the U.S. Air Force Arnold Engineering and Development Center in Tullahoma, Tenn., has been used to interface the overset grids. Flow simulations were carried out using an implicit, approximately factored, finite-difference code (F3D) for the three-dimensional, thin-layer Navier-Stokes equations. All calculations were carried out on the NASA Numerical Aerodynamic Simulator CRAY 2.

To reduce the complexity of the simulations, various engineering approximations were made. For

ORIGINAL PAGE
COLOR PHOTOGRAPH



Current level of configuration modeling showing surface pressure shading and flow Mach contours for $M_\infty = 1.05$

example, a sting was used to represent the orbiter plumes, SRB plumes were modeled with perfect gas assumptions, the orbiter vertical tail was removed because side slip is not of paramount interest, and so on. The current configuration modeling is shown in the first figure, which also shows computed flow results for Mach-1.05 conditions.

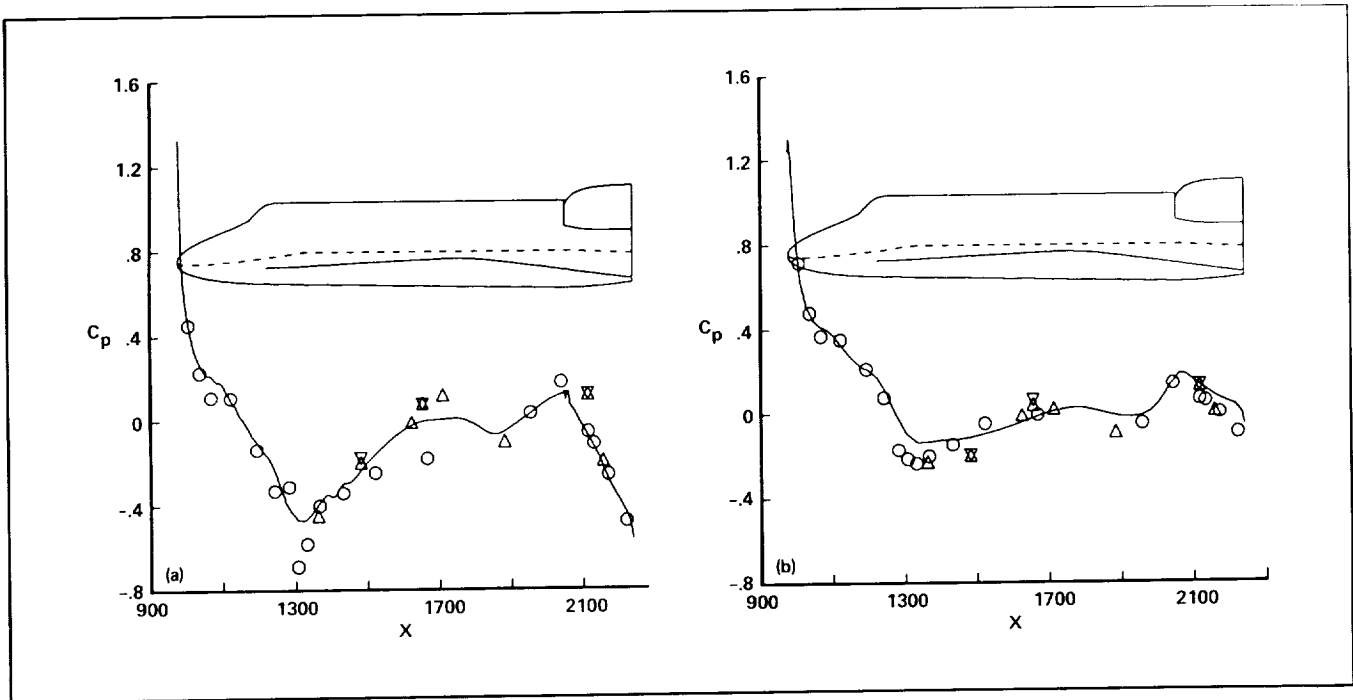
Numerical computations were carried out at Mach numbers of 2, 1.55, 1.05, 0.9, and 0.6 at angles of attack corresponding to flight conditions. This range of Mach numbers is near the maximum dynamic pressure encountered in ascent. Initial calculations used a coarse grid for the easier-to-compute supersonic flow conditions. As experience was gained, the more difficult subsonic and transonic Mach numbers were computed using finer grids and

better geometric fidelity. The $M_\infty = 1.05$ case was computed using nearly a million grid points.

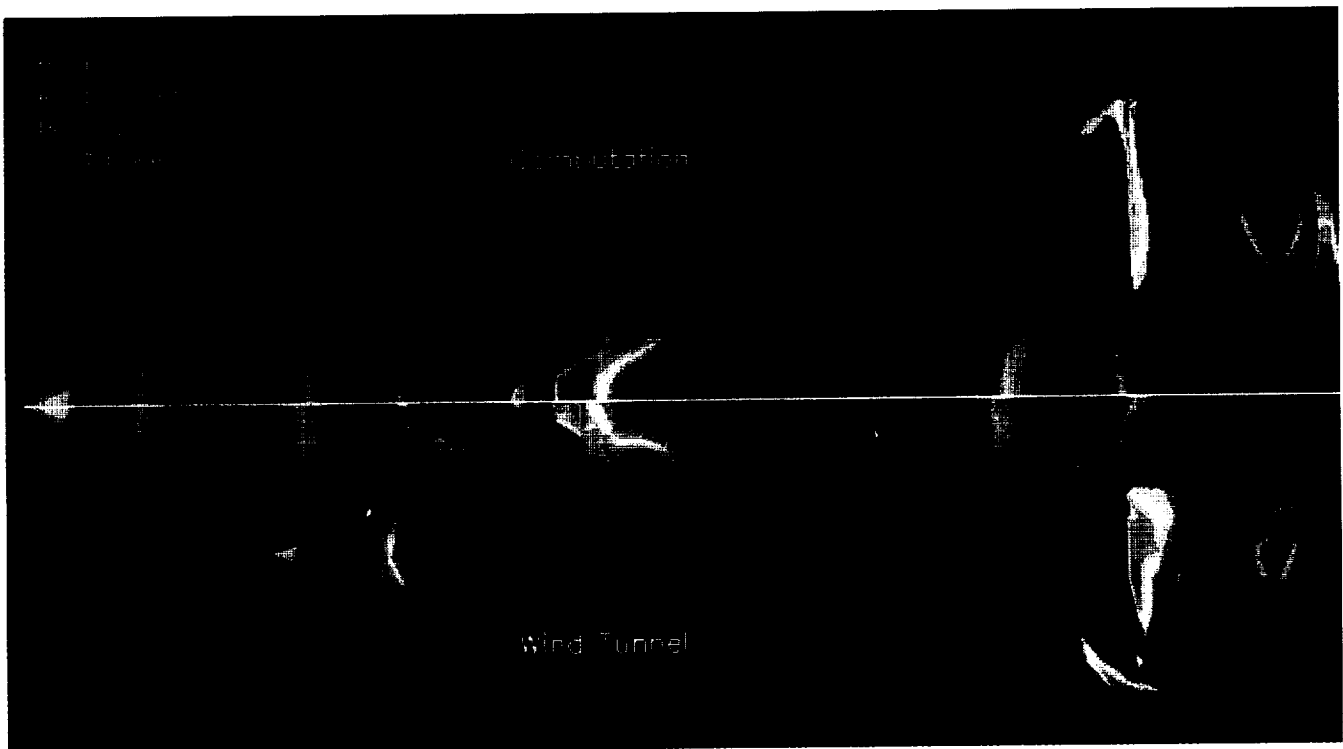
The experimental data base for the Shuttle includes an extensive wind tunnel data base as well as a limited amount of flight-test data. The second figure shows pressure comparisons between flight, wind tunnel, and computation at a station along the side of the orbiter for two of the computed Mach numbers. Pressure contours compared to wind tunnel data are shown in the third figure for the $M_\infty = 1.05$ case. This case has proper wing elevon settings and simplified attach hardware between the orbiter and the ET. It required about 15 hours of single-processor CRAY-2 time.

(J. Steger, Ext. 6459)

ORIGINAL PAGE
COLOR PHOTOGRAPH



Comparisons of pressure coefficient, C_p , from computation (—), wind tunnel (O), and flight (∇, Δ) along the side of the orbiter. a) $M_\infty = 1.05$, $\alpha = -3^\circ$, $Re = 4 \times 10^6/\text{ft}$, b) $M_\infty = 0.6$, $\alpha = -3^\circ$, $Re = 4 \times 10^6/\text{ft}$



Comparison of pressure coefficient between computation and wind tunnel, $M_\infty = 1.05$, $\alpha = -3^\circ$, $Re = 4 \times 10^6/\text{ft}$

ORIGINAL PAGE
COLOR PHOTOGRAPH

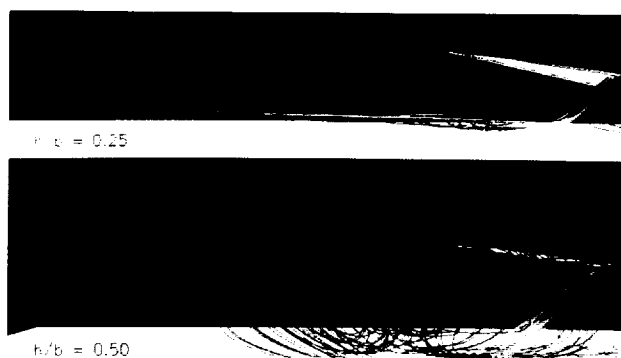
Simulation of the "Suckdown" Effect

Vertical and short takeoff and landing (V/STOL) aircraft use propulsive jets for lift and control during takeoff and landing. The Harrier AV-8B, for example, uses the movable nozzles of its Pegasus turbine engine to direct the engine exhaust to maintain a hover position or to control the flightpath while in ground effect. This results in complex fluid physics and intense thermal/acoustic loads.

To understand these complex interactions, a three-dimensional, implicit, flux-split Navier-Stokes solver (F3D) and a composite overset grid scheme (PEGASUS) have been used to study flow past a 60° delta wing equipped with two jets positioned symmetrically close to the inboard trailing edge. A number of cases with varying values of h/b have been simulated, where h is the height of the wing above the ground and b is the wingspan. These cases simulate landings at essentially zero rate of descent. For conventional takeoff/landing (CTOL) aircraft, lift actually increases slightly as the vehicle approaches the landing surface. However, because of the interaction among the propulsive jets, the airframe, and the ground, V/STOL aircraft (here modeled as a delta planform with jets) often encounter significant lift loss ("suckdown") during takeoff/landing.

As shown in the first figure, for $h/b = 0.25$ and 0.5, the jets penetrate far forward and roll up and back as a result of the interaction with the free stream, producing a ground vortex which engulfs most of the vehicle. The second figure shows that the leading-edge vortices are shed from the bottom of the wing rather than from the top. Although the vehicle is at a positive angle of attack, a negative lift coefficient is observed. The simulations indicate that this is due to the ground vortex producing an effective negative angle of attack and very low pressures on the lower surface of the delta planform because of the entrainment of flow into the high-speed jets.

This suckdown effect can prevent vertical takeoff and landing operations and, at present, it is difficult to determine the amount of suckdown for any given aircraft. These simulations are being validated against



Effect of h/b on ground vortex formation



CFD simulation of steady "suckdown" phenomena

experimental data from the NASA-Langley 14- by 22-Foot Wind Tunnel.

Experimental data and flight experience indicate that the amount of suckdown is reduced if the vehicle quickly leaves or approaches the ground. Fluid dynamicists suspect that if the aircraft moves fast enough, there is not enough time for the ground vortex (and related flow structures) to form and affect the aircraft. This effect will be studied next, which will require computing the flow around two objects in relative motion. To achieve this, the ground and vehicle are resolved on separate grids and the grids will move in relation to each other.

(K. Chawla and W. Van Dalsem, Ext. 4981)

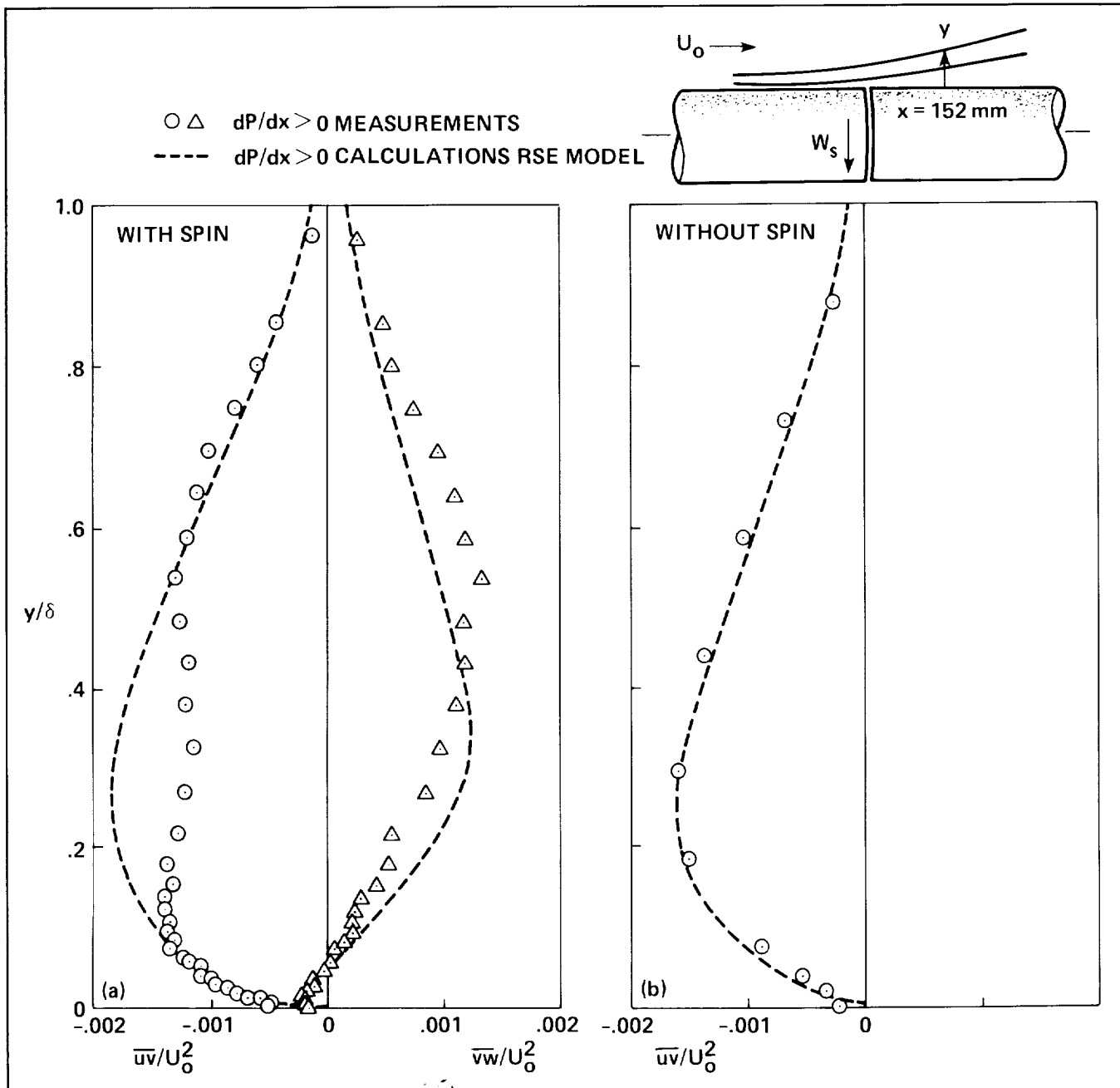
ORIGINAL PAGE
COLOR PHOTOGRAPH

Pressure Gradient Effects on a Three-Dimensional Turbulent Boundary Layer

Flows at the trailing edge of wings, fuselages, and diffusers experience rapid flow deceleration (and often flow separation) as a result of adverse pressure-gradient conditions. Drag and predictions

of drag in such flows are dictated by the degree of turbulent mixing (or Reynolds shear stress). The presence of crossflow (embedded in the streamwise flow) can alter this turbulent mixing.

Measurements in the flow about a spinning cylinder allow us to study the combined effects of adverse pressure gradient and transverse strain. Swirling flow, produced by a spinning section, flows



Reynolds stress distribution in adverse pressure gradient flow. a) With spin, b) without spin

over a nonspinning section of cylinder, where measurements are performed.

Measured \overline{uv} -Reynolds stress, responsible for redistributing (mixing) streamwise momentum, is overpredicted by calculations using a full Reynolds stress turbulence model (see part a of the figure). Predictions, with this same model, for the flow without swirl are accurate (part b of the figure). This model, like all others, lacks sensitivity to transverse flow gradients, which is needed to accurately predict three-dimensional flows in general. Reynolds stress component \overline{vw} , responsible for redistributing cross-flow momentum, is predicted fairly well with the exception of the location of the local maximum.

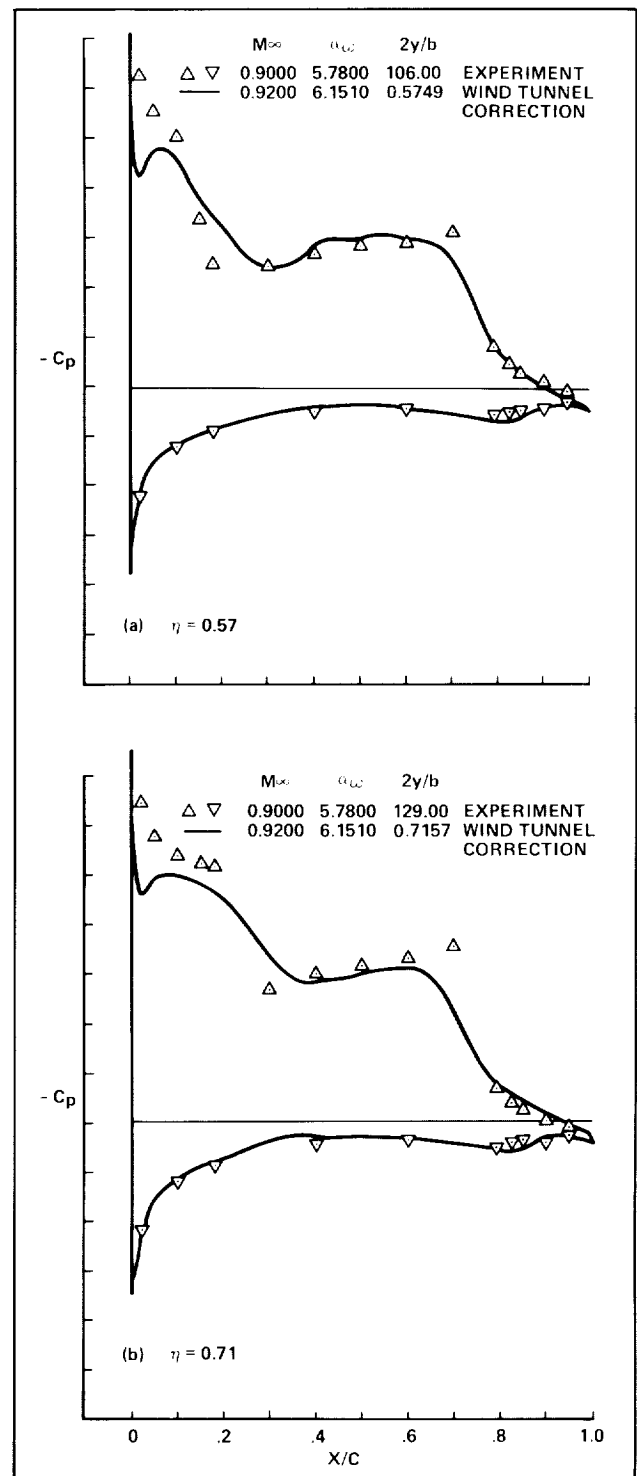
Experiments such as the one described above provide guidance for improving turbulence models.

(D. Driver, Ext. 6156)

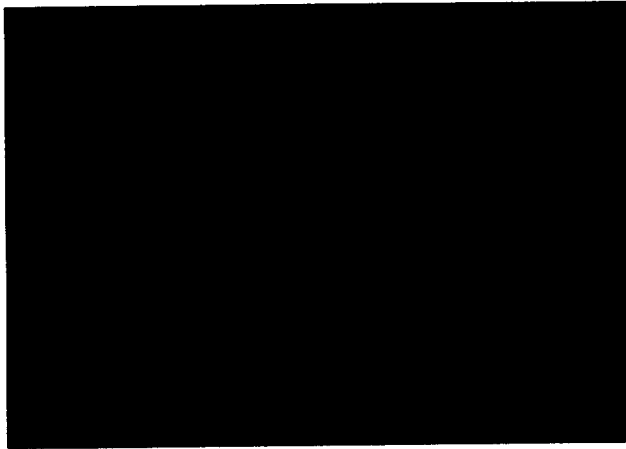
Transonic Navier-Stokes Project

The Transonic Navier-Stokes (TNS) Project has been initiated to develop computational procedures and associated computer codes for solving flow fields about complete three-dimensional aircraft configurations. Thin-layer, Reynolds-averaged, Navier-Stokes equations will be solved using a block- or zonal-grid structure.

This block-grid structure is used for two purposes. First (and most importantly), it improves the distribution of grid points about complicated geometries. That is, grid blocks far removed from large flow gradients can be relatively coarse, while grid blocks near large flow gradients can be fine. Second, because the solution from only one grid block at a time resides in the main memory, the block-grid approach provides a convenient mechanism for organizing the data base. Research opportunities associated with the TNS project are in the following areas: surface-geometry representation, grid-generation algorithm development, flow-solver algorithm development and/or improvement, and graphical display of geometric and flow-field results. Fundamental studies involving the numerical solution of flow-field physics about realistic configurations are anticipated.



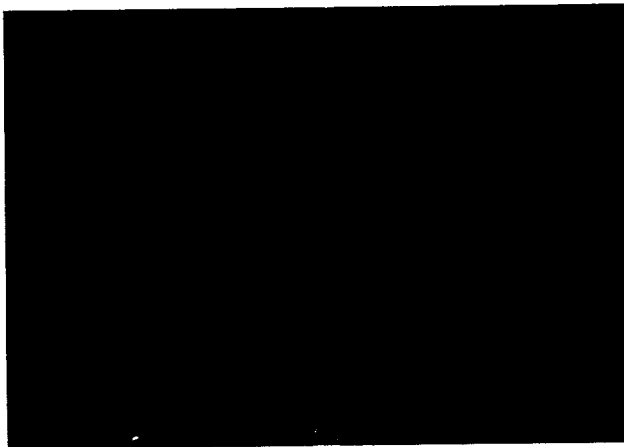
Computed pressure coefficients: $M_\infty = 0.9$, $\alpha = 6.0^\circ$, $Re = 4.5 \times 10^6$. a) $\eta = 0.57$, b) $\eta = 0.71$



Computed pressure contours on upper surface of F-16A: $M_\infty = 0.9$, $\alpha = 6.0^\circ$, $Re = 4.5 \times 10^6$



Computed temperature contours on symmetry plane of exhaust plume: $M_\infty = 0.9$, $\alpha = 6.0^\circ$, $Re = 4.5 \times 10^6$



Computed unrestricted particle traces for: $M_\infty = 0.9$, $\alpha = 6.0^\circ$, $\beta = 5.0^\circ$, $Re = 4.5 \times 10^6$

The first case computed was for Mach number and angle-of-attack conditions of $M_\infty = 0.9$, $\alpha = 6.0^\circ$, and a Reynolds number based on wing-root chord of 4.5×10^6 . The first figure compares the computed wing pressure-coefficient distributions with experimental data. The pressure-coefficient comparison at the semispan station $\eta = 0.57$ is shown in part a. Notice that the computed double-shock pattern on the upper surface of the wing compares well with the experimental data. The second shock position is well predicted as is the pressure coefficient on the wing lower surface. Part b shows the pressure coefficient comparisons at $\eta = 0.71$. The second shock position is well predicted, but slightly smeared. Pressures on the wing lower surface are also well predicted.

The second figure illustrates the pressure contours on the upper surface of the F-16A. Nine zones model this surface, and the smoothness of contours crossing zonal boundaries can be noted. For example, one zone ends at a streamwise location just downstream of the canopy, where another zone begins. High-pressure regions, indicating flow stagnation, can be seen at the fuselage nose, the front of the canopy, and at the leading edge of the vertical tail, as expected. Low-pressure regions around the strake and the wing upper surface near the leading edge indicate supersonic flow. There is a high-pressure region on the upper surface of the horizontal tail near the leading-edge root. This is due to the downwash from the main wing which, even at $\alpha = 6^\circ$, creates an effective negative angle of attack at the horizontal tail. Experimental data confirm this phenomenon.

To simulate power-on conditions and model the exhaust nozzle plume, two new overlapping grids were created in place of a sting. A nozzle exit to a free-stream pressure ratio of 2 was specified, as was a nozzle exit to a free-stream temperature ratio of 5. The nozzle exit-plane Mach number was specified to be 1.

The third figure shows static temperature contours which emanate from the nozzle exit plane. At Mach numbers near 1, the characteristics formed are essentially vertical expansion waves, which immediately expand the flow. (This is evident by the rapid drop in temperature.) Downwind of the expansion fan, a compression wave system develops because

ORIGINAL PAGE
COLOR PHOTOGRAPH

of the reflection of characteristics off the plume boundary.

The complete aircraft computed C_L underpredicts the experimental value by about 2.6%, while the computed C_D overpredicts the experimental C_D by about 1.6%. Overall, excellent agreement between computed and experimental force coefficients was obtained. Calculations were performed on a CRAY X-MP/48 computer using a single processor. This case took approximately 5000 iterations to lower the initial L_2 -norm three orders of magnitude, and required about 25 hours of central processing unit time.

Simulation of nonsymmetric flow with free-stream conditions: $M_\infty = 0.9$, $\alpha = 6.0$, and sideslip angle $\beta = 5.0^\circ$ was computed next. The fourth figure shows unrestricted particle traces released at a cross-sectional location just downstream of the nose. Particles released on the windward side are red, while the leeward particles are blue. The effects of yaw are clearly seen. Particle traces released from the leeward side are displaced by the canopy and proceed along the fuselage past the leeward side of the vertical tail. Particle traces released from the windward side are also displaced by the canopy; however, some cross over the fuselage centerline and proceed along the leeward side of the vertical tail while others proceed along the windward side.

(J. Flores, Ext. 5369)

Simulation of Rotor-Stator Interaction in a Multi-Stage Compressor

Flows within turbomachines are complex and are challenging to analyze computationally. Design constraints force the designer to place blade rows close to each other, causing significant potential and viscous interactions between blades. The interactions reduce the efficiency and cause unsteady stresses on the blades. A computational tool that can analyze these interactions can be useful in understanding these effects and will aid in designing more efficient and reliable turbomachines.

A two-dimensional, unsteady, thin-layer Euler/Navier-Stokes zonal code has been developed



Instantaneous temperature contours in a 2.5-stage compressor

to analyze these flows (STAGE-2). It is based on a third-order-accurate, upwind, implicit scheme. Body-conforming "O" grids are used to accurately resolve the viscous effects associated with each blade. These are overlaid on sheared Cartesian grids which resolve the inviscid flow field between blades. These Cartesian grids are allowed to slip past each other, simulating the unsteady rotor-stator geometry. STAGE-2 simulates multiple-stage machines and allows for differing numbers of blades in each row.

STAGE-2 has been used to model the flow in a 2.5-stage compressor for which a large body of experimental data exists. The Mach number at the inlet is 0.07 and the Reynolds number is 100000/inch. For the purposes of the calculation, the flow was assumed to be fully turbulent. The figure shows instantaneous temperature contours for this case. The wakes remain coherent for several chords. Their interaction with the downstream blades is one of the causes of the general unsteadiness of the flow. It should be noted that the contours are continuous across zonal boundaries, indicating a distortion-free transfer of information. Time-averaged pressures on the blades closely correspond to experimental data, indicating that the two-dimensional approximation can be used to simulate this on-design case.

(K. Gundy-Burlet, Ext. 4475)

ORIGINAL PAGE
COLOR PHOTOGRAPH

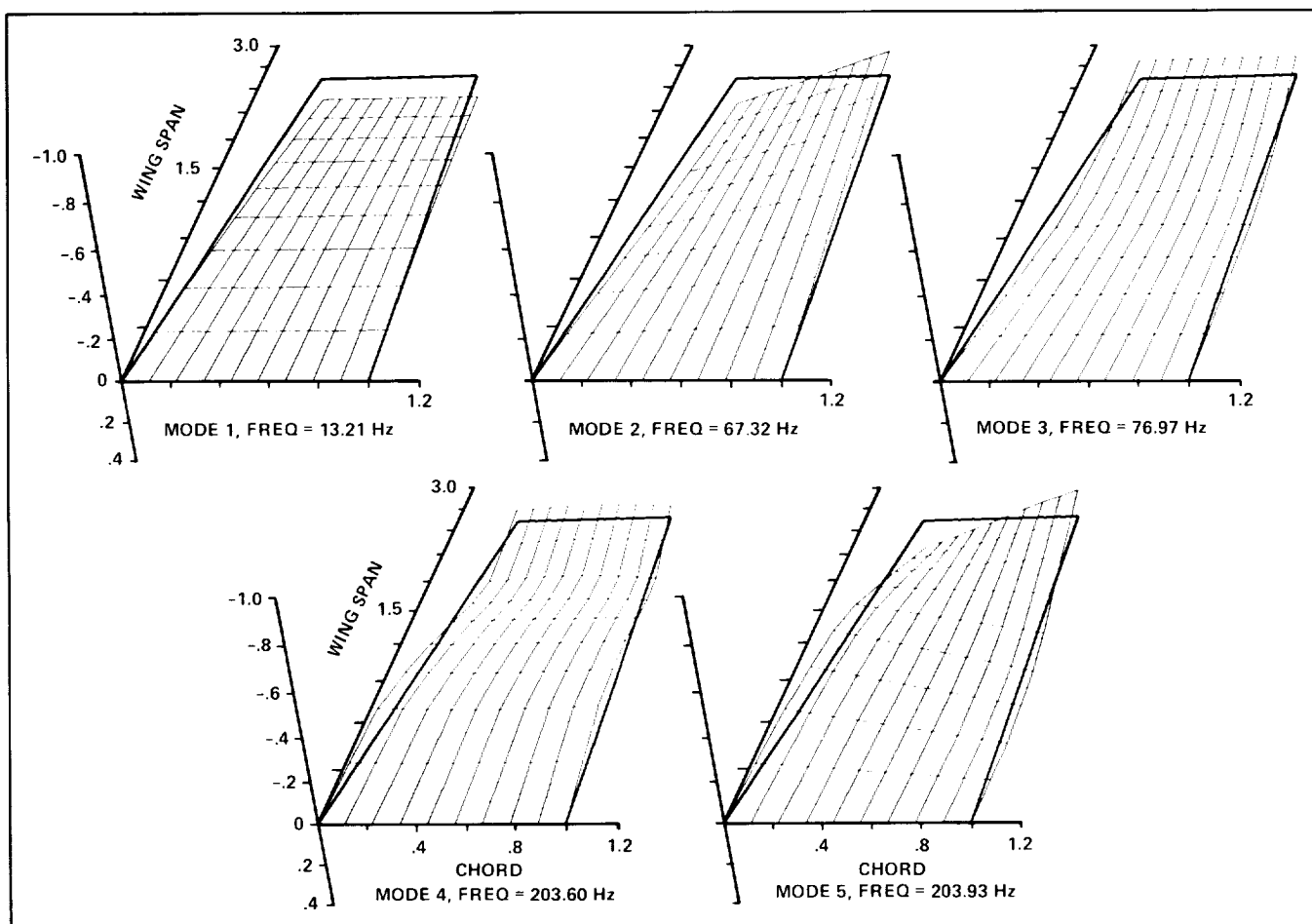
Aeroelasticity Using the Euler Equations

Aeroelasticity plays an important role in the design of efficient and safe aircraft. Aeroelasticity is a complex phenomenon that requires the understanding of both computational and experimental techniques. By conducting parallel computational and experimental studies, the overall cost of developing an aircraft can be considerably reduced. To date, most aeroelastic studies of aircraft have been conducted using potential flow equations.

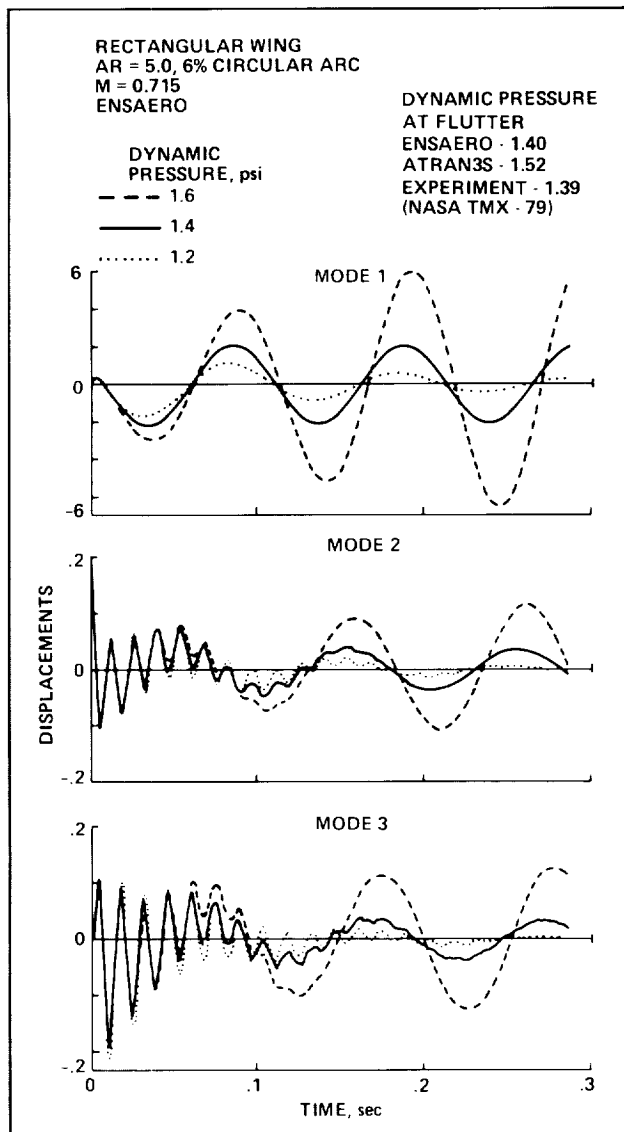
To study the aeroelasticity associated with separated and vortical flows, more advanced methods based on the Euler/Navier-Stokes equations, coupled with the structural equations, are required. With the availability of supercomputer facilities such as the Numerical Aerodynamic Simulator located at Ames Research Center, the Euler/Navier-Stokes equations

can be used for solving aeroelastic problems. At Ames, time-accurate procedures of coupling the Euler/Navier-Stokes equations with structural equations are being developed. ENSAERO version 1.0, a code based on the Euler equations coupled with the modal structural equations of motion, has been developed.

Computations in ENSAERO are made by simultaneously solving the Euler flow equations and the modal structural equations of motion. Time-accurate aeroelastic computations are made using configuration-adaptive dynamic grids. Grids are generated using the deformed shape obtained by solving the aeroelastic equations of motion. This is the first time such a technique has been successfully used for aeroelastic applications. Results shown in the figures demonstrate the application of ENSAERO. The line diagrams show the aeroelastic responses of a rectangular wing. The flutter dynamic



Modes of a rectangular wing

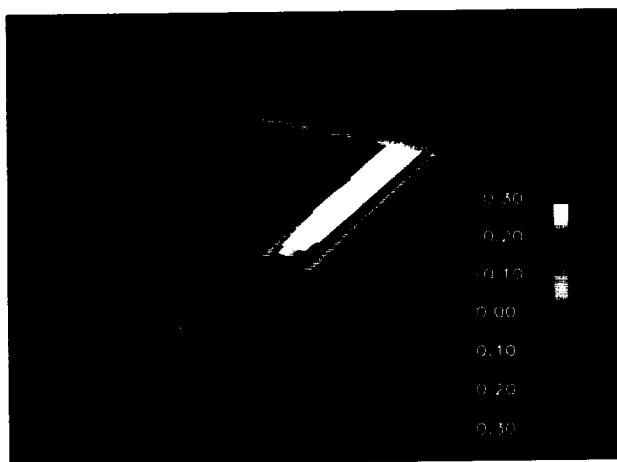


Aeroelastic responses using Euler equations

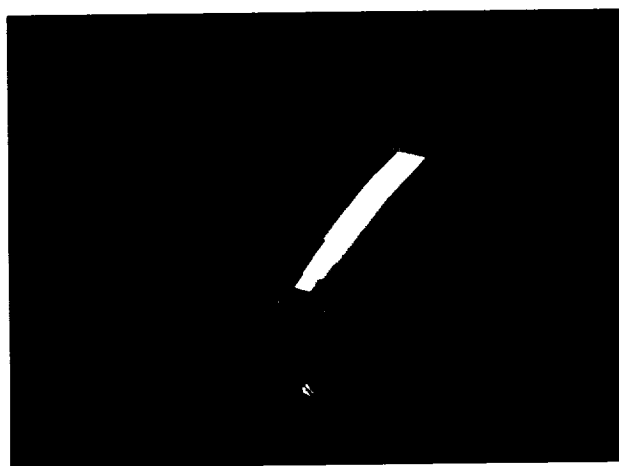
pressure computed by ENSAERO compares better with the experiment than that computed by ATRAN3S, an Ames code based on the potential flow theory. The color photograph shows three views of the aeroelastically oscillating wing. Configuration-adaptive dynamic grids appear in the photo. The colors on the wing represent surface pressures.

In this project the Euler equations are successfully coupled with the modal structural equations of motion for advanced aeroelastic applications. With this new computational tool, practically important aeroelastic phenomenon such as vortex-induced wing oscillations can be studied. This work has advanced the state of the art of computational fluid dynamics applications to aeroelasticity. ENSAERO will be extended to use the Navier-Stokes equations. Complex aeroelastic phenomena associated with vortical and separated flows will be studied.

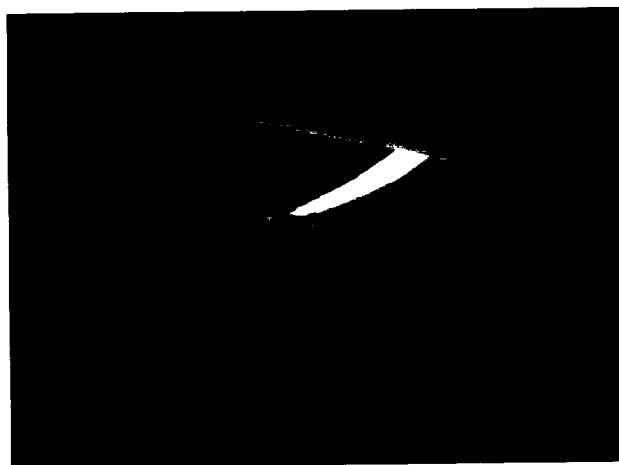
(G. Guruswamy, Ext. 6329)



(a) UNDEFORMED POSITION



(b) MAXIMUM DOWNWARD DISPLACEMENT



(c) MAXIMUM UPWARD DISPLACEMENT

Aeroelastic responses using Euler equations with configuration-adaptive grids

Aeroelasticity of Full-Span, Wing-Body Configurations

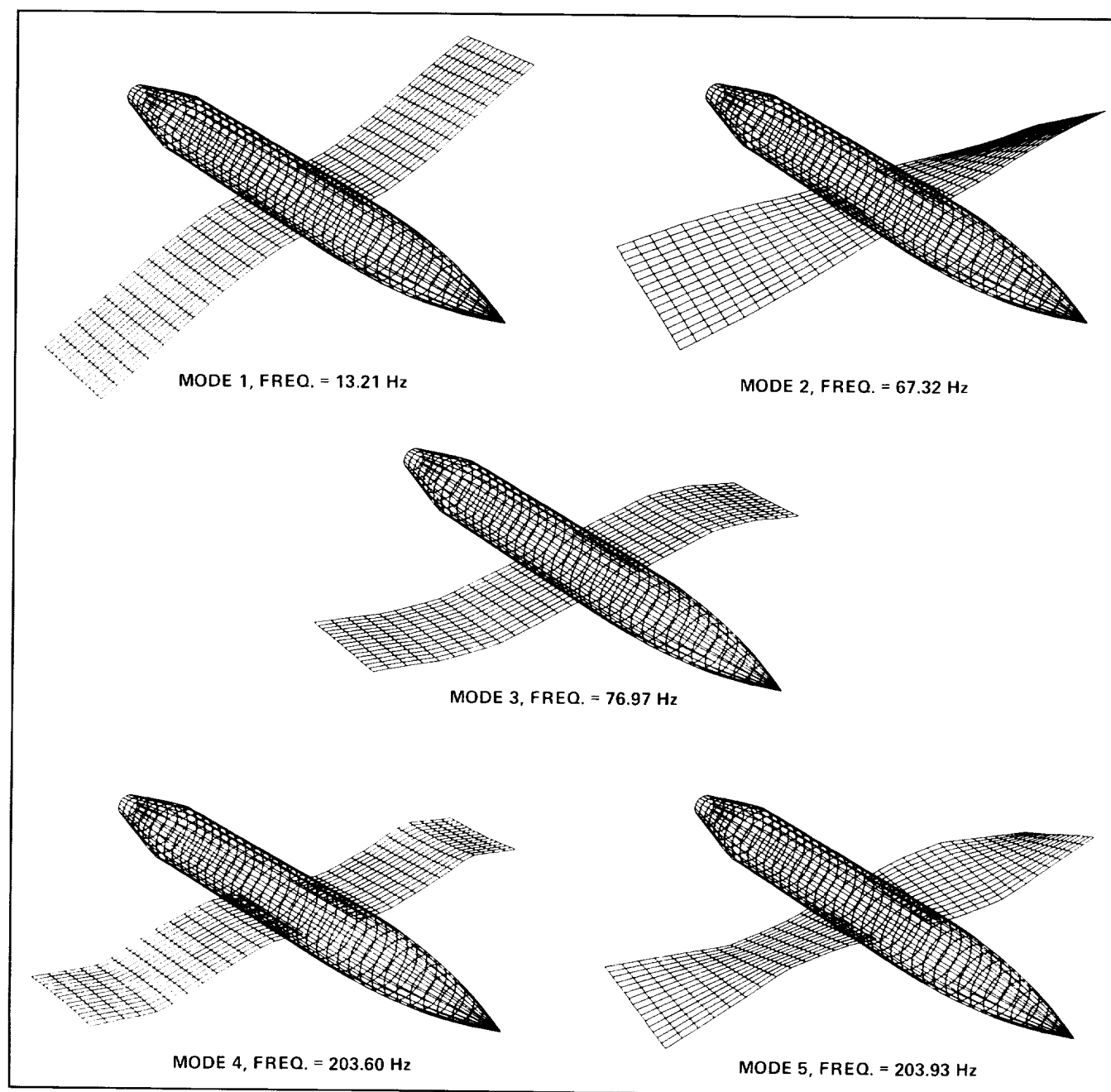
Modeling of full-span, wing-body configurations is necessary to accurately compute aeroelastic characteristics of aircraft, particularly those associated with asymmetric modes. Asymmetry can be encountered for an aircraft either in configuration (oblique-wing aircraft, fighters with stores on wings) or in flow conditions. Effects of asymmetry on aeroelasticity are more intense in the transonic regime where the flow is nonlinear and contains moving shock waves. Recently, an accurate method of computing unsteady transonics and aeroelasticity of full-span, wing-body configurations was developed using the transonic potential flow theory, and it has been incorporated in the code, ATRAN3S. Results illustrate the effects of symmetric and asymmetric modes of aeroelastic responses of full-span, wing-body configurations.

Computations in ATRAN3S are made by simultaneously solving aerodynamic and structural equations of motion. Modal data required in the analysis are computed by the finite-element method. Symmetric and asymmetric responses begin with the corresponding initial conditions. Results shown in the figures illustrate the effects of Mach number on the aeroelastic responses associated with symmetric and antisymmetric modes. Colors on the wing represent the surface pressures.

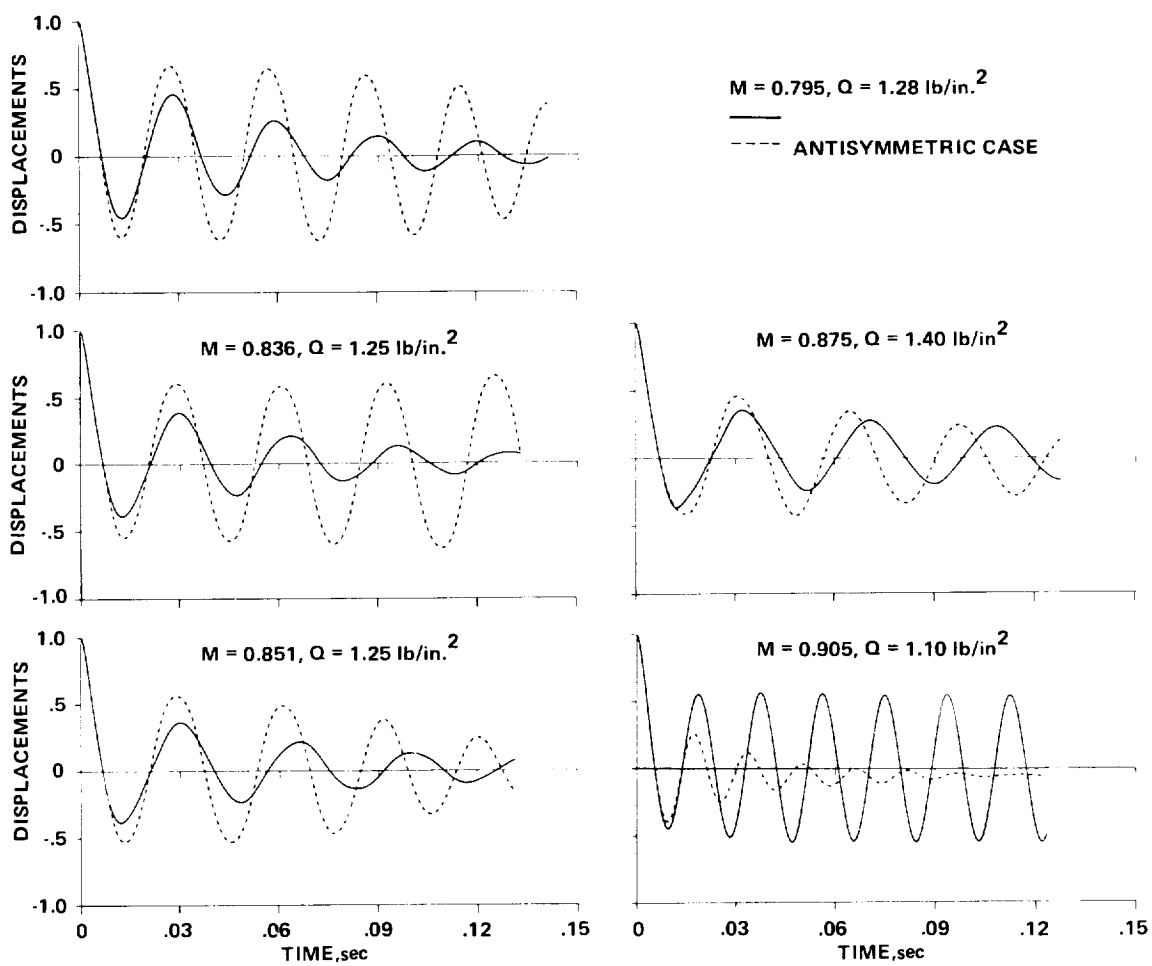
In this project a new computational tool to simulate the aeroelasticity of asymmetric wing-body configurations has been developed. It appears that the stability of aeroelastic responses changes with Mach number and depends on the type of wing modes. Using this computational tool, asymmetric aeroelastic responses of oblique-wing aircraft and aircraft carrying stores can be computed in the transonic regime.

(G. Guruswamy, Ext. 6329)

ORIGINAL PAGE
COLOR PHOTOGRAPH



Antisymmetric modes of a typical wing-body configuration

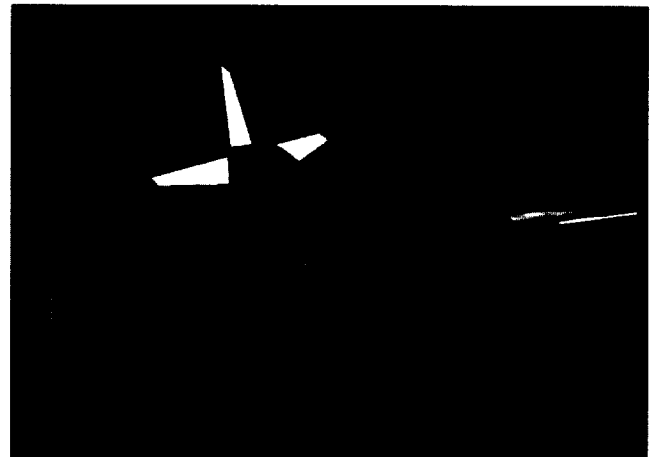


Effects of Mach number on aeroelastic responses associated with symmetric and antisymmetric modes

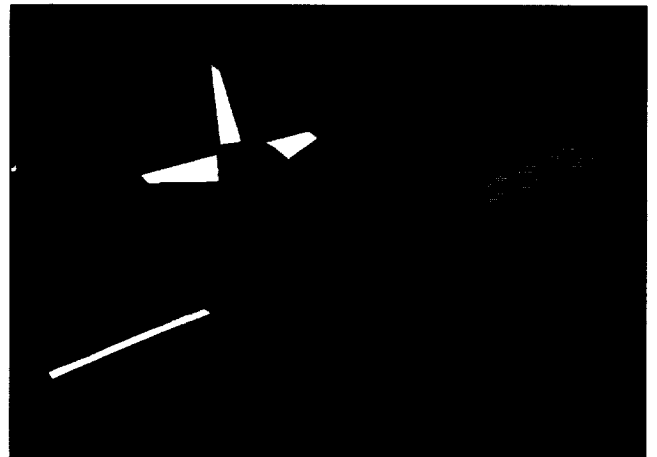
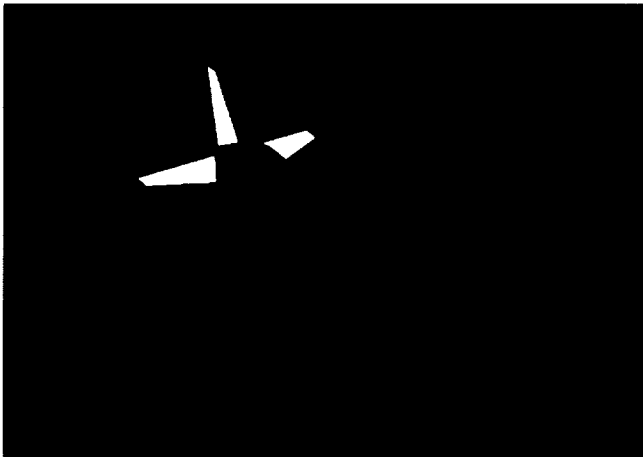
SYMMETRIC



ASYMMETRIC



INITIAL POSITIONS



AFTER SOME TIME



SYMMETRIC CASE IS STABLE



ASYMMETRIC CASE IS UNSTABLE

*Aeroelastic responses of full-span, wing-body configuration, $M = 0.795$, dynamic pressure = 1.29 psi
(Displacements are magnified and colors represent surface pressures)*

ORIGINAL PAGE
COLOR PHOTOGRAPH

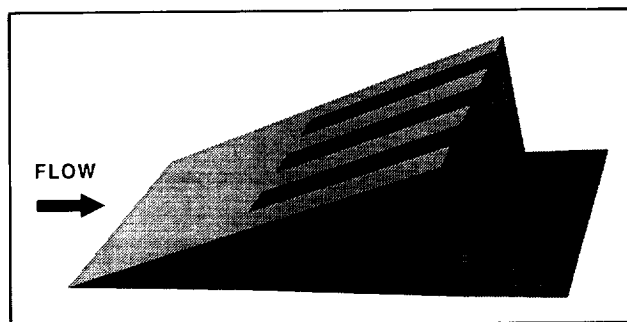
Hypersonic Flow Through a Narrow Expansion Slot for Scramjet Fuel Injection

In the development of a hypersonic vehicle, design of the propulsion system is one of the most important engineering problems. In hypervelocity flight, it is relatively easy to reach a condition of high pressure and temperature necessary for combustion. However, a hypersonic shear layer tends to be very stable. Therefore, a fuel injection system with enhanced mixing is of great interest to the design engineer. The first figure shows a generic model of an axial slot injector which consists of a compression ramp with a narrow expansion slot. The fuel is axially injected at the end of the compression ramp (not modeled in this study). The expansion slot is designed to induce high-speed fluid through the slot to mix air with the injected fuel side by side. This system has several advantages including:

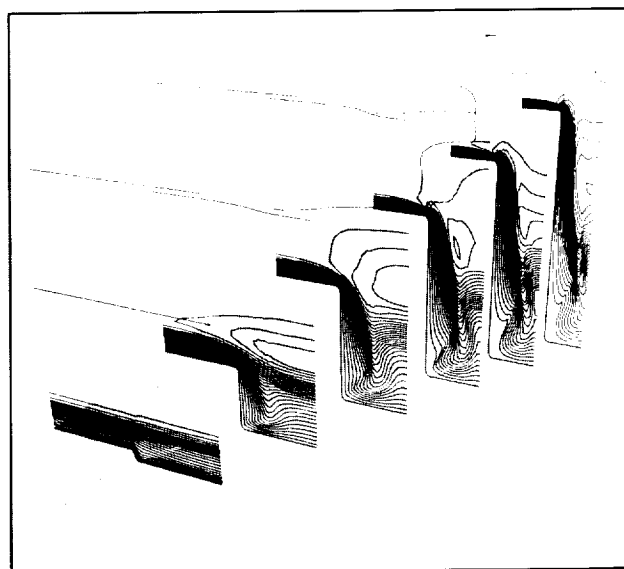
1. the side-by-side air-fuel mixing increases the air-fuel contact surface and ideally is devised to trigger the instability of the air-fuel shear layer, and
2. the streamwise injection alleviates the problem of high stagnation heat and high total pressure loss associated with wall injection.

In the present study, the three-dimensional (3-D) compressible Navier-Stokes equations are solved by a flux-difference splitting code. The computations are performed for a free-stream Mach number of 4.9 and a Reynolds number of 0.1×10^6 through a 20° expansion slot. A grid of $65 \times 49 \times 65$ is used for most of the calculations, with calculations on a finer grid of $129 \times 97 \times 129$ used to show grid independence.

In the second figure the computed Mach number contours show that viscosity plays an important role in the expansion process of hypersonic flow over a narrow slot. Note that in hypersonic flow over a convex corner, stream tubes will increase drastically in cross-sectional area. This compounds the viscous-layer thickening so much that the effectiveness of flow expansion is substantially reduced. This degradation is further aggravated in a narrow expansion slot because of the proximity of the three walls. In this adiabatic wall case, the slot is so dominated by the viscous layer that the flow through the slot loses about 73% of its total pressure. Cases with various wall temperatures and slot widths are also studied. Calculations show that wall cooling reduces the



Three-dimensional compression ramp with a narrow slot



Mach number contours for adiabatic wall case

thickness of the boundary layer, and hence increases the flow expansion.

An interesting characteristic of these flows is the relative insensitivity of mass flux through the slot gap, even though the viscous layer is very thick and is strongly affected by wall temperature and slot width. The mass flux is primarily contributed from the upper portion of the slot. In the lower portion of the slot, inviscidly, the flow is dominated by a highly expanded low-density fluid, and, viscously, by a viscous layer. As a direct consequence, as soon as the wedge angle is large enough, the mass flux through the slot is not affected significantly. Another point is that, in the 3-D case, the expansion around the axial corner induces cross flow that results in a higher mass flux than in the two-dimensional solutions.

(C. Hung and T. Barth, Ext. 5894/6740)

Computational Fluid Dynamics on a Massively Parallel Computer

Scientists and engineers continually seek additional computational power. New massively parallel computer architectures, with thousands of processors, attempt to provide such power. It is a significant problem to effectively use these novel architectures for solving problems in computational fluid dynamics.

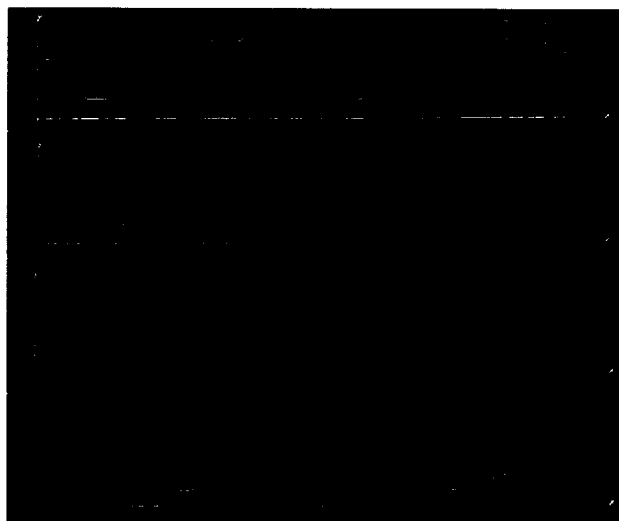
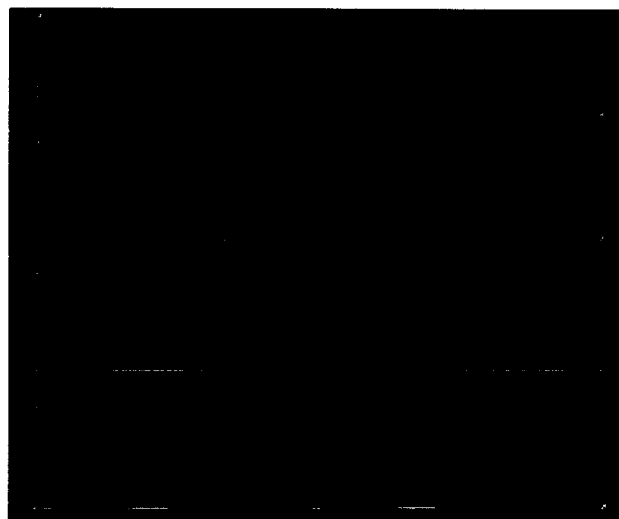
One massively parallel computer is the Connection Machine®. This machine has up to 65536 physical processors, and each processor can be configured into multiple virtual processors. A code solving the two-dimensional, compressible, Navier-Stokes equations has been developed for the Connection Machine. This code has been modeled on a well-known code developed at Ames Research Center, ARC2D. A comparison of the megaflop rate (millions of floating point operations per second) shows the massively parallel architecture can outperform conventional supercomputers. In the table, ARC2D was running on a CRAY XMP. The columns "explicit" and "implicit" refer to the method of advancing in time: the explicit algorithm is a three-stage, Runge-Kutta method, and the implicit algorithm uses a Beam-Warming approximate factorization scheme with a Pulliam-Chaussee diagonalization procedure. It is assumed that the megaflop rate of ARC2D on the CRAY XMP remains constant as the grid size increases.

(D. Jespersen and C. Levit, Ext. 6742/4403)

GRID SIZE	MEGAFLOPS			
	ARC2D (XMP)		CONNECTION MACHINE	
	EXPLICIT	IMPLICIT	EXPLICIT	IMPLICIT
128 X 128	51	63	63	58
256 X 128	51	63	123	86
512 X 512	51	63	241	106

Transition to Turbulence in Plane Poiseuille Flow

Numerical investigations of transition processes in plane Poiseuille flow were conducted. In one study, computations were performed with small ran-



Temporal evolution of internal shear layers in transition to turbulence in plane Poiseuille flow. The contours shown represent constant spanwise vorticity at a peak plane

ORIGINAL PAGE
COLOR PHOTOGRAPH

dom disturbances as an initial condition at a supercritical Reynolds number to mimic a natural transition. It was found that the theoretically predicted subharmonic-mode breakdown (a form of secondary instability) would not occur in the natural transition because of inherent characteristics associated with some modes that would exist for every natural transition situation. This resulted in a fundamental-mode breakdown in a situation where a subharmonic-mode breakdown was expected. When particular disturbances were suppressed artificially, the subharmonic breakdown was observed. Results of this study provide an explanation of the discrepancy in the behavior of the secondary instability between a theory and experimental observations.

In another study, later stages of the transition process were investigated. The initial condition was similar to a controlled experiment with forcing at a particular mode. Internal shear layers were formed because of the secondary instability, and later they were found to go through a roll-up process (a tertiary instability) in a manner similar to a free-shear mixing layer. The figure shows temporal evolution of the shear layers displayed by contours of spanwise vorticity at a peak plane. The structures of these shear layers are strikingly similar to those observed in a fully developed turbulent flow, suggesting a possible link between the two flows.

(J. Kim, Ext. 5867)

Direct Numerical Simulation of Compressible Free-Shear Flows

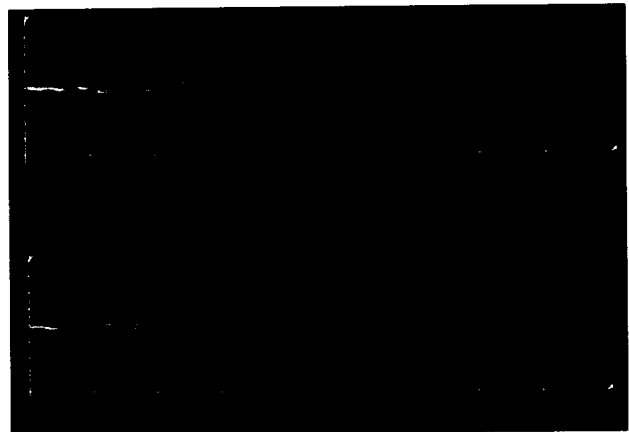
Experimental investigations have shown that compressibility has a stabilizing influence on turbulence, and greatly reduces associated mixing. To ensure proper combustion in devices such as the supersonic ramjet (scramjet) engine, the designer needs to understand the mixing process at supersonic speeds, but building a prototype to optimize design parameters is too expensive.

Direct numerical simulations of compressible free-shear layers have been conducted to understand this puzzle of turbulent mixing, and these simulations show the same effects seen in laboratory experiments. The stabilizing effect of compressibility is shown in the figure, in which two mixing-layer

flows have been simulated. The first corresponds to the mixing of two streams (Mach numbers of 2.0 and 1.2) of the same static temperature but of different flow speeds. The contours of vorticity in the figure show that the vorticity reorganizes into lumps (vortices) which then form larger vortices, which move at a certain speed. This process is known to generate vigorous turbulent mixing, which reduces the Mach number of the flow relative to the vortices to 0.4. In the second case the two streams have higher flow speeds; their Mach numbers are 4.0 and 2.4, and the mixing of the two streams is greatly reduced. The formation of vortices and their amalgamation into larger vortices occur much more slowly.

With numerical simulations it is possible to examine, in detail, the physical processes that lead to this dramatic reduction in mixing. This physical understanding may lead to new methods of enhancing the turbulent mixing.

(S. Lele, Ext. 4732)



Vortex formation in supersonic mixing layers

Accurate and Efficient Calculation of Equilibrium Gas Properties

The National Aerospace Plane and other future transatmospheric vehicles operate in flight regimes where air is dissociated and ionized, but thermodynamic and chemical equilibrium can be assumed. The design of the next generation of advanced engines also requires detailed computations at

ORIGINAL PAGE
COLOR PHOTOGRAPH

equilibrium conditions. Modern computational fluid dynamics (CFD) techniques, in which density, ρ , and internal energy, ϵ , are independent thermodynamic variables, have recently been generalized to cover arbitrary equilibrium equations of state. Solutions of the Navier-Stokes equations require the pressure, p , temperature, T , and their partial derivatives to be accurately given.

Previous equilibrium equations of state calculations were based on internal energy functions for the molecular species which are not accurate at high temperatures. More recent spectroscopic data and more rigorous quantum calculations for the molecular species have been used to develop a fully vectorized, chemical package. The program can compute equilibrium gas properties and their first and second derivatives for pure species and arbitrary gas mixture. Although the code operates at a speed of more than 100 million floating point operations per second (Mflops) on a CRAY 2 or XMP computer, the computation is tedious and cumbersome for most CFD applications.

To be useful in flow computations, one needs accurate and efficient piecewise interpolation for pressure and temperature, and their partial derivatives. Existing programs do not provide sufficient accuracy and continuity, and are inefficient on supercomputers. Furthermore, they are limited to a single particular gas mixture. An interpolation procedure based on a new, efficient, and vectorizable search algorithm with simple piecewise bilinear or bicubic polynomials has therefore been developed for this purpose. The program automatically con-

structs the data base by selecting the optimum, unequal spacing to achieve a desired accuracy.

As an example, the table compares central processing unit (CPU) times and Mflop rates of equilibrium air calculation on the CRAY XMP between the new interpolation procedures and the existing program. The new procedures are not only more than one order of magnitude faster than the existing program, but also can be as accurate as the exact calculation only at the expense of computer storage. Typically, to cover a range of density from 10^{-7} to 10^2 kg/m³ and internal energy from 10^5 to 1.5×10^8 J/kg for equilibrium air, the new interpolation using bicubic polynomials requires the storing of 800 data points for the pressure and 1200 data points for the temperature to obtain a maximum error of 1% for both functions and their derivatives.

(Y. Liu and M. Vinokur, Ext. 6667)

Splashes in Microgravity

The surface interface between a liquid and a gas plays a critical role in many problems of practical interest. The atomization of sprays in combustion applications depends upon the breakup of the fuel-gas interface. Ink-jet printers and other manufacturing applications use controlled forcing to break up jets into drops. In microgravity (μ -g) the interface between a liquid and a gas can play a critical role. Fuel containment is known to be an important problem in a μ -g environment. It can be shown that a liquid drop in μ -g will assume a spherical shape to minimize its surface energy. Small distortions on the drop will cause it to oscillate.

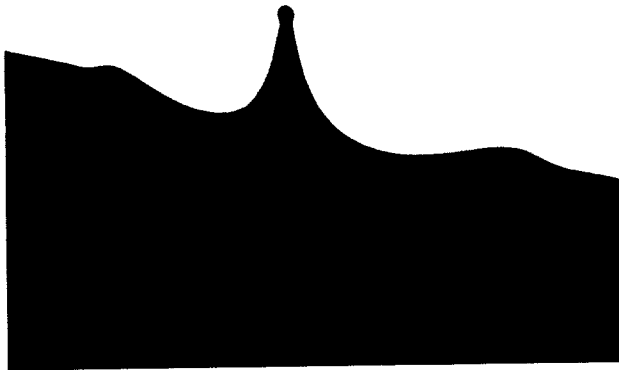
A numerical method that will track the liquid-gas interface has been developed. We treat the liquid as potential flow and track the interface using a boundary-integral method. The effect of small viscosity was included in the computation by retaining first-order viscous terms in the normal-stress boundary condition. Nonlinear oscillations and other motions of large axially symmetric liquid drops in μ -g were studied numerically. We found that small viscosity has a relatively large effect on the shape and frequency of the oscillation of the drop. Another application of the method has been the study of splashes off a liquid surface in a gravity and a μ -g

COMPARISON OF CPU TIMES FOR EQUILIBRIUM AIR CALCULATION

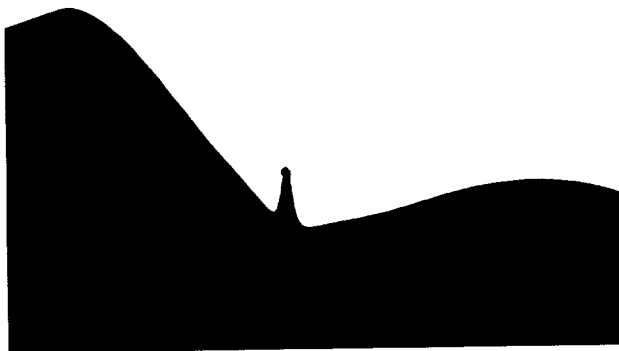
Method	Input	Output	CPU/point	Mflops
Bilinear interpolation	ρ, ϵ	$p, \frac{\partial p}{\partial \rho}, \frac{\partial p}{\partial \epsilon}, T, \frac{\partial T}{\partial \rho}, \frac{\partial T}{\partial \epsilon}$	1.04×10^{-6} sec	110
Bicubic interpolation	ρ, ϵ	$p, \frac{\partial p}{\partial \rho}, \frac{\partial p}{\partial \epsilon}, T, \frac{\partial T}{\partial \rho}, \frac{\partial T}{\partial \epsilon}$	1.93×10^{-6} sec	108
Existing program	ρ, ϵ	$p, \frac{\partial p}{\partial \rho}, \frac{\partial p}{\partial \epsilon}, T$	3.37×10^{-5} sec	12

environment (see figures). We find that in μ -g the crater of the splash is deeper and larger, the time scale is longer, and the ejected drops are smaller than they are in a gravity environment.

(N. Mansour and T. Lundgren, Ext. 6420)



Drop ejection in gravity environment



Drop ejection in zero-gravity environment

Passive Shock Control on a Supercritical Airfoil

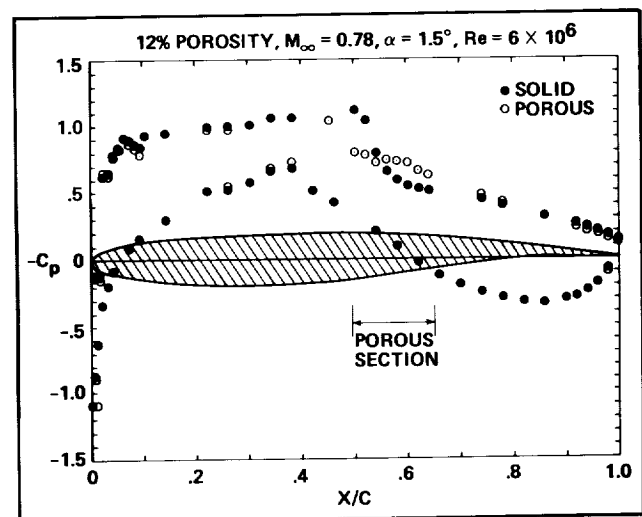
Drag reduction at transonic speeds has long been a goal of both NASA and the aircraft industry. One approach being studied at Ames Research Center attempts to reduce pressure drag by ameliorating the effects of shock waves that often form on the upper surfaces of wings in transonic flight. The concept involves the use of localized surface porosity in the region of interaction between the shock and the surface. A porous section in the airfoil at the base of the shock allows high-pressure air from

behind the shock to flow under the surface and exit into the low-pressure flow ahead of the shock wave. As shown on the accompanying figure, the effect of this passive circulation is to reduce the adverse pressure gradient created by the shock.

Attenuation of the pressure gradient reduces both the wave drag and the severity of the shock-wave/boundary-layer interaction. This latter result translates into less separation at the trailing edge and, consequently, lower pressure drag.

The investigation will provide sufficient data to validate numerical simulations. Once reliable computations can be made, the results can be used to optimize the technique for the greatest drag reduction.

(G. Mateer, Ext. 6156)



Pressure distribution on a supercritical airfoil

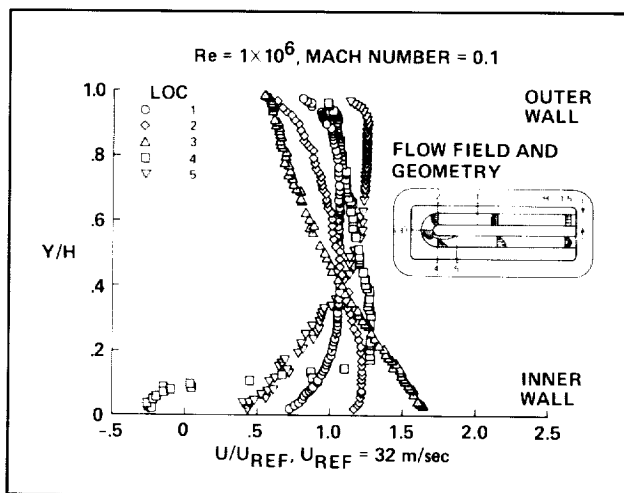
Space Shuttle Main-Engine Turnaround Duct Experiment

Considerations to be used in selecting a turbulence model for Navier-Stokes codes which calculate the internal flow in the Space Shuttle main engine (SSME) are virtually unknown. Few experiments to guide such a choice are available. A recent experiment in the Ames Research Center's High Reynolds Number Channel I should provide some guidance. Measurements were made in a two-dimensional turnaround duct test section that simulates many of

the flow features in the more complex SSME. Its main feature is a sharp 180° bend in the channel, as shown in the accompanying figure.

A two-component laser Doppler velocimeter was used to measure velocity and turbulence profiles in the flow. The longitudinal velocity profiles shown in the figure are examples of the data obtained. The measured data will be compared with Navier-Stokes calculations of the same flow using various turbulence models in a cooperative effort between the Ames Applied Computational Fluids Branch and Marshall Space Flight Center. These comparisons will advance turbulence modeling for internal flows, verify Navier-Stokes simulations of the SSME, and serve as a basis for improved rocket engine design.

(D. Monson, Ext. 6255)



Longitudinal velocity in Ames two-dimensional Space Shuttle main-engine turnaround duct

Low-Aspect-Ratio Wing Experiment

An ongoing project involving computational and experimental fluid dynamics continues in the Experimental Fluid Dynamics Branch. A low-aspect-ratio wing designed to reproduce some of the physical features of fighter wings is being tested in the Ames Research Center's High Reynolds Number Channel II (HRC-II). Surface pressure and surface flow patterns have been obtained on a "wing-alone" configuration. A second tunnel entry is planned to pro-

vide data on a wing/body/strake configuration and to extend the coverage of the wing-alone data to include flow-field velocity measurements with a laser Doppler velocimeter, flow-field visualization, and, possibly, surface-skin friction measurements.

The experiment is designed to provide data on realistic configurations for validating computer codes. Toward this end, the quantitative measurements have been qualified by the relative uncertainty in the quantities measured, and the wall pressures and wall boundary layers have been measured either to provide boundary conditions for the codes or to act as checks on the validity of the wind tunnel modeling.

The design of the low-aspect-wing experiment being run in HRC-II was influenced strongly by computational fluid dynamics (first figure). The experimental model is a simplified wing/fuselage made up of components which can be tested alone or together. The fluid dynamic codes used in this experiment ranged from the relatively old panel-method codes to transonic full-potential codes.

The panel-method code (PANAIR) was used to assess the wall interference (blockage) effects for subcritical flow. For this flow regime, the inviscid wall effects were predicted to be quite small, and this was substantiated by the wind tunnel data from the experiment when it was run. The full potential codes were used to check the design of the body, the wing, and the wing/body combination.

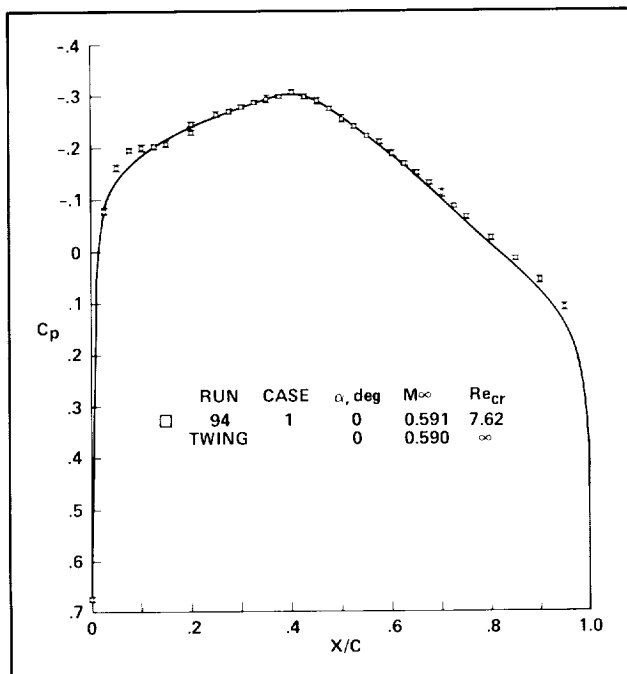
TAXI (transonic axisymmetric code) was used in the design of the body. It prompted a redesign of the nose after it predicted strong shocks on the original design which would have created unwanted strong interactions with the wind tunnel wall boundary layer.

TWING (transonic wing code) was used in the wing and wing/body design to obtain force and moment data in the supercritical regime, and to guide the placement of pressure tap locations on the experimental model. Predictions of this code, although limited because of both the full potential assumptions and the lack of wind tunnel walls in the computational model, proved to be accurate within the bounds of these limitations.

A priori estimates of the likely pressure fields of the model given by this code were a valuable asset during the design. Pressure taps were placed to provide the most comprehensive coverage of the pressure field possible with the limited amount of pressure taps which could be fitted within the wing. Additionally, the structural design of the wing could



Low-aspect-ratio wing/body in HRC-II



Low-aspect-ratio wing, $2y/b: 0.286$

be done with accurate knowledge of the distribution of structural loads over the wing. As this model had to withstand extremely high dynamic pressures to provide high Reynolds numbers, this was especially critical.

Angles of attack up to 8° have been tested at Reynolds numbers from 2 to 12 million, the latter which is equivalent to that which an F-16 would experience at transonic speeds at cruising altitude.

Flow regimes encountered in the test include shock/boundary-layer interaction and leading-edge vortical flow. Companion computations are being performed with the experiment.

Shown in the second figure is a relatively easily modeled case of low Mach number and angle of attack, compared with TWING, one of the codes used in the design of the experiment. This code does not model viscous effects or wind tunnel walls. For this case agreement with the experiment is relatively good, as expected. The current focus of the computational effort is to compare the experiment with the TNS (transonic Navier-Stokes) code, which will model both viscous effects and wind tunnel walls. Preliminary calculations with a coarse grid on the CRAY XMP have been performed and solutions with smoother, finer grids are being attempted on the CRAY-2. These calculations will be used to define the regimes that should be concentrated on in the experiment, and to define the limits of validity for the current version of the code.

(M. Olsen, Ext. 6200)

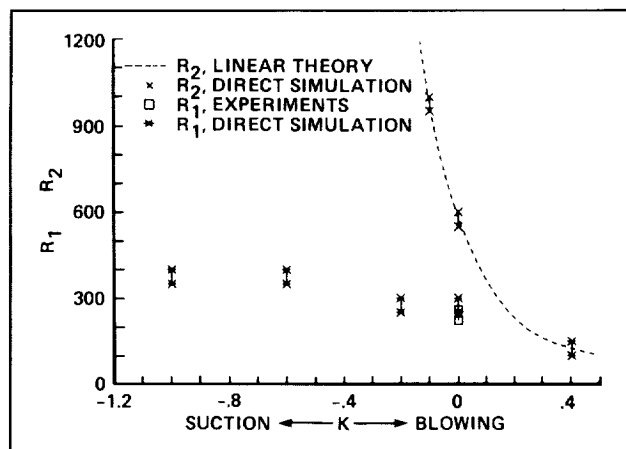
Direct Numerical Study of Leading-Edge Contamination

Instability, turbulence, and relaminarization in the attachment-line region of swept and unswept cylindrical bodies are studied by numerical solution of the full Navier-Stokes equations. The flow is simulated over a strip containing the attachment line and treated as homogeneous in the spanwise direction; the disturbances decay exponentially upstream. Transpiration through the wall may be prescribed. The new method, which admits completely general disturbances, agrees with published linear-stability results, which were limited to an apparently restrictive form of disturbance. Fully developed turbulent solutions with sweep are generated and compare well with experimentation. The turbulence is subcritical (except with blowing), resulting in large hysteresis loops. By lowering the sweep Reynolds number, or increasing the suction, the turbulent flow is made to relaminarize. The relaminarization Reynolds number is much less sensitive to suction than the linear-instability Reynolds number. Exten-

sive attempts to detect the postulated nonlinear instability of the unswept flow failed, suggesting that this flow is linearly and nonlinearly stable.

The figure shows the two critical Reynolds numbers (\bar{R} , based on strain rate and sweep component of velocity) versus the suction parameter K . R_2 is the threshold for instability of the laminar flow to small disturbances. The results agree with those obtained with linear theory. R_2 increases rapidly as suction is increased ($K < 0$). R_1 is the threshold for relaminarization and is the relevant parameter to prevent contamination of the leading edge by the fuselage boundary layer. Without suction, the results for R_1 agree with previous experimental results. They illustrate the hysteresis (R_1 is much lower than R_2). With suction, it was found that R_1 increases much less than R_2 , even proportionally. This result is important for laminar flow control. It is an example of new information that can be obtained only by direct simulation, and can be used directly by the designer.

(P. Spalart, Ext. 4734)



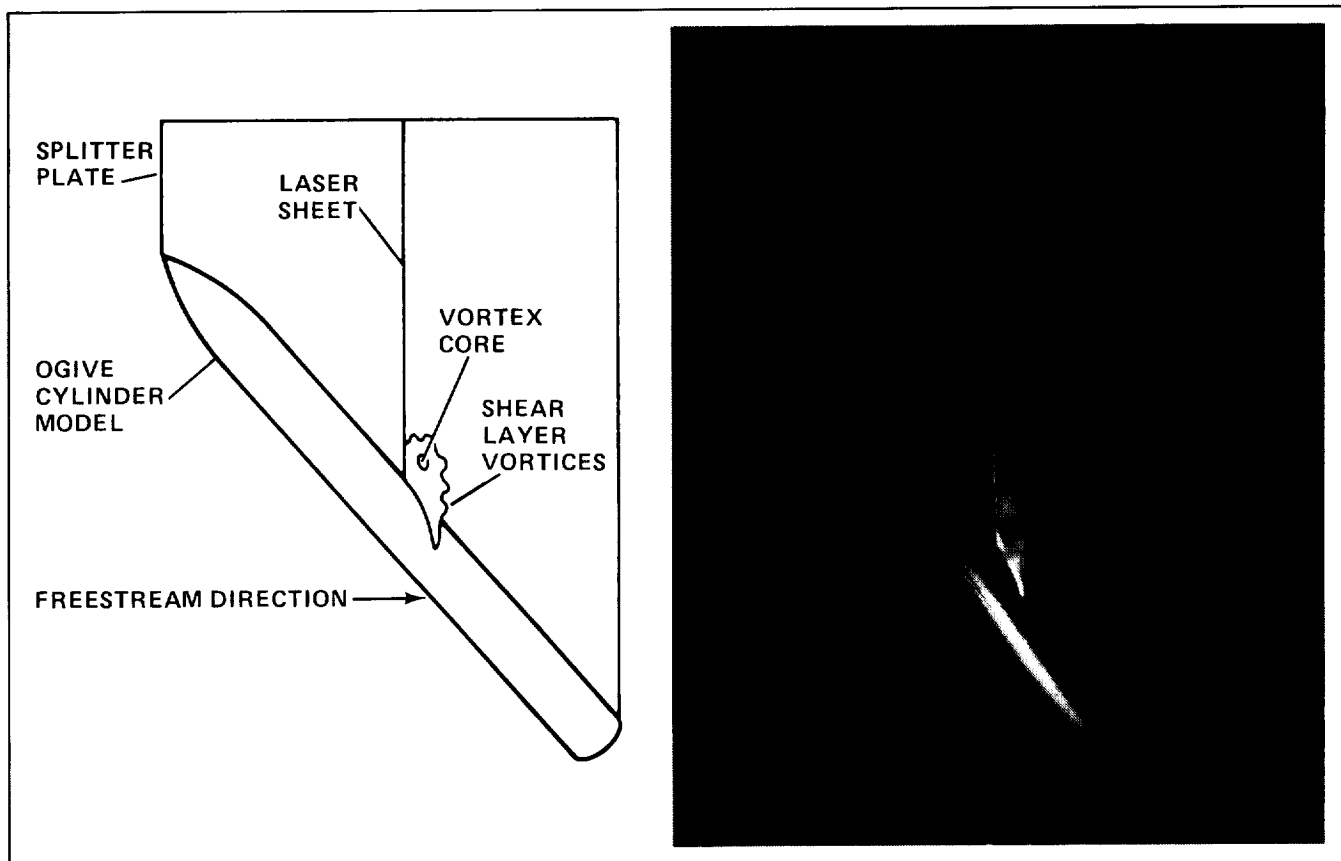
Critical Reynolds numbers at the leading edge

Experimental Study of Flow Unsteadiness Around an Ogive Cylinder at Incidence

This study of the flow past an ogive cylinder at a 20 to 85° angle of attack and Reynolds number of 26,000 is an example of a case where the phenomenon of interest was initially discovered computationally. Computations of a similar flow field, using a three-dimensional, time-dependent, thin-layer Navier-Stokes code, produced a time-dependent, normal-force coefficient history. Initially, it was thought that the code was having convergence problems. Closer examination of the solution showed what appeared to be shear-layer vortices being shed into the leeside vortex flow field at a frequency of 1200 Hz. Subsequent experiments have confirmed the high degree of flow-field unsteadiness. Several vortex phenomena have been observed and measured using hot-wire anemometers and surface-mounted pressure transducers. High-speed movies of the free shear layer show ripples in the layer near the separation point. These observed ripples (see accompanying figure) are indicative of the presence of shear-layer vortices.

Velocity fluctuations caused by shear-layer vortices significantly contribute to the overall unsteadiness of the ogive-cylinder leeside flow field at the Reynolds numbers studied. Additional questions about the origin and structure of the unsteady flow field and the effects of perturbations on the symmetry of the flow field are being investigated both experimentally and computationally.

(G. Zilliac and D. Degani, Ext. 4142/4470)



Smoke-laser visualization of ogive-cylinder leeside flow field at $Rn_D = 26,000$

1988 Bayesian Learning Accomplishments: AutoClass

The Bayesian learning group within Code RIA at Ames Research Center has developed the general theory for discovering patterns in noisy data. This theory is being tested in the relatively simple, but important, domain of automatic classification using an implementation called AutoClass. Here the goal is to find natural classes within a set of objects (examples, cases, etc.) that reflect some underlying cause. It has found classes that were unsuspected by workers in the field, and these classes have since been confirmed by further investigation. AutoClass has several important advantages over most previous work:

1. AutoClass automatically determines the most probable number of classes. The classes found represent actual structure in the data. Given random data, AutoClass discovers a single class.

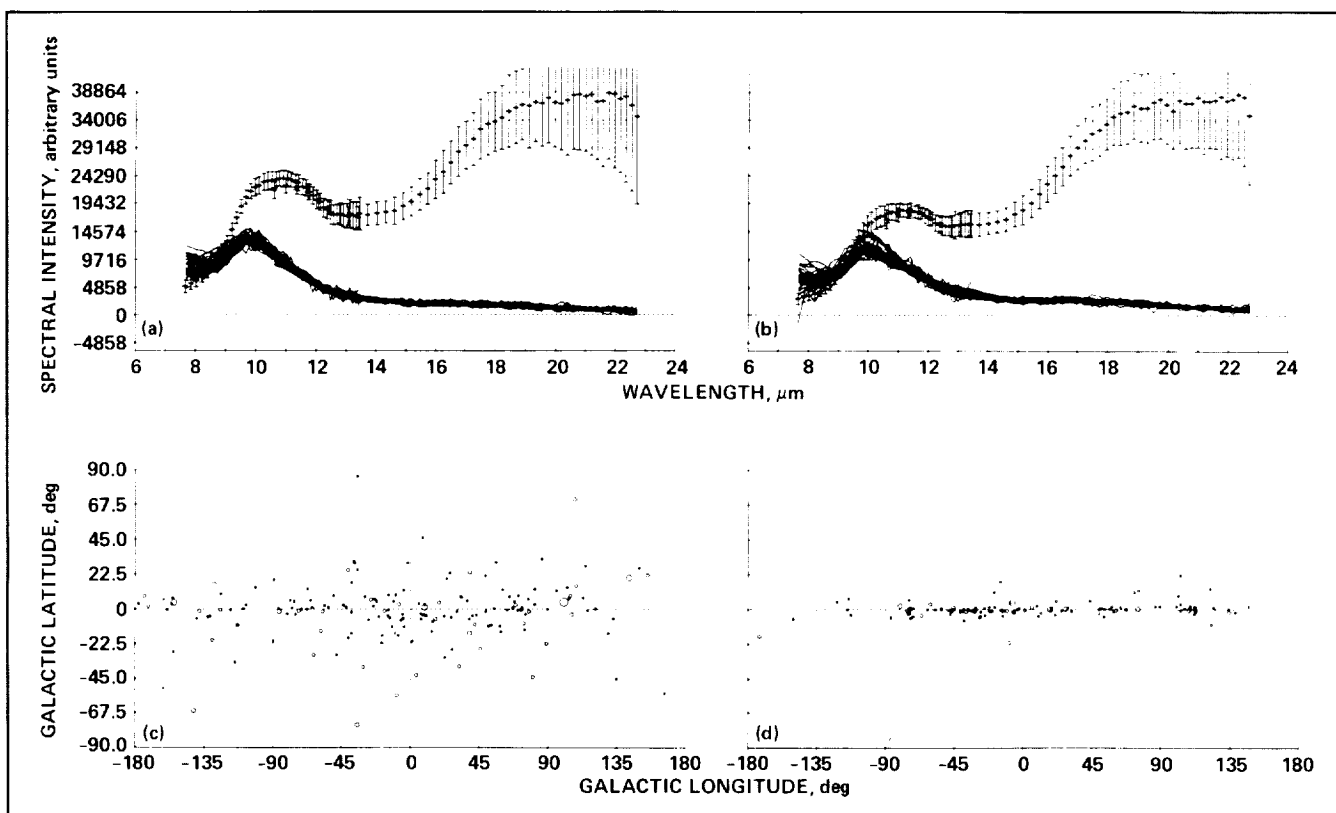
2. Bayes's theorem is all that is required to perform classification. No ad hoc similarity measure, stopping rule, or clustering quality criterion is needed. Decision theory applies directly to the probability distributions calculated by AutoClass.

3. Classification is probabilistic. Class descriptions and assignments of objects to classes are given as probability distributions. The resulting "fuzzy" classes capture the commonsense notion of class membership better than a categorical classification.

4. Real valued and discrete attributes may be freely mixed, and any attribute values may be missing.

AutoClass has classified data supplied by researchers active in various domains and has yielded some new and intriguing results. The following is a sample:

1. Infrared astronomy data base. The Infrared Astronomical Satellite (IRAS) tabulation of stellar spectra is not only the largest data base AutoClass has assayed (5,425 cases, 94 attributes), but is the



The spectra show two closely related IRAS classes with peaks at 9.7 and 10.0 μm . This discrimination was achieved by considering all channels of each spectrum. AutoClass currently has no model of spectral continuity. The same results would be found if the channels were randomly reordered. The galactic location data, not used in the classification, tend to confirm that the classification represents real differences in the sources.

least thoroughly understood by domain experts. AutoClass's results differed significantly from previous analyses. Evaluation of the new classes by infrared astronomers indicates that the hitherto unknown classes found by AutoClass have important physical meaning. An example of AutoClass discoveries from IRAS is shown in the figure.

2. Clouds data base. When applied to examples of two-dimensional cloud data (in both visual and infrared), AutoClass rediscovered the known cloud types as well as found finer structure within some of these types.

3. Miscellaneous. AutoClass has also found interesting results in a cardiac data base, Shuttle main

engine test data, IRAS point-source catalogue and the IRAS faint-source catalogue. Other data bases are being investigated.

The Bayesian theory on which AutoClass is based is sufficiently general that it can be applied to many other problems of interest to NASA, and other agencies, universities, etc., outside NASA. AutoClass has already been sent to a number of researchers.

(P. Cheeseman, Ext. 4946)

PI-in-a-Box: Intelligent On-Board Assistance for Spaceborne Experiments in Vestibular Physiology

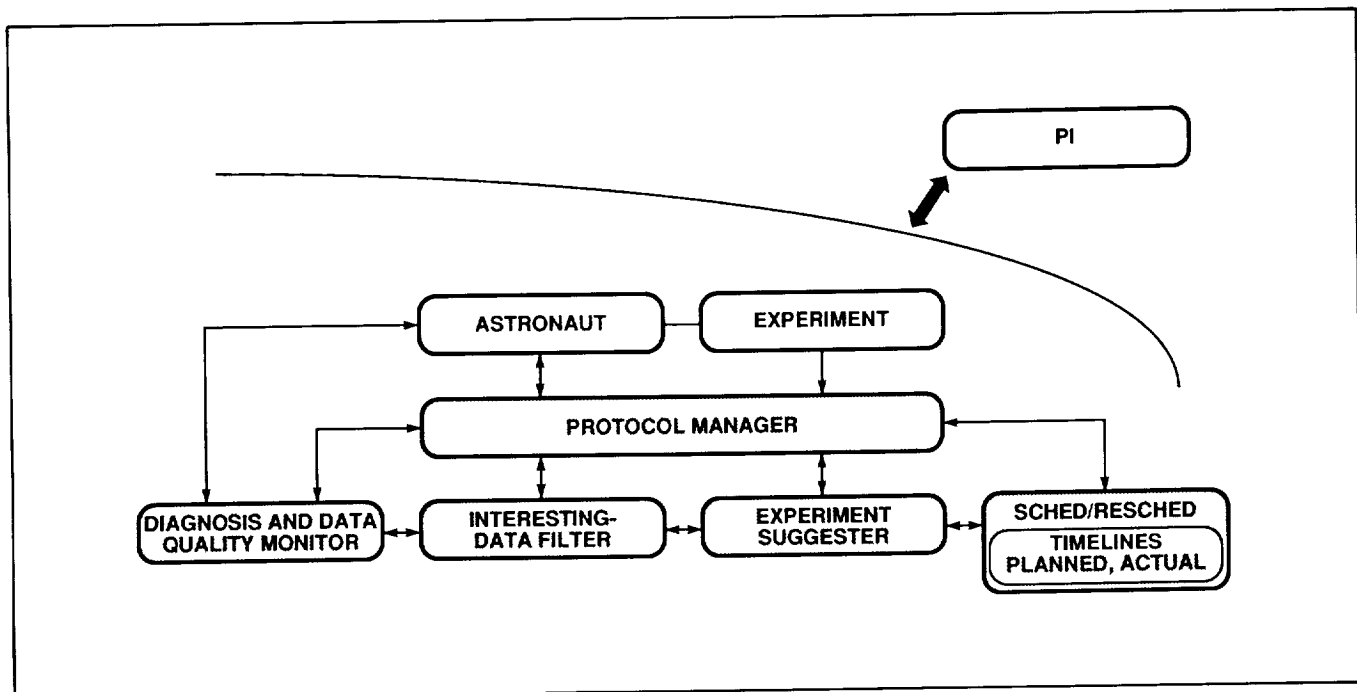
We are constructing a knowledge-based system that will aid astronauts in the performance of vestibular experiments. The system will provide real-time monitoring and control of signals, and it will help the mission specialists and payload specialists make decisions that are normally the province solely of a principal investigator, hence the name PI-in-a-box. Important and desirable effects of this tool will be to optimize the quality of the data obtained and to make the astronauts more productive and better integrated members of the scientific team.

The work begun in FY 1988 has been performed in collaboration with the Massachusetts Institute of Technology (MIT) and Stanford University. PI-in-a-box is initially designed to be used in the context of a series of vestibular physiology experiments to test theories on adaptation to weightlessness and space motion sickness. These experiments are being planned by Prof. Laurence Young, MIT, whose team has performed similar experiments in Spacelab missions SL-1 and D-1.

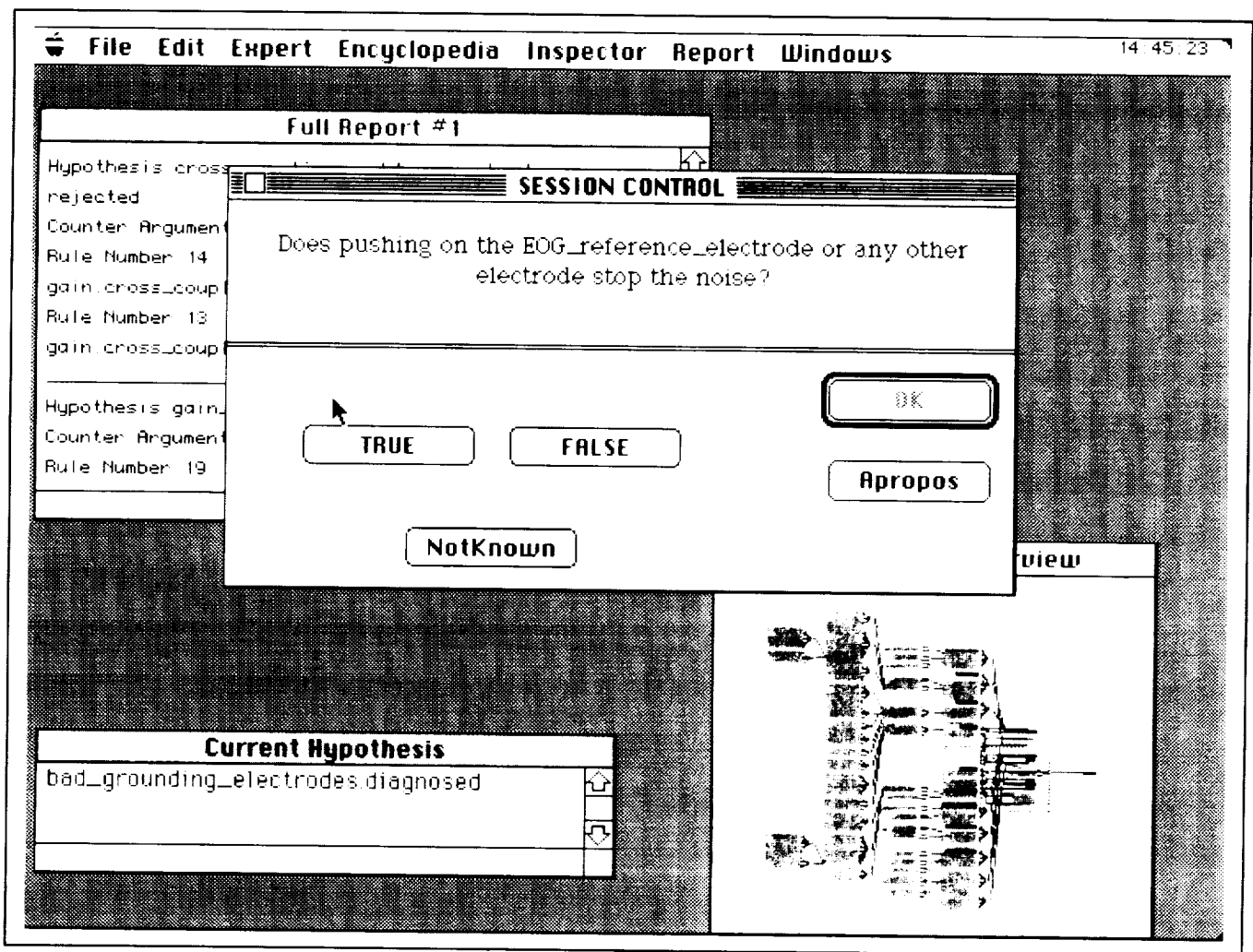
The initial top-level system design is illustrated in the first figure. The hub of the system is the Protocol Manager. This subsystem interacts with the astronaut and with the experiment, and serves as a controller for the remaining four major subsystem functions: (1) monitoring data quality and diagnosing fault, (2) detecting interesting data, (3) suggesting new experiments, and (4) scheduling or rescheduling experiments and resources.

As a first prototype we built a small diagnostic knowledge-based system for the electro-oculography (EOG) eye movement signal. The current knowledge base used to monitor and diagnose the EOG signal has been sufficient to produce a meaningful demonstration, although the user is still required to input data that will be input automatically in the operational system. Two typical interaction screens are shown in the second and third figures.

The second major thrust of our work in FY 1988 was a prototype for interesting-case detection. The cases we considered were related to a vestibular sled experiment in which the subject sits on a sled which rides back and forth on a track. The subject's eye movement is measured by EOG and relevant parameters are computed. Comparison of preflight, inflight, and postflight values of these parameters provides a test of the orientation model. The



Functional layout of "PI-in-a-box"



A prototype screen requesting input from the astronaut

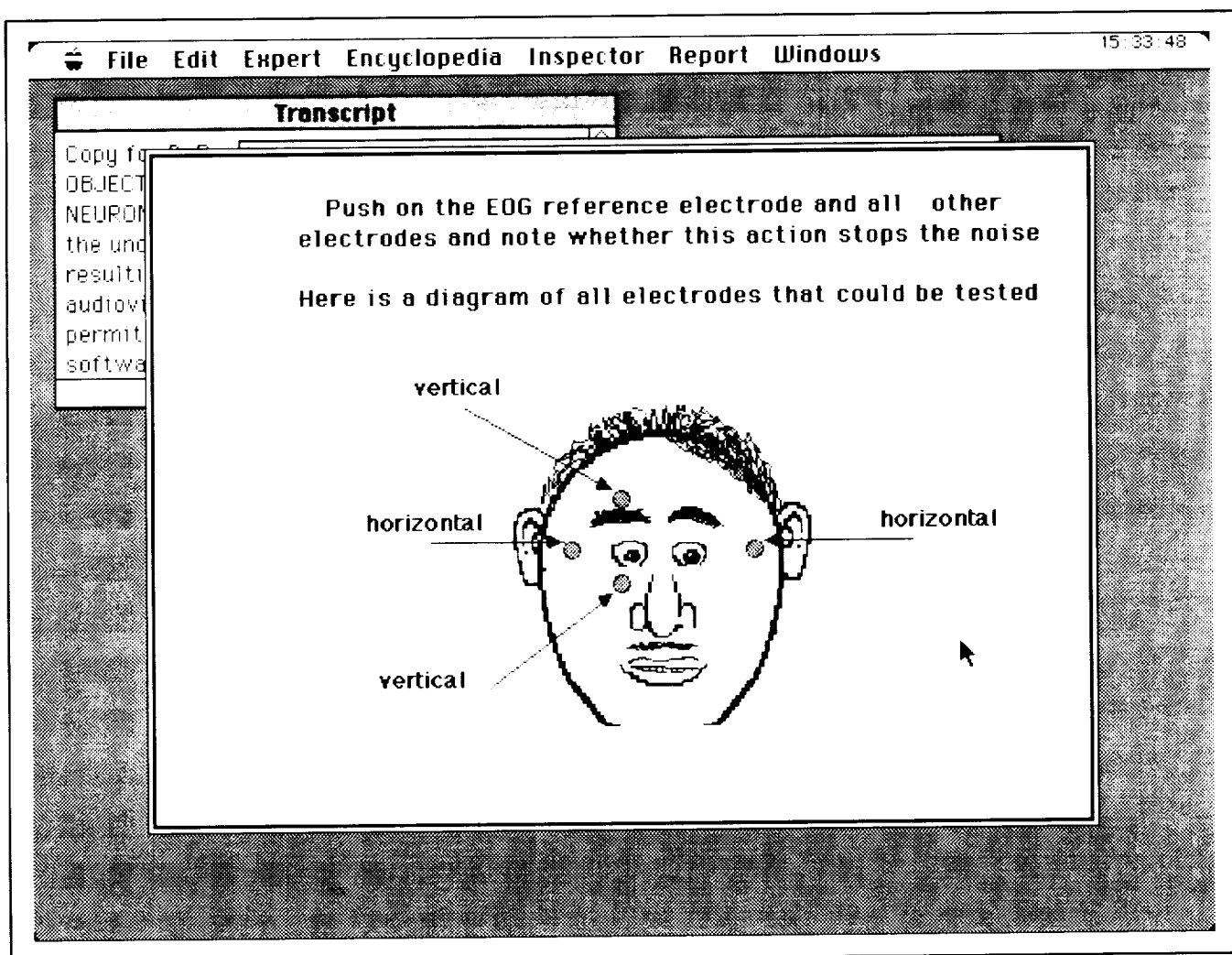
interesting-case detection prototype compares parameters for a preflight and an inflight experiment, and suggests whether the discrepancies detected should be viewed as interesting or not. This type of suggestion, in the final system, might lead to a recommendation for changes in the original experiment plan, either for a second look or for the exploration of previously unexpected possibilities.

Toward the end of FY 1988 work began on the protocol manager and on subsystems related to a

different vestibular experiment. In this new experiment, the subject looks into a rotating dome and experiences the illusion of self-rotation. Quantitative and qualitative parameters can be derived from these sensations, and other models of orientation in weightlessness can be tested. The functional requirements for the protocol manager were determined, and work on its implementation was started.

(S. Colombano and D. Rosenthal, Ext. 4380/4759)

ORIGINAL PAGE IS
OF POOR QUALITY



A prototype screen suggesting a course of action

Machine Learning and Planning

Code RIA, Ames Research Center, has a diverse program in machine planning and learning and concentrates specifically on the overlap of these two areas.

Planning is generally defined as the selection and sequencing of actions to achieve specified goals. As such, it involves reasoning about how actions affect the world, how resources are consumed by the occurrence of actions, and how actions can be used to effectively achieve goals.

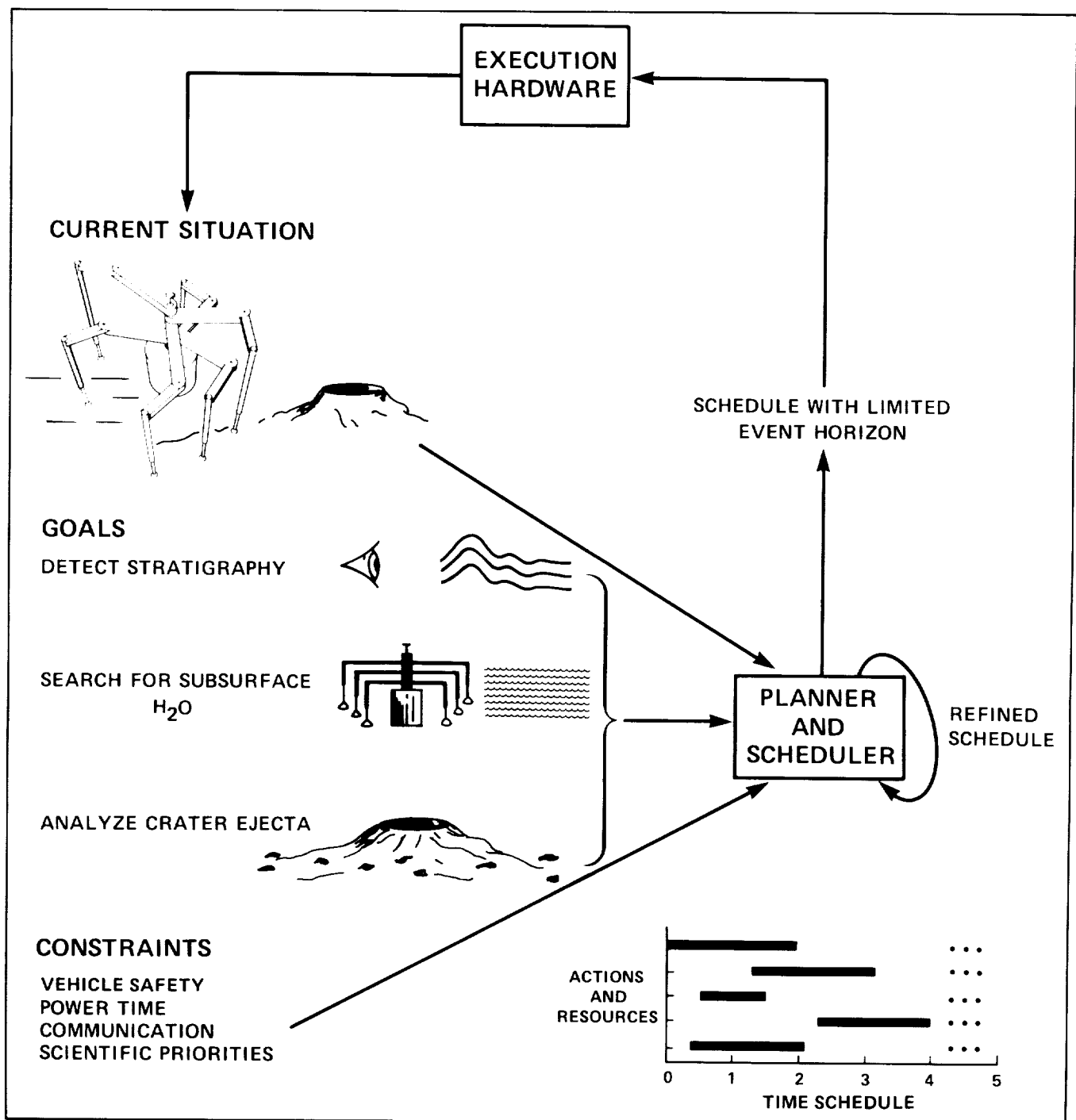
The goal of machine-learning research is the development of adaptive systems. Such systems improve their performance over time, increasing their

ability to deal with situations and events that cannot be predicted by the system's designer.

One aspect of machine learning studied is the acquisition of search control knowledge. One particular learning process, called Explanation-Based Learning (EBL), analyzes control decisions made during the course of planning in order to characterize the planner's successes and failures. The resulting search control knowledge can be used to guide future planning efforts. The idea of self improvement over time is graphically portrayed in the first figure.

Advanced EBL techniques have been incorporated in two systems built by NASA-supported research groups. One system, called Prodigy, developed primarily at Carnegie-Mellon University

ORIGINAL PAGE
BLACK AND WHITE PHOTOGRAPH



Planning and scheduling to achieve goals

(CMU), demonstrates that these learning techniques can dramatically improve the performance of a planning system. Subsequent collaborative work with the MITRE Corporation showed that approximating the learned knowledge improves its utility.

Our planning research integrates the predictive, goal-oriented aspect of classical planning with the reactive, situation-specific behaviors exhibited by traditional control systems. This research has resulted in a new paradigm in which the output of the

planner is a set of Situated Control Rules (SCR) that are applicable in certain contexts, and are used to suggest the performance of predetermined actions. This work begins to bridge the gap between classical control theory and artificial intelligence. The idea of incremental SCR generation is placed in the context of a Mars Rover Sample Return (MRSR) mission in the second figure.

Other work concerned with the seamless fit between planning and execution has been pursued in conjunction with various universities and corporations.

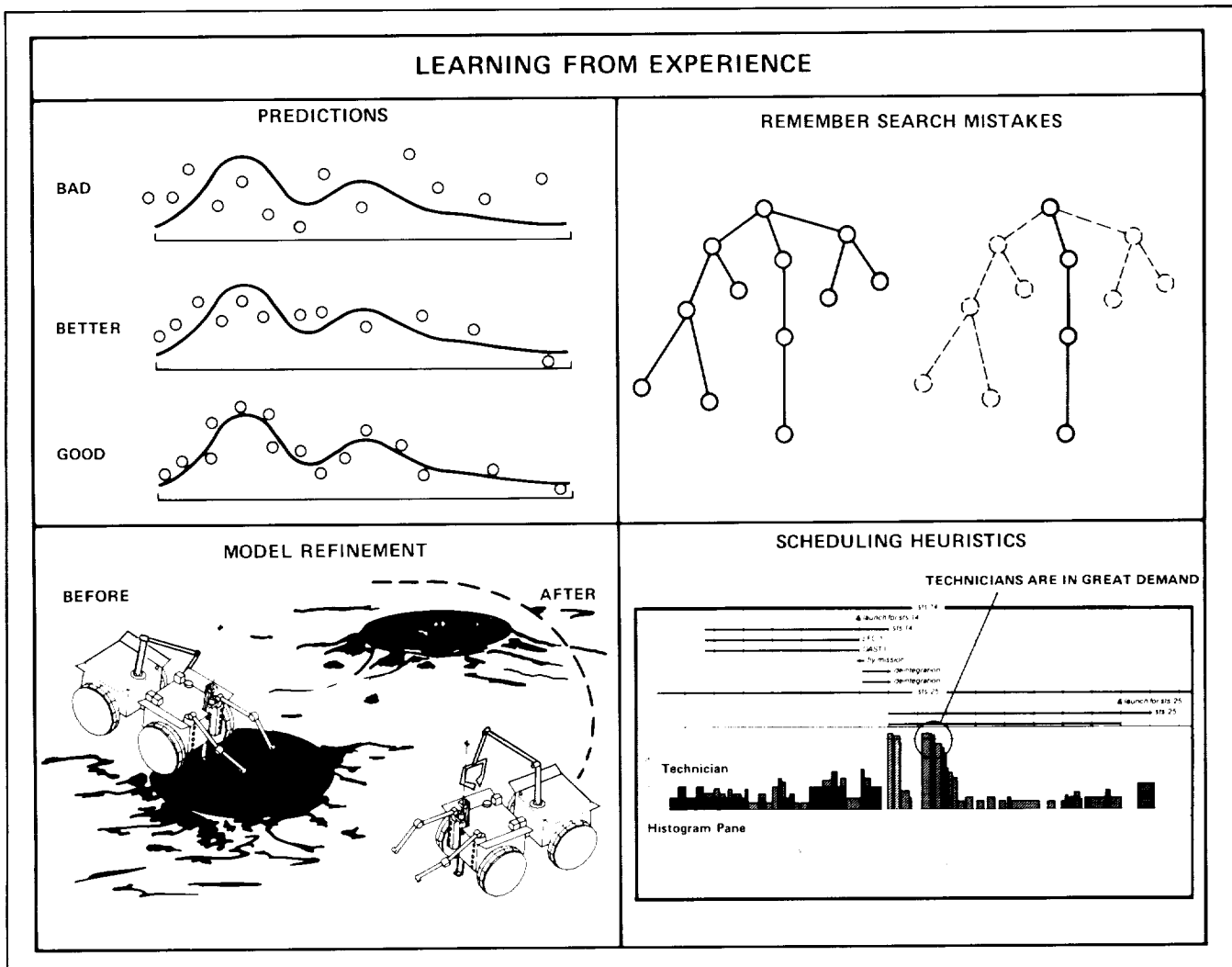
Theoretical work addressing the "Belief, Desire and Intention" model of rational action has been under way at SRI International. In connection with this work, a collaborative mobile robot demonstration put on by Stanford University, Rockwell International,

and SRI exhibited goal-directed autonomous behavior. One part of the overall control architecture of this robot employed a theory of knowledge and action developed at SRI called "Situated Automata."

Other collaborative work at SRI has been concerned with the representation and use of procedural knowledge. The Procedural Reasoning System was developed and applied to the problem of diagnosing a malfunction within the Reaction Control System of the Space Transportation System.

Work with CMU has resulted in the production of a hand-eye robotic test bed that can be used to study the formulation and solution of planning problems where the planning system is given incomplete information.

We have been involved with the development of SPIKE, a constraint-based scheduling system.



Learning from experience

SPIKE has been built at the Space Telescope Science Institute. The same problem has been addressed by CMU using their previously developed constraint satisfaction approach. These systems address the large-scale scheduling requirements of telescope science scheduling and related problems.

SOAR is a general cognitive architecture that integrates problem solving and learning. It was originally developed at CMU and is now being developed at CMU, Stanford University, Information Sciences Institute, and the University of Michigan. SOAR is notable for its use of universal subgoaling for problem solving and chunking for learning. Some of this year's accomplishments with SOAR include its integration with a robotic manipulator, its ability to accept and generalize external advice, and recent extensions in the area of analogical generalization.

(M. Drummond, Ext. 3388)

Spaceborne VHSIC Multiprocessor System

The Spaceborne VHSIC Multiprocessor System (SVMS) is to be used in Space Station Freedom for numeric and symbolic algorithms for large knowledge-based systems applications. The SVMS, which will have a sustained system performance of at least 100 million instructions per second, is a six-processor Ada/LISP machine consisting of a four-processor generic LISP Processor and two com-

panion processors: an RH32 and an i386. The programming languages are Ada, Common LISP with the Common LISP Object System, and a Concurrent Common LISP. The SVMS is to have at least a 40-bit tagged architecture, a 20-Mbyte main memory, and a paging device for large program executions.

The SVMS Project is divided into three phases.

1. Phase 0, system definition, was completed in June 1988 by a contractor team that consisted of Symbolics Display, Inc., and TRW Inc. The accomplishments of Phase 0 were the development and evaluation of a 1.6- μ m CMOS VHSIC LISP chip, fault-tolerant techniques, and integrated numeric and symbolic multiprocessor architecture.
2. Phase I is the fabrication of three SVMS brass-boards. The accomplishments of Phase I have been the issuance of RFP2-33369(LMV) on July 15, 1988, and the completion, in October 1988, of the evaluation of the proposals.
3. Phase II will fabricate the space-qualified SVMS. This phase is a collaboration of Ames Research Center, the Defense Advanced Research Projects Agency (DARPA), and the U.S. Air Force (USAF)/Rome Air Development Center (RADC), Griffiths Air Force Base. USAF/RADC is to provide the RH32 numeric processor.

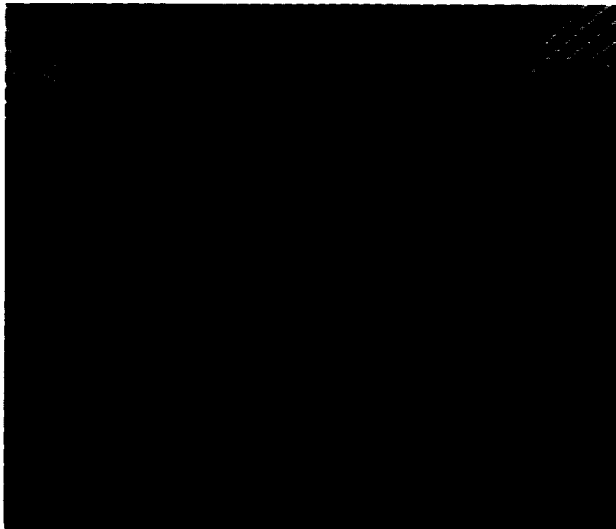
The delivery of the space-qualified SVMS is expected in early 1995, which is compatible with the initial operational capability schedule of Space Station Freedom.

(H. Lum, Ext. 6544)

rapidly address the device with a desired sequence of filters. This high-speed input/output capability is a key step in plans to integrate the optical processor with a knowledge-based system for image recognition and classification.

A new type of filter developed at Ames to recognize images at different aspect angles was further characterized. Specifically, the ability of the filter to recognize objects over a range of views (the "distortion range") was evaluated and was shown to be sensitive to the extent of the distortion range, but was relatively insensitive to the number of training images used to compute the filter. In general, a data base of filters would be required to cover a large distortion range. In support of this conclusion, methods of linking information and searching data bases for optical-image-recognition applications were investigated and reported.

(E. Ochoa, Ext. 6725)



Magneto-optic spatial light modulator displays pattern-recognition filter

Conservation of Design Knowledge

The long-term goal of the Conservation of Design Knowledge (CDK) project is to develop methodologies for creating and maintaining an accurate record of a system design throughout its life cycle. Currently, moving through the design, manu-

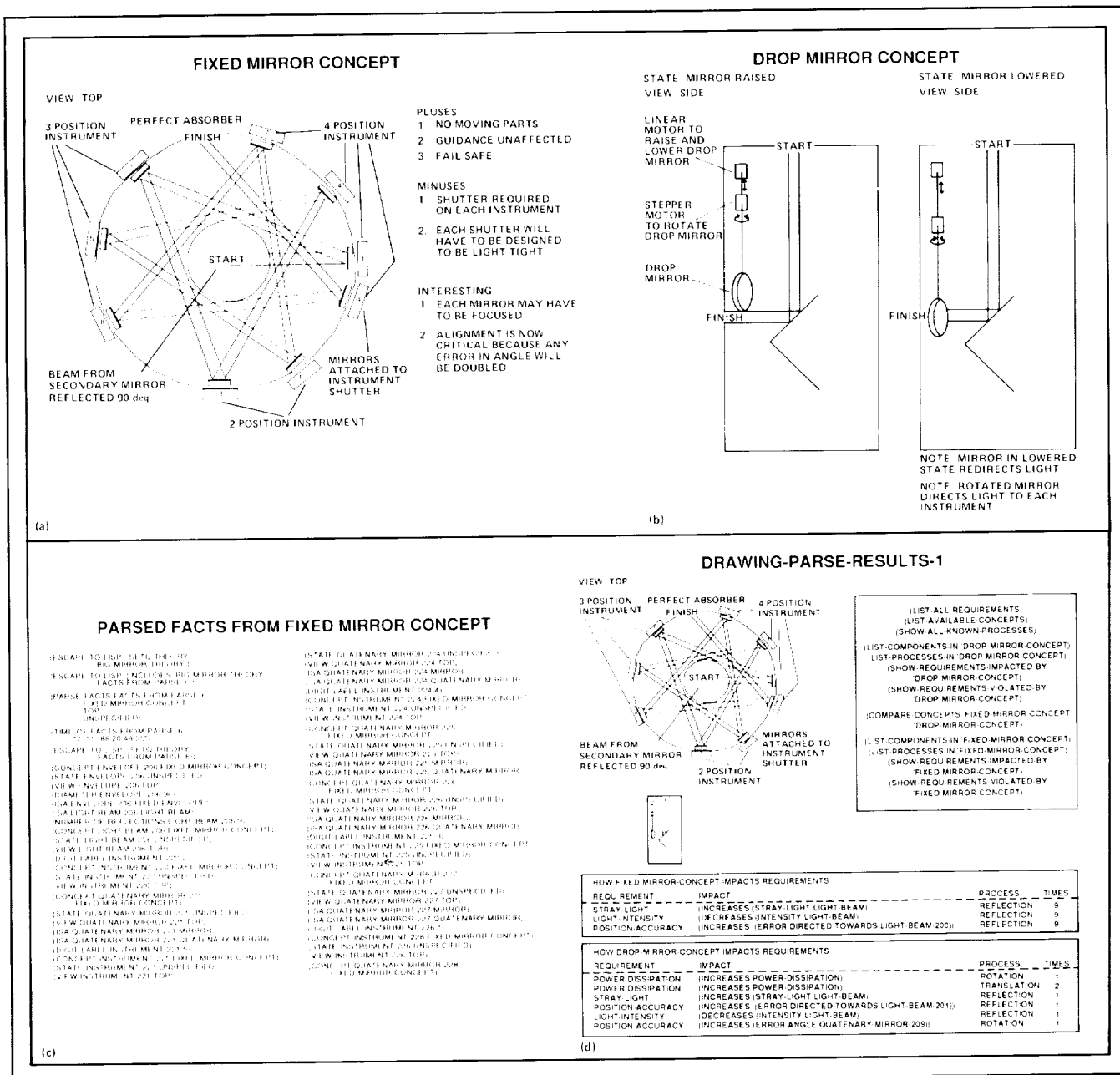
facturing, and deployment stages of NASA's large and complex space systems results in a considerable loss of information. If this information could be captured, the design and maintenance of such systems could be made more efficient and less error-prone.

To address the issues of acquiring design knowledge, a study was performed on the design of the Tertiary Mirror Assembly of Ames Research Center's Space Infrared Telescope Facility project. This study was performed together with the CDK project's third collaborator, the Center for Design Research from Stanford's Mechanical Engineering Department. The approach is to develop an electronic "designer's notebook," from which information can be extracted automatically, and for which methods can be developed for interacting with the designer. A text and graphics editor, vmacs™, is used as a basis for the electronic notebook. vmacs™ was developed by Fred Lakin, one of the Stanford collaborators, and is suited for studying the designer's behavior and for extracting design information.

During 1988 two prototype subsystems for capturing design knowledge from the Tertiary Mirror Assembly design have been developed: the "Rationale Inferencing System" and the "Page Set Summarizer."

The goal of the Rationale Inferencing System is to minimize the designer's extra effort to record design knowledge by automatically inferring the rationale for design decisions from the designer's notebook drawings. The system describes the rationale for a design change by comparing how the design meets the system requirements before and after the change. This comparison is done by interpreting the notebook sketches of the design alternatives (a and b of the figure) into a knowledge-based language (c of the figure). Models of the design alternatives' structures and behaviors are built by matching the interpreted information from the sketches with the knowledge base, which includes a component library and laws of physics. These models are evaluated as to how they meet the system requirements, and the result of a comparison of two design alternatives is a set of requirements, differently satisfied by each alternative (d of the figure).

The goal of the Page Set Summarizer is to automatically create a summary of the designer's notes that could serve as an explanatory introduction of the



A Knowledge-Based Approach to the Real-Time Control of Dynamical Systems

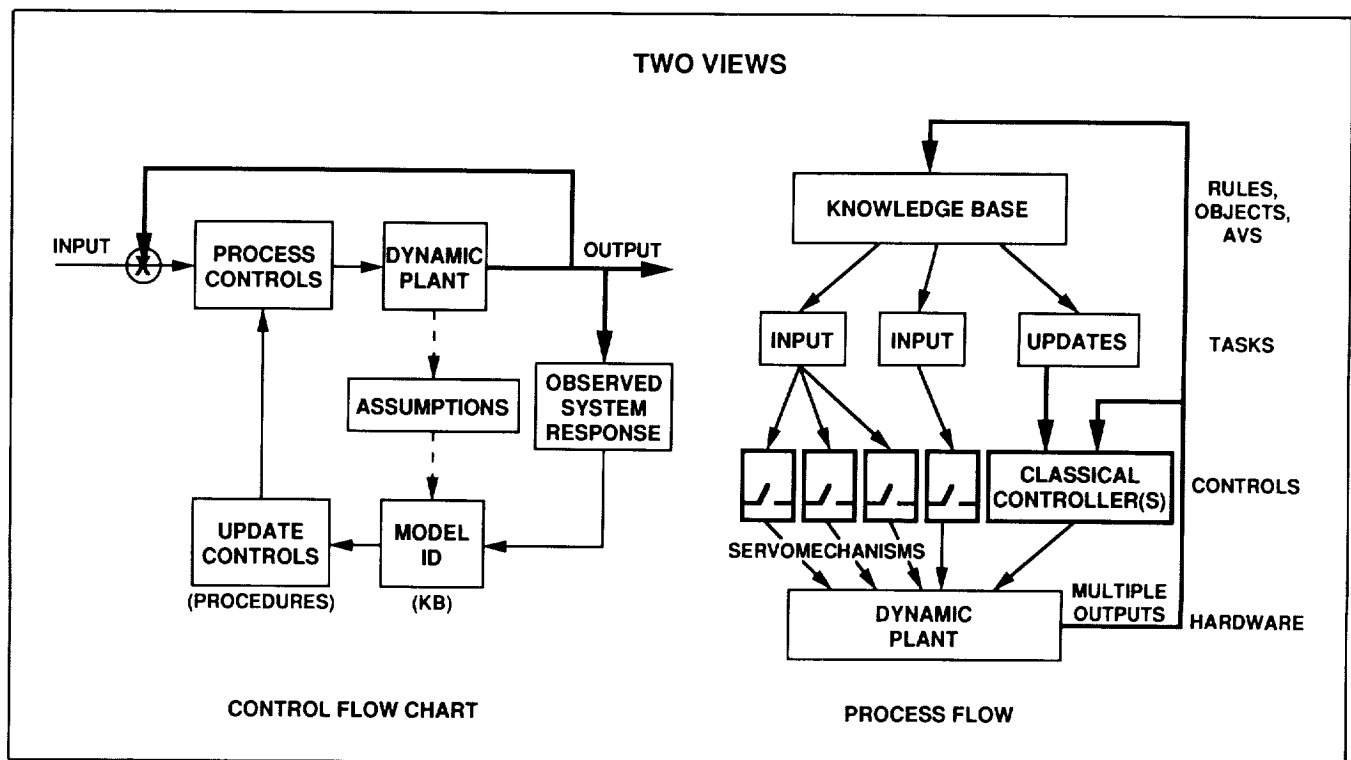
One characteristic of real-time thermal and electrical control systems is that component faults, unpredicted loads, and/or reconfiguration changes cause the system model to change. Presently, human operators update boundary conditions and/or adjust the model characteristics and parameters as changes occur. However, this procedure is slow and expensive, especially for real-time control in such advanced automation applications as are planned for Humans-in-Space missions; e.g., Space Station Freedom, Lunar base, or a manned Mars mission.

This work uses a combination of rule-based, object-oriented, and data-driven techniques for modeling, identification, and control. These techniques are applied to the real-time control of a thermal test bed as part of the Thermal Expert System (TEXSYS). When qualitative changes occur in the thermal test bed, a new model (including the component failure or system reconfiguration) is isolated

by the progressive application of rule sets over an object-organized knowledge base, and these model changes are used to either update or switch modes of the real-time thermal test bed controls. It follows that this approach places the knowledge-based software in a supervisory mode over conventional process controls.

The knowledge base representing expected thermal test bed configurations of faults makes use of a discrimination net at varying levels of abstraction. Qualitative process simulations are implemented as a network of frames with the Model Toolkit, and controller algorithms are implemented as procedures—which are triggered by the propagation of observed data through these simulations. By separating the knowledge about the thermal test bed from that governing the model identification and controls, the generality of this approach is preserved.

Translation between symbolic and algorithmic control domains is necessary to link knowledge-based software with algorithmic real-time systems. For the thermal test bed control, this translation is accomplished by first applying rule sets to map the identified model changes to a set of control model



Systems autonomy demonstration project: a knowledge-based approach to the real-time control of dynamical systems

changes; then, active values trigger numerical algorithms for estimating control parameter changes and/or procedures for control mode swapping so that minimum performance standards are satisfied.

Tests with TEXSYS and the thermal test bed are being used to demonstrate successful identifications of thermal test bed changes and to initiate corresponding controller modifications.

(C. Wong, Ext. 4294)

Human Interface to the Thermal Expert System

An important part of understanding most engineering systems is knowing how components are connected and how they interact. Much of this knowledge is captured in engineering schematics. Since this knowledge is crucial to understanding the functionality of a system, it is essential that the human interface provide the operator with the ability to examine a schematic.

The Human Interface to the Thermal Expert System (HITEX) is part of the Systems Autonomy Demonstration Project. The Ames Research Center's Code FL is responsible for developing HITEX in a cooperative effort with Code RI, which is responsible for developing the Thermal Expert System (TEXSYS) to monitor, control, advise, and do fault diagnosis on a thermal test bed developed by the Boeing Aerospace Corporation.

The goals of the HITEX are to provide a useful tool for thermal engineers to easily validate system performance, to provide flexible graphics to aid in finding and isolating information, and to accommodate users of varying skill levels. HITEX minimizes physical demands by using contact-sensitive displays and customization, memory demands through immediate feedback and direct manipulation, and cognitive effort through flexible data presentation.

The operator will interact with two screens: the HITEX expert system screen and the graphical information display. The HITEX expert system screen will be implemented on a monochrome monitor and the graphical information display will be on a color monitor. The screens will be placed side by side,

and will function as one large screen. A single keyboard and single mouse pointing device will be used, with the user being able to move the mouse from one screen to the other as if they were a single screen. Both screens will be driven by the single HITEX Symbolics, which will be in communication with both the Texas Data Acquisition System and the expert system.

Some desired capabilities for the graphical schematic for the TEXSYS are (1) the ability to use the mouse on any component and bring up a menu of options; (2) the ability to color code different types of fluid channels; (3) the ability to display sensor information dynamically updated, based on hardware readouts; (4) the ability to "flash" or color-code components to show an alarm or to focus the operator's attention; (5) the ability to customize the schematic by not showing certain sensors, components, or fluid channels; and (6) the flexibility to add or delete a component as the hardware configuration changes.

To achieve the flexibility and capabilities described above, an interactive graphical tool has been built to allow the user to easily construct and modify a complex schematic. The act of building a schematic involves creating a library of component classes (e.g., evaporators, valves, etc.). Once the library is constructed, a schematic is built by using the mouse on a library component, dragging it into a schematic window, and clicking to position it. Two components can be connected by clicking on the port for each component. Since it is unlikely that all of the components will be positioned correctly the first time, the schematic builder allows the user several ways in which components and flow channels may be moved.

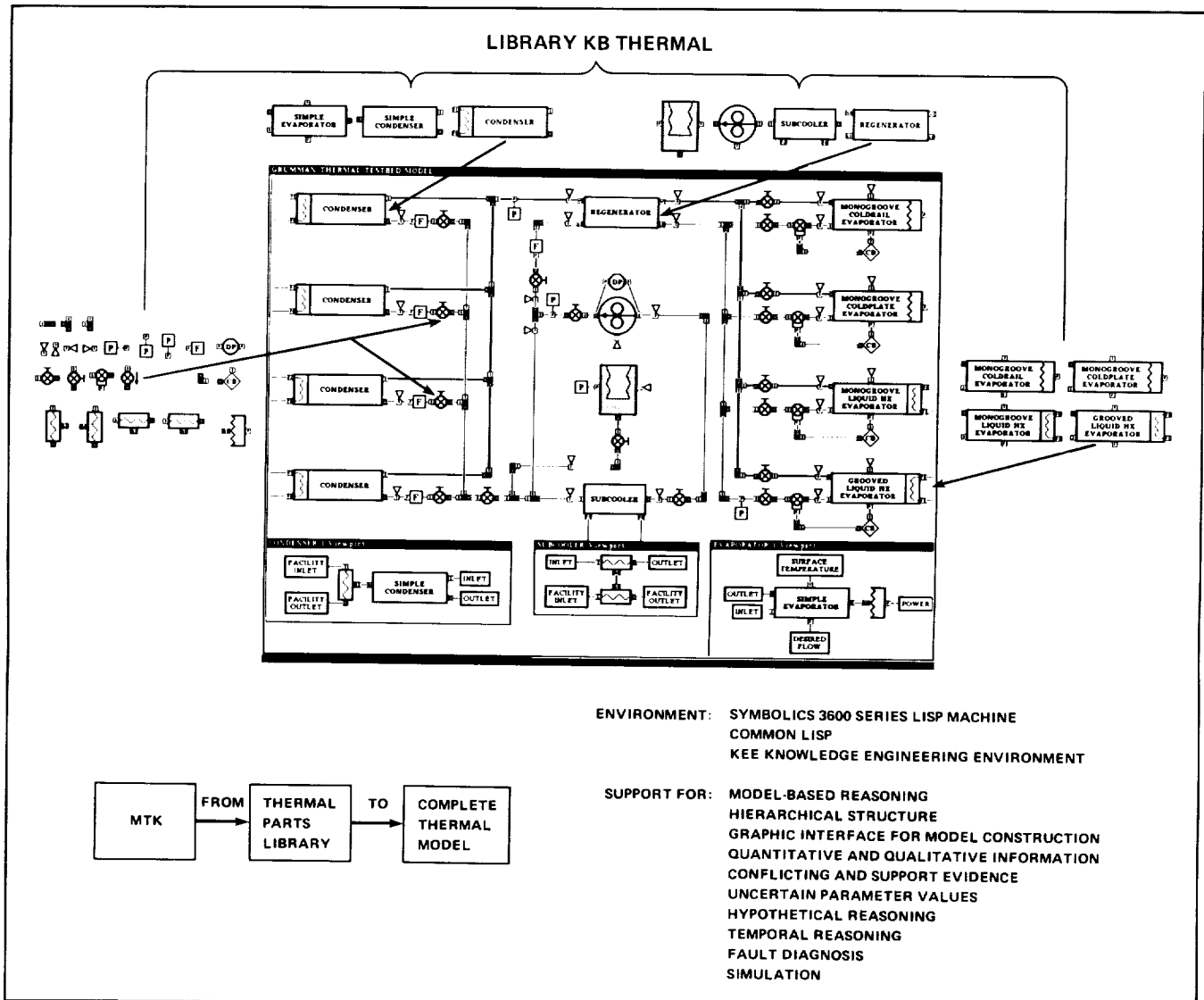
The schematic builder is similar to the graphical model-building capability available in the Model Toolkit (MTK) facility. The major differences are the ease of building the schematic and the professional quality of the schematic created. Comparing the two tools is similar to comparing the generation of a document by typing with a manual typewriter and the generation of the same document with a sophisticated word processor. The first figure shows an MTK-type interface; the second figure shows the additional capabilities in the new Human Interface.

The schematic-building toolkit has proven successful in building the schematic for the Ames

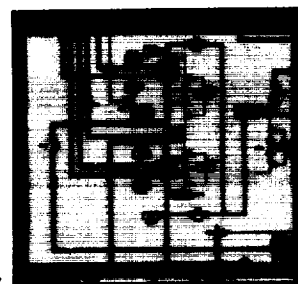
Brassboard model of the Boeing/Sundstrand thermal system. An attractive, fully functional schematic was

built in only 2 days using it.

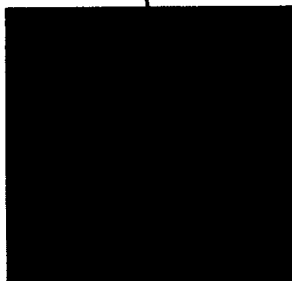
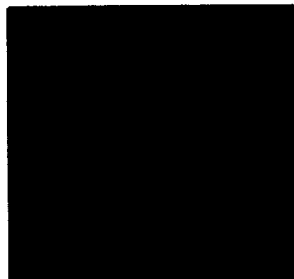
(C. Wong and N. Dorigi, Ext. 4294/3371)



Model toolkit for model-based reasoning in thermal expert system



- COLOR STATUS-AT-A-GLANCE
- INTERACTIVE SCHEMATIC
- ENGINEERING DIAGRAMS
- USER-DEFINED SENSOR MONITORS
- WARNINGS, ALARMS
- EXPLANATIONS
- ANALYSIS AIDS



Human interface for the thermal expert system

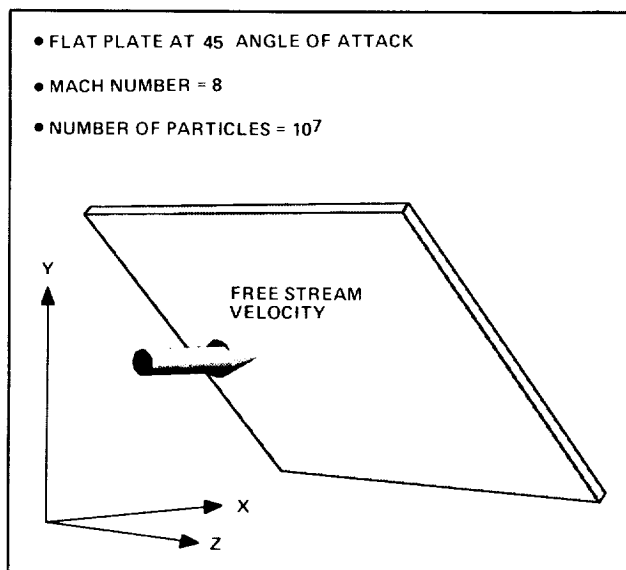
Discrete Particle Simulation of Compressible Flow

Future aerospace vehicles such as the aeroassisted orbital transfer vehicle will fly at times under rarified atmospheric conditions that lie outside the regime of applicability of continuum methods. Discrete particle simulations offer the possibility of calculating within this regime. Established methods of this class, such as direct simulation Monte-Carlo (DSMC), are computationally intensive, limiting their usefulness even on current computers. The new method developed is about two orders of magnitude

more efficient, allowing the simulation of realistic three-dimensional geometries.

The focus of this work was to develop the capabilities of the model to represent the physical processes inherent in this flight regime. At the same time, the algorithm has been optimized for the various machine architectures used. Although a supercomputer such as the CRAY-2 greatly augments the problem-solving capacity of the method through its large memory and speed, it is not viewed as the definitive architecture for this type of simulation. Careful consideration has been given to what would constitute an ultimate machine organization for this

ORIGINAL PAGE
COLOR PHOTOGRAPH



Three-dimensional flow around a flat plate at angle of attack

category of scientific problem. It is evident that a computer architecture conforming to this algorithm could be far less complex and costly than a general-purpose supercomputer.

Traditional DSMC methods model the flow as a large collection of discrete particles that interact with each other through mutual collisions. The physics of collisions are modeled in detail and the overall characteristics of the flow field are extracted from the statistical properties of many collisions. These methods show great promise but are computationally extremely intensive. They are difficult, if not impossible, to vectorize and, even with current machines, impractical for technically interesting geometries. However, it has been shown that modeling the exact physics of collisions is not necessary to accurately predict overall flow properties. It suffices to simplify the collision model, thereby reducing computational time and bringing realistic, rarified, three-dimensional flows with chemical effects within reach on current machines.

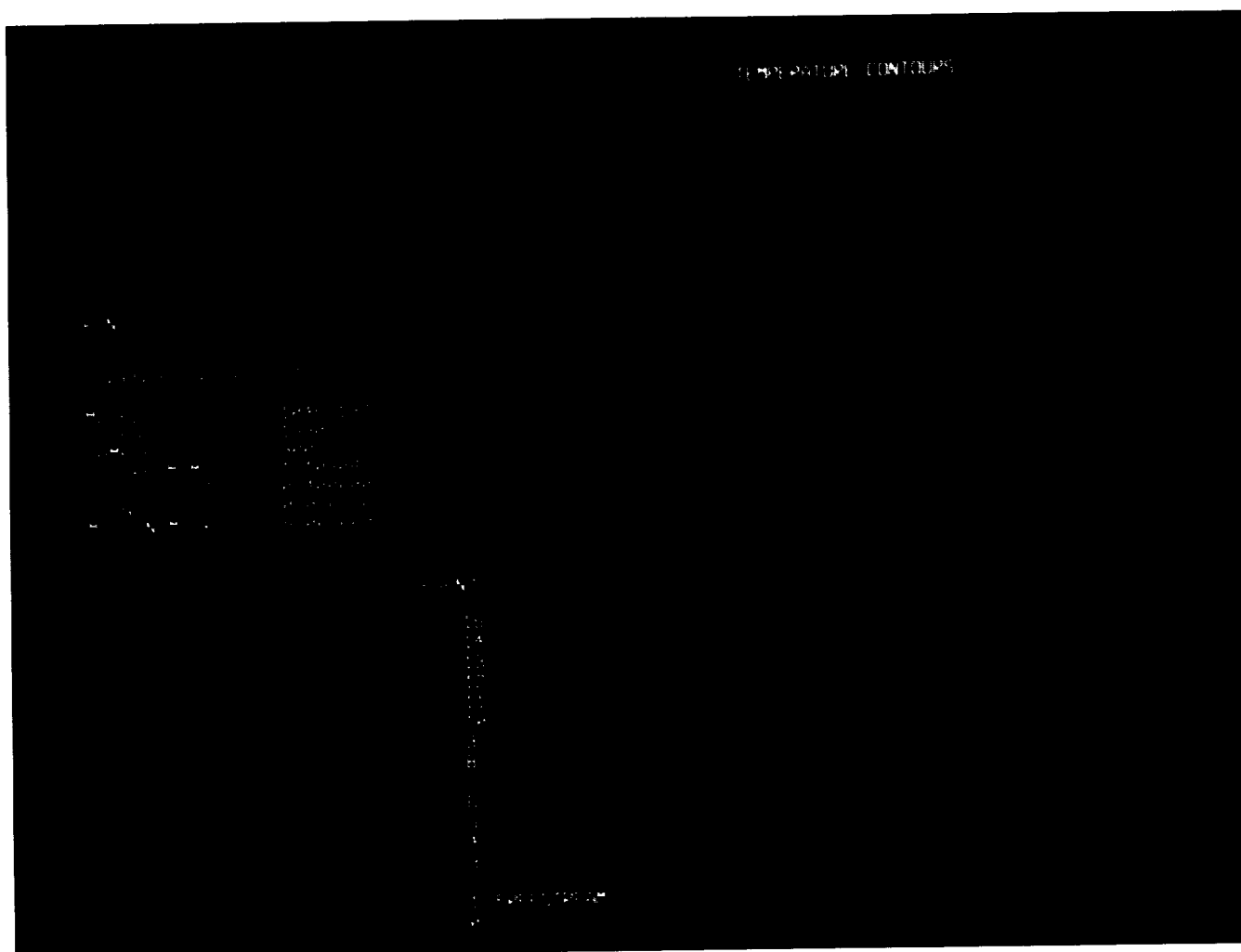
The algorithm may be divided into two parts, particle motion and collisions. The representation of

particle motion is the same for all particle methods, including DSMC. All particles move with their own constant velocity during a time step. After the new positions are integrated, boundary conditions are enforced and then the particles are collided. The present algorithm differs significantly from DSMC methods in the collision algorithm. Simplified physical models are used to represent the interaction between particles during collisions. Although the exact trajectories and interactions between particles are calculated in DSMC methods, the approach here is to restrict the possible outcomes of a collision to a small, previously enumerated subset of all possible outcomes and to choose among these outcomes on a quasi-random basis with minimal calculation. The allowable set of outcomes is defined by the usual conservation of mass, momentum, and energy. The outcomes of DSMC collisions may be thought of as an infinite set, whereas the current algorithm has discretized this space. The more complex particle models that are now under investigation allow the nonequilibrium partition of energy among translational, rotational, and vibrational states.

Three-dimensional calculations have been performed with 10^7 particles and 2.5×10^5 mesh cells that have produced good statistics while using less than 1 hour of CRAY-2 single-processor central processing unit time. This is more than two orders of magnitude more efficient than traditional DSMC methods.

The algorithm is extensively vectorized and has been used to study the suitability and adaptability of particle algorithms to vector architectures. The CRAY-2, with its large main memory, is essential for this type of simulation and provides a test bed for computer architectural aspects mentioned above. In this light, some portions of the algorithm were hand-coded in CRAY assembler language to take advantage of hardware characteristics.

(W. Feiereisen, Ext. 4225)



Temperature contours illustrating some characteristics of the flow field

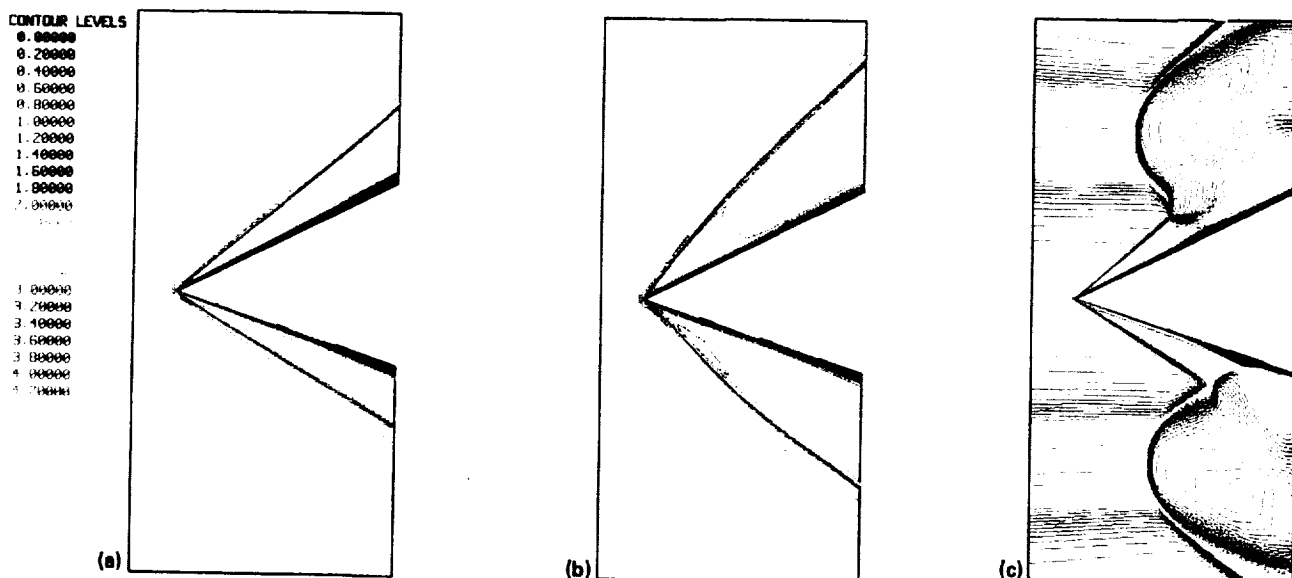
Simulation of Detonation-Wave-Enhanced Combustion

The use of detonation waves as a means to efficiently achieve combustion in a supersonic flow has recently been revived as an alternate design for the supersonic combustion ramjet (scramjet), or as an innovative engine design for hypersonic aircraft designed to reach orbital speeds. In detonation waves the reaction zone is strongly coupled to a preceding shock front and the combustion is completed within a very short distance. This alleviates some of the ignition problems that are expected to occur in conventional scramjet designs at high speed due to the finite ignition delays and very short residence times of the fuel-air mixture. At sufficiently high

Mach numbers, analytical arguments and computational experiments show that it is possible to stabilize an oblique detonation wave attached to a wedge or ramp.

Parts a and b of the figure show the transformation of a pure, oblique shock system into detonation waves. The wedge is inserted into a supersonic, stoichiometric, hydrogen-air mixture at an angle of attack, shown in part a of the figure. As the chemical reactions are allowed to proceed, the heat released by the combustion forces an upstream rotation of the wave fronts, shown in part b of the figure. (In this calculation, the chemistry model included 8 species and 16 reaction steps.) The combustion occurs just behind the shock and strongly affects the shock front, and a stable, standing detonation wave is thus

ORIGINAL PAGE
COLOR PHOTOGRAPH



*Mach contours for oblique detonation waves ($M_\infty = 4.2$, $p_\infty = 0.1$ atm, $T_\infty = 700$ K, H_2 fuel).
a) Shock waves, premixed fuel, no combustion; b) detonation waves, premixed fuel; c) detonation waves, stratified air-fuel mixture*

realized. This simple configuration is the basis of the oblique detonation wave engine design, which is being studied both experimentally and analytically at Ames Research Center.

Additional problems of fuel injection, penetration, and mixing delays will also plague the scramjet design. Therefore, it is necessary to estimate the behavior of the detonation waves in a more realistic environment, where the mixing between fuel and air is incomplete. Such a behavior has been qualitatively analyzed by modifying the free-stream flow conditions. In the extreme case of poor mixing, the flow patterns of two jets of fuel are studied by being convected into the shock pattern on either side of the wedge. Because of molecular weight and temperature variations, the flow has large variations in Mach number in the cross-stream direction. The shock curvature is then strongly fluctuating. The combustion takes place in very narrow regions, at the edge of the jets where most of the mixing occurs. The influence of the heat release onto the wave front is considerably lessened, and the shock curvature is

largely determined by the free-stream Mach number fluctuations, shown in part c of the figure. In this particular instance, the detonation is reduced to shock-induced combustion.

To obtain these numerical results, a shock-capturing, unsteady Navier-Stokes code has been developed. The code is based on a second-order total variation diminishing (TVD) algorithm extended to multiple species, and includes Fickian as well as multicomponent species diffusion. It is coupled to the chemical kinetics via a time-accurate, predictor-corrector algorithm and the operator-splitting method. It has a multigrid capability and uses a grid-patching algorithm that is fully conservative. A three-dimensional version of the code has also been developed. In order to simulate in more detail the nonequilibrium phenomena associated with shock and flame interactions, a $k-\epsilon$ TVD code is also being developed.

(J. Cambier, Ext. 4283)

ORIGINAL PAGE
 COLOR PHOTOGRAPH

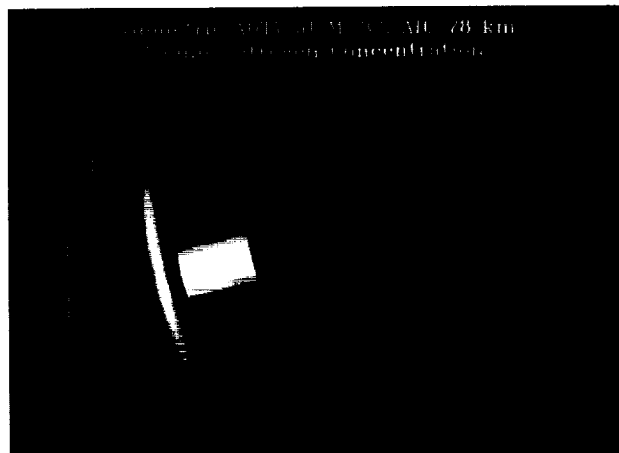
Computation of Nonequilibrium Hypersonic Flows

Several conceptual designs for vehicles that would fly in the atmosphere at hypersonic speeds have been developed. For the proposed flight conditions, the air in the shock layer that envelops the body is at a sufficiently high temperature to cause chemical reaction, vibrational excitation, and ionization. However, these processes occur at finite rates which, when coupled with large convection speeds, cause the gas to be removed from thermochemical equilibrium. This nonideal behavior affects the aerothermal loading on the vehicle and has ramifications in its design.

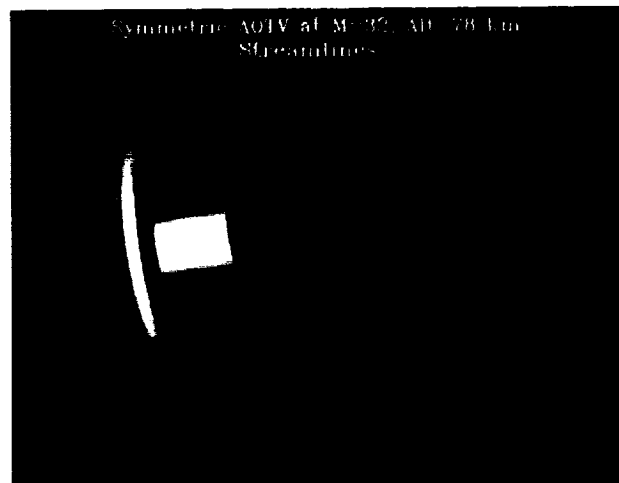
Air has been modeled with seven chemical species and its thermal state is characterized by six temperatures. The chemical species are diatomic and atomic oxygen and nitrogen, nitric oxide and its ion, and free electrons. The temperatures are a translational-rotational temperature, one vibrational temperature for each diatomic species, and an electron-electronic temperature. Mass is transferred between species according to finite-rate chemical reaction rates. The exchange of energy between energy modes is approximated with finite-rate models.

A numerical method to solve the fully coupled equation set that describes such a flow has been developed and computed results have been compared with experiment. It is a fully implicit algorithm and uses flux splitting to maintain stability in subsonic and supersonic regions. The method is two-dimensional or axisymmetric and includes all viscous terms, including binary mass diffusion.

The figures show a calculation of an axisymmetric aeroassisted orbital transfer vehicle (AOTV) at an altitude of 78 km and a speed of 9.0 km/sec. The first figure is a contour plot of the atomic nitrogen mass fraction in the flow field. The gas is highly reacted, with a maximum atomic nitrogen mass fraction of 0.68. Much of the wake is composed of atomic nitrogen because as the reacted gas expands around the shoulder of the body, the reactants



Contours of atomic nitrogen mass concentration in flow about an axisymmetric aeroassisted orbital transfer vehicle (color bar denotes local N mass concentration); $M_\infty = 32$ at 78 km altitude



Streamline tracings in flow about an axisymmetric aeroassisted orbital transfer vehicle; $M_\infty = 32$ at 78 km altitude

remain frozen in the flow because of the flow recombination rates. Thus, although the temperature is low, there are significant reaction products in the wake; this is a result of thermochemical nonequilibrium. The next plot shows the streamlines about the body, with the large recirculation region evident.

ORIGINAL PAGE
COLOR PHOTOGRAPH

This numerical method shows promise for application to recently proposed transatmospheric vehicles such as the AOTV, the National Aero-Space Plane, and the Mars mission vehicle. The physical model will be extended to include more ionic species and the effects of charge separation in highly ionized flows. The method also shows promise for extension to three dimensions.

(G. Candler, Ext. 4227)

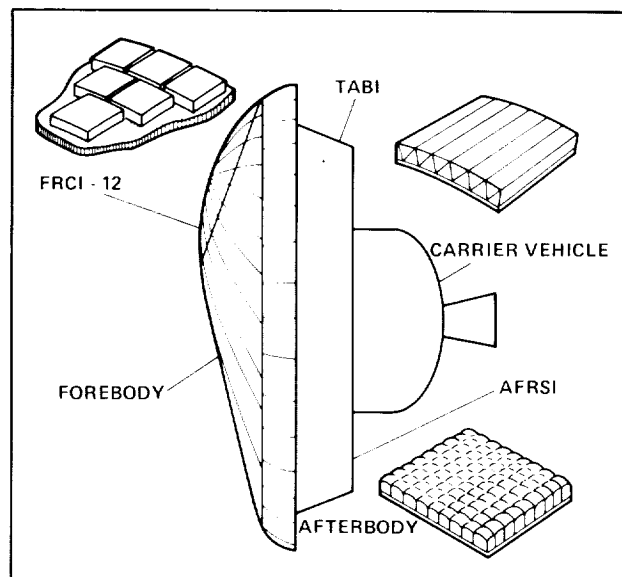
Aeroassist Flight Experiment to Use Ames-Developed Thermal-Protection Materials

An aerobraking orbital transfer vehicle aeroassist flight experiment (AFE) is planned by NASA for 1994. This experiment will contribute to the development of the technology necessary to build a reusable vehicle to carry payloads to geosynchronous orbit and return them to low Earth orbit using aerobraking to maximize payload mass fraction. Preliminary designs for both the aerobrake and carrier vehicle were produced during FY 1988 by Johnson Space Center (JSC) and Marshall Space Flight Center (MSFC), respectively. The thermal protection system used to protect the aerobrake during the aeropass is one of the most critical technologies required for the success of both the experiment and the design of an efficient, operational vehicle.

The thermal-protection system chosen for the AFE by JSC and MSFC, in consultation with Ames Research Center, consists primarily of materials developed by Ames. The forebody heat shield will be fibrous refractory composite insulation developed in the late 1970s by Ames and now manufactured by Lockheed Missiles & Space Co. The low heating ($<5 \text{ Btu/ft}^2\text{-sec}$) portions of the aerobrake afterbody and carrier vehicle will be protected by advanced flexible reusable surface insulation (AFRSI), which was developed by Ames with the Johns-Manville Corp. It is also used to protect most of the upper surface of the Space Shuttle orbiters. On those areas of the carrier vehicle where a flexible heat shield is needed with higher temperature capability than AFRSI, a newer material, being developed by

Ames with Woven Structures Inc., called tailorable advanced blanket insulation, is baselined. The figure shows the location of the heat shield components.

(H. Goldstein, Ext. 6103)



Thermal protection system for aeroassist flight experiment

Real-Gas Properties of Air and Air Plus Hydrogen Mixtures for Hypersonic Applications

Members of the Computational Chemistry Branch at Ames Research Center have been conducting an ongoing research project to compute selected properties of high-temperature gas mixtures such as those expected to be found in the shock layers surrounding both the National Aero-Space Plane (NASP) and the aeroassisted orbital transfer vehicle (AOTV). Calculated properties include molecular photoabsorption and photoemission cross sections, reaction rate constants, transport properties, and electron-impact cross sections. These basic chemical and physical data are needed as input to computational fluid dynamics calculations of the flow-field properties for these vehicles.

All the calculations have been carried out from first principles, using state-of-the-art quantum chemistry methods. Previous studies by members of the

Ames Computational Chemistry Branch have conclusively demonstrated that this approach can provide accurate reaction-rate constants and cross sections for conditions of temperature and pressure that are not amenable to experimental study.

Photoabsorption and photoemission cross sections have been determined for N_2 , NO, OH, N_2^+ , and O_2^+ . These calculations involve determining potential energy curves and electric dipole transition moments for each molecular band system. Reaction-rate constants have been computed for $N + O_2 \Rightarrow NO + O$, $O + N_2 \Rightarrow NO + N$ and $O + N + N$, and $H_2 + H_2 \Rightarrow H + H + H_2$. The latter process is an important three-body recombination reaction in the exhaust nozzle of the supersonic combustion ramjet (scramjet) engine of NASP. The transport properties computed to date are for atom-atom and atom-atomic ion collisions involving nitrogen and oxygen.

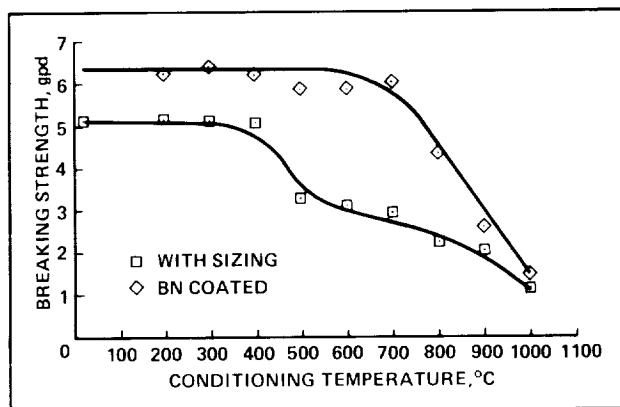
For the AOTV, the shock-layer temperatures will be high enough for limited ionization to occur. Previously, a first-principles theoretical study of the electron impact vibrational and electronic excitation of ground state N_2 had been carried out. During 1988, electron impact cross-section calculations were extended to include target molecules in excited electronic states. These cross sections are generally more than one order of magnitude larger than their ground-state counterparts. No measurements exist for any of these processes and yet they may control the ultimate degree of excitation or ionization in the AOTV shock layer.

As data are accumulated from these computational studies, they are recast in a suitable form for inclusion in the flow-field models and they are made available to others in the aerothermodynamics community.

(D. Cooper, Ext. 6213)

Boron Nitride Coatings for Silicon Carbide Fibers

Fibrous insulation blankets cover portions of the fuselage, wings, ailerons, and vertical stabilizers of the Space Shuttle orbiter. Similar flexible insulation blankets are being considered for use on other future space vehicles such as the aeroassisted orbital



Effect of temperature on breaking strength of SiC yarns

transfer vehicle (AOTV). However, postflight analysis on previous flights showed that some blankets were damaged. Analysis showed that this damage, which included missing or frayed fabric, was caused by aeroacoustic and aerodynamic effects. As a result, it is recommended that insulation fabrics which are more resistant to impact and aeroacoustic damage (especially at elevated temperatures) be used.

Silicon carbide (SiC) yarns and fabrics offer higher temperature capabilities and higher strength and modulus compared to the silicate fibers now used. These fibers retain considerable strength at elevated temperatures, as opposed to silicate fibers, which rapidly lose strength above about 700°C. Because SiC is a brittle material, it is very sensitive to flaws imparted during processing and use. Additionally, fiber degradation occurs not only from abrasion, but from the loss of material from reactions at elevated temperatures. To protect fiber yarns from degradation at elevated temperatures, it is necessary to coat the individual fibers with a material that provides resistance to abrasion. The commercially available fibers have a carbonaceous or polymeric coating or sizing to protect the surfaces from abrasion. However, this protective coating burns off at temperatures above 400°C, resulting in a significant degradation of the breaking strength of the yarn. In the accompanying figure, the breaking strength of the yarn is shown as a function of temperature in heated air. It can be seen in the curve labeled "with sizing" that there is a significant reduction in the strength of the yarn at 450°C.

A chemically vapor-deposited boron nitride (BN) coating enhances the mechanical properties of the SiC. As seen in the figure, the BN-coated yarn has initially higher breaking strength and retains its higher strength up to 900°C. The BN is deposited by chemical vapor deposition in a reducing atmosphere. The precursor used is diborane or a trichloroborazine compound. Deposition occurs at approximately 900°C and the coating thickness is approximately 1000-2000 Å. Because of the infiltration of the precursor gas, multifilament yarns can be coated with uniform coatings. The yarns can be coated continuously using a fiber-winding apparatus. The coated yarns will be used to weave fabrics for ultimate fabrication into insulation panels.

(D. Kourtides, Ext. 4784)

Fire-Resistant Composites for Aircraft Interiors

Aircraft interior sidewalls, ceiling panels, galley partitions, and other interior structures are being built primarily of composite panels with a face sheet consisting of epoxy resin and fiberglass. It has been demonstrated in the past, through laboratory and full-scale tests, that these materials emit large amounts of heat, toxic gases, and smoke when exposed to an interior in-flight or post-crash fire. The FAA recently

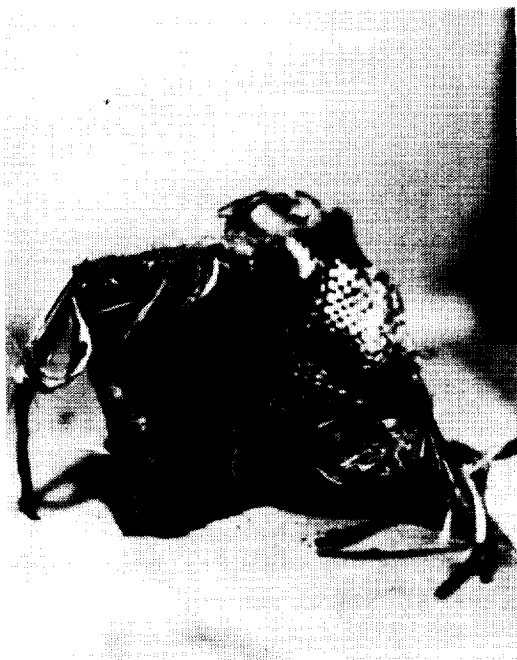
enacted regulations requiring that materials used in aircraft interiors meet a maximum heat-release rate and total heat release of 100 kW/m² and 100 kW-min/m², respectively. These values will drop to 65 kW/m² and 65 kW-min/m² in 1990.

A cooperative program between Ames Research Center and the FAA has resulted in the development of graphite, fiber-based composites which meet both the current and the future heat-release standards. These composites consist of a resin matrix of bis-maleimide/vinylpolystyrylpyrrole at a ratio of 65/35. The resin cures, using conventional curing equipment at 177°C, and is compatible with the curing schedule of epoxy and phenolic resins.

In the accompanying photograph, the two top composites are conventional epoxy-graphite composites shown after exposure to a heat flux of 3.5 W/cm². The left side is the front of the composite and the right side is the back. The composite was severely damaged and no structural integrity remained. In the bottom photographs the vinyl-polystyrylpyrrole/bismaleimide (VPSP/BMI) composites developed by Ames have been exposed to the identical heat flux. There was minimal structural damage to the composites and the heat-release rate was 51 kW/m², which meets the 1990 regulations. These composites are being evaluated for use in commercial transport aircraft and in the Ames DC-8 aircraft.

(D. Kourtides, Ext. 4784)

EPOXY/GRAPHITE, 3.5 W/CM²



FRONT



BACK

VPSP/BMI 3.5 W/CM²



FRONT



BACK

Epoxy/graphite and VPSP/BMI composites after exposure to 3.5 W/cm² heat flux

ORIGINAL PAGE
BLACK AND WHITE PHOTOGRAPH

Three-Dimensional Simulation of Flow About the Aeroassisted Flight Experiment Vehicle

The aeroassist flight experiment (AFE) vehicle will be deployed from the Space Shuttle, will pass through the Earth's atmosphere, and will be recovered by the Shuttle. Its purpose is to demonstrate the viability of aerobraking as a reentry technique and to provide data for the validation of real-gas computational fluid dynamic (CFD) codes, which can be used to design and analyze concepts for aeroassisted orbital transfer vehicles.

The design of the AFE vehicle and the experimental devices to be carried on it will depend upon numerical simulation of the flow about the body at flight conditions. Ballistic ranges and other experimental facilities cannot match the velocities the AFE will attain. Ballistic range data can be used to validate the gasdynamics of the CFD code. The code can, in turn, be extrapolated to simulate the flow field and predict the aerodynamic and aerothermodynamic loads encountered at flight conditions. Real-gas effects are important at flight conditions because of the high temperatures and pressures associated with hypersonic velocities.

A three-dimensional real-gas algorithm was developed and applied to the AFE configuration. Explicit differencing of the governing equations made the code robust and user-friendly. Real-gas effects



Three-dimensional flow simulation at conditions that reproduce ballistic range data (approximately 4 hours on the CRAY-2, 114,000 grid points)

are incorporated into the model by species conservation equations that include chemical source terms from finite rate reactions for dissociating and ionizing air. A unique way of coupling the chemistry to the gasdynamics allows flow solutions to be computed more efficiently than with other algorithms.

(G. Palmer, Ext. 4226)

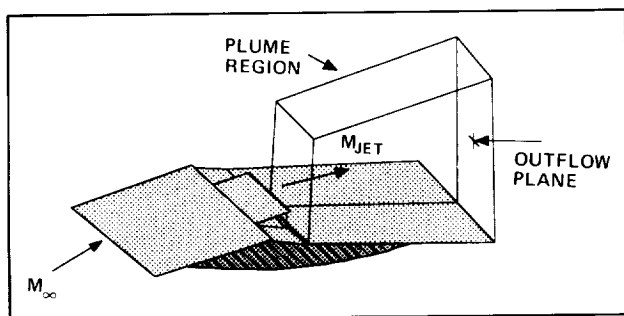
Computer Simulation of NASP Nozzle/Afterbody Flows

Three-dimensional (3-D) nozzle/plume flows are critical elements of the integrated propulsion systems of airbreathing transatmospheric vehicles such as the National Aero-Space Plane (NASP). These flow fields are highly interactive and geometrically complex, and contain regions of strong viscous/inviscid and viscous/viscous interactions. The interaction of the nozzle plume flow on the afterbody of the NASP strongly affects the vehicle's overall performance. A validated, accurate, and efficient computer code is needed to design and analyze potential NASP configurations.

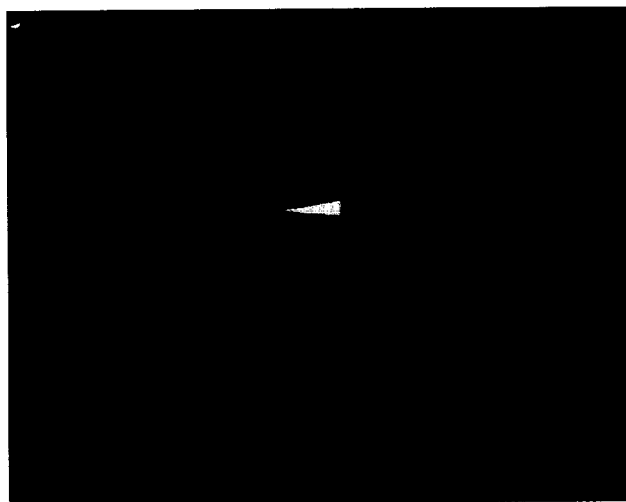
Significant advances have been made in developing a computer code, applicable to nozzle/afterbody flows, for predicting these flow fields. The 3-D nozzle code developed is an outgrowth of F3D, an implicit, perfect-gas Navier-Stokes solver that has been heavily modified to remedy problems encountered in shock capturing for these particular geometries. Patched and solution-adaptive grids are used to map the 3-D geometry and equilibrium real-gas chemistry has been incorporated into the solver.

Normally, appropriate experimental data for these types of flow fields are difficult to obtain. However, computed perfect-gas results from the 3-D nozzle code are being used to help design a nozzle/afterbody experiment to be conducted in Ames Research Center's 3.5-Foot Hypersonic Wind Tunnel. The experimental data will ultimately be used to validate the computer code.

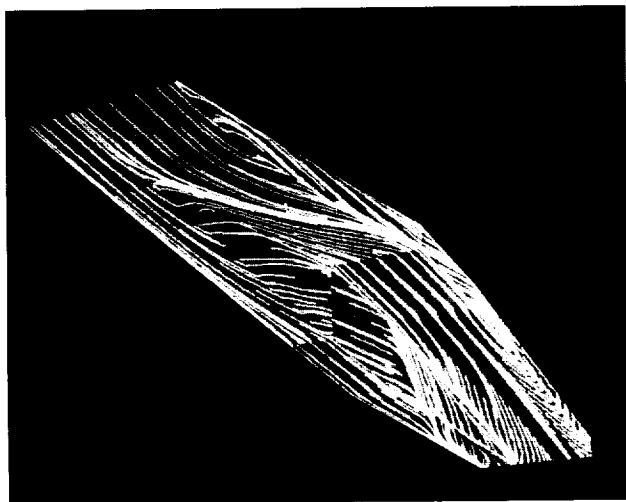
The experimental model consists of a rectangular slot nozzle with an angled afterbody ramp as shown in the first figure. Two-dimensional (2-D) symmetry plane calculations and 3-D calculations of the complete model geometry are being used to predict the plume flow field. Parametric studies of test



Schematic of NASP nozzle/afterbody experimental model



Computed Mach contours for NASP experiment



Simulated surface oil flow patterns for windward side of experimental model

conditions with free-stream Mach numbers from 5 to 14 and afterbody ramp angles from 0 to 20° have been computed. Mach contours in the symmetry plane and in the outflow plane at the end of the ramp are shown in the second figure. In the third figure predicted oil flow traces are shown for the underside of the model. These oil flow patterns show the complexity of the windward side flow which can "spill" over to the leeward side plume region.

The 2- and 3-D calculations aid design of the experiment in several ways. Calculations have helped determine afterbody ramp size (1) through parametric studies of M_∞ and ramp angle, (2) by predicting the location of free-stream pressure recovery, and (3) through static temperature predictions (static T must be less than air condensation temperature). The computed results were used to help predict model loads. The calculations have also helped to design model edge fences used to minimize spillage of the windward side flow onto the expanding plume region. Finally, the computed results have helped determine optimal locations for pressure probes and other instrumentation.

The 3-D nozzle code has demonstrated an ability to compute nozzle/afterbody flows for a variety of flow conditions and ramp angles and the code has been released to NASP researchers. After the experimental data are available, the final validated code will be a valuable design and analysis tool for the integrated propulsion systems of airbreathing hypersonic vehicles such as the NASP.

(S. Ruffin and E. Keener, Ext. 4210/5235)

Silicon Carbide Sewing Thread for a High-Temperature Thermal Protection System

Flexible ceramic insulation will be used on the aeroassist flight experiment (AFE) as part of the alternate thermal protection material experiment. In addition, the thermal protection system (TPS) for the avionics carrier panel will use a flexible ceramic insulation. For both cases, an integrally woven core

ORIGINAL PAGE
COLOR PHOTOGRAPH

of silicon carbide (SiC) yarn filled with either alumina or aluminoborosilicate insulation called tailorable advanced blanket insulation (TABI) will be the system used. This will require methods of sewing or stitching joints, closeouts, or blankets to fabricate the appropriate TPS article.

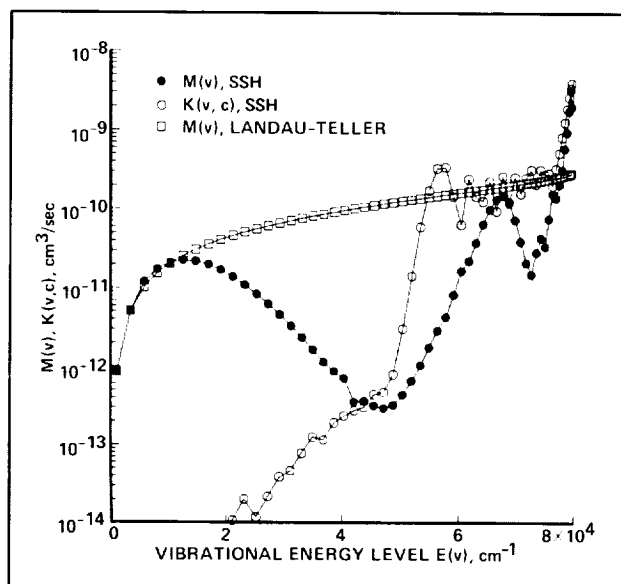
The objective was to determine the feasibility of developing a ceramic sewing thread using the same SiC yarn used in the TABI core structure. Two versions of this thread were prepared. One version used a polytetrafluoroethylene sizing coated over two twisted SiC yarns. The second version of SiC thread used a rayon service yarn over the SiC yarn followed by additional X-wrapping with Dacron. Both versions are able to be machine-sewn. A prototype 2- by 2-foot SiC blanket was prepared using each type of SiC sewing thread.

Because SiC yarns have already been shown to have high-temperature properties suitable for certain AFE-TPS applications, the use of these SiC threads could provide the methods of stitching or machine-sewing joints, edges, or holes required of these advanced TPS articles for such future vehicles as the aeroassisted orbital transfer vehicle or advanced launch systems.

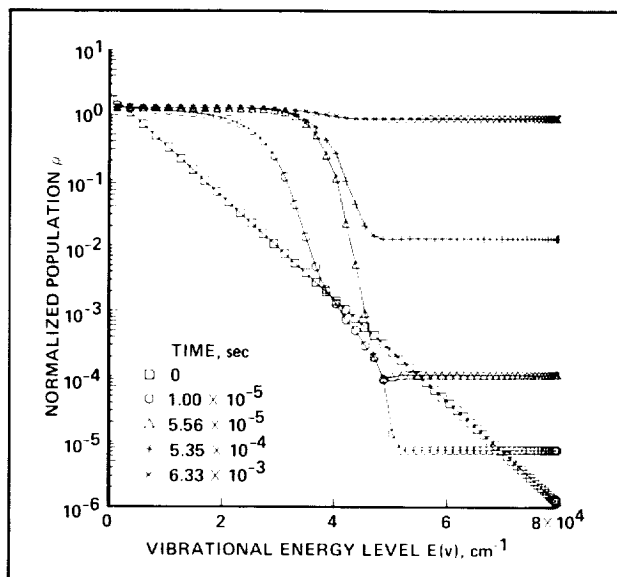
(P. Sawko, Ext. 6079)

VIBSSH: Approximate Quantum-Mechanical Calculation of Vibrational Relaxation

A method has been developed for calculating the approximate number densities of diatomic molecules in various vibrational levels during the nonequilibrium thermochemical relaxation process behind a shock wave or in an expanding flow. The number densities (populations) of various vibrational states in a molecule change during such a nonequilibrium flow because of the excitation, de-excitation, dissociation, and recombination processes caused by other colliding molecules or atoms. The colliding molecules themselves are at various different vibrational levels. Hence, the processes involve simultaneous transfers of vibrational and translational (and possibly rotational) energies between the two colliding molecules.



The overall vibrational transition rate coefficient $M(v)$ and the dissociation rate coefficient $K(v,c)$ for nitrogen at 4000 K



Number density of nitrogen molecules in various vibrational levels, normalized by their equilibrium values

The rate of transition of those molecules from one vibrational level to another is a sum of those caused by the collisions of molecules in various vibrational states. It is important to know how these processes

occur, because they dictate the rates of chemical reactions, and, thereby, the thermodynamic properties, in the flows around hypersonic objects.

In the first part of this work, the rate of transition of a particular vibrational state to another is calculated using a quantum-mechanical theory developed by Schwarz, Slawsky, and Herzfeld (SSH), which assumes that the transition process is characterized by the vibrational coordinates of the two colliding molecules only; that is, assuming that the rotational motion is irrelevant during the process. Although the general technique has been known for more than two decades, a comprehensive solution has never been obtained for any molecule because of existing limitations in computing capability. In the present work, a comprehensive solution has been obtained using the computing capability of CRAY computers, using a computer code named VIBSSH (Vibrational SSH-theory). The calculation was performed first for the nitrogen molecule under the assumption of zero rotational motion.

The first figure shows the result of such a calculation for nitrogen at 4000 K. In the figure, the abscissa shows the vibrational energy levels. The ordinate shows two quantities, $M(v)$ and $K(v,c)$. $M(v)$, shown with solid circles, is a weighted (by the square of the quantum jump involved) sum of the rates for all vibrational transitions out from a vibrational state, v , which is a measure of how fast a vibrational state is populated or depopulated. The calculated values are compared with the $M(v)$ values assumed in the so-called Landau-Teller model, which was used in most works. As we see here, the present method gives values considerably different from the Landau-Teller model. $K(v,c)$ is the rate of dissociation of the level v , which has never been calculated before.

These rate values are used to calculate the changes in the populations of various vibrational levels by integrating in time the rate equations describing the conservation of number density of each vibrational level. These equations, known as the master equation, are very stiff, and hence the calculation requires a computing machine of a high precision, such as CRAY, and considerable computing time.

In the second figure, a typical result of such a calculation is shown. Here, the ordinate is the number density of the molecules in various vibrational

levels, normalized by the values expected under thermodynamic equilibrium. The case is for the flow behind a normal shock wave in which the gas temperature is 8000 K. As seen here, the low vibrational levels reach equilibrium first, and then the equilibration process propagates to the high levels.

We plan to improve and extend this methodology to include rotational motion. When this is done, we should be in a position to predict from the first principles how the vibrational relaxation phenomenon affects the rates of chemical reactions in a high-temperature hypersonic flow.

(S. Sharma, Ext. 5235)

Real-Gas Experiments at Hypersonic Speeds

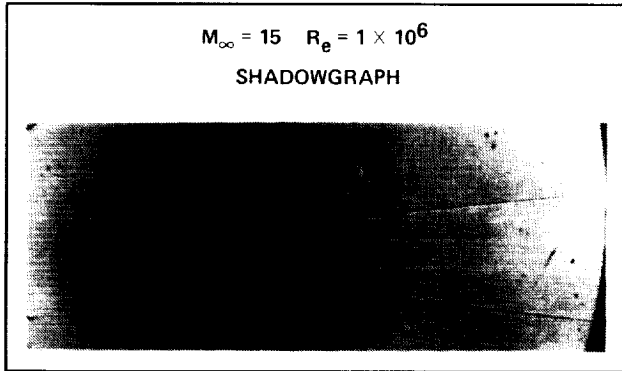
Experiments have been performed on sharp, slender cones in the Ames Research Center's Hypervelocity Free-Flight Aerodynamic Facility (HFFAF) in support of future hypervelocity vehicles, such as the National Aero-Space Plane (NASP). These experiments generate aerodynamic coefficients and shock shape data on models in the high-speed, high-altitude environment in which real-gas effects are important. The models, 5° half-angle cones with a tip radius 5% of the base radius, were launched at a velocity of 5 km/sec. The Reynolds number of the flow based on model length is 1×10^6 and the flow along the body is laminar.

A shadowgraph of the 5° cone in free flight in the HFFAF test section is shown in the first figure. The shock structure can be clearly seen in this figure. Model drag coefficient was determined using a more sophisticated data-reduction method than has previously been used. The results can be used to calibrate the physical models used in real-gas computer codes being developed at Ames. Calculations have shown that for the 5° cone at these conditions, 50% of the total drag is due to skin friction where real-gas effects will be felt.

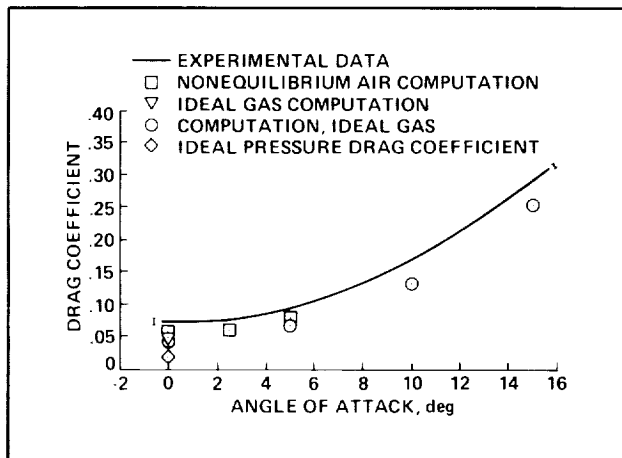
In the second figure, the drag results are compared with computational results obtained using both ideal-gas and nonequilibrium-air parabolized Navier-Stokes computer codes. The error in the experimental data is estimated to be $\pm 3\%$ and error bars

are provided in the figure. As shown, the ideal-gas computations fall below the nonequilibrium-air computations and all computations are lower than the experimental data. Experiments will be continued on other shapes and at other conditions where the effect of real-gas chemistry will be more obvious.

(A. Strawa, Ext. 3437)



5° half-angle cone, $M_\infty = 15$, $R_\theta = 1 \times 10^6$
shadowgraph



Experimental and computed drag coefficient versus angle of attack for 5° cone ($V_\infty = 5.03$ km/sec, $R_\theta = 1.0 \times 10^6$)

Mars Atmospheric Entry and Descent Using a High-Lift Vehicle

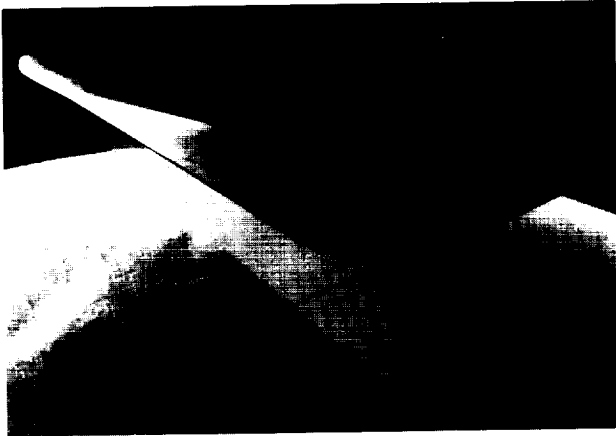
For the vehicle designed to land humans on Mars' surface, or to collect soil samples for return to Earth, a suitable landing site may be very important. The number of landing sites from which to choose can be increased and mission flexibility can be enhanced by using lifting vehicles, which can maneuver during atmospheric flight. High-lift vehicles have large longitudinal and lateral ranges. For example, a vehicle with a peak lift-to-drag (L/D) ratio of 2.3 would have a lateral range of 2500 km, making even the remote Martian polar regions accessible. Because the northern polar cap consists primarily of water ice, samples from the ice cap's edge may reveal indications of past biological activity. Lift can also be used to alleviate the deceleration loads and aerodynamic heating accompanying atmospheric entries, resulting in a benign environment for the crew and in lower structural and thermal protection weights.

The proposed vehicle configuration is illustrated in the figure. Aerodynamic characteristics were calculated, assuming a CO_2 atmosphere exists (the Martian atmosphere is 95.6% CO_2), and yielded a peak L/D ratio of 2.4. The vehicle would use atmospheric braking upon its arrival at Mars to decelerate from about 7 km/sec to a circular orbital speed of 3.5 km/sec. A gliding descent from orbit to the planet's surface will be made later. Maneuvering during the descent enables the vehicle to reach maximum lateral ranges up to 2500 km, while keeping the peak deceleration below 0.8 Earth gravity. It was also found that the atmospheric heating rates could be kept low enough to permit radiative cooling of the vehicle's surface. For example, during the descent from orbit, the peak stagnation point heating rate would be about 20 W/cm², resulting in an equi-

ORIGINAL PAGE
BLACK AND WHITE PHOTOGRAPH

librium wall temperature of under 1500 K. Therefore, the proposed vehicle configuration was found to be especially well suited for a manned Mars mission.

(M. Tauber, Ext. 6086)



Proposed high-lift vehicle configuration

Stagnation Streamline Reacting Flow Code Generalized for Any Gas Mixture

The stagnation streamline reacting flow (SPRAP) computer code has been extremely useful in estimating the nonequilibrium radiative heating of atmospheric entry vehicles such as the aeroassisted orbital transfer vehicle and aeroassist flight experiment (AFE). The code was originally written for only pure N_2 and a simulated air mixture of $0.79 N_2 + 0.21 O_2$. Past experience, however, with the planetary atmosphere experiments test program indicates that cyanogen (CN) is an important radiating species in the shock layer during Earth entry at high altitudes. This may be surprising as CO_2 , the source of the C in CN, is only 0.033% of the Earth's atmosphere.

SPRAP was rewritten recently to permit the introduction of any gas mixture, although the present data base of reactions, reaction rates, molecular properties, spectroscopic parameters, etc., is limited to those data involving N, O, Ar, and C.

The new program, called NONEQ, was used to estimate the radiative heating and optical spectrum emitted by the shock layer of the AFE along its flight trajectory. These calculations enabled the identification of the spectral features of importance to the AFE project and, in particular, the relative intensities of the N_2^+ and CN violet-band systems.

(E. Whiting, Ext. 4907)

ORIGINAL PAGE
BLACK AND WHITE PHOTOGRAPH

Space Research

Scientific Visualization of Geologic Data

U.S. Geological Survey (USGS) researchers are combining remote-sensing and image-processing technologies to investigate the scientific visualization of geologic and geographic data by computer-generated graphics and animation techniques. The results will lead to the development of tools that allow USGS scientists to view large quantities of data in multiple dimensions and thereby improve geologic analysis through visualization. The fields of image-processing and computer graphics are converging to provide the tools for interpreting data and for generating images from complex, multidimensional data sets.

USGS scientists have used computer graphics and animation techniques primarily to help illustrate geologic processes. Until recently these techniques were limited to the generation of single-frame, three-dimensional perspective views or crude black-and-white animations. These products were difficult to generate, relatively crude, and used simplified data layers. These limitations have hindered the use of visualization techniques for scientific analysis. Improved visualization will allow scientists to see previously unseen numerical information, and thereby gain insight into their data. Data represented visually will yield much more insight than data represented symbolically in computer printouts.

Scientists at the Menlo Park, CA, USGS who are studying volcanic processes are attempting to animate multidimensional seismic data to study a volcano's internal structure and the processes leading to volcanic eruptions. Researchers have created both two- and three-dimensional time series video sequences of seismic activity on the island of Hawaii. Shallow earthquake swarms and downrift migration patterns in response to magma movement are clearly seen. Major seismic zones are defined by a continually occurring background of seismicity and aftershocks. Earthquake patterns related to magma conduits, reservoirs, and buried rift-like structures are seen beneath Mauna Loa's summit caldera. Volume-rendering software was used to create a

three-dimensional, raster-image representation of the internal structure for the island of Hawaii.

Other investigations include the animation of shock-wave-deformation patterns along a fault rupture and the visualization of topographic structure derived from digital elevation data. Vector graphics techniques were used to animate the computed deformation patterns as wire frame models. The analysis of topographic structure in the study of landslide habitat will improve by visualization of the terrain using three-dimensional-terrain, stereoscopic, or shade-relief image rendering.

(W. Acevedo, Ext. 5299)

Pilot Land Data System (PLDS)

The Pilot Land Data System (PLDS) is a limited-scale, distributed-information system designed to explore scientific, technical, and management approaches to satisfy the needs of NASA's land science community both now and into the next century. The goal of the PLDS is to develop and implement a state-of-the-art data and information system to support research in the land-related sciences that will lead to a permanent research tool.

The PLDS is based on a distributed architecture that will use microcomputer workstations, supercomputers, and high-speed digital communications to form an operational capability with intelligent and useful services. From a local computer or terminal, an investigator can access a PLDS computer, conduct a complete search of the PLDS (and other) data holdings, and locate and possibly retrieve desirable data sets. Access to electronic mail, data analysis, a supercomputer, on-line help, and capabilities for file transfer are offered as additional services to scientists by the PLDS. The PLDS is managed by Goddard Space Flight Center, with Ames Research Center, Jet Propulsion Laboratory (JPL), and the university community participating.

The Ecosystem Science and Technology (ECOSAT) Branch at Ames is contributing to the development of the PLDS in the system-access and data-management areas. Ames is developing and implementing user-friendly procedures, simple access methods, electronic mail service, standard

protocols, and supporting documentation by which PLDS network users may access NASA facilities. In FY 1988, procedures and documentation to access selected supercomputers and data bases were developed and distributed. User-friendly menus which enable the use of PLDS resources were created and installed on all PLDS computers. By incorporating the input provided by each NASA center, a draft of the PLDS user's manual describing in detail the services of the PLDS was generated.

A data base of remotely sensed imagery collected by various instruments mounted on high- and medium-altitude aircraft based at Ames has been constructed and made available to land scientists via dial-up connection and national networks. Over 10,000 Daedalus TMS (Thematic Mapper Simulator), NS001 TMS, TMS (Thermal Infrared Multispectral Scanner), and aerial photographic images were inventoried on a MicroVAX at JPL using ORACLE data-base management software. A user's manual for the Ames Aircraft Data Base was written and distributed to interested scientists.

Future plans include the migration of the Ames Aircraft Data Base to a Sun4 computer in the Ecosystem Science and Technology Branch, the insertion of recent entries, and the production of an updated user's manual. In a possible joint effort with an ecosystem science project in the Branch, improved system-access capabilities (such as remote project computer connection, scientist communication, and efficient data transfer) may be developed. Services such as project data inventory with a user-friendly querying capability may also be provided. Development of all newly created capabilities will be coordinated with other PLDS nodes and will be offered to all scientists served by PLDS.

(G. Angelici, B. Phillips, and W. Likens,
Ext. 5947/3210)

Area Frame Development

The National Agricultural Statistics Service (NASS) of the U.S. Department of Agriculture and

the Ecosystem Science and Technology Branch (ECOSAT) of Ames Research Center have worked together for 10 years on integrating remote-sensing technology into the procedures used by NASS in its information-gathering activities. The latest manifestation of the cooperation between the two agencies is a NASS-sponsored research task at the Ecosystem Science and Technology (ECOSAT) Branch for developing software to create and edit area frames on a microprocessor-based workstation. A 3-year proposal was also awarded by NASA Headquarters starting in FY 1988 for additional hardware and personnel for the project.

An area frame is a construct used as a sampling vehicle for large-area surveys. It is compiled by dividing the area to be surveyed into contiguous parcels—each parcel being easily located on the ground and suitable for a sample-based survey. NASS uses area frames to select ground sample segments as part of a procedure for generating acreage estimates of agricultural commodities. The existing procedure to create and edit area frames is slow, labor-intensive, and sometimes inaccurate.

As an outgrowth of software development for the California Cooperative Remote Sensing Project in FY 1985 through FY 1987, ECOSAT proposed to NASS the possibility of performing the area frame functions with display software on a workstation. Prototype software for this computer-aided area frame procedure was completed and tested in FY 1988. Current efforts are directed toward completion and upgrading of the software and the implementation of an operational system.

Current configuration—A Sun 3/260 computer workstation was acquired in FY 1988 for the software development, and a color image display subsystem is being surveyed to interface with the workstation for the computer-aided procedure.

Future development—ECOSAT will add new functions to the software system and revise existing functions incorporated with NASS' requests. Additional peripheral devices, such as an optical disk drive and a scanner, are being considered to enhance the performance of the procedure.

(T. Cheng and R. Slye, Ext. 3326/6031)

Estimating Regional Methane Flux in Northern High-Latitude Ecosystems

The atmospheric concentrations of various trace gas constituents in the atmosphere have risen dramatically over the past century; very likely this has been in response to anthropogenic activities. To predict with confidence the effect of these increases on the Earth's climate and atmospheric chemistry, the present-day global budgets of these gases must be quantified in detail. Methane, one of the most chemically and radiatively active of these gases, participates in the chemistry of the troposphere and stratosphere and enhances the natural "greenhouse effect" that contributes to the Earth's energy balance. The atmospheric concentration of methane has increased over the past century in proportion to that of the human global population and is continuing to increase at a rate of about 1% per year.

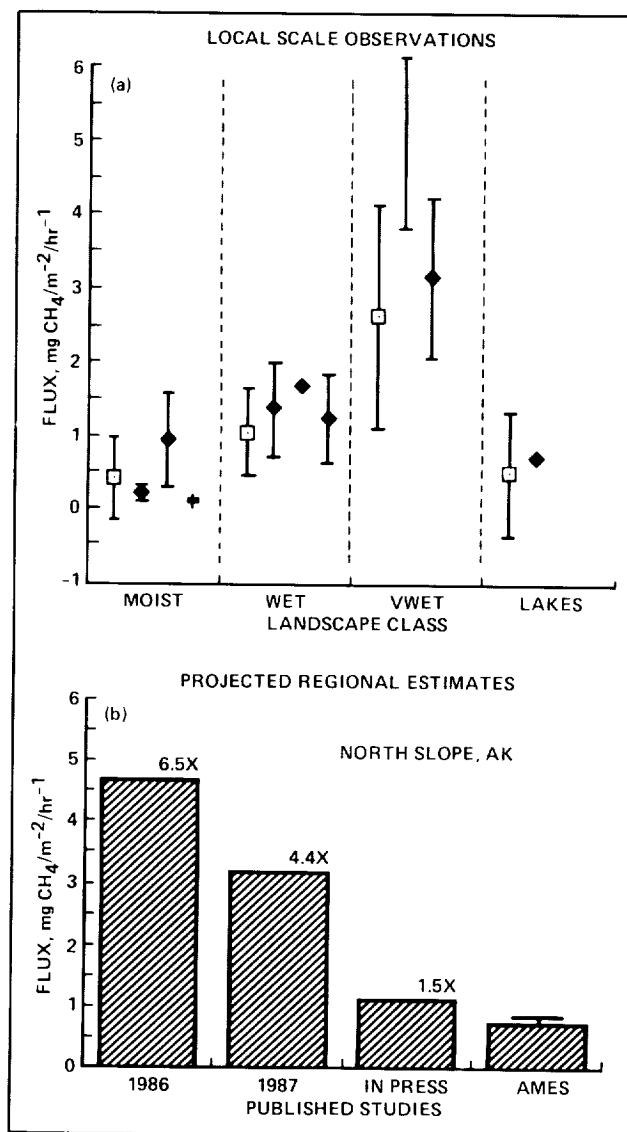
The need to understand both the natural and anthropogenic sources of methane is clear, although it is difficult because the sources are diverse, globally distributed, and very poorly quantified. The major natural source is most likely bacterial decomposition in wet, carbon-rich soils, such as the soils found in the northern high-latitude tundra (treeless wetlands) and taiga (forest) ecosystems. These ecosystems are of particular importance because of their extensive areal coverage and because of the vast carbon resources stored in these currently frozen soils that would become available for decomposition should a climatic warming be realized. The major obstacle to understanding these ecosystems has been the lack of information on their complexity and variability over space and time.

Within the Ecosystem Science and Technology Branch at Ames Research Center, a project is under way to quantitatively estimate the regional and seasonal methane flux from northern tundra and taiga ecosystems. The initial regions of study are the Arctic North Slope and the Tanana River Valley of Alaska.

The approach taken integrates surface and remote-sensing observations, by using the stratified sampling theory, to yield estimates of the aggregated flux of methane and its associated variance at the regional level. Surface observations of methane emissions, made in relation to local hydrological and

vegetation features, are scaled upward to landscape stratifications derived from data from the 80-m Landsat Multispectral Scanner and the multitemporal, 1-km, Advanced Very High Resolution Radiometer satellite.

Results to date in the Arctic tundra have demonstrated that rates of methane emissions, and the bio-



Comparison of observations and estimates of methane flux. (a) A comparison of observations of local scale methane flux for Arctic and subarctic wetlands. Data have been grouped by soil moisture and site descriptions provided in the literature. (b) A comparison of estimates of methane flux for the North Slope of Alaska using published regional estimation approaches

logical and physical processes controlling those emissions, can be effectively stratified both spatially and seasonally by using satellite-borne multispectral observations. The results confirm that wet tundra ecosystems are seasonally important to the global methane budget. However, although local emission rates are similar to independently published results, regional estimates for Alaskan study sites based upon the satellite stratifications are significantly lower than published results (see figure).

The need for incorporating remote sensing into regional ecosystems studies has been clearly identified, and the results suggest that current natural methane emission estimates for northern ecosystems on the global scale may be seriously biased because of inaccurate stratifications and areal estimates for these ecosystems.

(G. Livingston and L. Morrissey, Ext. 3617/6184)

Fast Airborne Gas Sensor

A new airborne instrument for fast, atmospheric trace-gas measurements has been developed and used in several field studies. This new sensor, the Airborne Tunable Laser Absorption Spectrometer (ATLAS) uses tunable solid-state lasers and other advanced electro-optical technology to provide in situ gas measurements at rates as fast as 1 Hz. ATLAS has been used to measure atmospheric CO and N₂O at altitudes of up to 21 km, and is capable of making CH₄ measurements as well. The ATLAS instrument is deployed on the NASA ER-2 high-altitude research aircraft, along with a suite of instruments designed to address specific key questions concerning the atmosphere.

In January 1987, ATLAS made CO measurements as a part of the Stratosphere-Troposphere Exchange Project deployed to Darwin, Australia. In Austral spring 1987 (August-September) the Antarctic ozone hole study was carried out from Punta Arenas, Chile. ATLAS took part in this study, measuring N₂O, as a dynamical tracer, on a dozen flights into the south polar vortex. The resulting data provide important new information about mean vertical motions within the polar vortex.

In an ongoing NASA program to study perturbed polar-winter atmospheric chemistry, ATLAS will take

part in a field trip to the Arctic to be deployed to Stavanger, Norway, in January 1989.

Several extensions of current ATLAS technology are being studied: First, extending the technique to higher sensitivity would allow us to measure less abundant, but still important, atmospheric trace gases such as HNO₃. Second, increasing the instrument sampling rate to 10-20 Hz would make this technique available for gas flux measurements in the atmospheric boundary layer to study bio-sources of gases such as CH₄ and N₂O.

(M. Loewenstein, Ext. 5504)

Trace-Gas Flux, Canopy Chemistry, and Remote Sensing in Coniferous Ecosystems

Many ecosystems around the world are now receiving anthropogenic inputs of nutrient elements such as nitrogen and sulfur as a result of acid deposition. Because greater nitrogen inputs and greater amounts of nitrogen are cycling within these systems, it is possible that they will also have increased losses of elements as trace gases, with potential effects on global atmospheric processes. A forest fertilization experiment is used to examine the degree to which nutrient turnover within ecosystems is reflected in trace-gas outputs and biochemical characteristics of the vegetation foliage.

Results show clearly that forests receiving inputs of fertilizer nitrogen respond with higher nitrogen turnover rates in the soil, and with three-fold increases in nitrous oxide flux during the wet part of the growing season. These forests have distinct foliar biochemical characteristics (higher concentrations of total nitrogen, chlorophyll, and amino acid, and lower concentrations of nonstructural carbohydrate and lignin than in the nonfertilized sites).

Remote sensing of these canopy characteristics would provide a key to estimating nutrient cycling and trace-gas fluxes over larger areas. Experimental remote-sensing techniques have been studied by using these sites. The results from this component of the research indicates that nitrogen and lignin foliar concentrations are significantly correlated to high-spectral-resolution reflectance data acquired

with the Airborne Imaging Spectrometer (an experimental sensor flown aboard the Ames C130 research aircraft). These results suggest that high-spectral-resolution remote-sensing data hold the potential for use in predicting ecosystem trace-gas flux.

(P. Matson, N. Swanberg, and T. Billow,
Ext. 6884/5896/3223)

Nitrous Oxide Flux from Tropical Forest Ecosystems

Understanding the sources and sinks of trace gases in the Earth's atmosphere, and the effects of human-induced change on them, is necessary for predictions of long-term climate change and the effect of anthropogenic changes on global habitability. Considerable evidence exists suggesting that tropical ecosystems, now undergoing very rapid change, are particularly important sources of many trace gases. The role of tropical forests in global energy and element cycling, and the extent to which land conversion will affect that role, is being examined as a component of the Biospheric Research Program, Earth Sciences Division, at Ames Research Center.

Nitrous oxide is one of several biogenic trace gases having important atmospheric roles whose atmospheric concentrations are increasing. To understand the role of tropical ecosystems in this flux, nitrous oxide flux and the nitrogen cycling processes that control flux have been measured across a range of tropical forests. Results have suggested a flux of 2.65 teragrams/year from humid tropical forests, a value considerably lower than is estimated in other tropical budgets, but still more than any other natural source. Not included in this estimate, or any others, is the contribution of nitrous oxide resulting from land clearing and conversion to pasture.

Studies of fluxes from several pastures in Amazonia have shown up to five-fold increases in flux from pastures compared to flux from intact forests. If this relationship is representative of other areas of the tropics, nearly one-half the measured increase in atmospheric nitrous oxide concentrations

can be accounted for by the conversion of tropical forests into pastures.

(P. Matson and G. Livingston, Ext. 6884/5896)

Biogeochemical Cycling in Terrestrial Ecosystems

In 1987-88, the first research to investigate the role of canopy biochemical properties in ecosystem behavior and in radiative reflectance was concluded, and it produced a number of significant accomplishments. Three years of intensive effort had led to several major findings. The lignin content of deciduous and coniferous forest canopies in Wisconsin could be statistically estimated by regression analysis of Airborne Imaging Spectrometer (AIS) data. Both the nitrogen and lignin content of coniferous forests in Oregon could also be estimated in this way. In related studies, the near-infrared reflectance spectra of foliar samples could be used, after calibration, to predict the concentrations of many biochemical components of the foliage. Many new analytical techniques were developed, or adapted from other research methods, to achieve these results. This is the first time such findings have been made in remote-sensing science, and they represent a major advance in the remote sensing of key biological parameters.

Lignin content is inversely related to nitrogen release from decomposing litter. Thus, the lignin prediction from AIS data leads to the mapping by inversion of nitrogen mineralization or release. A mineralization map for Blackhawk Island, WI, is the first instance of using remote sensing to estimate this key ecosystem property related to the fertility of the soil.

A unique method to estimate the signal to noise (S/N) performance of high-spectral-resolution (Airborne Visible/Infrared Imaging Spectrometer (AVIRIS)) data was developed by using geostatistical principles. This new technique has many advantages because it does not require a uniform spectrally flat target, can be applied to data from any site, and uses the actual data values. It was applied to forested site data from Florida and Oregon; to urban

and water data from Mountain View, CA; and to mineralogic data from Nevada. The results indicate that S/N performance of AVIRIS data acquired from the aircraft can be significantly lower than bench tests, flat-field tests, and other S/N techniques. Also, the results are target-dependent, indicating which spectral zones are likely to be useful for further analyses.

In 1987 the controls exerted by nutrient cycling and climate carbon exchange processes were mathematically incorporated in a new ecosystem simulation model, and the plant-climate aspects of the model were evaluated. Test areas as diverse as boreal taiga forests (Fairbanks) and subtropical humid pine (Florida), for example, were investigated.

In 1988, research was conducted on a fine scale by using digital terrain data to partition forested landscape into hydrologically and ecologically meaningful units, principally "hillslopes." The technique automatically determines the stream network, and the associated drainage divides for each stream link, thus forming irregular polygons. In a digital data base containing ecological and environmental parameters, the minimum area or stream order can be selected and used to aggregate data from these polygons. Statistical tests show that for this fluvial terrain, the within-partition variance is reduced while the between-partition variance is increased for remote sensing data when compared to simple rectangular grids of equal size.

Investigations of canopy chemistry and nutrient cycling continued in 1988. Research was carried out on a tropical forest on the island of Hawaii. Collaborative research is under way for forests treated by fertilization at sites in Florida and in Massachusetts, the latter to simulate the effects of chronic nitrogen deposition in acid rain. AVIRIS data acquisition could not be conducted in 1988 but will be in 1989.

At the same time, research is under way to establish the biophysical basis for the spectral results. Some initial success was achieved in 1988, with the analysis of about 100 leaf spectra which produce reasonable absorption characteristics of compounds such as lignin, cellulose, and sugar. Further attempts to analyze the spectra of recently cut, intact, and stacked whole deciduous leaves were unsuccessful because of spectral degradation of the samples (they aged quickly before measurement). Research was begun to perfect measurements of fresh, whole leaves of amaranth grown in green-

houses, to derive optical constants related to scattering for these leaves, and to analyze single leaf-reflectance spectra in relation to their chemical composition.

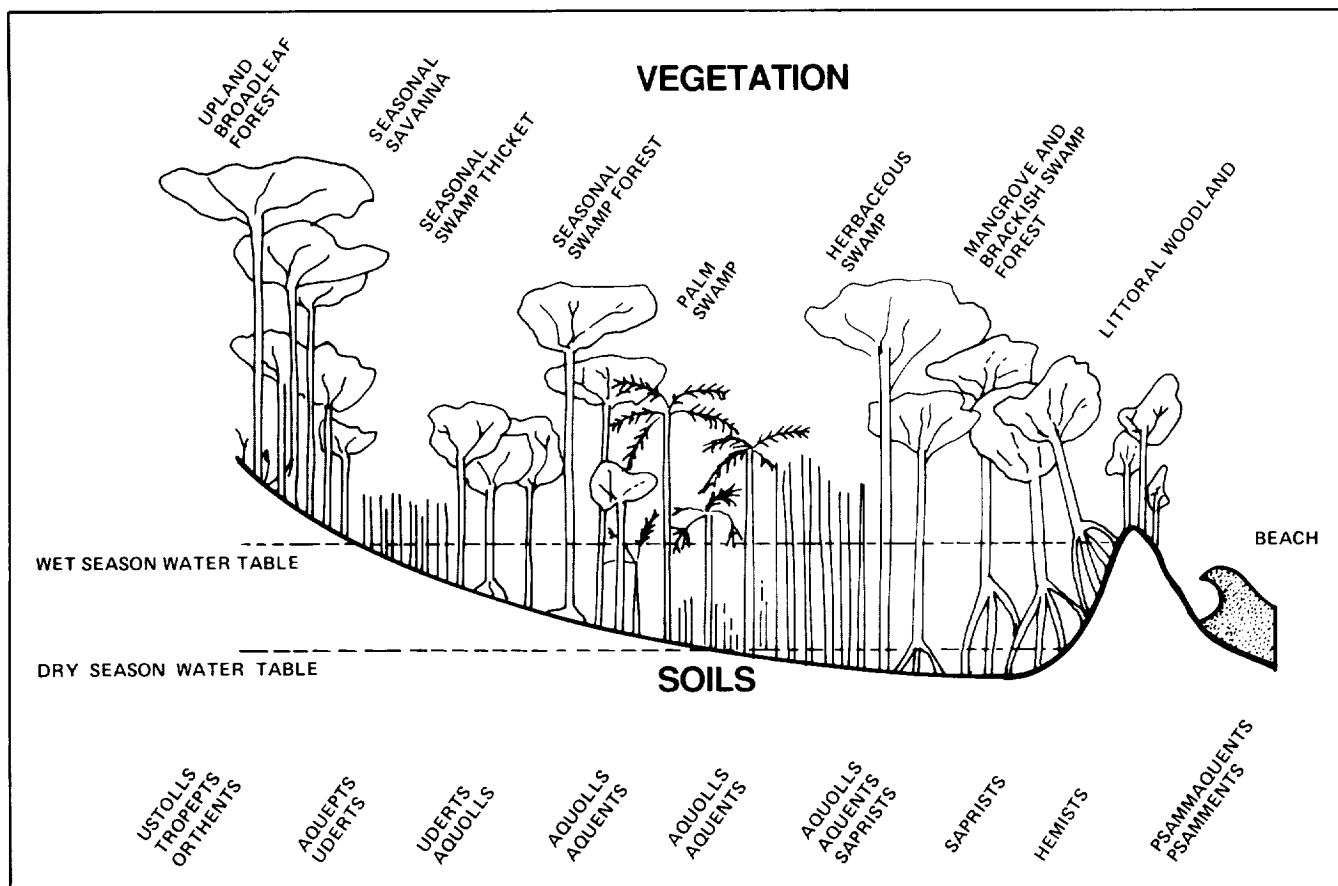
(D. Peterson, Ext. 5899)

Tropical Wetland Ecosystem Dynamics

Tropical wetlands research in the Ecosystem Science and Technology Branch at Ames Research Center focused on the use of spaceborne sensors to study short- and long-term hydrological changes and ancient Maya agriculture in the Yucatan Peninsula of southern Mexico and northern Central America. Wet season imagery on Sea Satellite (Seasat) Synthetic Aperture Radar (SAR) was used to identify areas of flooded vegetation by the high backscatter produced by L-band, HH-polarized microwave interactions between the vegetation and flooded surfaces. Seasonal changes in inundation beneath tropical forest canopies in Guatemala were detected in multitemporal Seasat SAR data sets by tracking spatial changes in areas with enhanced backscatter caused by flooding.

Landsat Thematic Mapper (TM) imagery of the study area was used to investigate wetland hydrology and to differentiate wetland vegetation types, as shown in the first figure. Marsh, savanna, semideciduous swamp forest, mangrove forest, and upland semievergreen forests were differentiated on false-color composite images of TM bands 5, 4, and 3. These images were enhanced by linear mapping of the contrast and intensity of each band for maximum discrimination of vegetation types.

Discrimination was possible largely because these plant communities contained significant differences in green leaf area, woody and dead biomass, and surface water, all of which have different reflectance characteristics in TM bands 5, 4, and 3. Remote-sensing interpretations were verified through comparisons with vegetation maps and field reconnaissance. Differences in reflectance between the infrared TM bands 5 and 4 and the visible bands 3 and 2 were examined in linear mapped false-color composite images. These images were used to dif-



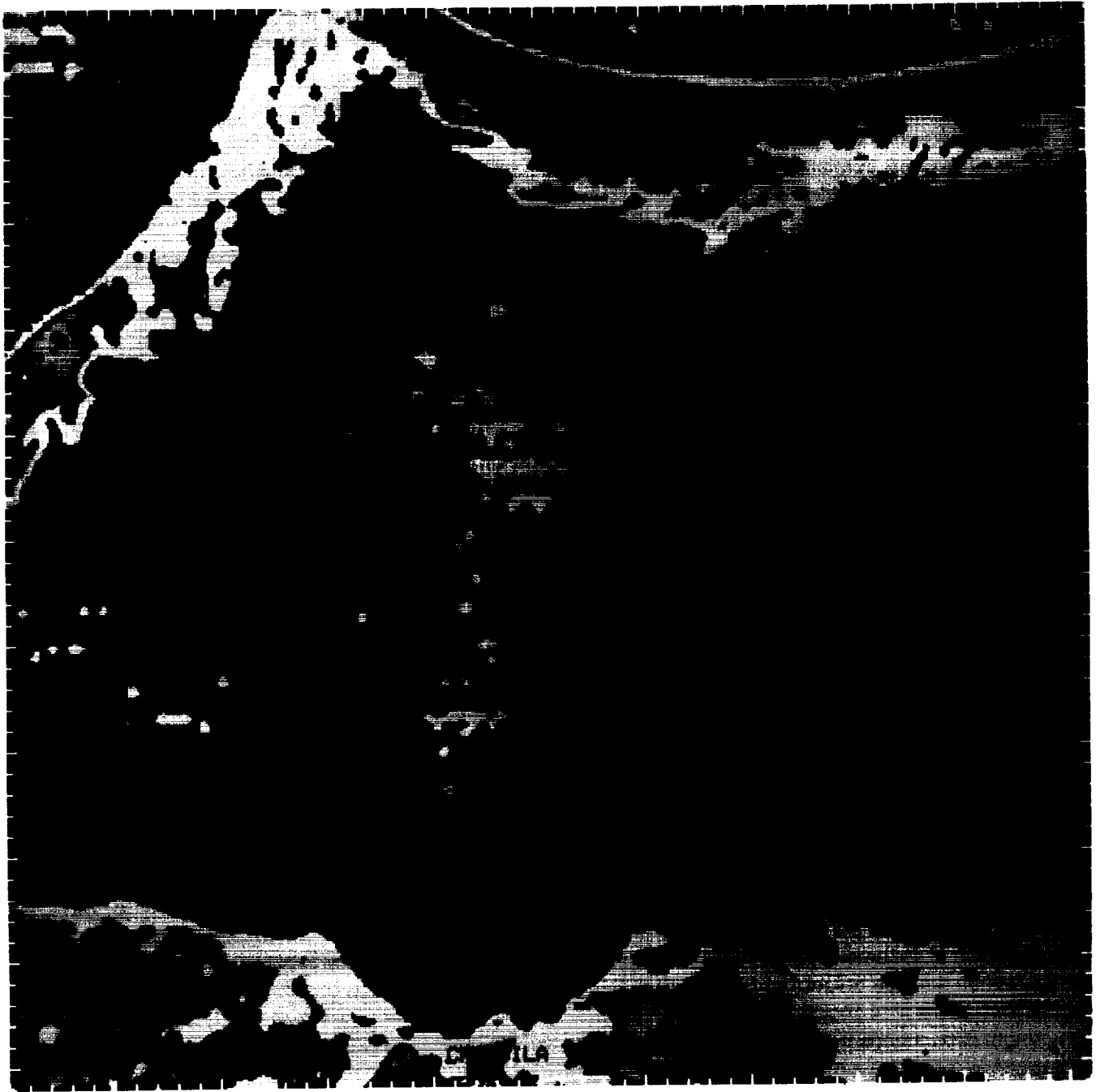
Tropical wetland ecosystems

ferentiate between dry and flooded surfaces, based on the much higher reflectance of water in the visible compared to the infrared part of the spectrum.

Large, ancient Mayan canals were mapped from Seasat SAR and TM imagery in northern Belize, southern Quintana Roo, Mexico, and along the upper Candelaria River in Campeche, Mexico. The TM imagery was found to be superior to the Seasat SAR for mapping ancient canals, but it lacked the spatial resolution for detecting small canals that are visible on color infrared photographs taken with low-flying aircraft. Large canal systems were found only in wetlands where the water table is perennially at or near the surface. Wetlands that undergo severe desiccation in the dry season do not contain canals, probably because the hydrology of these wetlands could not be controlled by the ancient Maya.

Thermal emission data from TM band 6 was used to map the distribution of thermal anomalies related to coastal freshwater springs along the north coast of the Yucatan Peninsula, as shown in the last figure. These springs were correlated with groundwater flow patterns interpreted from the distribution of solution features mapped from the false-color composite TM images described above. Comparison of wet- and dry-season imagery indicates that spring activity greatly increases in the wet season, suggesting rapid response of groundwater flows to seasonal rains.

(K. Pope and C. Duller, Ext. 5149/6031)



Landsat TM thermal infrared image of Conil Lagoon, northeastern Yucatan Peninsula. The freshwater springs appear as cold anomalies (black) along the coast in the warm salt water of the lagoon (blue)

ORIGINAL PAGE
COLOR PHOTOGRAPH

Atmospheric Optical Depths: Background Aerosols, Smokes, and Clouds

Adequate space and time averages of the optical properties of smokes, in relation to those of background aerosols and of natural clouds, are needed to assess the climatic implications of large-scale fires. One relevant measurement is the spectral optical depth, a measure of the degree by which the Sun's light rays are attenuated in the atmosphere by the combined effects of scattering and absorption by particles and gases. The Ames Research Center six-wavelength airborne autotracking sunphotometer was used over the past 3 years to measure atmospheric spectral optical depths in various climatic regimes. Results are as follows:

1. Langley-plot analyses of ground-based measurements taken at Mauna Loa Observatory, Hawaii, during a 10-day period exhibited variabilities in zero-airmass intercept voltages which were equivalent to instrument accuracy of 0.5%.

2. The optical depths of background aerosols varied between 0.001 and 0.1, depending on the wavelength of the sunlight and on geographic location. The Angstrom coefficient, a measure of the wavelength dependence of optical depth, varied between 0.75 and 2.5 as it was affected by both the presence of pollutants and the relative humidity to which the aerosol was exposed.

3. Smoke aerosols yielded optical depths that varied between 0.01 and 3.0. The spectral characteristics of these optical depths depended on the residence time of the smoke particles in the atmosphere and on the type of fuel that fed the fires. Smoke from forest fires showed a much steeper wavelength dependence than did natural hazes. Smokes therefore have a much higher potential to cool the Earth's surface than do background atmospheric aerosols of equivalent optical depths at a 1- μm wavelength.

4. Natural stratocumulus and cirrus clouds exhibited optical depths between 1 and 5, with neutral wavelength dependencies.

(R. Pueschel, Ext. 5254)

Condensed Nitrate, Sulfate, and Chloride in Antarctic Stratospheric Aerosols

It has been theorized that nitric acid condenses in the winter polar stratosphere to become an important component of polar stratospheric clouds. The removal of HNO_3 from the vapor phase, and its subsequent depletion from the stratosphere by sedimentation, may affect the polar ozone budget. The removal of NO_y from the gas phase inhibits the formation of ClNO_3 , resulting in a higher Cl_x concentration that will react with O_3 .

During the 1987 Airborne Antarctic Ozone Experiment, we estimated the NO_3 , the Cl and the SO_4 content of stratospheric aerosols by testing for the presence of condensed nitric, sulfuric, and hydrochloric acids. At various segments of the ER-2 research aircraft sample flights, aerosol particles were impacted on four 500- μm -diameter gold wires that were strung across a number of aluminum rings. The wires were pretreated to give results specific to certain physical and chemical aerosol properties.

One wire was carbon-coated, and was used for aerosol concentration and size analyses by scanning electron microscopy; the additional detection of S and Cl in individual particles was permitted by X-ray-energy-dispersive analyses. Three more wires were coated with nitron, barium chloride, and silver nitrate to detect, respectively, nitric, sulfuric, and hydrochloric acids in the aerosols. Wires were exposed at a number of locations and altitudes near 18 km. Immediately after collection, the acids were fixed as ammonium salts by exposing them in flight to NH_3 .

Results show that condensed nitrate was confined to latitudes south of 64° ; the atmosphere had to be colder than 200 K in order to find nitrate in particles. The negative correlation found between condensed nitrate and ozone concentrations is consistent with theories that postulate removal of gas-phase NO_y as a necessary step in allowing active chlorine-ozone reactions to occur. Condensed H_2SO_4 was present at concentrations between 0.1 and 0.9 parts/billion by mass, independent of the presence or absence of polar stratospheric clouds. The mass of condensed HCl was estimated to be approximately 3% of the mass of sulfuric acid.

(R. Pueschel, Ext. 5254)

Biospheric Monitoring and Vector-Borne Disease Prediction

Globally, more than 250 million humans suffer from malaria, and its occurrence is increasing in many regions. The World Health Organization (WHO) reports that the global malaria situation has deteriorated over the past 15 years. Factors influencing the current situation include reduced funding and manpower for control activities, increased resistance of the anopheline vector to insecticides, and development of drug-resistant forms of the *Plasmodium* parasite. Under these conditions, near-real-time data on the temporal and spatial dynamics of the vector populations are required for directing effective control measures.

NASA, with the assistance of world health agencies, has designed a phased multiyear research program to determine the feasibility of using remote sensing and related data-handling technologies to identify, monitor, and model the relationship between malaria vectors and their environment.

The first phase of this research was initiated in rice-growing areas of northern California. Rice fields are prime breeding habitats for *Anopheles freeborni*, the western malaria vector, and have been the subject of intensive study for the past 25 years. The density of mosquito breeding in rice fields has been shown to vary significantly from field to field, with a few fields often responsible for a large proportion of the mosquito production.

In 1985, a cooperative NASA/University of California study investigated the possibility of using remotely sensed data to monitor environmental parameters associated with the mosquito breeding habitat. In the results, *Anopheles freeborni* larval abundance appeared to be associated with specific vegetational characteristics of rice fields, and was correlated with spectral data acquired in June. Differences in plant biomass and rice phenology among fields, as monitored with spectral data, indicated that those fields supporting few mosquito larvae tended to develop more slowly than those with many larvae.

This suggested that differences in vegetational characteristics, identified and tracked with remote sensing during early-season rice development, might

provide the basis to predict larval mosquito production before its peak in late summer. These results encouraged a more comprehensive study in 1987.

In California's Sacramento Valley, 104 rice fields were surveyed for vegetation development and mosquito production between May and September 1987. Simultaneously, remote-sensing data were acquired from aircraft and satellite platforms. The results of the 1987 study were consistent with those from 1985: fields that developed early tended to have higher *A. freeborni* larval populations.

Of the 104 fields studied, 16 fields accounted for 50%, 36 fields accounted for 75%, and 52 fields accounted for 86% of the total seasonal mosquito production. Reflectance data were used to calculate a statistical function (canonical discriminant) to identify fields that were above and below a threshold of 0.09 larvae per dip, averaged over 10 weeks. Results showed that 52 fields were above, and 52 fields were below this threshold. In May and June, the accuracy of the discriminant function to identify the high-mosquito-producing fields was between 73 and 81%. The highest accuracy was on May 20, more than 2 months before peak mosquito production.

Work has been initiated on the second phase of this research in Chiapas, Mexico, where malaria transmission is a serious problem. In Chiapas, two mosquito species are responsible for malaria transmission: *A. albimanus* in the coastal plain and *A. psuedopunctipennis* in the foothills. The distribution and abundance of breeding habitats for these species are dependent on temporal and spatial changes in such environmental parameters as temperature and rainfall.

Preliminary analysis of Land Satellite Thematic Mapper data, acquired during the wet and dry seasons, indicates that the data can be used to characterize and monitor temporal and spatial changes in breeding habitat. Data on breeding habitats subsequently will be integrated with data on meteorology, hydrology, land use, and settlement patterns to develop a model to predict areas of potential malaria transmission.

(P. Sebesta and B. Wood, Ext. 5232/3326)

Remote Sensing of Biogeochemical Cycling Indexes of Western Coniferous Forests

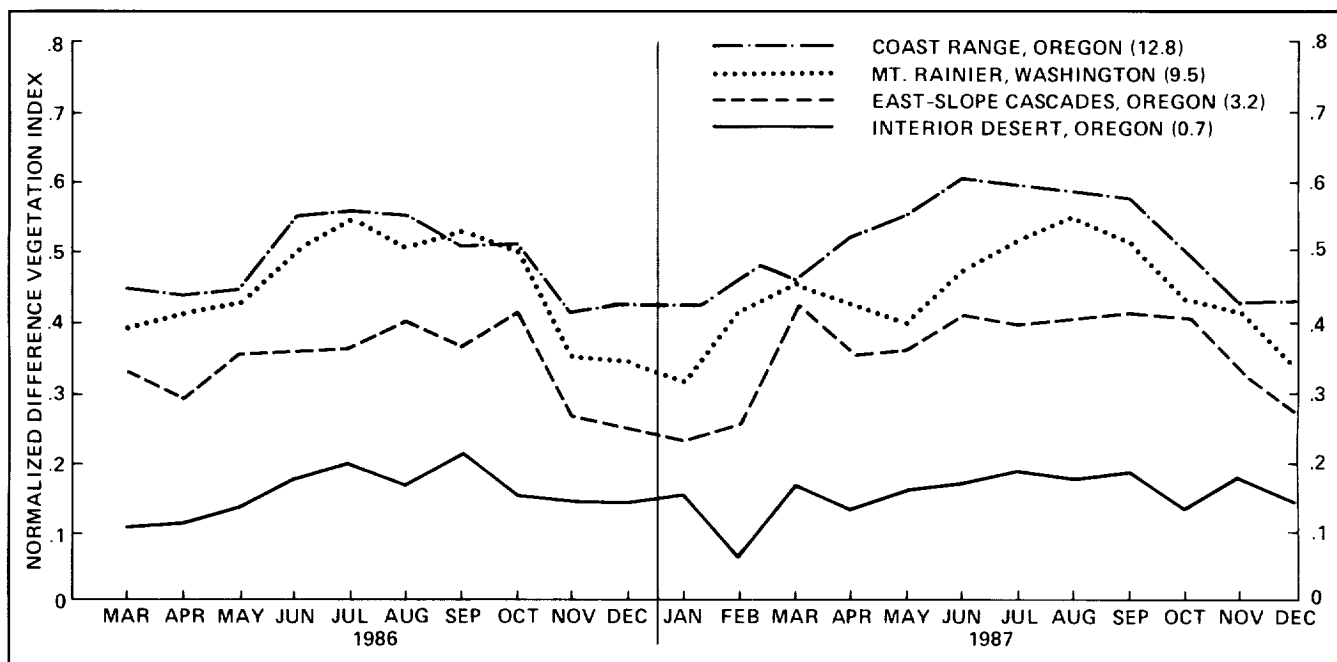
Coniferous forests occupy approximately one-third of the land area of the western United States. An important parameter of vegetation is the leaf area index (LAI), the projected leaf surface area per unit of ground area. The LAI of conifers is functionally related to the exchange of carbon dioxide, water, and oxygen, and is valuable in estimating the rate of canopy photosynthesis and evapotranspiration. In coniferous forests of the Pacific Northwest, the LAI has been shown to be linearly related to site water balance and net primary production.

One objective of this research is to analyze the relationship between the LAI of coniferous forests and the data acquired by the Advanced Very High Resolution Radiometer (AVHRR) on the National Oceanic and Atmospheric Administration-9 satellite to determine the spatial distribution of the LAI of coniferous forests in the western United States. The relationship between the AVHRR normalized difference vegetation index (NDVI) and the LAI of about 20 coniferous forest stands in Oregon, California,

Montana, and Washington was analyzed in the following manner. All cloud-free 1.1-km spatial resolution AVHRR scenes of the western United States were acquired, and the NDVI for each of the study sites was calculated. The highest NDVI for each site from each month was determined, and a composite data set of monthly maximum values was generated. These values have been calculated from March 1986 to December 1987.

Overall, there is good agreement between the LAI and the monthly maximum-value composites generated from the AVHRR data. The coefficients of determination range from approximately 0.50 to 0.80, with the strongest relationships occurring in the summer months. The seasonal variation in the NDVI maximum-value composite is not as high as has been observed by other investigators (see the figure).

The NDVI is reduced by about 30 to 40% in the winter months as compared to the summer maximum. This compares to a variation of about 70 to 80% observed from spatially averaged 4-km spatial resolution AVHRR data. We attribute the reduction of the NDVI to a combination of factors, including senescence of understory vegetation, needle loss, low Sun angle, and reduced absorbed photosyn-



AVHRR monthly trends for selected coniferous forest stands in the western United States. The LAI for each stand is in parentheses

thetically active radiation. The reduced seasonal variability of the 1.1-km data compared to the 4-km data is attributed to the spatial sampling of the 4-km data.

The second objective of this research is to determine the sensitivity of remote-sensing data to sites with varying nutrient cycling characteristics caused by forest disturbance. This is being accomplished by analyzing the relationship of both Thematic Mapper and AVHRR data to clearcut sites in various stages of regrowth. The stages range from newly cut, successional regrowth to mature coniferous forest. Preliminary results indicate that predictive disturbance stage-spectral relationships exist for these landscape features.

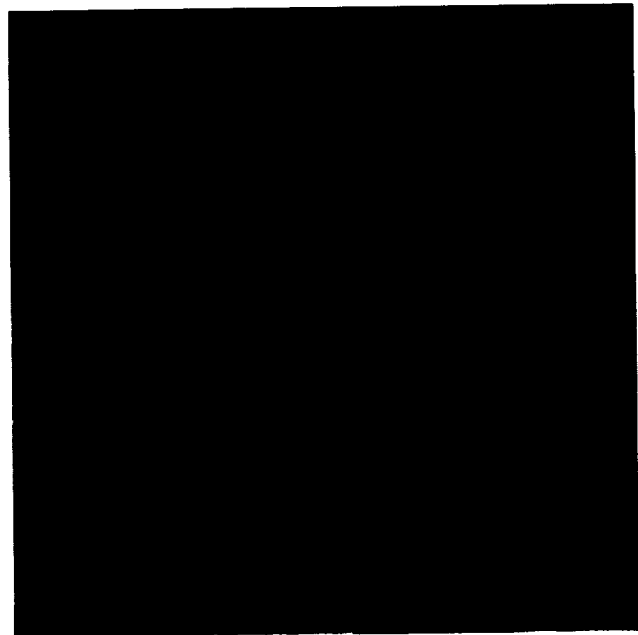
(M. Spanner, D. Peterson, Ext. 5896/5899)

Biodiversity Project

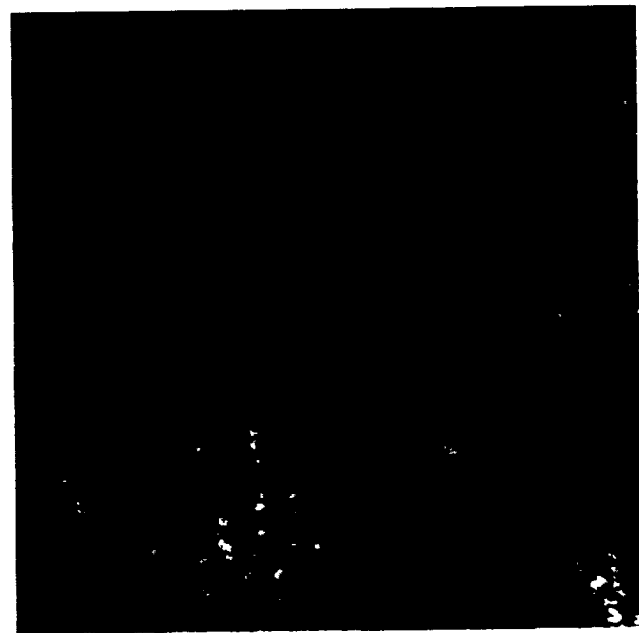
A pilot project is relating changes in the geographical distribution and condition of habitats detected with satellite imagery to species diversity and endangerment. Land Satellite (Landsat) multi-spectral scanner (MSS) scenes of two major forests in Uganda (Mabira and Kibale) were studied to assess long-term trends. Two frames of Mabira which were acquired in 1973 and 1988 were selected for detailed analysis (see figures).

The two frames were both registered to map Universal Transverse Mercator (UTM) coordinates so that each 60- by 60-meter area within the scene could be related to a habitat disturbance map created from ground observations. Thus, a matrix of changes in habitat over the 15 years could be constructed, rather than simple estimates of net changes.

MSS bands 2 and 4, the visual red and a portion of the near-infrared spectrum, were used to distinguish the forest from other types of land cover (savannah, agriculture, swamp, water) in the scene. This led to an estimate of a net decrease in forest acreage of 29% resulting from a 35% clearance and a 7% regrowth during 15 years. Within the forest, areas with high MSS-4 reflectance (generally the areas which corresponded to high-disturbance areas on the ground observation map) increased from 18% to 42% from 1973 to 1988, quantifying a greater



Landsat MSS coverage of Mabira, Uganda, on Feb. 2, 1973. False-color composite with MSS 2 in green, MSS 3 in blue, and MSS 4 in red. Mabira Forest appears as a brown blotch west of the Nile River



Landsat MSS coverage of Mabira on March 12, 1988. A large section of forest has disappeared from the eastern side. Disturbed areas of the forest, concentrated primarily on the western side, are a lighter shade of brown than the undisturbed areas

ORIGINAL PAGE
COLOR PHOTOGRAPH

decline in undisturbed forest than in overall forest. In addition, the forest perimeter measured on the imagery revealed an edge/area ratio increase roughly equal to the 29% decrease in area.

These changes potentially can be used to predict regional declines in biodiversity by using functional relationships between numbers of species and habitat area, and to predict changes in dominance between species that live in undisturbed, disturbed, or boundary (transitional) habitats.

Additional work evaluated the possibility of using Landsat MSS to identify four forest types, based on tree-species dominance or structure, and to differentiate among the other land-cover types present in the Mabira scene.

The spectral separability using all four MSS bands was first evaluated in a supervised mode, so that the mean and covariance matrices of spectral distributions for the land-cover/land-use types were estimated from sample areas. The forest samples were identified from a 1958 map of Mabira, sample agricultural areas from the ground observation map, and other samples (savannah, water, swamp) from visual interpretation of the Landsat imagery. Good separation was found among nonforest classes, between forest and nonforest classes, and even between forest and tree plantations. There was almost no separation among forest classes.

Spectral separability was then evaluated in an unsupervised mode by clustering spectra over all forest pixels and identifying the clusters with forest types on the sample areas. It was found that the clusters represented mixtures of types, with no one type predominating. This showed that it would be difficult to use Landsat MSS for determining the relative abundance of forest types and that experimentation with other types of remotely sensed data might be in order.

(L. Strong, C. Hlavka, Ext. 3325/3328)

AVIRIS Data Quality for Coniferous Canopy Chemistry

Before data from experimental sensors can be used to address scientific problems, it must be determined whether the quality is high enough to

address the particular question at hand. This study examined data from the Airborne Visible/Infrared Imaging Spectrometer (AVIRIS), which flies on the Ames ER-2 aircraft, to determine whether it was suitable for a study of forest canopy chemistry.

AVIRIS collects image data in 224, 9.8-nm bands ranging from 400 to 2400 nm. Both geometric and radiometric properties of AVIRIS data acquired over coniferous forest test sites in central Oregon were examined. Swath width, pixel size in the cross-track and along-track directions, and spectral locations of the bands were within preflight specifications, and were deemed to be suitable for a study of forest canopy chemistry. The signal-to-noise ratio in bands between 1400 and 2400 nm, however, was less than 10:1 over the forest test sites, too low to be used in the study of forest canopy chemistry.

These results and those of other AVIRIS investigators were presented at the AVIRIS Performance Evaluation Workshop and as a result, NASA Jet Propulsion Laboratory, Pasadena, CA, is making every effort to improve the signal-to-noise ratio of the AVIRIS instrument before the next field season. Future work with this data set will be restricted to bands located between 400 and 1400 nm.

(N. Swanberg, Ext. 5896)

Remote Sensing of Tropical Forest Types in Relation to Forest Fertility

Studies in the Biospherics Research Program at Ames Research Center have shown that the flux of nitrous oxide (an important greenhouse gas) varies among terre firme forest, campina forest, and cleared land which has been converted to pasture in the Amazon Boundary Layer Experiment (ABLE 2b) intensive study site near Manaus, Brazil.

In order to extrapolate these flux measurements, it is necessary to know the areal extent of each forest type. If these types have different spectral reflectance characteristics, then it is possible to assess their areal extent from the multispectral satellite images which we obtained over the study site. The results of a preliminary supervised classification of one such image suggest that 7.5% of the land had been cleared and converted to pasture by 1986. On

that basis, it can be estimated that pastures were responsible for a 20% increase in nitrous oxide fluxes from the area as compared to flux amounts before conversion to pasture. Additional classifications will attempt to determine the areal extent of terre firme and campina forests as well as to extrapolate flux measurements over larger areas.

(N. Swanberg, Ext. 5896)

ER-2 Ozone Measurements

Ozone is an important constituent and a useful tracer of stratospheric air. Measurements of the mixing ratio of ozone in the lower stratosphere have attained new importance with the discovery of the increased ozone depletion in the Antarctic region and the resultant fears of a global decline of ozone in the stratosphere. The Ames Research Center ultraviolet ozone photometer was designed for general use on the Ames ER-2 research aircraft in support of other measurements, and for accumulation of data on ozone trends and variability. Its location and operation does not interfere with most other instruments from various programs that use the ER-2 aircraft.

Reduction and interpretation continued on ozone data from the Antarctic mission of August and September 1987, and additional flight data were obtained. Latitudinal and vertical distributions were obtained on the ER-2 on its return from Puerto Montt, via Panama, to Moffett Field, CA, in October 1987.

In February 1988, the ER-2 carrying the Ames ozone photometer, the Harvard ClO and BrO instrument, and the whole-air sampler (jointly operated by Ames and the National Center for Atmospheric Research) made several flights from Moffett Field. The ozone photometer was essential for the interpretation of the ClO data. One flight reached the high-wind region of the northern polar vortex and produced data of interest for the Arctic ozone mission in 1989.

In telemetry tests on the ER-2, ozone measurements were transmitted to Ames to evaluate the usefulness of this feature in monitoring the status of instruments by the experimenters.

(J. Vedder, Ext. 6259)

Tracer Studies in the Stratosphere

Minor constituents play an important role in upper atmospheric photochemistry, and serve as tracers in the transport and mixing studies in tropospheric-stratospheric exchange processes. Measurements of trace gases are essential to understand the mechanisms by which minor constituents originating in the troposphere, both naturally occurring and anthropogenic, reach the stratosphere. Data on tracer distributions thus acquired are important in the development of models for predicting photochemical effects in the stratosphere.

In a joint effort in 1987, Ames Research Center and the National Center for Atmospheric Research (NCAR) developed and installed an automated whole-air sampler for the ER-2 research aircraft and installed NCAR's existing manually operated whole-air sampler on the DC-8 aircraft for the Antarctic ozone project.

Reduction of the data obtained in the Antarctic region in August and September 1987 continued for much of the year. At the base for operations in Punta Arenas, Chile, the mixing ratios of eight trace gases (including the chlorofluorocarbons CH₄, CO, and N₂O) were determined by gas chromatography. Additional analyses for these and other trace gases in the samples collected from the ER-2 and the DC-8 were done by NCAR in their laboratory. The data on the eight species measured in the field were presented at the Polar Ozone Workshop in May 1988. The results form an important contribution to interpreting the dynamics and chemistry of the depletion of ozone in the Antarctic atmosphere in winter and spring.

On February 13, 1988, the ER-2 carrying the whole-air sampler, the Harvard ClO and BrO instrument, and the Ames ultraviolet ozone spectrometer flew toward the northern polar vortex. Although the ER-2 did not enter the core of the vortex, it did reach the high-wind region around it. The mixing ratios of the eight trace gases provide information relevant to the Arctic ozone mission planned for January and February 1989. Preparations have begun for using the whole-air samplers on the DC-8 and ER-2 on this mission.

(J. Vedder, Ext. 6259)

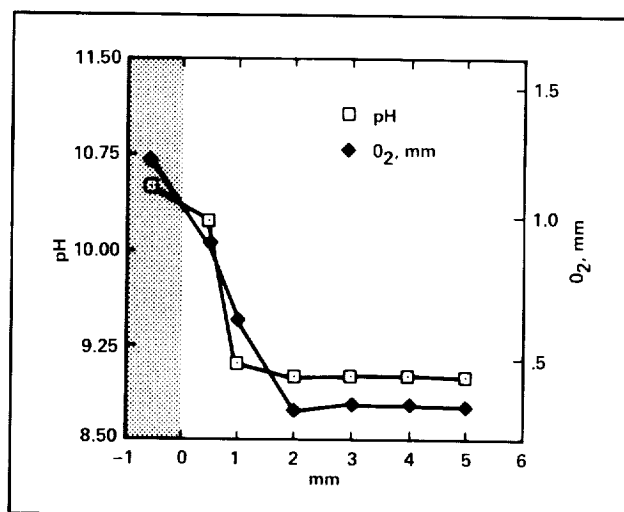
Remote Sensing of Aquatic Manganese Biogeochemistry

Manganese is a necessary micronutrient for all photosynthetic organisms—among other functions, it is a required cofactor for the O_2 -evolving enzyme of photosynthesis. In aquatic ecosystems, manganese is potentially limiting for algal growth and thus for primary production because the thermodynamically favored oxidized form is particulate, and it precipitates out of the water column.

Current research focuses on the manganese cycle in eutrophic Oneida Lake, NY. This research included the study of the mechanisms by which phytoplankton mediate manganese cycling and the role of bacteria in oxidizing and reducing manganese in sediments (especially in conjunction with carbon cycling), analysis and quantification of manganese cycling on a lakewide basis (supported by a suite of limnological parameters), analysis of the spectral reflectance signatures of natural blooms of phytoplankton (as well as laboratory cultures of algae), and digital data analysis of Thematic Mapper and Airborne Ocean Color Imager images of Oneida Lake.

The overall goal of this research is to determine the feasibility of using remote sensing to study a dynamic biogeochemical cycle in a moderate-sized lake. Remote-sensing image analysis is performed to extend our research on microbially mediated biogeochemical processes from microscale to lakewide synoptic data sets. The parameter which can be remotely sensed is the phytoplankton component, which we have shown plays a crucial role in manganese cycling in this lake.

The first figure shows that aggregates of naturally occurring phytoplankton, in this case the cyanobacterium *Microcystis*, can generate microenvironments of high pH and O_2 by photosynthetic activity. These microenvironments, under non-turbulent conditions, can extend several millimeters into the water column. Laboratory research has shown that manganese is catalytically oxidized at pH values greater than 9.5; therefore, when photosynthesizing phytoplankton raise the pH to (or above) this value, as shown in the first figure, the man-



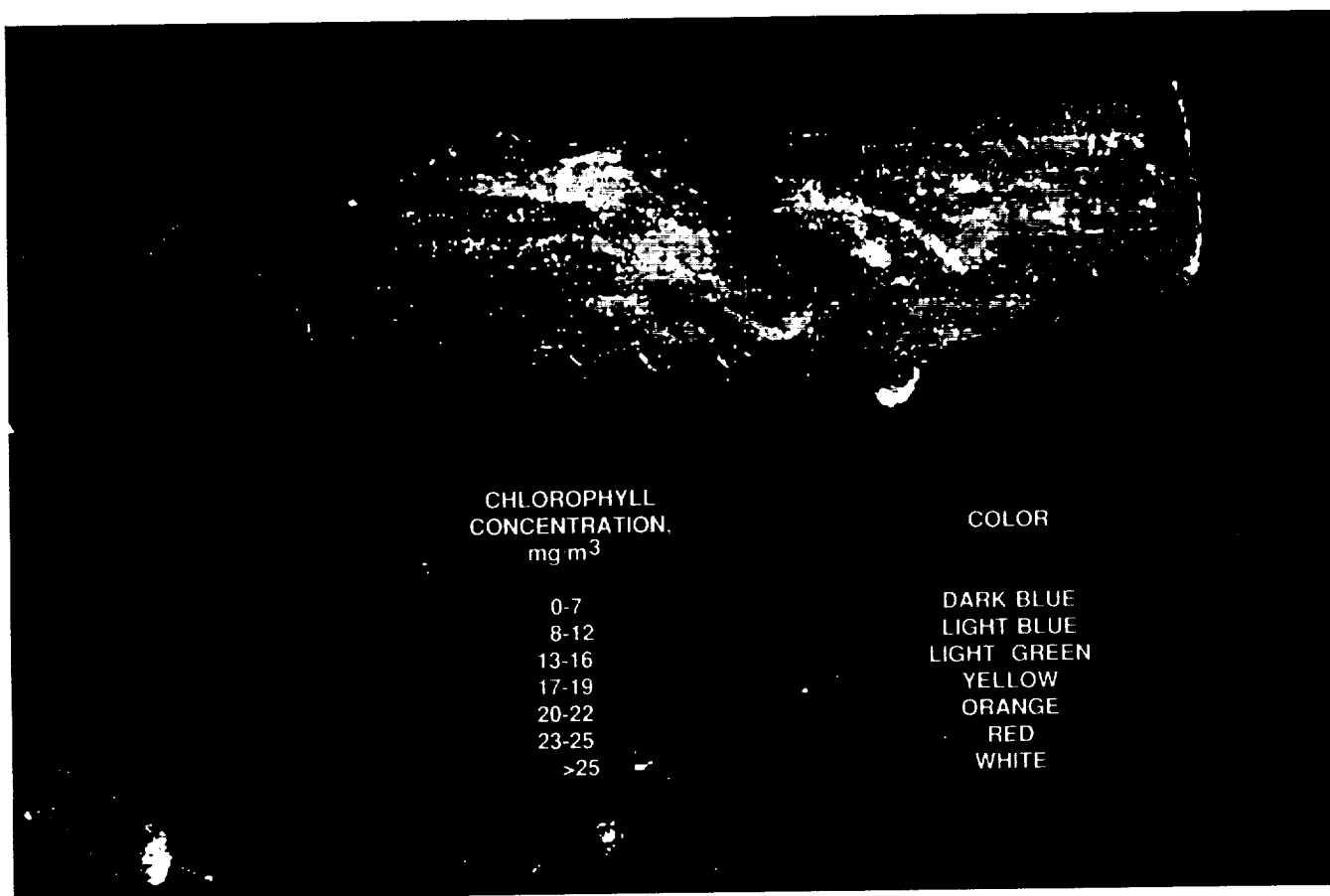
*Microgradients of pH and O_2 produced by naturally occurring, freshly collected clumps of *Microcystis*. These microenvironments were measured with pH and O_2 microelectrodes. The stippled area represents the phytoplankton cells, and the clear area represents the water column*

ganese oxidation reaction occurs. In addition to oxidizing manganese, phytoplankton suspend the oxides in photic surface waters where photoreduction of the particulate MnO_x back to biologically available $Mn(II)$ occurs.

Using data from the satellite Thematic Mapper and the Airborne Ocean Color Imager on the ER-2, we can map the surface phytoplankton of the entire lake. The final figure shows the surface chlorophyll concentration, calculated on a pixel basis, for Oneida Lake on June 14, 1986, when a massive phytoplankton-mediated, manganese-oxidation event was occurring. This image was processed at Ames Research Center, and was supported by field data acquired during the satellite flyover.

We are evaluating the relationship between phytoplankton carbon fixation, chlorophyll content, and manganese oxidation and uptake, and in the future we will intersect these results with the remotely sensed data to quantify the dynamics of carbon and manganese cycling in the lake.

(R. Wrigley, L. Richardson, Ext. 6060/3325)



Map of surface chlorophyll of Oneida Lake on June 14, 1986. An equation to estimate chlorophyll was derived from regression of Thematic Mapper digital data against surface chlorophyll measured in the lake, and was subsequently applied to the entire surface of the lake for each pixel

Gradients of Mineralization in Bone

The loss of bone mineral and, possibly, strength from the lower extremities of astronauts during spaceflight (and the possible risk of fracture during reentry) remains a challenging problem. To resolve this problem, the bone research program has taken two directions. One is aimed at developing techniques to maintain the integrity of the skeleton by a variety of means, including exercise and skeletal loading that mimic activities on Earth.

The second is a more basic approach that will enable us to understand the mechanisms of calcification of bone tissue.

A major advance in the more basic approach is the discovery of gradients of mineralization, with the same orientation as gravity, in human and animal

skeletons, reported from the following three separate laboratories.

1. Dr. M. Powell (Nuclear Diagnostics, Inc., San Francisco) in an Ames Research Center collaboration, evaluated the regional distribution of mineral by dual photon absorptiometry measurements of the entire skeleton of normal men after 30 days of head-down tilt bed rest. While decreases in mineral content in the lower extremities were not great enough to be detected, there were *increases* in skull bone mineral, averaging 10% above the prebed-rest measurements.

2. Drs. Dillaman and Roer from the University of North Carolina, Wilmington, working with the tail-suspended rat model for weightlessness, found ash weights of young rats (adjusted for body weight) reduced in the femur and tibia, unchanged in the

humerus and ulna, and increased in the skull and mandible. Both of these experiments are indicative of increased bone formation in the dependent regions of the body following postural change, a redistribution phenomena at 1 G that is most likely related to postural changes in hydrostatic pressures and in the cardiovascular system.

3. The third observation was made by Drs. J. Elliott and A. Boyde from the University College Hospitals in London. They used new image analysis techniques (backscattered electrons with scanning electron microscopy and computer microtomography) to analyze the distribution of mineral in the shaft of the femurs from young rats flown in the Cosmos 1887 flight. They found a linear gradient of decreasing mineralization from the upper to lower region of the femoral shaft that remained as steep in the 14-week-old flight bone as in the 12-week-old pre-flight bone. This indicates that bone mineral accretion in the femoral shaft in growing rats that proceeds in a pedal direction normally at 1 G, is impaired in 0 G.

These studies, at the whole bone level, clarify not only the role of gravity in bone formation in young rats and adult men, but also suggest the importance of changes in body fluid shifts in bone mineralization. How mineral and fluid shifts interact with the forces applied to bone through muscular activity are challenging questions.

(S. Arnaud, Ext. 6561)

Laboratory Studies of Reactions of Oxygen Atoms with Various Polymer Films

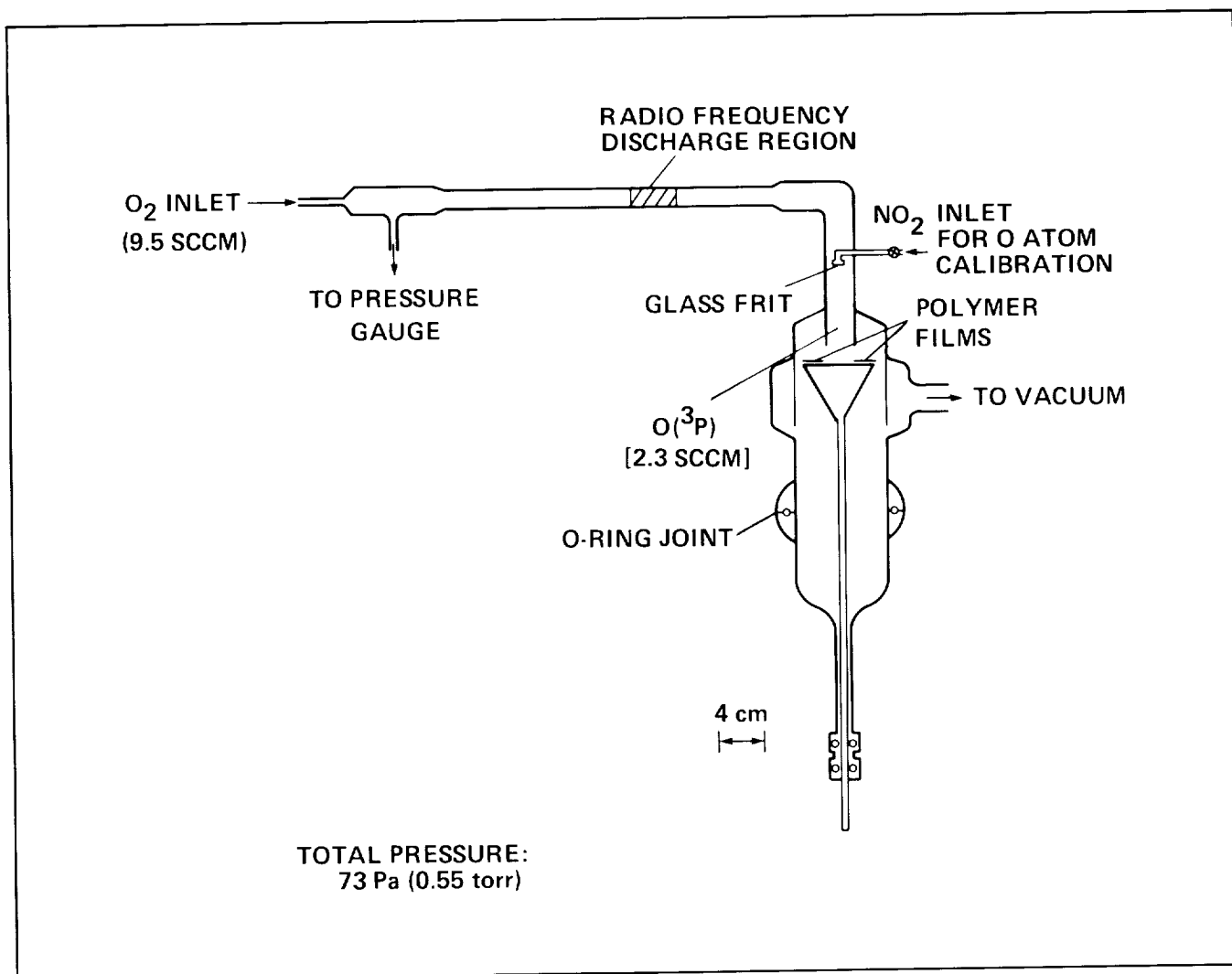
There is a need to understand the mechanism(s) of surface recession, or weight loss, occurring in polymeric films or coatings when exposed on the Space Shuttle to the low Earth orbital (LEO) environment. At the altitude of the Space Shuttle flights (~225 km above the Earth's surface), ground-state atomic oxygen, or $O(^3P)$, is the most abundant constituent (average density of 5×10^8 atom/cm³) in LEO, with an effective collisional energy of ~5 eV and a flux of $\sim 4 \times 10^{14}$ atom/cm²-sec, given spacecraft velocities of ~8 km/sec.

The importance of an understanding of the surface erosion, or etching, of polymers subjected to $O(^3P)$ in LEO lies in the need to develop a suitable data base for the design of the Space Station and to formulate new polymer structures resistant to O-atom attack. Although considerable data have been obtained on weight-loss measurements in polymer films exposed to $O(^3P)$, both in space and in ground-based experiments, there has been little effort to date to examine the mechanisms of the degradation processes or to compare the etch rates for various polymers subjected to the different types of $O(^3P)$ exposure.

Initial work involved a study of the reactions of $O(^3P)$ with polybutadienes having different amounts of vinylene (or 1,4) and vinyl (or 1,2) double bonds (or unsaturation), and with their polyalkenamer homologues. The major findings in that initial study of O-atom reactions with a family of closely related polymers were as follows: (1) vinyl double bonds exert a strong protective effect in polybutadienes against $O(^3P)$ -induced etching; (2) etch rates for polyalkenamers increase with decrease in $-CH=CH-$ unsaturation, culminating in the maximum rate for ethylene-propylene rubber or polyethylene; and (3) the reactions are confined to the polymer surfaces.

During FY 1988 the authors extended the range of polymers examined to include various commercial polymer films (e.g., Kapton, Mylar, Teflon, Tedlar, polystyrene, polyethylene) similar to those that had been exposed to $O(^3P)$ during Space Shuttle flight experiments. In both this and the earlier work, the polymer films were exposed to $O(^3P)$ *downstream* from the plasma in a low-pressure, oxygen discharge flow-tube apparatus. Apart from these two studies, nearly all prior publications reporting weight-loss measurements on films subjected to O atoms in oxygen discharge reactors involved exposure *in the plasma* (which contains various oxygen atomic and molecular ions and excited species, free electrons, and ultraviolet radiation, in addition to $O(^3P)$).

The aim of this followup study was thus to compare "out-of-glow" etch rates (see the first figure, where the O atoms have 0.04-eV translational energy) with literature values obtained from the following sources: "in-glow" exposures (also with 0.04-eV O atoms), STS-8 flight experiments (O atoms with 5.0-eV collisional energy), and beam



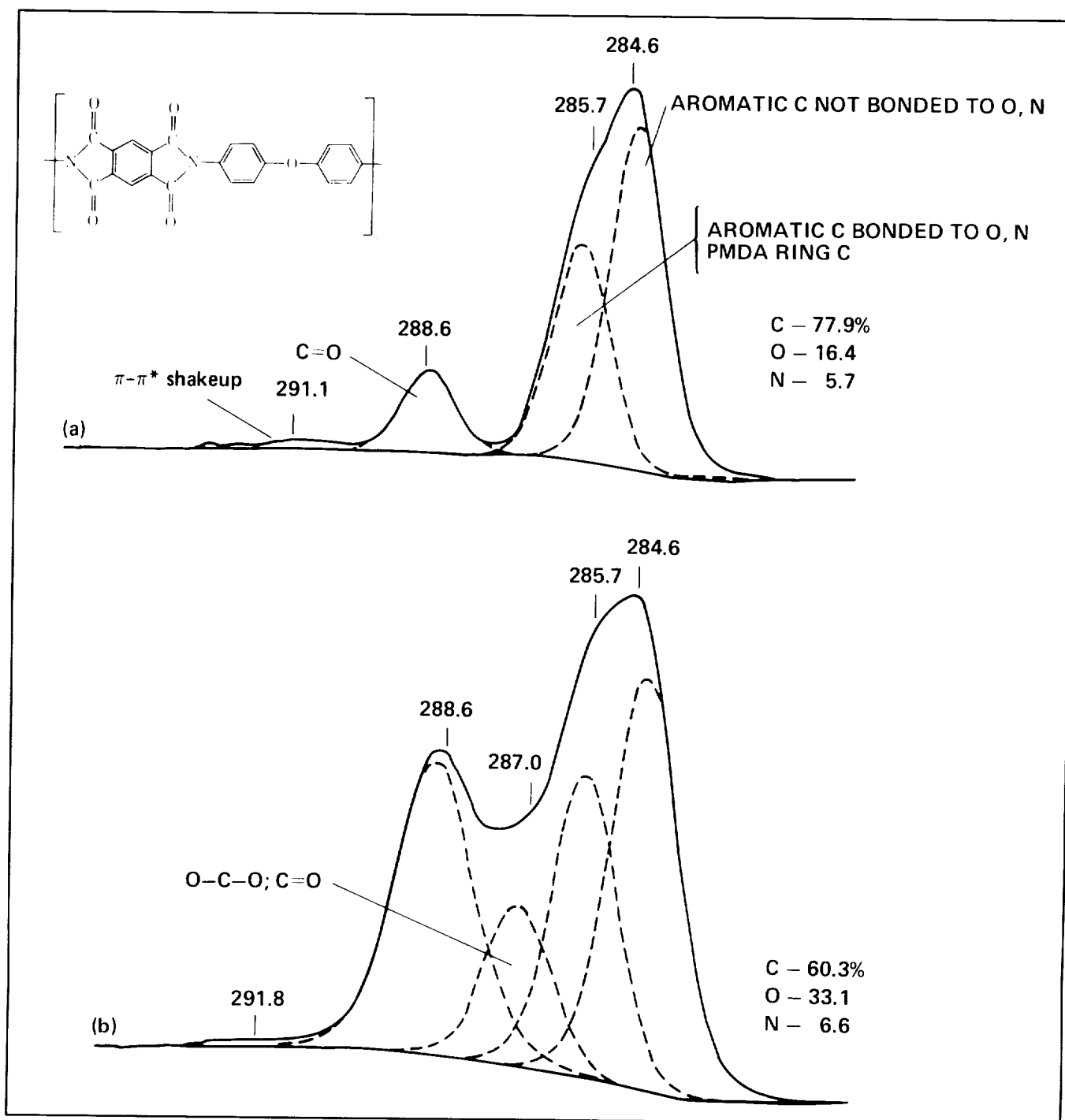
Apparatus for exposure to atomic oxygen [O(³P)]

experiments (with O atoms or ions ranging from 0.14 up to 800 eV in impact energy).

Etch rates (measured as mg/cm²-h) for all polymers exposed to O(³P) out of glow were one to four orders of magnitude smaller than the corresponding etch rates for in-glow exposures, reflecting in part the aforementioned difference in the respective "reactive" environments. Except for Teflon, *relative* etch rates (where the data are relative to Kapton as a standard) were found to be similar and more or less independent of polymer structure whether the polymers were subjected to in-glow plasma etching or to LEO exposure. However, out-of-glow relative etch rates showed a strong dependence on polymer structure. Although no explanation can be advanced

for these contrasting results, it was concluded that the use of RF discharge reactors—whether exposures to O(³P) are conducted "out of the glow" or "in the glow"—cannot serve as a routine, ground-based simulation of exposures of a polymer to the LEO environment. Another conclusion was that the etch rate data for Kapton fit reasonably well a logarithmic plot, with positive slope, of O-atom reaction probability versus O(³P) impact energy over a range of 0.01 to 1000 eV.

Examination of the Kapton surface, before and after reaction with O(³P) by means of Electron Spectroscopy for Chemical Analysis (ESCA), indicated steady-state competition between surface recession (etching) and oxidation (see the last fig-



C_{1s} spectra of Kapton before (a) and after (b) exposure to $O(^3P)$ for 0.5 hr in apparatus shown in the first figure

ure). Also, ESCA analysis of a series of fluorine-containing polyolefins exposed to $O(^3P)$ indicated that the maximum oxygen uptake increased regularly with decrease in fluorine content, again reaching the highest value in polyethylene (12-20 atom % O, depending upon type of $O(^3P)$ exposure). Finally, Teflon, which was known to be relatively very stable to LEO exposure but not to in-glow plasma etching, was found to be quite stable when exposed to O atoms in the apparatus shown in the first figure.

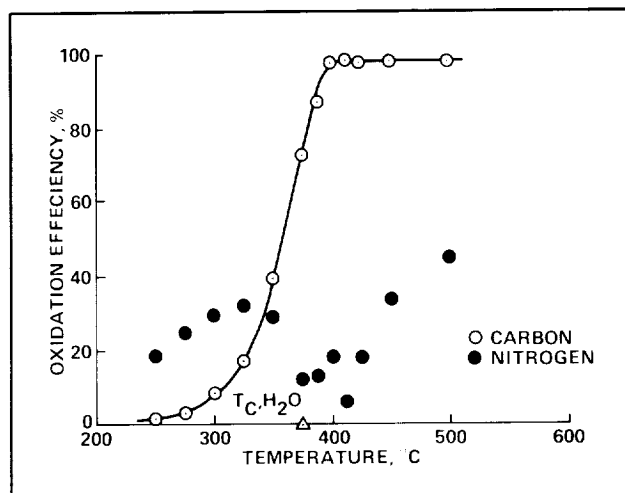
(M. Golub and T. Wydeven, Ext. 3200/5738)

Oxidation of CELSS Wastes Near the Critical Point of Water

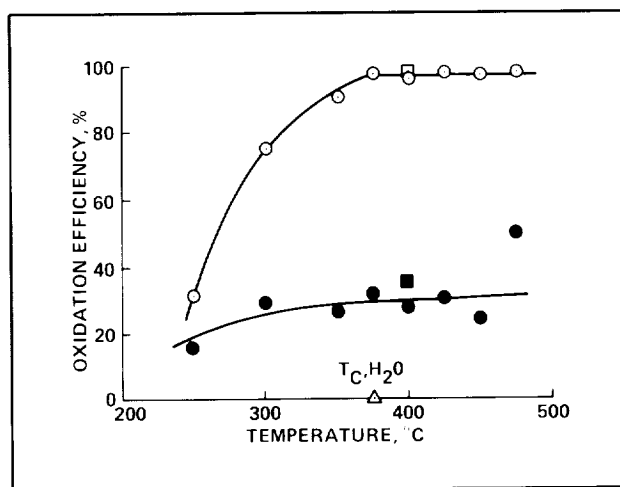
A controlled ecological life support system (CELSS) that uses higher plants to provide food for humans living in a space habitat will also include a waste processing subsystem. One of the major functions of the waste processing subsystem in a CELSS is to reclaim plant nutrients from waste streams. Among the candidate technologies for converting wastes into nutrients for plants is wet oxidation (WO). In WO, an aqueous waste solution or slurry is oxidized at an elevated temperature and pressure by using air or oxygen as the oxidant. If the oxidation is conducted above the critical point of water [374°C and 218 kg/cm² (3204 lb/in.²)], the method is generally referred to as supercritical water oxidation (SCWO).

Although a considerable amount of research and development has been devoted to WO and SCWO, many problems still remain, particularly when considering these processes for use in a CELSS in space. Among the concerns for a waste treatment subsystem in a CELSS are the fates of organic carbon and nitrogen. The fates of these elements are important because WO or SCWO is intended to work as a complete oxidizer of organic carbon and because the nitrogen is planned to be used as a fertilizer for higher plants. For nitrogen to be used as a fertilizer, it must be in a form such as nitrate ion or ammonia which can be easily and directly assimilated by plants.

During FY 1988 a comparative study of oxidation under WO and SCWO conditions was conducted.



Effect of temperature on the oxidation efficiency of ammonium hydroxide and acetic acid



Effect of temperature on the oxidation efficiency of human urine, feces, and wipes. Residence time was 60 min (open circle, carbon; solid circle, nitrogen) and 120 min (open square, carbon; solid square, nitrogen)

These experiments were carried out in the vicinity of the transition region between WO and SCWO, i.e., near 374°C and 3204 lb/in.². One of the goals of this work was to determine the extent of oxidation of organic carbon and ammonia near the critical point of water using a CELSS model waste and a waste composed of human urine, feces, and wipes. This task is one of several related tasks designed to identify the optimal oxidation conditions for processing

wastes for recycling in a CELSS and to uncover or identify any difficulties with this technology that are not anticipated.

Plotted in the first figure is the oxidation efficiency, or extent of oxidation, of the components in a model waste of acetic acid and ammonium hydroxide versus oxidation temperature. The data show that the oxidation efficiency of acetic acid is near 100% at slightly above the critical temperature for water, while only about 30% of the ammonia has been oxidized or lost from solution. This finding has an important implication for a CELSS-type application; namely, oxidation at low temperatures in the supercritical regime will destroy the organic carbon in solution (i.e., convert it to carbon dioxide so it may be reused in the plant growth chamber) while most of another important plant nutrient, ammonia, remains unoxidized.

Plotted in the second figure is the oxidation efficiency of the organic carbon and ammonia present in a representative CELSS waste of human urine, feces, and wipes. The data again show that if waste oxidation is carried out slightly above the critical point of water, i.e., above 400°C, organic carbon is completely oxidized and only about 30% of the ammonia is lost. Increasing the duration of oxidation from 60 to 120 min resulted in only a small additional loss of ammonia of about 5%.

In summary, the findings from this research suggest that if CELSS wastes are processed at temperatures slightly above the critical point for water, almost all of the organic carbon in the waste is converted to carbon dioxide while most of the ammonia is unoxidized and remains in solution. In earlier research, other investigators suggested that temperatures as high as 650-700°C would be necessary for waste treatment in a CELSS.

(T. Wydeven, Ext. 5738)

Research Animal Holding Facility

The rodent version of the Research Animal Holding Facility (RAHF) was delivered to the Ames Research Center Space Life Sciences Payloads Office from contractor facilities at Lockheed Sunnyvale.



Chief of the RAHF Project Office with the Rodent RAHF

Following delivery, the RAHF was subjected to an 11.75-day biocompatibility test using 24 male rodents installed in the 12 on-board cages. The test simulates an actual Spacelab mission, including animal loading at L - 12 hr, a contingency hold for weather, an 8-day mission, and animal unloading after landing.

All hardware functioned well, and the animals were clean, healthy, and growing normally at the conclusion of the test. Design modifications made to the hardware because of problems noted during the 1985 Spacelab-3 flight were tested and found to provide a positive barrier against contamination of the Spacelab cabin.

The RAHF will now be integrated into a ground rack in the proper configuration to support an Experiment Verification Test (EVT) at Ames in February 1989. The EVT is the final flight simulation before delivery of the hardware to the Kennedy Space Center for final integration and flight. The EVT is used to verify all procedures to be used by the mission and payload specialists in flight. The

astronaut crew will be in attendance for a major portion of the test.

The Rodent RAHF, along with the General Purpose Work Station and other associated hardware, is scheduled to fly on the Spacelab Life Sciences-1 (SLS-1) mission now scheduled for launch in June 1990.

(R. Hogan, Ext. 5248)

KC-135 Parabolic Flight Investigations

Seven life sciences investigations were conducted in parabolic flight on June 14 and 15, 1988, in the NASA Johnson Space Center KC-135 aircraft based at Ellington Air Field, Texas. These investigations supported a variety of ongoing payload projects and hardware development programs within the Space Life Sciences Payloads Office and Biological Research Projects Office at Ames Research Center.

1. Hardware and in-flight operations making up the Particulate Containment Demonstration Test (PCDT) were assessed. The PCDT is designed to challenge a Research Animal Holding Facility and a General Purpose Work Station (GPWS) with a typical 10-day accumulation of rodent debris (food crumbs, feces, and hair) to verify that the two systems and associated operations will adequately contain the debris and prevent contamination of the Spacelab cabin air. The GPWS cabinet will also be tested with a worst-case fluid spill to verify fluid containment under normal operating conditions.

2. Hardware and in-flight operations were evaluated for a future space flight study of the effects of microgravity-induced weightlessness on the development and function of gravity receptor structures of larvae (ephyrae) of the jellyfish *Aurelia*.

3. The Frog Embryology Experiment (FEE) is designed to investigate the effects of microgravity on fertilization and early development of the egg of the African clawed tree frog (*Xenopus laevis*). Hardware and portions of the in-flight procedures being developed to support the FEE were evaluated. Also studied was the zero-gravity behavior of the adult frogs.



Inflight transfer of animal from one cage to another

4. An evaluation was done on the effects of microgravity on the light output, in the blue wavelength, of a Gilway lamp. This lamp will be used in an experiment on Spacelab to investigate the response of seedling coleoptiles to blue light photostimulation while the plants are growing in microgravity.

5. We tested various designs for a cage door for a modular rodent habitat system currently under development at ARC to support life sciences research aboard the Space Station. The ease of capturing a rodent and extracting it from a cage via the cage door was evaluated.

6. Basic infant rat behavior in microgravity was studied, and an assessment was made of subsystem designs for an animal-development habitat. The habitat, an Orbiter middeck locker-size system for housing and maintaining a rat dam and her pups, is being developed for NASA by Star Enterprises of Bloomington, Indiana, under a Small Business Innovation Research (SBIR) contract.

7. A calorimeter system is being developed under a NASA SBIR contract by Geoscience, Ltd., of Solana Beach, California. We evaluated one of the design criteria, airflow, for the calorimeter, and assessed the performance of an animal watering

ORIGINAL PAGE
BLACK AND WHITE PHOTOGRAPH

system and a wet bulb psychrometer. We used a prototype calorimeter system for these assessments.

The objectives of each of the seven investigations were successfully met, and the use of the KC-135 aircraft was validated as an extremely useful testbed for conducting life sciences experiments and evaluating associated hardware and operations in advance of Spacelab flight operations.

(P. Savage, Ext. 5940)

General Purpose Work Station

The General Purpose Work Station (GPWS) fabrication and testing was completed in 1988, and custody of the GPWS has been turned over to the Johnson Space Center (JSC) Mission Management Office. Final work is currently under way to prepare the GPWS for its maiden trip on the Spacelab Life Sciences-1 (SLS-1) mission in June 1990.

The GPWS has been designed through the Ames Space Life Sciences Project Office to support a wide variety of life sciences experiments in the Spacelab. It consists of a main cabinet with internal airflow to entrain volatile gases, liquids, and particulate matter; support electronics; and a trace-contaminant control system to eliminate hazardous compounds. Temperature control, two-level lighting, and power, data, and video connections are available within the cabinet to support experiments.

The GPWS was thoroughly tested before it left Ames to ensure that it met the verification requirements imposed by JSC Mission Management. It also passed strict, internally imposed air-leak criteria and numerous functional tests. En route to the Kennedy Space Center (KSC), the GPWS was subjected to offgas testing at the Marshall Space Flight Center, providing assurance that it will not emit toxic gases onboard the Spacelab.

Integration of the GPWS into its flight rack at KSC is nearing completion. Its flight rack will be combined with the others to go on the SLS-1 flight, and will be installed in the Spacelab "can," which is in turn installed within the shuttle orbiter payload bay. The GPWS is intended for use in many future Spacelab missions.

(G. Schmidt, Ext. 6455)

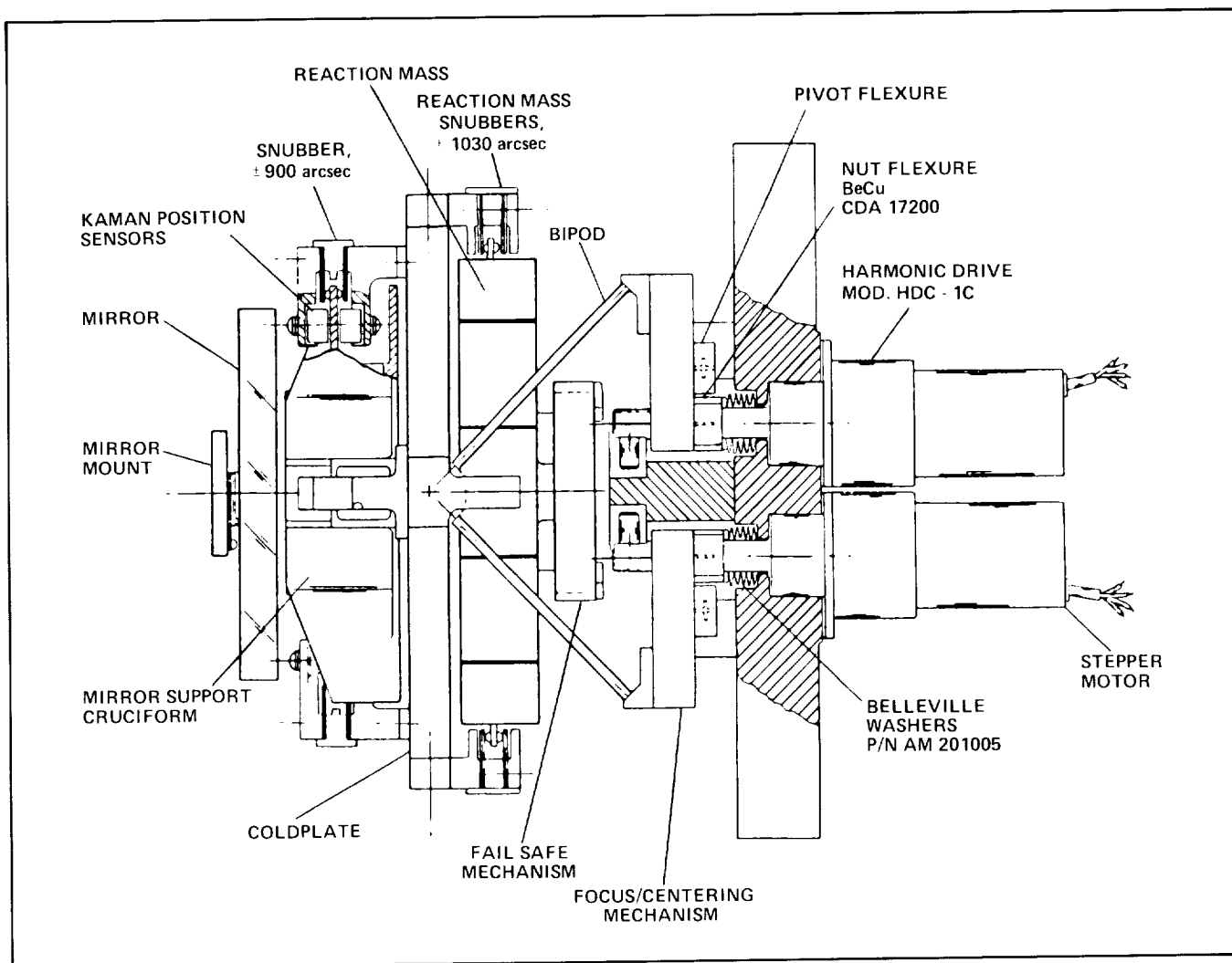


GPWS Project Manager with the GPWS at Ames

SIRTF Prototype Secondary Mirror Assembly

An important part of the Space Infrared Telescope Facility (SIRTF) design is the secondary mirror mechanism, which will tilt, center, and focus the secondary mirror. The tilt function will enable the telescope (1) to perform "chopped" observations, in which a source is rapidly and repeatedly compared with an adjacent area of blank sky; (2) to search regions of the sky for interesting sources; (3) to freeze the field of view for observation while the telescope slews; and (4) to direct the image of a source through "slits" to different instrument components sharing the field of view. During all these operations a precise position stability must be maintained (0.15 arcsec rms). The centering function will adjust the mirror laterally, and the focus function will adjust it along the telescope axis, to bring the mirror to its

ORIGINAL PAGE
BLACK AND WHITE PHOTOGRAPH



SIRTf prototype second mirror assembly design

correct position. Each of these motions is independently controlled.

To achieve these functions within SIRTf, the mechanism must operate at liquid helium temperature and dissipate a very small amount of heat (no more than about 5 mW). No device meeting all of these requirements has previously been constructed. The Perkin-Elmer Corporation in Danbury, CT, has been awarded a contract to design, build, and test the Prototype Secondary Mirror Assembly (PSMA).

During 1988, detailed requirements for the device have been intensively studied by Ames Research Center personnel, Sterling Software staff, the Perkin-Elmer staff, and outside experts chosen from the three SIRTf scientific instrument teams.

The studies have included (1) the relationship of the stability requirements to comatic blur introduced by tilting the mirror, (2) necessary tolerances in the event of fail-safe mechanism actuation, (3) propagation of launch loads to the PSMA, and (4) available space in which to house the mechanism.

The design, developed and analyzed at Perkin-Elmer, is shown in the accompanying figure. It includes a six-degree-of-freedom focusing and centering mechanism using stepper motors and harmonic drives to actuate a flexure lever system. The tilt mechanism itself includes an optimized reaction mass. Both the mirror and its mount, and the reaction mass, are mounted on a cold plate by flexure systems consisting of a cross-shaped blade flexure

and an axial stabilizer flexure. Mirror mount position is measured by four pairs of differential eddy current sensors. The position is controlled by four voice-coil actuators. Snubbers will limit the tilting components' motion during launch and in the event of erroneous control commands.

Extensive analysis at Perkin-Elmer indicates that the design has an excellent chance of meeting the many and demanding requirements. However, because of uncertainties and inadequate experimental data on material and device properties at liquid helium temperatures, a prototype will be built and tested to determine actual performance of the PSMA.

(P. Davis, Ext. 5916)

Spherical Bearing for an Airborne Telescope

Infrared astronomers have made significant discoveries using the NASA Ames Research Center Kuiper Airborne Observatory (KAO) with its 0.91-m telescope. The need for a 3-m-class airborne observatory to improve astronomy data-gathering capability has been established. The system envisioned by NASA and the international community of astronomers to meet this need is known as the Stratospheric Observatory For Infrared Astronomy (SOFIA).

A Cassegrain telescope configuration has been selected, to be installed in a Boeing 747SP-type aircraft. A mounting scheme fully compatible with the airborne environment, the aircraft characteristics,

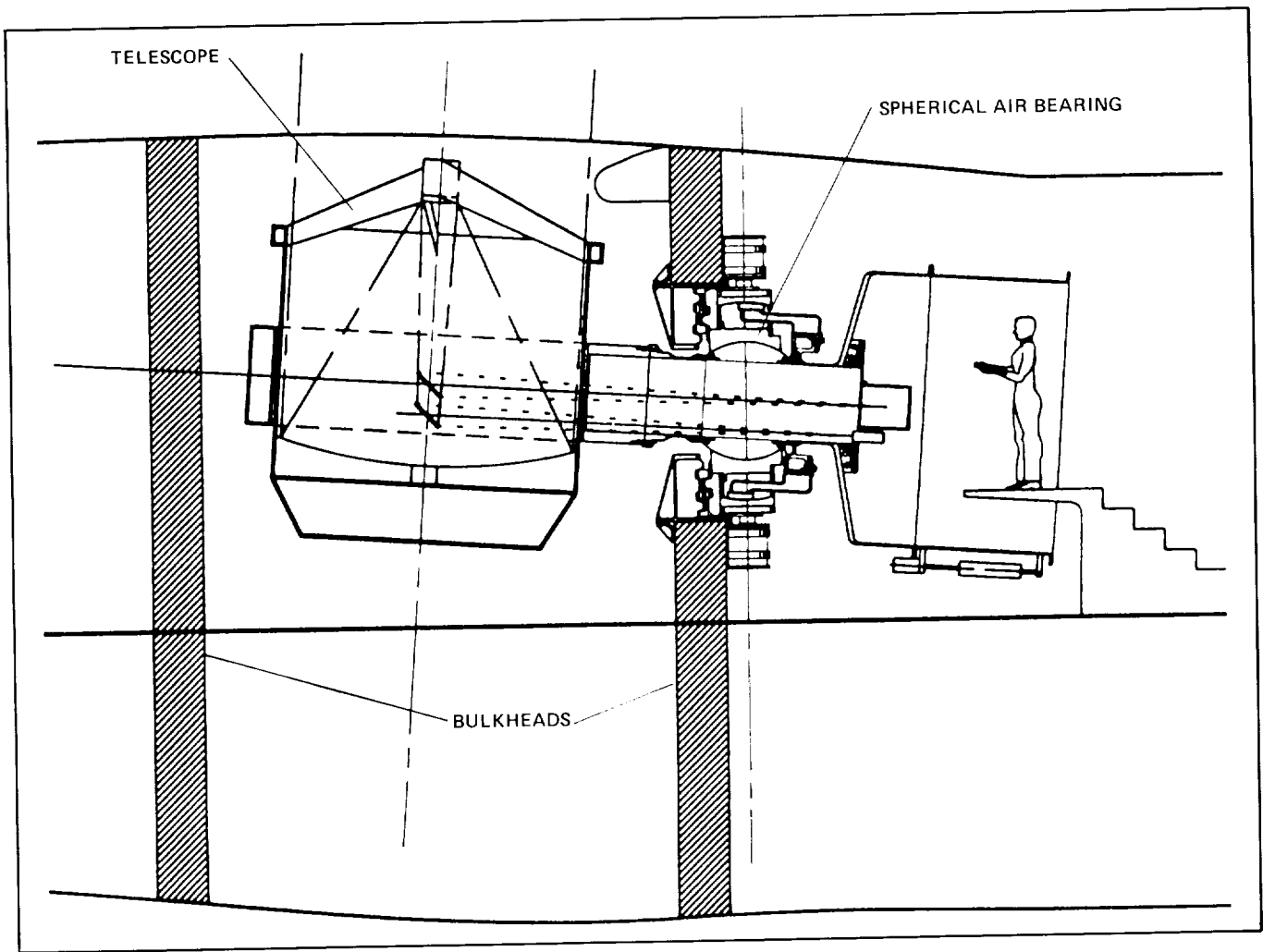
and the system specifications was required. A telescope mounting design was developed which uses a spherical bearing similar in concept to that used on the KAO system, differing primarily in its size.

The spherical bearing consists of a truncated ball, which forms the rotor, and a mating truncated spherical seat separated by a thin layer of pressurized air. This design was chosen mainly because of its compact configuration and its capability of isolating the telescope from aircraft motions in all three rotational degrees of freedom. The diameter of the rotor is 48 in. (121.92 cm), and a 31-in. (78.74-cm) bore was made through its center to accommodate the required optical path. The rotor allows unlimited rotation about the axis of the bore, and $\pm 4^\circ$ of motion about axes orthogonal to it. Air is introduced through 80 feed holes into the 0.00096-in. (24.38- μ m) gap separating the rotor from its seat.

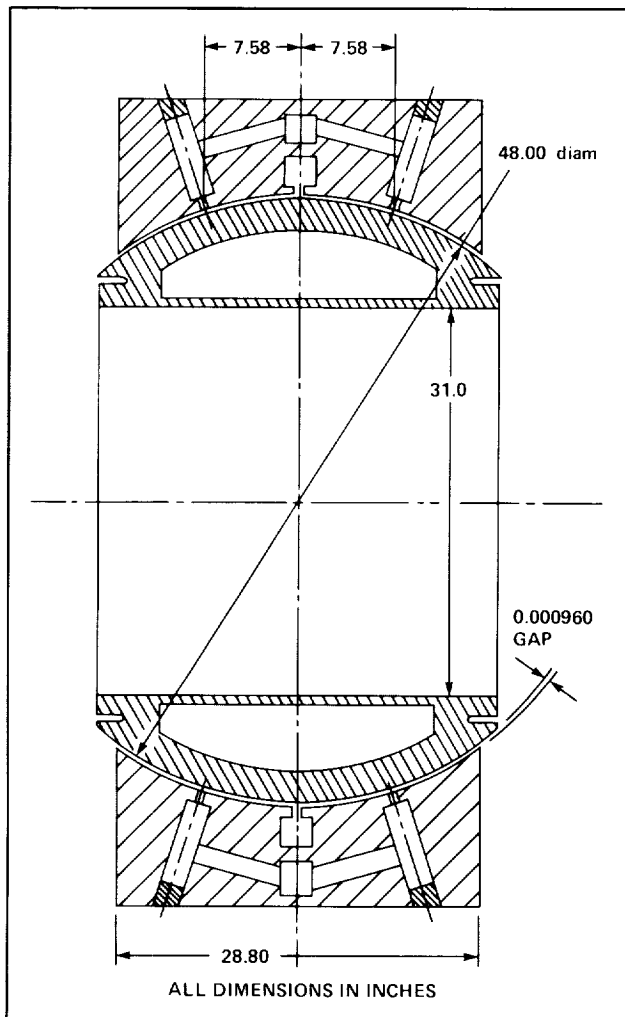
The first figure shows the spherical bearing integrated into the conceptual SOFIA telescope assembly. The second figure shows the bearing in schematic detail.

Engineering assessments and manufacturing risk evaluations have indicated that difficulties may be encountered in production of a bearing this large with a gap of roughly one-thousandth of an inch. Further studies to ensure feasibility have been initiated. This work supports the continuing efforts of the Center in maintaining a strong posture in infrared research in the atmosphere and in space.

(J. Eilers and R. Averill, Ext. 6536/4089)



SOFIA telescope



Spherical bearing

Helium-3 Cooler

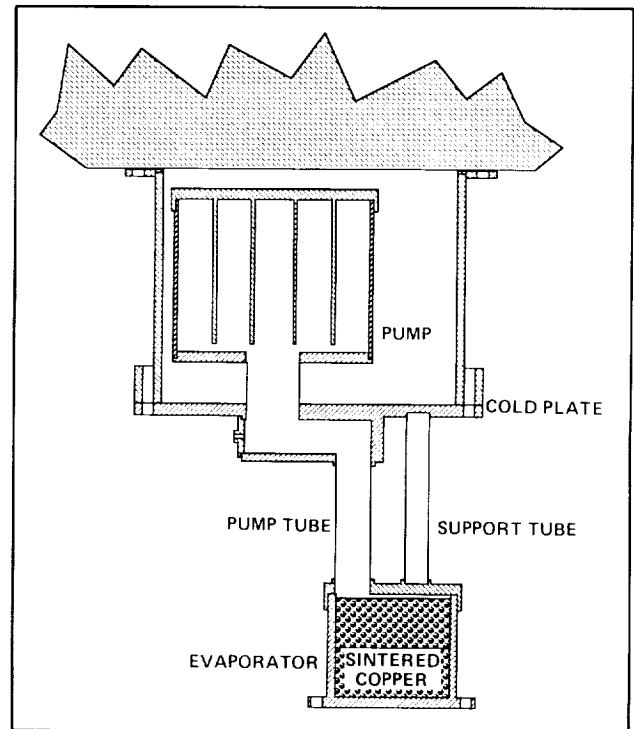
A ^3He cooler has been constructed for use in rocket-borne infrared astronomy and in zero-g physics experiments. The working fluid is ^3He , a rare isotope of helium. The cooler has no moving parts; rather, it uses a heater-activated sorption pump which contains activated charcoal. The cooler is started by heating the pump. The ^3He is driven off, and is condensed into the evaporator, which is filled with sintered copper. The sinter retains the liquid in zero g by surface-tension forces. At this point, the heater is turned off, allowing the pump to readsorb the ^3He , thus producing evaporative cooling in the evaporator. Temperatures as low as

0.25 K can be reached, starting from a 1.5-2 K heat sink provided by a superfluid He bath.

The surface tension (capillary) confinement of cryogenics for space applications was pioneered by Ames Research Center. By lowering the temperature available in a zero-g environment to 0.25 K, from the 1.5 K region provided by superfluid He (as was done in the Infrared Astronomy Satellite), this cooler allows a 10- to 50-fold improvement in bolometer sensitivity, and also permits the study of critical phenomena at the $^3\text{He}/^4\text{He}$ tricritical point. The cooler has no moving parts; hence, it is inherently long-lived. The operation is controlled by a single heater; therefore control is simple. The cooler is simple to incorporate into a superfluid He Dewar, as it may be bolted to the superfluid cooled cold plate and needs only a few electrical leads for control and monitoring.

This cooler is being developed under a cooperative research agreement between Ames and the University of California, Berkeley, and is scheduled for flight testing in a sounding rocket in February 1989. This will be the first flight test of a sub-1 K cooler in zero g.

(P. Kittel, Ext. 4297)



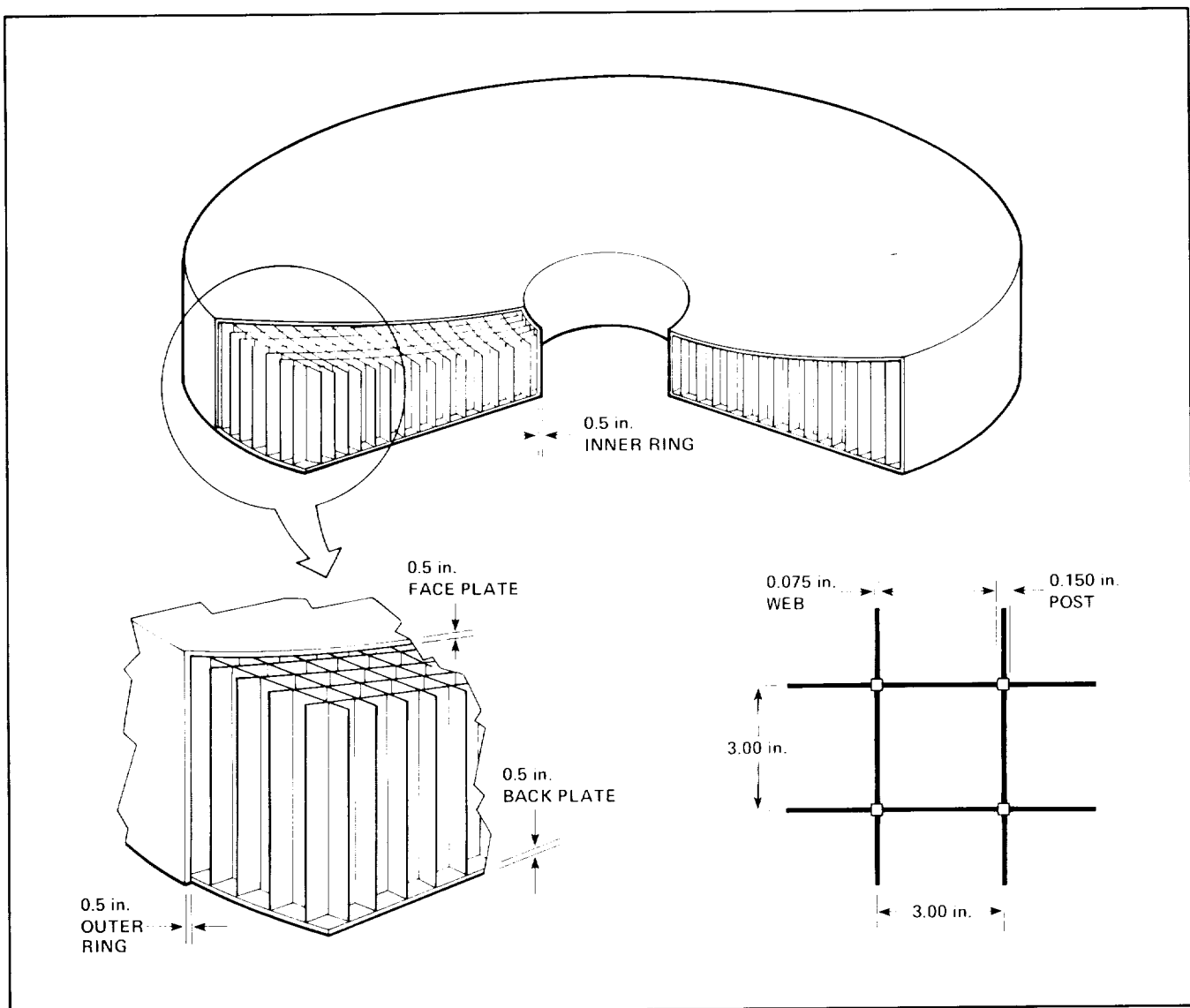
Rocket-borne helium-3 cooler

Cool-Down of Primary Mirror for the SOFIA Telescope

The Stratospheric Observatory for Infrared Astronomy (SOFIA) is a proposed airborne telescope with an aperture diameter of approximately 3 m. Past experience with the Kuiper Airborne Observatory indicates that the quality of the images obtained is strongly influenced by the temperature of the primary mirror, and precooling the mirror to near the operating ambient temperature (-25°F) is essential for producing good results.

In the preliminary study for SOFIA, Corning's ultra low expansion, frit-bonded quartz mirror was selected as a baseline design. The mirror consists of a 0.4-in. top plate, a 0.5-in. bottom plate, and a sandwiched honeycomb section with 3- by 3-in. cells. Overall thickness of the mirror ranges from 8.3 in. at the center to 15.8 in. at the outer edge. Small holes are cut in the bottom plate at the center of the cells to facilitate cooling. The figure shows the details of the primary mirror.

Nitrogen gas at -30°F will be used for the cool-down of the primary mirror. Several methods of



SOFIA primary mirror

introducing the cooling gas have been considered:

1. the gas moves at low velocity, and cooling is accomplished by natural convection only;
2. the gas blows along the top and the bottom surfaces at velocities of 10, 20, 30, and 40 ft/sec;
3. the gas flows into the cells through tubes at the rates of 1, 2, 3, 4, and 5 mirror masses/hr.

This problem has been analyzed with the computer programs SSPTA (Simplified Space Payload Thermal Analyzer) and SINDA (System Improved Numerical Differencing Analyzer). The results are presented in the table, which shows the time constants for all the cases analyzed. The time constant is defined as the time required for the temperature difference between the mirror and the gas to reach 37% of its initial value. For SOFIA, a time constant of 1 hr (maximum) has been specified. From the table, it can be seen that the time constant requirement can be met with surface blowing of 25 ft/sec or cell blowing of 1 mirror mass/hr. Surface blowing is recommended since cell blowing involves great mechanical complexity.

(S. Maa, Ext. 5915)

SOFIA PRIMARY MIRROR TIME CONSTANTS (hr)

Cases	Mirror surface	Strut (middle)	Bottom surface
No blowing	1.7	2.3	1.7
Blowing over top and bottom surfaces			
V = 10 ft/sec	0.75	1.5	0.78
V = 20 ft/sec	0.40	1.1	0.45
V = 30 ft/sec	0.25	0.95	0.28
V = 40 ft/sec	0.18	0.85	0.18
N ₂ blowing in cell			
1 mirror mass/hr (V = 3.7 ft/min)	0.35	0.45	0.80
2 mirror mass/hr	0.35	0.25	0.60
3 mirror mass/hr	0.30	0.20	0.50
4 mirror mass/hr	0.30	0.17	0.50
5 mirror mass/hr	0.30	0.17	0.50

Low-Background Evaluation of Large Integrated Infrared Detector Arrays

During FY 1988, further investigations into the performance characteristics of 58- by 62-element direct readout, extrinsic silicon infrared detector arrays were performed. This array technology, developed by Hughes Aircraft Co., has been adopted as the baseline for the Infrared Array Camera of the Space Infrared Telescope Facility (SIRTF). Tests on antimony-doped silicon (Si:Sb) and gallium-doped silicon (Si:Ga) arrays were conducted under conditions simulating space-based astronomical applications. Testing in FY 1988 concentrated on characterization of the Si:Ga array and on performance evaluation in a radiation environment simulating that to be experienced in Earth orbit.

Our test system has been used to accumulate a sizeable data base on the Si:Ga detector array. Measurements of responsivity, readout noise, dark current, input capacitance, linearity, well capacity, and power dissipation have been carried out in detail. All of these parameters are of critical importance in the determination of the suitability of this technology for use in an orbiting cooled telescope.

The Si:Ga array has demonstrated very encouraging performance, with high sensitivity and moderate dark current. Most performance parameters are well within the specifications required for SIRTF, and some are significantly better than specification. Sensitivities below 5×10^{-18} W/ $\sqrt{\text{Hz}}$, read noise below 60 rms electrons/read, dark currents below 1000 electrons/sec, and good uniformity with limited crosstalk between detector elements in radiation environments have all been demonstrated in the laboratory. However, questions about the transient response of this device, common to most bulk photoconductive devices, remain.

Radiation environment testing has begun using small (millicurie) sources of gamma and X-radiation



Si:Ga array output showing high uniformity and limited crosstalk around gamma ray hits (in red)

to simulate the on-orbit environment. Although the dose rates achieved so far are below those expected in space telescope applications, sufficiently long exposures have successfully deposited equivalent amounts of energy in these arrays. Changes in detector response similar to those observed on earlier orbiting astronomical missions have been produced in laboratory experiments. Further investigations are planned to identify the determining mechanisms and parameters of the observed radiation effects with the goal of controlling and minimizing them.

Additional research, including high-energy particle bombardment of these devices, will allow final judgment to be made on the suitability of this technology for SIRTf. Behavior of the Si:Sb devices in the on-orbit radiation environment and comparative studies of alternative detector technologies (e.g., Blocked-Impurity-Band detectors) are two areas where test effort will be concentrated in FY 1989.

(M. McKelvey and N. Moss, Ext. 3196)

ORIGINAL PAGE
COLOR PHOTOGRAPH

ORIGINAL PAGE
COLOR PHOTOGRAPH

Cryogenic Optics Test Facility for 1-M-Class Mirrors

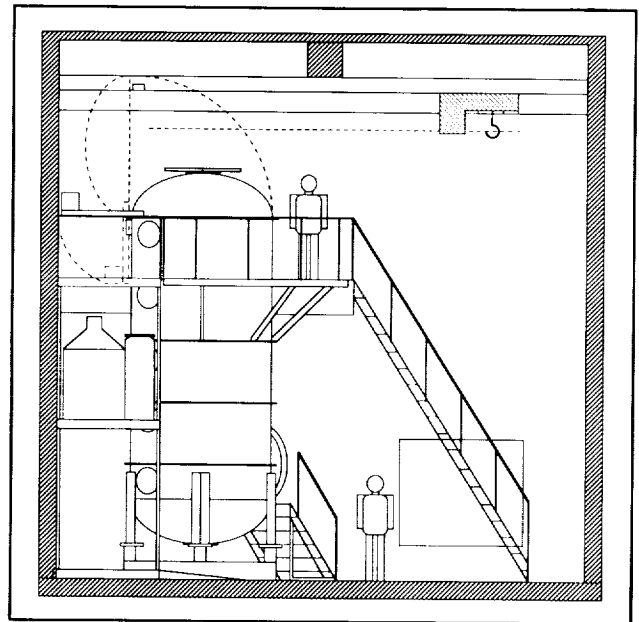
With the current high level of interest in infrared astronomy, the need has developed for optical characterization of 1-m-class (a maximum of a 1.25-m diameter with a 5.5-m radius of curvature) mirrors at cryogenic temperatures. The mirror of most interest is the primary mirror of the Space Infrared Telescope Facility (SIRTF). A cryogenic optics test facility, the One Meter Facility (OMF), is being developed which can interferometrically directly measure the optical figure quality of this and other 1-m-class mirrors at their operating temperatures (as low as 4 K).

The configuration of the OMF is shown in the figures. The first figure shows the layout of the OMF within the building. The second figure is a section drawing of the vacuum chamber showing the test setup for the SIRTF primary mirror.

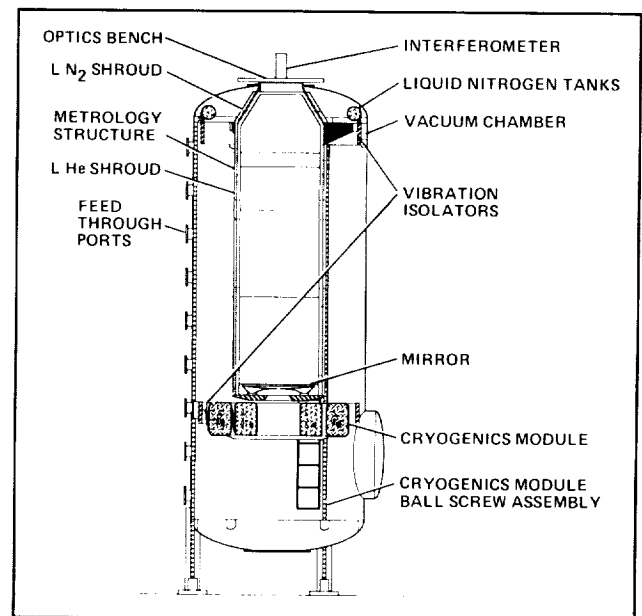
The OMF consists of a cylindrical vacuum chamber with a full-diameter door at its top. Inside the chamber, a cryogenics module rides on ball screws which allow it to be moved up and down to adjust for the radius of curvature of the mirrors to be tested. A test mirror is attached to the cryogenics module, which consists of liquid helium and liquid nitrogen tanks. The cryogenics module is thermally and acoustically isolated from the chamber. A fiberglass metrology structure mechanically links the mirror and the interferometer, which is located outside and at the top of the chamber. The metrology structure passes through the chamber wall via a flexible seal. The external mounting of the interferometer allows the use of commercially available interferometers as well as easy access. The adjustability of the height of the cryogenics module allows for all operations, such as mirror mounting, to be accomplished at table height from the platform at the top of the chamber and requires little work to be performed inside the chamber. The instrumentation for the interferometer is located on a platform next to the chamber.

Design considerations include future expansion of the OMF for testing entire optical assemblies and mirrors as large as 2 m in diameter. The OMF should be operational early in 1990.

(R. Melugin, L. Salerno, and G. Sarver, Ext. 3193/3189/3172)



OMF layout



Section view of OMF vacuum chamber

SIRTF Pointing Control System Studies

The Space Infrared Telescope Facility (SIRTF) is an orbiting space telescope with very stringent pointing-accuracy and stability requirements. It must perform a variety of rapid slew and nod maneuvers.

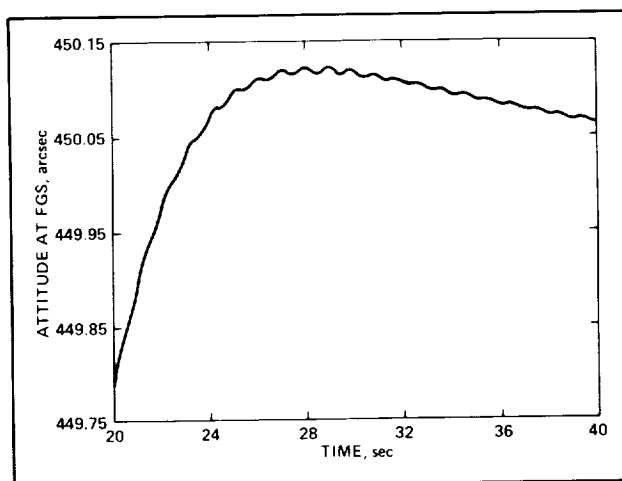
The observatory is cooled by superfluid helium (SFHe); it will carry a tank of this cryogen which will initially contain 4000 liters, accounting for 10% of the observatory weight. Over the lifetime of the observatory, the amount of fluid in the tank will vary from 1600 to 4000 liters. The design of a pointing control system (PCS) for the observatory is a general technical problem with several interesting aspects.

The initial design and simulation studies for SIRTf were done with a NASTRAN-derived model of the telescope and an end-mounted spacecraft. The very low damping coefficient (0.1%) assumed for the structural modes required the design of a bending compensator to stabilize the control system. Several engineering issues were explored, including the effects of variations in the structural model; the relocation of sensors and actuators; the influence of Fine Guidance Sensor (FGS) sampling period, resolution and noise on the system response; torque; and Rate Integrating Gyro noise and disturbances. Simulation studies were done using control-moment gyros and reaction wheels as actuators. A typical simulation result is shown in the figure.

Gain-switching of the controller, together with parameter-optimization of the Proportional-Integral-Derivative (PID) gains, was tried in an attempt to improve the small-angle slew performance. Significant improvements in settling time were seen in the simulation runs. However, as expected, this tuning of the PID gains was found to be very sensitive to the observatory model parameters. Therefore, this approach will eventually be coupled with a system identification effort that is currently ongoing.

The NASTRAN modeling of the observatory does not faithfully represent the effect of the SFHe slosh in the cryogen tank. The structural damping coefficients are also only estimates. Given that the SFHe depletes gradually over a 2-year period, it is likely that the observatory behavior will change with time. However, this variation in parameters can be assumed to occur over a much longer period than the duration of the slew maneuvers. Thus, for small slew maneuvers, a linear time-invariant model with uncertain parameters would be a representative model of the observatory.

In collaboration with Prof. Frank Alexandro, of the University of Washington, a system identification study for SIRTf was begun. An Auto Regressive Moving Average with exogenous signal (ARMAX)



Effect on settling time of reducing the moment of inertia by 25%

model was found to fit simulated RIG loop input-output data closely, both in the time and frequency domains. The modal parameters in the simulation were changed and a new set of test data was generated. A new ARMAX model fit to the data was obtained with good accuracy and computational efficiency using the PC-MATLAB software package on an IBM-compatible personal computer. Similarly, an autoregressive model with exogenous signal was fitted to simulated input-output data for the FGS loop. Currently, the closed-loop performance of the system represented by the identified models with a PID controller is being investigated.

Henning Schneider, at the University of Washington, designed a Linear Quadratic Gaussian controller for SIRTf, with the observatory represented by a NASTRAN-derived structural model. The nominal performance from this model is better than the PID, but worsens in the presence of disturbances.

The above investigations all concentrate on the design of the control algorithm. They assume that the motive power for the observatory comes from such conventional devices as reaction wheels. An alternate controller concept, in which the observatory and the spacecraft are connected through an extensible link, was studied. The telescope was pointed in a given direction by swinging the spacecraft in the opposite direction. The equations of motion were set up. They were linearized for two-dimensional motion through small angles. A PID controller was designed

using pole placement. The results showed good performance with low power consumption. Flexible body effects were ignored.

Besides their intrinsic interest, the above activities further the design and simulation effort on the SIRTf PCS. This space observatory is an important component of NASA's long-term program in space.

(R. Hanel, Ext. 5915)

SOFIA Pointing Control System Studies

The Stratospheric Observatory for Infrared Astronomy (SOFIA) is a planned 3-m-class airborne observatory to be mounted on a modified Boeing 747SP aircraft. The pointing and control system studies described below were part of the concept definition studies for SOFIA.

A three-axis controller was designed for the telescope. The observatory was modeled with 31 bending modes. The inputs were torques about three axes: azimuth, elevation, and line-of-sight. The corresponding angular rates were the outputs. A matrix transformation was employed to decouple the system, so that a command for motion about a given axis caused very little motion about the other two axes. Controllers of about 10-Hz bandwidth were designed for all three decoupled axes, using pole-placement techniques. The control law employed was a "generalized" Proportional-Integral-Derivative algorithm. The azimuth and the line-of-sight axes needed bending filters as well. Slew maneuvers of 300 arcsec about each axis were simulated. The 1% settling times for these maneuvers were found to be a little over 1 sec.

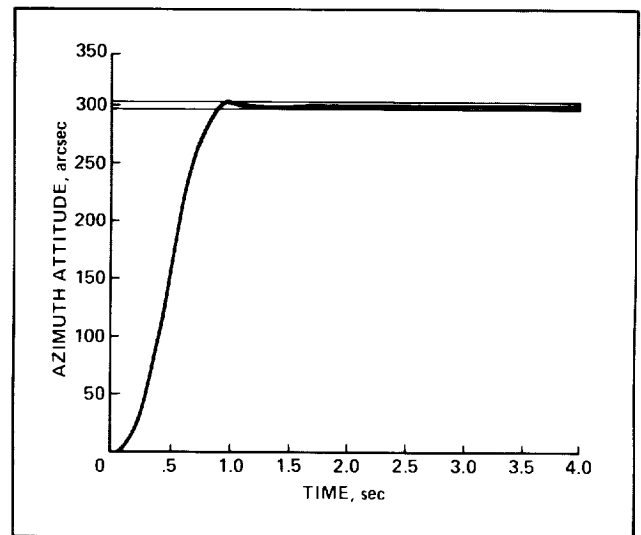
In each axis, a disturbance attenuation of over 100 dB was achieved over a 1- to 100-Hz frequency band. The peak torque requirement for the maneuvers was below 400 N·m, or well within the capabilities of currently available torquers. The response to a nod command about the azimuth axis is shown in the figure.

These studies are significant for control system design for SOFIA. It has been shown that a design which satisfies the performance requirements is fea-

sible. Such a design would also have sufficient stiffness to withstand the disturbances expected to act upon the system.

SOFIA is a logical progression from the existing Kuiper Airborne Observatory, and will be 11 times more sensitive. The SOFIA observatory can be expected to add greatly to human knowledge about the universe. It is an important component of NASA's long-term space program.

(R. Hanel, Ext. 5915)



Response in azimuth to nod command

Infrared Black Coatings for the Submillimeter Region

Because stray light can be a serious problem limiting the sensitivity of far-infrared telescopes, the Space Infrared Telescope Facility (SIRTf) program has supported a laboratory effort to characterize existing black telescope coatings and to develop new ones for the far-infrared/submillimeter region.

At Ames Research Center, a Non-Specular Reflectometer (NSR) has been built that is the only instrument in the world capable of measuring both specular and angle-resolved diffuse reflectance at wavelengths longer than 50 μm (0.5 mm). Because SIRTf works with very long wavelengths, a new

coating named Ames 24E has been developed. (A spectral survey of existing coating materials leading to its development was mentioned in the Ames 1985 R&T Report and also in a NASA Tech Brief.) Additionally, a better reflectance standard has permitted an internally consistent absolute reflectance calibration of the NSR at submillimeter wavelengths. This in turn has made possible comparison of earlier data on an older coating, Martin Black, with more recent data on Ames 24E and another new coating, Martin Infrablack. This comparison, described here, shows that the optically important characteristics of these coatings are markedly different.

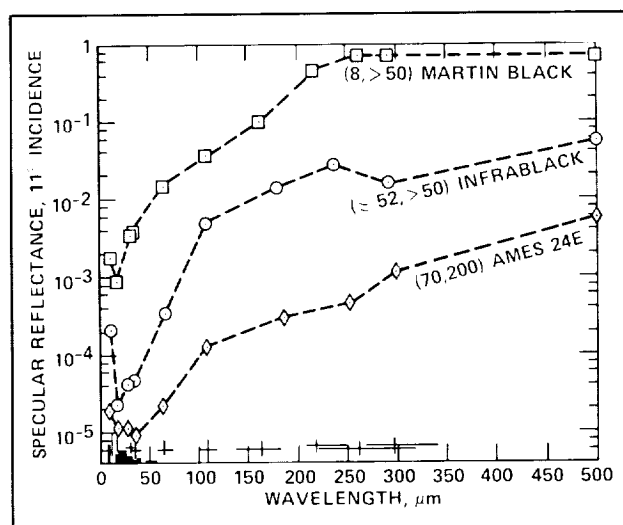
The specular reflectance of a telescope coating is its most important optical characteristic. Specular reflectance occurs when the angle of incidence (θ_i) equals the angle of reflection (θ_s). Specular reflectance spectra of the three coatings mentioned above are presented in the first figure. (Error in both reflectance and wavelength is represented by the crosses along the bottom of the figure.) The roughness and thickness, in micrometers, of each coating are given in parentheses preceding the coating name.

The most significant features of these data are the approximately one-order-of-magnitude lower reflectance of Infrablack, and the approximately two-orders-of-magnitude lower reflectance of Ames 24E, at most measurement wavelengths across the spectrum. These significantly lower specular reflectance values are consistent with the exponential dependence of specular reflectance on coating roughness and thickness (as described by the reflecting-layer theory of Smith in the Ames 1984 R&T Report) and with the greater roughness and thickness of the two newer coatings.

Given that nothing is perfect, all surfaces have some amount of diffuse reflectance as well as specular reflectance.

Diffuse reflectance occurs at nonspecular angles, and it is the second optically important characteristic of a coating. The angle-resolved, diffuse reflectance per unit projected detector solid angle is defined in National Bureau of Standards Monograph 160 as the bidirectional reflectance distribution function (BRDF).

Diffuse reflectance measurements of the three coatings made on the NSR at four separate wavelengths (indicated by different symbols) are shown in



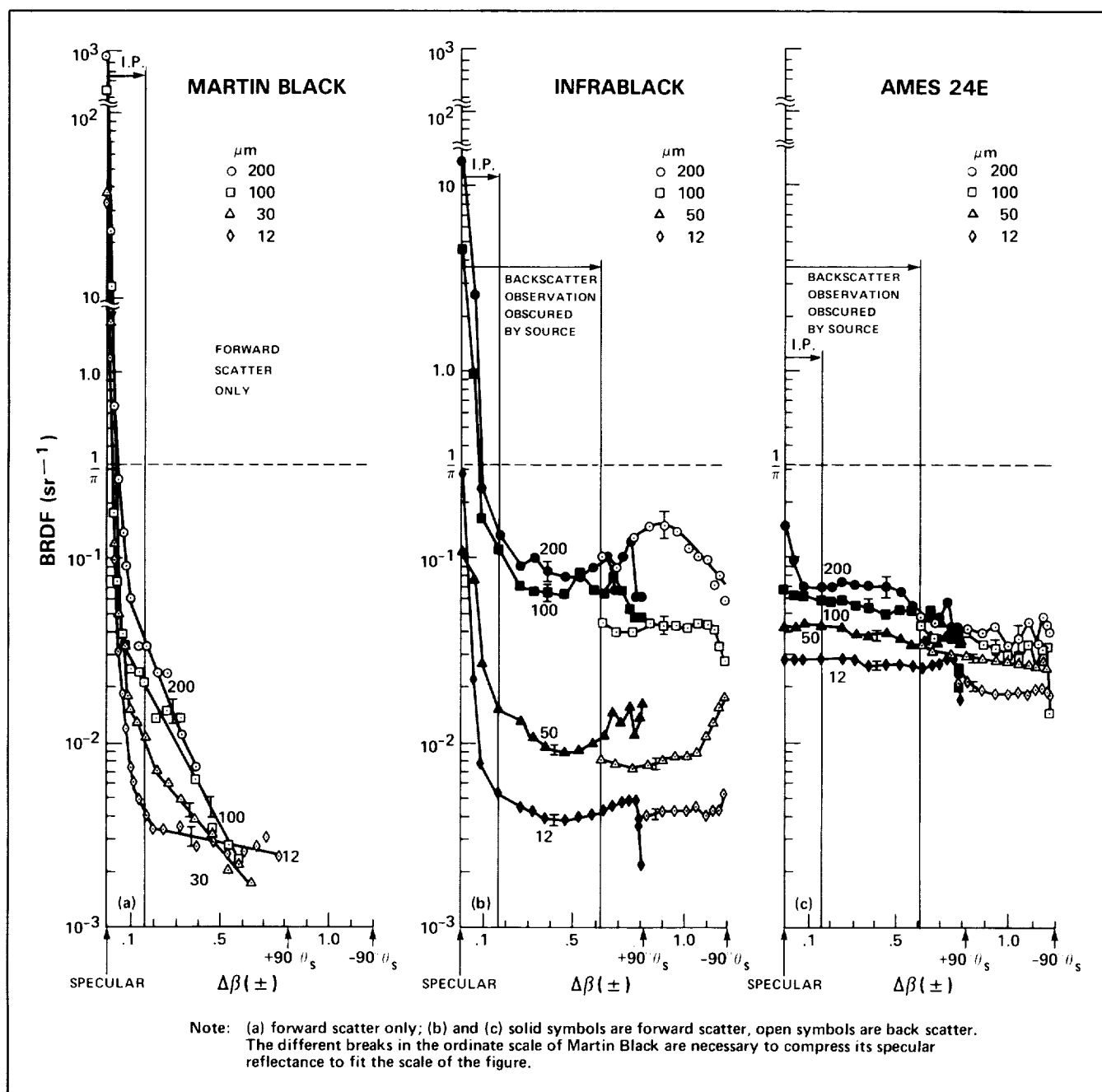
Specular photometric reflectance spectra

the second figure as absolute BRDF values. They are plotted versus $\Delta\beta$, which is the nonspecular angle in direction-cosine space ($\Delta\beta = \sin \theta_s - \sin \theta_i$). Statistical error bars are shown at representative values of $\Delta\beta$. For reference, the BRDF of a perfectly diffuse reflector is indicated by the dashed horizontal line at the value $1/\pi \text{ sr}^{-1}$. In contrast, the BRDF of a perfectly specular reflector would be indicated by a thin vertical line at $\Delta\beta = 0$.

A large amount of detailed information is shown in the second figure. The most significant feature is the increasingly diffuse character of the reflectance as one proceeds from Martin Black to Ames 24E (from a to c). At the shortest wavelength (12 μm), Martin Black is specular-diffuse; i.e., quasi-diffuse. But at longer wavelengths it is largely specular. Infrablack is specular-diffuse with a strong wavelength dependence, as well as having some angle-dependent features of lesser importance.

Ames 24E is almost perfectly diffuse with only a small wavelength dependence. The observed trend toward increasingly diffuse reflectance is not only consistent with the lower specular reflectance of the newer coatings as shown in the first figure, but it also partially explains those lower values. In effect, power from the specular peak of Martin Black has been redistributed to large nonspecular angles by the increasingly rough surfaces of the newer coatings.

Knowledge of the diverse nature of the optical characteristics of these as well as other coatings is critical to the design of far-infrared/submillimeter



Reflectance at 11° incidence

telescopes, because at certain places in a telescope a diffuse black coating is much more effective in reducing stray light than is a specular one, and the opposite may be true at other places. As demonstrated by these measurements, Ames' unique wavelength and reflectance measurement capability

provides necessary support for the design and development of the Center's far-infrared telescope projects, SIRTf and SOFIA (Stratospheric Observatory For Infrared Astronomy).

(S. Smith, Ext. 4392)

Tertiary Mirror Assembly

A design program to develop precision cryogenic mechanisms for application in space-borne infrared telescopes has been started by the Telescope Systems Branch at Ames Research Center. The Tertiary Mirror Assembly (TMA) is one of the critical optomechanical components in the Space Infrared Telescope Facility (SIRTF) optical train. The TMA is located on the telescope axis in the telescope instrument chamber. The functions of its dichroic tertiary mirror include directing the full 7-arcmin infrared field of view to each of the science instruments and the full 20-arcmin visible field of view to the guidance sensor. The TMA must satisfy stringent image-position repeatability (3.4 arcsec), focal-length repeatability (20 μ m), and jitter (3.4 arcsec rms) requirements. It must operate in a cryogenic, vacuum environment and have minimal power dissipation (<5 mW average). Its design life is 10 yr and 100,000 cycles at liquid helium temperatures (2 K).

The SIRTF Project Office is evaluating the feasibility of several TMA design concepts and critical cryogenic mechanism technologies which will enable the TMA to provide reliable, high-precision, infrared beam-steering capability. The current baseline tertiary mirror is inclined at an angle of 45° with respect to the telescope axis and has a compensator moving in conjunction with it. The flat, elliptical mirror and compensator are rotated about the telescope axis to any of seven fixed angles.

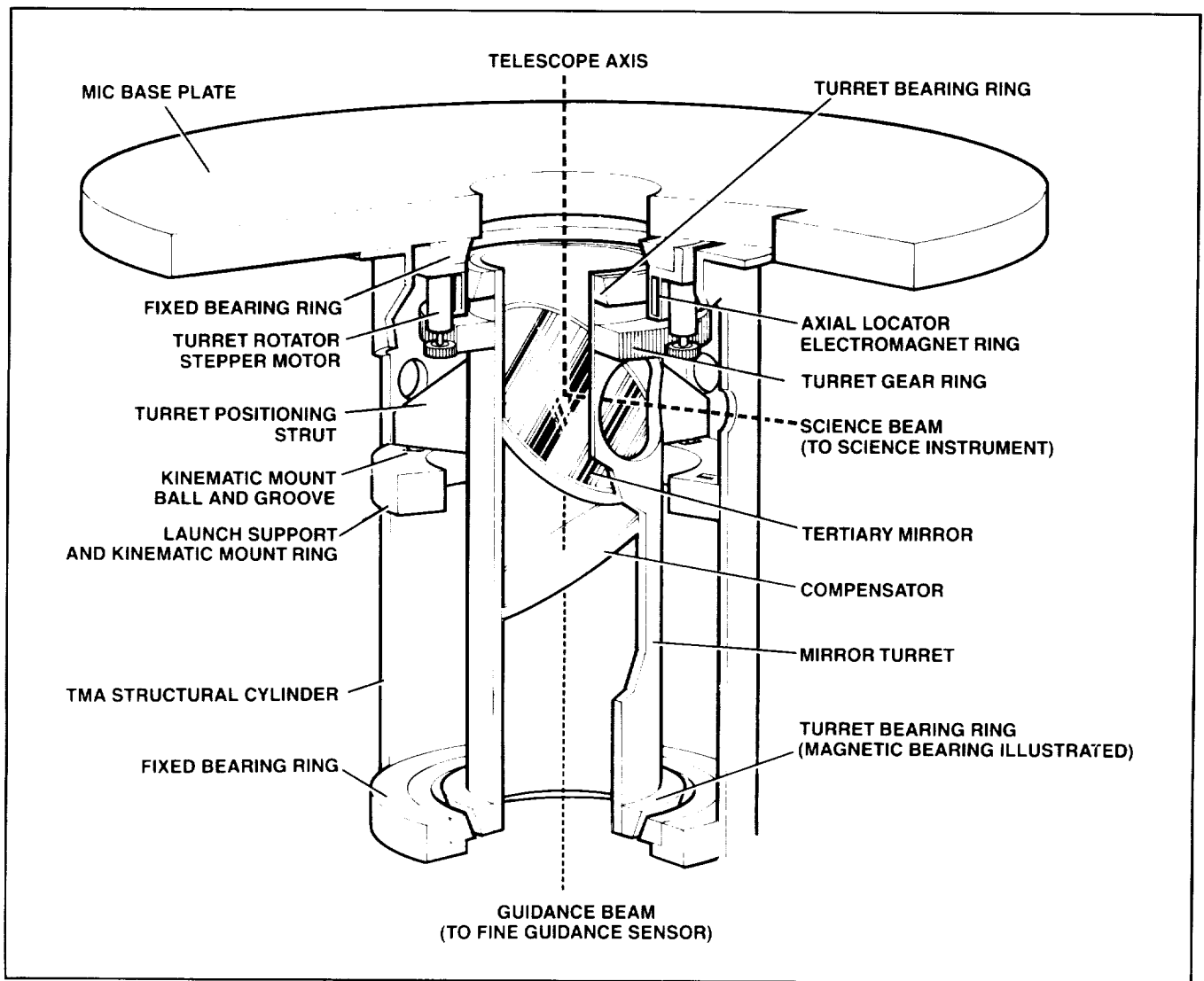
The first of the TMA designs under study, the rotating-mirror concept shown in the first figure, steers the science beam to each of the science instrument apertures by a turret mechanism. The cylindrical turret is suspended by bearings and a flexure system, and is rotated to rough alignment by a stepper motor. Once approximate alignment is achieved, linear actuators are turned off and the entire turret translates into a kinematic mount. The turret has three locator balls which seat into three locator V-grooves. The ball-and-groove arrangement provides the critical alignment required of the tertiary mirror. A variation of this design uses magnetic bearings in lieu of the friction-prone ball bearings.

The second TMA design, called the drop-mirror concept (second figure), uses a fixed tertiary mirror and compensator with a rotating quaternary mirror to provide beam steering. The basic design is similar to the rotating-mirror concept, except that the quaternary mirror can drop entirely out of the beam path, exposing an additional instrument aperture. This design uses a stepper motor for rough rotational positioning, and kinematic mounts for precise alignment. A linear motor provides translation out of and into the mounts and also a two-position fail-safe arrangement. The visible beam going to the guidance sensor is not disturbed by the beam-steering motion, but additional reflecting surfaces are required and light is provided in a nonuniform radial manner.

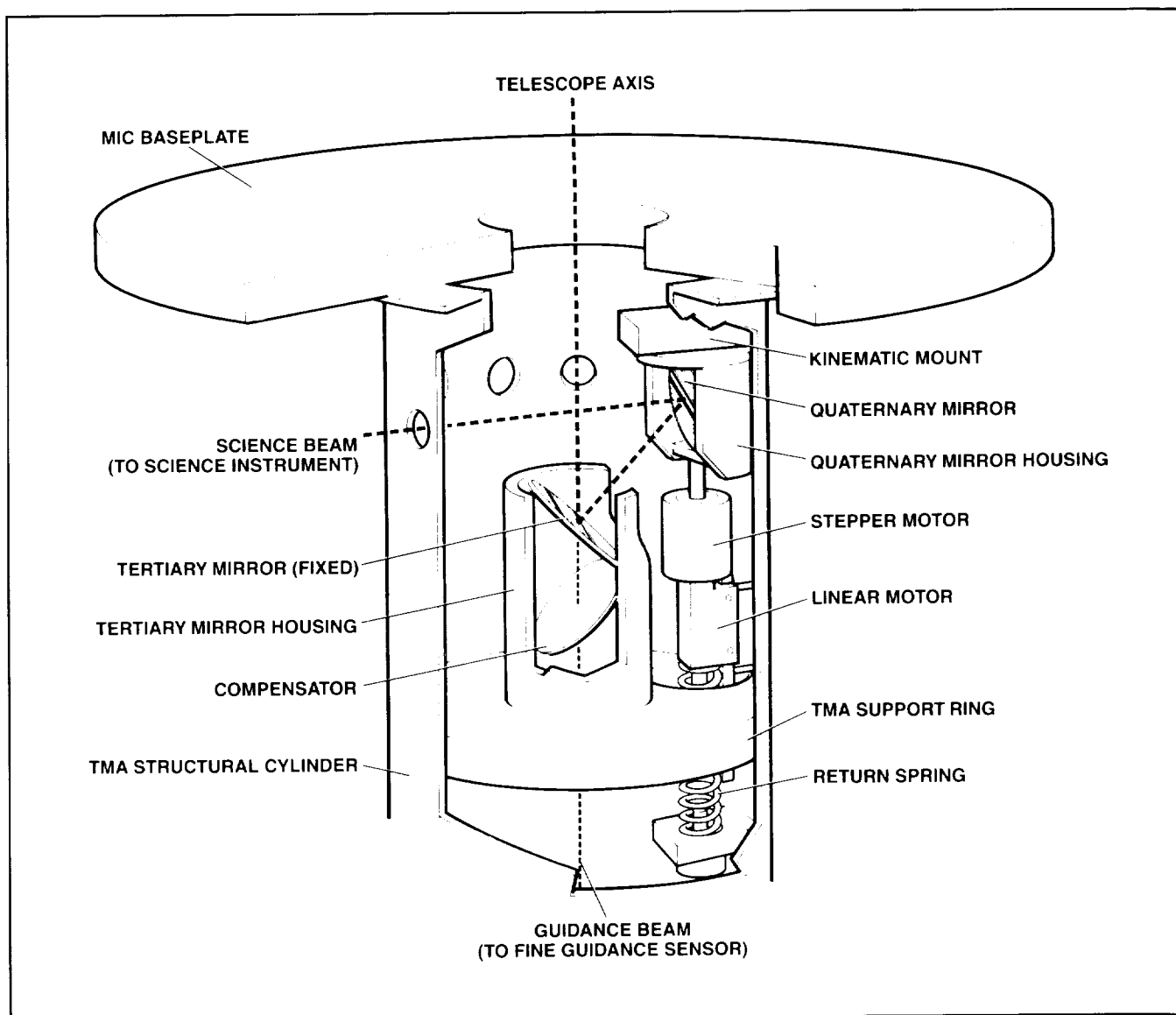
The third TMA design is called the small-tilt-mirror concept (third figure) and is an attempt to reduce the overall motion required of the TMA. For the small-tilt concept to be feasible, the tertiary mirror will have to move down farther into the instrument chamber, which increases the back focal distance. The small-tilt concept uses tangential rod flexures to support the tertiary mirror and compensator. The two are tilted at a small angle (<10°), using linear actuators which press locator balls against finely machined surfaces (kinematic design). When contact is achieved with these stops, the mirror and compensator are aligned. The design minimizes friction surfaces, but requires an additional reflecting surface and increases the back focal distance.

Almost all designs make use of relatively common engineering hardware and have no power dissipation or jitter in their aligned positions. The TMA design program should provide precision instrument designers with a range of developed cryogenic technologies that allow highly repeatable, minimal power-dissipation mechanisms. This program is being managed by the Infrared Astronomy Projects Office in collaboration with the Stanford University Mechanical Engineering Department's Center for Design Research and the Artificial Intelligence Research Branch.

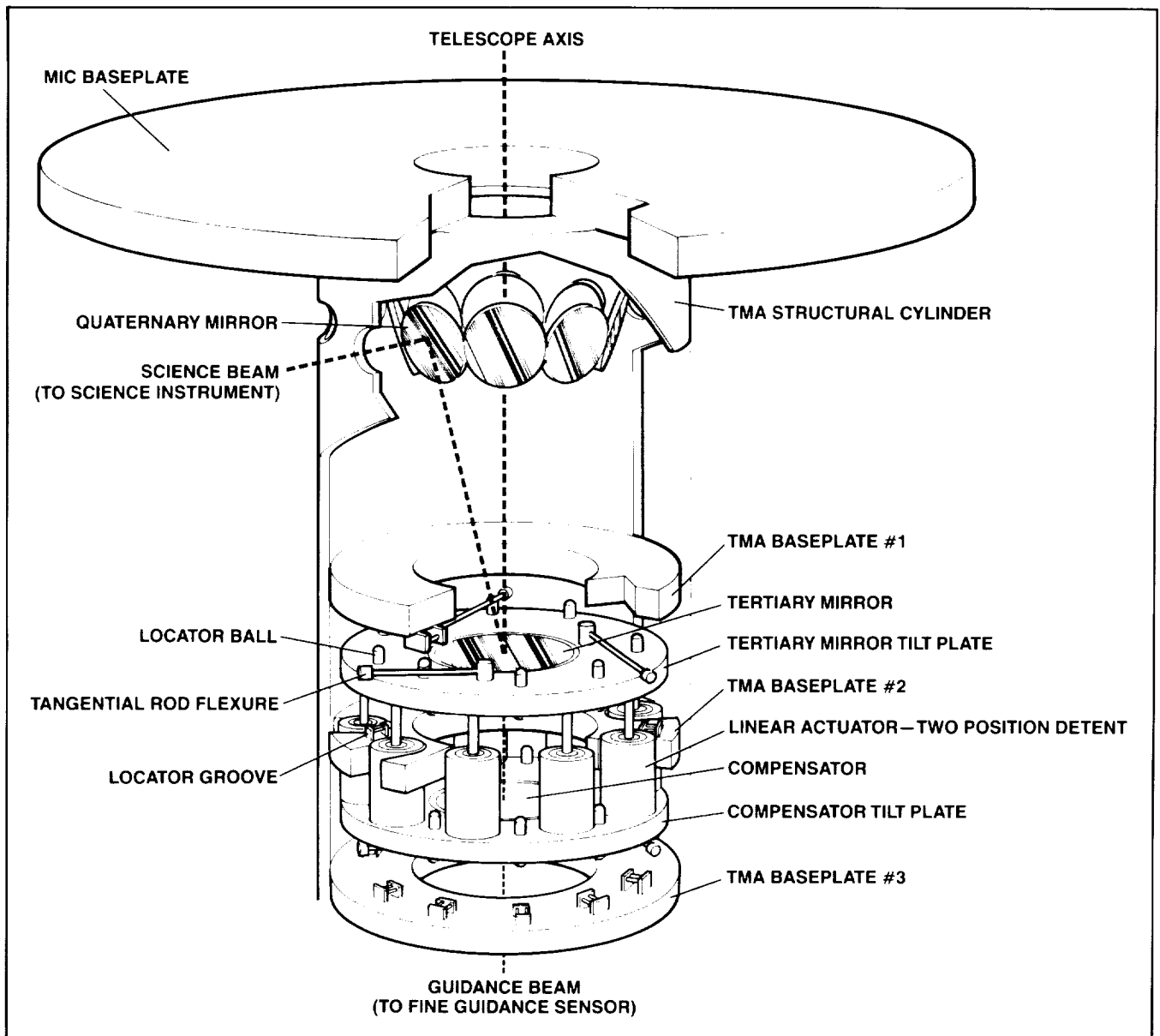
(M. Sullivan and J. Lee, Ext. 5914)



Tertiary mirror assembly—rotating-mirror concept



Tertiary Mirror assembly—drop-mirror concept

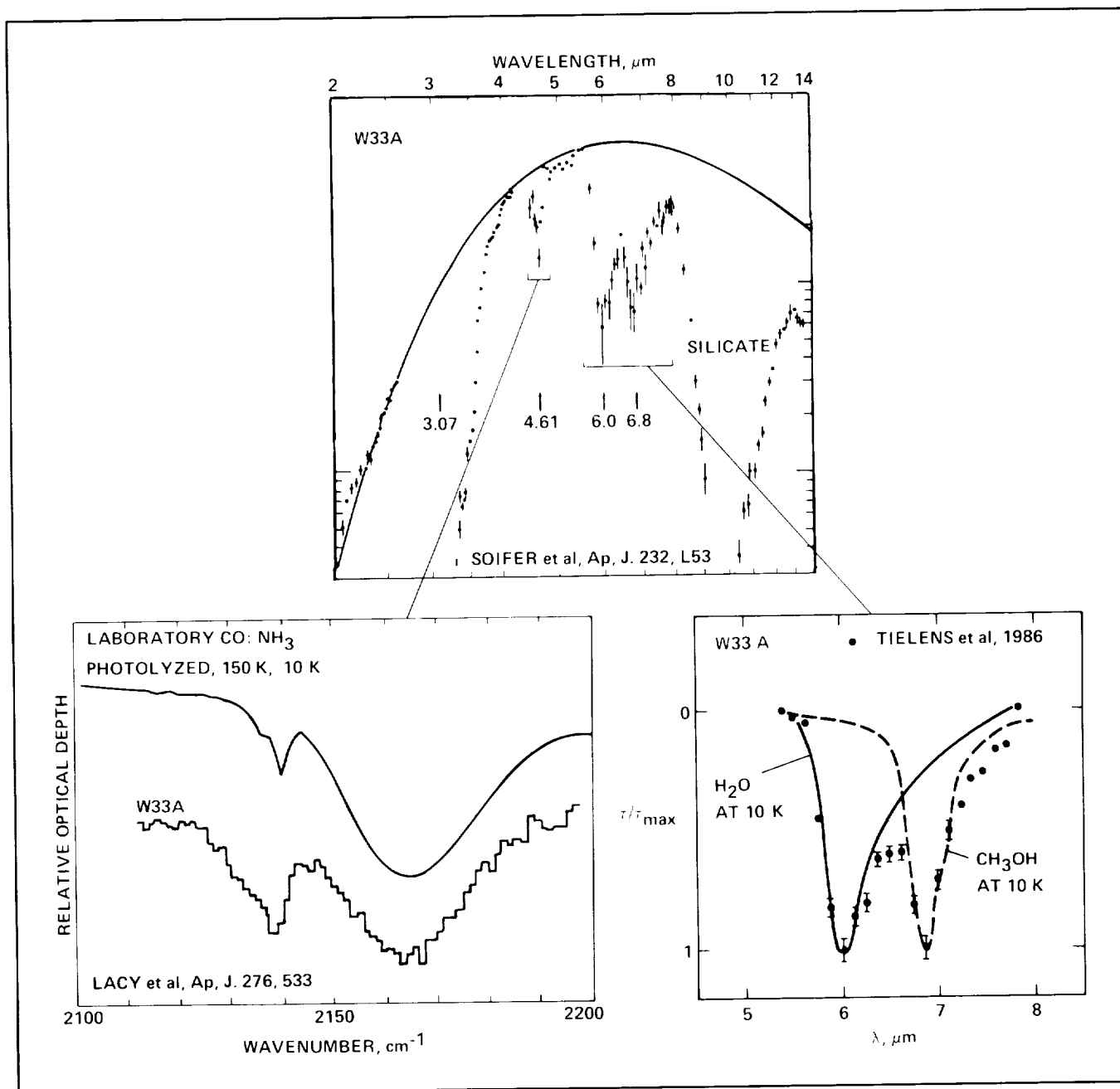


Tertiary mirror assembly—small-tilt-mirror concept

The Laboratory Study of Cometary and Interstellar Ice Analogs

During 1988 we made substantial progress in synthesizing ices believed to be important constituents of interstellar dust and comets. The spectra of these laboratory-made ices are compared to spectra taken using NASA's Kuiper Airborne Observatory

(KAO) stationed at Ames Research Center and NASA's Infrared Telescope Facility (IRTF) in Hawaii (as well as telescopes around the world). When it is found, after trial and error, which laboratory sample spectrum best matches the interstellar spectrum, we then know the constituents of interstellar and cometary material. In past years we have shown that KAO data (taken by using the Witteborn-Bregman spec-



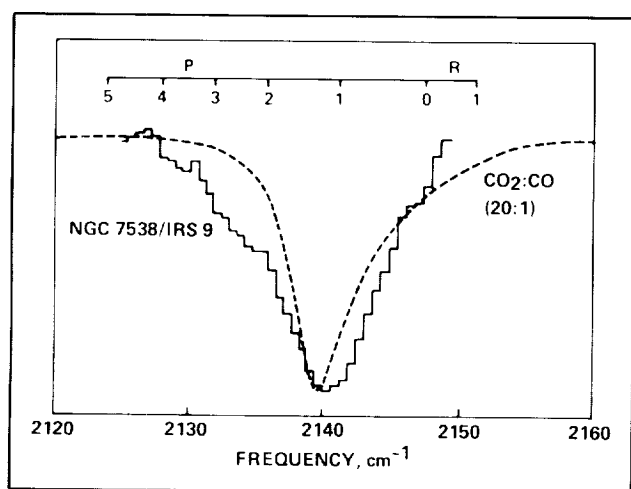
W33A is an infrared source in a dense molecular cloud. The comparisons between the laboratory spectra and the interstellar spectra show how well we can simulate the important conditions in space

trometer) indicate methanol (CH_3OH) to be a major constituent of interstellar and cometary ice, and not methane (CH_4) as was previously believed. Without these laboratory data, it is impossible to correctly interpret these observations.

In 1988 as well, we also made a very important finding. Laboratory simulations reveal that the spectrum of CO frozen in H_2O ice is different from the spectrum of CO when it is frozen in ices composed of CO_2 , O_3 , and other non-hydrogen-containing materials. IRTF observations carried out as a result of those experiments show that, in deep space, CO is not always frozen in H_2O ices; it is also in ices made up primarily of CO_2 -like molecules. This was a very fundamental observation because it showed, for the first time, that hydrogen is not important in determining the ice composition in all parts of space (as has been assumed for over 40 years); chemistry dominated by oxygen and carbon can also be important.

This information will have a strong impact on our understanding of the chemistry in molecular clouds that form before planets and comets form. It will guide instrument design for missions such as NASA's Space Infrared Telescope Facility, Comet Rendezvous and Asteroid Flyby, and the Comet Sample Return Mission.

(L. Allamandola, Ext. 6890)



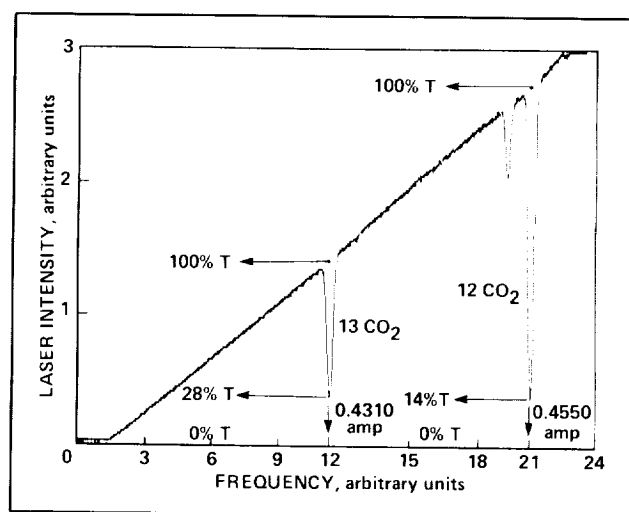
The infrared spectrum of solid CO in the interstellar object NGC 7538 (solid) is compared to the spectrum of CO frozen in CO_2 (dotted). This unexpected result shows that nonwater-rich ices are very important in space

Isotopic Ratio Measurements Using a Diode Laser Spectrometer

Semiconductor diode laser technology has now developed to the point where it can be realistically considered for application as a high-resolution molecular spectrometer that is reliable, lightweight, and flightworthy. Such a spectrometer can be used as a gas detector; moreover, it will have the capability to measure stable isotopic ratios without the problem of interference from impurity gases.

Using a lead-salt tunable diode laser, we have unambiguously identified two CO_2 rotational lines. These lines are in the $4.3\text{ }\mu\text{m}$ region of the spectrum, where $^{12}\text{CO}_2$ and $^{13}\text{CO}_2$ lines overlap in such a way that they have approximately equal absorbance at the expected isotopic concentrations of CO_2 on Earth and Mars. These two lines, P(37) of $^{12}\text{CO}_2$ at 2303.6953 cm^{-1} and R(28) of $^{13}\text{CO}_2$ at 2303.5301 cm^{-1} , can now be used to measure isotopic ratios of carbon in planetary samples when the carbon has been combusted to CO_2 . The effect of pressure on the line widths has been studied to further characterize these lines. Preliminary data suggest that it is possible to measure isotopic ratios over a wide range of gas pressures without any adverse effect on precision.

This technique can be extended to isotopic ratio measurements of other elements. Especially interesting is $^{14}\text{N}/^{15}\text{N}$, since this ratio may be useful in



Absorption of laser emission by the R(28) and P(37) lines of $^{13}\text{CO}_2$ and $^{12}\text{CO}_2$, respectively

dating Martian samples. The nitrogen isotopic ratio on Mars is significantly different from that on Earth, and it has been suggested that this ratio on Mars may have changed over the life of the planet, thus providing a means of dating Martian samples.

Furthermore, in addition to characterizing planetary samples (such as rocks and minerals) on Earth and on Mars, tunable diode laser spectroscopy has the potential of providing a technique to nondestructively measure the pressure and temperature of gases in laboratory applications, such as plasmas, shock tubes, and wind tunnels.

(J. Becker and C. McKay, Ext. 3213/6864)

Lightning Production of Hydrocarbons on Titan

Spacecraft observations show that lightning is present in many of the planetary atmospheres that have been observed. Theoretical calculations show that lightning in planetary atmospheres causes the formation and buildup of high-temperature compounds. Both field and laboratory measurements support these conclusions. Before the rise of life, lightning could have been even more significant in the evolution of the atmosphere by producing nitrogen compounds that were then rained out and deposited in the sea.

If the expected level of lightning activity is found in the atmosphere of Titan, then the results of laboratory measurements indicate that significant amounts of HCN, C₂H₆, C₂H₄, C₂H₂, and C₃H₈ are being formed in Titan's atmosphere. However, laboratory measurements are in disagreement with models based on equilibrium chemistry in the shock wave that is radiated by the lightning discharge column. Previous equilibrium chemistry models do not consider kinetic chemistry, nor do they consider the cooling core of the discharge. For this reason we have constructed a kinetic model of the chemistry occurring both in the shock wave and in the expanding core. A comparison of the laboratory measurements with the predictions of this model shows much better agreement than with the predictions of previous chemical equilibrium models.

(W. Borucki, Ext. 6492)

Star Sensor Search for Venusian Lightning

The existence of lightning activity on Venus is controversial. To help resolve the controversy, the Pioneer Venus Orbiter is being used to search for optical pulses from lightning flashes. During the spring of 1988, the star sensor was programmed to search the night side of Venus for 28 minutes near periaapsis for each of 90 orbits. Because the spacecraft rotates, the field of view of the star sensor is on the planet for only 50 seconds per orbit. Approximately 2% of the surface area of Venus is observed during each orbit. Nearly two-thirds of the total surface area between latitudes 40° south to 70° north was sampled at least once. Data analysis is under way.

(W. Borucki, Ext. 6492)

Clay Energetics

Among other goals, the Exobiology Program at Ames Research Center is charged with studying the origin, evolution, and distribution of life in the universe. Paradigms for modeling chemical evolution are based on the assumption that congruence must have existed between the geological conditions of the early Earth and those material and climatic requirements requisite for the prebiotic chemistry that precedes the development of cellular life forms. Modern paradigms for chemical evolution recognize the likelihood that much of prebiotic chemistry would have occurred at interfaces, rather than in single phases, and that the early atmosphere was not of a reducing nature.

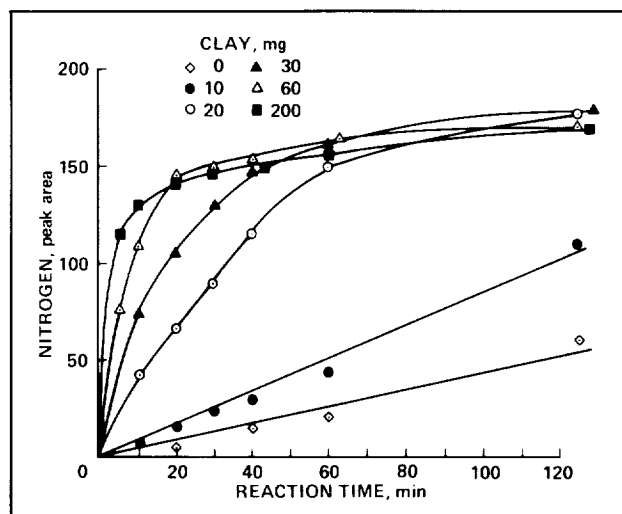
Mineral surfaces are excellent catalysts for organic chemistry. Among the more abundant and chemically active surfaces likely for the early Earth are clay minerals. A number of energy sources for driving prebiotic chemistry, which might have influenced the efficiency of mineral catalysts, are no longer as prevalent and they have been inadequately modeled by past laboratory studies. Among these energy sources are penetrating radiation and transmissible mechanical stresses. Clay minerals have an appreciable capacity for electronic energy stor-

age, which can be filled only by energy sources of the types mentioned. The impact of energy storage on the reactivity of clay surfaces has not been established, although much circumstantial evidence points to the conclusion that it must be significant.

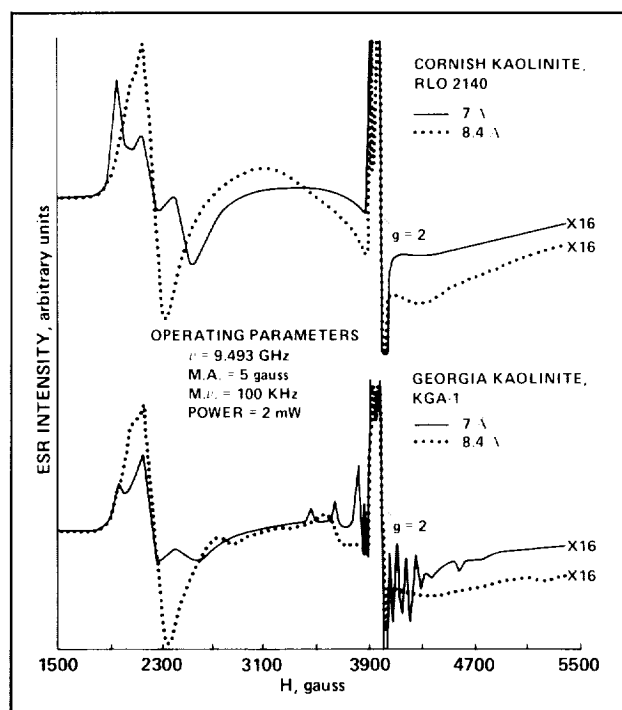
The following paragraphs will quantitate energy storage in clays, and help describe how energy is harvested, released, transduced, and used in the chemical reactions occurring on clay surfaces. The chemical reaction that has been chosen as a model for these studies is air-oxidation of hydrazine, which is the reverse of an important prebiotic chemical reaction—water splitting to produce reduced nitrogen. This reaction was chosen because wetting clays with hydrazine is associated with the release of substantial amounts of ultraviolet light, a novel phenomenon which is used to understand energy storage and release in clay minerals, and which may be a significant factor in understanding the mechanism of clay surface reactivity as well. Of necessity, several spectroscopic methods are also used in these studies: luminescence, electron spin resonance (ESR), and diffuse reflectance.

Studies developing the reaction protocol for measuring the rate of air oxidation of hydrazine were completed. Air oxidation was measured as a function of surface and structural iron content of the kaolinite, as determined by the relative intensities of the $g = 2$ and $g = 4$ ESR signals for iron. It was found that the oxidation rate was a strong function of the amount of kaolinite, over a broad range of kaolinite/hydrazine weight ratios, but the rate was more or less independent of iron content. A composite variable, total structural paramagnetism, composed of structural iron and stored electronic energy, was a preferable variable for correlating the rates. Results of these studies are summarized in the first figure.

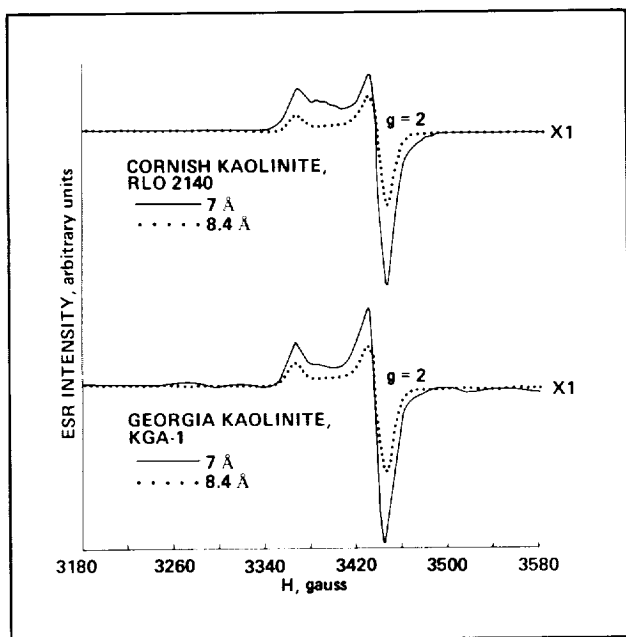
Studies determining a mutual dependence on interlayer hydration of the intensity of ESR signals for structural iron and stored electronic energy in kaolinites were completed and have proved the interdependency of a number of structural parameters of clays which are known, or postulated, to be of importance in clay surface reactivity. Therefore, models for surface reactivity cannot be developed without consideration of these parameters, which previously were thought to be independent of each other. Stored energy is one of the interdependent parameters, as are the ligand environment of structural iron and the degree of interlayer hydration.



Time profiles of the rate of oxidation as a function of the amount of Cornish kaolinite. The initial oxidation rate increases over the entire range of weights examined



Effects of intercalation of water on the ESR spectra attributable to structural ferric iron in two kaolinites. When measured shortly after preparation, the structural iron signal closely resembled that of the parent kaolinite. After several years, the complexity of the signal which has been associated with the degree of crystallinity in 1:1 clays deteriorated from that of the highly crystalline parent to that more characteristic of a natural halloysite



Effects of intercalation of water on the ESR spectra attributable to O^- -centers in two kaolinites. As in the case of the ESR signal from the structural iron, the initial signals much more closely resembled that of the parent material. Only after an extended interval between preparation and measurement can the diminution of the O^- -center signal be ascertained

The next figure shows the ESR signals associated with structural iron in two sets of hydrated, then aged, kaolinites. The last figure shows the ESR signals associated with stored energy in the same kaolinites. In the same time required to produce these changes, the capacity of these materials for emitting light upon drying is lost.

(L. Coyne, Ext. 5968)

Mars Exobiology Research Consortium

Determining whether there are clays on Mars, and estimating their abundance, is of particular interest because the presence of Martian clays would aid in resolving several dilemmas posed by the Viking analysis. The presence of clays would definitely establish the past existence of copious Martian water, and the clays would serve as reservoirs for

the vast inventory of Martian iron which is consistent with the Martian reflectance signature. The presence of clays could also explain much of the Viking surface chemistry, and the clays very likely have properties that will aid in determining the radiation history of the planet.

There is considerable controversy about the plausibility of finding substantial amounts of clays on Mars. A synthesis of information obtained from Viking analyses of surface elemental composition, simulations of Viking surface chemistry, geological considerations of the origins of clays, the probable history of Mars, and reflectance signatures of Mars would indicate a high probability for there being substantial amounts of clays on Mars. However, studies based simply on Martian surface reflectance have indicated that the diagnostic absorbance band for clays occurring at 2.2-2.3 micrometers is weak, and is in the region expected for iron or magnesium structurally substituted clays. However, many factors are known to suppress the intensity of bands in the near-infrared region of the spectrum, for which the ground-based data is either scanty or nonexistent.

The results shown are the initial results of the application of Near Infrared Reflectance Analysis (NIRA) to the spectroscopic characterization of a group of Mars Soil Analog Materials (MarsSAM). NIRA is a statistical spectroscopic method, developed by Karl Norris of the U.S. Department of Agriculture in the 1960s, which has been successfully applied in industry and agriculture to quantify individual constituents of multicomponent mixtures. It has not previously been applied to soil analysis. Independently determined values for various constituents of interest are used to determine analytical wavelength regions in which the amount of the constituent can be reliably quantitatively correlated with near-infrared diffuse reflectance data.

We have applied the method to the determination of analytical wavelengths for quantifying exchangeable iron and adsorbed water content in a series of variably Fe/Ca-cation-exchanged montmorillonite clays under conditions of varying relative humidity. We have found linearity of the absorbance, as a function of total iron over a range of exchangeable iron from 0-100% of the exchange capacity (1% to 7% total iron as Fe_2O_3), and as a function of water content over the range of relative humidity from 0-100%.

Among known materials suppressing contrast in spectral bands in the visible range are iron oxides. Our 1986-1987 studies and a variety of effects of surface hydroxylation reported in the literature have led us to believe that the iron-rich clays may be strongly hydroxylated. Surface hydroxylation would broaden the water bands in the 1.9 region, perhaps enough to serve as a previously uninvestigated source of contrast suppression for the near-infrared clay diagnostic band. Such hydroxylation might be, to some extent, irreversible. A long-term study of the spectra and reversibility of water adsorption on humidified iron-rich clays is planned.

(L. Coyne, Ext. 5968)

Particle-Gas Dynamics in the Protoplanetary Nebula

Over the last decade, a number of theoretical and observational studies have demonstrated the likelihood that flattened disks of dust and gas will form as a natural byproduct of stellar formation and have established their global thermal and dynamical properties. Collisional accretion of comet-sized planetesimals leads to the growth of solid planetary cores, followed by hydrodynamical accretion of nebula gas to form Jovian-type planets in the outer solar system. However, poorly understood stages connect these landmark events, and earlier stages of accretion are even less well understood. For instance, accretion of the planets has long been thought to result from settling of particulates into a layer that is sufficiently flattened so that gravitational instability may occur. However, gas drag and turbulent shear in and around the particle layer may result in diffusional spreading of the particle layer and prevent gravitational instability.

Clearly, a growing need exists for detailed theoretical and numerical modeling of the early nebula environment. Such modeling needs to adequately treat the processes occurring in a medium containing two distinct phases (gas and particles) which obey different forcing functions, but which are coupled by aerodynamic drag and are therefore able to influence each other's dynamical properties. We have been developing such a model in stages, and propose to

continue to do so, by drawing on our existing expertise in state-of-the-art computational fluid dynamics techniques and particle disk dynamics. Although the fullest and most detailed physics is never incorporated into the first version of any model, we have made a good beginning within a framework that is sufficiently general for all relevant physics to be ultimately represented.

During 1988, we developed a two-dimensional numerical model which obtains the two-phase dynamical behavior of the coupled gas-particle protoplanetary nebula. Our code uses a perturbation technique and several different parametrizations for the turbulence which have been successfully used in many similar situations in the past. We have now compared our code with previous analytical solutions in the inviscid (laminar) limit, with excellent agreement. The nebula gas, in general, is partly pressure-supported so that it orbits at a slightly slower rate than the particles. However, as the particles settle toward the midplane under gravity, their density begins to dominate. As the mass-dominant particles drive the locally intermingled gas at their higher orbital velocity, significant vertical wind shear is produced relative to the more slowly rotating pressure-supported gas above.

Previous inviscid models have been unable to predict the turbulence which will result from this shear at all, let alone in a fully self-consistent way. Our models use standard parametrizations of shear-driven turbulence. However, diffusive transport of the particles is one step removed and requires introduction of a nondimensional "Schmidt Number," which depends on the fluctuation time scales of the turbulence and the "stopping time" of the particles (a function of their mass and size). We have begun to explore reasonable ranges of Schmidt Number and have found that diffusive expansion of the particle layer, preventing gravitational instability, is indeed possible for certain particle sizes.

Other interesting aspects of the coupled behavior of the system have become clear for the first time as well, such as a radial flow in the gas in the vicinity of the particle layer, caused by momentum transfer between the particle layer and the intermingled gas. We are exploring all of these issues in greater detail.

(J. Cuzzi, Ext. 6343)

Planetary Ring Structure and Dynamics

Planetary rings as a class share many structural similarities, and presumably share similar controlling processes. The differences we see between the broad, opaque rings of Saturn; the nearly transparent rings of Jupiter; the dark, narrow rings of Uranus; and the incomplete ring arcs of Neptune may testify either to significantly different conditions of formation or merely to different operations of otherwise similar processes in different environments. Since the Voyager encounters with Jupiter (1977), Saturn (1980-81), and Uranus (1986), our understanding of ring structure has been greatly enhanced. From an understanding of the structure and dynamics of planetary rings, we hope to gain insight into the process by which planets form from their own protoplanetary particle disks. In several of the projects described below, faculty and student collaborators from Stanford University, Indiana University, and Cornell University have played important roles.

Planning for the Voyager Neptune encounter occupied a large part of our activity in FY 1988. The existence of narrow, incomplete partial ring "arcs" in the vicinity of Neptune's Roche zone is fairly well established, but nothing is known about their orbital or photometric properties. This lack of knowledge and the fainter illumination at Neptune than at previous encounters have caused us to adopt a survey-type imaging exploration of the inner Neptunian system. We do hope to place important new constraints on the existence of rings, ring arcs, and ring moons in the appropriate region, but we do not expect them necessarily to appear strikingly photogenic.

As one new insight leads to another, we are beginning to find several important ways in which the incessant "rain" of meteoroids can affect the structure and composition of the rings; this is especially true for Saturn's rings because of their enormous surface area.

Since 1982 we have been developing a numerical model for the redistribution of ring material following meteoroid impacts. Most of the bombardment is characterized by submillimeter-sized grains impacting ring particles from a centimeter to several meters in size; it has the aspect of cratering events for which the ejecta distribution is fairly well under-

stood. Our model includes a realistic parametrization of this ejection process, and carefully tracks the orbital trajectories of the ejecta to demonstrate how they redistribute mass and angular momentum within the rings. This redistribution is substantial, and produces nonintuitive but characteristic structure which is intriguingly reminiscent both of the well-known but poorly understood "record-groove" structure of Saturn's rings and of the curiously similar but completely mysterious structure inward of the inner edges of the A and B rings.

Another, related effect which we studied in 1988 is the compositional change caused by meteoroid infall. Saturn's rings are, at present, mostly icy material—thought to be greater than 90% water ice by mass—but a small amount of nonicy impurities is indicated. This year, members of our group carefully determined the ring particle brightness from Voyager observations, and modeled the dependence of ring particle brightness on the fraction of likely impurity material. If the mass infall rate of (presumably primitive carbonaceous) meteoroid material is as large as is currently believed, the estimated current fraction of nonicy material would be deposited in a period of only 1-10% of the age of the solar system. This puzzle is unsolved.

Yet one more related process involving meteoroid impact implies an extremely short evolutionary timescale for ring systems in general. In 1988, we showed that an aberration of the incident meteoroid flux, by the combination of a planet's orbital motion and that of its ring particles, creates an asymmetry in the deposition of angular momentum in the ring. This asymmetry can cause an inward evolution by the full ring width in the age of the solar system.

A final interesting byproduct of our aberration modeling is that impacts in the rings of relatively large meteoroids (10-cm radius) have the appropriate distribution with orbital longitude to help explain the mysterious "spokes" in the rings. However, this is only if the meteoroids are on nearly isotropic Oort Cloud-type orbits instead of low-inclination, prograde orbits. Further study of these various phenomena may produce greater insight into the distribution of the "debris" remaining from the creation of the planets.

Results in 1988 on meteoroid impact processes, and our less recent studies of spiral wave momen-

tum transport, have indicated that the current ring systems are probably highly evolved and structurally quite different from any possible "primordial" state. However, we are not yet convinced that all ring systems are geologically "young." As-yet-unknown stabilizing processes may be in force. We are seeking evidence for these as yet unrecognized processes observationally.

One such stabilizing process could involve a considerable amount of hidden mass in the rings, acting as ballast to slow the response of the ring to ongoing transfer of angular momentum. The hidden mass could be in the form of a myriad of small satellites with sizes between 1 and 10 km. We discovered one such "moonlet" inferentially from Voyager imaging and the occultation measurements of its perturbations of local ring structure. It lies within, and causes, the 325-km-wide Encke Gap in the outer part of Saturn's rings by a "shepherding" process which acts to repel nearby ring material. The mere presence of such large objects within the rings is inconsistent with local formation, because of the inability of large objects to grow in the presence of strong planetary tidal forces (the "Roche limit"), as well as the obvious difficulty of growing a moonlet in an empty gap which it creates itself. About a dozen similar gaps in the rings may be caused by similar, but smaller, moonlets.

In 1988 we published a related hypothesis which advocates the existence of a 1000- to 2000-km-wide "moonlet belt" of unseen 0.1- to 1-km-radius objects lying in the vicinity of Saturn's peculiar "kinky" F-ring. The primary evidence for these objects is the existence of several prominent and nonaxisymmetric depletions of magnetospheric electrons as measured by the close-approaching Pioneer 11 spacecraft. Our hypothesis presents a novel framework for explaining the existence of incomplete "ring arcs" in other planetary ring systems as transient "clouds" or clumps of particulate material released during collisions between members of such moonlet belts. It may be that ring systems blend into such moonlet belts, and subsequently into smaller numbers of successively larger satellites, as one moves outward from the planet and disruptive planetary tidal forces weaken. In this regard, one of the more interesting results of the Voyager Neptune encounter will be the distribution of ring clumps and asteroid-sized moon-

lets orbiting between the planet and the larger "classical" satellites far from the planet's Roche limit.

Along with the theoretical work just described, we carry on a program of data analysis using interactive image display and analysis programs designed specifically for ring image data, and for complementary stellar and radio occultation data. The bewilderingly complex structure of the B and inner A rings is now under study, as are the details of their unexplained inner edges. New radiative transfer programs are under development to address aspects of ring reflectivity which may be nonideal, such as closely packed particles and variable vertical structure. Inferences into these properties are necessarily indirect, but are extremely important in terms of understanding particle random velocities and the "viscosity" and evolutionary history of ring systems. In addition, we are participating actively in the planning of Cassini, a joint NASA-European Space Agency mission to explore the Saturn system intensively in the early 21st century.

(J. Cuzzi, Ext. 6343)

Early Biological Evolution and Atmospheric Carbon Dioxide— Searching for a Link

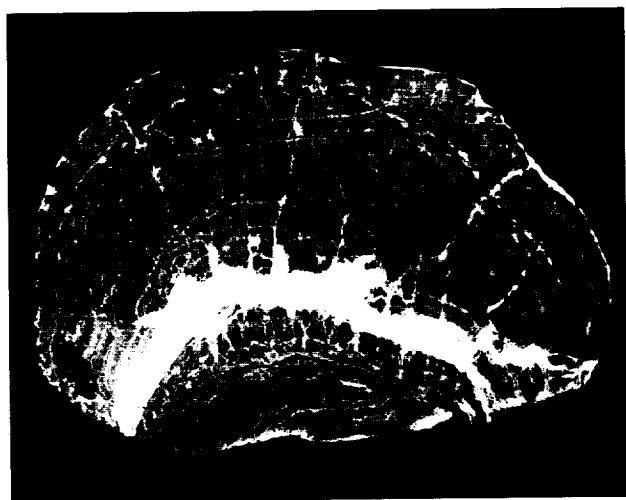
NASA's Exobiology Program supports research that explores the relationship between the origin and evolution of life and the origin and development of solar systems and planets. A key thrust of this research is to understand how planetary change affects biological evolution.

Geologists and atmospheric chemists have documented changes in the planet Earth during its 4.5-billion-year history. These changes include a decline in volcanism and an overall increase in both the mass and the land area of the continents. Volcanic gases and the weathering of rocks both exert strong influences upon the atmosphere. Indeed, earlier research at Ames Research Center illustrated how volcanos have helped to maintain atmospheric concentrations of carbon dioxide. Long-term changes in volcanism and land area probably have induced long-term trends in atmospheric composi-

tion. The most widely discussed of these trends has been a rise in oxygen levels and a decline in carbon dioxide levels.

Although the biological implications of increasing concentrations of atmospheric oxygen have been widely discussed, relatively little attention has been given to the decline in atmospheric carbon dioxide abundances. This decline must have been important biologically because photosynthetic organisms expend considerable amounts of energy to convert carbon dioxide to organic matter, and the amount of energy required increases as carbon dioxide levels decrease. The outcome of competition between organisms can be influenced by the efficiency with which competing biota convert resources, such as carbon dioxide and energy, into organic matter or biomass. Biological evolution reflects, among other things, the long-term consequences of competition between organisms.

To document the biological impact of changes in atmospheric carbon dioxide levels, investigators must search for and identify chemical changes, recorded in fossils, which were caused by changing carbon dioxide levels. Ames researchers have found that fossils of microbial communities, called stromatolites, are suitable test subjects for such a search.



Vertical cross section of a stromatolite (15 cm wide), showing the domical exterior shape and the internal laminations formed by successively deposited layers or "mats" of microorganisms. Many such stromatolites were found to contain organic matter deposited by ancient microorganisms (note dark layers in the figure)

These fossils, which are dome-shaped, laminated deposits found most frequently in limestones (see the figure), offer several advantages. They are the most abundant and ancient fossils known. They frequently grew in very shallow waters, in close contact with the ancient atmosphere. They have modern homologs, called microbial mats, whose constituent microorganisms and their responses to changing carbon dioxide levels can be investigated.

During 1988 we discovered that many stromatolites, some as old as 3.5 billion years, still contain remarkably well-preserved organic matter that was laid down by the original photosynthetic organisms. Such organic matter can be obtained from stromatolites having a variety of ages, which enables researchers to search for time-related trends in chemical composition. Indeed, a trend over time in the stable carbon isotopic composition of this organic matter has been found.

The abundance ratio of the heavier carbon isotope to the lighter isotope ($^{13}\text{C}/^{12}\text{C}$) has increased from 2.7-billion-year-old stromatolites to modern, living microbial mats. This trend in $^{13}\text{C}/^{12}\text{C}$ might have recorded a decline in the availability of carbon dioxide in ancient and modern shallow-water environments. Such microorganisms prefer to assimilate the ^{12}C isotope, but, if carbon dioxide supplies become limited, they will utilize more of the ^{13}C isotope. Thus, as atmospheric carbon dioxide levels declined, the $^{13}\text{C}/^{12}\text{C}$ value in stromatolitic organic matter might have increased accordingly.

Many of the well-preserved rock samples were discovered in Australia and North America, in collaboration with Dr. J. W. Schopf and others at the University of California, Los Angeles. These samples will be examined further to test the hypothesis that a meaningful relationship exists between the observed carbon isotopic trend and the proposed long-term decline in concentrations of atmospheric carbon dioxide.

(D. Des Marais, Ext. 6110)

Small-Particle Research on the Space Station

A wide range of fundamental scientific problems involving interactions between small particles can be

ORIGINAL PAGE
BLACK AND WHITE PHOTOGRAPH

addressed by conducting particle experiments in the microgravity environment of the Space Station.

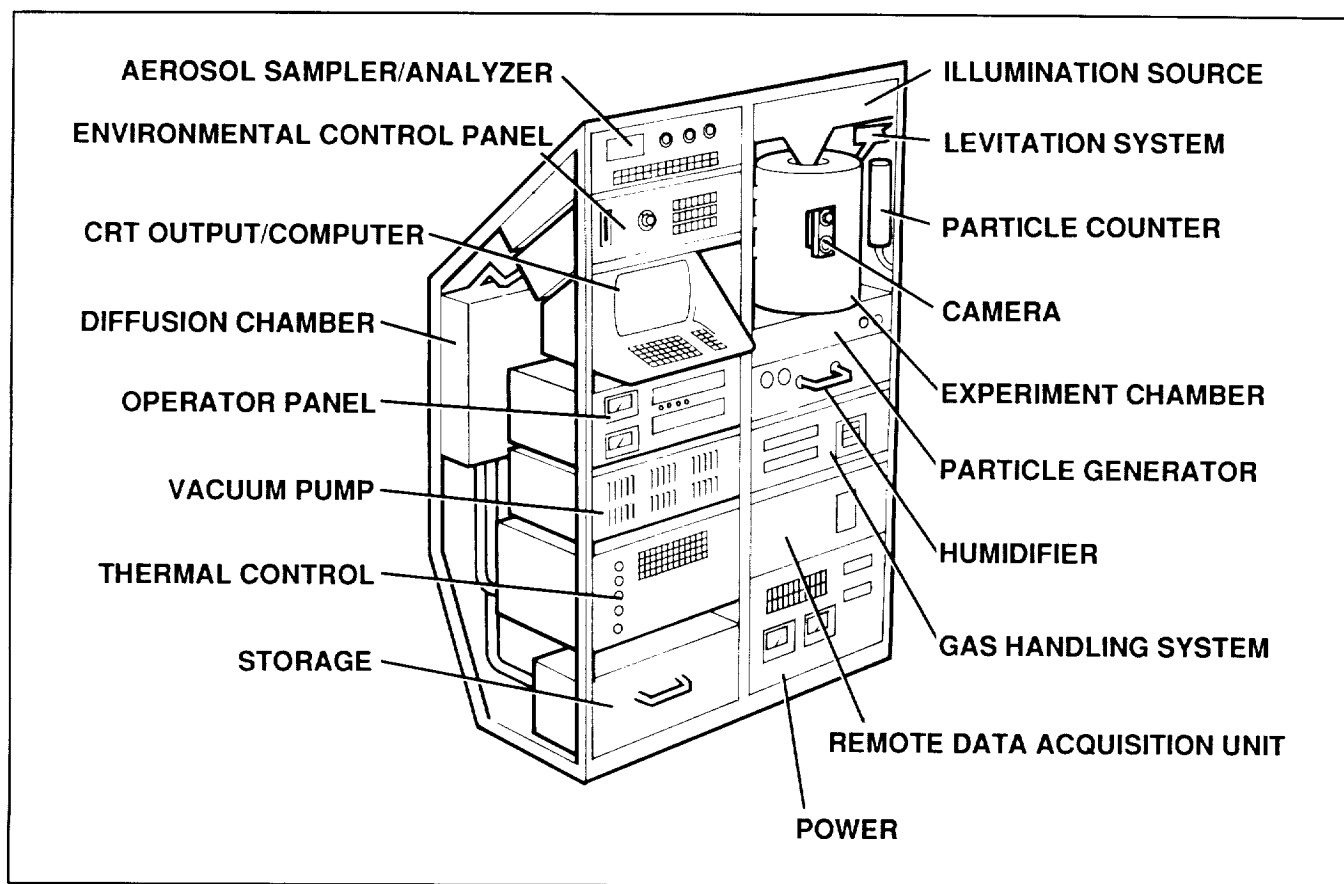
Examples of such experiments suggested by scientists at Ames Research Center include the following:

1. Particle-aggregation studies relevant to hypotheses concerning phenomena such as nuclear winter, species extinction caused by climatic changes, effects of volcanic eruptions, and the duration of Martian duststorms,
2. Investigations of the synthesis of amino acids (as well as other complex organic compounds necessary for the origin of life) on the surfaces of growing particles,
3. Determination of the growth, optical properties, and chemical composition of the organic aerosols produced in Titan's atmosphere by simulating the organic haze production in Titan's atmosphere,
4. Studies of dipolar grain coagulation and orientation as a possible mechanism for polarization of starlight shining through interstellar and intergalactic dust clouds,

5. Simulation of radiative emission by particles in various astrophysical environments, such as circumstellar shells, planetary nebulae, and protostellar disks.

Many other microgravity particle experiments have also been suggested by other NASA and university scientists representing such diverse disciplines as exobiology, planetary science, astrophysics, atmospheric science, and basic physics and chemistry. These experiments have in common the requirement that they be performed in an extremely low gravity ($<10^{-4}$ m/sec²) environment. For example, in many cases the microgravity environment is required because the particles must be suspended for times substantially longer than possible in Earth-based laboratories.

Ames Research Center is developing an interdisciplinary research facility, the Gas-Grain Simulation Facility (GGSF) (see the figure), for conducting small-particle research in the microgravity environment of the Space Station. The development of this



Gas-grain simulation facility

facility is sponsored jointly by the Life Sciences Division and the Solar System Exploration Division at NASA Headquarters.

The purpose of the GGSF is to simulate and study, in a microgravity environment, fundamental chemical and physical processes involving particles in the submicron- to millimeter-size range. Processes such as nucleation, growth, coagulation, condensation, and low-velocity collisions will be studied using this facility. The GGSF will occupy approximately 3.5 m³ and will provide the following: (1) an experiment chamber (4- to 10-liter internal volume); (2) environmental control subsystems (e.g., temperature, pressure, gas mixture, and humidity); (3) mechanisms for particle production, positioning, and removal; (4) measurement equipment (e.g., video cameras, optical particle counters, spectrometers, and photometers); and (5) energy sources. This facility will provide a means for extending existing ground-based experimental programs to a new domain.

Previously, Ames brought together scientists from a number of disciplines to determine the science requirements of the GGSF. Two workshops led to the establishment of a science community interested in microgravity particle research on the GGSF and to the collection of a data base of candidate GGSF experiments. In 1988, a number of theoretical and computer calculations were performed to analyze this set of candidate experiments and to refine the GGSF science requirements. These activities were conducted in preparation for response to the Space Station Pressurized Payloads Announcement of Opportunity, expected to be released early in 1989.

(G. Fogleman, J. Huntington, and G. Carle,
Ext. 4204/3675/5765)

Minerals as a Source of Free Oxygen in Planetary Evolution

The geological record indicates that the global-oxidation state of the Earth has risen slowly but continuously. While the present high level of atmospheric free oxygen, about 20%, is most certainly the result of the photosynthetic activity of plants, there

must have been a time when life had not yet "learned" to convert CO₂ and H₂O into organic matter and O₂ by using sunlight as an energy source. The question which forms the basis of our research is: Which reactions were responsible for the slow oxidation before the advent of photosynthesis, or is photosynthesis as old as the geologically documented Earth?

One abiogenic method for introducing oxygen into the atmosphere is by photolysis of traces of H₂O vapor in the stratosphere, where hard ultraviolet radiation from the Sun is available. Since hydrogen atoms escape into space, such a photolysis must accumulate oxygen in the atmosphere. Much hope had been attached to this reaction as being the most likely mechanism for the slow oxidation during the first 2- to 3-billion years of the Earth's recorded existence. Recent more refined model calculations for the early atmosphere, however, have dampened the expectations that stratospheric photolysis may have been productive enough to provide all the oxygen needed.

We have followed a completely different approach originating from research aimed at understanding defects and impurities in minerals. Among these impurities are traces of CO₂ and H₂O, which are incorporated by minerals deep in the Earth where the environment is dominated by hot, high-pressure H₂O- and CO₂-rich fluids.

When studying in greater detail the incorporation of H₂O and CO₂ into dense mineral structures, we found that they undergo surprisingly strange transformations. H₂O, for instance, first forms common hydroxyl anions (e.g., Si-OH), which have been known for many decades. In a second step, however, Si-OH pairs appear to convert into peroxy linkages Si^{OO}Si plus H₂ molecules. This is a mineral "water-splitting reaction." The incorporation of CO₂ is more complicated, but appears to lead to a similar "carbon-dioxide-splitting reaction" by forming Si^{OO}Si plus C.

These reactions occur internally at defects in the mineral structure, and are driven by thermodynamic nonequilibria which are common in the geological rock cycle. The elemental C precipitates out, while the mobile H₂ molecules escape from the mineral or react with the C to form organic matter. These abiogenic synthesis reactions clearly are of interest in the quest for the origin of life, which has been one of the

main thrusts of NASA-sponsored research for many years. These reactions may embody mechanisms to synthesize complex and stereospecific "organic" molecules which could be of particular interest in the development of earliest life forms.

The study of organic matter which may form abiogenically from minerals has met with severe experimental difficulties. Because it is difficult to separate small amounts of organic matter from natural minerals without contamination, we turned our attention to the other "half" of the H_2O and CO_2 splitting reactions, the peroxy entities $\text{Si}^{\text{OO}}\text{Si}$. Can we detect such peroxy in minerals and thus provide indirect support for the alleged abiogenic synthesis of organic matter?

As part of this effort, we developed a new technique, which we call Charge Distribution Analysis (CDA), that is apparently perfectly suited to the purpose. It uses one particular property of the peroxy predicted by theory—upon heating, the $\text{Si}^{\text{OO}}\text{Si}$ linkages break apart and generate two radical states, $\text{Si}-\text{O}^\bullet$, which represent positive holes in the mineral matrix.

Such positive holes are electronic defects which repel each other inside the mineral and so are forced to the surface where they impart a positive charge. We measure the charge by placing the sample on a sensitive balance in an inhomogeneous electric field. The field polarizes the sample—an effect which always leads to an attraction toward the bias electrode. If, however, the sample surface becomes positively charged and we apply a positive bias, the sample is repelled.

The first natural material we examined by CDA was obsidian, which is a volcanic glass widely associated with large-scale explosive volcanism. Chemically, it closely corresponds to the average composition of the continental crust. In some large volcanic eruptions, thousands of cubic kilometers of obsidian and its ejecta analogues, ash and pumice, are produced—thousands of times more than that produced during the eruption of Mount St. Helens in 1980.

Because obsidians erupt from a water-laden magma chamber, they are typically rich in dissolved H_2O and contain abundant $\text{Si}-\text{OH}$. By CDA we found that they also contain peroxy. The figure shows the apparent weight change as a function of the bias voltage. The strong repulsion which builds

up between 400° and 650°C provides evidence for highly mobile positive charges. Analysis of the data indicates that the charge carriers are positive holes which can only be generated thermally by dissociation of peroxy entities.

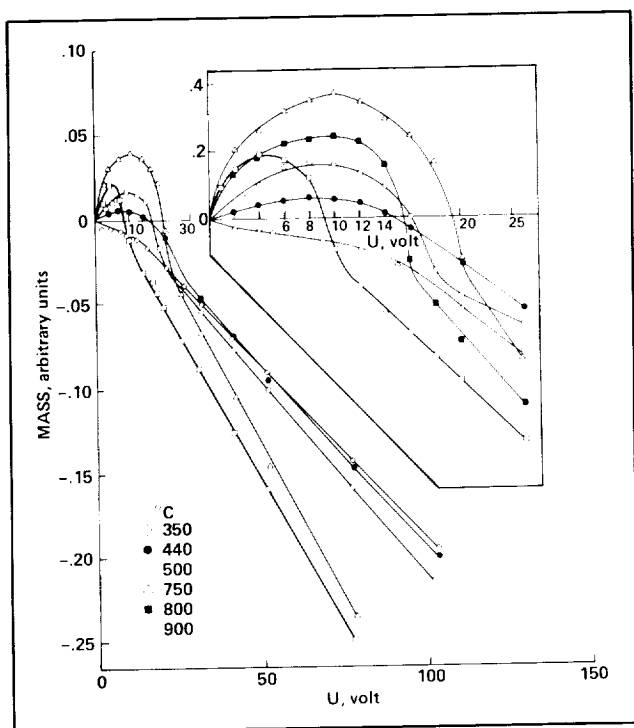
Other minerals in common rocks also appear to contain peroxy. This leads us to believe that peroxy "impurities" are extremely widespread and, hence, of global importance. To determine the peroxy content in minerals, we have also developed a wet chemical technique. The results are still somewhat preliminary but they indicate that the peroxy content in obsidian is about 0.01%. This may not appear to be a large amount, but we must look at this value in the context of the Earth as a whole.

The Earth has been volcanically and tectonically active over its entire recorded history, and it also has carried liquid water on its surface. Volcanoes and entire mountain ranges were continually eroded, and the debris, deposited into the ocean basins, was recycled through subduction and other mountain-building processes. The great cycle of uplift and subduction is estimated to take about 200 million years. This means that most of the continental mass currently available on the Earth has been recycled several times during the 3.7 billion years of Earth's history.

It also means that each cycle has reworked minerals which were potentially peroxy-containing. Upon weathering, they released hydrogen peroxide, which could be consumed as an oxidant (for instance oxidizing ferrous iron (Fe^{2+}) to ferric (Fe^{3+}), or it could decompose to yield free oxygen plus water.

By using estimates of the volumes of rock which currently weather every year, and some brave assumptions as to the validity of such estimates for the distant past, we can calculate how much oxygen would be injected into the geological environment, if the continental rocks contained on the average 0.01% peroxy. When added over 3 billion years, the quantities are enormous—sufficient to oxidize all the iron known to exist in ferric form in the iron-ore deposits in all the continents, with a remainder sufficient to raise the atmospheric oxygen level to about 1% of its present value.

The potential consequences are numerous. If the oxidation of the young planet Earth were largely controlled by peroxy release from minerals, early life (which in all likelihood originated in a nonoxidizing,



A charge distribution analysis of a volcanic glass, an obsidian from Glass Butte, OR, under positive bias at selected temperatures. The repulsion at low fields is evidence for a strong positive surface charge which grows dramatically above 400°C. This is indicative of positive hole charge carriers generated by peroxy dissociation

probably even reducing, environment) was under a constant constraint to adapt to a slowly rising oxygen level. In that case there would have been no need to "invent" photosynthesis early in the evolution of life in order to account for the observed global oxidation.

The presence of peroxy in minerals may also help us to better understand the highly oxidizing nature of Martian soil. Mars once possessed liquid surface water, and volcanic activity and weathering must have resembled that of early Earth. It is tempting to suggest that the oxidizing centers in Martian soil, detected during the Viking Mission, derived from structurally bound peroxy which the Martian minerals inherited from incorporated traces of H₂O.

Many more studies will be needed, but we appear to be on a promising road. Our capability to detect peroxy in minerals by a powerful novel physical technique, supplemented by an emerging chemi-

cal method, opens new vistas of knowledge of the evolution of Mars, of early Earth, and of the origin of life, which is still shrouded in mystery.

(F. Freund, Ext. 5183)

On Salt-Entrapped Bacteria, Evolution, and Martian Exploration

The ubiquitous energy-transducing ATPases appear to have originated early in the evolution of life. However, this notion is contradicted by the enzyme's complex structure and function. The study of the evolution of such complex biomolecules is confounded by the absence of a suitable fossil record because such molecules are extremely labile, barely survive the demise of their host, and leave no permanent record. Thus, studies of the evolution of macromolecular structures are horizontal rather than vertical (i.e., there is no well-defined time line). Clearly what is needed is an organism whose evolutionary clock has stopped running.

Salt crystals obtained from certain salt formations have been shown to contain viable bacteria which turn out to be extreme halophiles. These salt formations were laid down during the Triassic period, and there is reason to assume that the associated salt crystals were not subject to recent infiltration by either organic material or microorganisms. If this assumption is correct, the organisms found in these crystals were trapped in a nongrowing state for very long periods of time (possibly 200×10^6 yr). This has two implications for the NASA Program in Exobiology.

1. These bacteria represent "living fossils" whose biomacromolecules are available for study. These organisms may provide evolutionary biology with a time scale because their evolution was frozen for an extended time. We examined the ATPase from one of the organisms isolated from a salt crystal. This ATPase is structurally similar to the enzyme we characterized from a "contemporary" extreme halophile, from which it follows that this ATPase is similar to the halobacterial ATPase, but not to the ubiquitous energy-transducing ATPases. This suggests that the halobacterial ATPase may indeed be ancient (and not a product of recent evolutionary

change), and could well be an antecedent of the ubiquitous ATPase found in all other forms of life.

2. The other implication is related to the exploration of Mars. The absence of a recent history of water on the planet has led some to conclude that there is no extant life on the Martian surface and if life had ever arisen on the planet, it ended with the loss of liquid water. This is a logical conclusion based on the intuitive notion that life does not survive long in the absence of a food source. However, if organisms can indeed survive for extended periods without nutrients (as suggested by the presence of viable organisms in the salt crystals), then there is no a priori reason why a putative Martian biota could not also survive the last waterless episode on the planet. This possibility will have to be taken into account when developing strategies for Martian exploration, searching for life, and avoiding contamination of both the existing Martian life with terrestrial life and the terrestrial ecosystem with Martian organisms capable of survival and growth.

(L. Hochstein and H. Stan-Lotter, Ext. 5938/6052)

Are Magnesium Ions Primitive "Enzymes" in RNA-Type Replications?

To understand how the first living organism arose from "lifeless" chemicals, exobiologists must discover how important macromolecules, such as nucleic acids and proteins, were formed during the prebiotic era. A plausible pathway by which nucleic acids, the carriers of genetic information, may have been formed from simpler molecules in the absence of enzymes is via so-called "RNA-type replications." In this type of reaction, an RNA-type polymer serves as the template and directs the synthesis of its complementary daughter-polymer from its building blocks, the mononucleotides, available in solution. This polynucleotide-synthesizing system is similar to

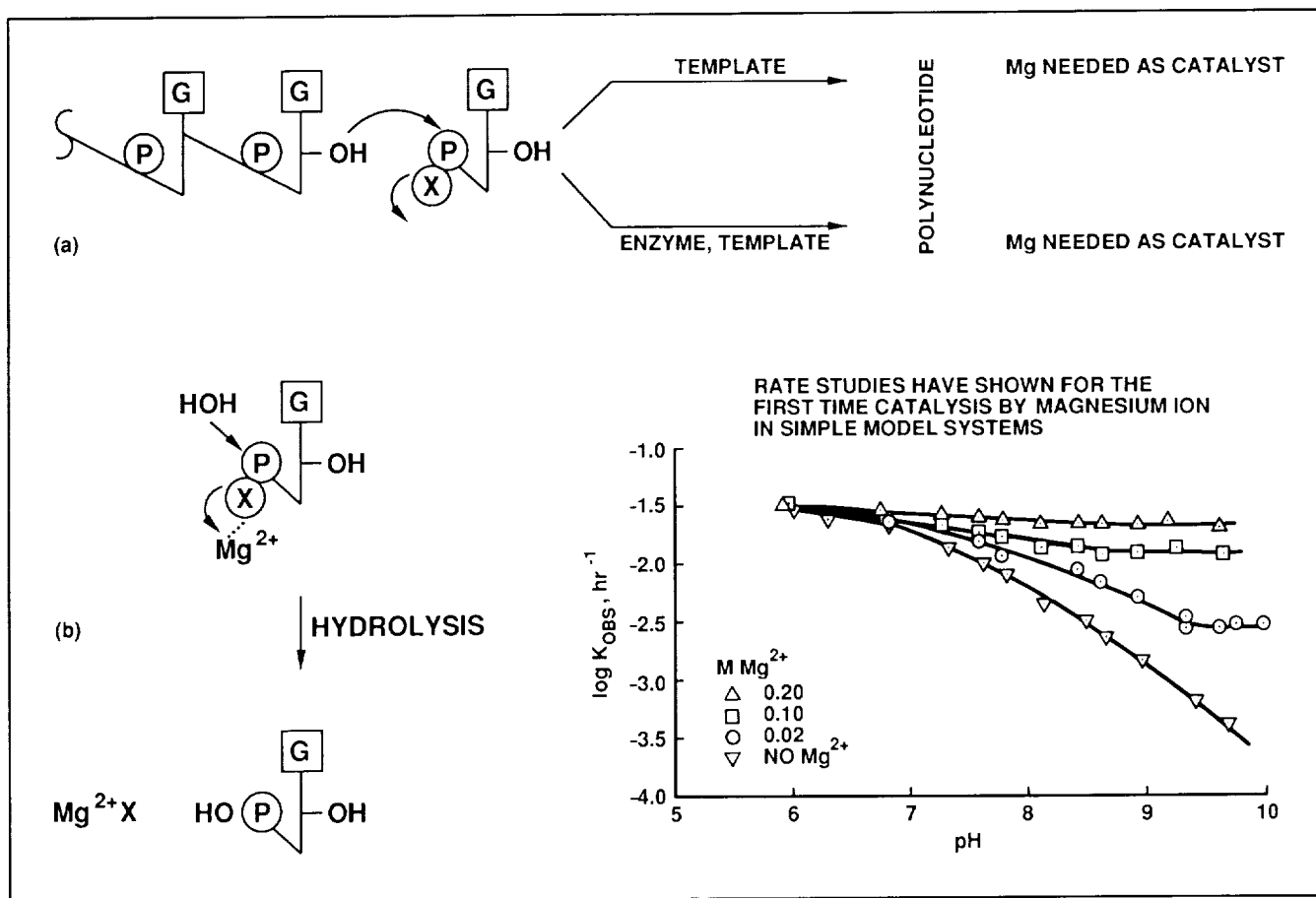
the naturally occurring, enzymatic (DNA/RNA replication) reactions, with the important difference that it is devoid of all enzymes.

One feature shared by both (i.e., enzymatic DNA/RNA and the nonenzymatic RNA-type replication reactions) is their dependence on magnesium ion. Since magnesium is necessary in both, this ion could be considered a primitive "enzyme." Even though the importance of magnesium in these reactions has been recognized for some time, the mechanism of its catalytic action has not been well established. This has been puzzling, because many studies in model systems that incorporate the phosphate group present in nucleotides showed the presence of magnesium inhibiting the reaction instead of acting as a catalyst.

This puzzle has now been partially resolved because of the discovery by investigators at Ames Research Center and the University of California at Santa Cruz of a model system that does exhibit strong catalysis in the presence of magnesium ion. This model system mimics the crucial step in the polynucleotide-synthesizing reaction where the OH group of a nucleotide attacks the phosphorus atom which leads to cleavage of the P-X bond and elongation of the nucleotide chain (see (a) in the figure). In the model system, attack on the phosphorus atom is initiated by the OH of the water molecule which results in hydrolysis (see (b) in the figure). Since chemically these reactions are so similar, the mechanism of the catalysis by Mg^{++} may reasonably be expected to be similar also.

A detailed kinetic study of the role of magnesium on the hydrolysis reaction is under way. In conjunction with a similar kinetic study on the polynucleotide synthesizing reaction, we hope to shed some light on the question of whether, in the presence of simply catalysts such as magnesium, "lifeless" chemicals really have the capacity to develop into complex molecules such as RNA and DNA.

(A. Kanavarioti and S. Chang, Ext. 6163/5733)



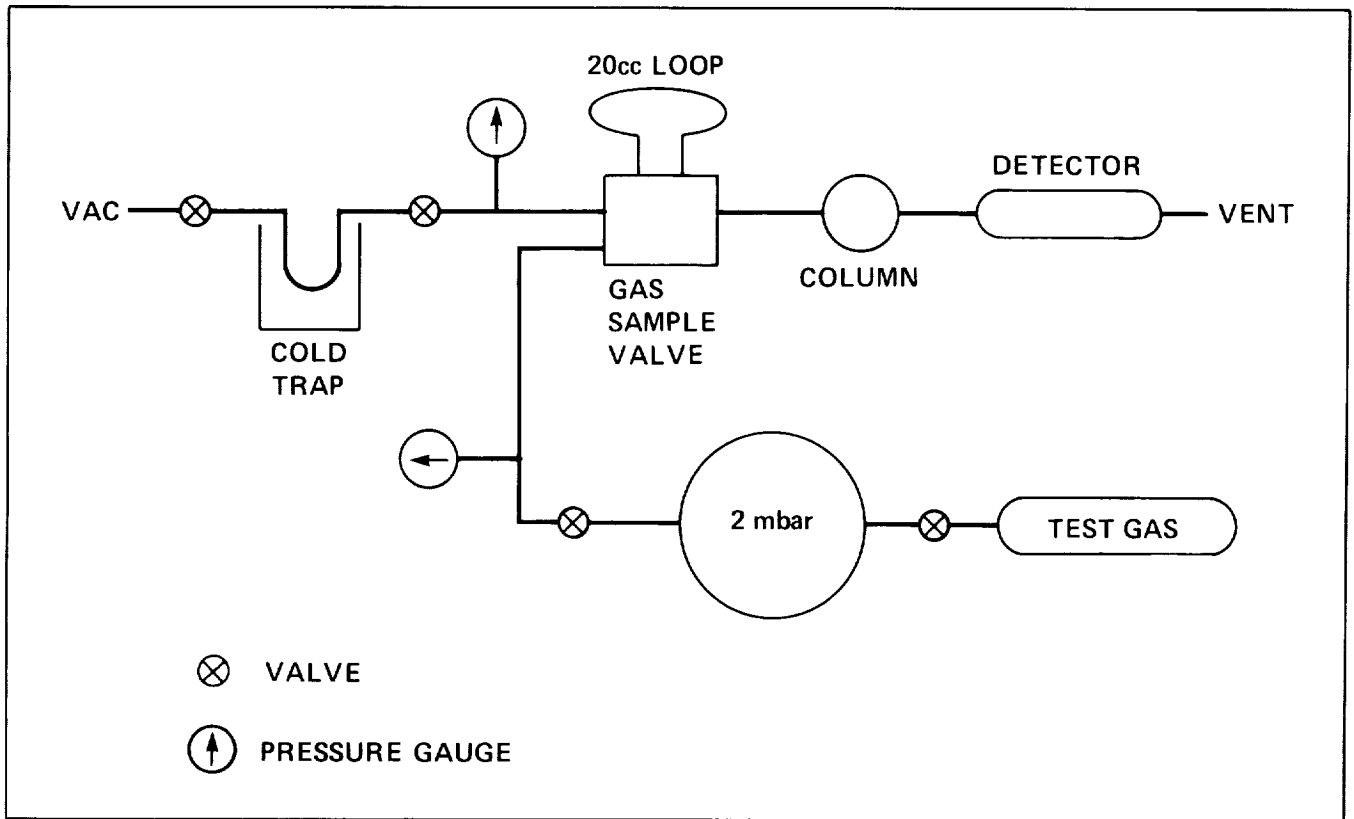
Role of magnesium ion in polynucleotide synthesis and in model systems; (a) polynucleotide synthesis reaction; (b) model hydrolysis reaction mimics synthesis

Gas Chromatographic Analysis of Model Titan Atmosphere at Low Pressures

Plans are being made to send a spacecraft to the Saturnian system to conduct studies of Saturn and one of its satellites, Titan. Gas chromatographic instrumentation to analyze the atmosphere of Titan is being developed by the Solar System Exploration Branch at Ames Research Center. The wide range of pressure regions to be sampled, from 2 mbar to 1.5 bars, will require specialized sample collection and analytical techniques. Gas analysis at first instrument deployment (180-km altitude) presents the most difficult scenario. The low ambient pressure at that altitude makes sample collection difficult and provides very little gas for analysis.

Preliminary studies done with a 20-cm³ sampling system and the very sensitive meta-stable ionization detector show that hydrocarbon components can be detected at very low concentrations. The first figure shows a schematic of the low-pressure sampling system that was used to analyze a model Titan atmosphere. A test gas of a model Titan atmosphere is used to pressurize a sample reservoir to 2 mbar. The sample is then allowed to expand into an evacuated sample loop for injection into the gas chromatograph.

The final figure shows the gas chromatogram of the mixture. Detection of the parts-per-million-level components was readily accomplished and the results can be extrapolated to yield detection limits of about 10 parts per billion. The time required to collect and analyze the gas sample should be as short

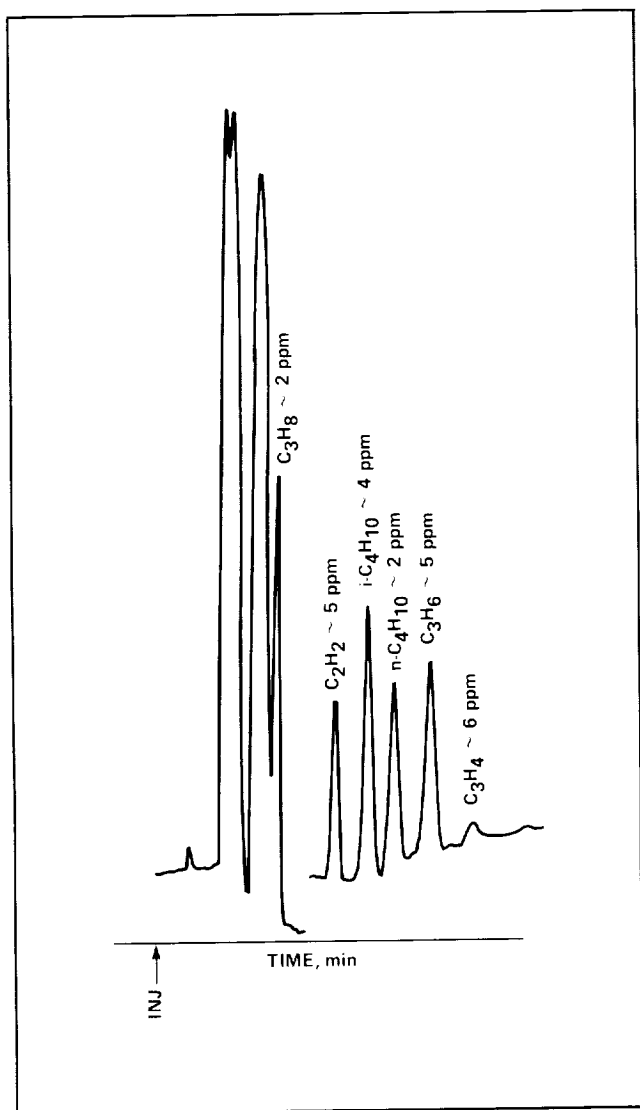


Low-pressure gas sampling system for analyzing a model Titan atmosphere

as possible, within mission time constraints. In this case, the time required to transfer a sample from the reservoir to the sample loop was about 100 seconds,

within the acceptable limits for the current mission plan.

(D. Kojiro, Ext. 5364)



Chromatogram of a hydrocarbon mixture analyzed using the system shown in previous figure. The total pressure of the mixture was 2 mbar, and the concentrations of the individual components are shown in the figure. All of the gases indicated have been found in or are expected to exist in Titan's atmosphere

Ecosystem Nitrogen Cycles as Modeled for Possible Ancient Martian Communities

The nitrogen cycle of the microbial communities inhabiting the Antarctic dry valleys is different from that found in other ecosystems and is influenced by

the harsh climatic conditions of the area. Two of the communities inhabiting this ecosystem include the cryptoendolithic microbial community living within the sandstone rocks and the microbial mat community living beneath the perennially ice-covered lakes within the valleys. The environments in which these communities live are very dissimilar; one within a lake and the other within a dry rock.

For the cryptoendolithic community, it has been determined that there is a net flux into the system of $17 \text{ mg NO}_3^- \text{ N m}^{-2} \text{ yr}^{-1}$ and $4 \text{ mg NH}_4^+ \text{ N m}^{-2} \text{ yr}^{-1}$ from the atmosphere. The concentration of both ions in the habitable zone of the colonized rock is approximately 60 mg N m^{-2} . The infall of NO_3^- results from atmospheric fixation by lightning and aurorae, while ammonium is probably blown in from the McMurdo Sound marine ecosystem. These sources obviate the need for in situ biological fixation, which is not observed. Based upon the uptake of radiocarbon, it has been determined that the biological incorporation of fixed nitrogen is $\leq 0.2 \text{ mg N}$, as NH_4^+ and NO_3^- . Although bacteria capable of denitrifying exist within the community, they are not denitrifying because of the physical structure of the system; in the hard porous sandstone there are no diffusive barriers that allow for the formation of anaerobic microsites. No nitrification could be detected by either the evolution of N_2O in control samples, or the accumulation of NO_2^- when NaClO_3 was used to block its oxidation by nitrification. The microbial community inhabiting this system performs the least number of transformations of nitrogen of any ecosystem reported to date, and therefore may represent the simplest nitrogen cycle in nature.

It has been determined that biological nitrogen fixation does not occur within the benthic microbial mat community inhabiting Lake Hoare. These data allow one to suggest that either (1) the demand for nitrogen is being met by the input of fixed nitrogen into the lake from meltwater flow into the lake and by the input of sediment entering the lake through the ice, or (2) high concentrations of oxygen in micro-zones within the sediment decrease significantly the areas that allow biological nitrogen fixation to occur.

Preliminary data gathered during the 1987-88 austral summer from Lake Hoare indicate that denitrification occurs only within the anaerobic sediment of this lake. In shallow portions of the lake, the high level of oxygen in the water column and

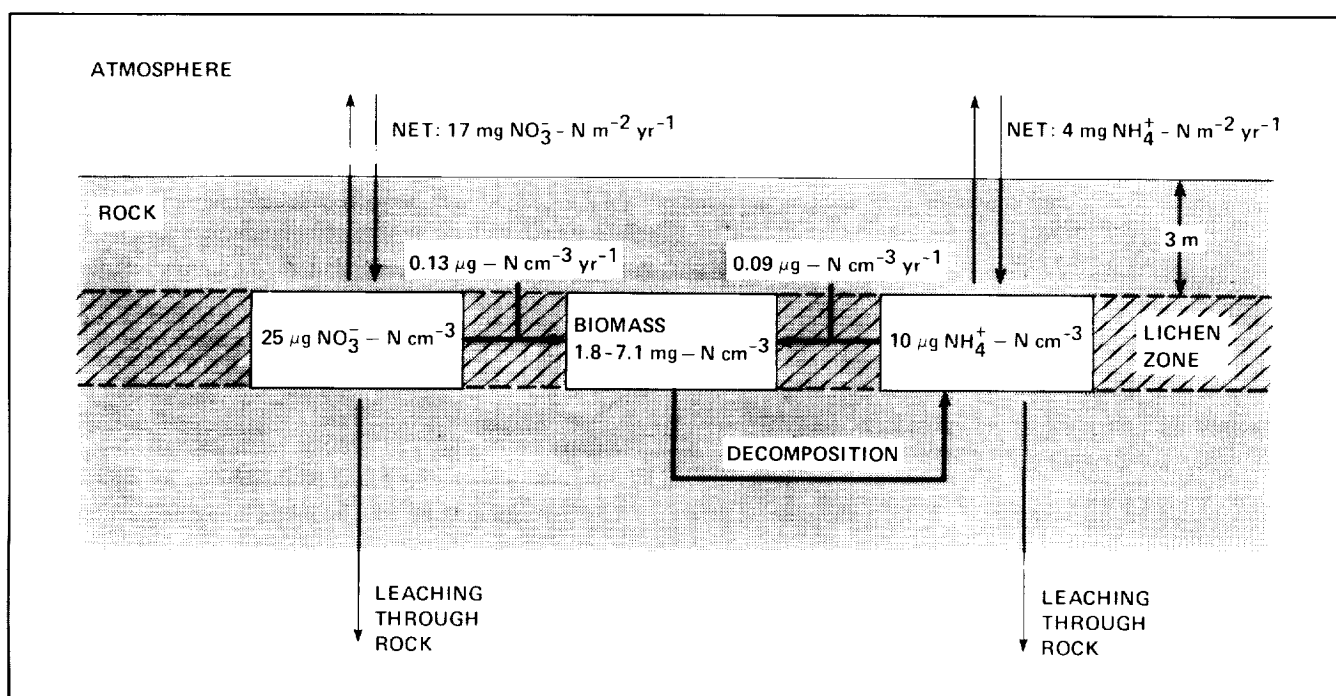
sediment appears to be inhibitory to denitrification. Nitrification within this community produces nitrous oxide at the bottom of the lake, causing the lake water to be about 490% supersaturated, compared to 140% saturation at the ice/water interface.

Studying such simple systems may have implications for understanding the evolution of the nitrogen cycle on early Earth. In addition, because it is thought that the environmental conditions on early Mars were much like those of early Earth, these systems may be regarded as analog or model systems for comparing what may have occurred on early Mars.

Because nitrogen is an important factor limiting primary productivity and microbial activity in Alpine ecosystems, it is important to understand the nitrogen cycle of this system. As part of the cycle, determining the rates of nitrogen fixation and denitrification is important in understanding the nitrogen bal-

ance within the ecosystem. The purpose of this project is to determine the rates of nitrogen fixation and denitrification for areas representative of Alpine tundra. Nitrogen fixation rates were determined *in situ* by using the acetylene reduction method. Rates of denitrification were similarly determined by using acetylene to block the reduction of nitrous oxide to dinitrogen and were monitored for the accumulation of N_2O .

Nitrogen fixation and denitrification appear to be at their peak during the spring in association with snowmelt, and at a minimum during the fall. Our previous work has shown that microbial activity, including nitrogen fixation and denitrification, is essentially zero from the time of first freeze to the time of spring thaw. One can approximate the overall nitrogen fixation and denitrification rates for Alpine tundra to be $\sim 5.2 \text{ mg N m}^{-2}/\text{yr}$, and $\sim 1.2 \text{ mg N m}^{-2}/\text{yr}$, respectively.



Representation of the nitrogen budget and cycle of the cryptoendolithic microbial community inhabiting the sandstone rocks of Linnæus Terrace, upper Wright Valley, Antarctica. The boxes represent the nitrogen pool sizes, and the arrows represent the nitrogen fluxes. The net annual flux of $\text{NO}_3^- \text{ N}$ and $\text{NH}_4^+ \text{ N}$ from the atmosphere into the rock is 17 mg m^{-2} and 4 mg m^{-2} , respectively, which creates reservoirs containing $25 \text{ mg NO}_3^- \text{ N m}^{-2}$ and $10 \text{ mg NH}_4^+ \text{ N m}^{-2}$ within the colonized zone of the rock ($\sim 3\text{-}5 \text{ mm}$ beneath the rock surface). The uptake rate for $\text{NO}_3^- \text{ N}$ is $0.13 \text{ mg m}^{-2}/\text{yr}$, and for $\text{NH}_4^+ \text{ N}$ it is $0.09 \text{ mg m}^{-2}/\text{yr}$. The time scale for replacement of biological nitrogen is $\sim 10^4 \text{ yr}$.

Rates of biological nitrogen fixation and denitrification are significantly positively correlated with soil moisture. The greatest rates of nitrogen fixation were in those areas containing nitrogen-fixing plants (e.g., *Trifolium* and *Dryas*), while the smallest rates were in dry sites associated with *Kobresia*. The balance between nitrogen fixation and denitrification on Niwot Ridge results in a net gain of $\sim 4.0 \text{ mg N m}^{-2}/\text{yr}$ to the system; while on the Martinelli slope, a net gain of $\sim 6.85 \text{ mg N m}^{-2}/\text{yr}$. This is not enough to meet the ecosystem's demand for fixed nitrogen. The primary source of fixed nitrogen for this ecosystem appears to result from atmospheric fixation by lightning and aurorae.

If one places the Antarctic dry valley crypto-endolithic microbial community (which we have shown to have no nitrogen cycle) at one end of a continuum, and forest ecosystems (which depend on biological nitrogen fixation and have a complete nitrogen cycle) at the other, this ecosystem bridges the gap in that continuum.

(R. Mancinelli, Ext. 6165)

Mars Penetrator Instrumentation Design for Exobiology

Penetrators have been proposed to explore the Mars subsurface as a relatively inexpensive method of deploying a network of scientific stations on the planet. A series of these free-falling, dart-like objects released from an orbiting space vehicle would provide access to a wide range of Martian environments. Upon impact with the surface, the forebody of the device separates from the afterbody and penetrates the soil to a depth of several meters. The afterbody, connected to the forebody by an umbilical, remains on the surface to transmit information to the orbiting satellite. The power unit for the penetrator is contained within the afterbody.

A penetrator dedicated to exobiological experiments would analyze Martian soil for evidence of past life by looking for organic materials and diagnostic soil chemistry. Evidence would also be sought for prebiotic chemical signatures. There is considerable geological, geomorphological, and climatological evidence that the early phases of Martian history were similar to those of Earth at a time when

life began on this planet. The relative (geological) quiescence of Mars since that time may have preserved evidence of early biological activity and, thus, could provide a window on ancient Terrestrial history. Exobiological analyses would be conducted with (for example) differential scanning calorimeters, evolved gas analyzers, alpha particle analyzers, and gas chromatographs. These are all stationary instruments remaining within the body of the penetrator.

An engineering design study has been conducted to investigate methods of acquiring soil samples for delivery to the internally housed instruments. The University of Wisconsin design, generated in conjunction with the Solar System Exploration

Branch at Ames Research Center, provides engineering concepts and specifications for

1. a suspension system that protects the sampling device during penetrator impact and maintains alignment of the sampler with the penetrator body,
2. a U-lever and plug mechanism that automatically provides an orifice for obtaining samples when the sampling device is activated,
3. a tracking system for guiding the sampling device through the orifice,
4. an innovatively designed boring tool that penetrates the soil and draws a soil sample into the penetrator body,
5. a miniature gearbox/motor assembly providing opposing rotations for the two intersleeving components of the boring tool,
6. a spring-driven, sample-placement device for delivering the internally acquired sample to onboard instruments for analysis,
7. a transfer mechanism that allows a sample to be passed from one instrument to another.

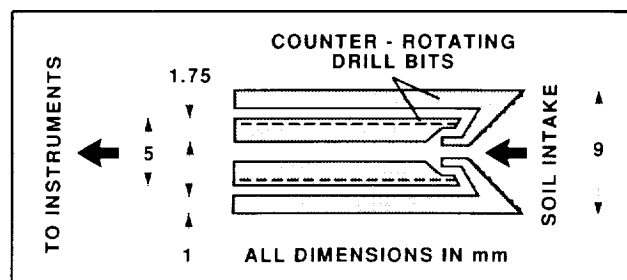
The design incorporates spring-driven mechanisms wherever possible because springs provide an extremely simple and efficient way of storing mechanical energy. Also, the compression-spring force used to push the rotating drill bit into the soil automatically compensates for resistance to drilling and thus prevents "stalling" of the mechanism.

The drill bit used by the sampling device (see figure) is composed of two hollow components, one inside the other. The outer bit has a tapered, diamond-impregnated cutting end that guides the sample to the inner bit while providing an excessive volume to minimize material cavities. The inner bit moves the sample back into the penetrator shell

where it can be deposited on a tray for analysis. Because the sample must be chemically and physically unaltered, the heat generated by the drilling operation is dissipated by the gas buffer between the two bits, and by the thermal conductivity of the drill's titanium alloy.

The study also provided some solutions to the forebody/afterbody coupling. An elastically deflected beam and locking-pin system provides a means of maintaining rigid forebody/afterbody coupling during flight, but shearing of the pins allows separation of the two units upon impact with the surface. The afterbody of the penetrator is flared so that deceleration of the unit is greater than that of the forebody, thus inducing the necessary differential motion for shearing the pins.

(J. Marshall, D. Schwartz, and G. Carle, Ext. 4204)



Penetrator drill

Cometary Impact and Chemical Evolution

Calculations of breakup altitude and deceleration of comets entering the primitive atmosphere of Earth indicate that comet nuclei were easily crushed by aerodynamic forces high above the Earth's surface. Comets smaller than 150 meters would have been completely decelerated by passage through the atmosphere and vaporized as they stopped, and the material would have been dispersed. Larger comets also would have been crushed, but the material would not have dispersed. They would have retained much of their cosmic velocity, and impact-generated shock waves would have shock-heated and vaporized these comets.

Vapor clouds of comets entering the atmosphere would have formed isolated clouds of material con-

taining excited cometary organic radicals. Comparing cometary composition and internal energies of cometary vapor clouds with the composition and internal energies of gases which have been exposed to experimental shock waves indicates that useful organic monomers, such as amino acids, may have been produced during the cooling of cometary vapor clouds. Thus, the potential exists for prebiotic chemical evolution in the atmosphere following cometary entry.

In order to examine this potential, we studied particle coalescence following cometary entry. The flux of cometary material entering the Earth's atmosphere during the first 700 million years would have been sufficient to cause the growth of particles that were large enough to sediment from the atmosphere in periods of a few months to a few years, depending upon the variations in the cometary entry rate.

Particle growth is an effective means of concentrating organic monomers from a dilute solution in the terrestrial environment. This is the next step in chemical evolution. Monomer concentration is an important requirement for formation of polymers because monomers must be close to other monomers in order to bond and form polymers. Thus, any monomers formed from cooling comet vapor clouds would have been brought close to other monomers by particle coalescence in the atmosphere. Coalescence following cometary entry may have satisfied an important need to concentrate prebiotic reactants.

Other processes operating during cometary entry were also found to be useful for prebiotic chemistry. For example, previous studies have indicated that wetting and drying cycles, heating, formation of aerosols, aqueous chemistry, and clay chemistry were all helpful for the formation of polymers. All of these processes or phenomena would have been present during sedimentation or scavenging of particles containing prebiotic monomers formed from cometary entry. Results indicate that prebiotic evolution may have been a common process in the universe because comets would have impacted during the late stage in accretion of the planets in any evolving solar system.

(V. Overbeck and C. McKay, Ext. 5496/6864)

Economical Signal-Processing Algorithms for SETI

Because of the very large volume of data, the high data rate, and the prevalence of terrestrial interference, NASA's Search for Extraterrestrial Intelligence (SETI) observational program must perform its signal-processing and recognition tasks in real time. The ability to extract weak signals having a wide range of potential characteristics, in real time, is what distinguishes the NASA SETI project from previous efforts. Detectable signals must be band-limited, either continuous wave (CW) or narrow band pulses, but they need not remain stationary in frequency. Relative acceleration between the transmitter and receiver (perhaps induced by planetary rotation) could introduce an arbitrary frequency drift as large as ± 1 part in 10^9 (± 1 Hz/sec at 1 GHz) and the SETI signal-detection algorithms must still be able to recognize the signal.

During 1988 we have made considerable progress in designing signal-processing algorithms that can detect drifting CW or pulsed signals with maximum economy of memory and computational load, and with minimum loss in sensitivity. For each of two polarizations, at 1-Hz resolution, the 10-million-channel spectrum analyzer to be used in SETI will produce 2×10^7 bytes of complex amplitude spectral data every second, plus an equal rate of data from each of the 2-, 4-, 7-, 14-, and 28-Hz resolutions. Thresholding on power for each of the resolutions can be used successfully to lower the data rate when one looks for periodic narrow band pulses. If we then apply an algorithm that looks for all possible pulse pairs and then a third pulse at the implied position, pulse detection in the presence of Gaussian noise can be accomplished, over a 10-MHz input bandwidth, in real time by using Microvax-class computers. The resulting detection sensitivity is within 3 dB of what is optimally possible if no threshold were applied and all the data were used.

The presence of one or more strong radio frequency interference (RFI) signals can greatly increase the number of events above a given threshold. Strong RFI will require that the threshold be raised or that segments of the data be discarded in order not to overload the computational capacity of any specific implementation of this pulse-detection scheme.

Coherently accumulating the complex amplitudes from a CW signal over a 1000-sec interval with a perfectly matched filter, appropriate to the drift rate, could achieve a signal-to-noise ratio (SNR) of -15 dB in a 1-Hz channel. In the SETI observations, using 10^7 channels of spectral data at 1-Hz resolution, and allowing for all possible discernibly different drift rates at the end of 1000 sec for each of these channels, a signal processor that would produce the optimal matched filter sensitivity in real time would require 2×10^{16} bytes of memory and a computational speed of 3×10^8 million instructions per second (MIPS). This is far beyond the capability of current hardware.

Incoherent accumulation of power spectra along the 1999 possible distinct drift lines for 1000 sec can be achieved with 10^{10} bytes of memory and 10^4 MIPS of computational capability. The best SNR that can be achieved with incoherent processing techniques is -6 dB, which is far below the coherent result, but substantially better than the 0 dB that has characterized previous SETI searches for nondrifting CW signals. The memory and computational requirements are still too costly for implementation in available general-purpose computers. Specialized processing hardware or algorithms that are more economical in memory or speed are required, and both are being investigated. Small Business Innovation Research awards to investigate special-purpose pulse and CW hardware detectors have been made and should produce results next year.

At Ames Research Center we have developed algorithms that implement the 1000-sec incoherent accumulations as sequences of shorter accumulation stages with "tree-pruning" at each stage, optimized to keep memory usage constant. These algorithms succeed in reducing the memory requirement to 3×10^8 bytes and the required processing speed to 300 MIPS, which is within reach of commercially available parallel architecture machines. The sacrifice in sensitivity for this economy is only 1 dB, in the absence of interference. The relative robustness against RFI of the algorithmic and special-purpose-hardware solutions has yet to be compared for cost effectiveness.

The amount of RFI that will typically be encountered during observations represents the greatest uncertainty in SETI signal processing today. There are a number of different ways in which RFI signals can be recognized and ignored, or excised, before



A data field containing the events above a threshold that passes 1% of the noise in the frequency-time plane. Frequency is displayed as individual spectral channels running horizontally, and each line represents a successive time sample of the spectrum. These data represent noise, plus a regular narrowband pulsed signal with a peak SNR of 8 dB and an average power of -4 dB times the mean noise



The same data field with the regularly spaced pulses identified by a three-pulse algorithm (Detection requires about 0.1 ms on a Microvax)

they can overload the signal-processing algorithms. However, all such schemes require additional hardware, firmware, and software that significantly increase the cost of the observational systems. Research in the future will focus on a categorization of the current RFI situation and on realistic projections so that the most cost-effective observing system can be specified.

(B. Oliver, Ext. 5166)

Progress in Signal Detection in SETI

In the Search for Extraterrestrial Intelligence (SETI) office at Ames Research Center, we are trying to detect signals generated by another technology. We do not consider complex signals whose energy is spread over a large area in the frequency-time plane, and thus appear noiselike. Instead, we limit the search to simple signals, such as monochromatic carrier waves (CW) whose energy is concentrated in frequency, or to regular trains of pulses whose bandwidth is no wider than that required by the duration of a single pulse. To get enough energy per pulse, the duration must be on the order of 1 sec. Thus we are looking for features only a few hertz wide in a broadband (~10 GHz) spectrum of thermal noise. To find these tiny "needles" of power in the broad "haystack" of noise in a reasonable time requires looking at many millions of possible frequencies at once. We need a multi-channel spectrum analyzer (MCSA) followed by pattern detectors.

The first prototype MCSA with 74,000 channels, each 0.5 Hz wide, was tested at the Goldstone, CA, tracking station beginning in March 1985. It filled one cabinet 6 ft high. Had it been expanded to cover 10 MHz in two polarizations, 30 such cabinets would have been needed. To cover the 300-MHz band proposed for use in a sky survey, 900 cabinets would have been needed.

ORIGINAL PAGE
BLACK AND WHITE PHOTOGRAPH

Realizing this, a design team at Stanford University, funded by a cooperative agreement with Ames, embarked on a program to reduce much of the hardware to a customized VLSI chip. This has resulted in more than an order-of-magnitude reduction in size and board count. The whole MCSA module, covering 10 MHz of spectrum in both polarizations and delivering simultaneously resolutions of 1, 2, 4, 7, 14, 28, and 643 Hz, can now fit into two racks. Further reduction of another factor of five or even ten may be possible.

Paralleling this hardware miniaturization effort has been the development at Ames of economical algorithms for the detection of the CW and pulsed signals. These algorithms save another order of magnitude or more in the computation rate and memory required, with little sacrifice in sensitivity.

(B. Oliver, Ext. 5166)



Custom Digital Fourier Transform Chip. This VLSI chip embodies in a pipelined structure the memory and arithmetic units required to perform a prime-factor fast Fourier Transform. The chip has 45,000 transistors and replaces the entire printed circuit board shown above it

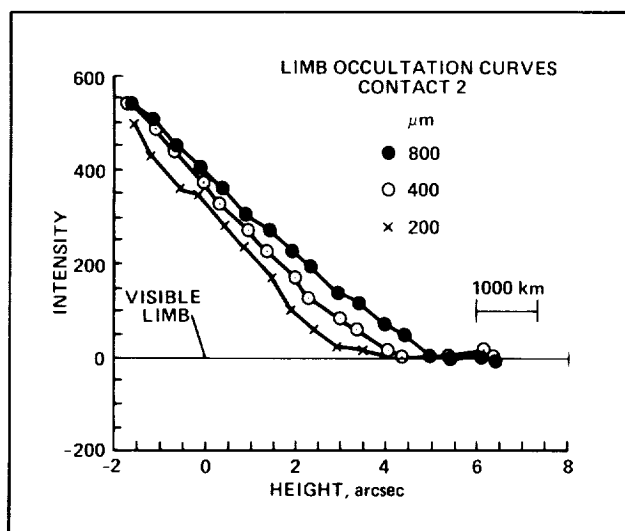
Submillimeter Observations of the Total Solar Eclipse of March 18, 1988

The path of the total solar eclipse of March 18, 1988, began in the Indian Ocean, passed over Borneo, and finally ended in the Gulf of Alaska. In order to intercept the eclipse path, the Kuiper Airborne Observatory was based in Guam and was flown along the eclipse path over the Pacific Ocean. This not only assured observation in the clear, but it also took the telescope above most of the absorbing atmospheric water vapor, which allowed observations to be made of the Sun at far-infrared wavelengths, wavelengths that would be invisible from even the driest sites on the Earth's surface. During the observations the limb of the Sun was simultaneously observed at visible, 30-, 50-, 100-, 200-, 400-, and 800- μ m wavelengths as the Moon slowly covered the limb. This technique produced a much finer spatial resolution of the different layers of the solar atmosphere than could have been obtained from even the largest telescopes on Earth.

Infrared observations are basically very sensitive measurements of the temperature and density of the different layers of that region of the solar atmosphere known as the chromosphere. The chromosphere is an interesting and poorly understood region of the Sun that is the location of the solar temperature minimum, since much higher temperatures are found both inside the Sun and out in the solar corona. Obviously the energy transport mechanism must change in this region so that energy can flow from a cooler to a hotter material. The eclipse results add to our understanding of the chromosphere and are needed to provide constraints on models of these energy-transport processes.

(T. Roellig and M. Werner, Ext. 6426/5101)

ORIGINAL PAGE
BLACK AND WHITE PHOTOGRAPH



The infrared signal at 200-, 400-, and 800-μm wavelengths from the Sun as the Moon covers the limb at second contact. Note that as the infrared wavelength increases, it originates at higher levels in the solar atmosphere

Modeling Metabolic Evolution on Mars

In the search for extraterrestrial life, we are faced with the dilemma of detecting and identifying life forms which may be quite different from those with which we are familiar. The Viking biology team used two main approaches in the search for life on Mars: visual (cameras), and metabolic (gas exchange, labeled release, and pyrolytic release experiments). The rationale for a metabolic approach was that all life had to metabolize to fuel life and reproduce. Furthermore, metabolism is a continuous process, detectable by several means.

While the Viking results suggest that there is no extant life on Mars, the possibility that life originated and became extinct persists. If the search for life on Mars is now to focus on extinct life, we suggest that visual and metabolic approaches again would be appropriate. Morphological fossils, although sometimes difficult to interpret, provide much information and have been extremely important in reconstructing extinct terrestrial life. Traces of metabolic activity, such as evidence of biological carbon or nitrogen fixation, are more likely to be preserved than are genetic attributes. Our work includes clarifying the

appropriate methods to search for a hypothetical extinct Martian biota based on metabolism.

Several methods have been used to analyze the physiology of extinct terrestrial life. First, the most obvious method is to use morphological fossils to extrapolate from what is known about extant relatives. For example, if a fossil looks like a plant, the extrapolation is that it had the metabolic attributes of extant plants, such as the ability to fix carbon, but not to metabolize exogenous organic carbon. This is a difficult criterion to apply to a planet such as Mars, where there are probably no extant representatives with which to compare. If fossils were found on Mars, the only possibility would be to compare morphologies with terrestrial analogs.

Second, when chemical signatures of extinct life are available, they are interpreted in light of what we know of their production. For example, the ratio of the stable isotopes of carbon, $^{12}\text{CO}_2$ to $^{13}\text{CO}_2$, is often used as an indication of biological carbon fixation. This criterion cannot be naively transferred to the search for extinct life on Mars. Similarly, magnetite deposits are produced both abiotically and biotically, and they can be distinguished from each other by comparing the crystal structure. Biologically deposited magnetite has a much smaller crystal lattice structure than abiotically deposited magnetite.

Third, the complexity of modern metabolic pathways may be used to place such pathways in a temporal sequence. This assumes that the complexity of a metabolic process on Earth would be indicative of its relative complexity in other, independently evolved, systems.

Fourth, phylogenetic speculation may be used to reconstruct metabolic evolution. A currently popular approach for determining phylogeny is to compare rRNA sequence data. These data can then be used to extrapolate to metabolic evolution. This is clearly a worthless approach with a hypothetical biota that does not have a recognizable analog to the terrestrial genetic code (i.e., that may not even contain nucleic acids, let alone ribosomes per se). If extant organisms were located on Mars, however, presumably they would contain some method for storing and disseminating information. This system would not necessarily resemble the nucleic acid-based terrestrial system. Thus, it would have to be analyzed de novo in the hope that an analogous system to rRNA sequence data might be found.

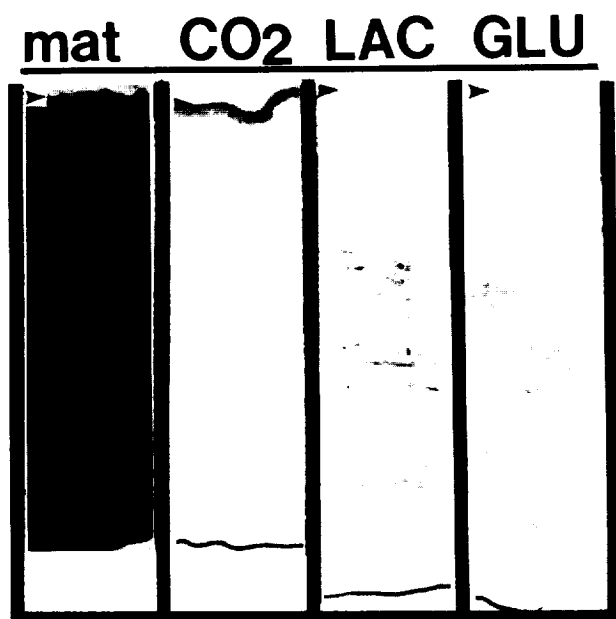
An approach that we think would be the most promising is to rationalize what the metabolic history of life might have been like on early Mars, based on what we know about the physical and chemical history of Mars and the vagaries of terrestrial metabolic evolution. For example, the physical environments on Earth and Mars probably were similar for the first billion years; then Mars became drier and colder. Because life arose on Earth during that time, it is possible that life also arose on Mars, was unable to adapt to the changing environment, and became extinct. If life arose, it may have been physiologically similar to microbial communities on Earth.

Our work has focused on carbon cycling in the microbial mat community of the hypersaline (7.2-9.1% salinity) ponds at Guerrero Negro, Baja California, as a model for such communities. These mats are finely laminate, with a 1- to 2-mm surface layer composed primarily of several blue-green algal species, and a small number of diatoms and sulfur-metabolizing photo- and chemo-autotrophs. Beneath this layer are layers of detrital material, facultatively

and obligately anaerobic bacteria, and the buried remains of former surface layers. We have exposed different faces of the mat to H^{14}CO_3 in order to locate and follow primary production; to ^{14}C -labeled lactate and glucose to follow heterotrophic activity; and to ^3H thymidine to follow DNA synthesis. Acid-stable radioactive carbon and hydrogen were visualized in longitudinal sections of the mat by a novel use of autoradiography.

These studies show that the primary site of biological carbon fixation is in the surface layers of the mat, with heterotrophic uptake of released fixed carbon occurring in the lower layers of the mat within a day of fixation. All layers of the mat of biological origin are able to incorporate lactate and glucose, with heavier labeling occurring in the surface layer. Dark and light incubations suggest that most surface labeling is due to heterotrophic uptake rather than to fixation or remineralization of carbon. The several dark, buried layers show an intermediate level of labeling and a higher level of carbonate, both of which suggest a higher level of metabolic activity. We suggest that within this community carbon fixation occurs on the surface, mostly by photosynthesis. Fixed carbon is utilized primarily in the dark layers, and secondarily in the remaining layers of biological origin. DNA synthesis, as assessed by ^3H thymidine incorporation, was detected only in the top 1 to 2 mm of the mat community.

(L. Rothschild and R. Mancinelli, Ext. 3213/6165)



Autotrophic and heterotrophic uptake of carbon. The mats were slit open, ^{14}C -labeled sodium bicarbonate, lactate, or glucose was injected (4 ml, $1\ \mu\text{Ci/ml}$), and the slit was closed quickly. Samples were incubated for 30 min. Note that carbon fixation occurs in the top layer, whereas heterotrophic uptake occurs throughout the mat

Astronomical Time-Series Analysis

The astronomical time-series analysis program is aimed at understanding the rapid and disordered luminosity fluctuations of quasars, active galactic nuclei, and radio galaxies. The current focus is the development of techniques for modeling random and chaotic processes by using time-series data. Chaos is a relatively recently discovered phenomenon in which nonlinear systems behave in a way that appears disordered, but is actually deterministic.

A simple modification of a standard method for modeling random processes has yielded a technique that works very well on chaotic processes. In addition, the method works surprisingly well on random processes, can distinguish randomness from chaos,

and, in simple cases, can even separate the two kinds of processes if both are present in the same time-series data.

A technique for computing Fourier transforms of unevenly spaced time series has been perfected. This approach allows computation of power spectra and autocorrelation and cross-correlation functions of unevenly spaced data.

(J. Scargle, Ext. 6330)

Collection of Model Titan Aerosols on Thin Wires

Titan, the largest satellite of the planet Saturn, has an atmosphere more dense and extensive than that of Earth. Based upon ground-based telescopic observations and measurements by the two Voyager spacecraft, this atmosphere is now known to consist primarily of molecular nitrogen (similar to the Earth's), with small amounts of methane, low-molecular-weight hydrocarbons, and nitriles (C-N compounds). In addition to these gases, the atmosphere contains at least three haze layers, one of which is colored and is responsible for Titan's red-orange color. At present, the composition and origin of these aerosol materials is unknown. To address, among others, the questions of the compositions of the gases and aerosols in Titan's atmosphere, NASA, in conjunction with the European Space Agency, plans to send spacecraft to Saturn and Titan (the Cassini mission) during the next decade. As part of this effort, there is an ongoing program in the Solar System Exploration Branch at Ames Research Center to develop instrumentation for the Titan probe that will collect and analyze the aerosols and gases in the atmosphere.

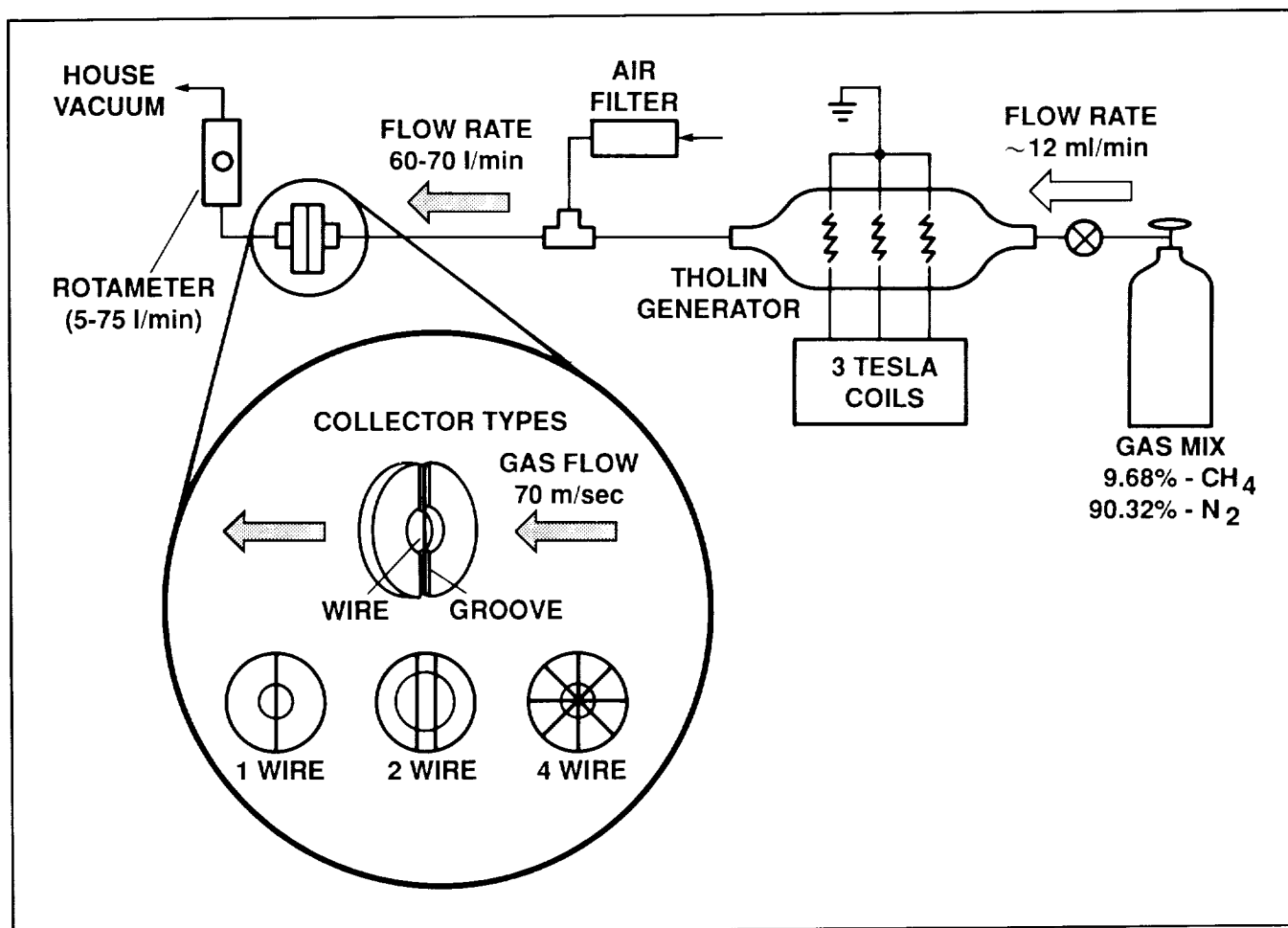
The sampling of aerosols in the atmosphere of Titan will involve collection of particles extending from nanometers (10^{-9} m) to micrometers (10^{-6} m) in size in a gas stream with velocities (owing to the

descent of the probe) ranging from 180 m/sec, at an altitude of ~ 170 km where the analytical instruments will first be deployed, to zero at the surface.

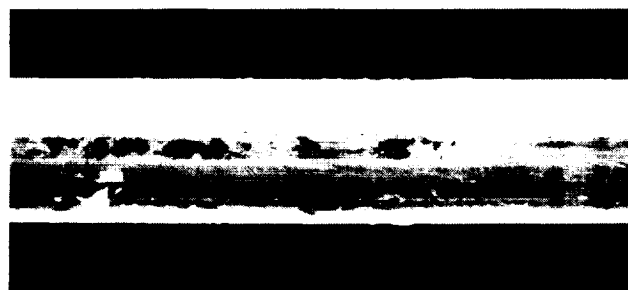
Because of their simple design and capability to collect small particles by impact, thin 25- μ m-diameter platinum wires are being examined for the aerosol collector for the Titan probe gas chromatograph. For these studies, the production of the model Titan aerosols was accomplished by exposing a mixture of 10% CH_4 -90% N_2 (modeling Titan's lower atmosphere) to three sparks powered by simple Tesla coils. The effluent of the aerosol generator was then mixed with carefully filtered room air at flow velocities of 40-56 m/sec and passed through the wire collector. This device consisted of a disk on which the wires were strung across a 0.5-cm hole through which the air passed. A schematic diagram of the aerosol generator and collector system is shown in the first figure. After about 30 min, the wires were removed from the collector and the collected aerosols were photographed with a scanning electron microscope.

A typical example of the results of these experiments is shown in the second figure. A view of the back (downstream) side of the wire is shown in the top photograph. As can be seen, the wire is clean, showing only a few particles and the marks from extrusion of the wire. In the two lower photographs, the front (upstream) side of the same wire at two magnifications is shown. The presence of numerous particles is easily seen. For the experiment shown in the figure, a mean radius of $1.4 \pm 0.5 \mu\text{m}$ for the particles was obtained. Smaller ($\sim 0.2\text{-}\mu\text{m}$) particles were collected in other experiments. Thus, submicron- to micron-size model Titan aerosols can be collected on thin wires. With further development of wire collectors now under way, it is expected that a wire array (mesh) device will be able to collect and prepare for analysis (by pyrolysis) any aerosols present in the lower region of Titan's atmosphere where the probe will be operational.

(T. Scattergood, V. Oberbeck, Ext. 6163/5496)



System used to generate and collect model Titan aerosols



(a) 1000 15 kV 741



1000 15 kV 539



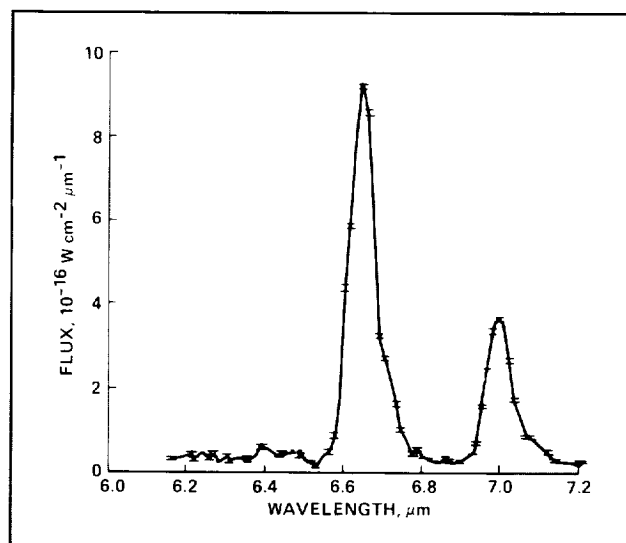
(b) 3000 15 kV 538

Collection of simulated Titan aerosols on a 25-μm-diameter wire (mixture 10% CH₄, 90% N₂).

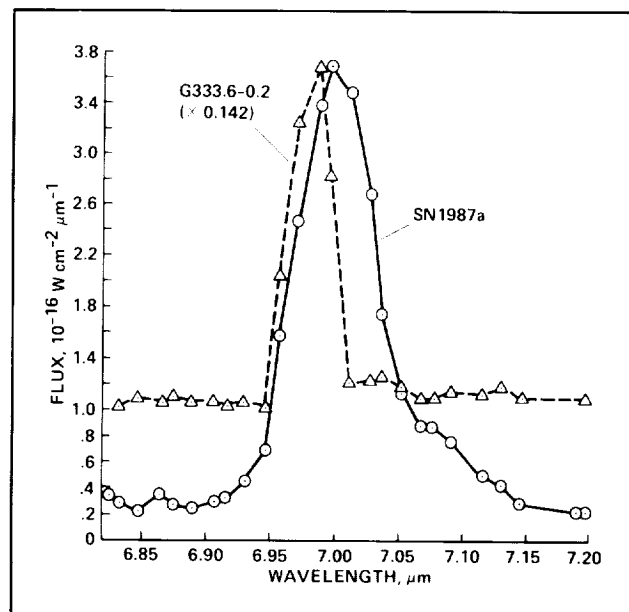
(a) Back view, (b) front views

Infrared Spectral Line Profiles of Supernova 1987a

Spectroscopic study of SN1987a (the supernova in the Large Magellanic Cloud (LMC)) from the Kuiper Airborne Observatory permits the determination of important details of the explosion that cannot be learned from ground-based observatories. The



Spectrum of Supernova 1987a showing NII and ArII lines. Note asymmetry on long wavelength side



Comparison of the ArII line in a nonexpanding, slow-moving ionized gas cloud with the same line in the supernova

forbidden lines of NII (6.634 μm) and ArII (6.983 μm) emitted by core products of the explosion (i.e., materials produced in the shock wave after core collapse) are unique in their strength and relative freedom from overlapping lines. Consequently their line profiles can be studied in detail.

ORIGINAL PAGE
BLACK AND WHITE PHOTOGRAPH

This study was accomplished with the Ames Faint Object Grating Spectrometer (FOGS), which covers the wavelength range in which the NIII and ArII lines appear with enough sensitivity to provide signal-to-noise ratios of 100 in the lines. FOGS provided resolving power sufficient to measure not only the average expansion velocity of 1400 km/sec, but also a red shift of the line centroids of 440 km/sec relative to the LMC recessional velocity (see figures).

An asymmetry is exhibited in the profiles of both lines. The asymmetry and the anomalous red shift can be explained in terms of scattering of the photons (emitted from NIII and ArII) by electrons in the expanding hydrogen envelope of the supernova in a

model that requires radial electron velocities up to 3000 km/sec and an electron optical depth of 0.4. Although evidence for this mechanism for producing red shifts has been searched for before (in quasi-stellar objects), this is probably the first time that it was ever observed.

This research was an application of the multiple-detector, infrared-spectroscopy capability developed by Ames Research Center scientists in collaboration with Lick Observatory over the past 10 years.

(F. Witteborn and J. Bregman, Ext. 4520/6136)

Report Documentation Page

1. Report No. NASA TM-101070		2. Government Accession No.		3. Recipient's Catalog No.	
4. Title and Subtitle Research and Technology Annual Report – 1988				5. Report Date August 1989	
				6. Performing Organization Code	
7. Author(s) Ames-Moffett and Ames-Dryden Investigators				8. Performing Organization Report No. A-89034	
				10. Work Unit No. 506-90	
9. Performing Organization Name and Address Ames Research Center Moffett Field, CA 94035-5000				11. Contract or Grant No.	
				13. Type of Report and Period Covered Technical Memorandum	
12. Sponsoring Agency Name and Address National Aeronautics and Space Administration Washington, DC 20546-0001				14. Sponsoring Agency Code	
15. Supplementary Notes Point of Contact: Dr. J. N. Nielsen, Chief Scientist, Ames Research Center, MS 200-1A, Moffett Field, CA 94035-5000 (415) 694-5500 or FTS 464-5500 or the Ames telephone number(s) at end of each item					
16. Abstract Selected research and technology activities at Ames-Moffett and Ames-Dryden are summarized. These accomplishments exemplify the Center's varied and highly productive research efforts for 1988.					
17. Key Words (Suggested by Author(s)) Space science, Life science, Space and terrestrial applications, Aeronautics, Space technology				18. Distribution Statement Unclassified-Unlimited Subject Category - 99	
19. Security Classif. (of this report) Unclassified		20. Security Classif. (of this page) Unclassified		21. No. of Pages 265	
				22. Price A12	